Discovery of Anti-Tuberculosis Lead Compounds from Actinomycetes

By

Wei Gao
B.S. China Pharmaceutical University, 2008

DISSERTATION

Submitted as partial fulfillment of the requirements
for the degree of Doctor of Philosophy in Medicinal Chemistry
in the Graduate College of the
University of Illinois at Chicago, 2014

Chicago, Illinois

Defense Committee:

Dr. Scott G. Franzblau, Advisor
Dr. Guido F. Pauli, Advisor
Dr. Birgit U. Jaki
Dr. James B. McAlpine
Dr. Brent J. Friesen, Dominican University

Copyright © by Wei Gao. All rights reserved. Printed in the United States of America. Except as permitted by United States Copyright Act of 1976, no part of this publication may be reproduced or distributed in any form or by any means without the prior written permission of the author.

DEDICATION

To my parents,

Chuanyu Gao and Li Xue.

ACKNOWLEDGEMENTS

This dissertation would not have been made possible without the enormous help from many people. I am grateful to all who have helped along the way and made the current work a reality.

First and foremost, my thanks go to my major advisor, Dr. Scott G. Franzblau, for sharing his knowledge and passion in searching for a cure for tuberculosis (TB). He impressed me not only by his dedication to quality science, but also by his humor, generosity, and unbounded enthusiasm. Secondly, I would like to thank my co-advisor, Dr. Guido F. Pauli, whose extensive knowledge and meticulous attitude showed me the example of an excellent scientist. I am very grateful to both my advisors for their patience, guidance and constant support throughout the course of my Ph.D. study.

I'd also like to thank others on my committee. I thank Dr. James B. McAlpine for his continued help for editing my scientific writings, and willingness to share his knowledge and experiences in both science and everyday life. I thank Dr. Birgit U. Jaki, for her help and kind advice in chemistry work and structure elucidation. I thank Dr. J. Brent Friesen for sharing his insightful knowledge of countercurrent chromatography and resolving many complex instrumentation problems.

I also thank Dr. Sanghyun Cho for his guidance and support in bioassays and in vitro experiments. I thank Dr. David C. Lankin for his support in NMR experiments as well as suggestions on my dissertation. I am also thankful to Dr. Shao-Nong Chen for his enormous help in maintaining various lab instruments and kind advice.

ACKNOWLEDGEMENTS (continued)

Many thanks go to Yuehong Wang. She is behind all the macrophage, cytotoxicity and mouse efficacy experiments in this dissertation. I also thank Baojie Wan and Dr. Chang Hwa Hwang for training me on various bioassays. I thank Dr. Larry Klein for the help discussion on Marfey's experiment. I thank Mr. Jeffrey R. Anderson for his great work on biochemistry.

My thanks also go to all my lab colleagues. Dr. José G. Napolitano ran many NMR experiments for my project, and showed me how to use the PERCH NMR software tool. Drs. Maria Florencia Rodrigues-Brasco, Charlotte Simmler, Johnathon Bisson, Joo-won Nam, René F. Ramos Alvarenga, Geping Cai, and Nan Zhang also provided their enthusiastic help in my research work. I feel privileged to work with all of them, as they never hesitated to share their expertise and experiences, asking nothing in return.

I would like to acknowledge ECUM at Myongji University, Korea, especially Dr. Joo-won Suh and Mr. Jin-Yong Lee, for sharing their huge actinomycete library, the contribution in identifying ecumicin's crystallographic structure and efforts in unveiling ecumicin's nonribosomal peptide synthetase.

I thank Drs. Alfred F. Goldberg, Olga Kandror and Tatos Akopian, from the Department of Cell Biology, Harvard University, for their work on ecumicin's mechanism of action.

I am thankful to NMR instrument support provided by the following individuals at the National Research Council, Halifax, Canada: Mr. Ian Burton as well as Dr. Tobias Karakach.

ACKNOWLEDGEMENTS (continued)

Finally, I am indebted to the Department of Medicinal Chemistry and Pharmacognosy for providing teaching assistantships and tuition waiver for my first two and half years here, and the College of Pharmacy for offering me a W.E. van Doren Scholarship.

WG

TABLE OF CONTENTS

1. Anti-Tuberculosis Drug Discovery from Microbes 1
   1.1 Introduction 1
      1.1.1 Tuberculosis remains a major public health threat 1
      1.1.2 Perspective on TB treatment 4
      1.1.3 Actinomycete as a viable source of new anti-tuberculosis agents 11
   1.2 Research goal and working hypothesis 15

2. High-throughput Screening of Actinomycetes 18
   2.1 Introduction to TB high-throughput screening 18
   2.2 Selection of screening methods 22
      2.2.1 Anti-TB activity 22
      2.2.2 Biological dereplication 22
      2.2.3 Anti-microbial inhibition spectrum 24
      2.2.4 Toxicity against mammalian cells 24
   2.3 Composition of actinomycetes extract library 25
   2.4 HTS Methodology 27
      2.4.1 High-throughput screening scheme 27
      2.4.2 Material and Methods 29
   2.5 Results 32
   2.6 Discussion 39
      2.6.1 Dereplication efficiency 39
      2.6.2 Potential false negatives 39

3. Strain MJM5123 identification and optimized growth condition 41
   3.1 Identification of strain MJM5123 41
   3.2 Optimized culturing conditions to improve ecumicin yield 44
      3.2.1 Lab-scale production of ecumicin from MJM5123 through a three stage fermentation procedure 46
      3.2.2 Large-scale production of ecumicin from MJM5123 47
   3.3 Material and methods 48

DISCOVERY OF ECUMICIN. 50

4. Isolation of Ecumicin 50
   4.1 Discovery of ecumicin via bioassay-guided fractionation 50
   4.2 Optimized fractionation scheme for mass production 52
   4.3 Discussion 56
   4.4 Material and methods 58

5. Structure elucidation 63
   5.1 Classification – the peptidic nature of ecumicin 63
   5.2 Connectivity solved by NMR experiments with the help of tandem mass analysis 68

TABLE OF CONTENTS (continued)

5.3 Stereochemistry identified by X-ray crystallography and Marfey's experiment 102
5.4 Verification of ecumicin's proposed structure by ^{1}H iterative Full Spin Analysis (HiFSA) 109
5.5 Material and Methods 113

6. Biosynthetic pathway of ecumicin 115
6.1 The non-ribosomal peptide synthetase gene cluster. 115
6.2 Material and methods 122

7. Ecumicin is a potent anti-TB agent in vitro and in vivo 123
7.1 *in vitro* biological profile of ecumicin 124
7.1.1 Ecumicin is a potent and selective anti-TB agent in vitro 124
7.1.2 in vitro microsomal stability 129
7.1.3 in vitro permeability – Caco-2 assay 129
7.1.4 Material and methods 129
7.2 Formulation development and animal studies 134
7.2.1 Suspension 136
7.2.1.1 Formulation preparation 136
7.2.1.2 Pilot PK study 136
7.2.1.2.1 Methodology 136
7.2.1.2.2 Result 137
7.2.2 Emulsion 138
7.2.2.1 Formulation preparation 138
7.2.2.2 Pilot PK study 138
7.2.2.2.1 Methodology 138
7.2.2.2.2 Result 139
7.2.2.3 Efficacy on an acute-infection TB mouse model 140
7.2.2.3.1 Methodology 140
7.2.2.3.2 Result 142
7.2.3 Micellar nanoparticle 144
7.2.3.1 Formulation preparation 144
7.2.3.2 PK study 149
7.2.3.2.1 Intravenous administration 149
7.2.3.2.1.1 Methodology 149
7.2.3.2.1.1 Result 150
7.2.3.2.2 Subcutaneous administration 150
7.2.3.2.2.1 Methodology 150
7.2.3.2.2.2 Result 151
7.2.3.3 Tolerance tests 154
7.2.3.3.1 Single dose tolerance test 154
7.2.3.3.2 Five-day tolerance test 154
7.2.3.4 Efficacy in an acute-infected TB mouse model 156

TABLE OF CONTENTS (continued)

7.2.3.4.1 Material and method 156
7.2.3.4.2 Result. 156

8. Target identification 158
8.1 Whole genome sequencing of ecumicin-resistant *M. tuberculosis* identified three potential targets. 158
8.2 Drug Affinity Responsive Target Stability (DARTS) determined supports ClpC1 as the target of ecumicin 161
8.3 Biochemical studies confirmed ClpC1 as the target 165
8.4 Discussion 169
8.5 Material and methods 173

9. Ecumicin analogs from strain MJM5123 176
9.1 Introduction 176
9.1.1 Isolation of ecumicin analogs 176
9.1.2 NMR structure sequencing 180
9.2 Deoxyecumicin 184
9.2.1 Isolation of deoxyecumicin (R10) 184
9.2.2 Structure elucidation of deoxyecumicin by HiFSA-assisted approach 185
9.2.3 HiFSA fingerprint of deoxyecumicin. 201
9.3 Norecumicin 203
9.3.1 Isolation of norecumicin (R7) 203
9.3.2 Structure elucidation of norecumicin using the NMR structure sequencing approach 204
9.3.3 HiFSA fingerprint of norecumicin. 218
9.4 Nordeoxyecumicin 220
9.4.1 Isolation of nordeoxyecumicin (R8) 220
9.4.2 Structure elucidation of nordeoxyecumicin by HiFSA-assisted approach 221
9.4.3 HiFSA fingerprint of nordeoxyecumicin. 235
9.5 Homoecumicin-11I 237
9.5.1 Isolation of homoecumicin-11I 237
9.5.2 Structure elucidation of homoecumicin-11I by HiFSA-assisted approach 238
9.5.3 HIFSA finger print of homoecumicin-11I 248
9.6 Homoecumicin-13I 251
9.6.1 Isolation of homoecumicin-13I 251
9.6.2 Structure elucidation of homoecumicin-13I by HiFSA-assisted approach 252
9.6.3 HIFSA fingerprint of homoecumicin-13I 263
9.7 Homoecumicin-6I 265
9.7.1 Isolation of homoecumicin-6I 265
9.7.2 Structure elucidation of homoecumicin-6I 266
9.8 R5 276
9.9 Discussion 278

TABLE OF CONTENTS (continued)

9.9.1 Using the upfield methyl signals to probe ecumicin congeners. 278
9.9.2 Sample purity and presumably conformational isomer(s). 281
9.9.3 The effect of sample purity and abundance on structure elucidation of new compounds. 285
9.9.4 The effect of pH on the ^{1}H NMR spectra of ecumicin and its analogs. 288
9.9.5 Comparison of the ^{1}H NMR fingerprints of the ecumicin congeners. 296
9.9.6 Structural-activity relationship concluded from ecumicin and its analogs. 299
9.9.7 Possible structures of other ecumicin analogs produced by *Nonomuraea* MJM5123. 300
9.10 Material and methods 302
10. Conclusion 305
REFERENCES 308
APPENDICES 320
VITA 445

LIST OF FIGURES

Figure 1. Global TB facts by the end of 2011. 3

Figure 2. Current global pipeline of new tuberculosis drugs. 7

Figure 3 Repurposed drugs for tuberculosis treatment. 7

Figure 4 New chemical entities for TB treatment. 9

Figure 5 The general process for discovery antimicrobial from actinomycetes. 11

Figure 6 Examples of anti-TB hits identified by whole-cell screening. 20

Figure 7.p High throughput screening publications indexed in MedLine. 21

Figure 8. Initial extraction of actinomycete culture. 26

Figure 9. High-throughput screening of actinomycete extract library for potential new anti-TB agents 27

Figure 10. Activity of all extracts follows the normal distribution with medium mean at 4.52% inhibition. 32

Figure 11. Distribution of anti-*M. tuberculosis* activity in all extracts analyzed by media and extraction types. 33

Figure 12. Media and/or extraction type dependence for production of active metabolites. 33

Figure 13. Scanning electron micrographs of mycelia and spores of MJM5123 grown on ISP medium 3 for 21 days at 28oC. 42

Figure 14. The neighbor-joining phylogenetic tree of MJM5123 based on 16S rRNA gene was constructed by using the MEGA 4.0 program. 43

Figure 15. Main fermentation profiles for the production of ecumicin by MJM5123 in a 7 L fermenter. 47

Figure 16 Bioassay-guided fractionation scheme of the methanolic extract of E5123 mycelia. . 51

Figure 17. ^{1}H NMR spectrum of fraction H14 (approximately 4 mg) in 200 µl methanol-d_4 (3 mm NMR tube, 600MHz, Bruker Avance 600). 51

LIST OF FIGURES (continued)

Figure 18. Thin Layer Chromatography of recombined fractions, in silica gel F254. 52

Figure 19. Optimized fractionation scheme for mass production of ecumicin. 53

Figure 20. Thin Layer Chromatography on silica gel F254 of (a) recombined ecumicin-containing fractions eluted from Sephadex™ column; (b) fractions eluted from vacuum liquid chromatography using silica gel. 55

Figure 21 Thin Layer Chromatography of distribution of peptides of interest in different solvent systems, in silica gel F254. 61

Figure 22. HR-LC-MS spectrum of ecumicin obtained on a Shimadzu IT-TOF instrument. 63

Figure 23. One-dimensional NMR spectra of ecumicin in methanol-d_4/d_3, 900/600/100MHz (Bruker Avance II 900, Bruker Avance 600, Bruker DPX 400).. 65

Figure 24. Circular dichroism spectrum of ecumicin. 66

Figure 25. IR Spectrum of ecumicin. 66

Figure 26. UV spectrum of ecumicin. Ecumicin was tested at 48.0 µM in methanol, 1 cm quart cuvette, 25°C (background subtracted). 67

Figure 27. Tandem mass spectrometry of ecumicin. 67

Figure 28. Comparison of ^{1}H NMR spectra (400 MHz) of the same ecumicin sample acquired on a same Bruker DPX-400 instrument in different solvents: (a) methanol-d_4 and (b) DMSO-d_6. 69

Figure 29. Typical long range ^{1}H,^{13}C coupling pattern of peptides, involving amide carbonyl carbon and neighboring α- and β-protons. 71

Figure 30. ^{1}H NMR Spectrum of ecumicin in CD_3OD (600MHz, Bruker Avance 600) with expansions and assignments. 76

Figure 31. DEPT135 spectrum (top) compared with ^{1}H,^{13}C-decoupled ^{13}C spectrum (bottom), (100 MHz, Bruker DPX-400). 78

Figure 32. ^{13}C NMR Spectrum of ecumicin in CD_3OH (100MHz, Bruker DPX-400) with expansions and assignments. 79

LIST OF FIGURES (continued)

Figure 33. HSQC Spectrum of ecumicin in CD_3OD (600MHz) with expansions. 81

Figure 34. COSY Spectrum of ecumicin in CD_3OD (600MHz) with expansions and assignment. . 83

Figure 35. HMBC Spectrum of ecumicin in CD_3OD (600MHz, Bruker Avance 600) with expansions and assignment on key correlations..... 88

Figure 36 Semi-selective HMBC spectrum on ecumicin's methyl region (F1 16-36 ppm) with expansions and assignment..... 93

Figure 37 Semi-selective HMBC on the carbonyl region (F1 164-184ppm) with expansions and assignment..... 95

Figure 38. Ecumicin's two possible structures (a) and (b) constructued from NMR analysis. 98

Figure 39. Fragmentation pattern of ecumicin in tandem mass spectroscopy..... 100

Figure 40. Oak Ridge Thermal-Ellipsoid Plot Program representation of the asymmetric unit of ecumicin, shown at 50% probability displacement ellipsoids..... 102

Figure 41. Parameters defining $n \rightarrow \pi^*$ interaction..... 103

Figure 42. Electron density map of selected residues, tryptophan (W10), phenylalanine (F12), threonine (T5) and isoleucine (I3) at 0.83 Å resolution. 105

Figure 43. LC-ESI-MS (Shimadzu 2020) on a RP C18 column. 106

Figure 44. Structure of ecumicin..... 107

Figure 45. Observed ROESY correlations for ecumicin (methanol-d_4, 600 MHz, Bruker Avance 600). 108

Figure 46. The crystal structure of ecumicin explains how the shielding aromatic cones give rise to the two up field proton resonances) in NMR spectra at 0.16824 ppm (H-5 of the *N*-Me-L residue) and 0.33065 ppm(H-6 of the *N*-Me-L residue). 110

Figure 47. ^1H iterative Full Spin Analysis by Perch software (v.2011.1, PERCH Solutions Ltd., Kuopio, Finland). 112

Figure 48. Circular representation of the *Nonomuraea sp*. MJM5123 chromosome. 116

LIST OF FIGURES (continued)

Figure 49 Genomic organization of the ecumicin biosynthetic gene cluster. 118

Figure 50. Predicted catalytic domain organization of the NRPS gene. 118

Figure 51 Gene inactivation of *ecu11* by λ Red mediated recombination and HPLC analysis of ecumicin production. 121

Figure 52. Ecumicin has time and concentration-dependent bactericidal activity against *M. tuberculosis*. 125

Figure 53. Ecumicin is bactericidal against *M. tuberculosis* in murine macrophages. Bars represent *M.* 126

Figure 54 (a) Cyclosporin A. (b) Representative cyclosporine blood concentration profiles from a renal transplant patient given the currently marketed formulation Sandimmune® (SIM) versus the new Neoral® formulation, without (a.m.) and with food (p.m.). 135

Figure 55 Limited oral absorption was observed for ecumicin in emulsion. 139

Figure 56. Timeline of efficacy using an acute-infected TB mouse model. 141

Figure 57. No significant anti-TB activity observed for ecumicin (ECM) in emulsion in an acute-infected mouse model. 142

Figure 58. ^{1}H NMR spectrum of mPEG(5)-PLA(4) in $CDCl_3$. 146

Figure 59. Particle size of ecumicin micelle formulation 148

Figure 60 Mean plasma and lung tissue concentrations of ecumicin in mice (n = 3) after a single i.v. dose of ecumicin at 5 mg/kg. 150

Figure 61. Plasma and lung exposures in mice (n = 3) following single or multiple s.c. doses of ecumicin at 20mg/kg. 153

Figure 62. Timeline of efficacy study in an acute-infected TB mouse model. 156

Figure 63 Twelve s.c. doses of micellar ecumicin (ECM) inhibit *M. tuberculosis* growth in the lungs of mice during acute infection. 157

Figure 64 The basic strategy of DARTS. 162

LIST OF FIGURES (continued)

Figure 65. Ecumicin does not protect either wild-type or mutated *M. tuberculosis* EspG3. 163

Figure 66. Ecumicin protects wild-type but not mutated *M. tuberculosis* ClpC1..... 164

Figure 67. (A) Crystal structure of ClpC1 from *M. tuberculosis*. (B) Cyclomarin docked in ClpC1 from *M. tuberculosis*..... 167

Figure 68. (A) Ecumicin enhances ATPase activity of wild-type ClpC1 derived from *M. tuberculosis*. (B) Hill Coefficient for Activation of ClpC1 by ecumicin..... 167

Figure 69. Ecumicin selectively activates wild-type ClpC1 derived from *M. tuberculosis.*..... 168

Figure 70. ClpC1 does not activate degradation of casein by ClpP1P2 in the presence of ecumicin..... 168

Figure 71 Model of ClpP mechanism of function. Shown is a cartoon model of the ClpP tetradecamer with the axial loops indicated. 171

Figure 72 Structures of cyclomarin A and lassomycin. 171

Figure 73. HPLC chromatogram of a Sephadex^{TM} LH-20 fraction of MJM5123 crude extract... 176

Figure 74 Separation scheme of ecumicin and its analogs. 179

Figure 75. Each amino acid has its own spin system(s). 181

Figure 76. relative qHNMR analysis of deoxyecumicin sample. 185

Figure 77. Proposed structure of deoxyecumicin. 186

Figure 78. High-resolution MS spectrum of deoxyecumicin. 186

Figure 79. Overlay of deoxyecumicin's pseudo HiFSA profile (blue) and experiemntal ^{1}H NMR spectrum of deoxyecumicin (red, 600 MHz, Bruker Avance 600)..... 193

Figure 80. Overlay of the deoxyecumicin's improved pseudo HiFSA profile (blue) and 1H NMR spectrum of deoxyecumicin (red)..... 194

Figure 81. ^{1}H profile of the different amino acid in deoxyecumicin..... 195

Figure 82. ^{13}C spectra of deoxyecumicin (blue) and ecumicin (red) with expansions. 196

LIST OF FIGURES (continued)

Figure 83. DEPT-135 spectra of deoxyecumicin (blue) and ecumicin (red) with expansions. ... 197

Figure 84. Comparison of COSY spectra of deoxyecumicin (grey) and ecumicin (yellow). 198

Figure 85. Comparison of HSQC spectra of deoxyecumicin (grey) and ecumicin (Red) with expansions. 199

Figure 86. Comparison of the HMBC spectra of deoxyecumicin (grey) and ecumicin (Red). 200

Figure 87 The ^{1}H iterative full spin analysis of (A) ecumicin and (B) deoxyecumicin. 202

Figure 88 (A) Proposed structure of norecumicin. (B) Structure of ecumicin. 204

Figure 89 High resolution MS data of norecumicin. 205

Figure 90. Overlay of norecumicin's pseudo HiFSA profile (blue) and ^{1}H NMR spectrum (red) indicates norecumicin does not contain *N*-methyl-isoleucine. 209

Figure 91 The spectrum of the different amino acid in norecumicin (in expansion) revealed by comparing ^{1}H NMR spectrum of norecumicin (red) and spectrum of those amino acids commonly observed in norecumicin and ecumicin (blue). 210

Figure 92. DEPTQ-135 spectrum of norecumicin (blue) compared with DEPT-135 (green) and ^{13}C (red) spectra of ecumicin. 211

Figure 93. Expansions of DEPTQ-135 spectrum of norecumicin (blue) compared with DEPT-135 (green) and ^{13}C (red) spectra. 212

Figure 94 Comparison of COSY spectra of norecumicin (red) and ecumicin (yellow). 213

Figure 95 expansions on comparison of COSY spectra of norecumicin (NECM, red) and ecumicin (ECM, yellow). 214

Figure 96 Comparison of HSQC spectra of norecumicin (HECM-3V, grey) and ecumicin (ECM, yellow-red) with expansions. 215

Figure 97 Comparison of HMBC spectra of norecumicin (HECM-3V, grey) and ecumicin (ECM, yellow-red). 216

LIST OF FIGURES (continued)

Figure 98 Comparison of semi-selective HMBC spectra of norecumicin (NECM, grey) and ecumicin (ECM, red). 217

Figure 99. The ^{1}H iterative full spin analysis of (A) ecumicin and (B) norecumicin, including the simulated amino acid sub-spectra, their mathematical sum, and observed ^{1}H NMR spectrum. 219

Figure 100. (A) Proposed structure of nordeoxyecumicin. (B) Structure of ecumicin. 221

Figure 101 High resolution MS data of nordeoxyecumicin. 222

Figure 102. Overlay of nordeoxyecumicin's pseudo HiFSA profile (blue) and the ^{1}H NMR spectrum (red). 228

Figure 103. The overlay of the second ecumicin-based HiFSA profile (blue) and the ^{1}H NMR spectrum of nordeoxyecumicin (red). 229

Figure 104. The overlay of the third ecumicin-based HiFSA profile (blue) and the ^{1}H NMR spectrum of nordeoxyecumicin (red). 230

Figure 105. (A) DEPTQ-135 spectrum of norecumicin (NDECM, blue), compared with DEPT-135 (ECM, green) and ^{13}C (red) spectra of ecumicin. (B) Expansions of DEPTQ-135 spectrum of norecumicin-3V (blue), compared with DEPT-135 (green) comparison. 231

Figure 106. Comparison of the COSY spectra of nordeoxyecumicin (grey) and ecumicin (yellow). 232

Figure 107. Comparison of the HSQC spectra of nordeoxyecumicin (grey) and ecumicin (red) with expansions. 233

Figure 108. Comparison of the HMBC spectra of nordeoxyecumicin (grey) and ecumicin (yellow) with expansions. 234

Figure 109. The ^{1}H iterative full spin analysis of (A) ecumicin and (B) nordeoxyecumicin, including the simulated amino acid sub-spectra, their mathematical sum and observed ^{1}H NMR spectrum. 236

Figure 110. (A) Proposed structure of homoecumicin-11I. (B) Structure of ecumicin. 238

LIST OF FIGURES (continued)

Figure 111. High resolution MS data of homoecumicin-11I. 239

Figure 112. Overlay of the first ecumicin-based HiFSA profile (blue) and ^{1}H NMR spectrum of homoecumicin-11I (red) led to two possible explanations for their structural difference. 244

Figure 113. Comparison of the COSY spectra of homoecumicin-11I (grey) and ecumicin (yellow) with expansions. 245

Figure 114. Comparison of the HMBC spectra of homoecumicin-11I (grey) and ecumicin (yellow) with one expansion. 246

Figure 115. Comparison of the HMBC spectra of homoecumicin-11I (grey) and ecumicin (yellow) with one expansion. 247

Figure 116. ^{1}H NMR spectrum (700 MHz, methanol-d_4) and HiFSA profile of homoecumicin-11I with or without simulated impurity. 250

Figure 117 (A) Proposed structure of homoecumicin-13I. (B) Structure of ecumicin. 252

Figure 118. High resolution MS data of homoecumicin-13I. 253

Figure 119. Comparison of homoecumicin-13I's experimental ^{1}H spectrum (red) with the spectrum generated from the first PMS file (blue). 258

Figure 120. Comparison of homoecumicin-13I's experimental 1H spectrum (red) and the spectrum generated from the second PMS file (blue). 259

Figure 121. Comparison of the COSY spectra of homoecumicin-13I (grey) and ecumicin (yellow) with expansion pf one region. 260

Figure 122. Comparison of HSQC spectra of homoecumicin-13I (grey) and ecumicin (yellow) with expansions 261

Figure 123. Due to the limited amount of sample (0.27 mg) of sample, the HMBC spectrum of homoecumicin-13I using a 700 MHz 1.7 mm cryoprobe NMR (NS = 64, TD1= 300) only showed the correlations of the methyl and a few select ^{1}H resonances. 262

Figure 124. ^{1}H NMR spectrum (700 MHz, methanol-d_4) and HiFSA profile of homoecumicin-13I with or without simulated impurity. 264

LIST OF FIGURES (continued)

Figure 125 (A) Proposed structure of homoecumicin-6I. (B) Structure of ecumicin. 266

Figure 126 High resolution MS data of homoecumicin-6I. 267

Figure 127. Comparison of the ^{1}H spectra of homoecumicin-6I (red) and ecumicin (blue). 270

Figure 128. Comparison of the COSY spectra between homoecumicin-6I (grey) and ecumicin (yellow) revealed an additional isoleucine coupling pathway. 271

Figure 129. Comparison of the HSQC spectra of ecumicin (red) and homoecumicin-6I (grey). 272

Figure 130. The HMBC spectrum of homoecumicin-13I using a 700 MHz 1.7 mm cryoprobe NMR (NS = 64, TD1= 300) only showed the correlations of the methyl and a few select ^{1}H resonances. 273

Figure 131. HR-MS spectrum of R5. The ecumicin analog signal $[M+2H]^{2+}$ = 793.5032, indicated an exact mass of 1584.9918. 277

Figure 132. Comparison of the ^{1}H NMR spectrum of ecumicin (blue) and R5 (red) revealed an ecumicin analog that is only one component of R5. 277

Figure 133. The crystal structure of ecumicin explains how the shielding aromatic cones give rise to the two up field proton resonances in NMR spectra at 0.16824 ppm (H-5 of the *N*-Me-L residue) and 0.33065 ppm(H-6 of the *N*-Me-L residue)..... 280

Figure 134. HR-MS spectrum of fraction H14 suggests the presence of only ecumicin and its isomer(s). 283

Figure 135. Differential chemical shifts (Δδ) of the ecumicin analogs norecumicin and deoxyecumicin, caused by residual acid, represented by (a) bar chart, and (b) heat maps. 290

Figure 136. Differences in the chemical shifts of ecumicin and its analogs that reflect their structural differences. (a) The one hydroxyl group difference between Ph-L-THREO-S and L-F, and (b) the one methylene group difference between *N*-Me-L-ALLO-L and *N*-Me-L-V. 298

Figure 137. Other possible ecumicin analogs. 301

LIST OF FIGURES (continued)

Figure 138. Semi-preparative HPLC separation of norecumicin-3V, nordeoxyecumicin and ecumicin..... 302

Figure 139. Semi-preparative HPLC separation of ecumicin, deoxyecumicin, homoecumicin-11I, homoecumicin-13I and homoecumicin-6I. 303

LIST OF TABLES

TABLE I. MOST ADVANCED TB VACCINE CANDIDATES IN CLINICAL TRIALS. (Paternership 2013) . 5

TABLE II REPURPOSED DRUGS FOR TUBERCULOSIS TREATMENT. 8

TABLE III. BIOLOGICAL PROFILE OF PRIORITY GROUP 1 – 3..... 37

TABLE IV. BIOLOGICAL PROFILING OF METHANOLIC EXTRACT OF PRIORITIZED CULTURE MJM5123, AND ITS FRACTIONS GENERATED BY SOLID PHASE EXTRACTION ON AN RP-18 CARTRIDGE AND METHANOL/WATER GRADIENT ELUTION..... 38

TABLE V. GENETIC RELATEDNESS OF MJM5123 WITH CLOSELY RELATED STRAINS BY DNA-DNA HYBRIDIZATION..... 43

TABLE VI. CULTURAL FEATURES OF MJM5123. 43

TABLE VII. PHYSIOLOGICAL AND BIOCHEMICAL PROPERTIES OF MJM5123. 44

TABLE VIII. ^{1}H (900 MHZ) AND ^{13}C (100 MHZ) NMR DATA OF ECUMICIN IN METHANOL-D_4 (CD_3OD)..... 73

TABLE IX. A SUMMARY OF CARBONYL GROUPS THAT MAY CONTRIBUTE TO N→Π* INTERACTIONS IN ECUMICIN. 104

TABLE X. GENERAL FEATURES OF MJM5123 GENOME. 117

TABLE XI. PREDICTED FUNCTIONS OF THE ORFS IN THE PUTATIVE ECUMICIN-PRODUCING GENE CLUSTER. 119

TABLE XII. SPECIFICITY-CONFERRING CODE OF ADENYLATION DOMAINS IN THE PARTIAL ECUMICIN-PRODUCING NRPS ANALYZED BY NRPSPREDICTOR2. 120

TABLE XIII. ECUMICIN MICS (μM) AGAINST CLINICALLY-ISOLATED *M. TUBERCULOSIS* CLADES, REPRESENTING WORLD-WIDE GENETIC DIVERSITY. 126

TABLE XIV. MIC (μM) OF ECUMICIN (ECM) VS *M. TUBERCULOSIS* CLINICAL STRAINS ISOLATED FROM PULMONARY TB PATIENTS HOSPITALIZED IN NATIONAL MASAN HOSPITAL, KOREA. 127

TABLE XV. *IN VITRO* BIOLOGICAL ACTIVITIES OF ECUMICIN (ECM). 128

LIST OF TABLES (continued)

TABLE XVI. IN VITRO ACTIVITY OF ECUMICIN MICELLE COMPARED WITH FREE ECUMICIN..... 148

TABLE XVII. 5-DAY TOLERANCE TEST WITH MICELLAR ECUMICIN IN BALB/C MICE..... 155

TABLE XVIII. MIC (μM) PROFILE OF WILD-TYPE AND ECUMICIN (ECM)-RESISTANT *M. TUBERCULOSIS* STRAINS. 158

TABLE XIX. MUTATIONS OF *CLPC1* IN ECUMICIN RESISTANT STRAINS..... 159

TABLE XX. PPSC WAS NOT THE TARGET OF ECUMICIN (ECM)..... 160

TABLE XXI. SUMMARY OF ECUMICIN CONGENERS. 177

TABLE XXII ^{1}H AND ^{13}C NMR DATA OF DEOXYECUMICIN IN CD_3OD (600, 400 MHZ). INTERPRETATION OF ^{1}H NMR WAS DONE BY ^{1}H ITERATIVE FULL SPIN ANALYSIS..... 187

TABLE XXIII. ^{1}H (900 MHZ, BRUKER AVANCE II 900) AND ^{13}C (100 MHZ, BRUKER DPX 400) NMR DATA OF NORECUMICIN IN CD_3OD. 205

TABLE XXIV ^{1}H (900 MHZ, BRUKER AVANCE II 900) AND ^{13}C (100 MHZ, BRUKER DPX 400) NMR DATA OF NORDEOXYECUMICIN IN CD_3OD. 222

TABLE XXV. ^{1}H AND ^{13}C NMR DATA OF HOMOECUMICIN-11I IN CD_3OD. 239

TABLE XXVI. ^{1}H AND ^{13}C NMR DATA OF HOMOECUMICIN-13I IN CD_3OD. 253

TABLE XXVII. AVAILABLE ^{1}H AND ^{13}C NMR DATA OF HOMOECUMICIN-6I IN CD_3OD..... 274

TABLE XXVIII. SUMMARY OF THE NMR ANALYSES OF THE ECUMICIN CONGENERS..... 281

TABLE XXIX. (A) RESIDUAL ACID AFFECTS THE ^{1}H NMR SPECTRA (METHANOL-D_4) OF NORECUMICIN. 291

TABLE XXX. BRIEF SUMMARY OF ECUMICIN AND ITS ANALOGS PRODUCED BY *NONOMURAEA* MJM5123, AND THEIR ANTI-TB ACTIVITY..... 299

LIST OF ABBREVIATIONS

Å	Ånstrom
bid	twice daily
BGF	bioassay-guided fractionation
CAP	capreomycin
CCC	counter-current chromatography
CD	Circular dichroism
$CHCl_3$	chloroform
COSY	^1H–^1H correlation spectroscopy
CS	countercurrent separation
δ	chemical shift (ppm)
DARTS	Drug Affinity Responsive Target Stability
DMSO	dimethyl sulfoxide
ECM	ecumicin
ECUM	Extract Collection of Useful Microorganisms
EtOAc	ethyl acetate
F	phenylalanine
FID	free induction decay (in NMR)
FVM	Frozen vegetative mycelia
H_2O	water
H_2SO_4	sulfuric acid
HEMWat	CS solvent system consisting of hexanes, ethyl acetate, methanol and water
HChEMWat	CS solvent system consisting of hexanes, chloroform, ethyl acetate, methanol and water

LIST OF ABBREVIATIONS (continued)

HiFSA	^{1}H iterative full spin analysis
HMBC	heteronuclear multiple-bond correlation spectroscopy (^{1}H–^{13}C)
HSQC	heteronuclear single quantum coherence spectroscopy (^{1}H–^{13}C)
HPLC	high-performance liquid chromatography
HSCCC	high-speed countercurrent chromatography
HTS	high-throughput screening
Hz	Hertz
I	isoleucine
IC_{50}	the concentration at which the curve passes through the 50% inhibition level
Ile	isoleucine
INH	isoniazid
ip	intraperitoneal injection
IR	infrared spectroscopy
iv	intravenous injection
K	partition coefficient
KM	kanamycin
λ	wavelength (nm)
L	leucine
Leu	leucine
LG	Lorentzian–Gaussian window function in NMR processing
LOD	limit of detection
LOQ	limit of quantitation

LIST OF ABBREVIATIONS (continued)

M	mole(s)/L
MABA	microplate Alamar blue assay
MBC	minimum bactericidal concentration
MDR	multiple drug-resistant
Me	methyl group
MeOH	methanol
mg	milligram(s)
mL	milliliter(s)
Mox	moxifloxacin
NRP	non-ribosomal peptide
NRPS	non-ribosomal peptide synthetase
µg	microgram(s)
µL	microliter(s)
ng	nanogram(s)
MHz	mega Hertz
MIC	minimum inhibitory concentration
min	minute(s)
mm	millimeter(s)
mol	mole
MS	mass spectrometry
NMR	nuclear magnetic resonance
NS	number of scans
o1p	transmitter offset (in NMR)

LIST OF ABBREVIATIONS (continued)

PCR	polymerase chain reaction
PEG	Polyethylene glycol
pH	$-\log_{10}[H^+]$ (measure of acidity)
Phe	pheynlalanine
Ph-S	phenyl-serine
PK	phamacokinetics
PLA	poly lactic acid
po	by mouth
ppb	parts per billion
ppm	parts per million
qd	once a day
qHNMR	quantitative proton (^{1}H) NMR
qod	once every other day
R_f	retention factor: migration distance of an analyte as a fraction of distance of origin to solvent front in thin-layer chromatography
RMP	rifampin
RP	reversed phase (chromatography)
rpm	rotations per minute
sc	subcutaneous injection
SDS-PAGE	Polyacrylamide gel electrophoresis
S_f	retention factor: volume of stationary phase as a fraction of total coil volume in countercurrent chromatography
SM	streptomycin
T	threonine

LIST OF ABBREVIATIONS (continued)

TB	tuberculosis
TLC	thin layer chromatography
Thr	threonine
Trp	tryptophan
UV	ultraviolet light, i.e., 20–400 nm
V	valine
Val	valine
vis	visible light, i.e., 400–700 nm
VLC	vacuum liquid chromatography
vvm	volume of air per volume of broth per minute
WGS	whole genome sequencing
WT	wild type
XDR	extensively drug-resistant
Y	tryptophan

SUMMARY

The development and spread of drug-resistant tuberculosis has led to the urgent demand to find new drug leads with novel modes of action. The present study focuses on the discovery of ecumicin and its analogs from an actinomycete extract, originating from an actinomycete extract library. Ecumicin is an in vivo active anti-*M. tuberculosis* macrocyclic tridecapeptide with a novel mode of action. This work demonstrated that it is possible to find new anti- *M. tuberculosis* secondary metabolites from actinomycetes by direct whole-cell based high-throughput screening. It also suggests that ClpC1 is a valid drug target against *M. tuberculosis* and that ecumicin may serve as a lead compound for anti-tuberculosis drug development.

Chapter 2 describes the high-throughput screening campaign of more than 65,000 actinomycete extracts for inhibition of *Mycobacterium tuberculosis* viability. This campaign led to the ecumicin-producing strain, *Nonomuraea sp.* MJM5123. The mycelial methanolic extract of this strain demonstrates selective anti-*M. tuberculosis* activity.

Strain MJM5123 was mass cultured (Chapter 3), and extracted. The mycelial methanolic extract underwent a chemical fractionation process in parallel with biological characterization (Chapter 4). Through the process, several small peptides with potent and selective anti- *M. tuberculosis* activity were isolated.

The structure elucidation of the major active peptide, ecumicin (Chapter 5), was achieved by combining an array of modern techniques with traditional methods. The large

molecular weight of 1599 amu by high resolution mass spectrometry precluded the initial inference of its molecular formula. The individual building blocks were identified by extensive NMR experiments. The resulting two possible planar structures were distinguished by tandem mass spectrometry. Determination of the absolute configuration and unambiguous structural confirmation was achieved by X-ray crystallography and Marfey's analysis. The structure of ecumicin has been confirmed by its nonribosomal peptide synthetase (Chapter 6). The 1D ^{1}H NMR spectrum of ecumicin was registered as a 1H iterative full spin analysis (HiFSA) profile, which provides a complete list of accurate proton chemical shifts and ^{1}H,^{1}H-coupling constants.

Chapter 7 details the biological profile of ecumicine. Ecumicin is a potent, selective bactericidal compound against *M. tuberculosis* in vitro, including non-replicating cells. This compound is equally active against drug-resistant *M. tuberculosis* including clinically isolated multiple and extensively drug-resistant strains. Subcutaneous administration to mice of ecumicin in a micellar formulation at 20 mg/kg resulted in plasma and lung exposures exceeding the MIC. Complete inhibition of *M. tuberculosis* growth in the lungs of mice was achieved following 12 doses at 20 or 32 mg/kg.

Genome mining of lab-generated, spontaneous ecumicin-resistant *M. tuberculosis* identified the ClpC1 ATPase complex as the putative target. This was confirmed by a drug affinity response test (Chapter 8). ClpC1 functions in protein breakdown with the ClpP1P2 protease complex. Ecumicin markedly enhanced the ATPase activity of wild type ClpC1, but

prevented activation of proteolysis by ClpC1. Less stimulation of the ATPase activity was observed with ClpC1 from ecumicin-resistant mutants.

The structure elucidation of six ecumicin analogs, which were also isolated from strain MJM5123, is discussed in Chapter 9. Based on the high level of similarity in the 1D- and 2D-NMR spectra of all the ecumicin congeners and the assumption that they are synthesized by the same biosynthetic pathway, it is reasonable to assume that these peptides are structurally very similar. With the comprehensive knowledge on ecumicin's structure and the availability of its HiFSA profile, the structures of its analogs were elucidated using a new method – NMR structure sequencing. This method mainly uses information from the most sensitive NMR experiment, the 1D ^{1}H NMR, and treats each new peptide as a mixture of individual amino acid residues, for expedited structure elucidation.

1. Anti-Tuberculosis Drug Discovery from Microbes

1.1 Introduction

1.1.1 Tuberculosis remains a major public health threat

Mycobacterium tuberculosis is the cause of one of the most deadly diseases known to man. Despite the availability of effective chemotherapy and BCG vaccine, tuberculosis (TB) remains a major public health threat. Worldwide, new cases of TB have been falling for several years, reaching a rate of 2.2% between 2010 and 2011. However, as the world's population is growing at about 2% per year, the total number of new TB cases is still enormous. In 2011, there were an estimated 8.7 million new cases of TB (13% co-infected with HIV) and 1.4 million TB related mortalities (30% were HIV-positive individuals) (WHO 2012). Two factors that contribute to the continued morbidity and mortality rates are the appearance of drug-resistant TB and its association with the HIV epidemic.

Although the present WHO recommended regimen for drug-susceptible TB is highly efficacious, with cure rates of around 90% in HIV-negative patients, it requires 6 months of treatment with first-line drugs [a combination of rifampicin (RMP), isoniazid (INH), ethambutol (EMB) and pyrazinamide (PZA) for 2 months, followed by a 4-month continuation phase of RMP and INH].

It is necessary to have the whole 6-month therapy in order to kill a sub-population of slow-growing *M. tuberculosis* persisters and to prevent relapse by allowing sufficient host immunity development. (Zhang, 2011) During the disease process, *M. tuberculosis* resides in microenvironments with different oxygen content and/or pH, which affect the bacilli's metabolic

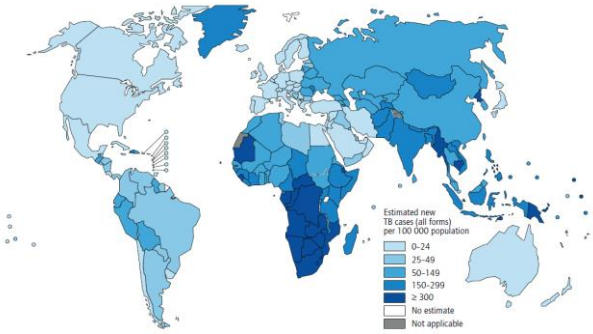
status. *M. tuberculosis* in lesions are divided into four different subpopulations according to their metabolic status and susceptibility to TB drugs (Mitchison 1985) : (a) the actively growing ones are most susceptible to INH (in case of INH resistance, the bacteria are killed by RMP or inhibited by EMB); (b) the ones that have bursts of metabolism are most susceptible to RMP, (c) the ones with low metabolic activity that reside in acidic environment are killed by PZA; (d) the "dormant". (Zhang, 2011)

Partially due to the lengthy treatment, poor patient compliance is common, leading to drug-resistant TB cases and treatment failure. The number of cases of multi drug-resistant TB (MDR-TB, resistant to at least INH and RMP, the two most powerful first-line treatment anti-TB drugs) reached almost 60 000 worldwide in 2011, with an estimated 3.7% of new cases and 20% of previously treated cases to be MDR-TB (WHO 2012). Regimens for MDR-TB treatment currently recommended by WHO entail 20 months of treatment with second-line drugs for most patients, and are associated with multiple (and sometimes serious) side-effects and lower cure rates. Extensive drug-resistant TB (XDR-TB, MDR-TB plus resistance to a fluoroquinolone and at least one of three injectable second-line drugs) has been reported in 84 countries, and it accounts for 9.0% of all MDR-TB cases (WHO 2012). The remaining treatment options for XDR-TB are therefore less effective, have more side effects, and are more expensive.

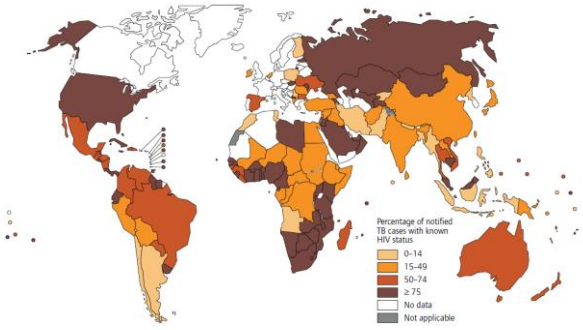
HIV co-infection is the most significant known risk factor for susceptibility to *M. tuberculosis* infection and progression to active disease. The combination of HIV and TB accelerates the development of each disease. The development of active TB is accelerated by co-infection with HIV, which increases *M. tuberculosis* reactivation rates from 3%–10% per life-time to 5%–10% per **life-year** (Corbett, et al. 2003). Furthermore, there are also interactions between

TB treatment and antiretroviral therapy (ART) for people living with HIV, making those TB drugs ineffective in such cases.

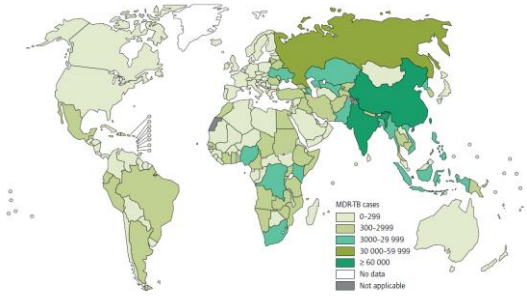
HIV and drug-resistance constitute two distinct obstacles for TB control. When combined, their synergistic effect is marked. For example, in an outbreak of XDR-TB occurring among HIV-infected individuals in KwaZulu-Natal, South Africa, 52 of 53 affected patients died, with a median time of death after detection of 16 days (Gandhi, et al. 2006).



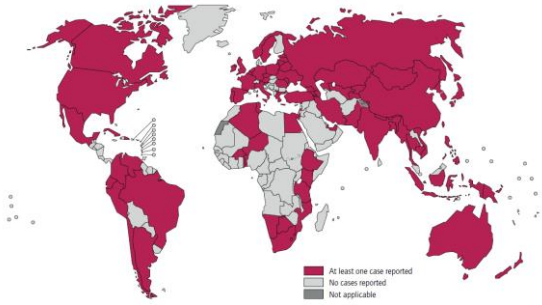
(a) Estimated TB incidence rates



(b) Percentage of TB patients with known HIV status by country



(c) Number of MDR-TB cases estimated to occur among notified pulmonary TB cases



(d) Countries that had notified at least one case of XDR-TB

Figure 1. Global TB facts by the end of 2011. (WHO 2012)

1.1.2 Perspective on TB treatment

Currently the two main strategies of TB treatment are vaccination and chemotherapy.

Developed in 1921, the Bacille Calmette-Guérin (BCG) vaccine remains the only vaccine against TB today. It provides some protection against server forms of childhood TB, but is unreliable in cases of adult pulmonary TB. Unfortunately the latter is responsible for the major disease burden worldwide. (WHO)

Since the early 1990s, when the World Health Organization (WHO) declared TB a global emergency, significant efforts have been made in the study of TB (Kaufmann and Parida 2007), including research on new TB vaccines development. The development of new TB vaccines has followed two basic avenues (Ottenhoff 2009, Kaufmann 2010, Ottenhoff, et al. 2010). One approach is directed at replacing the BCG protocol by either improved recombinant BCG or by genetically attenuated *M. tuberculosis*, to produce safer, more immunogenic priming vaccines that could induce longer lasting protection against highly virulent clinical isolates; the other direction being pursued focuses on the development of subunit vaccines, primarily aiming to boost (recombinant) BCG-induced responses.

As of 2013, more than a dozen TB vaccine candidates entered clinical Phase II and Phase III trials (as summarized in **TABLE I**), and many more are in the pre-clinical pipeline to be considered for testing in phase I clinical trials. At least 16 vaccine candidates are in advanced pre-clinical development and well over 20 next-generation candidates are in the discovery pipeline(Ottenhoff and Kaufmann 2012).

However, it is worth noting that these vaccines are not "designed to prevent infection or to achieve sterile eradication, but rather to better prime and/or boost infection control". So at the best they will only be able to inhibit or delay TB reactivation (Wang, 2012). Additionally, there are concerns that vaccination of HIV-infected individuals may not confer the same degree of protection experienced by immunocompetent persons due to their altered immune function. Prior to the arrival of the new generation vaccines that are able to provide sufficient protection to HIV-negative as well as HIV-positive individuals by preventing infection or achieving sterile eradication, chemotherapy will remain the essential weapon in the battle against TB.

TABLE I. MOST ADVANCED TB VACCINE CANDIDATES IN CLINICAL TRIALS. (Paternership 2013)

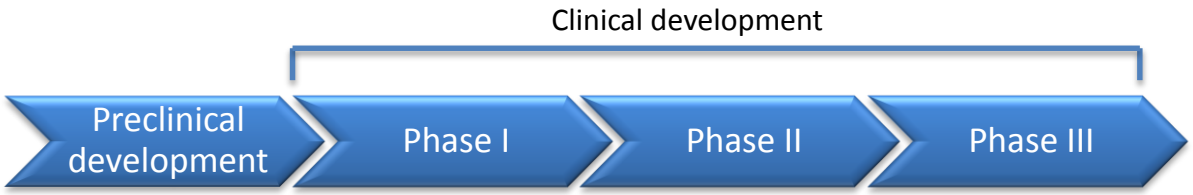
Type	Candidate	Clinical Trial status
Recombinant BCG	VPM 1002	Phase II
Viral vector	Oxford MVA85A/Aeras-485	Phase IIb
	Crucell Ad35/Aeras-402	Phase II
	AdAg85A	Phase I
	Crucell Ad35/MVA85A	Phase I
Fusion Protein in adjuvant	Hybrid 1+IC31	Phase II
	Hybrid 56/Aeras-456+IC31	Phase II
	M72+AS01	Phase IIb
	Hybrid 4/Aeras-404+IC31	Phase II
	ID93+GLA-SE	Phase I
Whole bacterial vaccine	RUTI	Phase II
	M. vaccae	Phase III
	M. TUBERCULOSISVAC	Phase I

In the absence of an effective vaccine to prevent TB in adults, TB treatment has for decades largely relied on anti-TB chemotherapy. TB chemotherapy began in 1944 when Schatz

and Waksman discovered streptomycin from a soil-derived actinomycete. Afterwards, several synthetic compounds were developed as TB drugs, including para-aminosalicylate, INH, PZA, ethionamide/prothionamide, EMB, and quinolones. The discovery of cycloserine, kanamycin and its derivative amikacin, viomycin, capreomycin, rifamycins and the derivative RMP were as a result of further screening of soil microbes for antibiotics. (Zhang, 2011)

After a long hiatus during which no new TB drugs were discovered, pharmaceutical companies rekindled research programs to develop anti-TB drugs in the 1990s. In over forty years, bedaquiline (also known as TMC207; Janssen Infectious Diseases/TB Alliance) is the first new TB drugs to be approved by the FDA for use as part of combination therapy for adults with MDR-TB. However, it was also found to pose a significant cardiotoxicity risk.

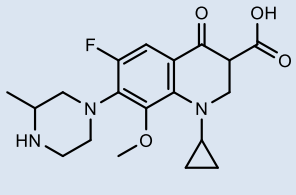
Apart from the clinically available drugs, a number of new therapeutic agents are currently under investigation and new treatment regimens are in clinical trials (Figure 2) (Parternership 2013, Zumla, et al. 2013). Many of the new TB drug candidates are drugs that were developed for the treatment of other infectious diseases and have since been repurposed or new dosages of known drugs (Figure 3, TABLE II). Others (PA-824 and SQ-109, Figure 4) were initially discovered as antimycobacterial agents and have subsequently been developed as potential TB drugs with novel modes of action. Several additional novel compounds are in preclinical development for TB (Figure 4), including the TBA-354, DC-159a, SQ609, SQ641, BTZ043 and CPZEN-45 (Figure 4).



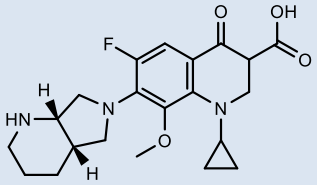
TBA-354	PA-824	Gatifloxacin
TBI-166	Sutezolid	Moxifloxacin
CPZEN-45	Bedaquiline	Delamanid
DC-159a	SQ-109	Rifapentine
SQ609	Linezolid	
SQ641	Rifapentine	
Q203	AZD-5847	
PBTZ169	Clofazimine	

Figure 2. Current global pipeline of new tuberculosis drugs. Agents currently in discovery or development for the treatment of tuberculosis (TB) are shown. (Parternership 2013, Brigden, et al. 2014)

Fluoroquinolones:

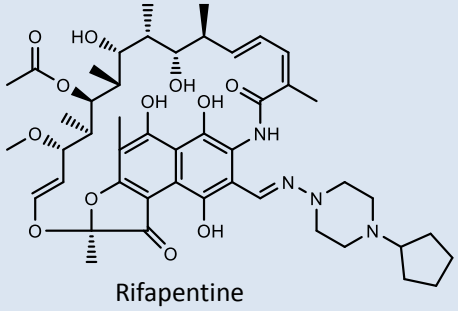


Gatifloxacin



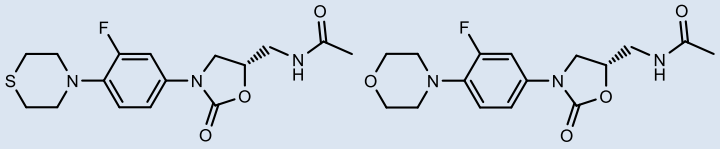
Moxifloxacin

Rifamycin:



Rifapentine

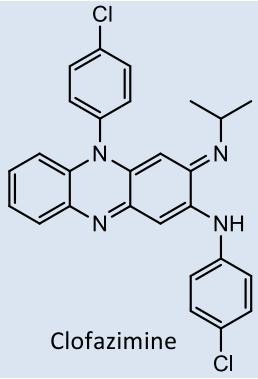
Oxazolidinones:



Sutezolid

Linezolid

Riminophenazine:



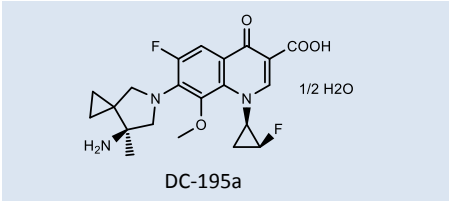
Clofazimine

Figure 3. Repurposed drugs for tuberculosis treatment and new dosages of known drugs (rifapentine). The chemical structures of anti-infective agents that were initially developed for the treatment of other infectious diseases that are now being evaluated in clinical trials for tuberculosis treatment. Sutezolid is also known as PNU-100480.

TABLE II REPURPOSED DRUGS FOR TUBERCULOSIS TREATMENT.

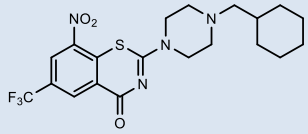
Drug class repurposed for TB treatment	**Drug Name**	**Original usage**
Fluoroquinolones	Moxifloxacin Gatifloxacin	Broad-spectrum antibiotics (effective for both gram-negative and gram-positive bacteria) to treat serious bacterial infections, esp. hospital-acquired infections and those in which resistance to older antibacterial classes is suspected.
Oxazolidinones	Linezolid Sutezolid	To treat infections caused by gram-positive bacteria that are resistant to other antibiotics, including *Enterococcus faecium*, *S. aureus*, *S. pneumonia*, *S. pyogenes*.
Riminophenazine	Clofazimine	Leprosy

Fluoroquinolone:



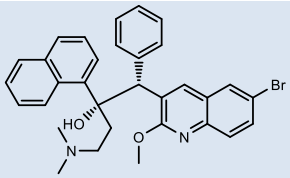
DC-195a

Benzothiazinone:



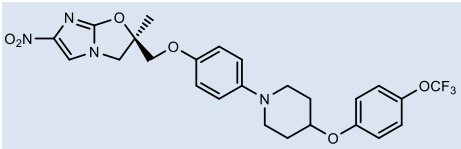
PBTZ169

Diarylquinoline:

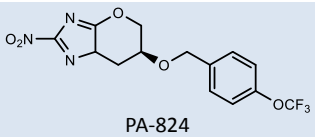


Bedaquiline

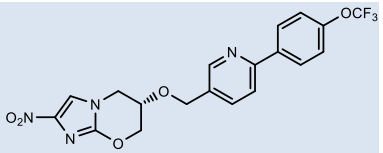
Nitroimidazole:



Delamanid

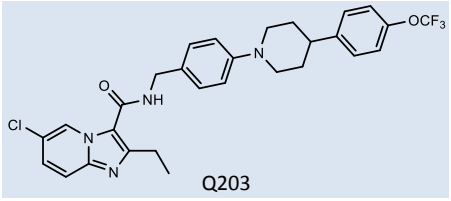


PA-824



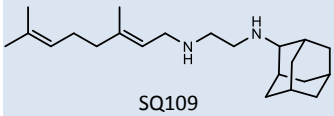
TBA-354

Imidazopyridines:



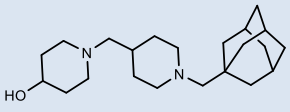
Q203

Ethlenediamine:



SQ109

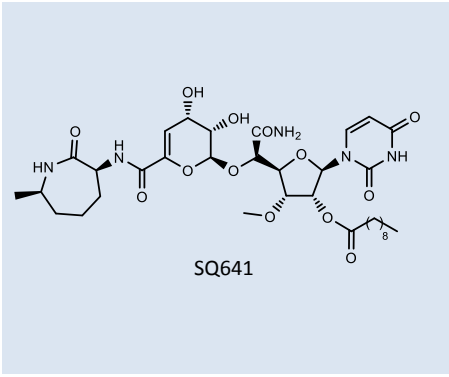
Dipiperidine:



SQ609

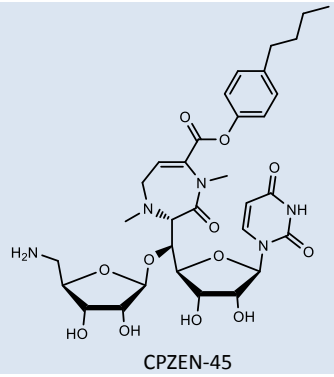
Actinomycete-derived antibiotics:

Capuramycin analog



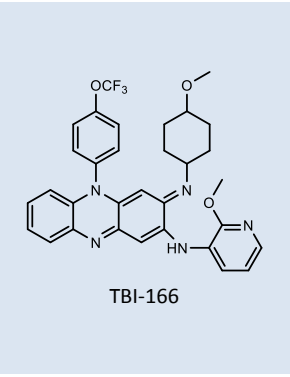
SQ641

Caprazamycin analog



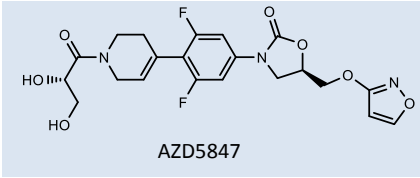
CPZEN-45

Riminophenazine:



TBI-166

Oxazolidinone:



AZD5847

Figure 4. New chemical entities for TB treatment.

Even with this promising pipeline of new TB drugs, given the low success rate of drug candidates in clinical development and the emergence of drug resistance, there is still a strong need for the discovery of other clinical candidates. (Pethe, 2013) The current criteria for the development of new TB drug candidates are stricter than ever before. The ideal candidate should have the following properties:

1) a fully validated safety profile,
2) more potent than existing drugs in order to reduce the duration of therapy;
3) able to inhibit new targets so that MDR-TB and XDR-TB can be treated;
4) compatible with antiretroviral therapy, as many patients are co-infected with HIV;
5) no antagonism to other TB drugs or drug candidates so that a regimen comprising at least three active drugs can be constituted;
6) able to kill *M. tuberculosis* in its different physiological states including the subpopulation of persisters.

1.1.3 Actinomycete as a viable source of new anti-tuberculosis agents

Among soil microorganisms, actinomycetes have served as the origin of the largest number of new antibiotic drug candidate and lead molecules that have been used clinically for the treatment of a variety of bacterial infections (Berdy 2005). Beginning in the 1940s, numerous antibiotics have been discovered from actinomycetes, including streptomycin, tetracycline, erythromycin, rifampin. The general process for discovery has not changed significantly over the years and is outlined in Figure 5.

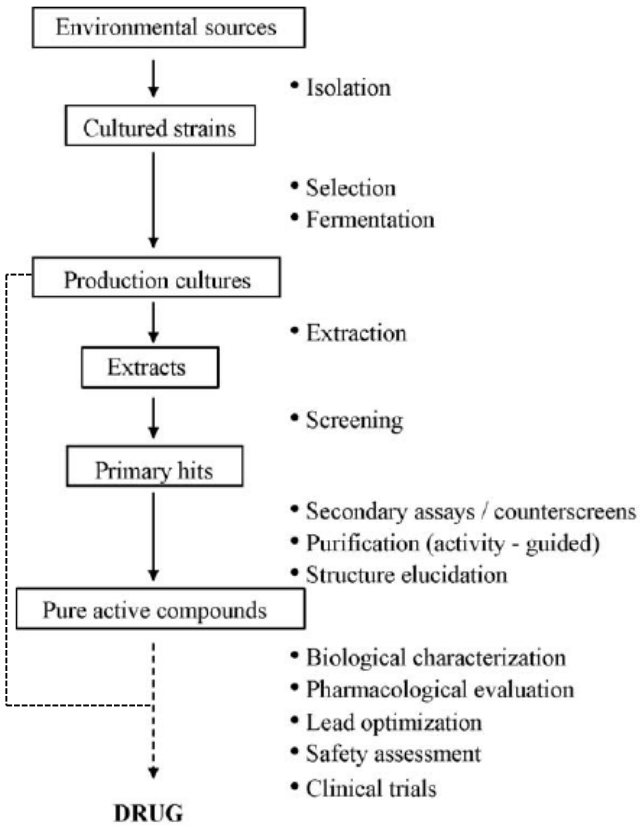


Figure 5. The general process for discovery antimicrobial from actinomycetes.

The traditional method used to find new antibiotics from soil microorganisms such as actinomycetes is first to isolate them on solid agar-based media and then to either culture them or place an extract of their culture broth onto an agar surface on which a "lawn" of the target bacterium has been made. The target microorganism is often a species of gram-positive *Staphylococcus* or *Bacillus* or a gram-negative *E. coli*, as these organisms grow easily and abundantly and are fairly good representatives of gram-positive and gram-negative bacteria in general. Following incubation of the plates, one looks for the presence of a "zone of inhibition" – a clear area where a diffusible actinomycete metabolite has inhibited the growth of the bacterium. In general this type of test is known as an agar-diffusion assay.

Although several actinomycete derived TB drugs (rifampin, streptomycin and cycloserine) were discovered by using agar diffusion assays to detect their presence, these screens were not initially conducted using *M. tuberculosis*. This was due to its contagious nature and often fatal outcome (at the time) if infected. Also, the extremely slow growth rate of *M. tuberculosis* makes the use of agar diffusion tests very difficult as "the size of the zone of inhibition depends both upon the rate of diffusion of the active agent and the rate of growth of the target organism". (Pauli, 2005) Instead, it was later found that the actinomycete antibiotics identified by their ability to inhibit other bacteria were also capable of inhibiting or killing *M. tuberculosis*, and in all three cases tuberculosis became the primary disease for use of these drugs.

Today, it is known that certain other drugs – in this case purely synthetic compounds – are only active against *M. tuberculosis* or the genus Mycobacterium either because of a unique molecular target that does not exist in other bacteria or because of a unique "activating" property

of an otherwise inactive “prodrug”. Therefore, there is the distinct possibility that many other potential novel anti-TB agents were not detected during the heyday of actinomycete screening during the 1940s-80s.

Indeed, out of the thirteen new chemical entities in current TB drug pipeline (Figure 2), two (SQ641 and CPZEN-45) are derived from actinomycete secondary metabolites. SQ641 (Reddy, et al. 2008) is an chemically modified capuramycin, which was discovered in *Streptomyces griseus* 446-S3 based on antibacterial activity against *S. pneumoniae* and *M. smegmatis* (Yamaguchi, et al. 1986). CPZEN-45 (Takahashi, et al. 2013) is a semi-synthetic antibiotic from caparazamycin. Caparazamycin was discovered from *Streptomyces sp*. MK730-62F2 in a project to screen for narrow spectrum anti-mycobacterial antibiotics from microbial products (Igarashi, et al. 2003).

In recent years, the low efficiency of finding new antibiotics from actinomycetes has been attributed to the current absence of “low hanging fruit” and the failure of the pharmaceutical industry to alter their historical approach. In the 1990s, there was a trend to move away from screening against whole bacteria to screening against isolated molecular targets. Because crude extracts are often not suitable for screening in molecular assays due to non-specific interference, and because combinatorial chemistry was new and in vogue, natural products were de-prioritized.

However, the trend for screening has now reversed back to whole cell screens. The effectiveness of high-throughput screening largely depends on the quality of the library screened. Although there has been increasing recognition that synthetic compound libraries represent only a tiny fraction of all possible chemical diversity (Campbell 2010, Drewry and Macarron 2010), there is still relatively little innovation with respect to natural products. In an industry that runs

on short timelines, there is a great hesitancy to go through the bioassay guided fractionation/isolation process and run the risk of isolating a previously known compound.

Thus, actinomycetes remain a viable source for the discovery of new anti-TB agents. Using the technology present today in a modern Biosafety Level 3 laboratories, we are able to safely screen tens of thousands of natural product extracts against the virulent *M. tuberculosis* H37Rv strain in microplates with speed. Modern technologies, e.g., high speed countercurrent chromatography, HPLC-MS, and NMR, enables rapid isolation and identification of new natural products. These together equip us with the ability to look for potentially novel anti-TB agents from Actinomycetes with higher workflow efficiency.

1.2 Research goal and working hypothesis

This study is part of a project between the Institute for Tuberculosis Research (ITR), at the University of Illinois at Chicago (UIC), Chicago (USA) and the Extract Collection of Useful Microorganisms (ECUM), at Myongji University (Korea).

The broad goal of this study is to discover from actinomycetes new potential anti-TB chemotherapy agents with the ability to treat existing MDR- and XDR- strains and shorten the duration of TB treatment. The underlying central hypothesis is that there are still many undetected novel anti-TB agents in actinomycetes, with the ability to treat existing MDR- and XDR- strains, shorten the duration of TB treatment, and have the potential to be developed as potent anti-TB chemotherapy.

The first aim of the project involved the biological screening of a choice of 65,000 extracts of 7,000 cultured actinomycete strains originating from different habitats. From those initial screenings, strain *Nonomuraea sp.* MJM5123 was one of the top hits selected for large-scale cultivation, based on its ability to produce selective anti-tuberculosis activity. This already validated the working hypothesis that there are actinomycete strains with the ability to produce selective anti-TB activity.

The second aim involved the bioassay-guided fractionation of *Nonomuraea sp.* MJM5123 extracts, to isolate the biological active compounds. Ecumicin and several of its analogs were isolated, with their anti-TB activity confirmed, validating the working hypothesis that the anti-TB activity produced by strain MJM5123 is a result of its production of anti-TB active agents.

The third aim was to solve the structure of ecumicin and its analogs. These compounds were found to be peptolides with *N*-methylations.

Based on the characteristics of ecumicin's structure, we hypothesized that ecumicin and its analogs were produced non-ribosomally. The fourth aim was to identify ecumicin-producing gene clusters from MJM5123.

The fifth aim involved extensive in vitro and in vivo testing of ecumicin, in order to understand ecumicin's in vitro biological profile, pharmacokinetics in mice and eventually efficacy in mice. The working hypothesis was that ecumicin is an in vitro and in vivo active anti-TB agent. Among all anti-tuberculosis peptides produced by MJM5123, ecumicin was selected for all the testing because a) all of the isolated peptolides have similar activity vs *M. tuberculosis*, and b) compared to its analogs, ecumicin is the most abundant metabolite.

As the same high potency has been observed with any of the test mono-drug resistant *M. tuberculosis* strains, as well as clinical isolates including XDR- and MDR- strains, we hypothesized that ecumicin exerts its anti-TB activity via a novel mode of action. The sixth aim of the project was to understand this new mechanism of action. This was achieved through two sub-aims: 1) to identify ecumicin's target by whole genome sequencing of the spontaneous ecumicin-resistant *M. tuberculosis* strains; 2) to confirm that ecumicin binds to the target by drug affinity responsive test; and 3) to identify ecumicin's mechanism of action by biochemical studies. Ecumicin was found to stimulate ClpC1's APTase activity while inhibiting the ClpC1-dependant protein degradation in *M. tuberculosis*.

The anti-*M. tuberculosis* activity for each of the ecumicin analogs was assessed, in order to get some initial understanding of the structure-activity relationship of this peptide class. However, all compounds showed similar activity, so the structure-activity relationship remains undetermined.

2. High-throughput Screening of Actinomycetes

2.1 Introduction to TB high-throughput screening

Two key factors that determine the effectiveness of an HTS campaign are the choice of screening method and the quality of the sample library.

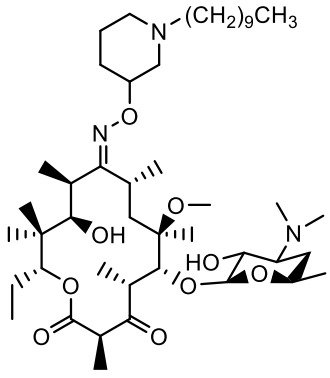
Choosing a suitable screening method has always been an important part in the discovery of new antimicrobials. Current approaches to the discovery of anti-TB compounds range from whole cell screening against *M. tuberculosis* or a surrogate, to cell-free, target-based screening.

The use of intact bacteria as a simple test for antibiotic activity has been responsible for the discovery of most of the drugs currently used to treat bacterial infections. All TB drugs, including the new diarylquinoline bedaquiline (Andries, et al. 2005, Diacon, et al. 2012), were either identified or derived from a whole cell screening lead. Similarly, the discovery/development of drug candidates in current TB drug pipeline relied on whole cell screenings, as seen in the development of the nitroimidazoles PA-824 (Stover, et al. 2000) and OPC-67683 (Matsumoto, et al. 2006), and diamine SQ-109 (Protopopova, et al. 2005), as well as the early discovery of benzothiazinones (BTZ) (Makarov, et al. 2009) and the 2-aminothiazole-4-carboxylates (ATCs) (Al-Balas, et al. 2009).

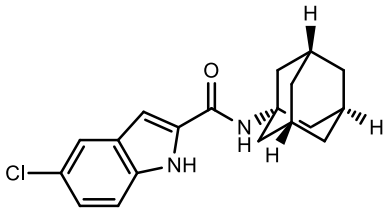
With the growing need to discover more clinical candidates for TB treatment, several recent campaigns were carried out with *M. tuberculosis,* and have led to a large number of potential lead compounds (Ananthan, et al. 2009, Goldman and Laughon 2009, Maddry, et al. 2009, Sivendran, et al. 2010, Stanley, et al. 2012). Recently, GlaxoSmithKline (GSK) conducted a

large (2M compounds) phenotypic screening campaign using *M. bovis* BCG for the primary screening, and *M. tuberculosis* for activity confirmation. GSK identified 177 *M. tuberculosis* hits from the campaign (Cooper 2013). A few of the recent hits are presented in **Figure 6**.

Since the sequencing of the *M. tuberculosis* genome in 1998, a continuing effort has been made to identify specific, essential TB biochemical targets. The high throughput assays developed against such targets could lead to the identification of novel chemical hits with potential to become novel TB drugs. Unfortunately, cell free assays have so far been unsuccessful in finding anti-bacterial drug candidates (Singh, et al. 2011); the underlying problem remains the translation of in vitro activity into whole cell, antimycobacterial activity. Nevertheless, a range of target-based screens has been employed in recent years of TB drug discovery, with the identification of several potential lead compounds (Manger, et al. 2005, Soellner, et al. 2007, Rawls, et al. 2009, Rawls, et al. 2010, Vasan, et al. 2010, Humnabadkar, et al. 2011, Jean Kumar, et al. 2013).



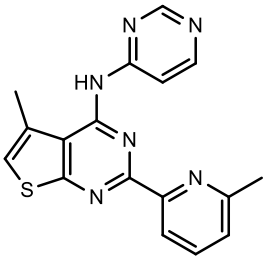




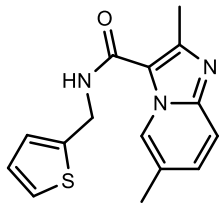
(1) MIC = 0.125 µM

(2a) R1 = CH3, R2 = H, MIC = 0.06 µg/ml
(2b) R1 = benzyl, R2 = H, MIC = 0.06 µg/ml

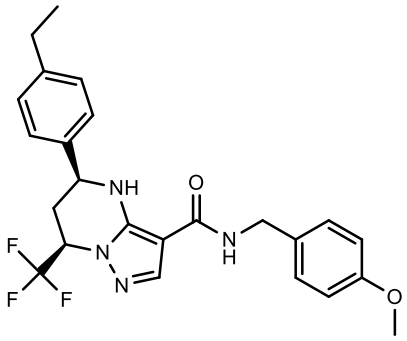
(3) MIC=0.47 µM



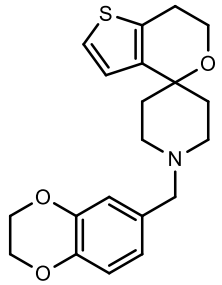
(4) MIC = 0.76 µM



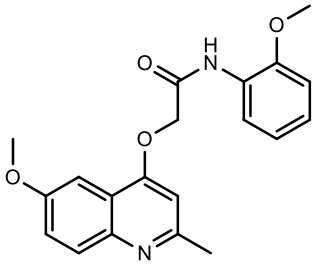
(5) MIC = 0.19 µM



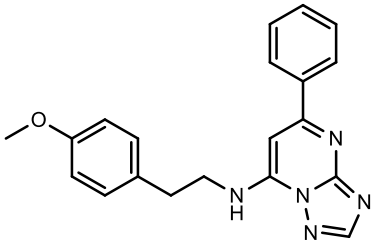
(6) MIC = 0.25 µM



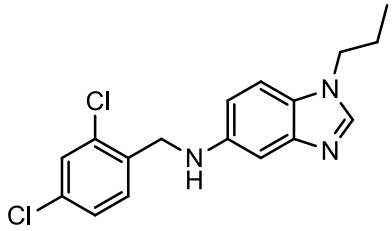
(7) MIC = 0.38 µM



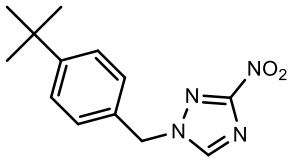
(8) MIC = 0.70 µM



(9) MIC = 0.94 µM



(10) MIC = 16 µM (2012)



(11) MIC = 0.5 µM (2012)

Figure 6. Examples of anti-TB hits identified by whole-cell screening. 1 is a macrolide derivative; 2a and 2b are 2-aminothiazole-4-carboxylates (ATC); 3-9 are GSK anti-tubercular whole-cell active chemotypes of interest; 10 is a novel inhibitor of MmpL3; and 11 is a novel DprE1 inhibitor.

Although there has been increasing recognition that even the largest, most carefully designed synthetic compound libraries access only a tiny fraction of possible chemical diversity (Campbell 2010, Drewry and Macarron 2010), application of HTS for identification of biologically active natural products has remained a relatively uncommon activity (Figure 7). (Henrich and Beutler 2013). Admittedly high-throughput assessment of natural products is fraught with a

variety of obstacles associated with the complex nature of the crude extracts. However, even for some successful natural product screening campaigns, e.g., the one responsible for the discovery of caparazamycin (Igarashi, et al. 2003), there was very limited information published regarding the screening process. This potentially hinders the growth of this already slow-growing field.

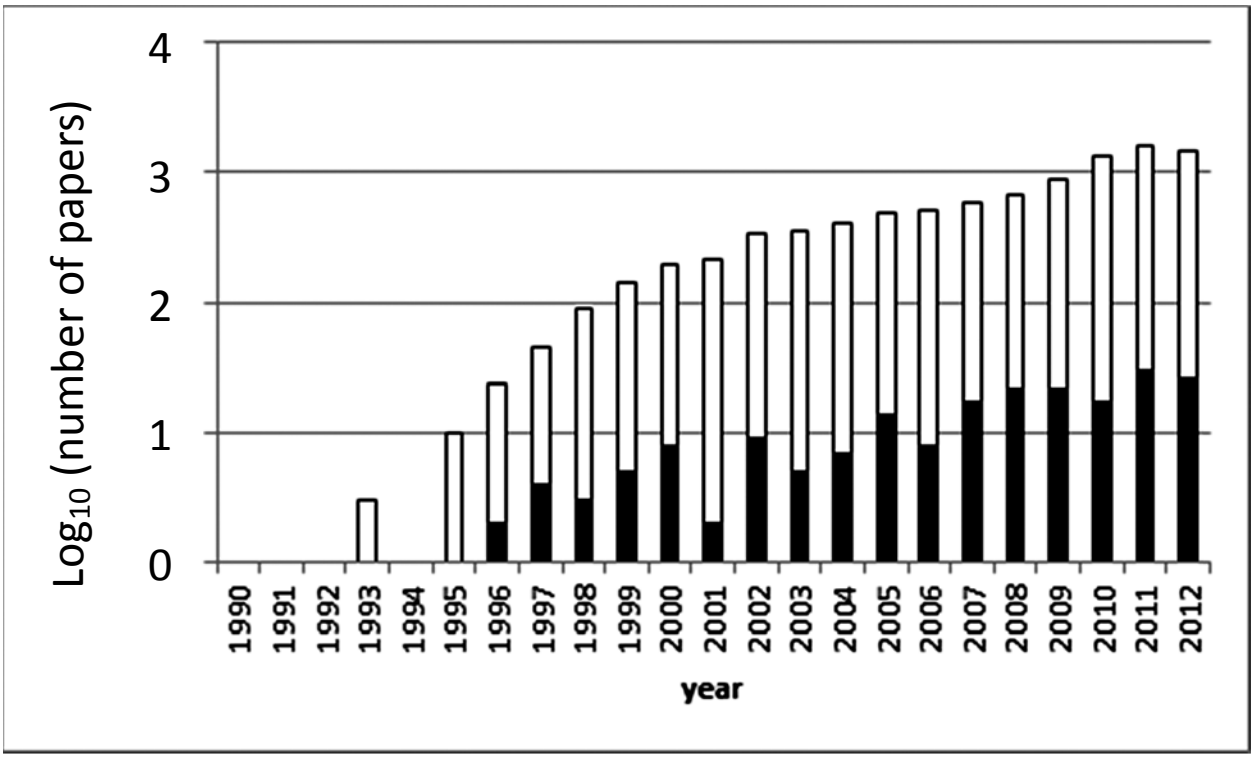


Figure 7. High throughput screening publications indexed in MedLine. The number of publications combining “high throughput screening” and “natural products” (black bars) is a small fraction of the total references indexed under “high throughput screening” (open bars). (Henrich and Beutler 2013)

2.2 Selection of screening methods

2.2.1 Anti-TB activity

To look for selective anti-TB agents that would fulfill the criteria mentioned in Chapter 1, we opted for whole cell screening over target-based screening, so that we were not limited to a few known TB drug targets, but remained open to finding agents with novel modes of action.

Admittedly, there is no single in vitro assay that could represent the in vivo TB development process. *M. tuberculosis* in lesions are divided into four different subpopulations according to their metabolic status and susceptibility to TB drugs (Mitchison 1985). So far, no TB assay could represent all these subpopulations. However, a combination of different in vitro assays, each representing a different *M. tuberculosis* subpopulation, should provide a better estimation on a test agent's in vivo activity. Having established techniques for the high throughput screening (HTS) against both replicating and non-replicating cultures of the virulent strain H_{37}Rv in a modern Biosafety Level 3 laboratory, we decided to use the microplate Alamar Blue assay (MABA) with a fluorescent readout (Collins and Franzblau 1997) for hit identification, and the low oxygen recovery assay (LORA) against non-replicating *M. tuberculosis* (Cho, et al. 2007) for hit characterization/prioritization.

2.2.2 Biological dereplication

Prioritizing the initial hits was required for identification of novel anti-TB actinomycete extracts, due to high prevalence of very common compounds, such as streptothricin or streptomycin. The methods used to distinguish novel compounds from known compounds at the earliest stage possible in the discovery process are known as "dereplication". Chemical dereplication, e.g. UV-visible, IR, NMR, or LC-MS analysis either requires a higher degree of purity

to become meaningful, or is expensive and time-consuming, making it inappropriate in early HTS phase on a large number of initial hits. We used a biological dereplication method that involved the use of a panel of *M. tuberculosis* isolates that have been selected as resistant to specific common compounds. This idea was initially proposed by Stansly (Stansly 1946) and put into practice by Stapley (Stapley 1958). We included a panel of resistant *M. tuberculosis* isolates, each resistant to one actinomycete-derived TB drug [streptomycin (SM), rifampin (RMP), kanamycin (KM) and cycloserine (CS)] to screen our test samples. If the test sample contained a compound to which one of the test panel is resistant, then the sample was classified as containing a known or at least a compound cross-resistant with a known, and therefore de-prioritized.

This method may result in false positives, especially in the highly unlikely case of an extract containing a number of known anti-TB agents. Activity of such an extract against the panel of mono-drug resistant strains may look as if it contains a new compound.

For better dereplication, it is necessary to track the biological (antibiotic) activity as well as the chemical entity (Singh and Barrett 2006). For chemical classification or identification sufficient to recognize whether an activity is novel or previously seen, a common method is to follow the activity through several, usually orthogonal, fractionation steps, in order to correlate the biological activity with the chemical signature. Potent activities present in small quantities may be practically chemically invisible in the face of more major components.

Due to the limitation of manpower, we decided to include only one fractionation step as the final step of prioritization/dereplication.

2.2.3 Anti-microbial inhibition spectrum

A spectrum of antibacterial activity provides additional information for dereplication, as a mean of early, rapid and inexpensive fingerprint for identification. By creating a large "deck" of results from a panel of organisms, patterns can be recognized that indicate the presence of a previously seen compound. In the present study, four microorganisms were used in our prioritizing screen panel, including one Gram-positive bacterium – *Staphylococcus aureus*, one Gram-negative bacterium – *Escherichia coli*, one fungal species – *Candida albicans*, and one non-tuberculous mycobacterium – *M. smegmatis*. These four microbes have been extensively used in different HTS campaigns. If the test sample contains a compound to which one of the test panel is very susceptible, then a possibility for the sample to contain a known compound is high, and, therefore, the sample should be de-prioritized.

2.2.4 Toxicity against mammalian cells

One key requirement of a promising new TB drug lead is having a fully validated safety profile. Aiming at finding from actinomycetes new potential anti-TB chemotherapy agents, prioritization of test samples should also reflect their toxicity against mammalian cells. Activity against VERO cells (IC_{50}) was taken as a sample's cytotoxicity, and the selectivity index was calculated as IC_{50}/MIC (replicating and non-replicating *M. tuberculosis*).

2.3 Composition of actinomycetes extract library

Our source actinomycete extract library was generously provided by ECUM, an institution at Myongji University in Korea, that maintains a growing collection of actinomycete isolates from various locations, including Korea, China, Nepal, the Philippines, Vietnam, Antarctica and the Arctic. (also see Geping, 2013) At the time of the described screening was performed, ECUM had a collection of over 7000 actinomycete isolates. The number is still growing as ECUM is actively collecting and isolating actinomycetes. The inclusion of rather exotic locations with different climates was an attempt at isolating rare and novel species, and increasing the chemical diversity of natural products in the library.

While primary metabolites are essential for the microbe's proper growth and survival, secondary metabolites are not, at least under laboratory conditions. (White, 2012) To increase the chance of secondary metabolite production, initial fermentation of actinomycetes involved three different media. Each isolate was first fermented in 20 ml of three different liquid cultures – G.S.S. (rich medium), Bennett's (normal medium), and D.Y.C. (minimal medium).

The mycelia and culture media supernatant were separated by centrifugation. The former was extracted with methanol, and the latter was partitioned with ethyl acetate, creating three extracts (Figure 8). The insoluble material was discarded. All fractions were then concentrated by speedvac or lyophilization. Nine extracts were thus generated from each microbial isolate. An un-weighed aliquot of each extract was placed in 96-well plate. To create the initial stock solution, 100 µl of DMSO (Sigma-Aldrich®) was added to each well. The plate was allowed to sit for 24

hours before screening to ensure all samples were sterilized, as full strength DMSO stock solutions act as sterilizing agents (Schmitz and Skoog 1970).

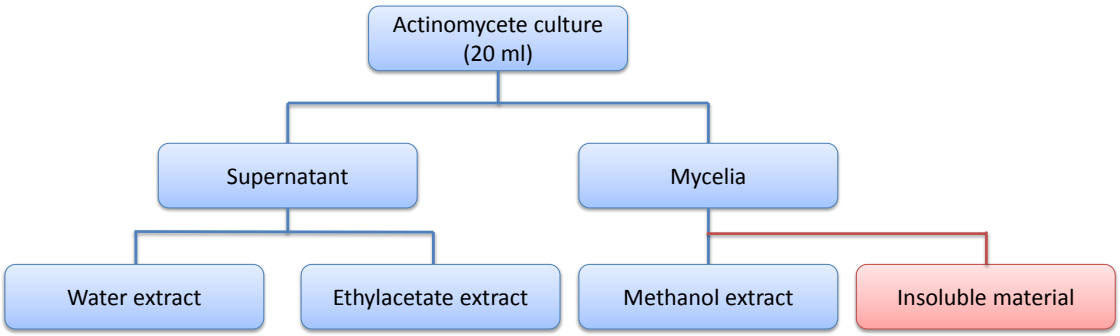


Figure 8. Initial extraction of actinomycete culture.

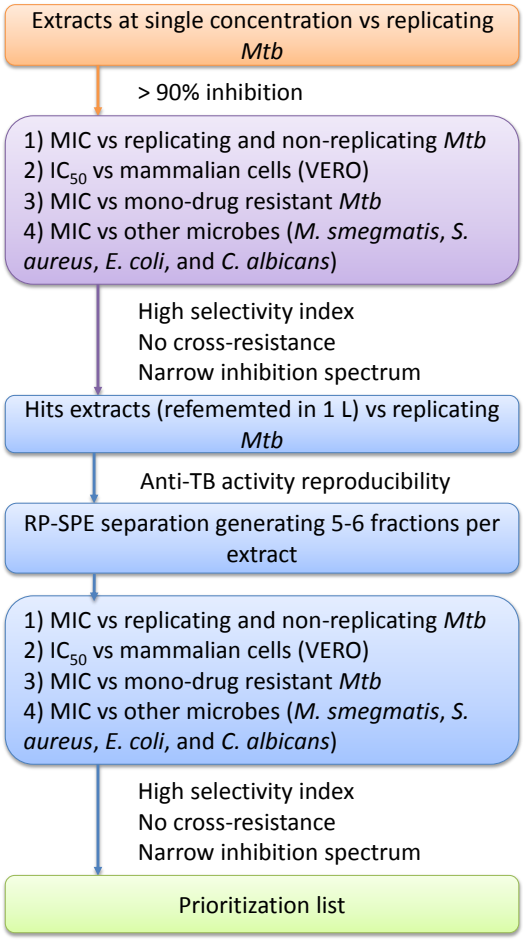


Figure 9. High-throughput screening of actinomycete extract library for potential new anti-TB agents.

2.4 HTS Methodology

2.4.1 High-throughput screening scheme

The scheme of our high-throughput screening campaign is shown in Figure 9.

To select anti-TB active extracts from the library, all actinomycete fermentation extracts were first screened for inhibition of replicating *M. tuberculosis* at a single concentration (1% v/v) using the MABA assay with fluorescence readout (Collins and Franzblau 1997). Those that exhibited ≥ 90 % inhibition of fluorescence relative to untreated control cultures were selected as initial hits.

Pseudo MIC values were determined for all initial hits, with the assumption that the concentrations of all extracts were 1 mg/ml, against: replicating *M. tuberculosis*, and isogenic *M. tuberculosis* strains that are resistant to SM, RMP, KM and CS in MABA, to ensure that we were not merely re-discovering one of these actinomycete-derived antibiotics.

Toxicity against mammalian cells (pseudo IC_{50} vs VERO cells) was also tested for initial hits.

Although the pseudo MIC and pseudo IC_{50} values were meaningless themselves, when put into the formula "selectivity index (SI) = IC_{50}/MIC (replicating *M. tuberculosis*)", they created an informative parameter, the selectivity index, which is independent of the testing concentrations by definition. This parameter can be viewed as a first estimation of a sample's therapeutic window. A high selectivity index is always desired, therefore only those extracts with selective anti-*M. tuberculosis* activity were prioritized.

The initial hits were further prioritized using: 1) MIC values against non-replicating *M. tuberculosis* in the LORA assay, to look for agents with the potential to shorten TB treatment duration, and 2) their activity against a panel of other microorganisms (*S. aureus*, *E. coli*, *C. albicans*, and *M. smegmatis*). Extracts with LORA activity were prioritized. Those with non-specific activity were deprioritized, due to a higher possibility of a hit extract containing a known compound, as the four microorganisms have been widely used in HTS.

Source organisms of the prioritized hits were re-fermented at medium scale, e.g. 1L, and extracted following the same scheme as discussed above (Figure 8). Stock solutions of these newly prepared extracts were prepared with accurate concentration, and were re-tested against replicating *M. tuberculosis*. Those that failed to reproduce anti-TB activity were removed from the hit list.

The confirmed hit extracts were fractionated by solid phase extraction using C18 cartridges with a gradient elution ranging from 20% to 100% methanol in 20% increments, with a final chloroform wash, creating six fractions for each sample. Stock solutions of these fractions with accurate concentrations were prepared in DMSO and screened against replicating *M.*

tuberculosis, including wild type and mono-drug resistant strains, non-replicating *M. tuberculosis*, mammalian VERO cells, as well as the four other microorganisms (*E. coli*, *S. aureus*, *C. albicans*, and *M. smegmatis*). The fractions were prioritized using the same criteria that was applied to initial hits.

Producing actinomycete strains of the *top prioritized fractions* were selected for further study. Strain MJM5123 is an example of a strain that produced a top prioritized fraction; the follow-up studies are discussed in following chapters.

2.4.2 Material and Methods

Activity vs. replicating *M. tuberculosis* H37Rv (ATCC 27294). All compounds were evaluated for MIC vs. *M. tuberculosis* H37Rv using the microplate Alamar Blue assay (MABA) as previously described (Collins and Franzblau 1997) except that we now use 7H12 media (instead of 7H9 + glycerol + casitone + OADC) (Falzari, et al. 2005), and freshly prepared 0.6 mM resazurin (Sigma-Aldrich®) solution instead of Alamar Blue dye. The percent inhibition was recorded as inhibition of fluorescence relative to untreated control cultures. The MIC was defined as the lowest concentration effecting a reduction in fluorescence of 90% relative to controls.

Cytotoxicity. Extracts and fractions were routinely tested for cytotoxicity against mammalian cells using VERO cells (ATCC CRL-1586, purchased from ATCC) (Cantrell, et al. 1996, Mangalindan, et al. 2000, Falzari, et al. 2005). After 72 hours exposure, viability was assessed on the basis of cellular conversion of MTS [3-(4,5-dimethylthiazol-2-yl)-5-(3-carboxymethonyphenol)-2-(4-sulfophenyl)-2H-tetrazolium, inner salt, purchased from Fisher

Scientific] into a soluble formazan product using the Promega™ CellTiter 96™ Aqueous Non-Radioactive Cell Proliferation Assay. Rifampin was included as a control.

MIC against mono drug-resistant isolates. MABA was used to assess MICs against isogenic *M. tuberculosis* H37Rv derived strains from ATCC with mono-resistance to rifampin (ATCC 35838), streptomycin (ATCC 35820), kanamycin (ATCC 35827), and cycloserine (ATCC 35826).

Activity against non-replicating persistent (NRP) *M. tuberculosis*. The test was performed as described earlier. (Cho, et al. 2007) Briefly, the assay involves three steps: "1) adaptation of *M. tuberculosis* to low oxygen through gradual, monitored, self-depletion of oxygen during culture in a sealed fermentor, 2) exposure for 10 days of the low-oxygen adapted culture to test compounds in microplates that are maintained under an anaerobic environment, thus precluding growth and 3) subsequent evaluation of *M. tuberculosis* viability as determined by the ability to recover." (Gill, 2012) Recovery/viability is determined by the extent to which a luciferase-expressing strain can recover the ability to produce luminescence. This procedure is termed the Low Oxygen Recovery Assay (LORA) and is HTS-compatible.

Spectrum of activity. *Staphylococcus aureus* (ATCC29213), *Candida albicans* (ATCC90028), *Escherichia coli* (ATCC25922), *Mycobacterium smegmatis* MC2155, were purchased from ATCC. MICs against these organisms were measured by micro dilution with a spectrometric readout at 570 nm as described by the National Committee on Clinical Laboratory Standards(NCCLS 1990, NCCLS 1991). The activity against *M. smegmatis* was determined by MABA with variation – after incubating with test samples for three days at 37^{o} in a 96-well microtiter plate, 12 µl of 20%

Tween80 and 20 µl of Alamar Blue dye (Thermo Scientific™) was added to each well; after an additional four hours incubation, viability was assessed by the measurement of fluorescence with a Victor^3 spectrophotometer (PerkinElmer).

2.5 Results

The primary screening encompassed 63,329 actinomycete extracts from ECUM. A total of 318 extracts (0.55%) exhibited ≥ 90% inhibition of fluorescence relative to untreated control cultures when screened against replicating *M. tuberculosis*. (Figure 10). The activity was mostly found in the organic solvent extracts of normal or rich media (Figure 10). The majority of active samples were found in only one of the 9 extracts that were produced from each culture. However some were found in as many of four of the extracts (usually both of the organic extracts and of the richer media). As a result, the secondary library of only active anti-*M. tuberculosis* actinomycete extracts contained a total of 208 source strains (3.0% of whole library).

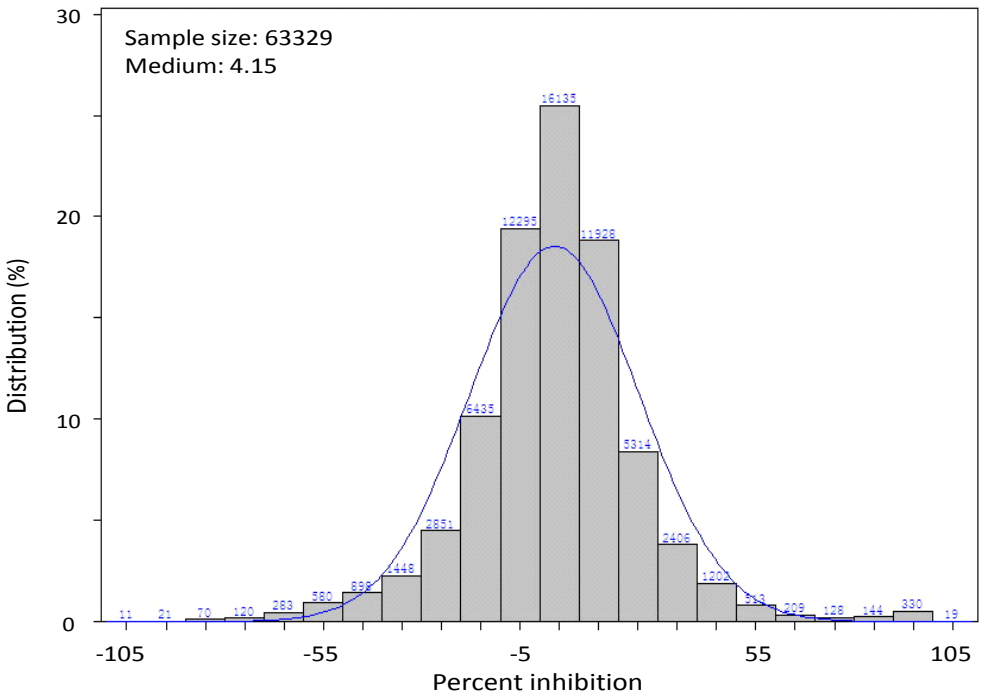


Figure 10. Activity of all extracts follows the normal distribution with medium mean at 4.52% inhibition. Number on top of each bar represents number of samples found with corresponding percentage inhibition range.

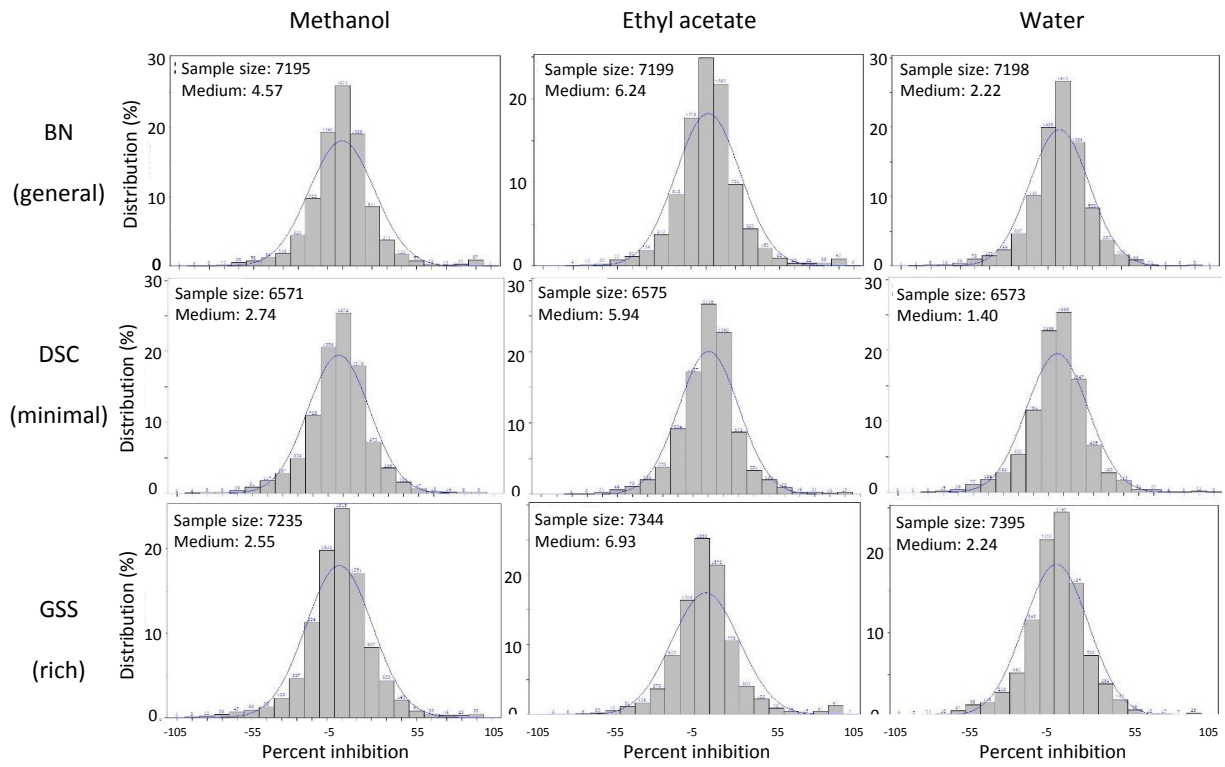


Figure 11. Distribution of anti-*M. tuberculosis* activity in all extracts analyzed by media and extraction types.

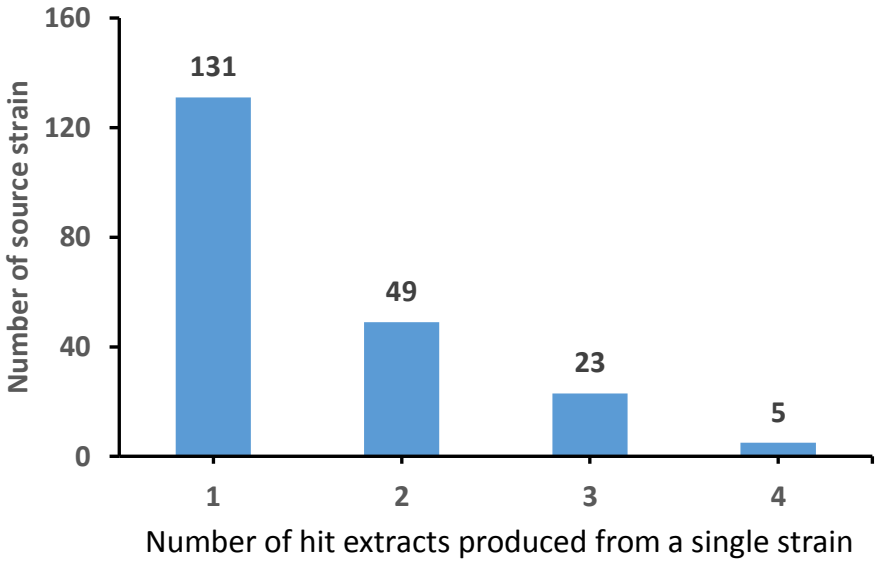


Figure 12. Media and/or extraction type dependence for production of active metabolites. Most hit strains (63%) would only produce anti-*M. tuberculosis* activity in one extract when cultured in a certain media.

Retesting against $H_{37}Rv$ for MIC determination confirmed 278 hits from the initial hit list (87.4%). When tested against mammalian VERO cells, 154 of the confirmed hits showed no obvious toxicity (IC_{50} > 10 µl/ml or SI > 10). When tested against the isogenic strains that are resistant to KM, RMP or SM, 124 of the confirmed non-toxic hits showed no cross-resistance with any of these drugs.

Most (67) of the 124 prioritized hits were found in only one of the 9 extracts that were produced from a single culture; 38 were found in two of the extracts; and 18 were found in three extracts. Removal of duplicate strains resulted in a list of 93 hits, representing 1.3% of strains in the original library. Only 10 of the 93 hits were water fractions.

The screening profiles for all nine extracts produced by the 93 strains were examined, to pick the most active fraction for further prioritization. Although the methanolic extract of strain MJM7049 cultured in Bennett's medium had a selectivity index of only 6.5 and the ethyl acetate extract of the same strain cultured in GSS medium had IC_{50} > 10, the former was included in the hit list in place of the later due to its over 10-fold higher activity against all tested *M. tuberculosis* strains.

The activity of the final 93 hits against non-replicating *M. tuberculosis* as well as a spectrum of other microbes (*S. aureus*, *E. coli*, *C. albicans*, *M. smegmatis*) were identified.

Together with their anti-TB activity profile, they were divided into four priority groups. The first group contained three hits – two were selected for their highly selective potency against replicating *M. tuberculosis* with no cross-resistance with RMP, KM, SM or CS; another one was

included for its high potency against non-replicating *M. tuberculosis*. Compared to hits in group 1, hits in the second group had one of the following undesirable features, (a) less active against replicating *M. tuberculosis*, (b) active against at least one of the nontuberculous microbes, (c) some toxicity against mammalian cells. Compared to group 2, hits in group 3 had some of the following undesirable features, (a) even less active against replicating *M. tuberculosis*, (b) highly active against at least one nontuberculous microbe, (c) toxicity against mammalian cells, (d) cross-resistance with RMP, SM or KM. Group 4 consisted of hits with the least favorable biological profile; they were the hits with lest activity against replicating *M. tuberculosis*, bearing cross-resistance to RMP, SM or KM.

After the groups were determined, an *M. tuberculosis* strain resistant to CS became available, and the top three groups were tested against it. The biological profile of the top three groups (22 hits) is summarized in TABLE III.

An analysis of their 16S rRNA suggests that the majority of the hits in the top three groups (17) were produced by strains belonging to the *Streptomyces* genus, and only one by a *Nonomuraea* species. The source strains of the remaining four were to be identified.

A new batch of the 22 hits were prepared from a medium scaled fermentation (1L), with their anti-TB activity confirmed by MABA. Subsequently, six fractions were generated for each extract by solid phase extraction on a RP-18 cartridge. TABLE IV shows the screening result of one top priority hit, strain MJM5123. The fractionation process concentrated the selective anti-TB activity of the methanolic extract of MJM5123 (MJM5123GM) into the two most lipophilic

fractions. Furthermore, undetected in MJM5123GM, activity against non-replicating culture was seen in these two fractions.

TABLE III. BIOLOGICAL PROFILE OF PRIORITY GROUP 1 – 3. EXT, EXTRACT; M, METHANOL; E, ETHYL ACETATE, W, WATER; RKM, KANAMYCIN-RESISTANT STRAIN; RRMP, RIFAMPIN-RESISTANT; RSM, STREPTOMYCIN-RESISTANT; RCS, CYCLOSERINE-RESISTANT. MIC, THE LOWEST CONCENTRATION OF A TEST AGENT THAT WILL INHIBIT 90% OF THE GROWTH OF A MICROORGANISM.

				MIC vs *M. tuberculosis* in µl/ml (%, at 10µl/ml)					IC50 in µl/ml		MIC vs *M. tuberculosis* in ul/ml (%, at 10µl/ml)				LORA	
Priority group	ID	Media	Ext	Rv	rKM	rRMP	rSM	rCS	1	2	*E. coli*	*S. aureus*	*C. albicans*	*M. smegmatis*	% inhibition at 10µl/ml	MIC in µl/ml
1	5123	GSS	M	0.51	0.31	0.89	0.84	2.49	> 10	> 40	0%	0%	64%	0%	17%	>10
	7483	BN	E	1.55	2.25	2.27	2.26	4.68	> 10	> 40	17%	4.34	8.03	0%	101%	0.48
	8412	GSS	E	2.86	0.30	2.03	0.58	0.25	> 10	> 40	0%	12%	0%	2.3	22%	>10
2	1526	GSS	E	1.66	2.35	2.16	2.36	89%	> 10	> 40	23%	3.71	86%	0%	100%	1.68
	1543	BN	E	1.20	2.38	2.19	2.32	1.22	> 10	28.2	0%	2.94	7.22	0%	101%	0.11
	2526	BN	E	1.44	2.06	1.38	1.08	1.15	> 10	29.9	12%	1.78	4.27	0%	99%	0.08
	4824	BN	M	2.34	1.69	2.33	1.45	1.48	> 10	29.2	22%	2.01	4.26	56%	100%	4.23
	4977	BN	M	2.42	2.45	2.32	2.01	2.33	> 10	> 40	22%	2.14	4.84	44%	100%	0.04
	5560	GSS	E	2.28	2.29	3.66	1.90	3.74	> 10	> 40	0%	0.46	7.02	59%	99%	0.23
3	7049	BN	M	0.85	0.60	0.60	0.62	0.57	5.5	9.4	14%	0.90	1.88	77%	100%	0.58
	1401	GSS	E	4.66	4.88	4.46	4.68	4.30	> 10	> 40	13%	4.48	65%	16%	101%	0.30
	4302	GSS	M	4.76	4.84	4.90	4.44	4.77	> 10	> 40	26%	8.02	4.97	11%	98%	0.45
	4413	BN	M	2.49	2.52	4.36	2.24	2.50	> 10	> 40	19%	3.02	85%	19%	101%	>10
	4721	BN	M	4.94	4.73	6.81	4.59	4.66	> 10	> 40	15%	4.22	22%	16%	101%	8.85
	4887	BN	E	4.83	5.94	4.82	4.66	4.74	> 10	> 40	10%	4.82	6%	6%	101%	>10
	5132	BN	E	4.53	4.82	4.19	4.45	21%	> 10	> 40	1%	39%	0%	11%	58%	7.58
	5960	DYC	E	2.20	0.63	2.40	3.59	0.96	> 10	3.2	13%	0.22	64%	12%	14%	0.25
	6477	DYC	W	2.57	2.36	3.34	4.81	4.80	> 10	> 40	2%	35%	73%	87%	101%	0.24
	6833	GSS	W	1.51	3.60	1.16	0%	0%	> 10	> 40	0%	26%	88%	24%	101%	0.15
	8106	DYC	W	8.14	2.42	1.00	2.26	2.92	> 10	> 40	4.75	4.42	4.91	2.38	83%	0.26
	8427	BN	M	2.92	2.60	2.40	4.02	2.35	> 10	> 40	4%	3.17	88%	17%	100%	0.46
	8915	BN	M	2.37	3.74	3.48	3.87	3.73	> 10	> 40	2%	4.20	87%	8%	100%	>10

TABLE IV. BIOLOGICAL PROFILING OF METHANOLIC EXTRACT OF PRIORITIZED CULTURE MJM5123, AND ITS FRACTIONS GENERATED BY SOLID PHASE EXTRACTION ON AN RP-18 CARTRIDGE AND METHANOL/WATER GRADIENT ELUTION. G, GSS; M, METHANOLIC EXTRACT. RKM, KANAMYCIN-RESISTANT STRAIN; RRMP, RIFAMPIN-RESISTANT; RSM, STREPTOMYCIN-RESISTANT; RCS, CYCLOSERINE-RESISTANT.

Sample	MIC vs *M. tuberculosis* (µg/ml)					IC50 vs VERO (µg/ml)	LORA (µg/ml)	Spectrum Activity (% inhibition at 100µg/ml)			
	Rv	rRMP	rSM	rKM	rCS			*E.coli*	*S. aureus*	*C. albican*	*M. smegmatis*
MJM5123GM	5.01	9.10	2.42	9.83	4.91	> 100	> 100	0%	12%	0%	33%
20% Methanol	25%	7%	6%	1%	7%	> 100	> 100	0%	5%	29%	12%
40% Methanol	13%	16%	0%	7%	12%	> 100	> 100	0%	3%	0%	18%
60% Methanol	17%	17%	0%	3%	0%	> 100	> 100	0%	5%	36%	10%
80% Methanol	8.48	9.34	2.46	9.42	4.80	> 100	> 100	0%	0%	0%	22%
100% Methanol	0.14	0.25	0.04	0.60	0.15	> 100	1.57	0%	1%	38%	9.72
Chloroform	0.19	0.51	0.08	0.40	0.15	> 100	6.70	0%	7%	71%	9.99

2.6 Discussion

2.6.1 Dereplication efficiency

Bioactivity-guided isolation and structural elucidation following the HTS revealed that the major anti-TB components in the top strain MJM8412 were several ilamycin analogs as previously patented by Eli Lily Co. (Kulanthaivel Palaniappan 2000), and in MJM5123 were ecumicin and its analogs (see following chapters). The result confirmed that our biology-chemistry coupled dereplication method is successful in ruling out the known actinomycete-derived TB drugs. On the other hand, this method's efficiency in excluding known anti-TB active agents other than TB drugs is limited. In the future, a combination fast bioassay-guided isolation of active component with small-scale starting material, and modern spectrometric techniques (LC-MS, NMR, etc.) that require sub-milligram quantity to achieve full/partial structural elucidation, should be applied for early identification of known agents other than TB drugs.

2.6.2 Potential false negatives

The initial hits list and the prioritized hits list both suggested that anti-TB activity was mostly found in the organic solvent extracts. Only 46 hits (14%) on the initial list, and 10 hits (11%) on the prioritized list were water extracts. This observation might be explained by the better permeability through the hydrophobic outer layer into *M. tuberculosis* of hydrophobic compounds, which tend to be present in the organic phase when extracted against water.

Poor solubility of test samples, esp. hydrophilic samples, in DMSO is the other possible cause of the low hit rate found in aqueous extracts. Several hydrophilic TB drugs, e.g. the purchased SM in the salt form, do not have good solubility in DMSO. When used as positive

controls in TB assays, it is usually dissolved in sterilized water (instead of DMSO) to make the stock solution.

Poor solubility of potential hydrophilic anti-TB agents in DMSO may have caused false negative hits in our HTS campaign. This issue might be solved by including both water and DMSO to make stock solutions. It could be done by 1) either preparing stock solutions of aqueous extracts in water, and utilizing the antibiotic mixture (BBL™ MGIT™ PANTA™ antibiotic mixture) to avoid contamination during testing, or 2) preparing two sets of stock solution for the whole library, one set with DMSO and the other with water. It is also possible that a fine-tuned mixture of DMSO and water could be used as a single solvent for stock solution preparation, so that both typical hydrophobic and hydrophilic anti-TB agents could achieve reasonable solubility.

3. Strain MJM5123 identification and optimized growth condition

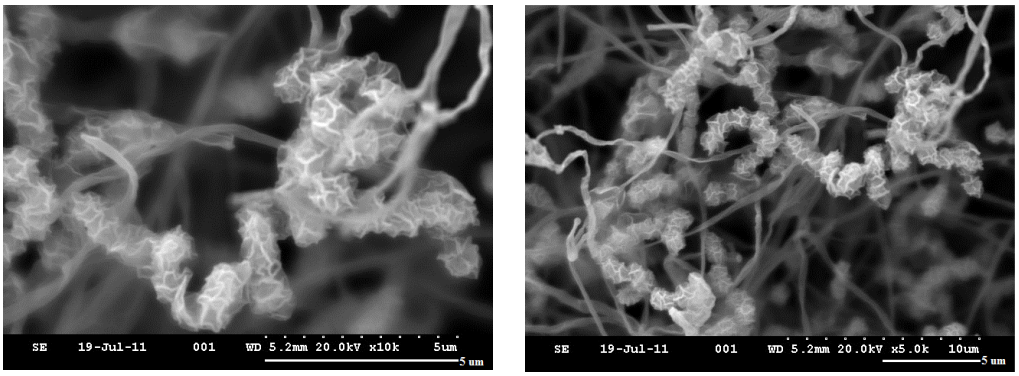
The methanolic extract of actinomycete strain MJM5123 was selected as one of the top hits from a library of over 63,500 actinomycete extracts. Study on the 16S rRNA of MJM5123 suggested it is a new strain of the genus *Nonomuraea*.

For efficient production of the anti-TB active compounds, culturing conditions, including culture media, temperature and time, were optimized. Under lab conditions, a titered yield of 373 mg/L was calculated for the major anti-TB active compound, using the optimized culturing conditions.

3.1 Identification of strain MJM5123

Phylogenetic relatedness based on the 16S rRNA gene of MJM5123 indicated that the strain was located on a coherent and monophyletic subclade, with neighboring strains and genome-wide comparison between MJM5123 and the most closely related strains showed 34.8 % similarity to *Nonomuraea rubra* DSM 43768^T (98.2% 16S rRNA gene similarity), 65.5 % similarity to *Nonomuraea roseola* DSM 43767^T (98.0 % 16S rRNA gene similarity) and 65.8 % similarity to *Nonomuraea dietziae* DSM 44320^T (97.5 % 16S rRNA gene similarity) (Figure 14, TABLE V). Hence, MJM5123 can be considered as a novel genetically separate strain of the genus *Nonomuraea*. The spores of MJM5123 have an open spiral with a rugose surface (Figure **13**). Filamentous aerial and substrate mycelium were beige color on all tested media and the mycelium was not fragmented. Atypically, aerial mycelium and spores were formed only on ISP3 agar medium (TABLE VI). MJM5123 did not produce any diffusible pigments nor melanin (TABLE VII). The

growth temperature was in the range of 20 to 40°C. MJM5123 could grow at pH 5.0 to 9.0 and tolerate up to 3% NaCl. It utilized diverse sugars, e.g. hexoses, pentoses, alcohol sugars and disaccharides, as sole carbon sources. It was susceptible to apramycin, kanamycin, vancomycin and thiostrepton, but was resistant to ampicillin. Whole cell hydrolysates of MJM5123 contained glycine and meso-diaminopimelic acid, glucose, galactose, mannose, and xylose. The major fatty acid and menaquinone were palmitic acid (25.53%) and MK-9(H_4). Phosphatidylethanolamine, diphosphatidylglycerol, phosphatidyl-monomethylethanolamine, phosphatidylinositol mannoside, unknown phospholipid and lipids were also detected.



(a) (b)

Figure 13. Scanning electron micrographs of mycelia and spores of MJM5123 grown on ISP medium 3 for 21 days at 28°C. Microscope magnification 10,000× (a) and 5,000× (b), respectively (white bars represent 5 µm).

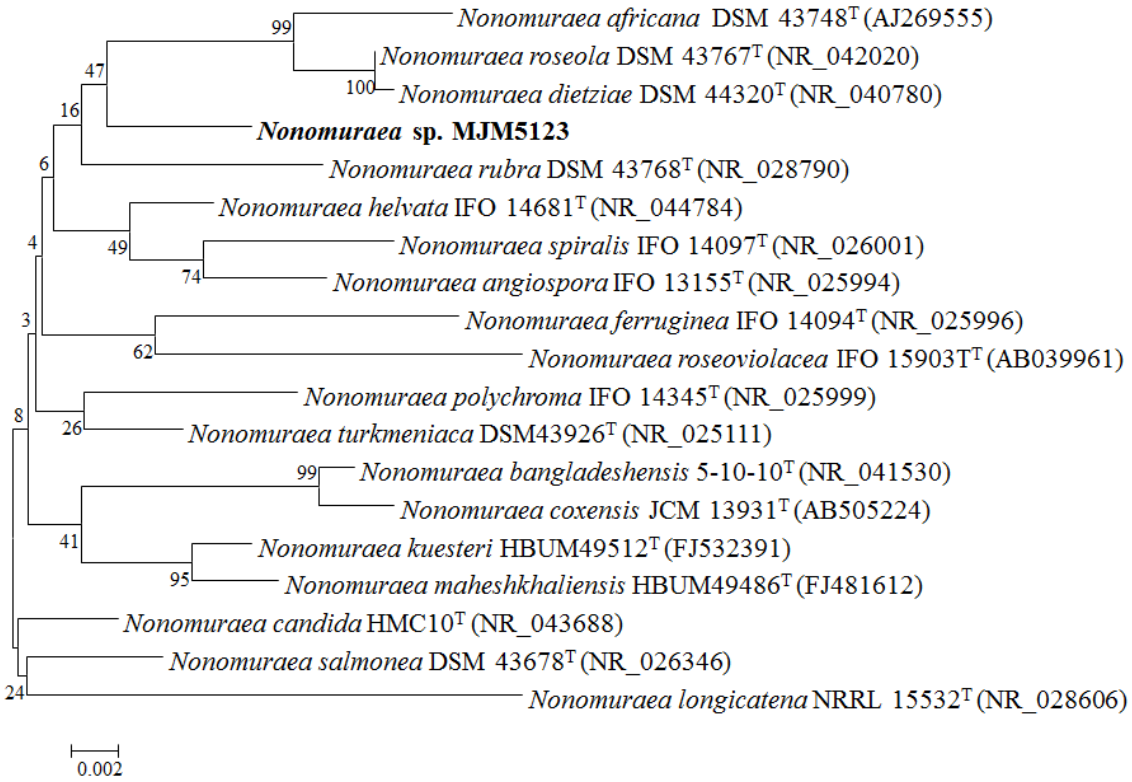


Figure 14. The neighbor-joining phylogenetic tree of MJM5123 based on 16S rRNA gene was constructed by using the MEGA 4.0 program. Numbers at the branch nodes represent bootstrap values (%) based on 1,000 replicates. Bar number indicates 0.002 substitutions per nucleotide.

TABLE V. GENETIC RELATEDNESS OF MJM5123 WITH CLOSELY RELATED STRAINS BY DNA-DNA HYBRIDIZATION. THE SELF-HYBRIDIZATION SIGNAL OF MJM5123 GENOMIC DNA WAS 100%, AND RELATIVE SIGNALS WITH OTHER STRAINS GENOMIC DNA WERE EVALUATED AS THE PERCENT SIMILARITY.

Taxa	MJM5123 (%)
MJM5123	100.0
N. dietziae DSM 44320^T	65.8
N. roseola DSM 43767^T	65.5
N. rubra DSM 43768^T	34.8

TABLE VI. CULTURAL FEATURES OF MJM5123. GROWTH AND SPORULATION ON AERIAL MYCELIUM WERE SCORED AS: ++, GOOD; +, MODERATE; ±, POOR; –, NO GROWTH AND NO SPORE FORMED.

	MJM5123
ISP medium	Growth/reverse color/aerial mycelium/sporulation
ISP2	++ / beige/ - / -
ISP3	+ / beige / ++ / ++
ISP4	+ / beige / - / -
ISP5	+ / beige / - / -
ISP6	+ / beige / - / -
ISP7	+ / beige / - / -

TABLE VII. PHYSIOLOGICAL AND BIOCHEMICAL PROPERTIES OF MJM5123. [1]CHARACTERISTICS WERE SCORED AS (++), POSITIVE; (+), MODERATE; (-), NEGATIVE. [2]CHARACTERISTICS WERE SCORED AS (+), DETECTED; (ND), NON-DETECTED.

Characteristics[1]	Description	Characteristics[2]	Description
Utilization of sole carbon source:		Cell wall amino acids: Glycine	+
Glucose	++	MESO-Diaminopimelic acid	+
Sucrose	++		
Fructose	+		
Mannitol	++	Whole cell saccharide analysis:	
Xylose	++		
Arabinose	++	Glucose	+
Rhamnose	++	Galactose	+
Raffinose	±	Mannose	+
Inositol	±	Arabinose	ND
Galactose	++	Ribose	ND
Maltose	++	Xylose	+
Mannose	++	Rhamnose	ND
Melanin pigment		Antibiotic resistance	
With tyrosine	-	(50 µg/ml)	
Without tyrosine	-	Apramycin	-
		Kanamycin	-
pH range for growth	5.0 ~ 9.0	Vancomycin	-
Growth temperature	20°C ~ 40°C	Thiostrepton	-
Growth salinity	Up to 3 %	Ampicillin	+

3.2 Optimized culturing conditions to improve ecumicin yield

As the anti-TB activity of strain MJM5123 was concentrated in the methanolic extract of its mycelia, in order to acquire maximum mycelia, an optimized three-stage fermentation procedure was applied, including activation of frozen vegetative mycelia stage, seed culture growth stage, and main fermentation stage.

3.2.1 Lab-scale production of ecumicin from MJM5123 through a three stage fermentation procedure

Frozen vegetative mycelia (FVM) of MJM5123 were used for routine and reproducible processing. It was prepared as follows. MJM5123 was inoculated into a 500 ml baffled flask containing 70 ml of activation medium, which is composed of soluble starch (2.0 %), yeast extract (0.5 %), beef extract (0.3 %), tryptone (0.5 %), $CaCO_3$ (0.2 %), $CoCl_2$ (0.0001 %), $MgSO_4 \cdot 7H_2O$ (0.05 %), and NE-302 (0.05 %) at pH 7.2. The flask was incubated on a rotary shaker at 34 °C, 200 rpm for 72 hours. The culture broth was later thoroughly mixed with 50 % glycerol at a 1:1 ratio (v/v) and serve as FVM. Aliquots of 5 ml FVM were stored at -80^{o}C until use.

Activation. A 5 ml FVM aliquot was transferred into a 500 ml baffled flask containing 50 ml activation medium. This was incubated on a rotary shaker at 34 °C, 200 rpm for 54 hours to yield activated young vegetative culture.

Early fermentation. A 5 ml aliquot of activated young vegetative broth was inoculated into a 500 ml baffled flask containing 50 ml of seed culture (SC) medium [glucose (1.0 %), dextrin (3.0 %), soytone (1.0 %), corn seed meal (0.5 %), yeast extract (0.5 %), K_2HPO_4 (0.1 %), $CaCO_3$ (0.4 %), $MgSO_4 \cdot 7H_2O$ (0.086 %), $CaCl_2$ (0.01 %), $(NH_4)_2SO_4$ (0.1 %), soybean oil (0.08 %), and NE-302 (0.05 %) at pH 7.2], and incubated on a rotary shaker at 34^{o}C, 200 rpm for 60 hours to yield seed culture.

The main fermentation was carried out in a 7 L fermenter (KoBiotech, South Korea) with 5 L working volume. A total of 500 ml of seed culture was transferred to 4.5 L of main fermentation medium [glucose (2.0 %), soluble starch (6.0 %), corn steep liquor (1.6 %), corn seed

meal (0.6 %), yeast extract (0.8 %), soytone (1.25 %), $CaCO_3$ (0.3 %), K_2HPO_4 (0.1 %), $MgSO_4 \cdot 7H_2O$ (0.086 %), $CaCl_2$ (0.01 %), $FeSO_4 \cdot 7H_2O$ (0.001 %), L-valine (0.05 %), NE-302 (0.05 %) at pH 7.2]. The culture was incubated at 34°C, 600 rpm and 0.3 vvm (volume of air per volume of broth per minute) of aeration for 144 hours.

Ecumicin production was quantified by HPLC at 373 mg/L. Analysis was performed on a Waters Delta Prep 4000 Preparative Chromatography System with a YMC-Pack ODS-A column (5 µm, 10 × 250 mm, YMC Co., Ltd., Japan) by isocratic elution using 40 % aqueous acetonitrile solution containing 20 mM sodium phosphate (pH 8.0) at ambient temperature. The flow rate was kept at 4.0 ml/min and eluents were monitored by a UV detector at 280 nm.

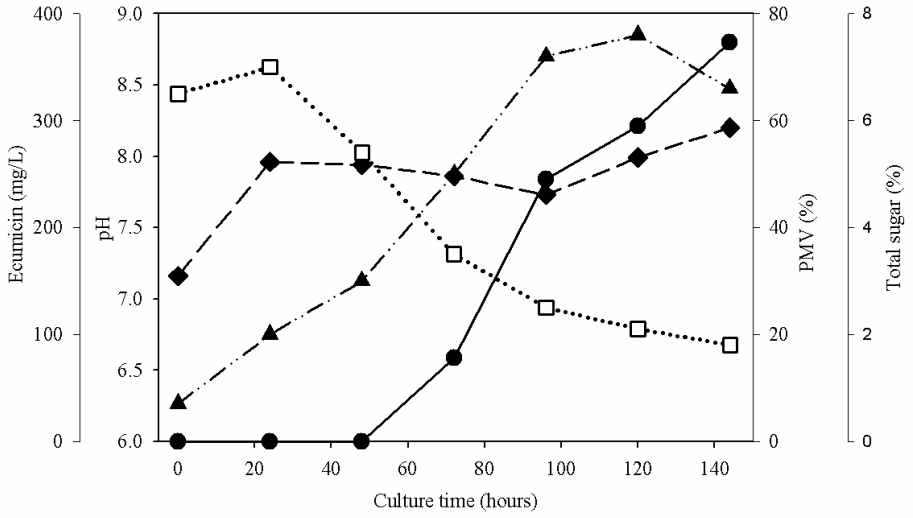


Figure 15. Main fermentation profiles for the production of ecumicin by MJM5123 in a 7 L fermenter. The fermentation processed at 34°C, 600 rpm agitation speed and an aeration rate of 0.3 v/v/m for 6 days. Twenty milliliters of broth were taken and analyzed for ecumicin titer (mg/L, ●), total sugar concentration (%, □), packed mycelia volume (PMV, %, ▲) and pH (◆) every 24 hours.

3.2.2 Large-scale production of ecumicin from MJM5123

Large-scale production of ecumicin from MJM5123 was performed by B&C Biopharm. A 500 L fermenter was used with 350 L working volume, and the yield of ecumicin was 98 mg/L by HPLC.

3.3 Material and methods

Isolation of a new actinomycete strain

The ecumicin-producing strain MJM5123 was isolated from a soil sample from Hallasan National Park in Jeju Island, South Korea. The strain is maintained at the Extract Collection of Useful Microorganisms (ECUM) library at Myongji University, South Korea (Yoon, et al. 2006), and has been deposited at the Korean Collection for Type Cultures (KCTC) with the access number KCTC 12178BP.

Molecular approaches for the identification of MJM5123

The 16S rRNA gene of MJM5123 was compared with related sequences and the similarity was evaluated using the NCBI BLAST available at http://www.ncbi-nlm-nih.gov/. The sequences were aligned using CLUSTAL X (Thompson, et al. 1997), and the phylogenic tree was constructed by the neighbor-joining method (Saitou and Nei 1987) using the MEGA 4.0 software (Tamura, et al. 2007). The relationship of each taxon in the phylogenic tree was calculated by 1,000 bootstrap replications (Felsenstein Jul, 1985). The genetic relatedness of MJM5123 with its most related strains was evaluated by the DNA-DNA slot-bolt hybridization method (Kafatos, et al. 1979). The self-hybridization signal was taken as 100 %, and the relative intensities of genomic DNAs of other strains were determined as the percent similarity.

Morphological and cultural features

The International Streptomyces Project (ISP) media were used to determine the color of aerial and substrate mycelia, and diffusible pigment (Shirling and Gottlieb 1966). The morphological features of spores and mycelia were observed by scanning electron microscopy (SEM, Hitachi, S-3500N, Japan). Temperature, pH, and salinity conditions for growth were tested on ISP3 medium, and antibiotic susceptibility was performed on ISP2 medium containing individual antibiotic. Incubation was carried out at 28°C for 2 weeks. The utilization of different sugars (1%, w/v) as sole carbon source was evaluated on ISP9 medium.

Chemotaxonomic characters

The meso-diaminopimelic acid (DAP), glycine and whole cell wall sugars were analyzed by TLC (Becker, et al. 1964). Polar lipids were analyzed according to a previously published method (D.E. Minnikin 1984). Menaquinone was analyzed by HPLC (Tamaoka 1986). The cellular fatty acid methyl esters were analyzed by using the ACTIN1 database (version 6.10) of the Sherlock Microbial Identification System (MIDI) (Sasser 1990).

DISCOVERY OF ECUMICIN.

The major anti-TB component in strain MJM5123 was found to be ecumicin (Figure 45) through a three-step bioassay-guided fractionation scheme. The structure elucidation was only made possible by combining an array of modern techniques with traditional methods, e.g., high-resolution mass spectrometry (MS), tandem MS, one- and two-dimensional NMR, X-ray crystallography, the Marfey's experiment, UV, IR, and circular dichroism.

4. Isolation of Ecumicin

4.1 Discovery of ecumicin via bioassay-guided fractionation

The MJM5123 mycelial cake was obtained by centrifugation of the fermented whole broth at 4 °C at 9,000 g for 20 min. The cell cake was extracted with an equal volume of methanol, and the extract was dried under vacuum. The methanolic extract (128.7g) went through a 3-step bioassay-guided fractionation (Figure 16): Vacuum liquid chromatography (VLC) of the extract on reversed phase silica gel using a water/methanol gradient in 20% steps and a chloroform wash, yielded seven chemically distinct fractions, VC-1 to 7. MICs of < 0.76 and 0.74 µg/mL were observed for fractions VC-6 & 7 eluting with 100% methanol and 100% chloroform, respectively. VC-6 & 7 were recombined (8.47 g) and further separated into 81 fractions on a Sephadex^{TM} LH-20 open column with 100% methanol as the eluent, yielding a panel of 16 recombined (on the basis of TLC) fractions, S-1 to 11. MICs were <0.21 µg/mL for subfractions S-2 and S-3. S-2 (177 mg) was separated into 140 fractions by HSCCC (Friesen and Pauli 2008) with HEMWat+2, which is a mixture of hexanes, ethyl acetate, methanol and water (3:7:5:5, v/v). As an even distribution

of sample S-2 was achieved with HEMWat+2 (P = 0.926), HEMWat+2 was selected as the most suitable two phase solvent system. Following their bioactivities (Figure 18), these 140 fractions were recombined to a panel of 26 fractions, H-1 to H-26. MICs were <0.5 µg/mL for H-3, H-5, H-7, H-9 to H-23. Among the active peptide fractions, H-14 was the purest by ^{1}H-NMR analysis (91 %, Figure 17) and, therefore, selected for structural elucidation. This compound was later named ecumicin.

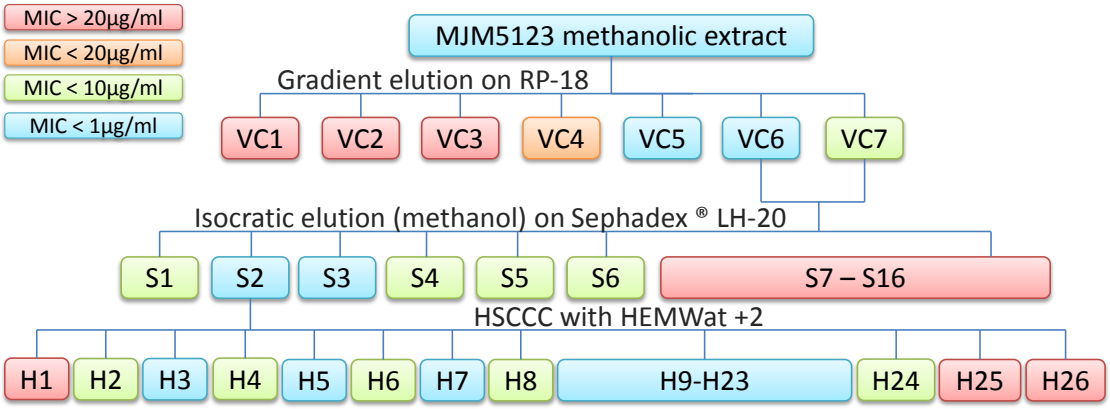


Figure 16. Bioassay-guided fractionation scheme of the methanolic extract of E5123 mycelia.

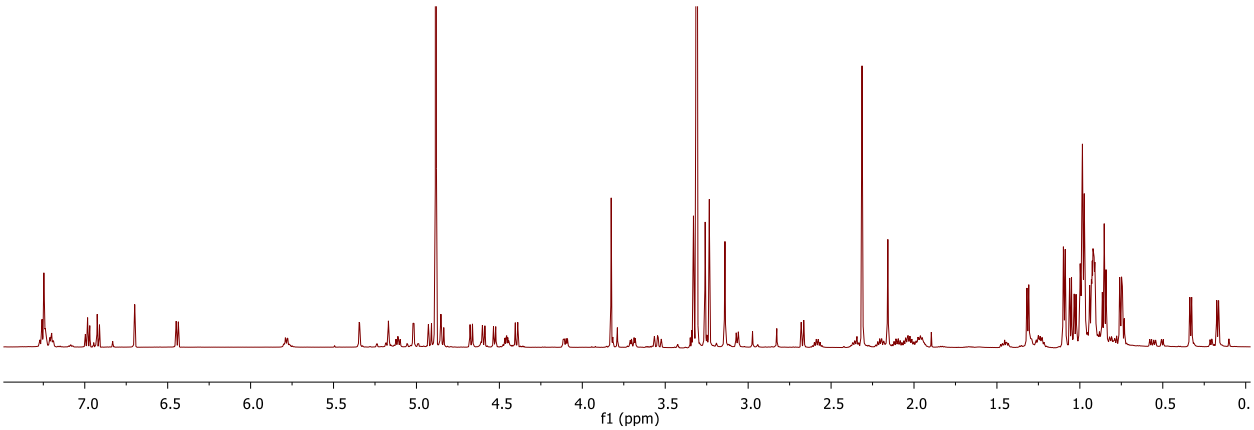


Figure 17. ^{1}H NMR spectrum of fraction H14 (approximately 4 mg) in 200 µl methanol-d_4 (3 mm NMR tube, 600MHz, Bruker Avance 600).

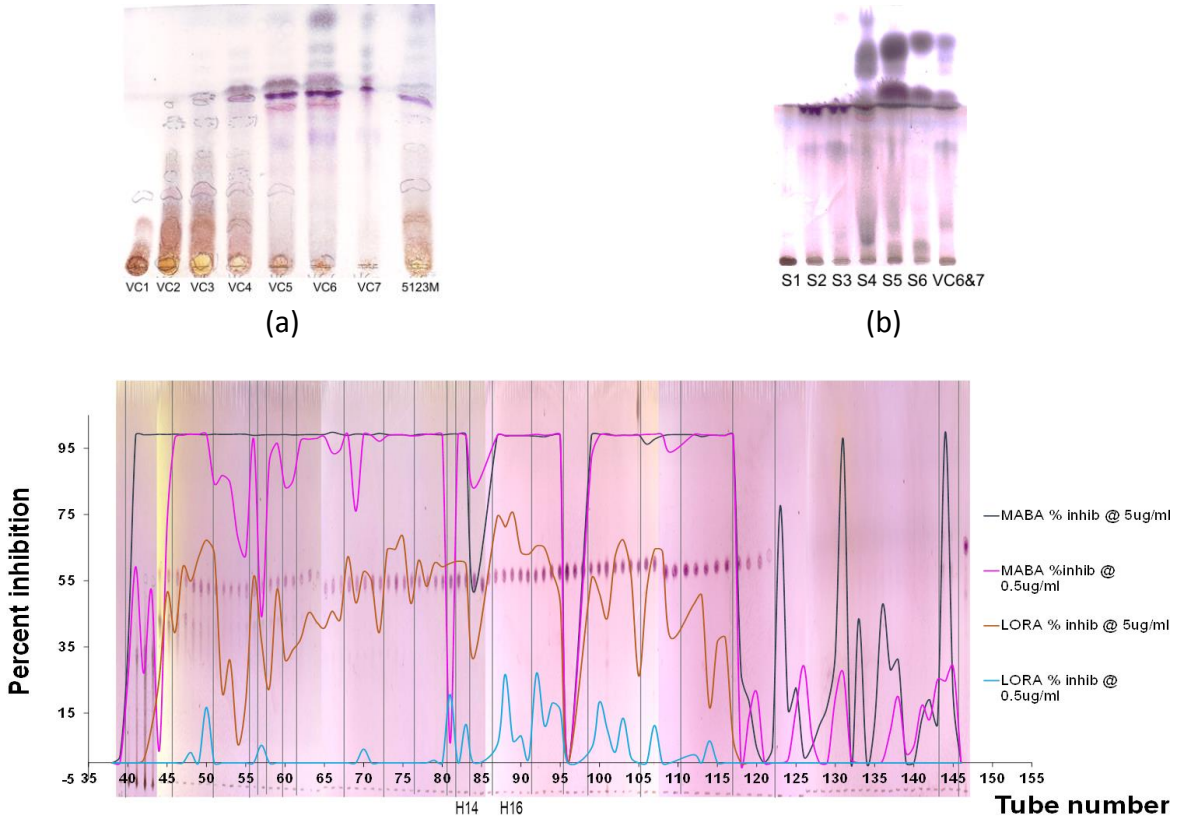


Figure 18. Thin Layer Chromatography of recombined fractions, in silica gel F254. The plate was eluted with toluene: methanol = 7:3 (v/v) mixture, revealed with UV at 254 & 366 nm (marked with pencil) and vanillin spray. (a) Fractions collected from VLC; (b) active fractions eluted from Sephadex^{TM} LH-20; and (c) bio-autography of fraction S-2, which was presented as fractions collected from HSCCC overlaid with chart of their anti-*M. tuberculosis* activities, with grey lines indicate the recombination according to their bioactivity.

4.2 Optimized fractionation scheme for mass production

After its identification, the outstanding in vitro biological activity of ecumicin was recognized, and we were interested in studying its anti-TB activity in a mouse model. As a result, gram quantities of ecumicin were needed, so an optimized fractionation scheme (Figure 19) was developed for the mass production.

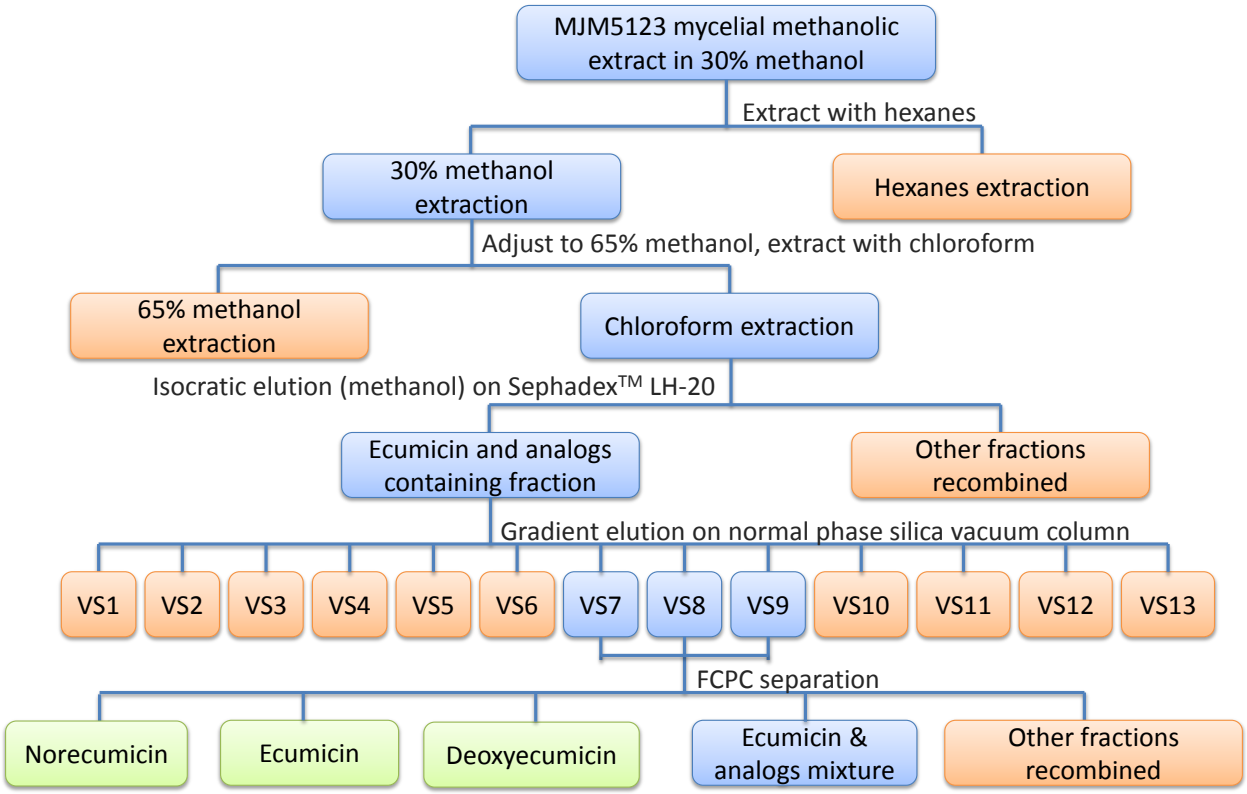


Figure 19. Optimized fractionation scheme for mass production of ecumicin [VS1, hexanes; VS2, hexanes: chloroform = 1:1 (v/v); VS3, chloroform; VS4, chloroform:ethyl acetate = 6:4 (v/v); VS5, chloroform: ethyl acetate = 4:6 (v/v); VS6, chloroform: ethyl acetate = 2:8 (v/v); VS7, ethyl acetate; VS8, ethyl acetate: methanol = 85:15 (v/v); VS9, ethyl acetate: methanol = 8:2 (v/v); VS10, ethyl acetate: methanol = 7:3 (v/v); VS11, ethyl acetate: methanol = 6:4 (v/v); VS12, ethyl acetate: methanol = 1:1 (v/v); and VS13, methanol].

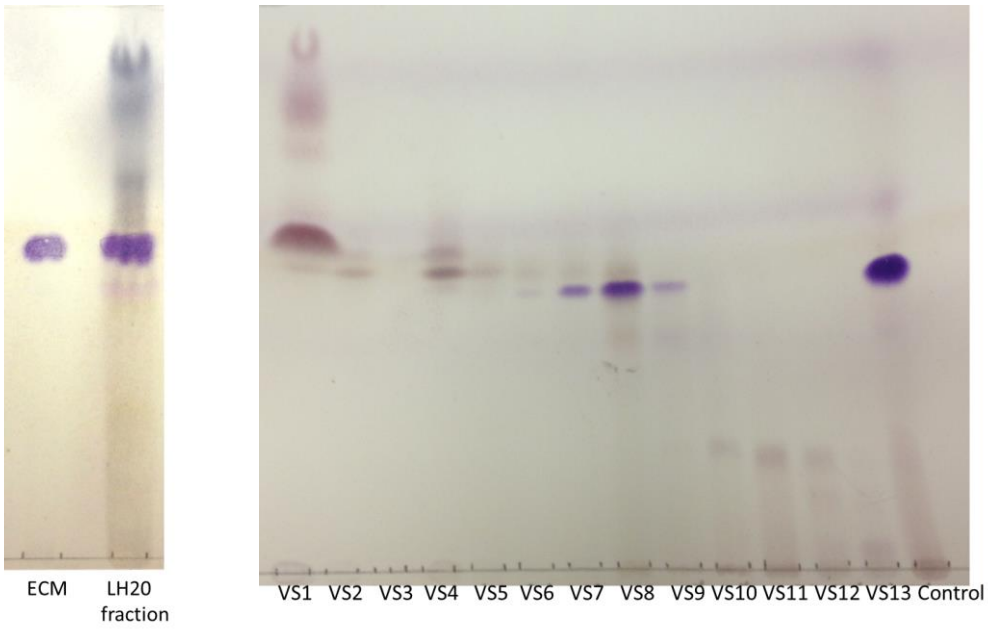
The MJM5123 mycelial cake was obtained by centrifugation of the fermented whole broth at 4°C at 9,000 g for 20 min. The cell cake was extracted with an equal volume of methanol. The extract was concentrated under vacuum at 37°C to 1/5th volume. It was diluted to 30% methanol by adding deionized water to the concentrated solution. This mixture was defatted by partitioning with n-hexane. One volume of methanol was added to the methanol-water phase, making it a 65% methanol solution. The 65% methanol solution was then extracted with one

volume of chloroform, and the chloroform layer was back-extracted by shaking with deionized water. The chloroform layer was evaporated to dryness to yield a yellowish solid, which was then dissolved in methanol at 100 mg/ml and applied to Sephadex^{TM} LH-20 open column equilibrated with 100% methanol.

After TLC analysis (Figure 20), ecumicin-containing fractions were recombined and further fractionated by vacuum liquid chromatography using normal phase silica gel. A gradient elution was applied, ranging from hexanes (VS1), hexanes : chloroform = 1:1 (v/v, VS2), chloroform (VS3), chloroform: ethyl acetate = 6:4 (v/v, VS4), chloroform: ethyl acetate = 4:6 (v/v, VS5), chloroform: ethyl acetate = 2:8 (v/v, VS6), ethyl acetate (VS7), ethyl acetate: methanol = 85:15 (v/v, VS8), ethyl acetate: methanol = 8:2 (v/v, VS9), ethyl acetate: methanol = 7:3 (v/v, VS10), ethyl acetate: methanol = 6:4 (v/v, VS11), ethyl acetate: methanol = 1:1 (v/v, VS12); and pure methanol (VS13). TLC analysis suggested that ecumicin was mainly concentrated in VS7, VS8 and VS9. Therefore, the three fractions were recombined for further purification.

The final purification step was carried out by the fast centrifugal partition chromatography (FCPC), with a HChEMWat solvent system [hexanes: chloroform: ethyl acetate: methanol: water (with 1% formic acid) = 4:7:9:10:10 (v/v)]. The separation was performed in reverse phase, using a Kromaton Technologies (Angers, France) apparatus with a 1L rotor, equipped with a Rheodyne injector and 50ml sample loop. Rotation speed was kept at 1,000 rpm and mobile phase (upper phase) flow-rate at 30 ml/min. Fractions were collected at 0.5 min/tube by a fraction collector, 100 min for elution and 40 min for extrusion. Fractions from the final step were analyzed by q^{1}HNMR (Pauli, et al. 2012), and those containing > 80% ecumicin were

recombined for bioassays. Fractions that contain ecumicin analogs, and the remaining fractions were recombined respectively for further studies (see Chapter 5 and 6).



(a) (b)

Figure 20. Thin Layer Chromatography on silica gel F254 of (a) recombined ecumicin-containing fractions eluted from Sephadex™ column (LH-20 fraction) compared with ecumicin standard; (b) fractions eluted from vacuum liquid chromatography using silica gel [VS1, hexanes; VS2, hexanes: chloroform = 1:1 (v/v); VS3, chloroform; VS4, chloroform: ethyl acetate = 6:4 (v/v); VS5, chloroform: ethyl acetate = 4:6 (v/v); VS6, chloroform: ethyl acetate = 2:8 (v/v); VS7, ethyl acetate; VS8, ethyl acetate: methanol = 85:15 (v/v); VS9, ethyl acetate: methanol = 8:2 (v/v); VS10, ethyl acetate: methanol = 7:3 (v/v); VS11, ethyl acetate: methanol = 6:4; VS12, ethyl acetate: methanol = 1:1 (v/v); and VS13, methanol]. ECM, ecumicin. The plates were developed with toluene : methanol = 7:3 (v/v) mixture, revealed with vanillin spray.

This process is very effective at separating ecumicin related peptides from other components (133 mg/L yield). However, the yield for ecumicin, which composed over 40% of all anti-TB active peptides, is only 30 mg/L. This reflects the tiny structural differences between

ecumicin and its analogs, which leads to similar chromatographic behavior, and therefore difficulties in isolating each peptide. Further purification with preparative or semi-preparative HPLC of the “ecumicin & analogs mixture” fraction would partially solve this problem (see Chapter 9), and in the meantime, produce a little more of purified ecumicin sample. But to get a reasonable amount of any pure peptide using HPLC would require repeated injections of small amount of samples (up to 40 µl of 5 mg/ml peptide mixture on a semi-prep HPLC column, otherwise analog peaks would overlap severely). At this stage, this is impractical due to the time limitations (approximately 20 min to separate 0.2 mg peptide mixture).

4.3 Discussion

Both orthogonal separation schemes were effective in isolating ecumicin from the crude extract of MJM5123. The first protocol yielded approximately 10 mg/L ecumicin from un-optimized MJM5123 fermentation, while the second one yielded approximately 30 mg/L ecumicin from optimized MJM5123 fermentation. With better understanding of ecumicin’s properties, liquid-liquid extraction could later be used to replace the vacuum liquid chromatography as a simple yet effective first step separation, with the advantage of straight forward and inexpensive scale-up.

Countercurrent separation (CS, including HSCCC and FCPC) provided a loss-free fractionation technique, due to the lack of a solid stationary phase.

With HSCCC instruments with 20 ml to 300 ml coils, and FCPC with 200 ml to 1 L rotors readily available, another advantage in liquid-liquid chromatography is easy scale-up. In this study, this technique has made possible fast separation of a relatively large amount of sample

with high resolution. An FCPC instrument equipped with a 1 L rotor is able to fractionate up to 5 g sample in a single run. Importantly, within a few hours, compounds with very similar structures, e.g. norecumicin, deoxyecumicin (see Chapter 9) and ecumicin, could be well separated.

However, one major problem exists in the separation of ecumicin and its other analogs by liquid-liquid chromatography. The peptides can emulsify the two liquid phases, which lead to a constant loss of stationary phase, and therefore caused reduction in the resolution power of CS. This problem might be solved by increasing rotation speed after sample injection in FCPC, as rotation assists settling of two phases in the system. Unfortunately this solution is merely not practical, as the design of FCPC sets a limit in the maximum system pressure, which is directly related to rotation speed. Exceeding the maximum allowed pressure causes leakage of the partition disk stacks.

4.4 Material and methods

Vaccum liquid chromatography

The methanolic extract of MJM5123 (128.7g) was dissolved in 200 ml methanol (distilled, reagent grade from Fisher®), and mixed with 200g reversed phase silica gel. The mixture was dried by rotovap, and the dry powder was placed on top of a vacuum column packed with 800g reversed phase silica gel. A water (purified by Milli-Q water purification system)/methanol (distilled, reagent grade from Fisher®) gradient in 20% steps (1 L/step) and a chloroform (distilled, reagent grade from Fisher®) wash (2 L) was applied.

Liquid-liquid extraction

Approximately 100g of the methanolic extract of MJM5123 was dissolved in 1 L of 25% methanol solution (water - purified by Milli-Q water purification system, methanol - distilled, reagent grade from Fisher®). The solution was washed with 500 ml hexanes (distilled, reagent grade from Fisher®) three times. The methanol solution was kept and 500ml methanol (distilled, reagent grade from Fisher®) was then added to make it 65% methanol solution. The 65% methanol solution was extracted by 500 ml chloroform (distilled, reagent grade from Fisher®) three times. The chloroform solution was recombined and dried.

Sephadex™ LH-20 separation

Approximately 1.5 g sample was dissolved in 10 ml methanol (distilled, reagent grade from Fisher®) loaded on a Sephadex™ LH-20 open column (5 cm × 30 cm, with approximately 200 g dry LH-20) that was equilibrated in methanol. Fraction collection started just before the light yellow band reached the bottom of the column; 9 ml eluent was collected in each test tube.

For the discovery run, eluents were collected until all colored bands on the column were gone (approximately 75 tubes). For scaled-up separation, only the first 25 tubes were collected to cover the fractions containing ecumicin and its analogs. An aliquot from each tube was spotted on normal phase thin layer chromatography (TLC) plate, developed by methanol:toluene = 7:3, and spots were revealed by vanillin spray. The vanillin reagent was prepared by dissolving 0.8 g vanillin in a mixture of 76 g of non-denaturized ethanol and 4 g of concentrated sulfuric acid. The reagent was evenly sprayed to the dried TLC plate in an operating fume hood. The plate was heated at approximately 120° C for 3-5 min, and observed under white light. Positive reaction will yield colored spots. Fractions with similar TLC patterns were recombined.

HSCCC solvent system selection

Approximately 2 mg of sample was placed in 4 ml glass vial, to which 2 ml of a HEMWat (hexanes, ethyl acetate, methanol, and water mixture) solvent system was added and mixed well. The settling time was recorded. The two phases of solvents were separated, dried and weighed. HEMWat +2 (hexanes, ethyl acetate, methanol, and water mixture in the ratio of 3:7:5:5) had the shortest settling time (~ 40 s), and even distribution of sample in both phases (P = 0.926). Therefore HEMWat +2 was initially selected as the most suitable solvent system for HSCCC separation.

HSCCC experiment

The small scale purification was carried out on a PTR CCC-1000 machine equipped with 118 ml coil with a rotation speed of 1100 rpm. The organic phase (upper phase) was used as stationary phase, and retention (Sf) of 57.6% was achieved with a mobile phase flow-rate of 0.5

ml/min. Fractions were collected at 2 ml/tube by a fraction collector for 400 min during elution (until K_{calc} = 2.5). Afterwards, extrusion was performed – the organic phase was pumped at 1 ml/min for 130 min, and fractions were also collected at 2 ml/min. As a constant loss of stationary phase was observed during the elution, the actual retention (Sf) value decreased during the run, and as a result, the elution end point had a $K_{real} > 2.5$.

FCPC solvent system improvement

With the understanding that ecumicin is a slightly basic compound with a free tertiary amine group (See Chapter 5 Figure 45), we decide to use a pH refined solvent system for the scale-up separation of the compound, in the hope of sharpening the peaks of ecumicin and its analogs.

Instead of deionized water, an aqueous solution with 1% formic acid (reagent grade, from Sigma-Aldrich®) was added to the solvent system. However, when using this solution, all HEMWat solvent systems were found to be too non-polar – all peptides of interest were found only in the aqueous phase. ChEMWat (a mixture of chloroform, ethyl acetate, methanol and 1% formic acid) solvent systems were tried, and were found to be too polar – all peptides of interest were only found in the organic phase. When combining the chemistry of the two solvent system, peptides of interests had near even distribution in the two phases. When the solvent system was composed of hexanes, chloroform, ethyl acetate, methanol, water with 1% formic acid in the ratio of 4:7:9:10:10, the peptides were distributed evenly in the two phases (by TLC), and a settling time of 45 s was recorded. This was used as the working solvent system in large scale

ecumicin isolation. The organic phase (lower phase) was used as the stationary phase, whereas the aqueous phase (upper phase) was used as the mobile phase.

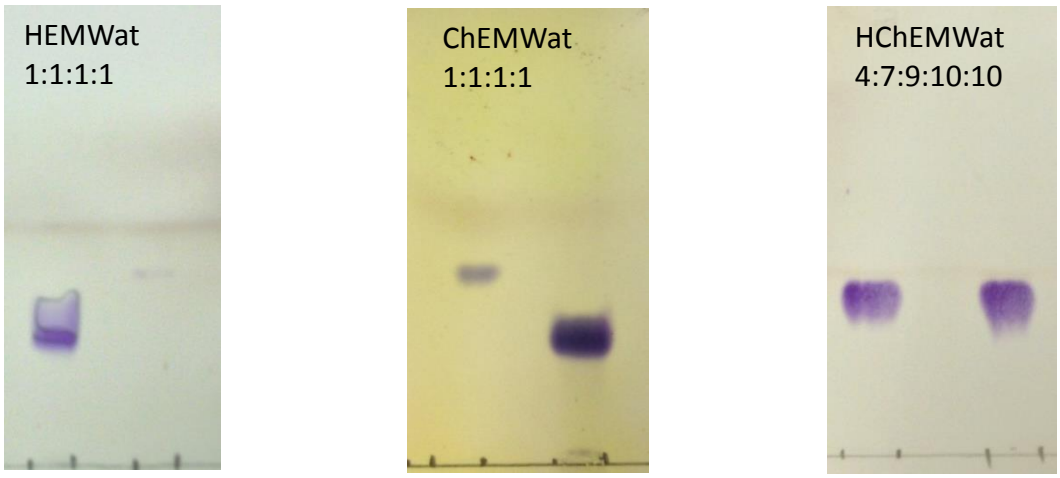


Figure 21. Thin Layer Chromatography of distribution of peptides of interest in different solvent systems, in silica gel F254. The plate was eluted with toluene: methanol (7:3, v/v) mixture, revealed with UV at 254 & 366 nm (marked with pencil) and vanillin spray. aq., aqueous phase; org., organic phase. Purple spots corresponds to peptides of interest. The differences in R_f value in (b) was due to residual solvent used to apply the sample. (a) HEMWat 0, hexanes: ethyl acetate: methanol: 1% formic acid water solution = 1:1:1:1 (v/v); (b) ChEMWat 0, chloroform: ethyl acetate: methanol: 1% formic acid water solution = 1:1:1:1 (v/v); (c) HChEMWat, hexanes: chloroform: ethyl acetate: methanol: 1% formic acid water solution = 4:7:9:10:10 (v/v). Aq, aqueous phase; org, organic phase.

Purity determination by the 100% qHNMR method

The ^{1}H NMR spectrum of fraction H14 (900 MHz, CD_3OD,Figure 17) was acquired under quantitative conditions (90 degree excitation pulse, acquisition time 4.0 s, relaxation delay 60.0

s) using a Bruker Avance II 900 instrument. Processing, used zero filling (2x), Lorentzian-Gaussian apodization (LB = -0.3, GB = 0.05), and polynomial baseline correction.

The aromatic singlet (δ_H 6.698) of **1** was selected as the most pure signal, and used to quantitate **1** by applying the following integral-based 100% qHNMR method. The integral of the singlet was set to 1.000, representing the integral of one proton (1H). All other proton signals between δ_H 0.0 to 7.5 in the spectrum, except for the solvent signals (HOD and CHD_2OD), were integrated, and the sum of these integrals was determined to be 137.36.

A total of 125 non-exchangeable protons are present in **1**. Considering that all resonances not belonging to **1** (i.e., the impurity signals) were typical peptide resonances, and assuming that they have the same molecular weight as **1** (i.e., isomeric impurities), the purity of **1** in fraction H14 was calculated as:

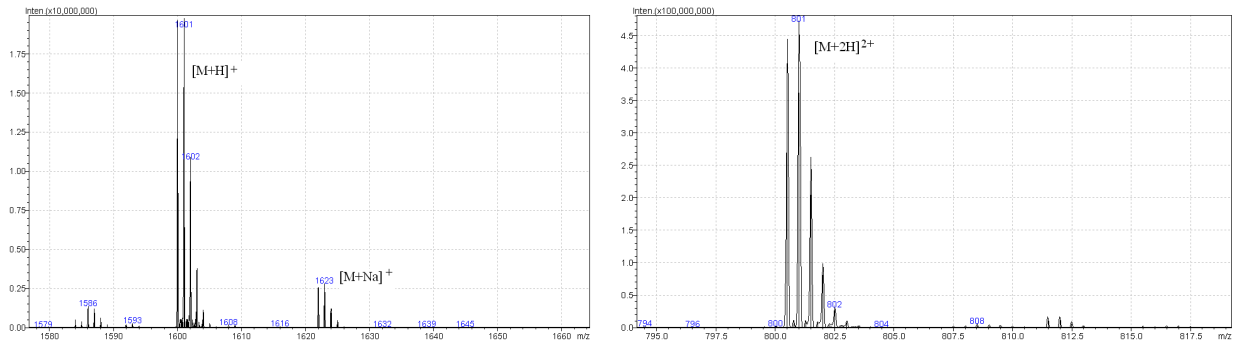
Purity = 125×1.00/137.36×100 % = 91.0 %

5. Structure elucidation

Pure ecumicin forms pale yellow to colorless needle-shaped crystals; m.p. 165 ~ 168°C; $[\alpha]^{24}_{D}$ = 138.0 (c = 0.09, $CHCl_3$); UV (MeOH) λ_{max}(log ε) 219(4.74), 225sh(4.48), 277(3.61) nm ; IR ν_{max} 3315, 2962, 1632, 1508, 1255, 1089, 737 cm^{-1}; ^{1}H NMR and ^{13}C NMR data, see TABLE VIII; HR-ESI-MS m/z data, see Figure 22; ESI-MS2 m/z data see Figure 27.

5.1 Classification – the peptidic nature of ecumicin

High resolution ESI-MS analysis of ecumicin showed pseudo molecular ions at *m/z* 1600.0189 $[M+H]^+$, 1621.9982 $[M+Na]^+$, and 800.5131 $[M+2H]^{2+}$ (Figure 22), which indicated an exact mass of 1599.0111. Such high exact mass precludes a good prediction of the molecular formula without further evidence.



(a) (b)

Figure 22. HR-LC-MS spectrum of ecumicin obtained on a Shimadzu IT-TOF instrument.

The distribution of signals in one-dimensional NMR spectra indicated the peptidic nature of the compound. The ^{1}H NMR spectra in methanol-d_3/-d_4 displayed eight exchangeable proton signals from 7.72 – 9.20 ppm, which are likely to be amide proton signals; the ^{13}C NMR spectrum revealed 12 carbonyl signals, which, taking into account peak intensities, indicated 13 carbonyl groups (Figure 23). In the ^{1}H NMR spectra, "the distribution of signals with doublets in the amide proton region and signals covering the complete range between 5.4 and 0.7 ppm was a clear indication that the investigated compound was indeed a peptide." (Jaki, 2001)

The presence of amide carbonyl moieties was supported by a strong IR band at 1632 cm^{-1} (Figure 25), as well as UV bands at 211 and 219 nm (Figure 26). An additional IR band at 1508 cm^{-1} and UV bands at 263, 281, and 291 nm were an indication for the presence of aromatic residues.

Tandem mass spectrometry's failure to suggest any uniform fragmentation proteomics pattern indicated that the peptide was a cyclic one (Figure 27).

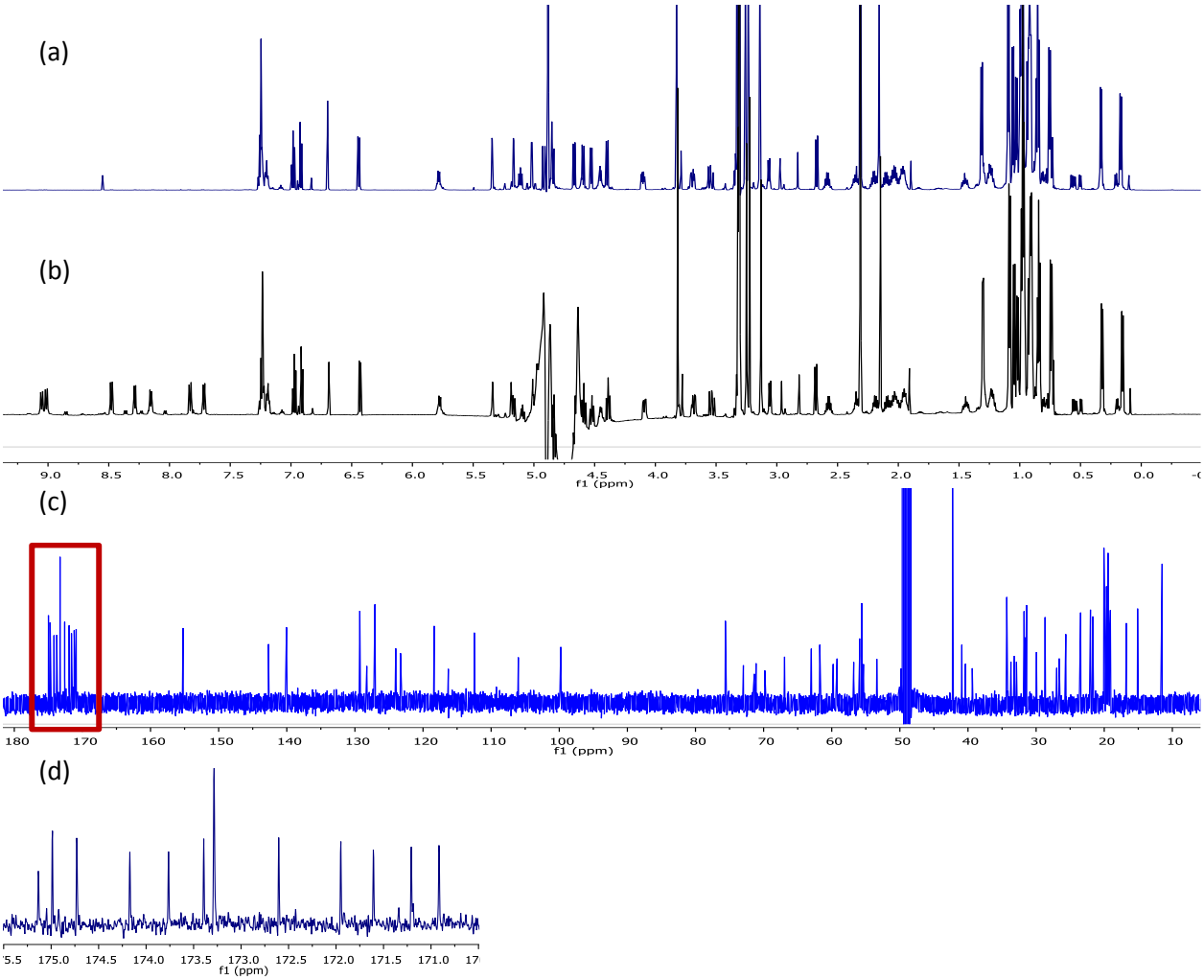


Figure 23. One-dimensional NMR spectra of ecumicin in methanol-d_4/d_3, 900/600/100MHz (Bruker Avance II 900, Bruker Avance 600, Bruker DPX 400). (a) ^{1}H spectrum in methanol-d_4 (CD_3OD); (b) ^{1}H spectrum in methanol-d_3 (CD_3OH), processed with water subtraction; (c) ^{13}C spectrum in methanol-d_3 (CD_3OH); (d) expansion on the carbonyl carbon region from the ^{13}C spectrum in methanol-d_3 (CD_3OH).

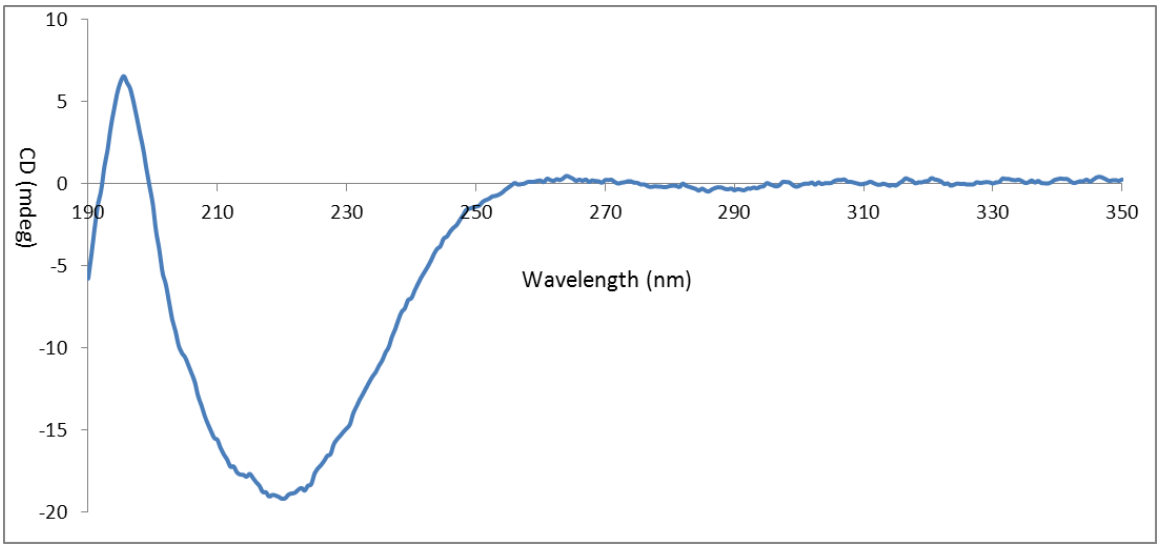


Figure 24. Circular dichroism spectrum of ecumicin. Ecumicin was tested at 10 µM in acetonitrile, 1 cm quartz cuvette, 25°C (background subtracted), on a Jasco J 715 polarimeter.
$[\theta]_{molar}$ = -1.92×10^6 deg·cm^2·mol^{-1} (220 nm)
$[\theta]_{molar}$ = 6.16×10^5 deg·cm^2·mol^{-1} (196 nm)

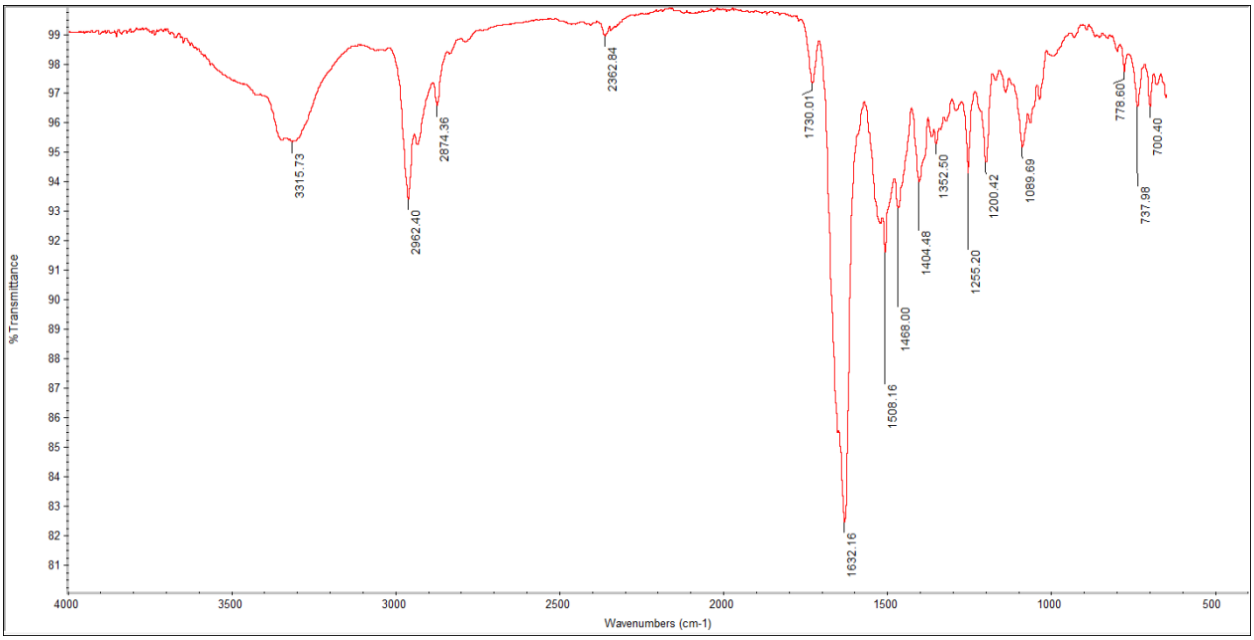
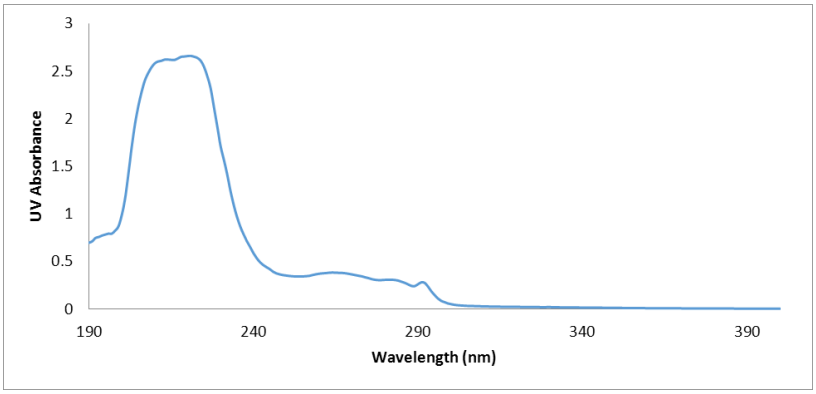


Figure 25. IR Spectrum of ecumicin.



$\varepsilon = 5.42\times10^{4}\ M^{-1}\cdot cm^{-1}$ (211 nm)
$\varepsilon = 5.53\times10^{4}\ M^{-1}\cdot cm^{-1}$ (219 nm)
$\varepsilon = 7.92\times10^{3}\ M^{-1}\cdot cm^{-1}$ (263 nm)
$\varepsilon = 6.47\times10^{3}\ M^{-1}\cdot cm^{-1}$ (281 nm)
$\varepsilon = 5.84\times10^{3}\ M^{-1}\cdot cm^{-1}$ (291 nm)

Figure 26. UV spectrum of ecumicin. Ecumicin was dissolved at 48.0 µM in methanol, 1 cm quart cuvette, 25°C (background subtracted).

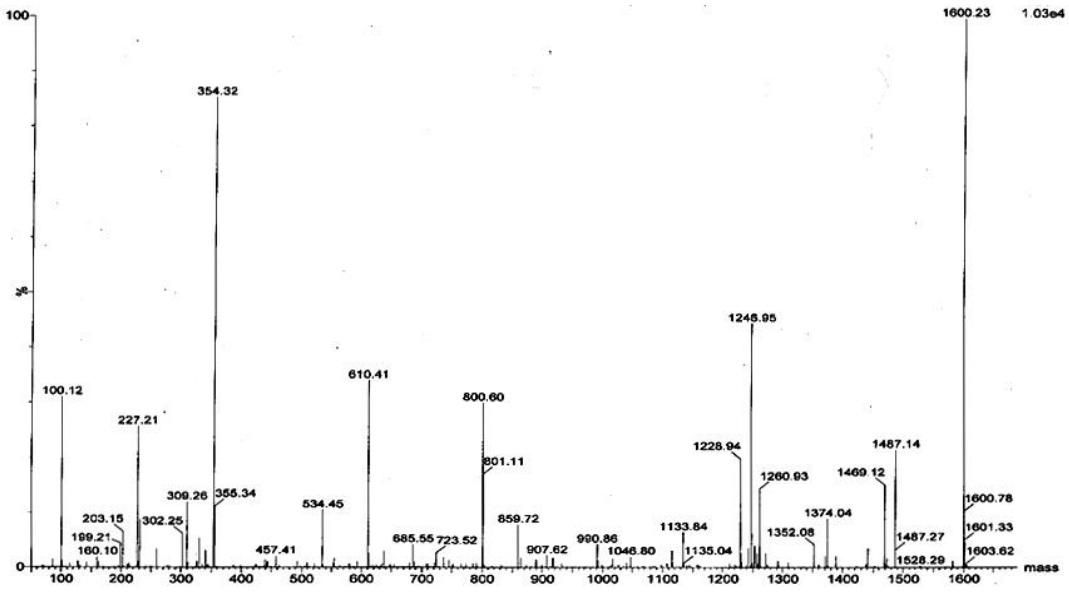


Figure 27. Tandem mass spectrometry of ecumicin.

5.2 Connectivity solved by NMR experiments with the help of tandem mass analysis

Information gathered from a combination of one-dimensional (^{1}H- and ^{13}C-NMR) and two-dimensional NMR experiments (COSY, TOCSY, HSQC, HMBC, semi-selective HMBC) in two different deuterated solvents (methanol-d_3/d_4) at 400MHz, 600MHz and 900MHz, was well as from a tandem mass spectrometry (MS/MS), was assembled to reveal the connectivity of amino acid residues in ecumicin.

The inclusion of methanol-d_3 (CD_3OH) was an attempt to obtain information related to the exchangeable amide protons. Such information would usually be obtained by using an aprotic NMR solvent, e.g. DMSO-d_6. However, although ecumicin dissolves well in DMSO-d_6, the broader ^{1}H signals resulted from this solvent's higher viscosity (compared to methanol-d_3/d_4), and the large number of protons in ecumicin (considering its 1599 amu molecular weight), led to a heavily overlapped spectrum that is hard to analyze (Figure 28). Therefore, we decided to use methanol-d_3/d_4 in our NMR experiments.

Despite the relatively large molecular weight (1599.0111 amu), the 1D-NMR spectra in methanol-d_3/d_4 provided sufficient signal dispersion and, therefore, were rich in structural information. At this stage, we were not able to extract full information from the ^{1}H NMR spectrum. However, as discussed in Chapter 9, with the new NMR structure sequencing method, extraction of information from a new ^{1}H NMR spectrum is possible when an appropriate portal NMR profile is available.

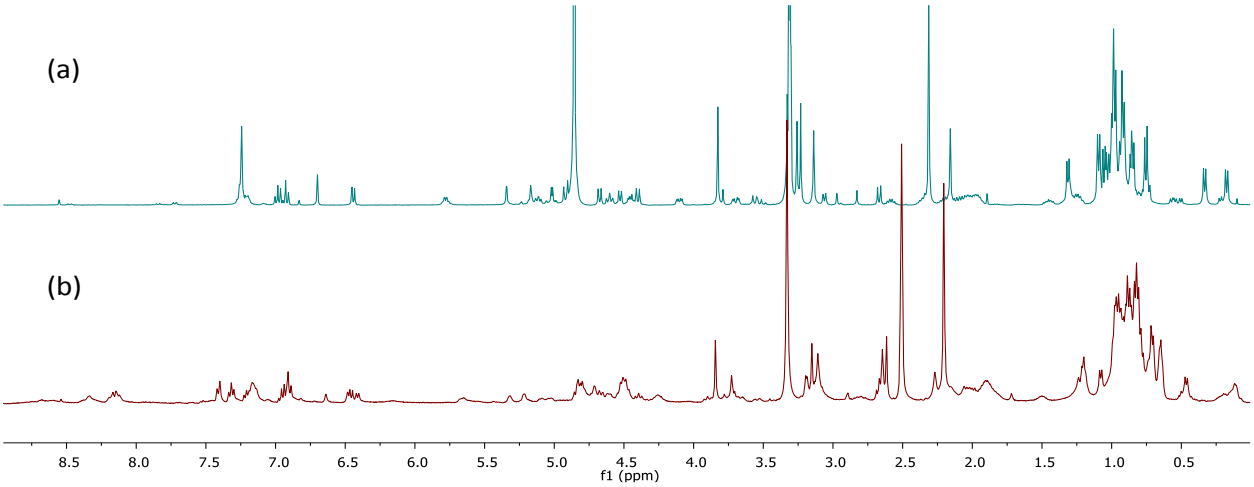


Figure 28. Comparison of ^{1}H NMR spectra (400 MHz) of the same ecumicin sample acquired on a same Bruker DPX-400 instrument in different solvents: (a) methanol-d_4 and (b) DMSO-d_6. The two spectra were processed with identical parameters.

Eight exchangeable proton signals between 9.20 and 7.72 ppm were observed by comparing the ^{1}H NMR spectra in methanol-d_3/d_4 (Figure 23). In addition, signals occurred in the aromatic region, coding for one phenyl group and another aromatic system. In addition, doublets/triplets were found between 0.73 and 1.33 ppm, corresponding to 20 aliphatic methyl groups. Surprisingly, for the case of a peptide, singlets at 2.16, 2.31, 3.14, 3.23, 3.26, 3.33, and 3.82 ppm appeared, indicating 8 *N*-methyl and/or methoxy groups. More details of the ^{1}H NMR spectrum in methanol-d_4 are shown in Figure 30, and summarized in TABLE VIII.

The ^{13}C NMR spectrum (Figure 32, TABLE VIII) revealed a total of 12 (amide-) carbonyl signals in the range between 170.92 and 175.14 ppm, corresponding to 13 carbonyl carbons. By using DEPT-135 (Figure 31) and HSQC experiments (Figure 33), 34 methine, 3 methylene, and 28 methyl signals were identified. These signals, along with 5 quaternary carbon signals at 155.23, 142.68, 140.04, 118.36, and 112.47 ppm indicated a total of 83 carbons present in ecumicin.

The cross peaks in the HSQC spectrum (Figure 33) in general were well dispersed and, therefore, readily assigned. The only exception was the region of methyl signals, where 13 carbon signals integrating for 15 carbons were found in a range of 1.0 ppm (19.1 – 20.1 ppm), and their corresponding proton signals crowded within only 0.4 ppm range (0.73 – 1.13 ppm). Five strongly overlapped signals were observed in this region, making it almost impossible to assign the C-H connections for these methyl groups by HSQC alone. This region was later assigned with the ^{13}C-^{1}H single bond correlations extracted from a semi-selective HMBC experiment (Claridge and Perez-Victoria 2003). Such correlations were observed with a coupling constant around 126 Hz along the F2 dimension (Figure 36, F1 sw = 20 ppm, P02 = 26 ppm). The semi-selective HMBC experiment yields high resolution signals in the indirect ^{13}C dimension by suppressing homonuclear proton coupling modulations, and, therefore, suitable for resolving highly crowded regions of NMR spectrum.

A COSY experiment revealed the presence of 15 discrete ^{1}H,^{1}H spin systems (Figure 34). Combined with information obtained from HMBC experiment (Figure 35), these subsequently indicated the following 13 amino acids: *N,N*-dimethyl-valine (*N,N*-Me_2-V), five valines (V^{1-5}), *N*-methyl-isoleucine (*N*-Me-I), threonine (T), *N*-methyl-threonine (*N*-Me-T), *N*-methyl-leucine (*N*-Me-L), *N*-methyl-valine (*N*-Me-V), *N*-methyl-4-methoxy-tryptopahn (*N*-Me-4-OMe-Y),and phenyl-serine (Ph-S). The connection of *N*-methyl groups were confirmed by using the ^{1}H,^{13}C long-range correlations (^{4}J) between methyl proton signals and α-carbon signals, and/or methyl carbon signals and α-proton signals. The connections of spin systems within the *N*-Me-4-OMe-Y and Ph-S units were also confirmed by a standard HMBC experiment.

As expected for peptides, each amide carbonyl signal correlates with two α-protons from both sides of the amide bond, but only one β-proton from the same side of the amide bond (Figure 29). Therefore it is possible to piece together individual amino acids by following such $^{1}H,^{13}C$ long-range couplings. However, the standard HMBC experiment failed to provide sufficient resolution in the carbonyl region, where twelve signals (integrating for thirteen carbons) were found to crowd within a 4.5 ppm range. A semi-selective HMBC experiment focusing on this region (Figure 37) allowed the pin-point positioning of almost every carbonyl group, and gave a general view about ecumicin's overall 2D structure. In addition to the amide bonds, one ester bond was also observed as the β-proton of T correlates with the carbonyl carbon of V^{5}.

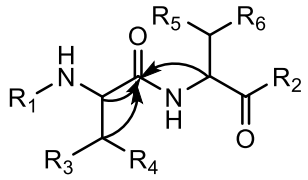


Figure 29. Typical long range $^{1}H,^{13}C$ coupling pattern of peptides, involving amide carbonyl carbon and neighboring α- and β-protons.

Although the carbonyl carbons of *N,N*-Me_2-V and *N*-Me-L resonate at the same frequency (173.29 ppm) and, thus, left two structural possibilities (Figure 38), it was concluded that ecumicin is a cyclic depsipeptide composed of thirteen amino acids, including five valines (V^{1}-V^{5}),

one *N*-methyl-valine (*N*-Me-V), one *N*-methyl-leucine (*N*-Me-L), one *N*-methyl-isoleucine (*N*-Me-I), one *N*-methyl-threonine (*N*-Me-T), one threonine (T), one *N,N*-dimethyl-valine (*N,N*-Me_2-V), one phenyl-serine (Ph-S), and one *N*-methyl-4-methoxy-tryptophan (*N*-Me-4-OMe-Y). This composition suggested a molecular formula of $C_{83}H_{134}N_{14}O_{17}$ and a calculated exact mass of 1599.0051 amu, which was in excellent agreement with results from high-resolution mass spectrometry (1599.0111 amu).

TABLE VIII. ^{1}H (900 MHZ) AND ^{13}C (100 MHZ) NMR DATA OF ECUMICIN IN METHANOL-D_4 (CD_3OD). THE CHEMICAL SHIFTS OF THE AMIDE PROTONS WERE OBSERVED IN METHANOL-D_3 (CD_3OH). INTERPRETATION OF THE ^{1}H NMR SPECTRUM (CD_3OD) WAS PERFORMED BY ^{1}H ITERATIVE FULL SPIN ANALYSIS.

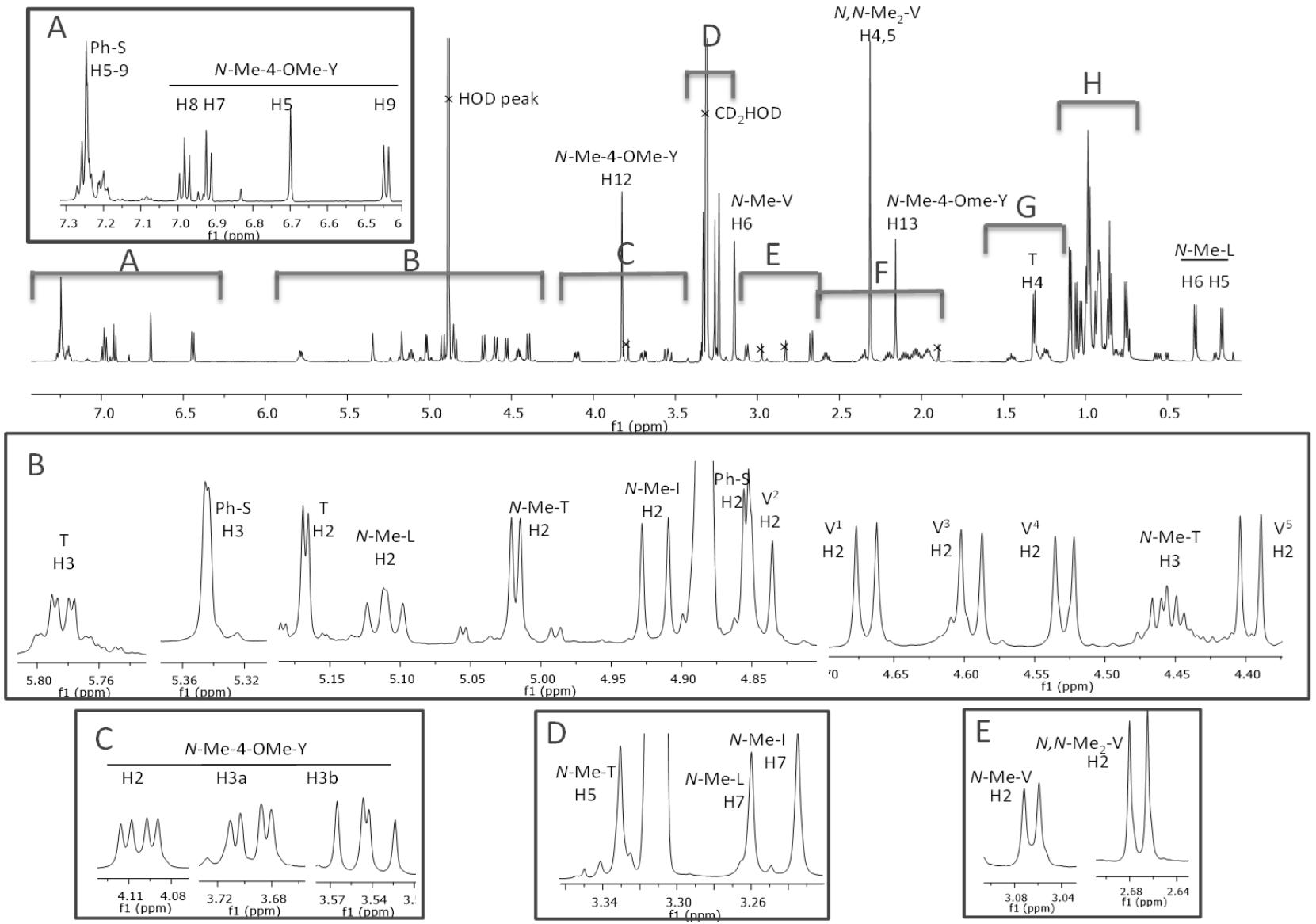
Amino Acid		^{1}H δ in ppm (mult, *J* in Hz)	^{13}C δ in ppm
N,N-Me_2-V	1		173.28
	2	2.671561(d, 9.17)	75.61
	3	2.04238 (dqq, 9.17, 6.62, 6.29)	28.68
	4,5	2.31275 (s)	42.26
	6	0.84714 (d, 6.59)	19.35
	7	0.97824 (d, 6.62)	20.05
l-V^1	1		174.99
	2	4.66906 (d, 8.75)	55.91
	3	2.10140 (dqq, 8.75, 6.78, 6.72)	31.62
	4	0.99220 (d, 6.78)	19.62
	5	1.05540 (d, 6.72)	19.36
	NH	8.17 (d, 8.2)	
N-Me-l-*allo*-I	1		172.6
	2	4.91828 (d, 11.23)	61.76
	3	1.95748 (dddq, 11.23, 0.46, 2.93, 6.63)	34.33
	4	0.98913 (ddq, 0.46, -12.27, 7.29)	26.61
		1.25532 (ddq, 2.93, -12.22, 7.63)	
	5	0.75394 (dd, 7.29, 7.63)	11.5
	6	0.74389 (d, 6.63)	15.1
	7	3.23392 (s)	31.4
l-T	1		171.95
	2	5.16694 (d, 2.34)	53.39
	3	5.78316 (dq, 2.34, 6.51)	69.82
	4	1.31314 (d, 6.51)	16.76
	NH	8.50 (d, 9.1)	
N-Me-l-T	1		171.21
	2	5.01758 (d, 3.73)	63
	3	4.45748 (dq, 3.73, 6.47)	66.93
	4	0.91184 (d, 6.47)	19.91
	5	3.32951 (s)	34.3
l-V^2	1		174.73

Amino Acid		^{1}H δ in ppm (mult, *J* in Hz)	^{13}C δ in ppm
	2	4.84222 (d, 8.92)	56.77
	3	2.35035 (dqq, 8.92, 6.69, 7.03)	31.76
	4	1.09227 (d, 6.69)	19.64
	5	0.97929 (d, 7.03)	19.7
	NH	7.73 (d, 8.6)	
N-Me-l-L	1		173.28
	2	5.11038 (dd, 6.24, 8.38)	55.59
	3	1.23883 (ddd, 8.38, -13.30, 5.79)	39.37
		1.45226 (ddd, 6.24, -13.30, 8.22)	
	4	0.95701 (ddqq, 8.22, 5.79, 6.55, 6.59)	25.64
	5	0.16824 (d, 6.59)	21.67
	6	0.33065 (d, 6.55)	23.47
	7	3.25886 (s)	31.63
l-V[3]	1		173.39
	2	4.59437 (d, 8.87)	55.34
	3	2.02671 (dqq, 8.87, 6.55, 6.78)	32.88
	4	0.91510 (d, 6.55)	19.66
	5	0.85858 (d, 6.78)	19.21
	NH	9.07 (d, 9.5)	
N-Me-l-V	1		170.92
	2	3.06545 (d, 7.63)	71.37
	3	2.58294 (dqq, 7.63, 6.50, 6.78)	29.94
	4	0.9759 (d, 6.78)	19.76
	5	1.09381 (d, 6.50)	22.02
	6	3.13992 (s)	40.37
N-Me-4-OMe-l-Y	1		171.61
	2	4.10202 (dd, 11.16, 4.71)	71.11
	3	3.54489 (dd, 11.16, -13.73)	26.97
		3.69383 (dd, 4.71, -13.73)	
	4		112.47
	5	6.69837 (d, 0.49)	124
	6		140.04
	7	6.91805 (ddd, 0.49, 0.67, 8.18)	106.01
	8	6.98170 (dd, 8.18, 7.80)	123.3
	9	6.44182 (dd, 0.67, 7.80)	99.77

Amino Acid		^{1}H δ in ppm (mult, *J* in Hz)	^{13}C δ in ppm
	10		155.23
	11		118.36
	12	3.825517 (s)	55.59
	13	2.15732 (s)	40.9
	NH	10.22 (d, 2.0)	
l-V[4]	1		174.17
	2	4.52858 (d, 7.91)	59.21
	3	2.20008 (dqq, 7.91, 6.75, 6.81)	33.7
	4	1.02824 (d, 6.75)	19.44
	5	0.98912 (d, 6.81)	19.97
	NH	7.85 (d, 9.6)	
Ph-l-*threo*-S	1		173.76
	2	4.85369 (d, 1.90)	59.78
	3	5.34385 (d, 1.90)	72.97
	4		142.68
	5, 9*	7.23959 (dddd, 1.33, 7.65, 0.78, 1.28)	127.06
	6, 8*	7.25549 (dddd, 7.65, 7.480, 1.70, 0.78)	129.28
	7*	7.20063 (dd, 1.27, 7.65)	128.25
	NH	8.30 (d, 7.8)	
l-V[5]	1		175.13
	2	4.39608 (d, 8.89)	59.26
	3	1.96782 (dqq, 8.89, 6.84, 6.41)	33.19
	4	0.91936 (d, 6.42)	19.1
	5	0.93496 (d, 6.84)	19.44
	NH	9.02 (d, 9.9)	

* Signals observed from an AA'BB'C spin system.

Figure 30. ^{1}H NMR Spectrum of ecumicin in CD_3OD (600MHz, Bruker Avance 600) with expansions and assignments.



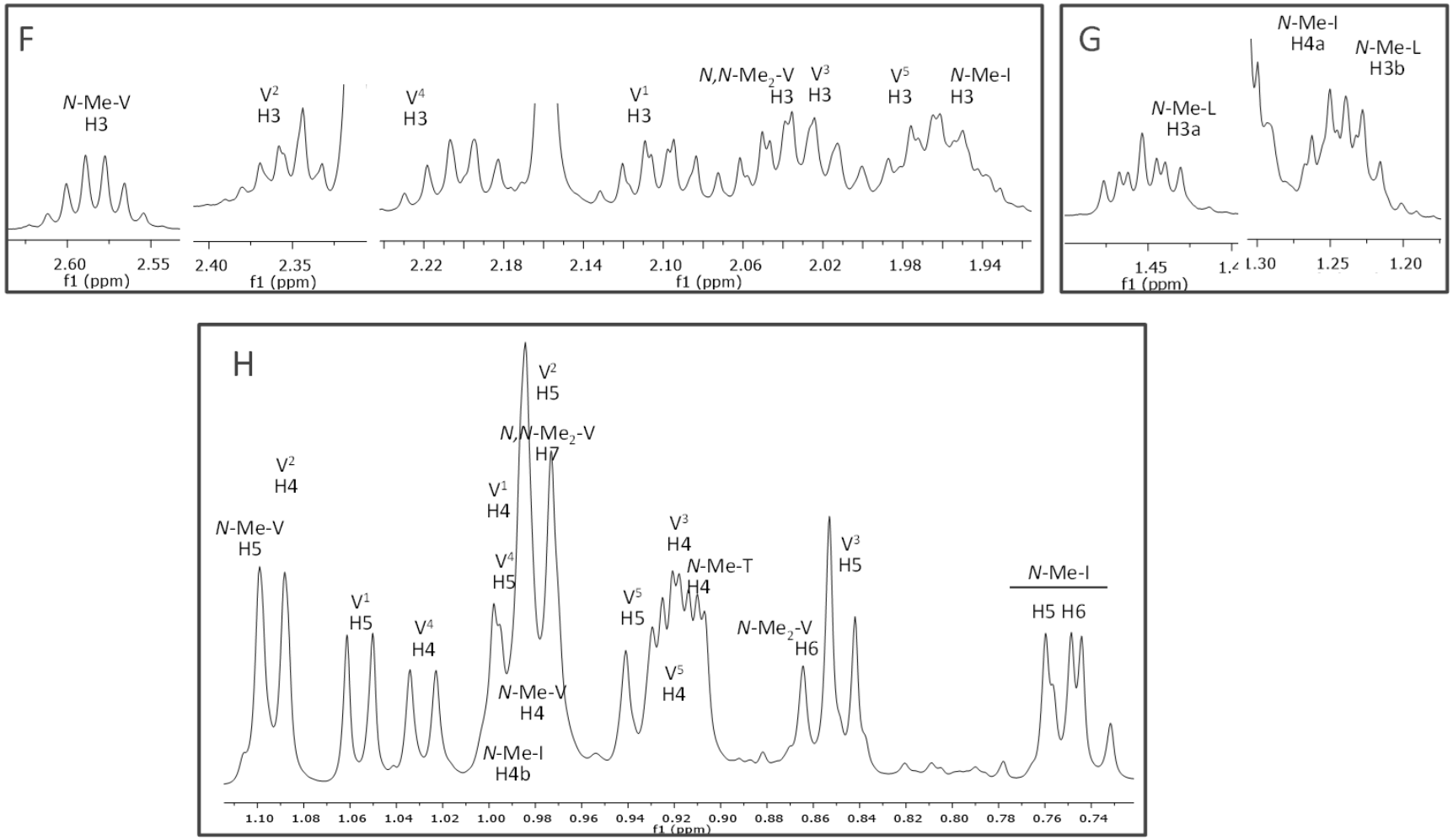

F
N-Me-V H3
V2 H3
V4 H3
V1 H3
N,N-Me2-V H3
V3 H3
V5 H3
N-Me-I H3
2.60 2.55 f1 (ppm)
2.40 2.35 f1 (ppm)
2.22 2.18 2.14 2.10 2.06 2.02 1.98 1.94 f1 (ppm)
G
N-Me-L H3a
N-Me-I H4a
N-Me-L H3b
1.45 f1 (ppm)
1.30 1.25 1.20
H
V2 H5
N,N-Me2-V H7
V2 H4
V1 H4
N-Me-V H5
V3 H4
N-Me-T H4
V3 H5
V4 H5
V1 H5
V4 H4
V5 H5
N-Me2-V H6
N-Me-I H5 H6
V5 H4
N-Me-V H4
N-Me-I H4b
1.10 1.08 1.06 1.04 1.02 1.00 0.98 0.96 0.94 0.92 0.90 0.88 0.86 0.84 0.82 0.80 0.78 0.76 0.74 f1 (ppm)

Figure 31. DEPT135 spectrum (top) compared with ^{1}H,^{13}C-decoupled ^{13}C spectrum (bottom), (100 MHz, Bruker DPX-400).

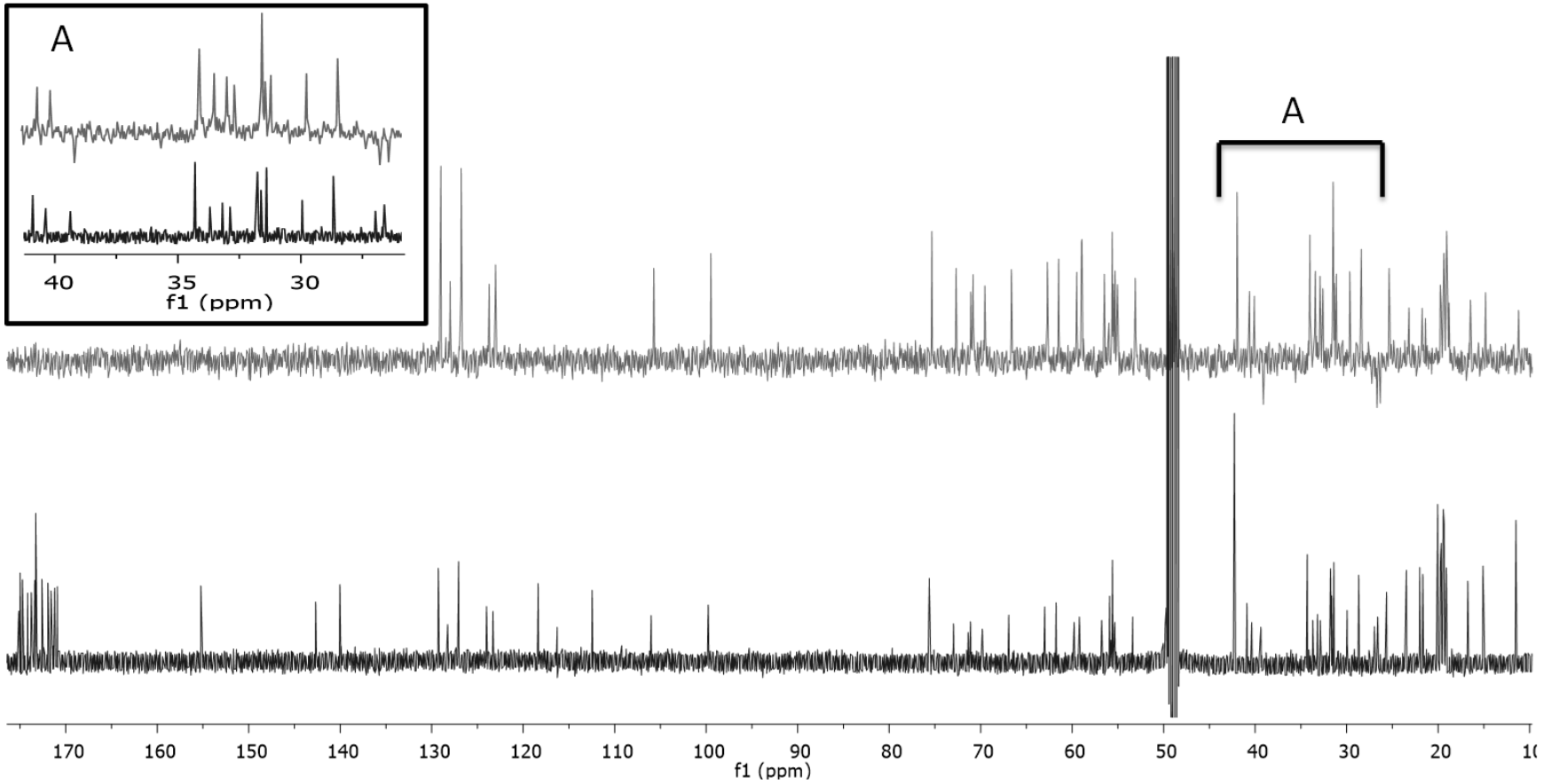
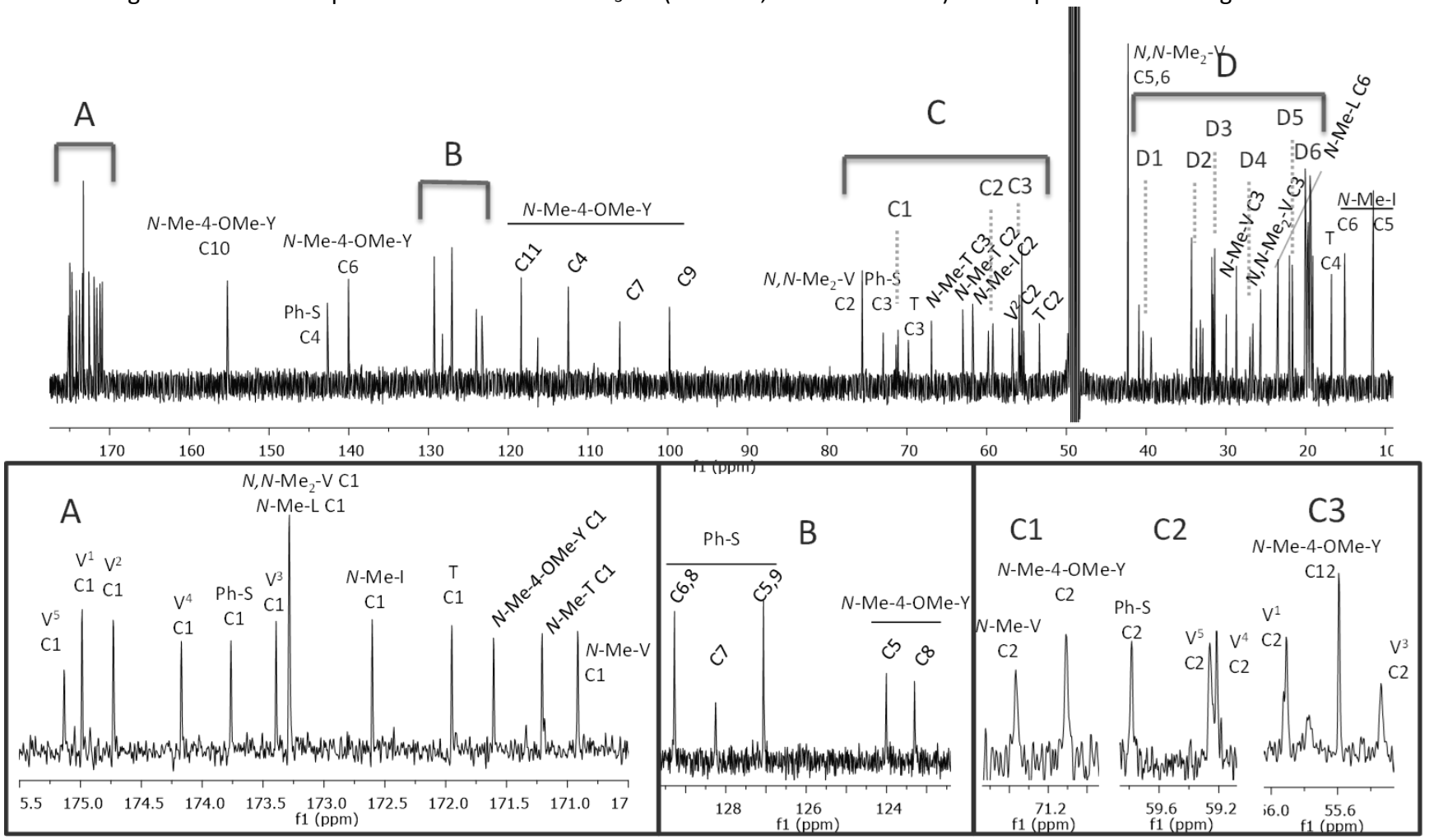


Figure 32. ^{13}C NMR Spectrum of ecumicin in CD_3OH (100MHz, Bruker DPX-400) with expansions and assignments.



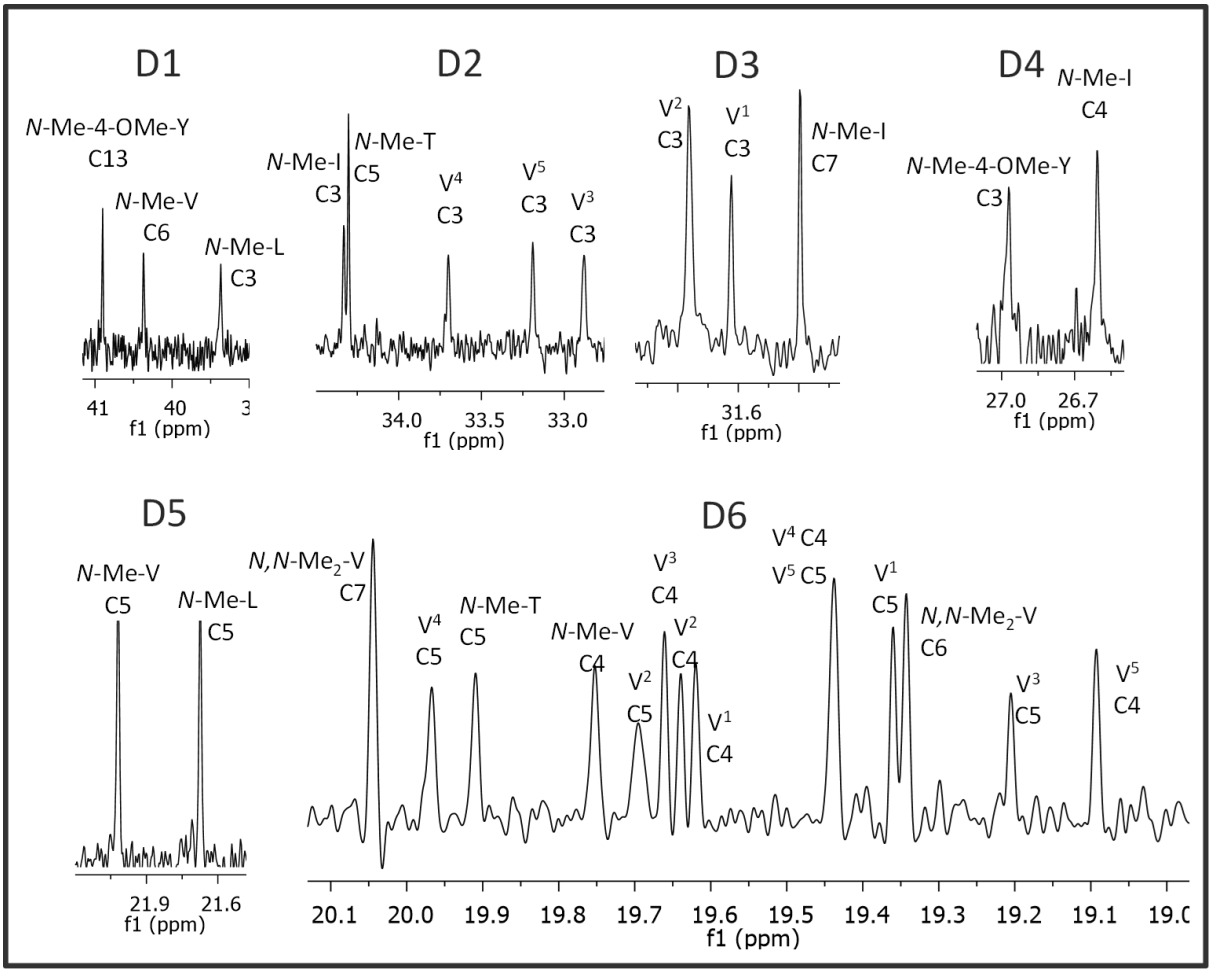
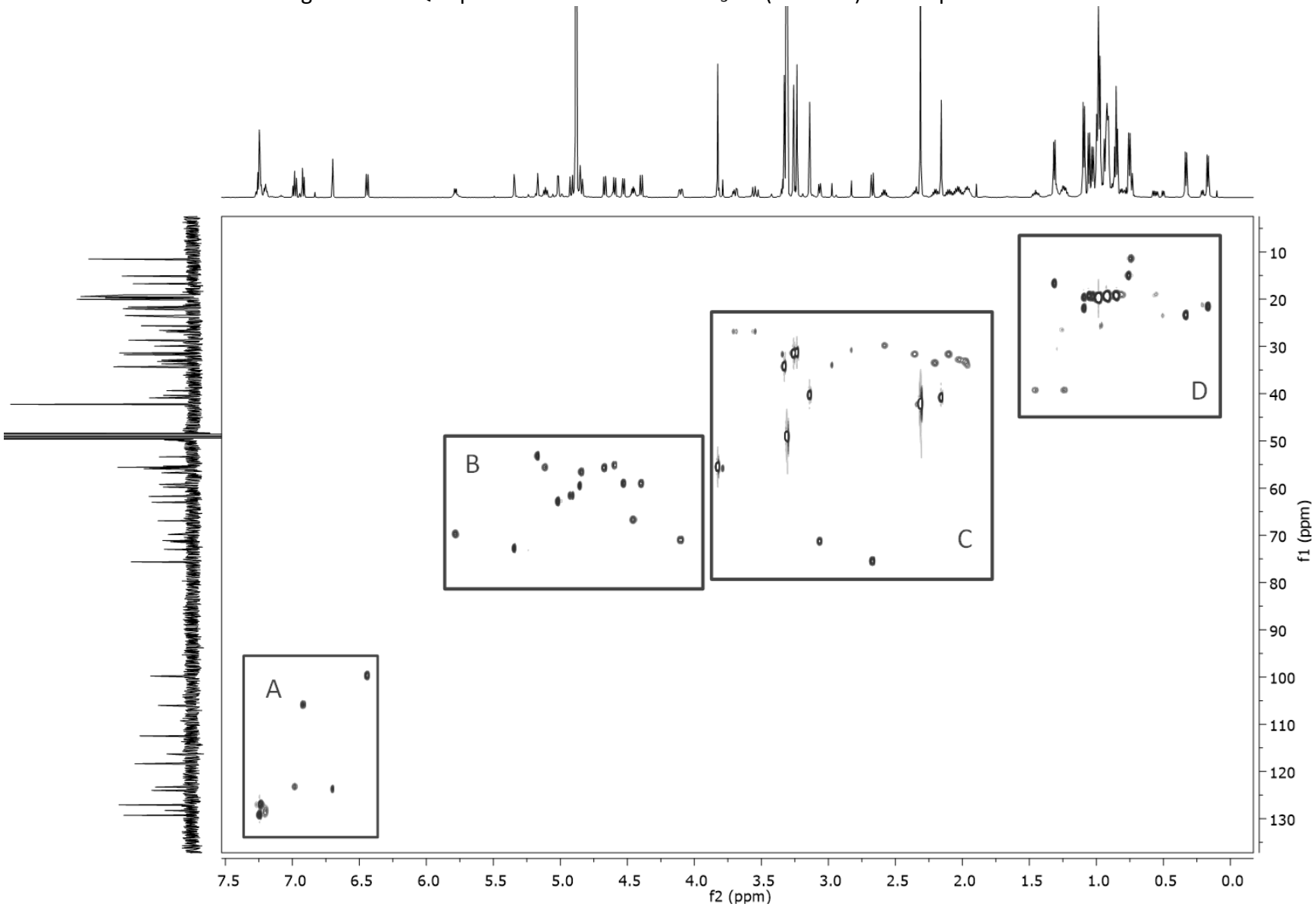

D1
N-Me-4-OMe-Y C13
N-Me-V C6
N-Me-L C3
41
40
f1 (ppm)
D2
N-Me-I C3
N-Me-T C5
V4 C3
V5 C3
V3 C3
34.0
33.5
33.0
f1 (ppm)
D3
V2 C3
V1 C3
N-Me-I C7
31.6
f1 (ppm)
D4
N-Me-I C4
N-Me-4-OMe-Y C3
27.0
26.7
f1 (ppm)
D5
N-Me-V C5
N-Me-L C5
21.9
21.6
f1 (ppm)
D6
N,N-Me2-V C7
V4 C5
N-Me-T C5
N-Me-V C4
V3 C4
V2 C4
V2 C5
V1 C4
V4 C4
V5 C5
V1 C5
N,N-Me2-V C6
V3 C5
V5 C4
20.1
20.0
19.9
19.8
19.7
19.6
19.5
19.4
19.3
19.2
19.1
f1 (ppm)

Figure 33. HSQC Spectrum of ecumicin in CD_3OD (600MHz) with expansions.



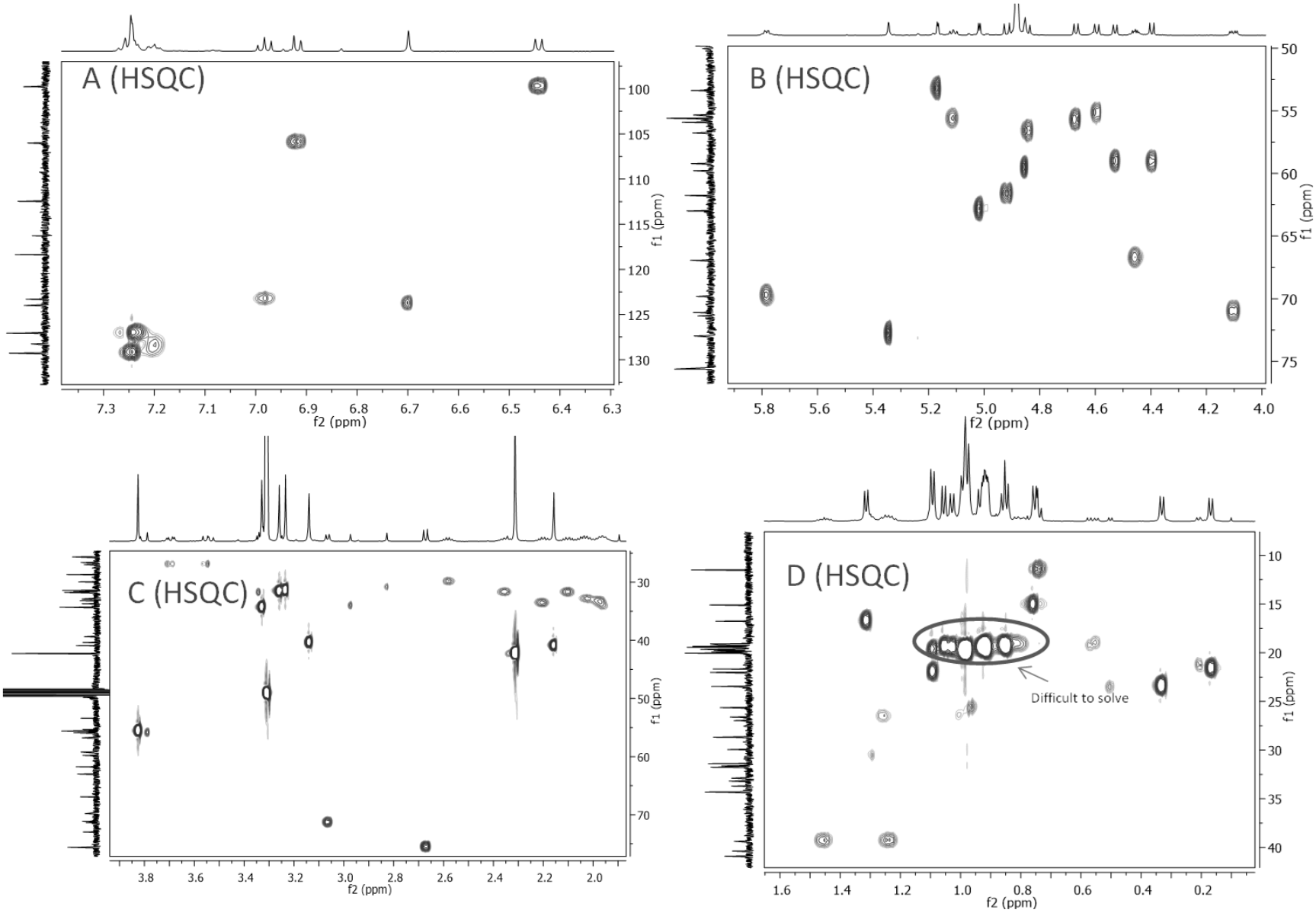
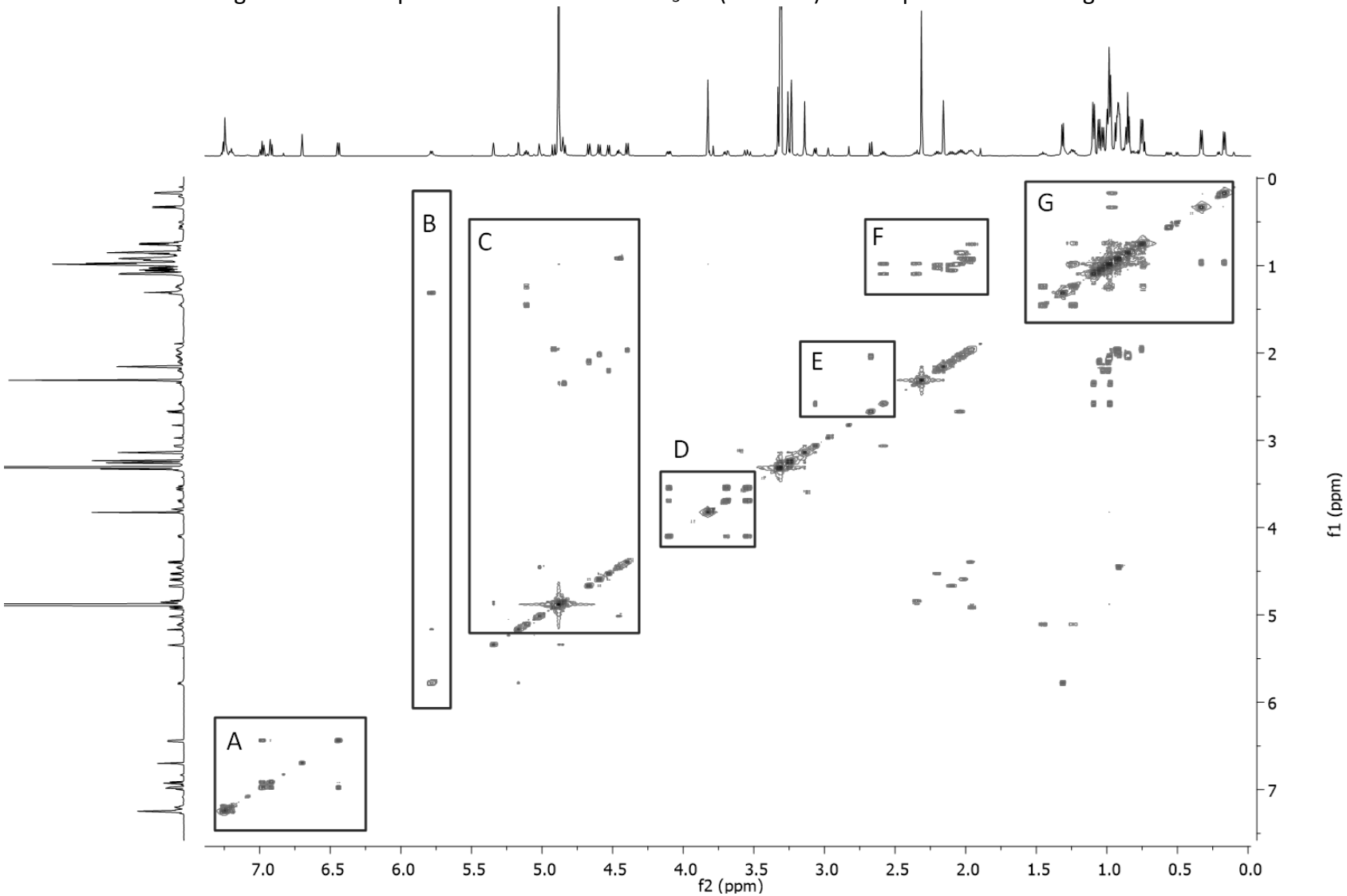
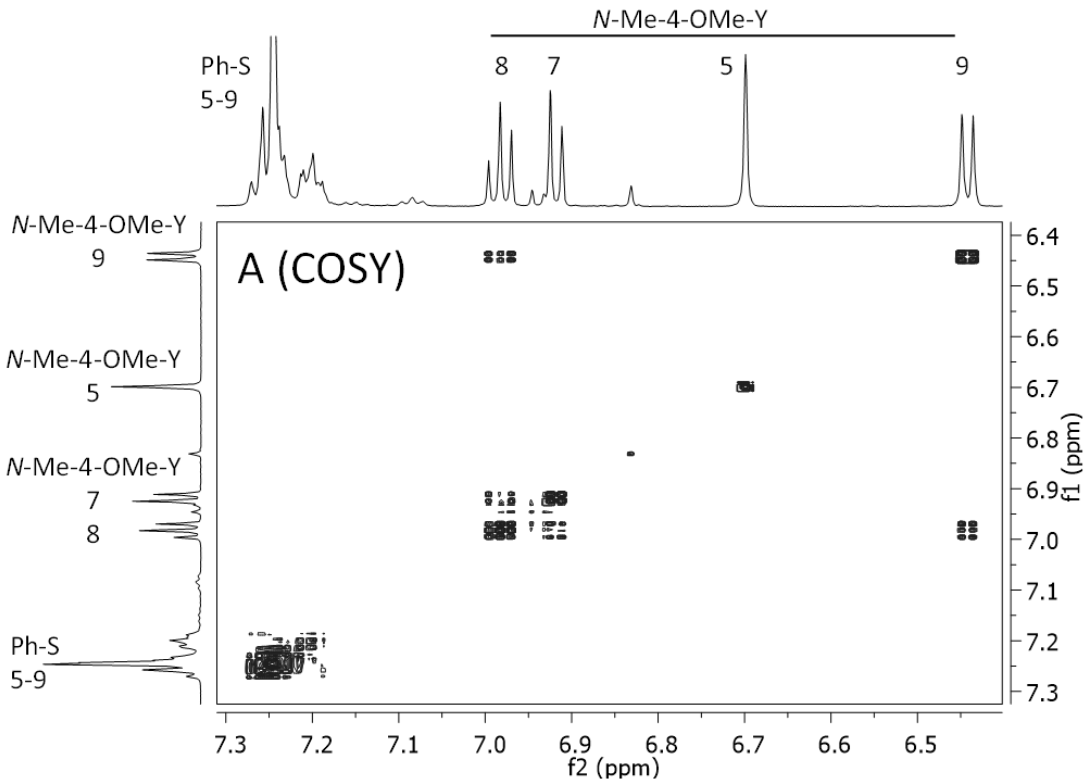
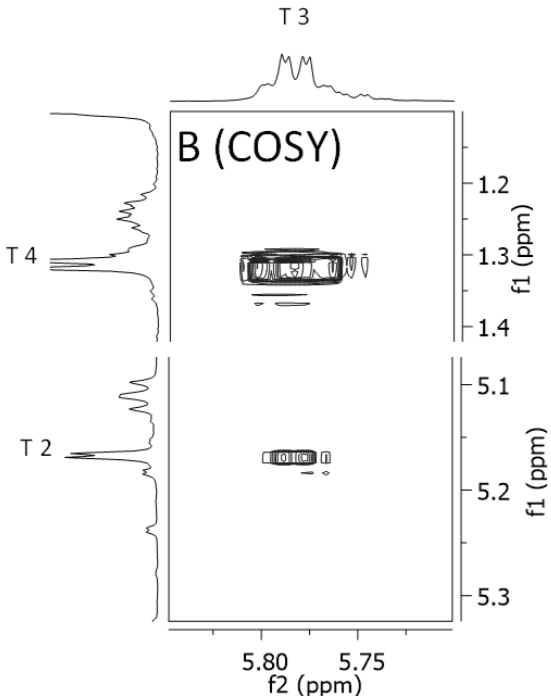
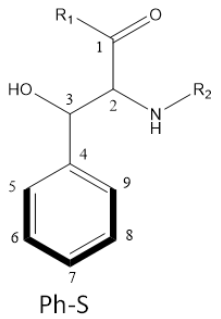

A (HSQC)
B (HSQC)
C (HSQC)
D (HSQC)
Difficult to solve
f1 (ppm)
f2 (ppm)

Figure 34. COSY Spectrum of ecumicin in CD_3OD (600MHz) with expansions and assignment.

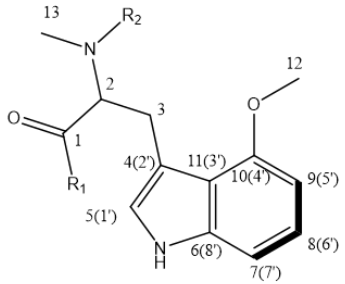




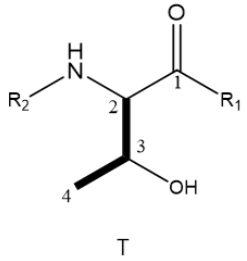




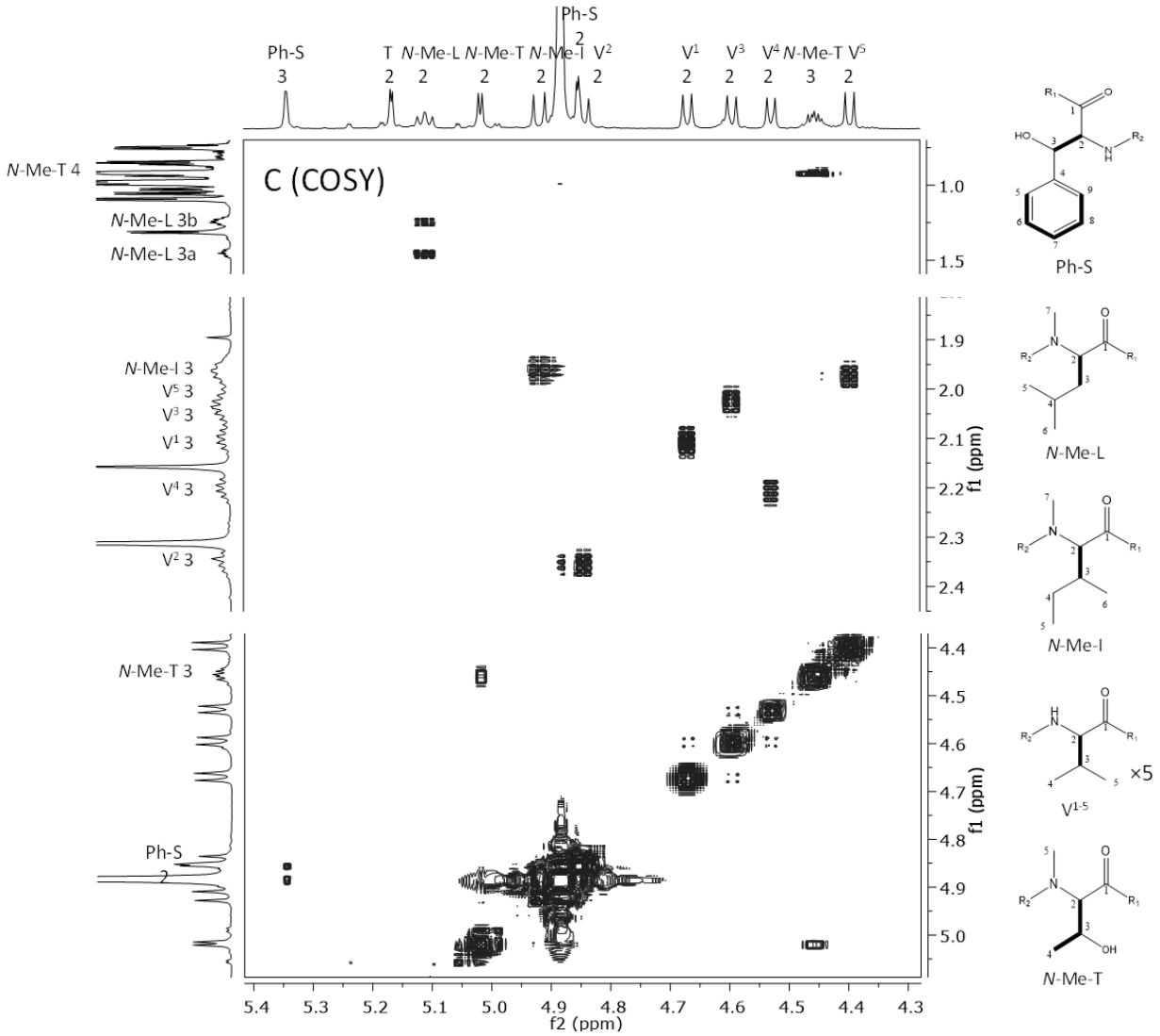
Ph-S

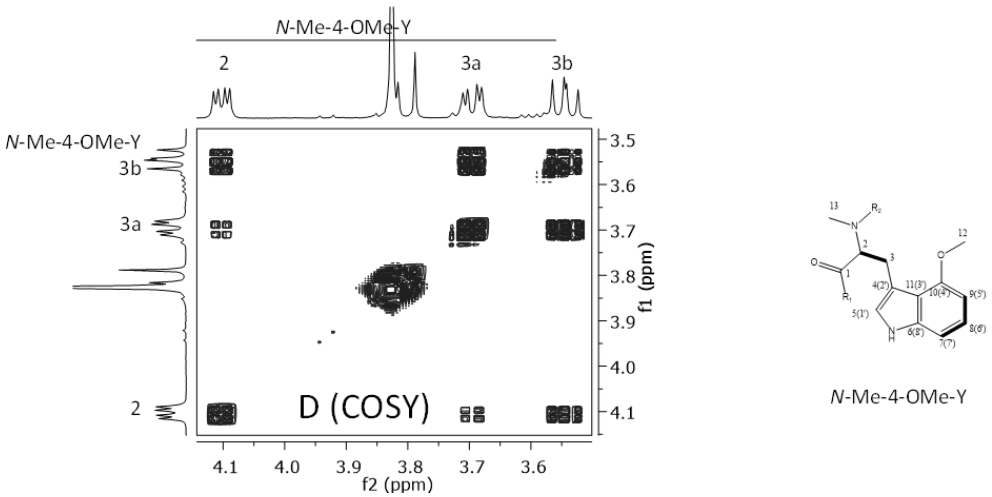


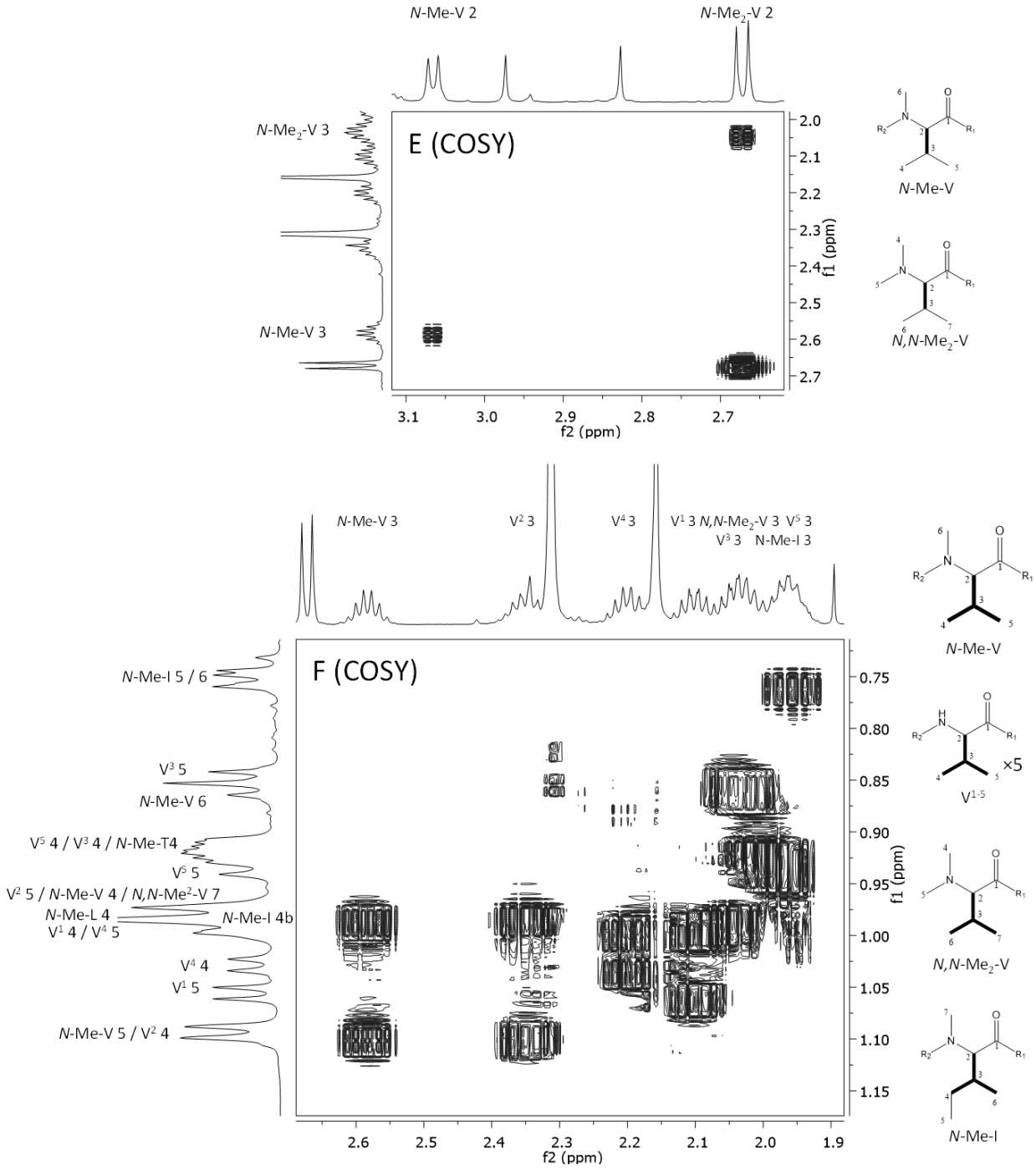
N-Me-4-OMe-Y



T


Ph-S
T
N-Me-L
N-Me-T
N-Me-I
V2
V1
V3
V4
N-Me-T
V5
C (COSY)
N-Me-T 4
N-Me-L 3b
N-Me-L 3a
N-Me-I 3
V5 3
V3 3
V1 3
V4 3
V2 3
N-Me-T 3
Ph-S
f1 (ppm)
f2 (ppm)
Ph-S
N-Me-L
N-Me-I
V1-5
×5
N-Me-T


N-Me-4-OMe-Y
2
3a
3b
N-Me-4-OMe-Y
3b
3a
2
D (COSY)
f1 (ppm)
f2 (ppm)
N-Me-4-OMe-Y


N-Me-V 2
N-Me2-V 2
N-Me2-V 3
E (COSY)
N-Me-V 3
f1 (ppm)
f2 (ppm)
N-Me-V
N,N-Me2-V
N-Me-V 3
V2 3
V4 3
V1 3 N,N-Me2-V 3 V5 3
V3 3 N-Me-I 3
F (COSY)
N-Me-I 5 / 6
V3 5
N-Me-V 6
V5 4 / V3 4 / N-Me-T4
V5 5
V2 5 / N-Me-V 4 / N,N-Me2-V 7
N-Me-L 4
V1 4 / V4 5
N-Me-I 4b
V4 4
V1 5
N-Me-V 5 / V2 4
×5
V1-5
N-Me-I

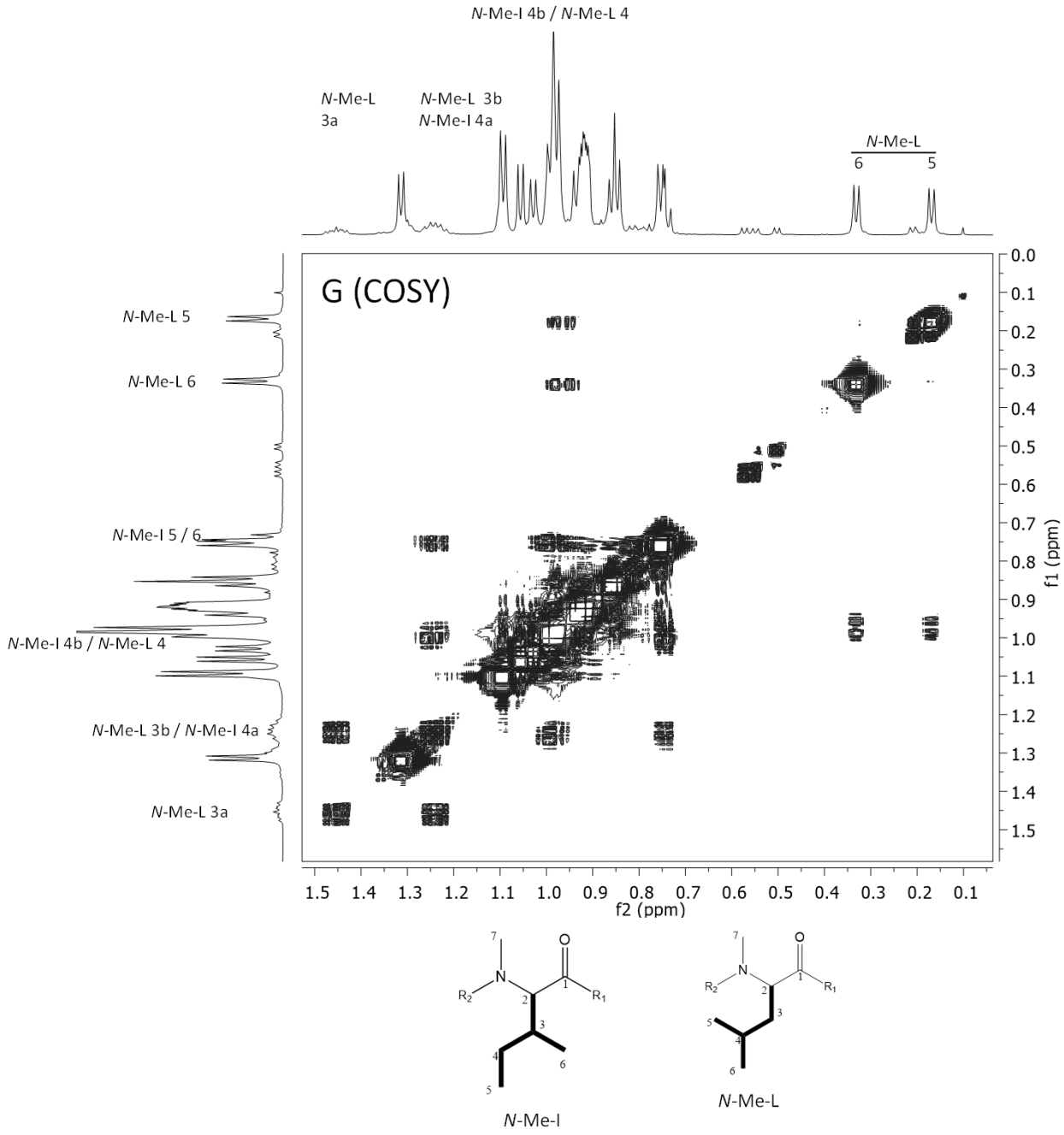
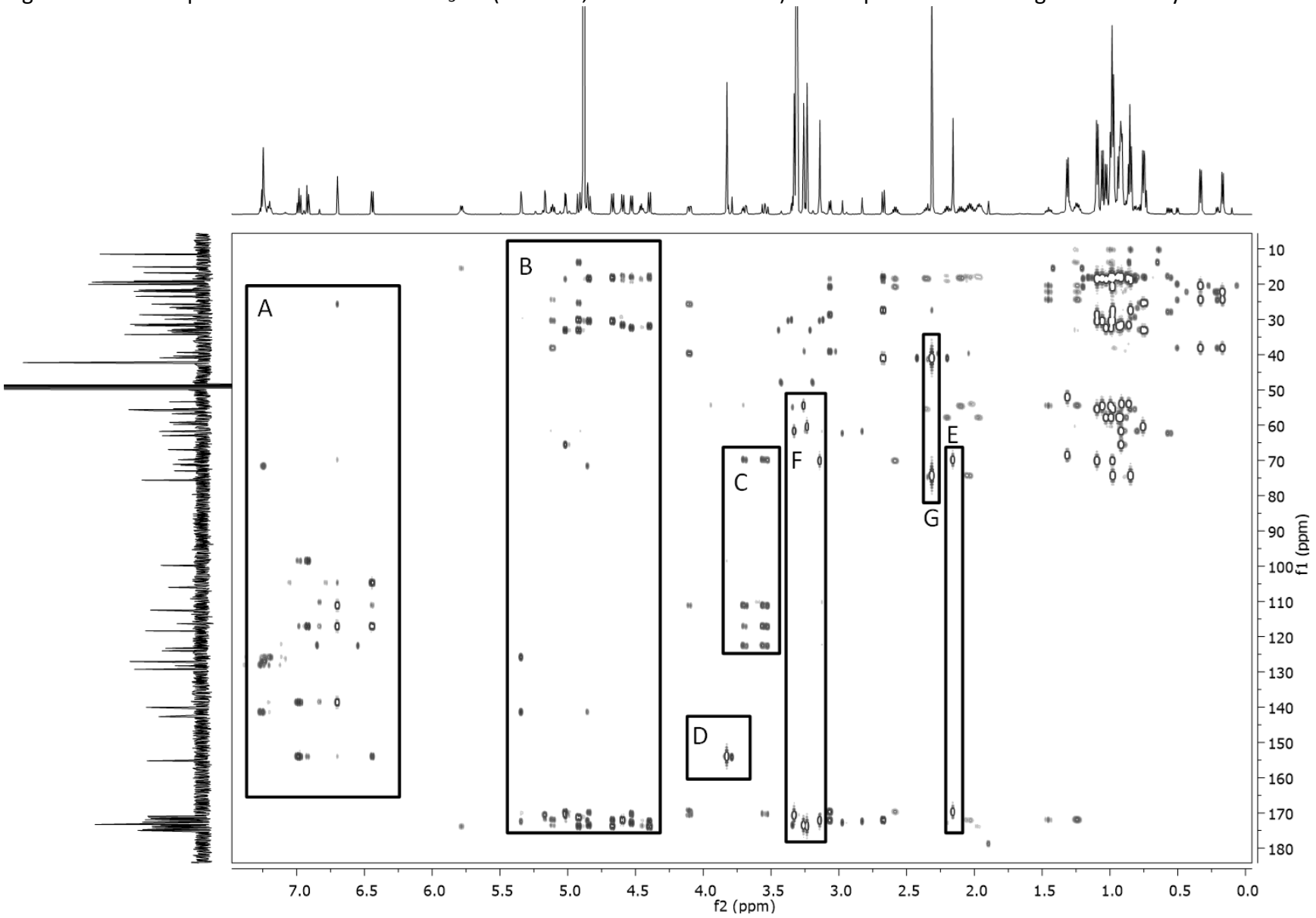
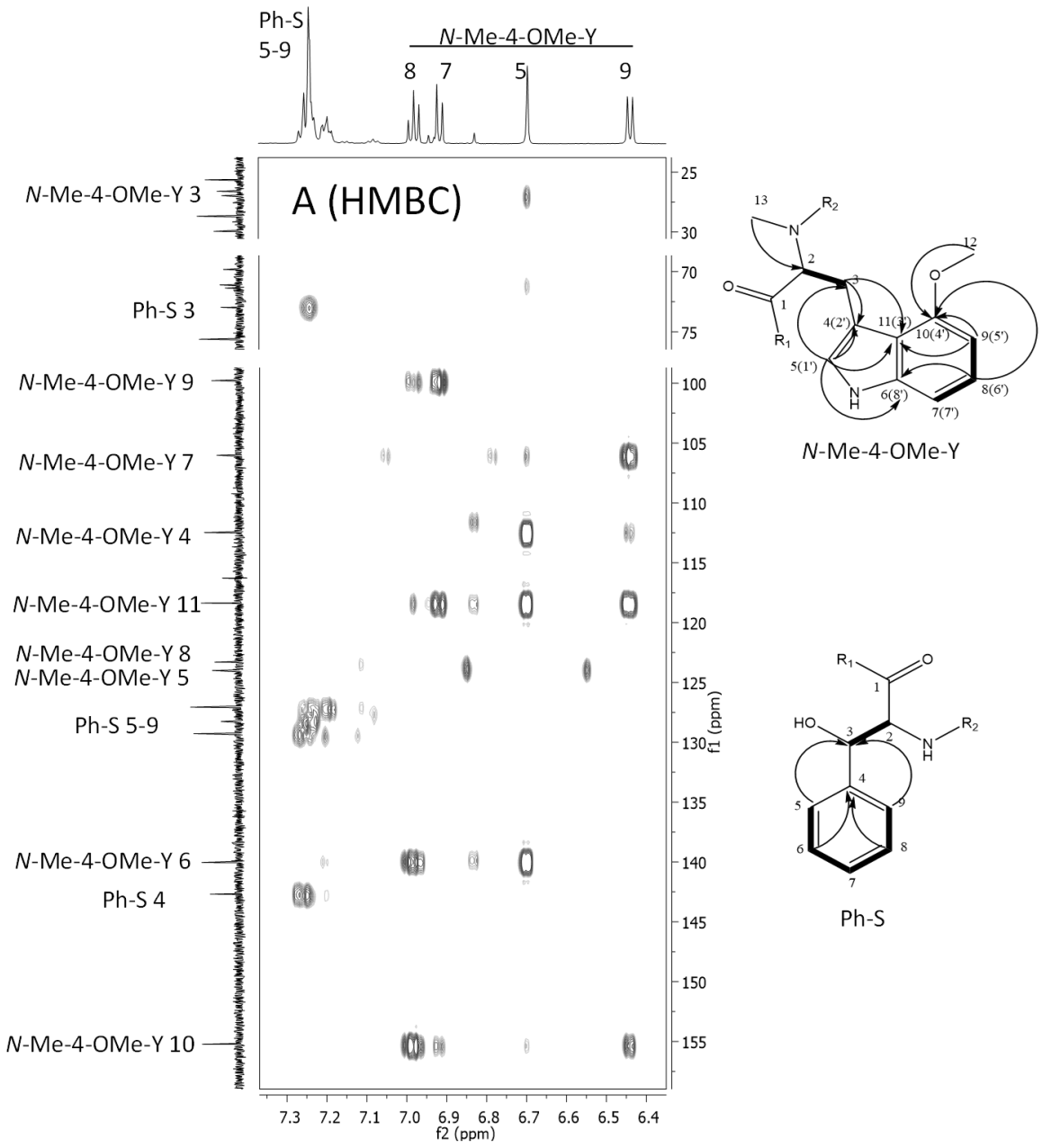
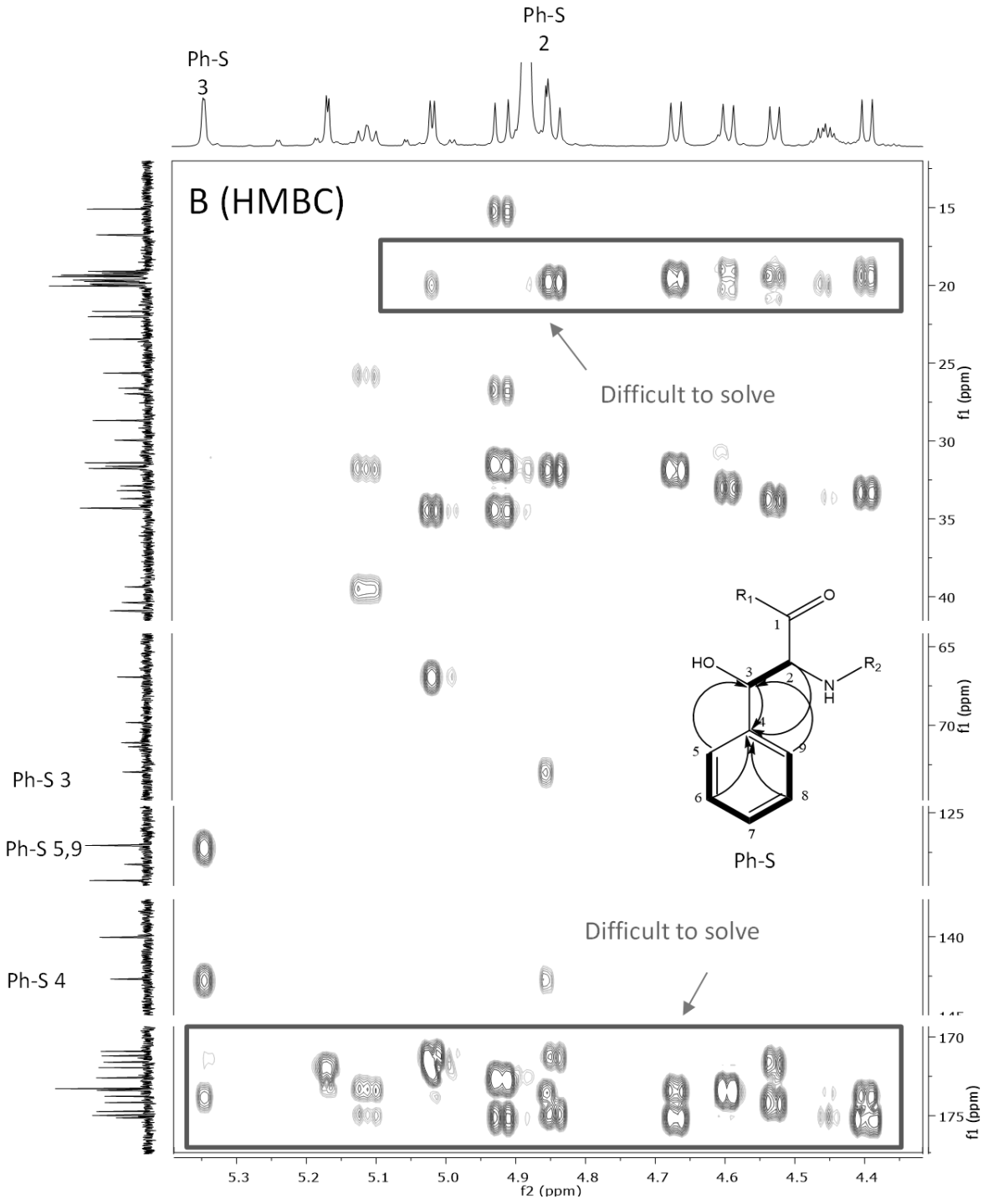
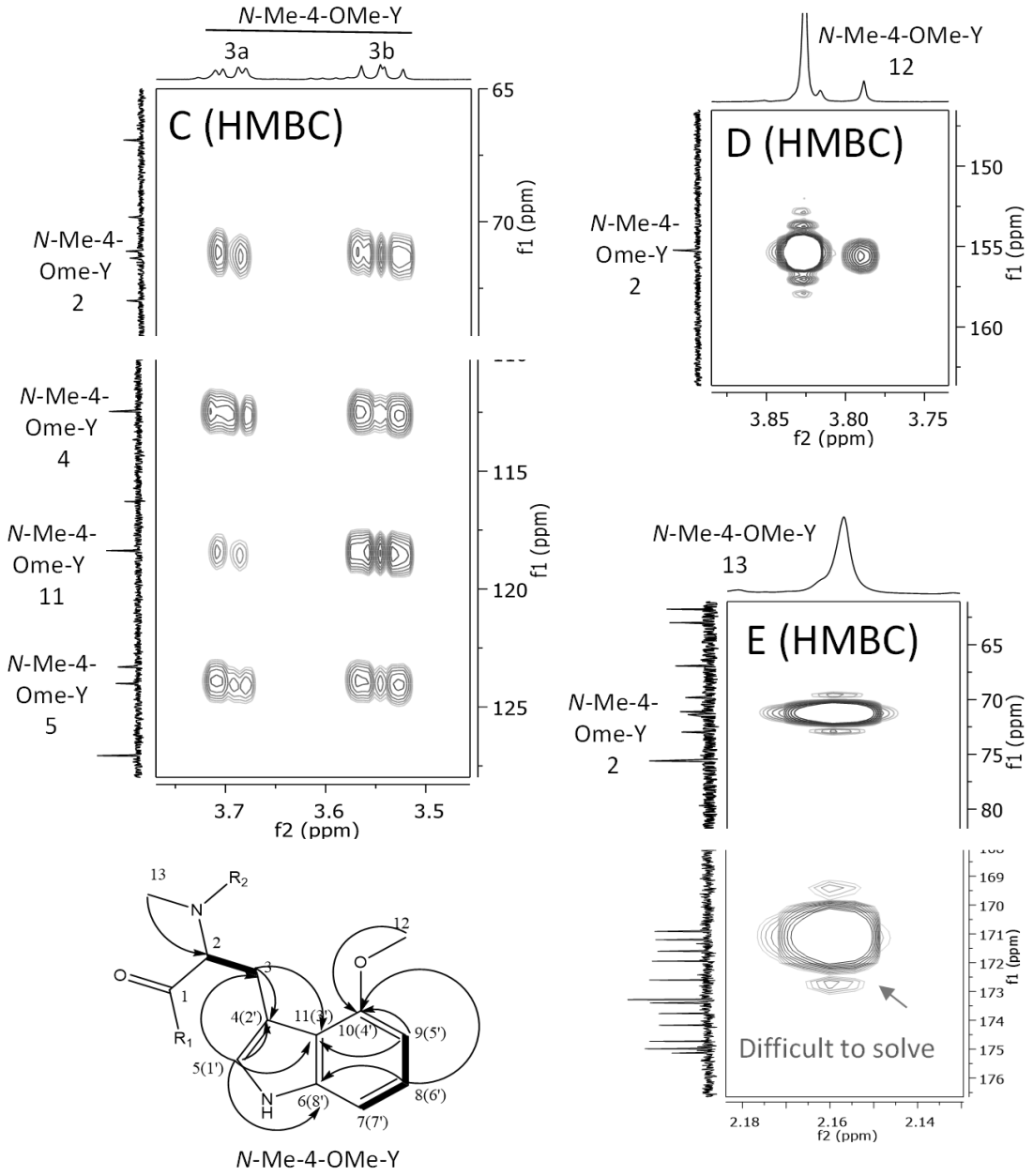

N-Me-I 4b / N-Me-L 4
N-Me-L 3a
N-Me-L 3b
N-Me-I 4a
N-Me-L 6 5
G (COSY)
N-Me-L 5
N-Me-L 6
N-Me-I 5 / 6
N-Me-I 4b / N-Me-L 4
N-Me-L 3b / N-Me-I 4a
N-Me-L 3a
f1 (ppm)
f2 (ppm)
N-Me-I
N-Me-L

Figure 35. HMBC Spectrum of ecumicin in CD_3OD (600MHz, Bruker Avance 600) with expansions and assignment on key correlations.




Ph-S
5-9
N-Me-4-OMe-Y
8 7 5 9
A (HMBC)
N-Me-4-OMe-Y 3
Ph-S 3
N-Me-4-OMe-Y 9
N-Me-4-OMe-Y 7
N-Me-4-OMe-Y 4
N-Me-4-OMe-Y 11
N-Me-4-OMe-Y 8
N-Me-4-OMe-Y 5
Ph-S 5-9
N-Me-4-OMe-Y 6
Ph-S 4
N-Me-4-OMe-Y 10
f1 (ppm)
f2 (ppm)
N-Me-4-OMe-Y
Ph-S


Ph-S
2
Ph-S
3
B (HMBC)
Difficult to solve
Ph-S 3
Ph-S 5,9
Ph-S 4
Difficult to solve
Ph-S
f1 (ppm)
f2 (ppm)


N-Me-4-OMe-Y
3a
3b
C (HMBC)
N-Me-4-Ome-Y 2
N-Me-4-Ome-Y 4
N-Me-4-Ome-Y 11
N-Me-4-Ome-Y 5
f1 (ppm)
f2 (ppm)
3.7
3.6
3.5
65
70
115
120
125
N-Me-4-OMe-Y
12
D (HMBC)
N-Me-4-Ome-Y 2
150
155
160
3.85
3.80
3.75
N-Me-4-OMe-Y
13
E (HMBC)
N-Me-4-Ome-Y 2
65
70
75
80
169
170
171
172
173
174
175
176
Difficult to solve
2.18
2.16
2.14
13
R2
N
2
3
O
1
R1
12
O
4(2')
11(3')
10(4')
9(5')
5(1')
N
H
6(8')
7(7')
8(6')
N-Me-4-OMe-Y

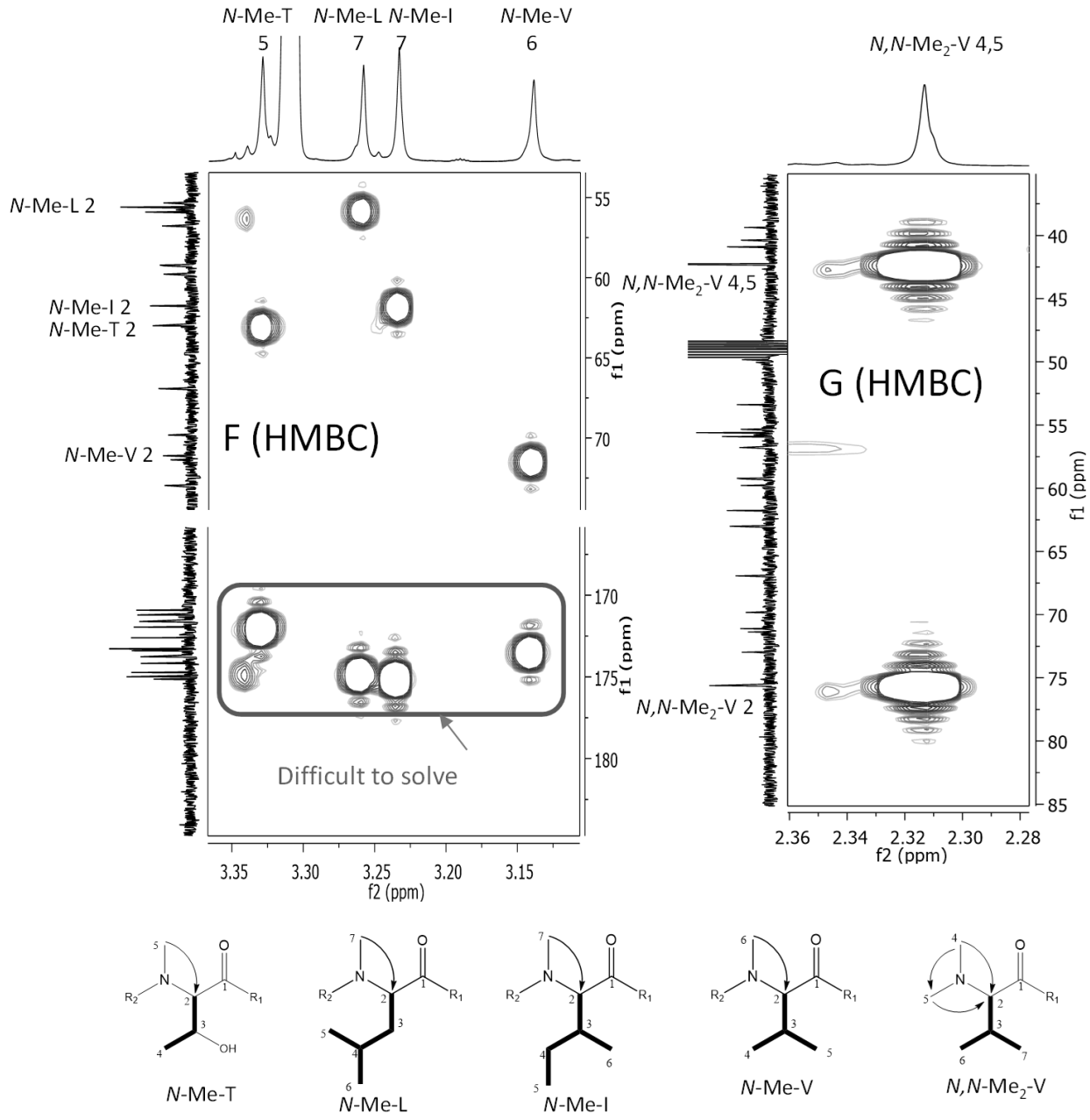
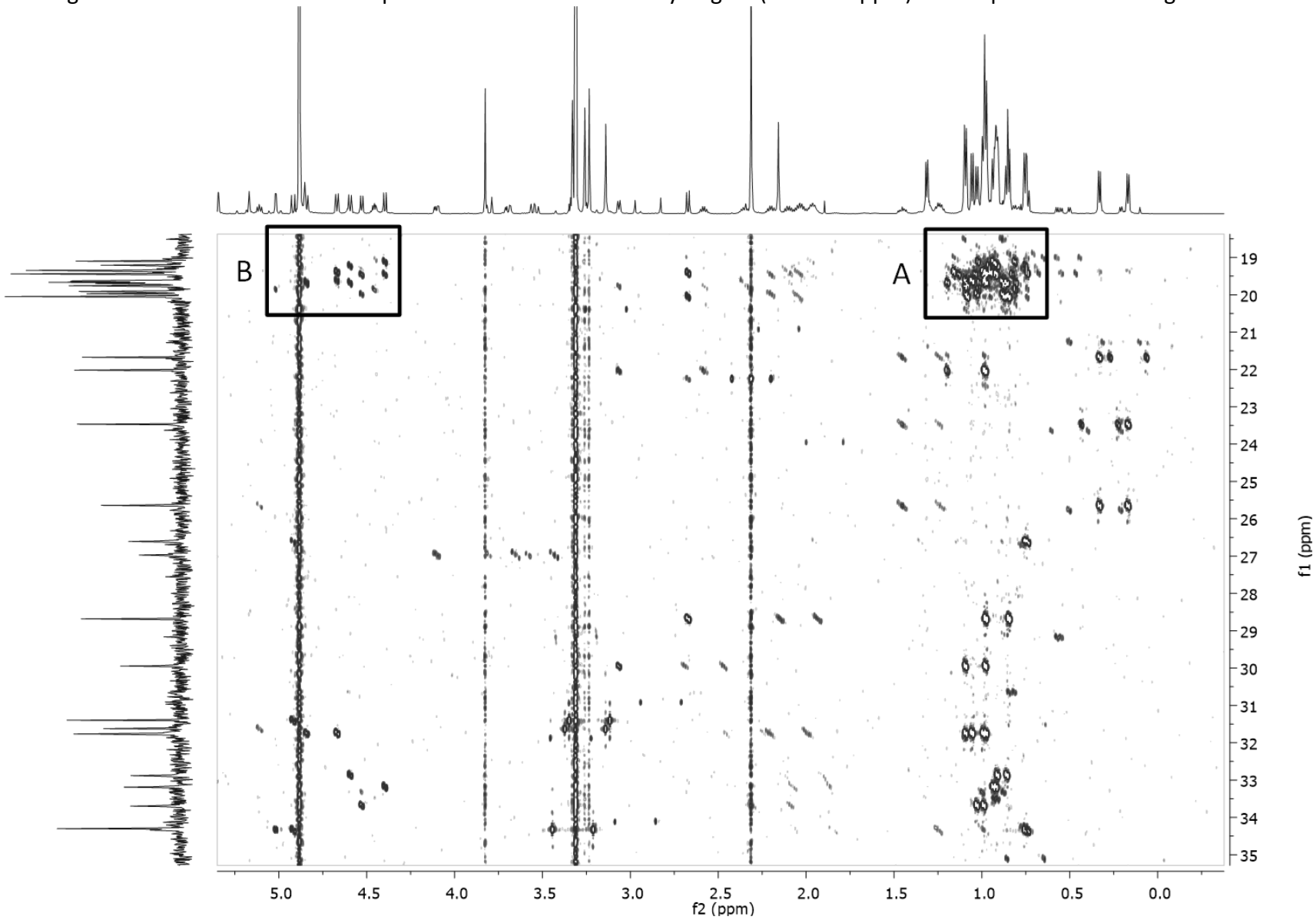
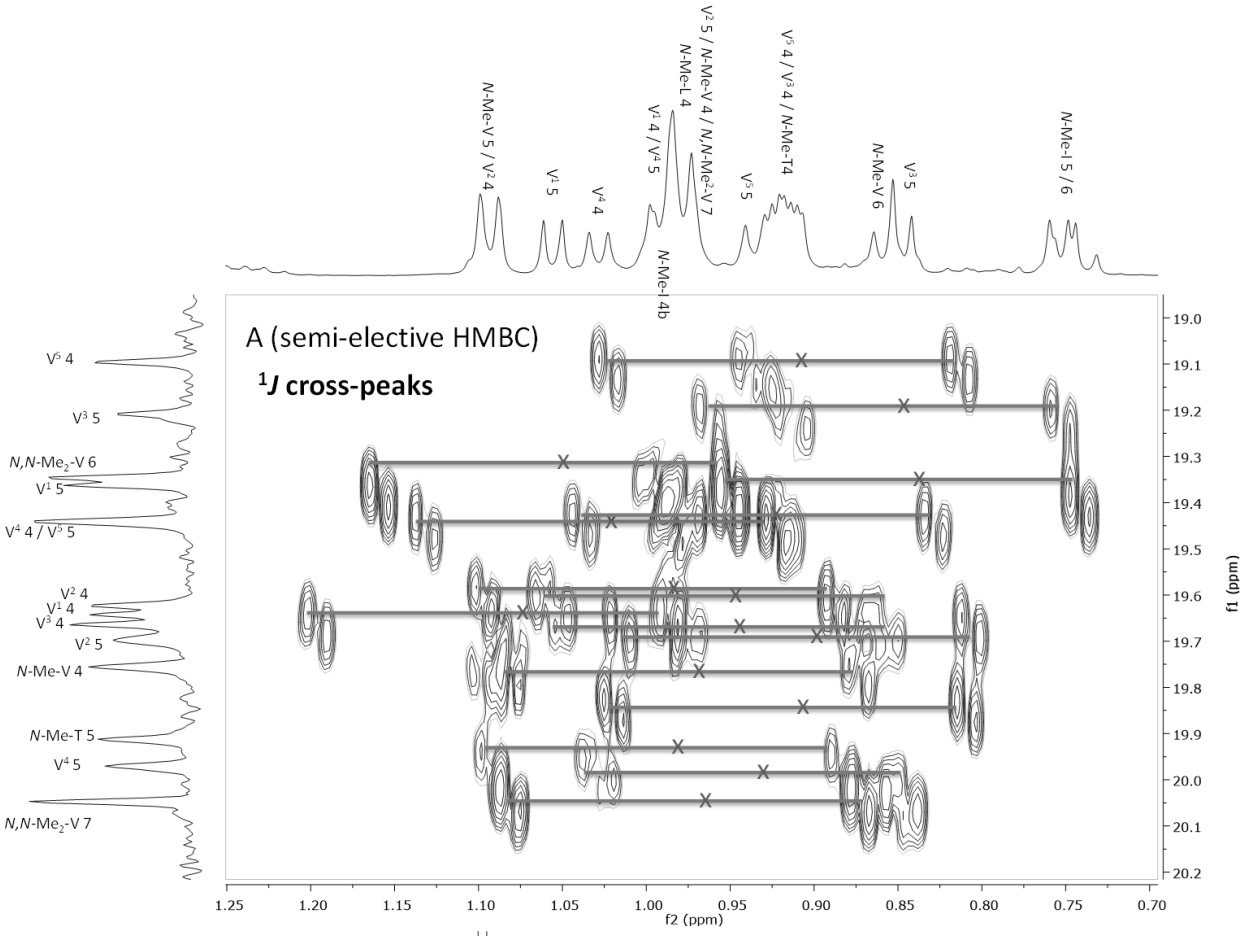

N-Me-T
N-Me-L
N-Me-I
N-Me-V
5
7
7
6
N-Me-L 2
N-Me-I 2
N-Me-T 2
N-Me-V 2
F (HMBC)
Difficult to solve
f1 (ppm)
f2 (ppm)
3.35
3.30
3.25
3.20
3.15
N,N-Me2-V 4,5
N,N-Me2-V 2
G (HMBC)
2.36
2.34
2.32
2.30
2.28
N-Me-T
N-Me-L
N-Me-I
N-Me-V
N,N-Me2-V

Figure 36. Semi-selective HMBC spectrum on ecumicin's methyl region (F1 16-36 ppm) with expansions and assignment.




A (semi-elective HMBC)
1J cross-peaks
N-Me-V 5 / V2 4
V1 5
V4 4
V1 4 / V4 5
N-Me-L 4
N-Me-I 4b
V2 5 / N-Me-V 4 / N,N-Me2-V 7
V5 5
V5 4 / V3 4 / N-Me-T4
N-Me-V 6
V3 5
N-Me-I 5 / 6
V5 4
V3 5
N,N-Me2-V 6
V1 5
V4 4 / V5 5
V2 4
V1 4
V3 4
V2 5
N-Me-V 4
N-Me-T 5
V4 5
N,N-Me2-V 7
f2 (ppm)
f1 (ppm)

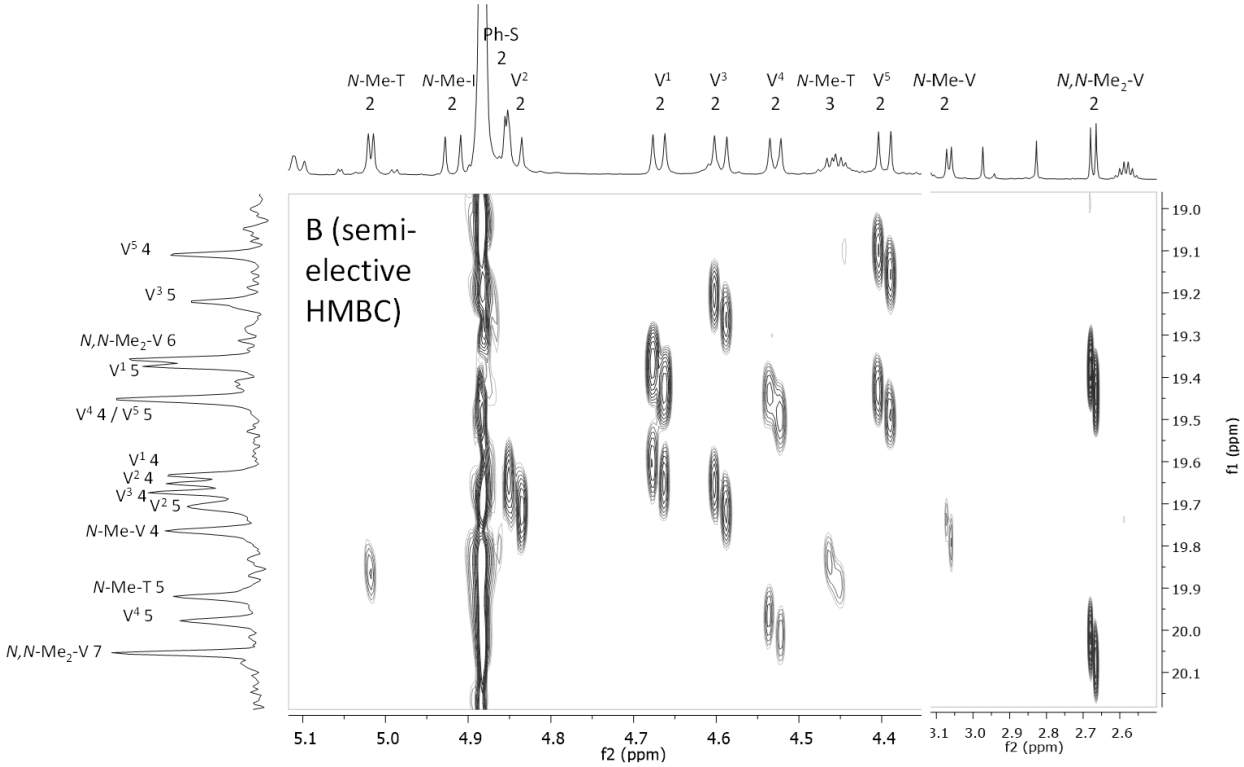
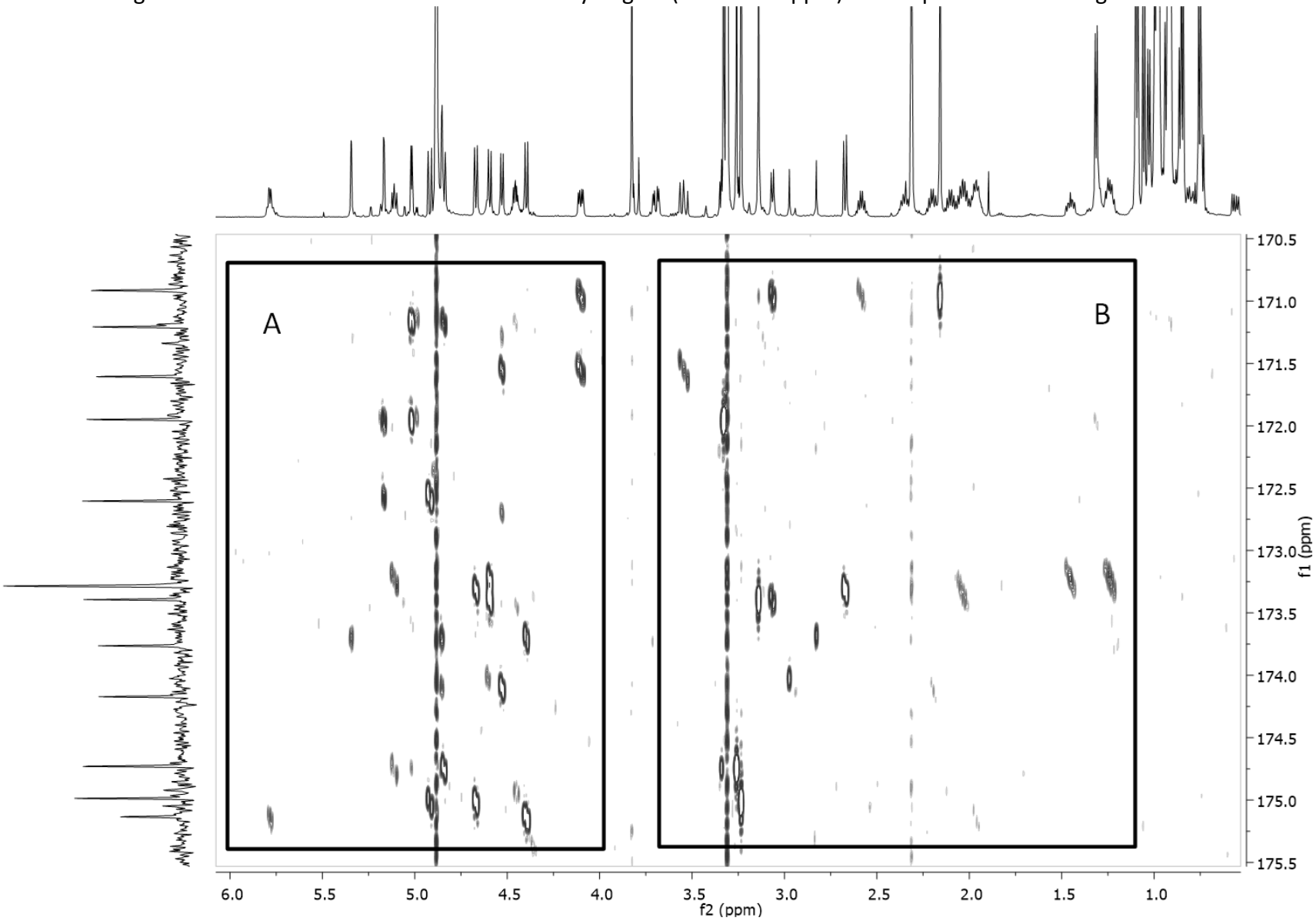
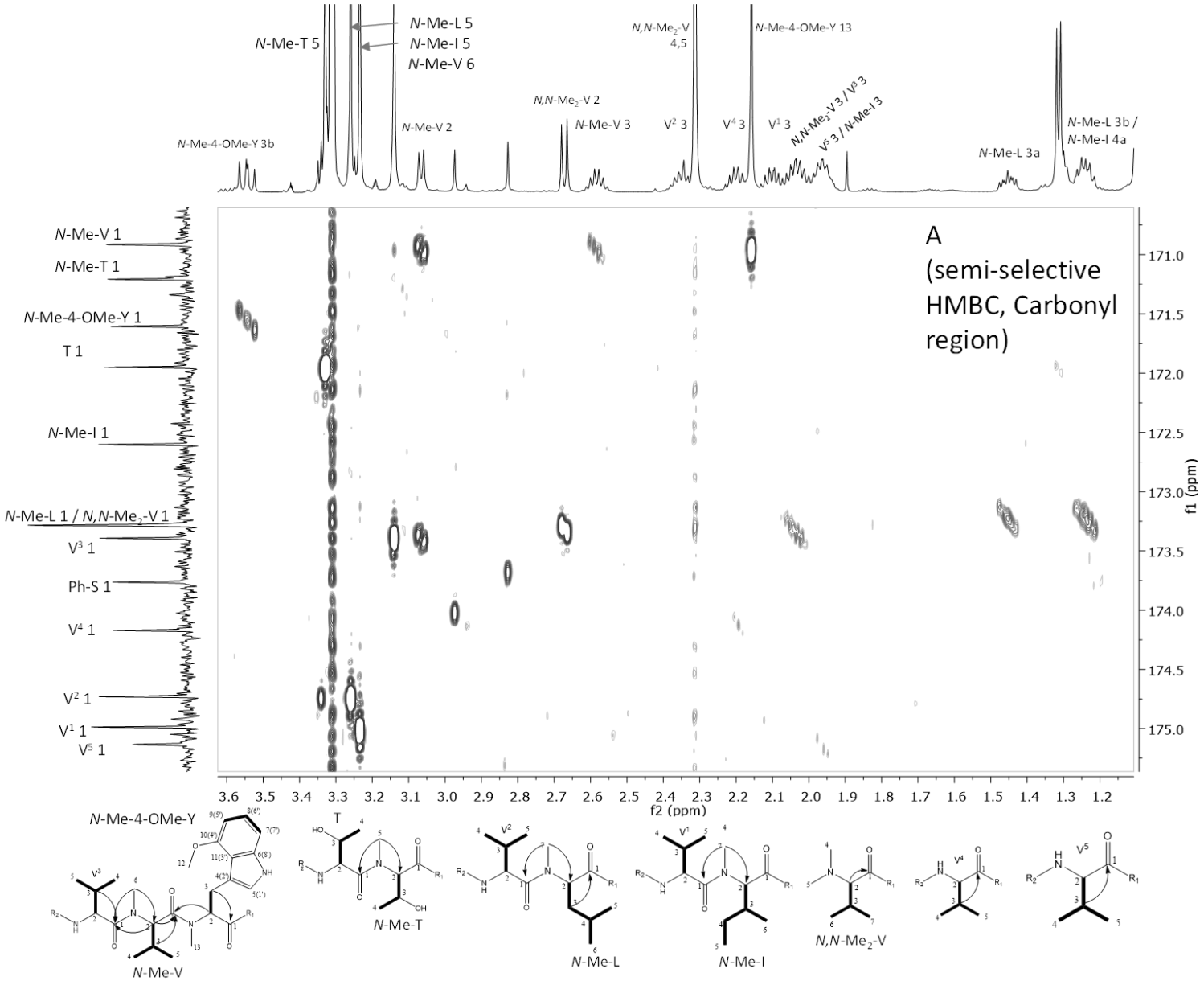
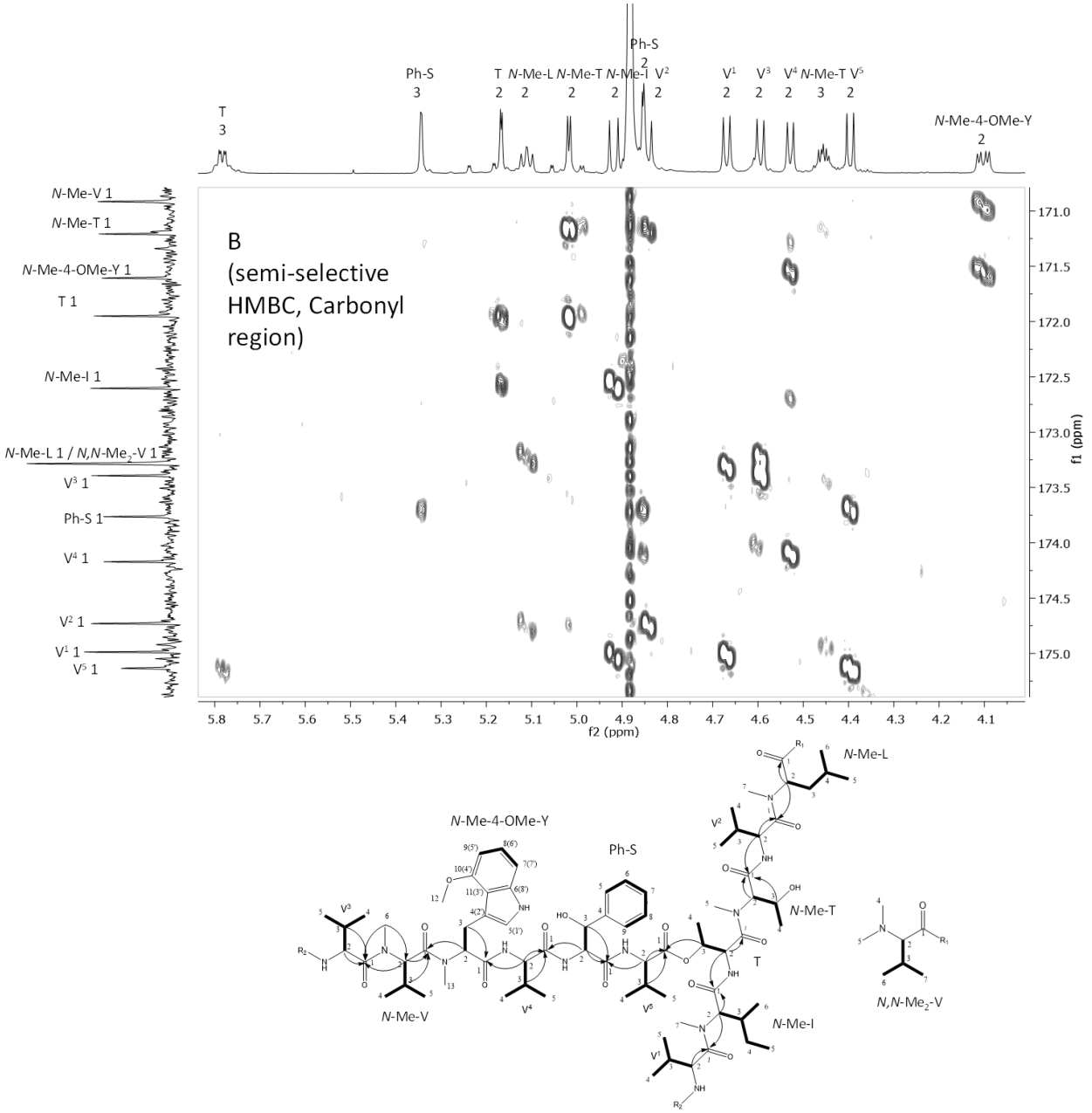

B (semi-elective HMBC)
Ph-S 2
N-Me-T 2
N-Me-I 2
V2 2
V1 2
V3 2
V4 2
N-Me-T 3
V5 2
N-Me-V 2
N,N-Me2-V 2
V5 4
V3 5
N,N-Me2-V 6
V1 5
V4 4 / V5 5
V1 4
V2 4
V3 4
V2 5
N-Me-V 4
N-Me-T 5
V4 5
N,N-Me2-V 7
f2 (ppm)
f1 (ppm)

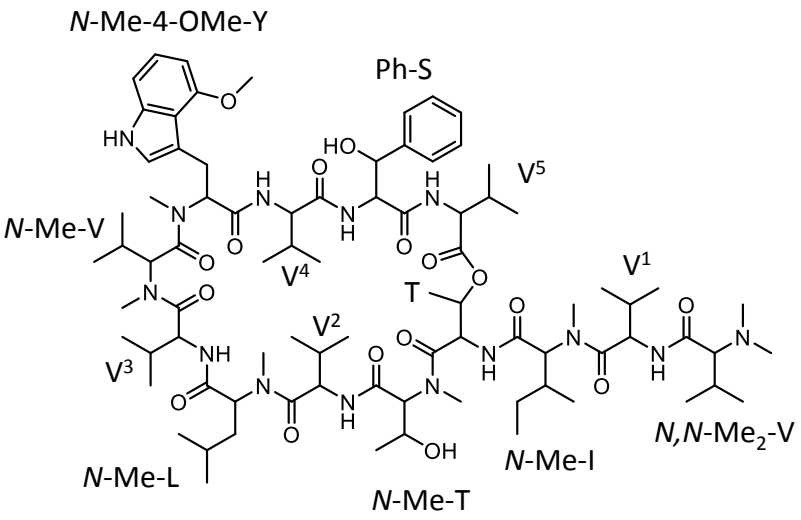
Figure 37. Semi-selective HMBC on the carbonyl region (F1 164-184ppm) with expansions and assignment.




N-Me-T 5
N-Me-L 5
N-Me-I 5
N-Me-V 6
N,N-Me2-V 4,5
N-Me-4-OMe-Y 13
N,N-Me2-V 2
N-Me-V 3
V2 3
V4 3
V1 3
N,N-Me2-V 3 / V3 3
V5 3 / N-Me-I 3
N-Me-4-OMe-Y 3b
N-Me-V 2
N-Me-L 3a
N-Me-L 3b / N-Me-I 4a
N-Me-V 1
N-Me-T 1
N-Me-4-OMe-Y 1
T 1
N-Me-I 1
N-Me-L 1 / N,N-Me2-V 1
V3 1
Ph-S 1
V4 1
V2 1
V1 1
V5 1
A
(semi-selective HMBC, Carbonyl region)
f1 (ppm)
f2 (ppm)
N-Me-4-OMe-Y
N-Me-V
T
N-Me-T
N-Me-L
N-Me-I
N,N-Me2-V


B
(semi-selective
HMBC, Carbonyl
region)
T 3
Ph-S 3
T 2
N-Me-L 2
N-Me-T 2
N-Me-I 2
Ph-S 2
V² 2
V¹ 2
V³ 2
V⁴ 2
N-Me-T 3
V⁵ 2
N-Me-4-OMe-Y 2
N-Me-V 1
N-Me-T 1
N-Me-4-OMe-Y 1
T 1
N-Me-I 1
N-Me-L 1 / N,N-Me2-V 1
V³ 1
Ph-S 1
V⁴ 1
V² 1
V¹ 1
V⁵ 1
f2 (ppm)
f1 (ppm)
N-Me-L
N-Me-4-OMe-Y
Ph-S
N-Me-T
T
N-Me-V
N-Me-I
N,N-Me2-V

(a)



(b)

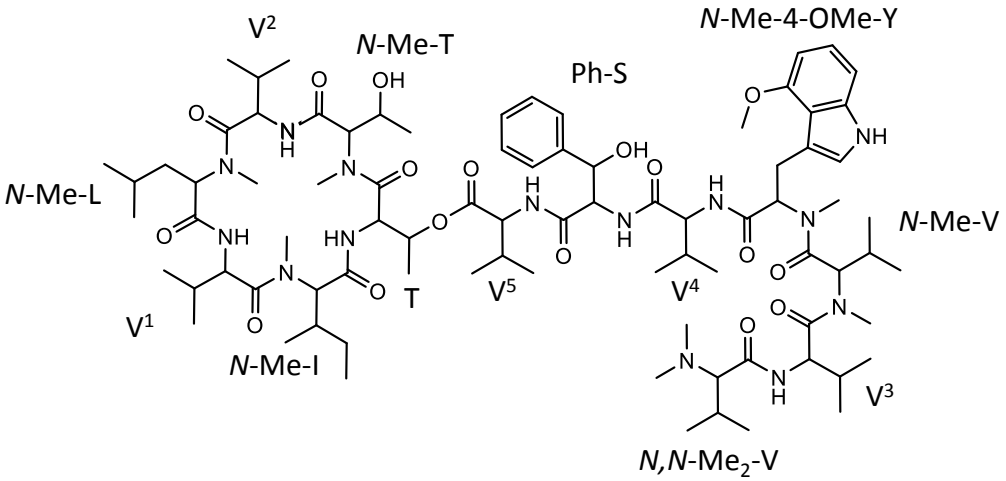


Figure 38. Ecumicin's two possible structures (a) and (b) constructued from NMR analysis.

Examination of the tandem mass spectrum, which is summarized in Figure 39, revealed evidence to support the structure as proposed in Figure 38a. Connection between *N,N*-Me_2-V and V^1 was indicated by a fragment ion [*N,N*-Me_2-V + V^1 + *N*-Me-I]$^+$ at m/z 354.32.

The following fragments confirmed the assigned structure in Figure 38a: m/z (rel. int.) 1600.23 [M+H]$^+$ (8), 1246.95 [M – *N,N*-Me^2-V – V^1 – *N*-Me-I + 2H]$^+$ (48), 990.86 [M – *N,N*-Me^2-V – V^1 – *N*-Me-I – T – V^5 + 2H]$^+$ (7), 800.60 [M+2H]$^{2+}$ (50), 610.41 [*N,N*-Me_2-V + V^1 + *N*-Me-I + T + V^5]+ (36), 354.32 [*N,N*-Me_2-V + V^1 + *N*-Me-I]+ (87).

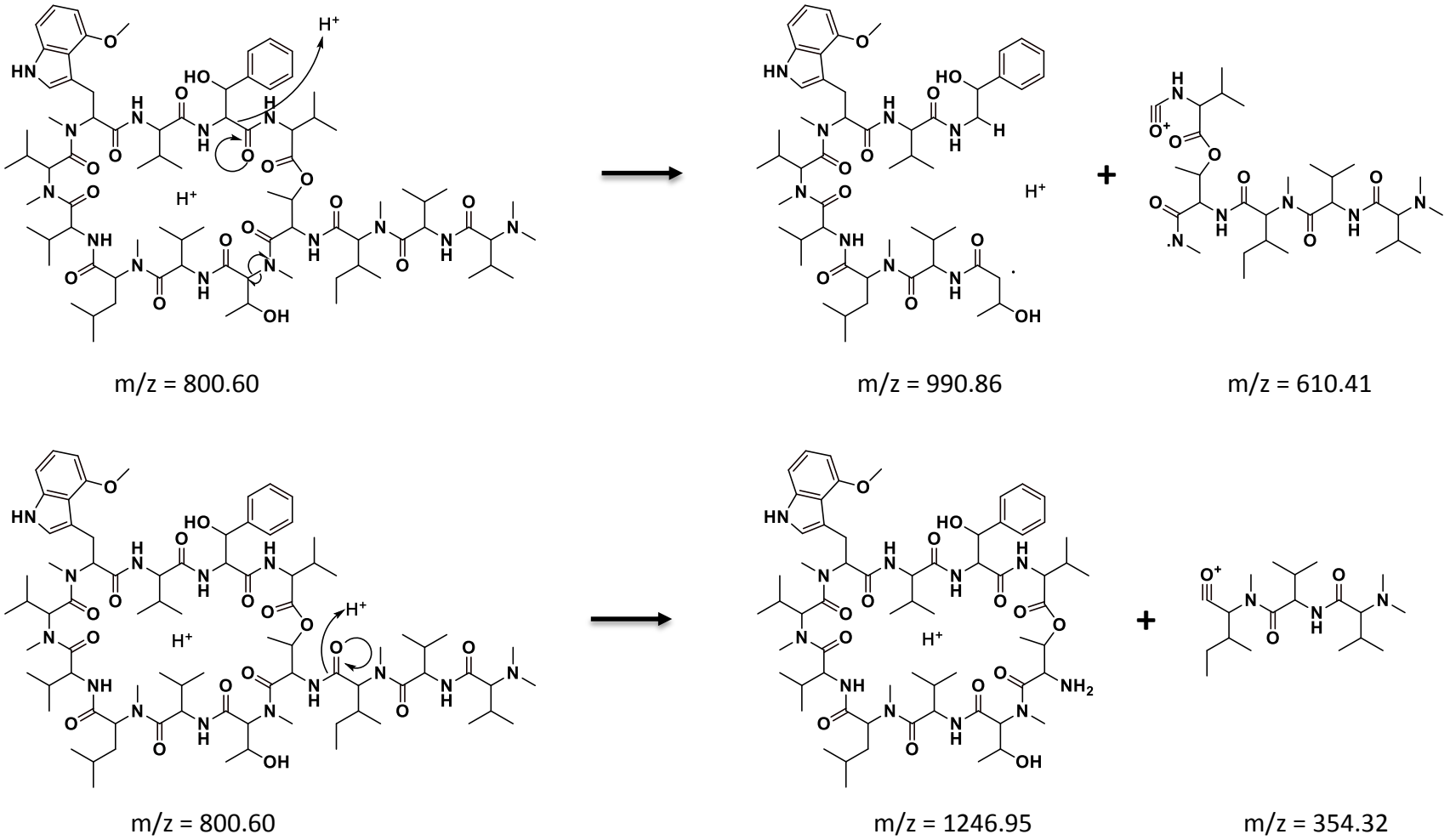


Figure 39. Fragmentation pattern of ecumicin in tandem mass spectroscopy.

5.3 Stereochemistry identified by X-ray crystallography and Marfey's experiment

A needle shaped crystal of ecumicin was obtained by slow evaporation from a solvent mixture of methanol, acetonitrile and water, initially in a 2:2:1 ratio. Crystal dimensions were approximately 0.1 mm × 0.15 mm × 0.5 mm. X-ray data were collected at room temperature on a Bruker D8 discover X-ray system and the crystal diffracted X-ray to 0.83 Å. The crystal belonged to the orthorhombic space group P2(1)2(1)2 with unit cell parameters a=71.64 Å, b=11.43 Å, c=12.70 Å. One molecule was observed per asymmetric unit.

As shown in Figure 40, ecumicin has a twist anti-parallel hairpin structure. Five intermolecular hydrogen bonds stabilize the overall structure. Surrounding water molecules were also involved in hydrogen bonding and presumably further stabilized the structure.

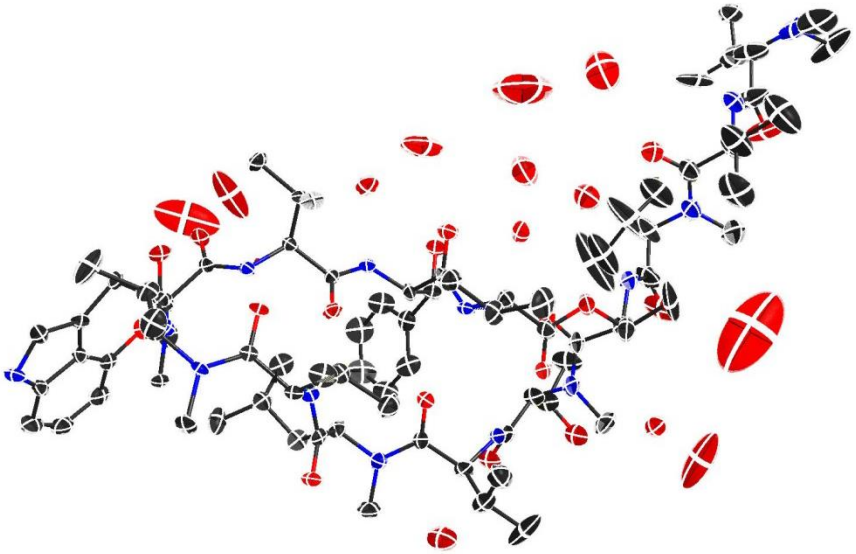


Figure 40. Oak Ridge Thermal-Ellipsoid Plot Program representation of the asymmetric unit of ecumicin, shown at 50% probability displacement ellipsoids.

In addition, the n→π* interaction, an electronic delocalization effect analogous to the hydrogen bond, may also play a role in stabilizing the peptide's secondary structure(Bartlett, et al. 2010). The stabilization offered by the n→π* interaction to proteins' secondary structures ranges from 0.5 kcal/mol for an α-helix, 1.3 kcal/mol for a 3_{10}-helix, to 0.1 kcal/mol for a π-helix (Bartlett, et al. 2010). Based on observation of proteins with α-helix structure, a previous publication has recommended two parameters that define n→π* interaction between two carbonyl carbon groups (Figure 41): $d_{n\to\pi^*} \leq 3.22$ Å (the sum of van der Waals radii of oxygen and carbon), $95° \leq \vartheta \leq 125°$ (a range centered on the approximate angle of the Burgi-Dunitz trajectory for nucleophilic attach at a carbonyl carbon, ~109°) (Bartlett, et al. 2013). Following such criteria, two n→π* interactions were found, as highlighted in TABLE IX. The two pairs of carbonyl groups resided in the turning point of the β-sheet, and therefore contributed to the stabilization of the turn. An additional five pairs of carbonyl groups were recorded in TABLE IX, although they all had some parameter(s) slightly outside the recommended region and may not be considered as n→π* interactions.

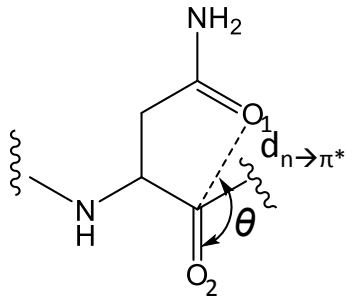


Figure 41. Parameters defining n→π* interaction. $d_{n\to\pi^*} \leq 3.22$ Å, and $95° \leq \vartheta \leq 125°$.

TABLE IX. A SUMMARY OF CARBONYL GROUPS THAT MAY CONTRIBUTE TO N→Π* INTERACTIONS IN ECUMICIN. CARBONYL GROUPS THAT FULFILLED RECOMMENDED PARAMETERS WERE HIGHLIGHTED IN YELLOW; THE REST WERE HAVING PARAMETER(S) SLIGHTLY OUTSIDE THEIR RECOMMENDED REGION (IN RED). AA, AMINO ACID RESIDUE.

AA (C=)O_1	**AA C(=O_2)**	**$d_{n\rightarrow\pi^*}$ (Å)**	**ϑ**
V^3	*N*-Me-V	2.647	97.6°
N-Me-V	*N*-Me-4-OMe-Y	2.911	124.4°
V^1	*N*-Me-I	3.346	99.0°
V^4	Ph-S	3.319	111.8°
T	*N*-Me-L	3.410	102.2°
N-Me-L	T	3.304	107.7°
V^5	T	2.866	91.0°

The structures of non-standard amino acids were confirmed by inspecting the position of each atom using the electron density map (Figure 42). As the hydrophobic side chains of alternate residues point up and down from the β-hairpin axis, the surface of ecumicin is hydrophobic and neutral.

The crystallographic data were deposited in the Cambridge Crystallographic Data Centre (CCDC) under the deposition number 940680. These data may be obtained free of charge via http://www.ccdc.cam.ac.uk/data_request/cif, or by e-mailing data_request@ccdc.cam.ac.uk, or by CCDC, 12 Union Road, Cambridge CB21EZ, UK; fax: +44(0)-1233-336033.

A Marfey's experiment resulted in incomplete hydrolysis; however, distinctive L-valine and *N*-Me-L-valine residues were identified (Figure 43 and 44). The analysis was carried out as described (Bhushan and Bruckner 2011).

Combining information from the X-ray structure and the Marfey's experiment, we concluded that ecumicin consisted of 12 L-configured amino acids or their analogs (Figure 45). The chirality of the 13th amino acid, the *N*,*N*-dimethyl valine residue, could not be determined at

this stage, as this amino acid does not react with Marfey's reagent. In addition, X-ray crystallographic distinction is complicated by the close similarity of the electron density maps of the corresponding C and N atoms.

A ROESY experiment confirmed the cross-ring correlations (Figure 46) and suggests that when dissolved in methanol, the three amino acid tail either does not exist in the conformation suggested by crystallographic analysis, or there is inter-molecular correlation due to relatively high concentration (5mM).

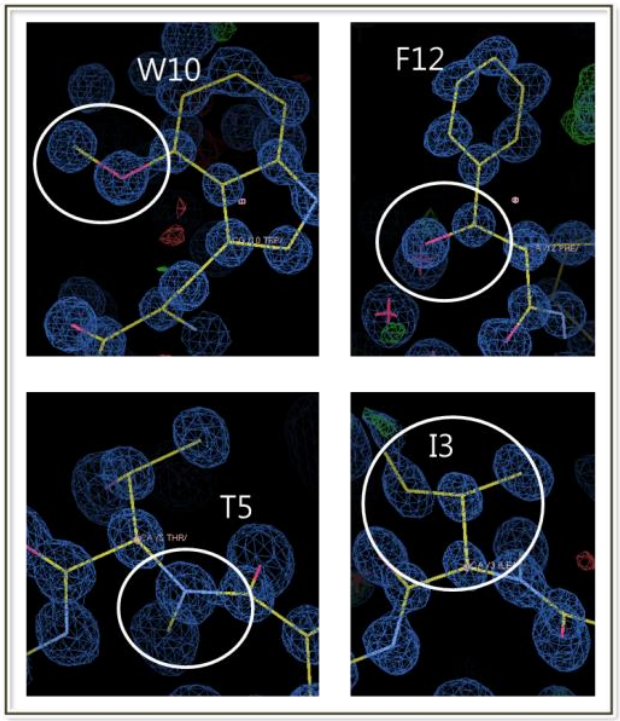


Figure 42. Electron density map of selected residues, tryptophan (W10), phenylalanine (F12), threonine (T5) and isoleucine (I3) at 0.83 Å resolution.

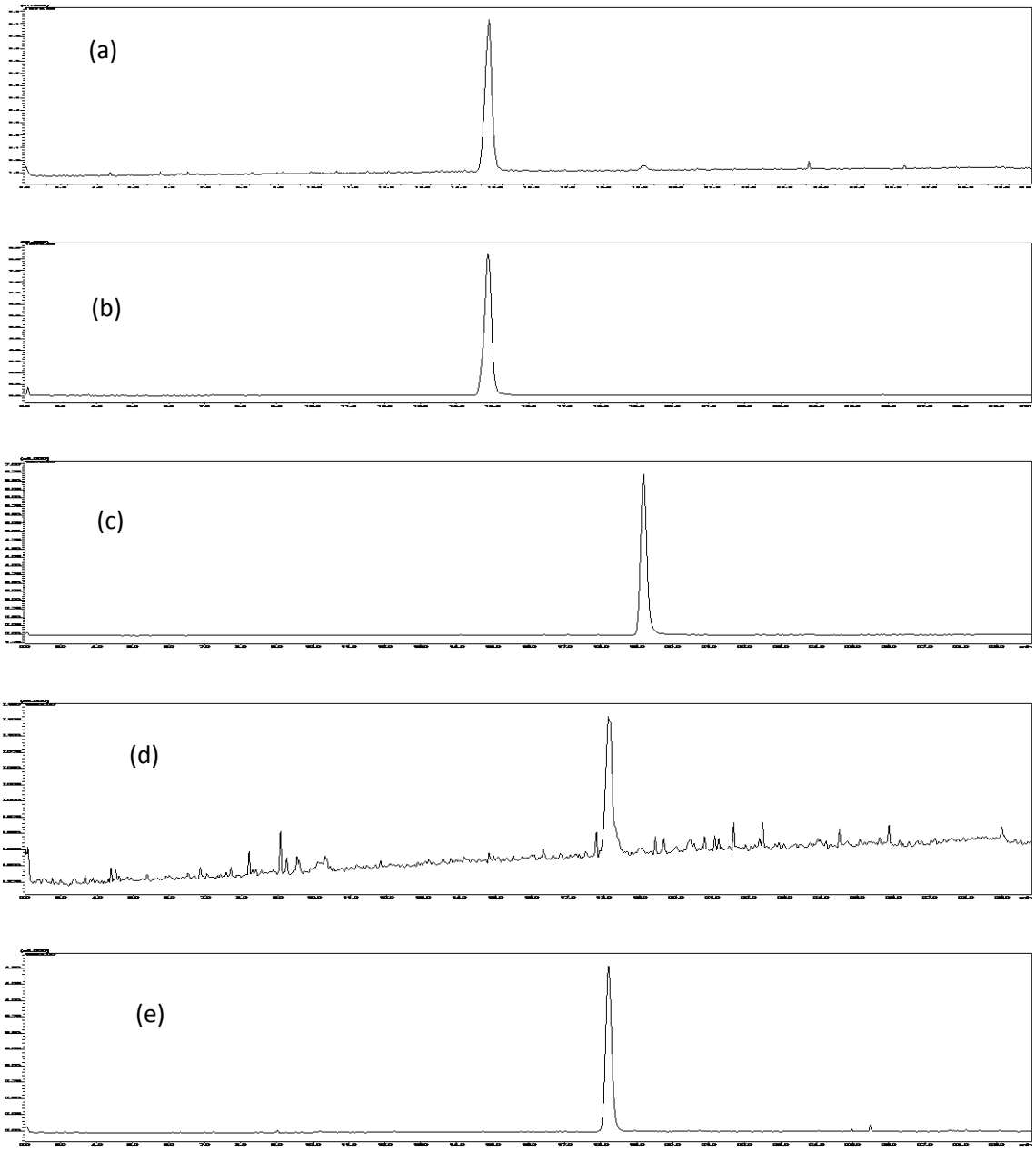


Figure 43. LC-ESI-MS (Shimadzu 2020) on a RP C18 column; peaks shown in (a), (b), and (c) were detected with SIM mode at m/z = 370.3; peaks shown in (d) and (e) were detected with SIM mode at m/z = 384.0.

(a) Hydrolizate of ecumicin reacted with L-FDAA, r.t. = 14.87 min.
(b) L-ala-NH_2-DNP-L-valine, r.t. = 14.87 min.
(c) L-ala-NH_2-DNP-D-valine, r.t. = 19.19 min.
(d) Hydrolizate of ecumicin reacted with L-FDAA, r.t. =18.22 min.
(e) L-ala-NH_2-DNP-*N*-methyl-L-valine, r.t. =18.22 min.

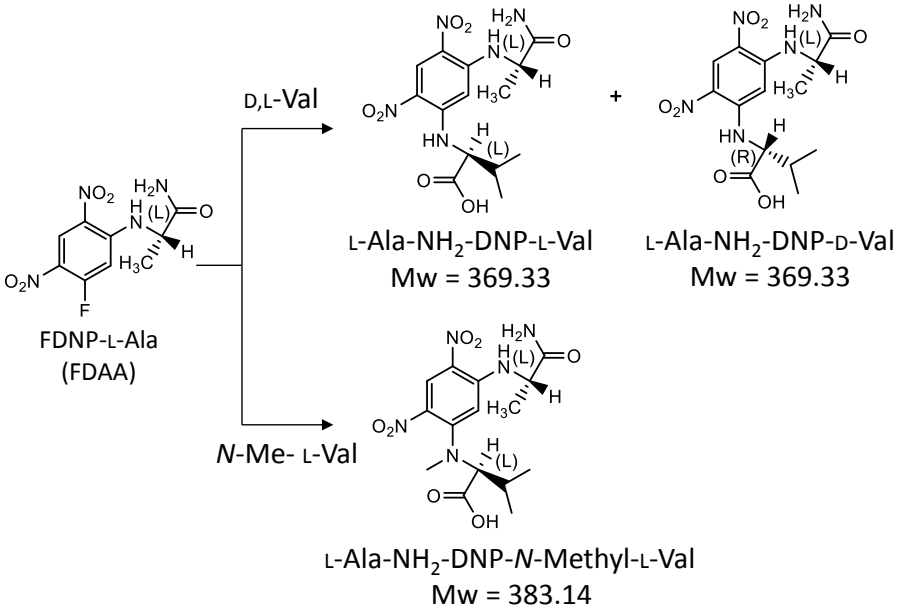


Figure 44. The Marfey's reaction and formation of L-L- and L-D-diastereomers.

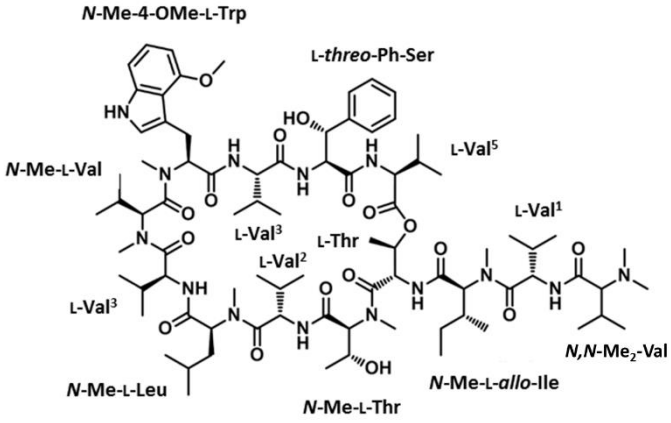


Figure 45. Structure of ecumicin

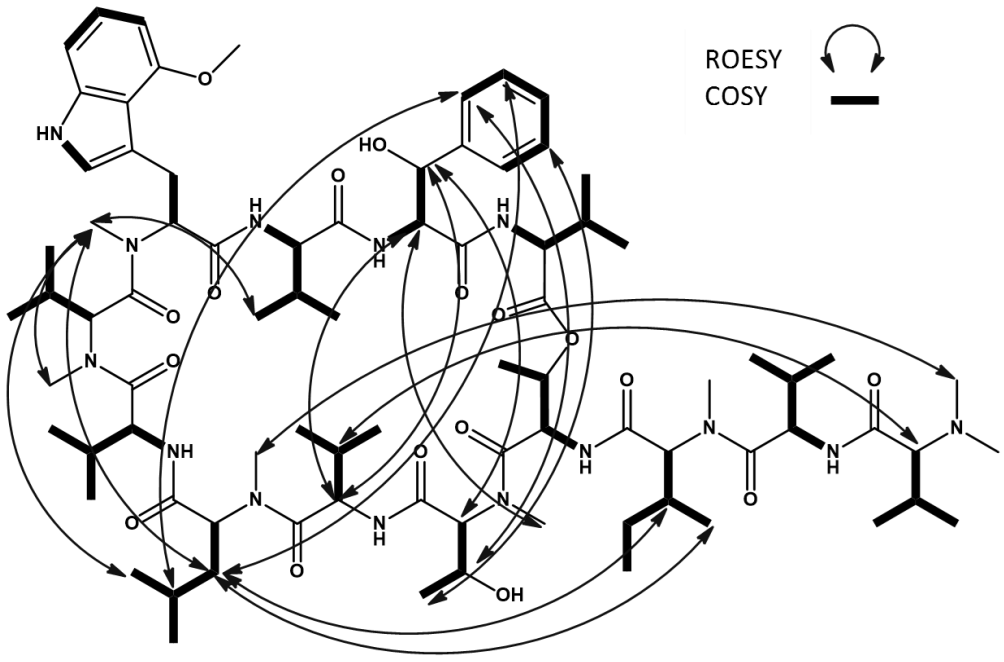


Figure 46. Observed ROESY correlations for ecumicin (methanol-d_4, 600 MHz, Bruker Avance 600).

5.4 Verification of ecumicin's proposed structure by ^{1}H iterative Full Spin Analysis (HiFSA)

Final evidence for the ecumicin structure and important data for future rapid and precise dereplication came from a complete interpretation of all ^{1}H NMR spectral spin parameters [^{1}H chemical shift (δ), and scalar couplings (J)], achieved by performing a ^{1}H iterative Full Spin Analysis (HiFSA) using the PERCH software tool, the procedure follows a recently established approach to produce detailed ^{1}H NMR profiles based on field-independent parameters (Laatikainen, et al. 2007, Napolitano, et al. 2012). HiFSA analysis enables full interpretation of complex ^{1}H resonances that otherwise is hardly or unachievable by standard visual inspection due to spectral overlap, especially overlap like that seen in the methyl and methylene regions (0.9 – 2.1 ppm) of the ecumicin spectrum. The 3D crystal structure was used for spectral prediction of the initial NMR spin parameters. The final calculated spectrum showed congruence with the experimental one (RMSD = 0.114% when solvent peaks and impurity peaks were excluded, Figure 48). In addition to providing unambiguous and highly accurate δ and J values, the HiFSA analysis revealed small, long-range couplings that influence the overall line shape of the ^{1}H NMR signals, such as the coupling between H-5 and H-7 of the *N*-Me-4-OMe-L-Trp unit, $^5J_{H,H}$ = 0.5 Hz. Overall, HiFSA led to the determination of 65 ^{1}H chemical shifts and 53 ^{1}H-^{1}H coupling constants for ecumicin (TABLE VIII). To date, ecumicin represents the largest molecule for which a full ^{1}H NMR spin analysis has been achieved.

The crystal structure of ecumicin also provided an explanation for the occurrence of two up field proton signals (0.16 ppm and 0.33 ppm). As shown in Figure 47, the two terminal methyl groups of the *N*-Me-L residue that corresponded to the two up-field proton signals, are positioned in the shielding cones of two aromatic systems – Ph-S and *N*-Me-4-OMe-Y. This

suggests that when dissolved in methanol, ecumicin's macro cycle maintains the conformation as was observed in crystal, which produces the unusual high field chemical shifts.

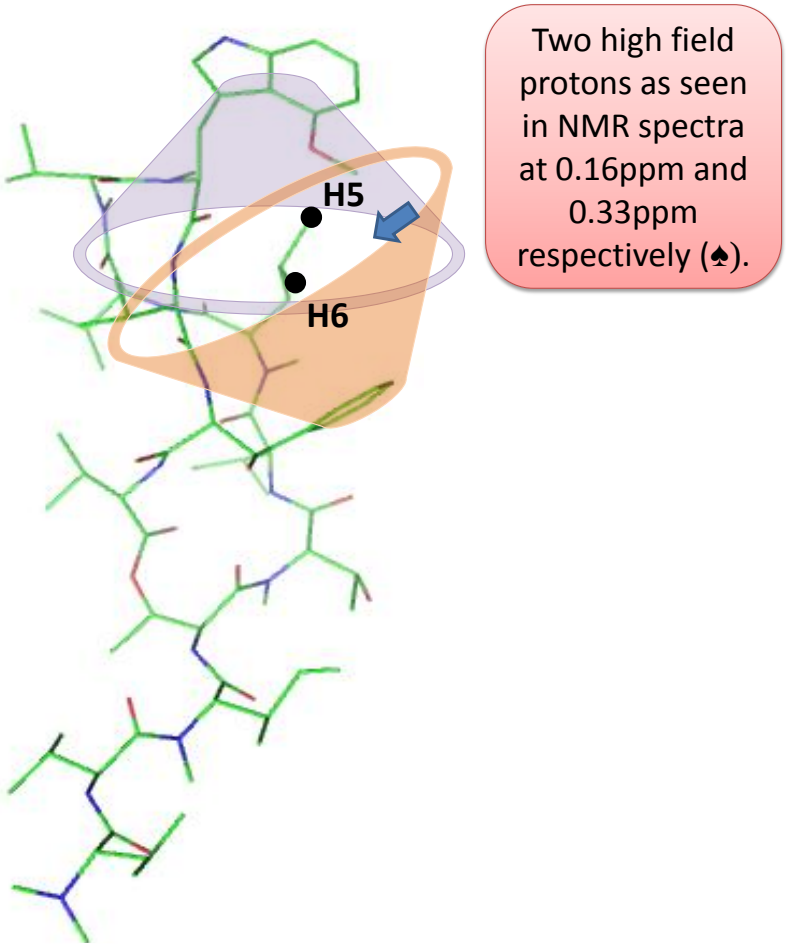


Figure 47. The crystal structure of ecumicin explains how the shielding aromatic cones give rise to the two up field proton resonances in NMR spectra at 0.16824 ppm (H-5 of the *N*-Me-L residue) and 0.33065 ppm(H-6 of the *N*-Me-L residue).

In addition, that all amino acid residues in ecumicin are connected by amide groups, makes them discrete spin systems. As a result, it is possible to study the ^{1}H sub-spectrum of individual amino acid without affecting the rest of the ^{1}H spectrum. As a complete list of accurate δ and J values is available, ^{1}H sub-spectra of all ecumicin's 13 amino acids were generated (Figure 48). The mathematical sum of these 13 sub-spectra gives rise to a calculated HiFSA spectrum of ecumicin that is congruent with the experimental one (RMSD = 0.114%). This observation suggests a possibility to study a new oligo-peptide as a mixture of individual amino acid residues. The advantage in this method is obvious, as information on a large number of amino acids is readily available. Furthermore, the ^{1}H sub-spectra of a certain type of amino acid residue should share a same pattern, with variations on chemical shift values, which reflect the differences in each amino acid's surrounding chemical environment. This is true for the ^{1}H sub-spectra of ecumicin's seven valine residues (*N,N*-Me_2-Val, *N*-Me-Val, and Val^1 – Val^5, Figure 48). So, theoretically, ^{1}H NMR patterns of known amino acid residues can be directly used in the structure elucidation of a new peptide.

In Chapter 9, we developed a NMR structure sequencing method for the structure elucidation of ecumicin's analogs, by analyzing each new peptide as a mixture of individual amino acid residues.

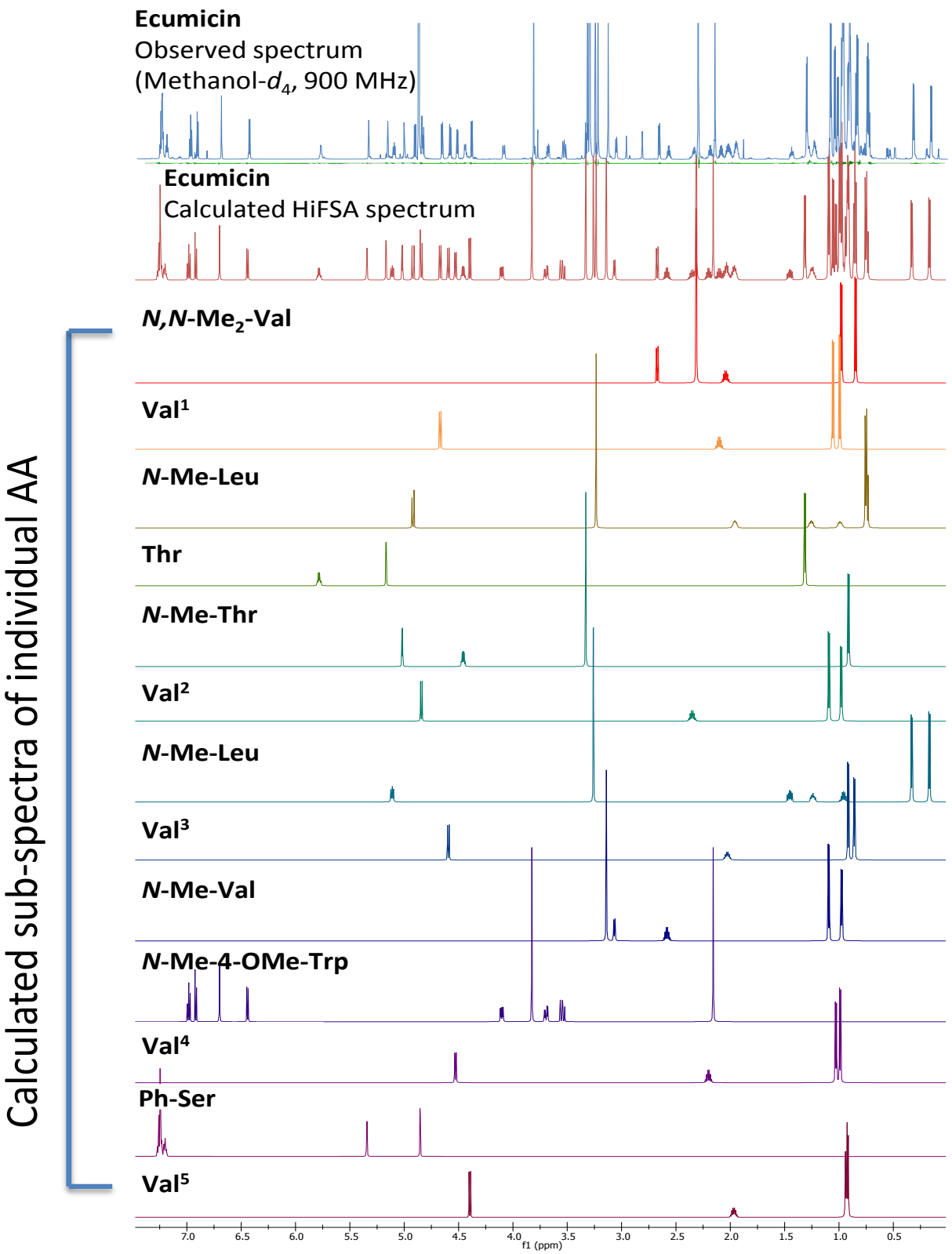


Figure 48. ^{1}H iterative Full Spin Analysis by Perch software (v.2011.1, PERCH Solutions Ltd., Kuopio, Finland). The experimental ^{1}H spectrum (methanol-d_4, 900 MHz) was obtained from a Bruker Avance II 900 instrument.

5.5 Material and Methods

The melting point (m.p.) was determined using a Stuart™ melting point apparatus SMP3 and was uncorrected. Optical rotation was recorded on a JASCO P-2000 digital polarimeter, NMR spectra were recorded on Bruker DPX 400, Avance 600 and Avance II 900 instruments. The IR spectrum was recorded on a Nicolet™ 6700 FT-IR instrument, and the UV spectrum was recorded on a SpectraMax® Plus 384. The X-ray diffraction data were collected on a Bruker D8 discover X-ray system, and the structures were solved by direct methods using ShelxD software.

Pure ecumicin is a colorless needle-shaped crystal; m.p. 165 ~ 168°C; $[\alpha]^{24}_{D}$ 138.0 (c = 0.09, $CHCl_3$); IR ν_{max} 3315, 2962, 1632, 1508, 1255, 1089, 737 cm^{-1}; UV data see Figure 26; ^{1}H NMR and ^{13}C NMR data, see TABLE VIII; HR-ESI-MS *m/z* data, see Figure 22; ESI-MS^2 *m/z* data see Figure 27.

Peptide structure elucidation by X-ray crystallography

Colorless needle-like crystals of ecumicin were obtained using a slow evaporation method over 5 to 7 days. X-ray data were collected on a Bruker D8 discover X-ray system at room temperature and the crystal diffracted X-ray to 0.83Å. Crystal data for ecumicin: $C_{83}H_{134}O_{17}N_{14}$, M = 1599. 01, space group $P2_12_12$ (no. 18), a = 71.64(7) Å, b = 11.434(11) Å, c = 12.697(13) Å, V= 10400 (110 Å3, Z = 4, F(000) = 3972, Dc = 1.172 g/cm^3, μ (MoKα) = 18.71 cm^{-1}, T = 293(2), 1142 variables refined with 10140 reflections with I > 4σ(I) to R_1 = 0.1722.

Marfey's experiment

0.3 mg peptide was mixed with 0.5 ml 6N HCl solution. The mixture was heated at 110°C for 16 hours, and the resultant solution was dried under vacuum. 100 μg dried hydrolyte, or 100 μg amino acid standard [L-valine (Sigma-Aldrich), D-valine (Sigma-Aldrich), and *N*-methyl-L-valine

(Sigma-Aldrich)] was mixed with 20 µL 1M $NaHCO_3$ in water and 10 µL 10% L-FDAA (Sigma-Aldrich) in acetone. The solution was heated to 80°C for 3 min, and then cooled down to room temperature. 20 µL 1M HCl was then added to neutralize the solution. The derivatized sample was then diluted to approximately 1 µg/ml with acetonitrile. 5 µL of diluted sample was injected into a RP-C18 column (Xterra® MS C18 3.5 µm 2.1x150 mm), and a bi-phase gradient method starting from 1% FA acetonitrile solution: 1% FA water solution = 20:80 to 50:50 in 30min was applied. The MS detector was first set to scan mode with m/z from 200 to 600 on a test run, and later to SIM mode with m/z of 370, and 384 for analysis.

6. Biosynthetic pathway of ecumicin

6.1 The non-ribosomal peptide synthetase gene cluster.

That ecumicin is a cyclic depsipeptide with several *N*-methylations suggests that it is likely synthesized by a non-ribosomal peptide synthetase (NRPS). Genome sequencing of MJM5123 via a combination of 454 sequencing platforms, the ion torrent PGM system, and the Sanger sequencing method produced 587,383 reads and 342,400,680 base pairs, and the PGM generated 1,564,568 reads and 258,317,577 base pairs in total (Figure 49). The combined genome sequencing dataset covered 40.6× genome. The assembled sequence data provided 13,246,849 bp in 170 contigs and 70.8% G+C content. Genome annotation results revealed that 12,719 genes could be predicted, containing 12,654 protein coding genes and 65 RNAs (TABLE X). The putative function of 9,184 protein coding genes could be assigned.

Ecumicin is a cyclic depsipeptide composed of 13 amino acids, six of which are *N*-methylated, including the N-terminal valine which is di-*N*-methylated. The genome of strain MJM5123 was sequenced and a portion identified as the putative ecumicin biosynthetic locus (Figure 50). This gene cluster includes *ecu11*, an NRPS gene encoding 13 modules with a thioesterase domain at its *C*-terminal. The predicted substrate specificity of adenylation domains, together with the occupancy of *N*-methyltransferase domains, is consistent with the ecumicin structure (Figure 51, TABLE XI andTABLE XII). Auxilliary genes in the locus include Ecu1, predicted to encode a cytochrome P450, and with significant homology to NovI of the novobiocin biosynthetic locus. NovI was shown to catalyze β-hydroxylation of a Tyr residue loaded on a peptidyl carrier protein (PCP), which leads us to propose that Ecu1 mediates β-hydroxylation of

L-Phe encoded by the PCP domain of module 12. Ecu2 displays a significant homology to Trp dioxygenase and Ecu3 is predicted to encode an *O*-methyltransferase. Hence Ecu2 and Ecu3 are proposed to be involved in the generation of the 4-OMe-L-Trp moiety. The lack of any epimerization domains in this NRPS suggests that ecumicin is composed of only L-amino acids, including an *N,N*-Me_2- L-Val.

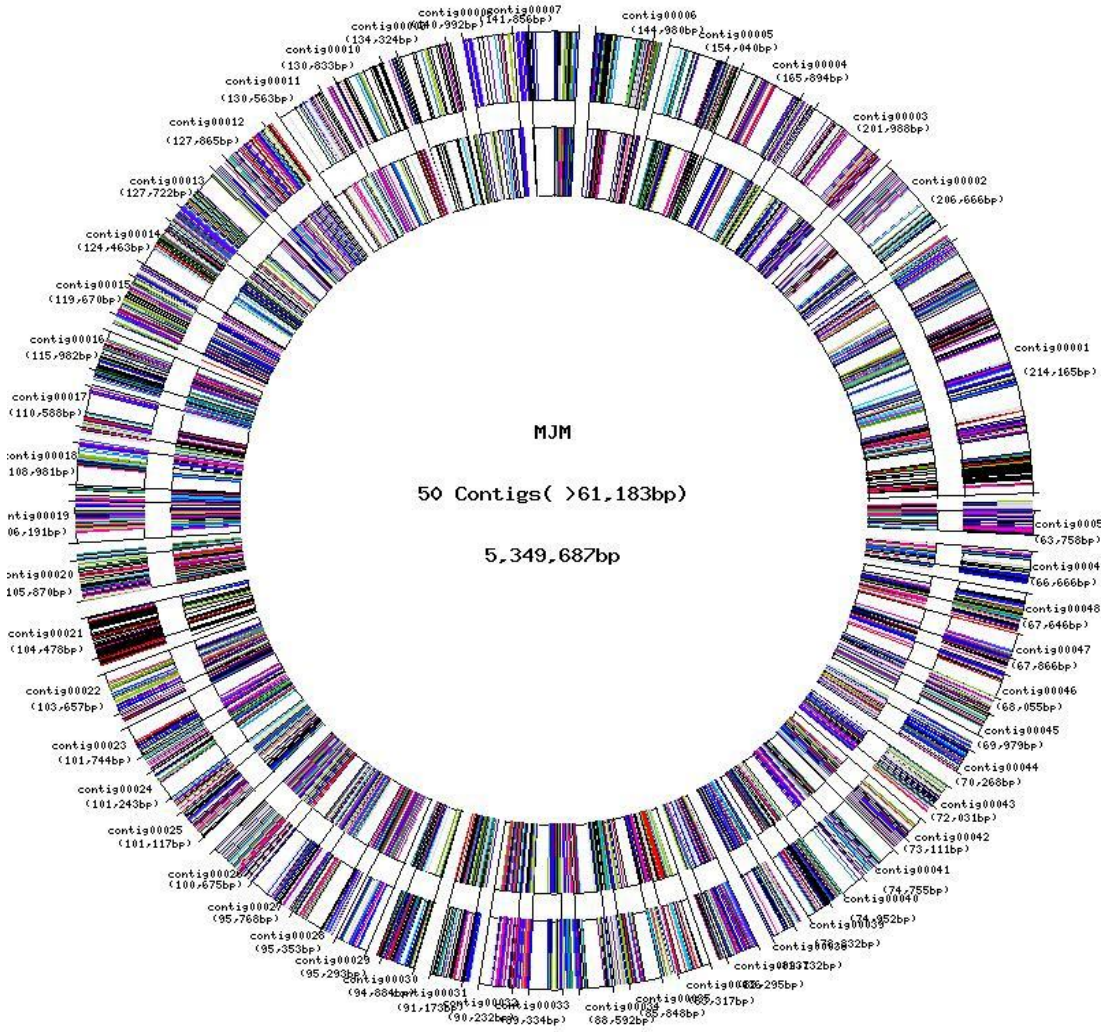


Figure 49. Circular representation of the *Nonomuraea sp*. MJM5123 chromosome.

TABLE X. GENERAL FEATURES OF MJM5123 GENOME.

Feature	Mjm5123
TOTAL SIZE	13,246,849 bp
G+C	70.8 %
Protein Coding Region	89%
Transfer RNAs	63
Ribosomal RNAs	2
Protein Coding Genes	
Conserved with protein function assigned	9,184
Conserved with unknown protein function	2,288
Nonconserved	1,182
Total	12,654

To verify the role of Ecu11 in ecumicin biosynthesis, *ecu11* was inactivated by integration of an *aac(3)IV*/*OriT* cassette using the λ Red mediated recombination technique. An apramycin-resistant and neomycin-sensitive phenotype strain was selected, and the correct gene inactivation was confirmed by PCR. The Δ*ecu11*::*aac(3)IV* mutant did not produce ecumicin as verified by HPLC analysis (Figure 52). This result provides convincing evidence that *ecu11* is indeed the gene encoding the NRPS responsible for ecumicin biosynthesis.

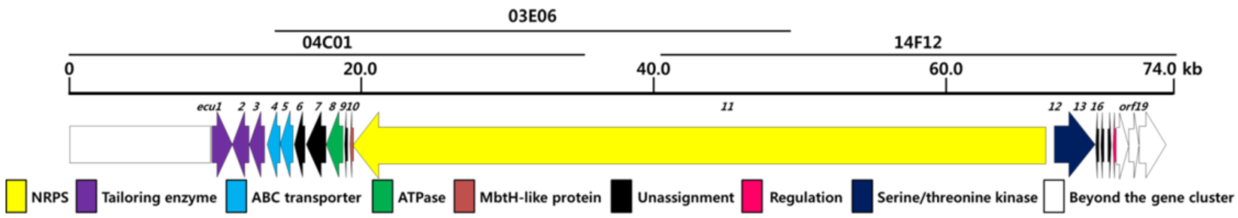


Figure 50. Genomic organization of the ecumicin biosynthetic gene cluster.

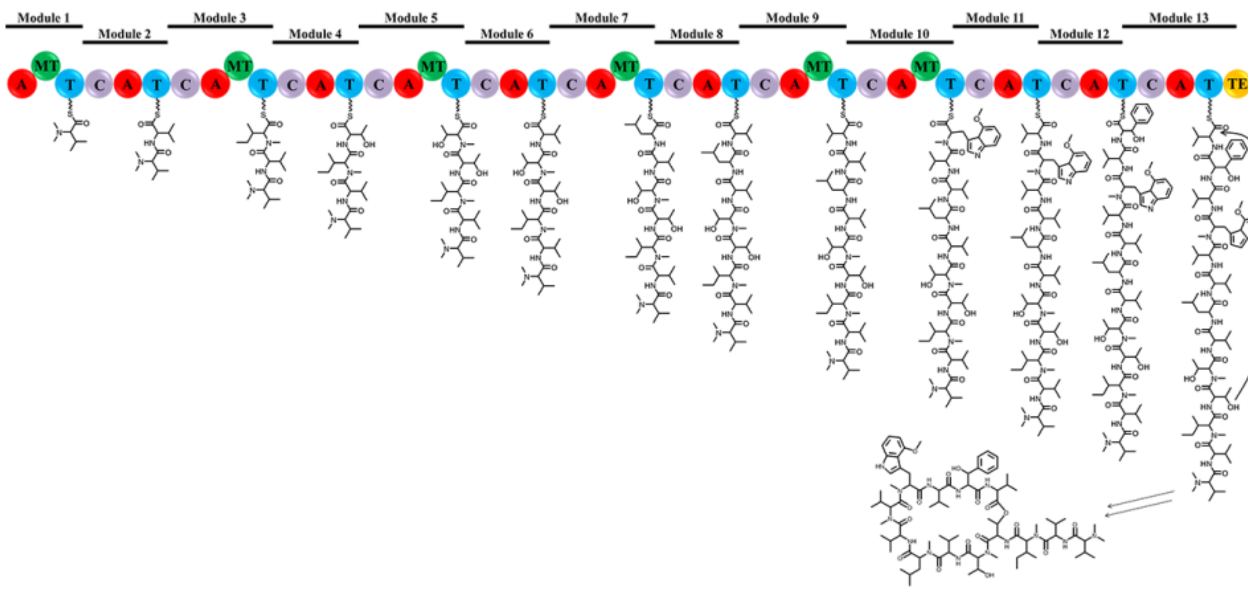


Figure 51. Predicted catalytic domain organization of the NRPS gene. According to their presumed functions, genes and domains are color-coded. Abbreviations for NRPS domains are: A, adenylation; C, condensation; T, thiolation; MT, methyltransferase; TE, thioesterase.

TABLE XI. PREDICTED FUNCTIONS OF THE ORFS IN THE PUTATIVE ECUMICIN-PRODUCING GENE CLUSTER.

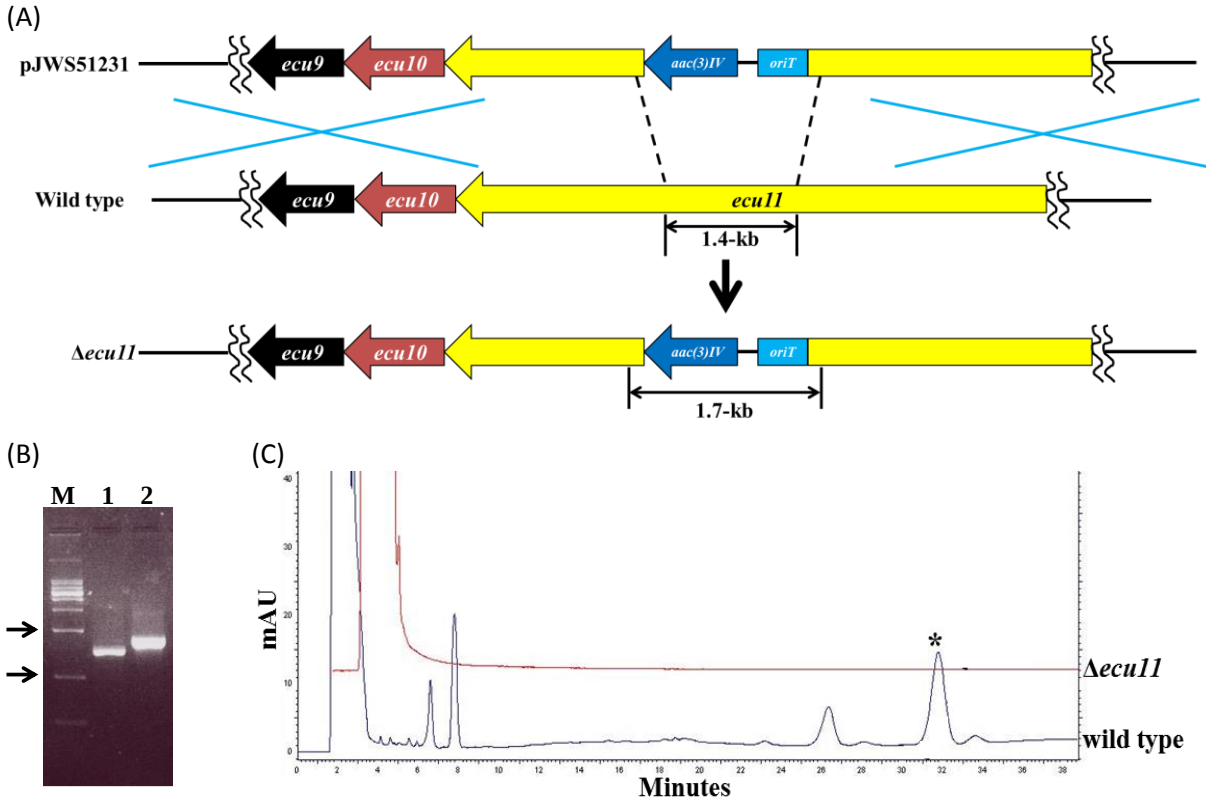
Protein	Amino Acids	Predicted function in ecumicin biosynthesis (reference)	Identity/similarity (%)
Ecu1	396	Cytochrome P450 (YP_001539312.1)	66/80
Ecu2	368	Tryptophan dioxygenase (ZP_08007658.1)	27/42
Ecu3	333	*O*-methyltransferase (ZP_09402183.1)	52/68
Ecu4	276	ABC transporter (ZP_23072754.1)	57/75
Ecu5	320	Hypothetical protein (WP_019436373.1)	72/84
Ecu6	329	Hypothetical protein (ZP_03710192.1)	50/65
Ecu7	446	Hypothetical protein (YP_003680853.1)	55/67
Ecu8	362	ATPase AAA family (ZP_07402977.1)	57/67
Ecu9	78	Hypothetical protein (YP_003381857.1)	65/77
Ecu10	72	MbtH-like protein (YP_003101336.1)	75/90
Ecu11	15,258	NRPS (ZP_20966573.1)	56/67
Ecu12	892	Putative serine/threonine kinase (AAP03109.1)	46/55
Ecu13	65	Hypothetical protein (XP_001935968.1)	37/47
Ecu14	144	Hypothetical protein (WP_021592209.1)	46/57
Ecu15	67	Hypothetical protein (WP_017593885.1)	82/94
Ecu16	267	LmbU and CloE-like protein (BAF98638.1)	53/73
Orf17	111	Integrase (WP_009719320.1)	59/79
Orf18	590	Integrase (YP_003273711.1)	59/72
Orf19	324	Integrase (YP_003273712.1)	74/83

TABLE XII. SPECIFICITY-CONFERRING CODE OF ADENYLATION DOMAINS IN THE PARTIAL ECUMICIN-PRODUCING NRPS ANALYZED BY NRPSPREDICTOR2 (RAUSCH, ET AL. 2005, ROTTIG, ET AL. 2011).

Domain	**Specific-conferring code**										**Predicted AA**	**AA in ecumicin**
A_1	D	A	Y	W	W	G	G	T	F	K	Val	*N,N*-Me_2-Val
A_2	D	A	Y	W	W	G	G	T	F	K	Val	Val
A_3	D	A	Y	W	W	G	G	T	F	K	Val*	*N*-Me-Ile
A_4	D	F	W	N	I	G	M	V	H	K	Thr	Thr
A_5	D	F	W	S	V	G	M	V	H	K	Thr	*N*-Me-Thr
A_6	D	A	Y	W	W	G	G	T	F	K	Val	Val
A_7	D	A	L	L	L	G	A	V	V	K	Phe*	*N*-Me-Leu
A_8	D	A	Y	W	W	G	G	T	F	K	Val	Val
A_9	D	A	Y	W	W	G	G	T	F	K	Val	*N*-Me-Val
A_{10}	D	V	A	L	V	G	A	V	H	K	Trp	*N*-Me-4-OMe-Trp
A_{11}	D	A	Y	W	W	G	G	T	F	K	Val	Val
A_{12}	D	A	W	T	V	A	A	V	C	K	Phe	Ph-Ser
A_{13}	D	A	Y	W	W	G	G	T	F	K	Val	Val

* Although the predicted AAs of A_3 and A_7 do not match corresponding AAs in ecumicin, given that both cases involves non-polar amino acid, it is possible that in real life A3 and A7 domains have high reorganization specificity on Ile and Leu residues respectively.

Figure 52. Gene inactivation of *ecu11* by λ Red mediated recombination and HPLC analysis of ecumicin production. (A) Construction of a *ecu11* inactivation mutant (Δ*ecu11*) (B) Electrophoretic analysis of the correct inactivation of *ecu11* by *aac(3)IV*/*OriT* cassette was verified by PCR with the chromosomes of wild type (1.4 kb) (1) and Δ*ecu11* mutant (1.7 kb) (2). Lane M indicates the DNA molecular marker (Elpis-biotech 1 kb Marker). Arrows emphasized 1.0 and 2.0 kb fragments. (C) HPLC analysis of mycelial extracts from wild type and gene inactivation of mutant Δ*ecu11*. Ecumicin peak marked (*) at 32 min. Production of ecumicin was not observed in Δ*ecu11* mutant compared to the wild type.



6.2 Material and methods

The MJM5123 genome was sequenced to obtain information on ecumicin biosynthetic gene cluster(s). The genomic DNA was prepared according to the protocol published by Pospiech (Pospiech and Neumann 1995). A draft genome sequence of MJM5123 was obtained with the 454 GS-FLX (Roche) and the ion torrent PGM system and the traditional whole-genome Sanger sequencing method which generated cosmid libraries (insert size ~35 kb) by random shearing of genomic DNA. The sequence data were assembled using the Newbler, Phred/Phrap/Consed package and in-house scripts. The protein encoding genes were predicted using Glimmer 3.0 (Delcher, et al. 2007). tRNA and rRNA were identified with tRNAscan-SE (Lowe and Eddy 1997) and RNAmmer (Lagesen, et al. 2007). The functions of predicted protein-coding genes were then annotated through comparisons with the databases of UniRef90 (Suzek, et al. 2007), NCBI-NR (Benson, et al. 2008), COG (Tatusov, et al. 1997), and KEGG (Kanehisa, et al. 2008). The putative ecumicin biosynthetic gene clusters were assigned by in silico analysis of the annotated non-ribosomal peptide synthetase (NRPS) genes. The domain feature and each adenylation domain's substrate specificity were analyzed by web-based platform (Rausch, et al. 2005, Rottig, et al. 2011).

7. Ecumicin is a potent anti-TB agent in vitro and in vivo

In vitro biological profiling suggested that ecumicin's selective anti-*M. tuberculosis* activity was comparable or superior to current first line anti-TB drugs. Ecumicin maintained high potency against MDR- and XDR-TB clinical isolates, as well as H37Rv-isogenic strains mono-resistant to RMP, INH, SM, CS, kanamycin, and the cyclic peptide capreomycin, suggesting a molecular target not shared with these drugs. It was highly bactericidal against replicating *M. tuberculosis* cultures, and more modest but still potent against non-replicating cultures, indicating the possibility of shortening the duration of treatment.

Several attempts were made to formulate ecumicin in order to prove its anti-*M. tuberculosis* activity in vivo. Simple suspension and emulsion formulation failed to deliver sufficient quantities to the target organ (lung tissue) in the mouse, and thus no efficacy was observed. However, the two nano-formulations had good in vivo bio-availability, and suggested that with minimum treatment, ecumicin is at least bacteriostatic in vivo.

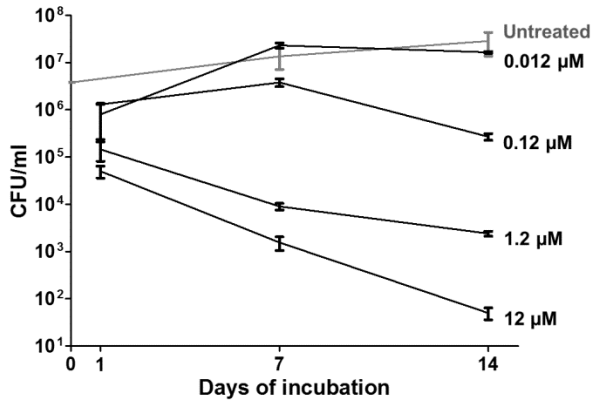
7.1 *in vitro* biological profile of ecumicin

7.1.1 Ecumicin is a potent and selective anti-TB agent in vitro

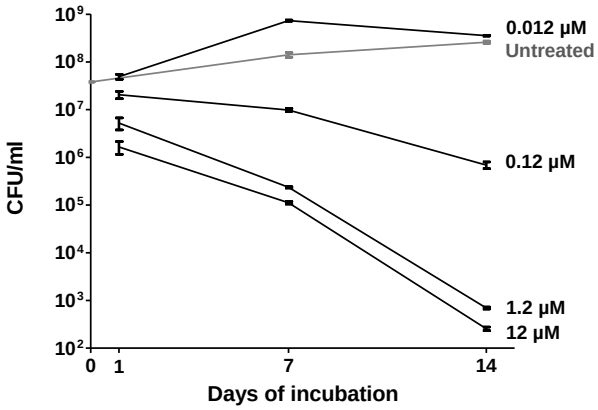
Ecumicin has an *in vitro* anti-*M. tuberculosis* activity profile comparable or superior to current first line anti-TB drugs (TABLE XV). Minimum inhibitory concentrations (MICs) against replicating *M. tuberculosis* $H_{37}Rv$ are 0.16 μM, 0.09 μM, and 0.47 μM for ecumicin, RMP, and isoniazid (INH), respectively. Ecumicin maintains this level of activity against *M. tuberculosis* $H_{37}Rv$-isogenic strains mono-resistant to RMP, INH, SM, CS, kanamycin, and the cyclic peptide capreomycin, suggesting a molecular target not shared with these drugs. When tested against nine clinical strains isolated from pulmonary TB patients hospitalized in the National Masan Hospital (Korea), ecumicin showed equally high potency towards all strains, including the MDR and XDR *M. tuberculosis* isolates (TABLE XIV). Ecumicin also maintained this level of *in vitro* potency against *M. tuberculosis* clinical isolates representing the six major global clades (Filliol, et al. 2006) (TABLE XIII), as well as against five of six non-tuberculous mycobacterial species (TABLE XV). No activity was observed against *S. aureus*, *E. coli,* or *C. albicans* at 32 μM. Moreover, ecumicin is selective with respect to mammalian cells (VERO and mouse macrophage J774 cell lines), with a selectivity index (IC_{50}/*M. tuberculosis* MIC) greater than 640. Ecumicin is highly bactericidal against *M. tuberculosis* replicating in culture broth medium (MBC = 0.34 μM) and the extent of kill was both time and concentration-dependent (Figure 53). More modest but still potent activity was observed against non-replicating cultures (MBC = 1.5 μM), indicating the possibility of shortening the duration of treatment. In J774 macrophages, the concentration of ecumicin yielding a $2\times\log_{10}$ CFU reduction of *M. tuberculosis after* 7 days incubation (compared to initial CFU) was calculated to be 0.12 μM, thereby extending its bactericidal activity to the

intracellular environment (Figure 54). The MIC only increased by 2-4 fold in the presence of 4% bovine serum albumin (physiological concentration) or 10% fetal bovine serum (TABLE XV), suggesting that protein binding may not have any significant functional effect.

Figure 53. Ecumicin has time and concentration-dependent bactericidal activity against *M. tuberculosis*. Each data point was represented by two measurements, error bars = SD. (a) Initial inoculation size = 3.8×10^6 CFU/ml, (b) initial inoculation size =3.8×10^7CFU/ml.



(a)



(b)

Figure 54. Ecumicin is bactericidal against *M. tuberculosis* in murine macrophages. Bars represent *M. tuberculosis* CFU prior to treatment (T0) or after 7 days incubation without (untreated) or with rifampin (RMP) or ecumicin (ECM) at the indicated concentrations (μM). Values are means ± SD. According to Bonferroni's method (Godfrey 1985), significant differences ($P < 0.01$) were observed between untreated and each ecumicin treated group, T0 and ECM 1.2, and T0 and ECM 0.12.

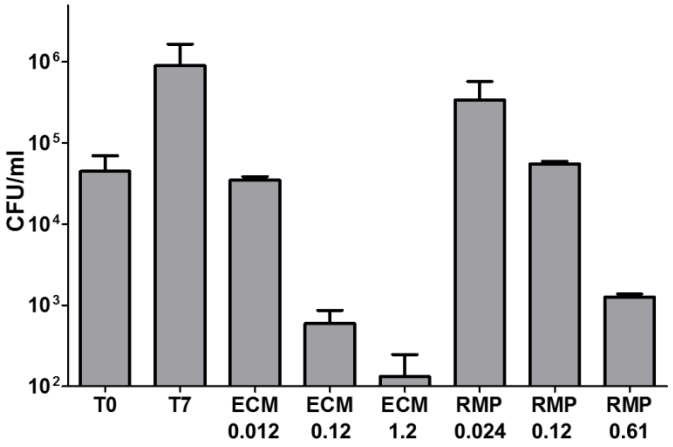


TABLE XIII. ECUMICIN MICS (μM) AGAINST CLINICALLY-ISOLATED *M. TUBERCULOSIS* CLADES, REPRESENTING WORLD-WIDE GENETIC DIVERSITY.

M. tuberculosis Lineage	Geographical Location	Strain Code	MIC (μM)
$H_{37}Rv$	-	$H_{37}Rv$	0.38
Indo-Oceanic	East Africa, South East Asia, South India	X003899	0.23
East Asian	East Asia, Russia, South Africa	X004439	0.29
		X004244	0.13
Euro-American	Americas, Europe, North Africa, Middle East	X005282	0.14
		X005319	0.36
East African Indian	East Africa, North India, Pakistan	X001354	0.38

TABLE XIV. MIC (μM) OF ECUMICIN (ECM) VS *M. TUBERCULOSIS* CLINICAL STRAINS ISOLATED FROM PULMONARY TB PATIENTS HOSPITALIZED IN NATIONAL MASAN HOSPITAL, KOREA.

		INH	RMP	SM	KM	MOX	ECM
H37Rv		0.91	0.08-0.15	0.86	4.1	0.31	0.16-0.31
Pan-susceptible	S2	1.82	0.30-0.61	0.86	4.1	0.62	0.31
	S3	0.91	0.30	1.7	4.1	0.31	0.31
	S4	0.91	0.61	0.86	2.1	0.31	0.63
RMP-resistant	R3	0.91	>9.7	0.86	4.1	0.31	N.D.
	R4	0.91	>9.7	0.86	4.1	0.31	N.D.
MDR	1	15	2.4-4.9	6.9	4.1	0.31	0.31
	2	29	>9.7	3.4	4.1	0.62	0.31
	3	29	>9.7	3.4	4.1	0.62	0.31
XDR	1	>29	>4.9	>55	>66	>9.96	0.63
	2	>58	>4.9	14	>66	4.98	0.31
	3	>58	>4.9	14	>66	>9.96	0.63

TABLE XV. *IN VITRO* BIOLOGICAL ACTIVITIES OF ECUMICIN (ECM). RMP, RIFAMPIN; INH, ISONIAZID; MOX, MOXIFLOXACIN; SM, STREPTOMYCIN; KM, KANAMYCIN; CS, CYCLOSERINE; CAP, CAPREOMYCIN; RC, REPLICATING CULTURE (MABA); NRC, NONREPLICATING CULTURE (LORA); BSA, BOVINE SERUM ALBUMIN; FBS, FETAL BOVINE SERUM.

			ECM	RMP	INH	CAP	MOX	SM	KM	CS	PA-824
MBC (μM) vs. *M. tuberculosis* $H_{37}Rv$		RC	0.34	-	4.9	4.9	-	-	-	-	-
		NRC	1.5	-	8.4	8.4	-	-	-	-	-
MIC (μM) vs. *M. tuberculosis* (RC)	$H_{37}Rv$	0.5% BSA	0.16	0.08	0.29	1.9	0.05	1.2	2.1	-	< 0.08
		4% BSA	0.58	0.10	0.44	1.0	1.8	0.96	-	-	0.22
		10% FBS	0.36	0.23	0.22	4.5	0.47	3.2	-	-	0.47
	strains resistant to:	RMP	0.19	>1	0.47	3.4	0.11	0.72	-	-	0.06
		INH	<0.12	0.01	>8	7.5	0.11	0.48	-	-	0.06
		MOX	0.31	0.06	0.24	3.6	>8	0.49	-	-	-
		SM	<0.12	0.02	0.23	3.7	0.06	>8	-	-	0.18
		KM	<0.12	0.03	5.6	>16	0.12	3.1	>50	-	-
		CS	<0.12	0.01	0.42	3.8	0.12	0.89	-	> 100	-
		CAP	0.29	0.06	0.46	52	0.24	3.3	-	-	-
	6 Global Clade Representatives		0.13-0.38	0.03-0.06	0.03-0.06	0.24-0.45	-	0.43-1.5	-	-	0.31-2.0
	Clinical isolates	3 Pan-susceptibles	0.31-0.62	0.30-0.61	0.88-1.8	-	0.30-0.62	0.86-1.7	2.1-4.1	-	-
		3 MDR strains	0.31	≥1.2	15-29	-	0.12-0.25	3.4-6.9	4.1	-	-
		3 XDR strains	0.31-0.62	>1.2	>15	-	≥1.9	≥14	>66	-	-
IC_{50} (μM)		Vero cell	>63	86	-	-	-	-	-	-	-
		J774	>32	-	-	-	-	-	-	-	-
MIC (μM) vs.		*E. faecalis*	>32	12	-	-	-	-	-	-	-
		P. aeroginosa	>32	0.10	-	-	-	-	-	-	-
		S. pneumonias	>32	0.05	-	-	-	-	-	-	-
		A. baumannii	>32	-	-	-	-	-	-	-	-
		E. coli	>32	-	-	>50	-	-	-	-	-
		S. aureus	>32	-	-	>50	-	-	-	-	-
		C. albicans	>32	-	-	>50	-	-	-	-	-
	Mycobacterium	*smegmatis*	1.7	12	49	0.48	-	0.48	-	-	-
		chelonae	0.97	-	-	-	-	-	-	-	-
		abscessus	>63	-	-	-	-	-	-	-	-
		kansasii	<0.24	-	-	-	-	-	-	-	-
		avium	0.35	-	-	-	-	-	-	-	-
		marinum	0.95	-	-	-	-	-	-	-	-

7.1.2 in vitro microsomal stability

The cyclic structure and *N*-methylation pattern of ecumicin is likely to contribute to the observed resistance to enzymatic degradation. After 30 min incubation with human or mice liver microsomes, ecumicin remained substantially unchanged (95% and 91% remaining, respectively).

7.1.3 in vitro permeability – Caco-2 assay

The permeability coefficients calculated from a Caco-2 cell assay were 16 nm/s apical to basolateral, and 28 nm/s basolateral to apical. This predicts poor to modest intestinal absorption and, serves to explain why initial attempts of direct oral administrations in mice have failed to produce detectable quantities in blood or lung tissue.

7.1.4 Material and methods

Activity vs. replicating *M. tuberculosis* $H_{37}Rv$, cytotoxicity, MIC against mono drug-resistant isolates and activity against non-replicating persistent *M. tuberculosis* were determined as described in Chapter 2 (2.3.2).

MIC against non-mycobacteria

MICs against *Escherichia coli* (ATCC 25922), *Staphylococcus aureus* (ATCC 29213), *Acinetobacter baumannii* (ATCC BAA-747), *Enterococcus faecalis* (ATCC 29212), and *Pseudomonas aeruginosa* (ATCC 27853) were determined by photometry at OD570 after 16 h incubation in 2.2 % Mueller Hinton II broth (Becton Dickinson, Sparks, MD, USA), for Streptococcus pneumonia (ATCC 49619) at OD490 after 20 h in 2.2 % Mueller Hinton II broth with addition of 2 % horse blood, and for *Candida albicans* (ATCC 10231) at OD570 after 48 h in 1 %

Cellgro RPMI 1640 media (Mediatech Inc., Manassas, VA, USA) with addition of 1.8 % d-(+)-dextrose (ICN Biomedicals, Aurora, OH, USA) and 3.5 % MOPS (Acros, NJ, USA). MICs were also defined as the lowest concentration resulting in > 90 % reduction in absorption relative to untreated control cultures.

MIC against non-tuberculous mycobacteria

MICs against *M. smegmatis* (ATCC 700084) and *M. abscessus* (ATCC 19977), were determined by the MABA in a manner similar to that used for *M. tuberculosis* except that cultures were incubated at for 72 h prior to addition of 0.6 mM resazurin and Tween 80 and then fluorescence was recorded after an additional 4 h of incubation. *M. chelonae* (ATCC 35752) and *M. marinum* (ATCC 927) were cultured in 7H9 media at 30 °C for 72 h and 120 h respectively. *M. avium* (ATCC 15769) and *K. kansasii* (ATCC 12478) were cultured in 7H9 media at 37 °C for 6 days and 7 days respectively. MIC against *M. bovis* BCG (ATCC 35734) was determined by the MABA.

Time and concentration-dependent bactericidal activity against *M. tuberculosis*

One test plate was prepared for the experiment according to the MABA protocol. A luciferase-expressing strain was used so that both luminescence and CFU readout could be obtained. CFU of initial bacterial inoculum was recorded as T0 CFU for comparison. The entire range of assay (ecumicin in three concentrations 1 × MIC, 10 × MIC and 100 × MIC plus bacterial control) was repeated nine times (9 ×) on the plate, so that the plate will allow the analysis of three time points.

On days 1, 7 and 14, luminescence of the sample plate was first recorded, and then the sample plate was used for CFU plating. Three repeats of entire range of assay were transfered

from the assay plate into 1.5ml microcentrifuge tubes (total volume 600 µL= triplicate × 200 µL in each well). Samples were centrifuged at 10,000 rpm for 2 min. Then supernatant was discanted carefully; then 600 µL media were added to the pellet for re-suspension. This wash step was repeated three times. The final re-suspension was ready for dilutions. A 50 µL aliquot of each sample was added onto the plates in duplicate (changing tips for every well). The plates were sealed with Petri-seal tape and incubated at 37°C for 3-4 weeks. Colonies were counted after incubation and recorded.

MIC against clinical isolates (including multi drug-resistant and extremely drug-resistant *M. tuberculosis*)

Twelve *M. tuberculosis* strains were utilized in this study; one reference (H37Rv) and 11 clinical strains isolated from pulmonary TB patients hospitalized in National Masan Hospital. All clinical strains were isolated and stored in the TB Specimen Biobank, National Masan Hospital. The clinical strains were identified as *M. tuberculosis* by both IS6110 specific PCR kit (Seegene, Seoul, Korea) and Antigen Test kit (SD, Seoul, Korea). Additionally, for purity assessment, all isolates were plated on blood agar plates and incubated for 3 days. When the purity was confirmed, the *M. tuberculosis* strains were evaluated for drug susceptibility by the agar proportion method for INH and RIF and by the absolute concentration method for injectable and fluoroquinolone (FQ) drugs. The DNA of *M. tuberculosis* strains were extracted from the bacterial colonies grown on Ogawa medium. The extracted DNA samples were used for molecular drug susceptibility tests (MTBDRplus and MTBDRsl, HAIN Lifesciences, Germany) against INH, RIF,

injectable, and FQ drugs. The *M. tuberculosis* strains freshly grown on 7H11 agar medium for 2 weeks were used for MIC.

The MICs of anti-TB drugs (INH, RIF, SM, KM, and Moxi) and ecumicin were measured by the MABA (Collins and Franzblau 1997) with a modification in which Alamar Blue was replaced with resazurin (0.6 mM). Each drug was tested in triplicate. The MIC was defined as the lowest drug concentration that prevented a color change from blue to pink.

MIC against genetically diverse *M. tuberculosis*

M. tuberculosis isolates collected from throughout the world have been grouped into six major SNP clusters (Filliol, et. al. 2006). MICs were determined by MABA against isolates from each cluster (total of six isolates) to ensure lack of major heterogeneity with respect to susceptibility. The isolates are X001354 corresponds to Indo Oceanic lineage, X004439 and X004244 to East Asian lineage, X005282 and X005319 to Euro-American lineage, and X001354 to East African Indian lineage. (Filliol, et. al. 2006)

Activity in macrophage culture

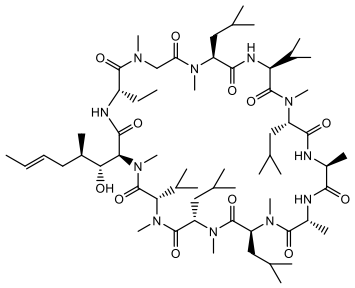
Inhibition of growth of *M. tuberculosis* Erdman (ATCC 35801) in a macrophage cell culture was assessed as previously described (Zhou, et. Al. 2010) except that cultures were not activated with interferon. Briefly, J774A.1 cells were cultured on 13 mm coverslips in 24-well plates, infected with *M. tuberculosis* Erdman, extracellular bacilli removed by washing and cultures incubated in DMEM containing ecumicin at 0.012, 0.12 and 1.2 µM, rifampin at 0.024 0.12 and 0.61 µM. All experimental conditions were set up in triplicate. At T0 (for untreated controls) and

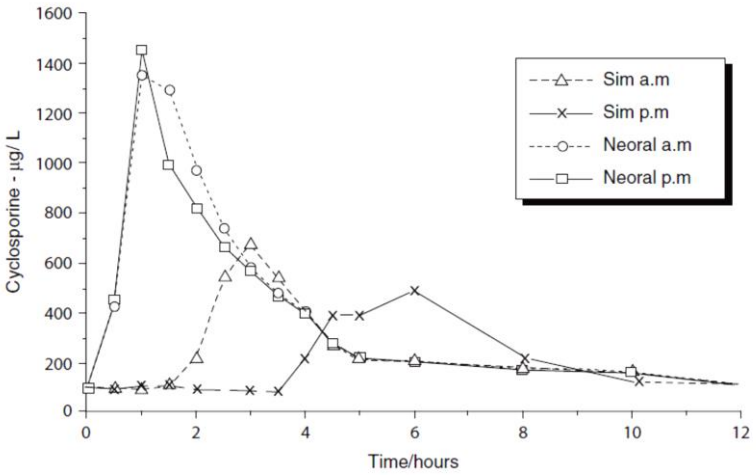
after seven days the incubation medium was removed and macrophages were lysed with 200 µl of 0.25 % SDS. After 10 min of incubation at 37 °C, 200 µl of fresh media were added. The contents of the wells were transferred to a microtube, sonicated (Branson Ultrasonics model 1510, Danbury, CT) for 15 s, and 1:1, 1：10, 1：100, and 1：1000 dilutions were plated on 7H11 (Difco) agar plates. Colonies were counted after incubation at 37 °C for two to three weeks.

7.2 Formulation development and animal studies

The initial development of a formulation for ecumicin was inspired by the successful case of cyclosporin A. Despite its violation of the generally accepted Lipinski's Rules, cyclosporin A (Figure 55a) is a hydrophobic cyclic peptidic immune-suppressant drug. Currently, cyclosporine A is marketed in a self-emulsifying drug delivery system (Neoral®), which has an improved oral absorption profile compared to the original suspension formula (Sandimmune®) (Figure 55b) (2008). Similar to cyclosporin A, ecumicin is also a hydrophobic cyclic peptide with *N*-methylations. As a result, suspension and emulsion formulations were prepared for ecumicin and were tested for oral-bioavailability in mice, despite Caco-2 assay results that suggested poor to moderate intestinal absorption. While very poor absorption, if any, was observed in mice with suspended ecumicin, some degree of absorption was observed for the emulsion. As the lung exposure with emulsion formulation was above ecumicin's MIC value, an efficacy study was carried out using an acute infection mouse model, but no efficacy was observed.

Subsequent experiments focused on parenteral administration as a prelude to a proof of concept efficacy study. The formulation development therefore focused on improving ecumicin's aqueous solubility. A copolymer micellar formulation was developed for this purpose.





(a) (b)

Figure 55. (a) Cyclosporin A. (b) Representative cyclosporine blood concentration profiles from a renal transplant patient given the currently marketed formulation Sandimmune® (SIM) versus the new Neoral® formulation, without (a.m.) and with food (p.m.).(Lawrence and Rees 2000)

7.2.1 Suspension

Inspired by cyclosporine A, the oral bioavailability of ecumicin in suspension was analyzed in a pilot pharmacokinetic (PK) experiment. Poor absorption was observed.

7.2.1.1 Formulation preparation

A total of 50 mg ecumicin was suspended in 2.5 ml of 12.5 mM HCl solution. The mixture was vortexed and sonicated to create an ecumicin suspension of 20 mg/ml.

7.2.1.2 Pilot PK study

7.2.1.2.1 Methodology

Eight healthy female BALB/c mice weighing approximately 20 g were used for this study. The mice were fed normally and had free access to water. To each mouse, 200 µl of ecumicin suspension was administrated orally, so the actual dosage was approximately 200 mg/kg. Experimental animals were humanely euthanized. Blood and lung tissue samples were collected at 1, 2, 3, and 4 h post treatment. Each sampling time point involved 2 mice.

Blood was centrifuged at 4,000 g for 20 min at 4 °C. Fifty microliters of resulting supernatant was mixed with 50 µl cold acetonitrile, and centrifuged again at 4,000 g for 20 min at 4 °C. The supernatants were diluted by 100-fold in acetonitrile and analyzed by LC-MS^2 on an ABSciex Q-trap 4000 instrument with an ESI ion source.

The lung samples were washed in phosphate buffer solution (PBS), dried with a towel paper, and weighed. To each gram of lung tissue 3ml PBS was added, and each sample was homogenized by sonication until the homogenate showed even consistency without any visible

chunks. The homogenate was centrifuged at 4,000 g for 20 min at 4 °C. An aliquot (50 µl) of resulting supernatant was mixed with 50 µl cold acetonitrile, and centrifuged again at 4,000 g for 20 min at 4 °C. The supernatant were diluted by 100-fold in acetonitrile and analyzed by LC-MS^2 on an ABSciex Q-trap 4000 instrument with ESI as ion source. A standard curve was built by analyzing acetonitrile solutions of ecumicin at different concentrations under identical analytical condition.

Samples were analyzed by HPLC (Shimadzu)-MS (AB SCiex QTRAP 4000), using a RP column (Xterra® C8, 2.5µm, 2.1 × 50 mm) and a bi-phase linear gradient. The flow rate was kept at 0.2 ml/min. After sample injection, mobile phase ramped from 50% acetonitrile (0.1 % formic acid) to 70 % in one minute; then in 4 minutes, ramped further up to 95% acetonitrile (0.1 % formic acid), and was kept at this concentration for 2 minutes; and finally re-equilibrated with 50% acetonitrile (0.1 % formic acid) for 2 minutes.

The MS^2 transition 800.6 (m/z) to 100.2 (m/z) was used to quantitate ecumicin, and an additional transition 800.6 (m/z) to 227.3 (m/z) was used for qualification. Reserpine was used as internal standard, and was quantitated by measuring the transition 609.3 (m/z) to 195.1 (m/z).

7.2.1.2.2 Result

The ecumicin concentrations in plasma samples were all below the instrument's limit of detection (LOD = 10 ng/ml), while ecumicin concentrations of lung samples were all below the instrument's limit of quantitation (LOQ = 30 ng/ml), suggesting very limited, if any, oral absorption of ecumicin in suspension.

7.2.2 Emulsion

Inspired by Sandimmune®, the oral bioavailability of ecumicin in emulsion was analyzed in a pilot pharmacokinetic (PK) experiment. Limited absorption was observed, but the lung exposure was above ecumicin's MIC value.

7.2.2.1 Formulation preparation

A total of 80 mg ecumicin was dissolved in 120 µl ethanol, which was subsequently added to 360 µl Labrafil M 1944 CS and mixed well. To this mixture 320 µl soy oil was added. The resultant solution (approximately 800 µl) was stored at 4 °C. Before administration, 3.2 ml deionized water was added to the solution. After inverting the container several times, a homogenous emulsion was achieved. Each ml of the emulsion contained 20 mg ecumicin.

7.2.2.2 Pilot PK study

7.2.2.2.1 Methodology

Fourteen healthy, female BALB/c mice weighing approximately 20 g were used for this study. Mice were fed normally and had free access to water. To each mouse, 200 µl of ecumicin emulsion was administrated orally, so the actual dosage was approximately 200 mg/kg. Experimental animals were humanely euthanized. Blood and lung tissue samples were collected at 0.5, 1, 2, 4, 6, 8 and 24 h post treatment. Each sampling time point per experimental phase is represented by 2 animals.

The blood and lung samples were processed and analyzed as described in 7.2.1.2.1

7.2.2.2.2 Result

Since all samples were diluted 100-fold prior to analysis, the ecumicin concentrations of all samples were below the instrument limit of quantitation (30 ng/ml, 100×LOQ = 3 μg/ml), except for the lung samples at 0.5 h, suggesting limited oral absorption of ecumicin in the emulsion formulation. However, ecumicin concentrations of lung tissue seemed to have remained well above its MIC value (0.26 μg/mlin 7H12 medium, 0.93 μg/ml at the presence of 4% BSA, TABLE XV) for 24 h post administration.

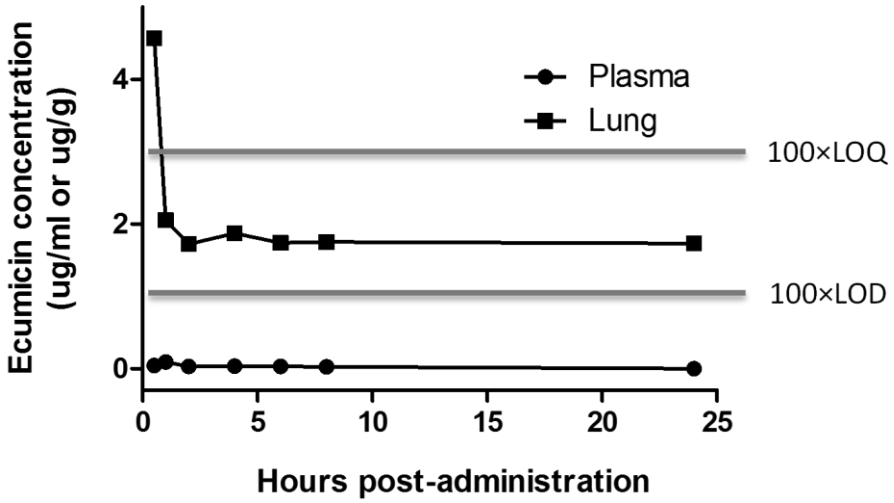


Figure 56. Limited oral absorption was observed for ecumicin in emulsion. All ecumicin concentrations were below the instruments limit of quantitation, except for lung tissue concentration at 0.5 h. The experiment gave a rough estimate of the absorption of ecumicin in emulsion.

7.2.2.3 Efficacy on an acute-infection TB mouse model

Although the plasma level of orally dosed emulsified ecumicin was very limited, the concentrations in the target organ (lung) were surprisingly high and seemed to have remained above the ecumicin MIC (0.26 μg/ml under regular test condition, 0.93 μg/ml at the presence of 4% BSA, TABLE XV) for 24 h post administration.

Following the PK experiment, ecumicin's efficacy was assessed in an acute TB-infected mouse model (Falzari, et al. 2005) using this formulation, but unfortunately no efficacy was observed.

7.2.2.3.1 Methodology

Eight-week-old female BALB/c mice were infected via aerosol with a suspension of 5×10^6 CFU of *M. tuberculosis* Erdman per ml by using a Glas-Col inhalation system. Ecumicin emulsion was prepared as described in 7.2.2.1, and administered by oral gavage in a maximum volume of 200 μl. Mice were treated daily during the acute phase of infection from day 10 until day 29 post-infection. Each treated group was composed of 7 mice.

The mice were sacrificed two days after the last day of treatment, and the lungs were removed, homogenized, and serially diluted 10-fold in HBSS. Fifty microliter aliquots of diluted lung homogenate sample were plated in duplicate on 7H11 agar. The plates were incubated at 37°C for 2 to 3 weeks and then CFU recorded.

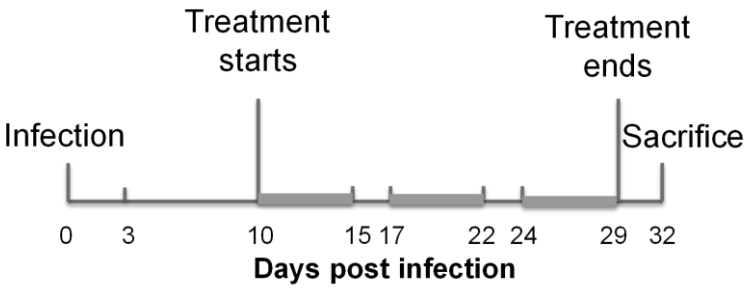


Figure 57. TB acute-infection mouse model.

7.2.2.3.2 Result

In preliminary tolerance tests, no signs of overt toxicity were observed in mice dosed orally at 200 mg/kg daily for five consecutive days. A preliminary evaluation of the activity of the ecumicin emulsion was performed in a low-dose aerosol infection mouse model, in comparison with 20mg/kg isoniazid and 10mg/kg rifampin (Figure 58). In conclusion, ecumicin in emulsion was not significantly active at 200 mg/kg po in this model.

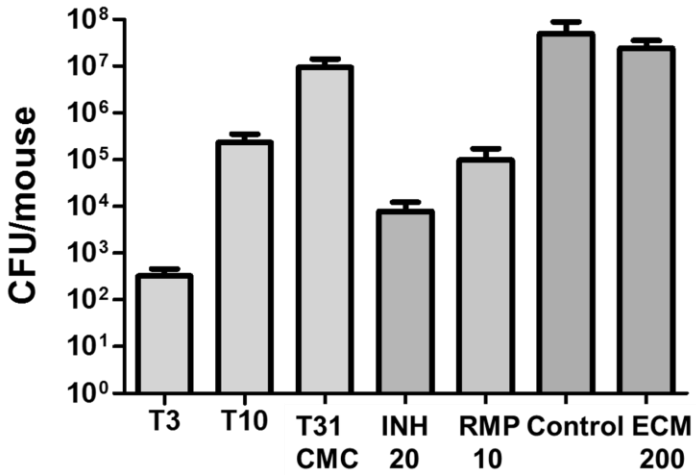


Figure 58. No significant anti-TB activity observed for ecumicin (ECM) in emulsion in an acute-infection mouse model. For all groups, n=7 except T3 (n=4). T3, untreated, sacrificed 3 days post-infection; T10, untreated sacrificed 10 days post-infection; T31 CMC, treated p.o. with 0.5% carboxymethyl cellulose (CMC); INH 20, treated p.o. with 20 mg/kg isoniazid in 0.5% CMC; RMP 10, treated p.o. with 10 mg/kg rifampin in 0.5% CMC; Control, treated p.o. with blank emulsion; ECM 200, treated p.o. with 200 mg/kg ECM. CMC, RMP 15, blank micelle, ECM 20, and ECM 32 mice were sacrificed 31 days post-infection. Values are means ± SD. Multiple comparisons among pairs were performed by Bonferroni's method (Godfrey 1985). There were significant differences between all ($P < 0.01$) except between T31, Control, and ECM 200 groups.

Failure to observe any efficacy with emulsified ecumicin might indicate that ecumicin is not active in vivo. However, as determined in the PK study, mouse lung concentrations between 1 h to 24 h falls between the LOD and LOQ, thus only indicating the presence of, but not the concentration of ecumicin in the lung sample but not the exact concentrations. The conclusion that the ecumicin concentrations in lung tissues remained above ecumicin MIC value, was weak. It is reasonable to assume that oral administration of ecumicin in emulsion did not achieve the required result in enough lung exposure, and therefore, cannot lead to any obvious efficacy.

7.2.3 Micellar nanoparticle

Because ecumicin has very poor oral absorption, efforts were made to develop a parenteral administration to be used in proof of concept efficacy studies. The formulation development, therefore, focused on improving ecumicin's aqueous solubility. A copolymer micellar formulation was developed for this purpose.

Block copolymers have a self-assembling tendency, as they usually have low critical association concentrations compared to low molar mass surfactants (Kwon, et al. 1995). Polymeric micelles resemble many properties of micelles formed by low-molecular weight surfactants. The assembled spherical micelle has a core-shell structure in aqueous solution. The core is formed by aggregation of hydrophobic segments, which is able to accommodate hydrophobic drugs. The shell consists of a protective brush-like corona of hydrophilic segments.

Polymeric micellar nano-particles possess several advantages, e.g. solubilization of poorly soluble molecules, sustained release, size advantages, and protection of encapsulated substances from degradation and metabolism (Croy and Kwon, 2006). In addition, targeting ligands can be attached for selective targeting, imaging moieties can be incorporated for tracking micelles *in vivo*, and pH-, thermo-, ultrasound-, or light-sensitive block copolymers can be used for controlled micelle dissociation and drug release (Oerlemans, et. al. 2010). Genexol-PM, nanoparticle formulation of paclitaxel, has been approved by FDA to treat breast cancer.

7.2.3.1 Formulation preparation

A number of polylactide (PLA) based amphiphilic block copolymer micelles have been used for solubilizing hydrophobic drugs (Le Garrec, et al. 2004, Kumar, et al. 2011, Fischer, et al.

2013). In this study, PLA was chosen as the hydrophobic segment of a block copolymer, due to its biocompatibility, degradability and nontoxicity. Polyethylene glycol (PEG) was chosen as hydrophilic segment for the same reason .

mPEG-PLA diblock copolymers were synthesized by ring-opening polymerization of D,L-dilactide by using mPEG(5) as initiator and stannous 2-ethylhexanoate as a catalyst (Lucke, et al. 2000). Briefly, D,L-dilactide was recrystallized in ethyl acetate at room temperature until the racemic mixture melting point was attained (124–126 °C), and mPEG(5) was used without further purification. The synthesized diblock copolymers were referred to as mPEG(x)-PLA(y), where x and y represented the weight-averaged molecular weight of the mPEG and PLA block in kDa.

mPEGx-PLAy was obtained by modulating the feed ratio of D,L-dilactide and mPEG. The molecular weight of the mPEG block was 5,000, and the desired molecular weight of the PLA block was 4,000.

To remove any trace of water, the starting materials [5 g of mPEG(5) and 4 g of D,L-dilactide] were each dissolved in 100 mL toluene in a round-bottomed flask. About 40 mL of toluene was distilled off. The water-free solutions were united in a three-neck flask, a precisely weighed amount of 25 mg stannous 2-ethylhexanoate was added, and the mixture was refluxed for 24 h at 120 °C under a nitrogen atmosphere. After the toluene was distilled off with a rotary evaporator, the residue was re-dissolved by the addition of an appropriate amount of chloroform, vigorously stirred and precipitated in diethyl ether at 0 °C, and then filtered. The precipitated polymer was dried in a desiccator at room temperature under high vacuum. After drying for 2 days, a white powder of the copolymer was obtained.

The synthesized copolymers were characterized with regard to their composition by ^{1}H-NMR. A Bruker DPX-400 instrument was used to obtain the spectra of the sample dissolved in $CDCl_3$. Figure 59 shows the ^{1}H-NMR spectrum of mPEG(5)-PLA(4). The peaks at 3.65 and 3.36 ppm corresponded to methylene units and terminal methoxy group in the mPEG block, signals at 1.58 and 5.18 ppm could be attributed to the hydrogen atoms of the methyl and methine groups for PLA segments, respectively. From the peak integrity ratio of their methylene and methyl groups, the mass ratio of repeating units in mPEG and PLA blocks was calculated to be 5:4.

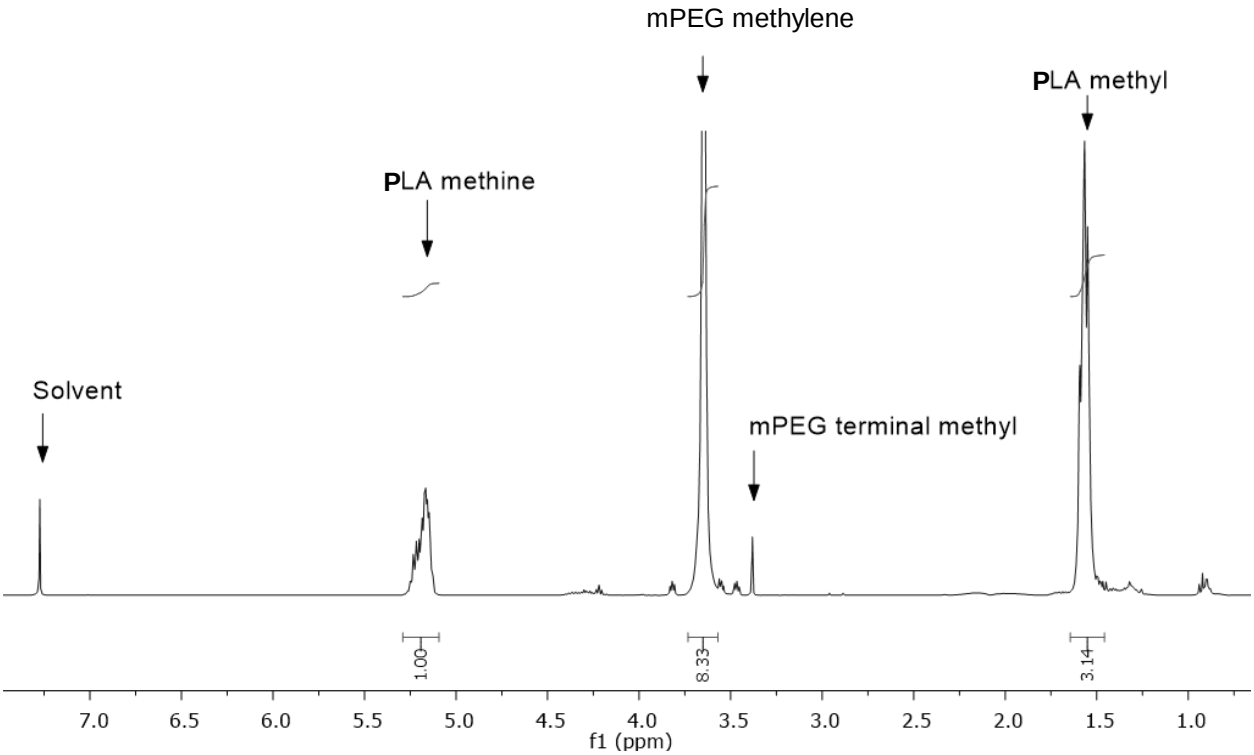


Figure 59. ^{1}H NMR spectrum of mPEG(5)-PLA(4) in $CDCl_3$.

Ecumicin loaded polymeric micelles (ECM-PM) were prepared by the dialysis method. Briefly, 10 mg mPEG(5)-PLA(4) was dissolved in 0.9 mL DMF, to which 1 mg ecumicin dissolved in

0.1 mL DMF was added. The solution was transferred to a dialysis bag (MWCO 3,500) and dialyzed against D.I. water for one day, changing the water frequently. The resultant clear solution in the dialysis bag was then lyophilized. To determine the drug loading content (LC, w/w %) and entrapment efficiency (EE, w/w %), an aliquot of dry micelles were dissolved in acetonitrile by sonication for 15 min, and the ecumicin content was measured by LC-MS^2 on an ABSciex Qtrap 4000 instrument. The LC and EE of the micelles were then calculated based on the following formula:

$$\text{LC (\%)} = \frac{\text{Mass of ecumicin extracted from freeze-dried micelle}}{\text{Total mass of freeze-dried micelle}} \times 100\%$$

$$\text{EE (\%)} = \frac{\text{Mass of ecumicin extracted from freeze-dried micelle}}{\text{Total mass of ecumicin initially used}} \times 100\%$$

The LC was found to be 5.03%, and the EE was 55.3%.

The average hydrodynamic radius of the micelles was determined by dynamic light scattering of another aliquot of dry micelles re-suspended in D.I. water. As shown in Figure 60, the average particle sizes were 51.5 nm, (STD = 9.5 nm, Vol = 96.6 %) and 691.1nm (STD = 105.0 nm, Vol = 3.4 %).

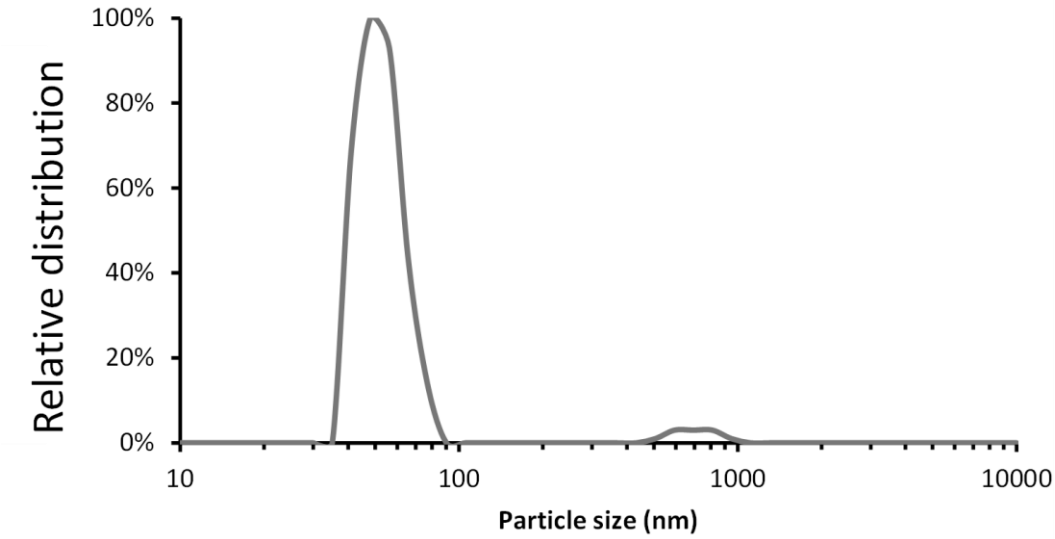


Figure 60. Particle size of ecumicin micelle formulation

The in vitro activity of this ecumicin micelle formulation was analyzed by the MABA assay against the *M. tuberculosis* H37Rv strain (TABLE XVI). ECM-PM was equally potent as free ecumicin in this assay.

TABLE XVI. IN VITRO ACTIVITY OF ECUMICIN MICELLE COMPARED WITH FREE ECUMICIN

Sample	MIC (μM)
ecumicin	0.06
ECM-PM dissolved in DMSO	0.08
ECM-PM dissolved in PBS	0.06
mPEG(5)-PLA(4)	>200 ug/ml

To test the drug loss during filtration, PBS solution containing 10 mg/ml ecumicin micelles (5% loading) was filtered through a 0.22 µm filter. A 2 µl aliquot of the resultant solution was dissolved in 998µl acetonitrile and centrifuged at 4000 g for 20 min. From each sample, the top 100 µl of supernatant was used for LC-MS^2 analysis by on an ABSciex Qtrap 4000 instrument. The result suggested that filtration removed 97% ecumicin from the solution, with 0.015 mg/ml ecumicin left. This indicates that sterilization by filtration is not suitable for this formulation. To ensure that the final PBS solution was sterile and suitable for repeated parental dosing, ecumicin micelles used in mouse studies were prepared in clean hoods.

7.2.3.2 PK study

7.2.3.2.1 Intravenous administration

7.2.3.2.1.1 Methodology

Ecumicin micelles were prepared as described (see 7.2.3.1), and stored at -20^{o}C, and was re-suspended in sterile saline to achieve a final ecumicin concentration of 0.7 mg/ml before use.

Twelve healthy male CD-1 mice weighing approximately 28 g were involved in this study. Mice were fed normally and had free access to water. To each mouse, 200 µl of ecumicin suspension was administrated via i.v., so the actual dosage was approximately 5 mg/kg. The animals were humanely euthanized. Blood and lung tissue samples were collected at 0.5, 1, 2, and 4 h post treatment. Each sampling time point per experimental phase is represented by 3 animals. The blood and lung samples were processed and analyzed as described in 7.2.1.2.1. The standard curve was established by spiking acetonitrile solution into blank mice plasma or lung homogenate.

7.2.3.2.1.1 Result

After a single intravenous (i.v.) administration of 5 mg/kg body weight, ecumicin was eliminated from plasma with a distribution half-life of approximately 30 min, and showed a terminal half-life of 3 h (Figure 61). Concentrations in lung ranged from 1.5–2.8 µg/g. Areas under the curve for concentration versus time ($AUC_{0\rightarrow 4h}$) were 9.6 and 8.9 mg·h/ml for plasma and lung tissue, respectively.

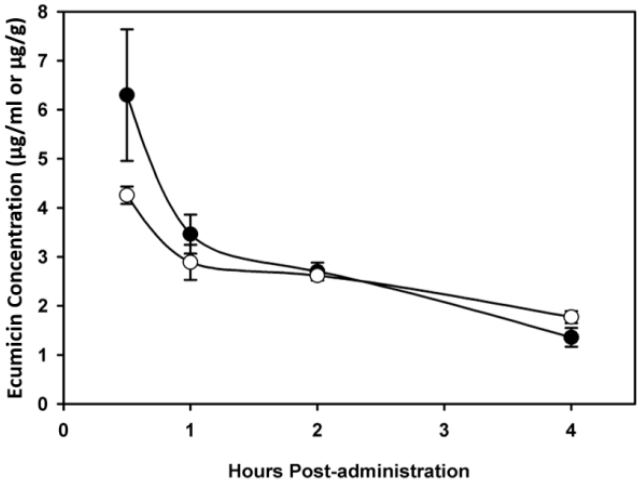


Figure 61 Mean plasma and lung tissue concentrations of ecumicin in mice (n = 3) after a single i.v. dose of ecumicin in mPEG-PLA formulation at 5 mg/kg. Solid circles, plasma; open circles, lung tissue.

7.2.3.2.2 Subcutaneous administration

7.2.3.2.2.1 Methodology

Ecumicin micelles were prepared as described (see 7.2.3.1), and stored at -20^{o}C, and was re-suspended in sterile saline to achieve a final ecumicin concentration of 0.7 mg/ml before use.

Fourty two healthy male CD-1 mice weighing approximately 28 g were involved in this study. Mice were fed normally and had free access to water. To each mouse, 800 µl of ecumicin suspension was administrated via s.c., so the actual dosage was approximately 20 mg/kg.

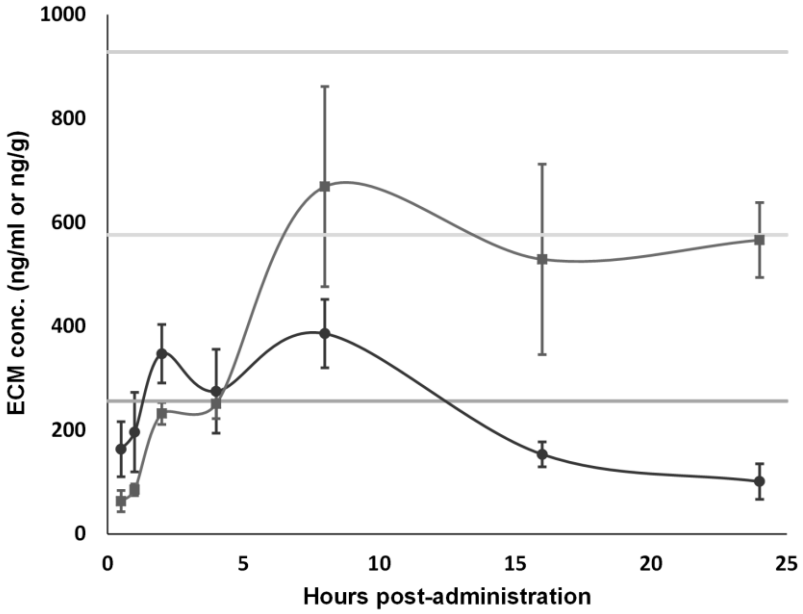
One group of animals (n = 21) were humanely euthanized after a single administration. Another group of mice (n = 21) received 5 daily administrations before being humanely euthanized. Blood and lung tissue samples were collected at 0.5, 1, 2, 4, 8, 16 and 24 h post treatment. Each sampling time point per experimental phase is represented by 3 animals. The blood and lung samples were processed and analyzed as described in 7.2.1.2.1. The standard curve was established by spiking acetonitrile solution into blank mice plasma or lung homogenate.

7.2.3.2.2.2 Result

After a single subcutaneous (s.c.) administration of 20 mg/kg of the micellar ecumicin, the maximum plasma concentrations (C_{max}) was reached at 0.30 – 0.40 µg/ml within 2 h, and this level was maintained at 8 h post-administration. In lung tissue, a plateau of 0.60 – 0.73 µg/g was achieved at 8 h post-administration, and maintained for 24 h. $AUC_{0\rightarrow 24hr}$ were 5.5 and 11.7 mg·h/ml for plasma and lung tissue, respectively.

Ecumicin in the micelle formulation appeared to accumulate in lung tissue when mice were administrated five consecutive daily s.c. doses of 20 mg/kg, achieving a range of 1.5–3.4 µg/g throughout the 24 h dosing interval following the last dose (Figure 62). This exceeded the MIC, even in the presence of physiological albumin (0.58 µM or 0.93 µg/ml).

(A)



(B)

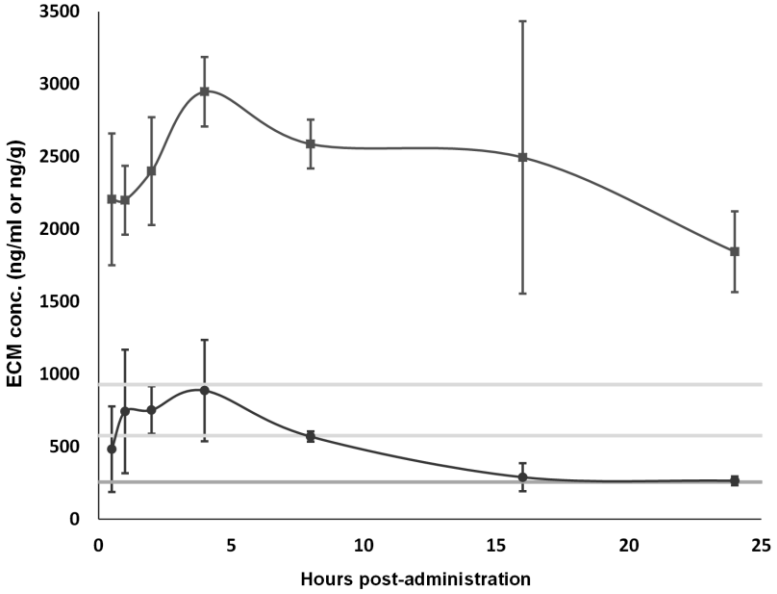


Figure 62. Plasma and lung exposures in mice (n = 3) following (A) single or (B) five daily s.c. doses of ecumicin at 20mg/kg. Solid circles, plasma levels; solid squares, lung levels. The three horizontal lines indicated ecumicin in vitro MIC at the presence of 4 % BSA (928 ng/ml), 10 % FBS (576 ng/ml) or 0.5 % BSA (256 ng/ml).

7.2.3.3 Tolerance tests

7.2.3.3.1 Single dose tolerance test

Five healthy BALB/c female mice weighing approximately 20 g were used in the single dose tolerance experiment. Six milligrams of micellar ecumicin and 10 mg of blank micelles were dissolved in sterile 5 % dextrose solution to yield a final concentration of 10 mg/ml, respectively. 1.5 ml of the ecumicin micelle solution was diluted to a final concentration of 5 mg/ml. The solutions were heated in a 50 °C water bath for 3 min to become clear. Two mice were each administrated i.v. 200 µl of 10 mg/ml micelle solution by (5 mg/kg ecumicin); one mouse was administrated i.v. 200 µl of 5mg/ml micelle solution (2.5 mg/kg ecumicin); and two mice were administrated 200 µl of 10mg/ml blank micelle solution (100 mg/kg micelle). The mice were observed for 15 min, immediately and 1 day after the administration. All mice survived and behaved normally at both time points.

7.2.3.3.2 Five-day tolerance test

Nine healthy BALB/c female mice of weights ranging from 20 to 30 g were used in the 5-day tolerance experiment (TABLE XVII). Stock solutions of 10 mg/ml and 20 mg/ml micellar ecumicin were prepared as described above (see 4.9.1.1). The 10 mg/ml solution was used for intravenous (iv, 5 mg/kg) administration every other day (qod), and subcutaneous (sc, 20 mg/kg) administrations daily (qd) or twice every day (bid). The 20 mg/ml solution was used for gavage (po) administrations (20 mg/kg, qd; 10 mg/kg, bid).

After five days, signs of toxicity were observed for mice treated via i.v. (qod), and s.c. (bid), e.g., less active, weak, ruffled fur and weight loss. However, sc (qd) and po (qd or bid) were tolerated well by tested animals.

TABLE XVII. 5-DAY TOLERANCE TEST WITH MICELLAR ECUMICIN IN BALB/C MICE.

Route	Dosing frequency	Vol. (µl)	Dosage (mg/kg)	No. of mice	Weight (g)		Toxicity observed at day(s)				
					Day 1	Day 5	1	2	3	4	5
iv	qod	200	5	1	30	25	-	-	-	Less active	Weight loss
				2	30	24	-	-	-	Less active	Weight loss
sc	qd	800	20	1	24	23	-	-	-	-	-
				2	24	23	-	-	-	-	-
sc	bid	800	20	1	29	27	-	-	Less active	Ruffled fur, weak	Ruffled fur, weak
				2	30	27	-	-	Less active	Ruffled fur, weak	Ruffled fur, weak
po	qd	300	20	1	25	24	-	-	-	-	-
po	bid	200	10	1	23	22	-	-	-	-	-
				2	23	22	-	-	-	-	-

7.2.3.4 Efficacy in an acute-infected TB mouse model

7.2.3.4.1 Material and method

The in vivo efficacy study was carried out as described in 7.2.2.3.1, with the following modifications (Figure 63). Briefly, BALB/c mice infected by aerosol inhalation with a low dose of *M. tuberculosis* Erdman and mice were treated on days 10-14, 17-21, and 24-25 post-infection with 20 or 32 mg/kg ecumicin by s.c. administration in a micellar vehicle. Forty-eight hours after the last treatment, mice were sacrificed, and viability of *M. tuberculosis* was determined by CFU from lung homogenates.

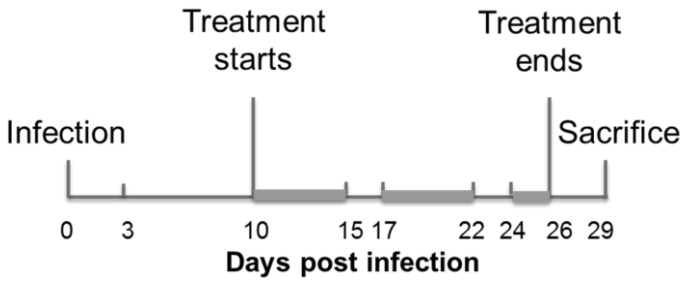


Figure 63. Timeline of TB acute infection model.

7.2.3.4.2 Result.

Compared with untreated groups, mice treated with 20 mg/kg and 32mg/kg ecumicin had reductions in *M. tuberculosis* lung CFU of $1.3\times\log_{10}$ and $1.6\times\log_{10}$ respectively (Figure 64). In the latter case, this represents essentially complete inhibition of growth. The micelle vehicle used in

this experiment was sufficient to demonstrate a proof-of-concept that ecumicin is active in vivo. However, although ecumicin demonstrates bactericidal activity in vitro, only bacteriostatic activity was observed in this in vivo study. Considering that ecumicin's in vitro bactericidal activity is time- and concentration-dependent (Figure 53), it is possible that with higher dosage or longer treatment time, ecumicin would show in vivo bactericidal activity.

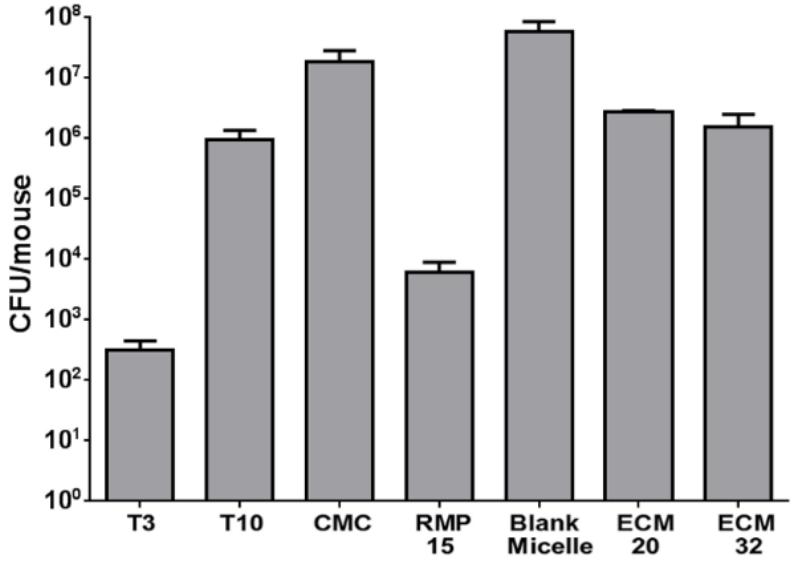


Figure 64 Twelve s.c. doses of micellar ecumicin (ECM) inhibit *M. tuberculosis* growth in the lungs of mice during acute infection. For all groups, n=7 except T3 (n=5) and RMP 15 (n=6). T3, untreated, sacrificed 3 days post-infection; T10, untreated sacrificed 10 days post-infection; CMC, treated p.o.with 0.5% carboxymethyl cellulose; RMP 15, treated p.o. with 15 mg/kg rifampin in 0.5% CMC; blank micelle, treated s.c. with 640 mg/kg blank micelle; ECM 20, treated s.c. with 20 mg/kg ECM; ECM 32, treated with 32 mg/kg ECM s.c. CMC, RMP 15, blank micelle, ECM 20, and ECM 32 mice were sacrificed 29 days post-infection. Values are means ± SD. Multiple comparisons among pairs were performed by Bonferroni's method (Godfrey 1985). There were significant differences between all ($P < 0.01$) except between T10, ECM 20 and ECM 32.

8. Target identification

8.1 Whole genome sequencing of ecumicin-resistant *M. tuberculosis* identified three potential targets.

Spontaneously-arising ecumicin-resistant mutants of *M. tuberculosis* H37Rv were selected in vitro to determine the frequency of mutation to resistance and to investigate ecumicin's mechanism of action. Single-step mutants at 1×MIC were selected at a frequency of 3×10^{-8}, then inoculated onto 7H11 plates with ecumicin at 2×MIC, and finally onto 7H11 plates with ecumicin at 4×MIC.

To investigate whether the phenotype of these resistant mutants of *M. tuberculosis* were specific for ecumicin, the parent strain and the resistant mutants were tested for sensitivity to a panel of antibiotics with various mechanisms of action. Based on their relatively high level of selective resistance to ecumicin (TABLE XVIII), four strains – *M. tuberculosis* ITR6, ITR7, ITR12 and ITR13 - were selected for whole genome sequencing.

TABLE XVIII. MIC (µM) PROFILE OF WILD-TYPE AND ECUMICIN (ECM)-RESISTANT *M. TUBERCULOSIS* STRAINS. RMP, RIFAMPIN; INH, ISONIAZID; CAP, CAPREOMYCIN; SM, STREPTOMYCIN.

		ECM	RMP	INH	CAP	SM	PA-824
M. tuberculosis H37Rv		0.16	0.08	0.29	1.9	1.2	<0.08
ECM-resistant *M. tuberculosis* strains	ITR6	1.5	<0.02	0.08	0.37	<0.06	<0.031
	ITR7	1.4	<0.02	0.12	0.49	0.08	<0.031
	ITR12	1.5	<0.02	0.12	0.91	0.89	<0.031
	ITR13	1.0	<0.02	0.07	0.42	0.16	<0.031

Comparison of the genome sequences of the four selected resistant strains with that of *M. tuberculosis* H37Rv revealed that the selected mutants all harbored non-synonymous mutations in *clpC1* (Rv3596c), *ppsC* (Rv2933) and *espG3* (Rv0289). All resistant strains had the same mutations to *espG3* (GGT>AGT; G191S) and *ppsC* (CAG>TAG; Q695stop), but harbored one of four mutations in the N-terminal Repeat I of *clpC1* (Kar, et al. 2008) that resulted in proline for leucine 96, serine or phenylalanine for leucine 92, or proline for alanine 95 (TABLE XIX). PCR and Sanger DNA sequencing confirmed mutations in all three genes of each resistant strain.

TABLE XIX. MUTATIONS OF *CLPC1* IN ECUMICIN RESISTANT STRAINS. ALL RESISTANT STRAINS HAD THE SAME NON-SYNONYMOUS CHANGES TO *ESPG3* (GGT>AGT; G191S) AND *PPSC* (CAG>TAG; Q695STOP).

Resistant Strain	Codon Mutation	Amino Acid Change
ITR1	TTG>TCG	L92S
ITR2	CGG>CCG	L96P
ITR3	CGG>CCG	L96P
ITR5	TTG>TCG	L92S
ITR6	CGG>CCG	L96P
ITR7	CGG>CCG	L96P
ITR8	TTG>TCG	L92S
ITR9	TTG>TTT	L92F
ITR10	TTG>TCG	L92S
ITR11	GCG>CCG	A95P
ITR12	TTG>TCG	L92S
ITR13	TTG>TCG	L92S

Previous studies have suggested that *clpC1* and *espG3* are essential for viability and infectivity of H37Rv (Brodin, et al. 2006, Raju, et al. 2012, Raju, et al. 2012), while *ppsC* is non-

essential (Lamichhane, et al. 2003, Rengarajan, et al. 2005, Griffin, et al. 2011). As the *M. tuberculosis* CDC1551 *ppsC* transposon mutant harboring a disrupted *ppsC* was found to be fully sensitive to ecumicin (TABLE XX), we concluded that PpsC is not the ecumicin molecular target.

TABLE XX. PPSC WAS NOT THE TARGET OF ECUMICIN (ECM). RMP, RIFAMPIN; INH, ISONIAZID; SM, STREPTOMYCIN; CAP, CAPREOMYCIN. *M. TUBERCULOSIS* CDC1551 *PPSC* TN MUTANT (NR-18565) WAS ACQUIRED FROM ATCC.

	MIC (μM) v.s.					
	ECM	RMP	INH	SM	CAP	PA-824
M. tuberculosis CDC1551 *ppsC* Tn Mutant	0.16	0.08	0.29	1.2	1.9	<0.08
M. tuberculosis H37Rv	0.16	<0.012	0.29	1.2	1.9	<0.08

8.2 Drug Affinity Responsive Target Stability (DARTS) determined supports ClpC1 as the target of ecumicin

To further examine potential targets, recombinant *E. coli* over-expressing recombinant mycobacterial ClpC1 and EspG3 (wild type and mutants) were tested for Drug Affinity Responsive Target Stability (DARTS) (Lomenick, et al. 2009).

Drug Affinity Responsive Target Stability is a general methodology for identifying and studying protein-ligand interactions, by using crude cell lysates and other complex protein mixtures (without requiring purified proteins), and native, unmodified small molecules. The technique is based on the principle that when a small molecule binds to a protein, the interaction stabilizes the target protein's structure such that it becomes protease resistant (Figure 65). (Lomenick, et al. 2009).

As shown in Figure 66, ecumicin failed to protect either the wild-type or mutated *M. tuberculosis* EspG3. Therefore, we concluded that EspG3 is not likely an ecumicin molecular target.

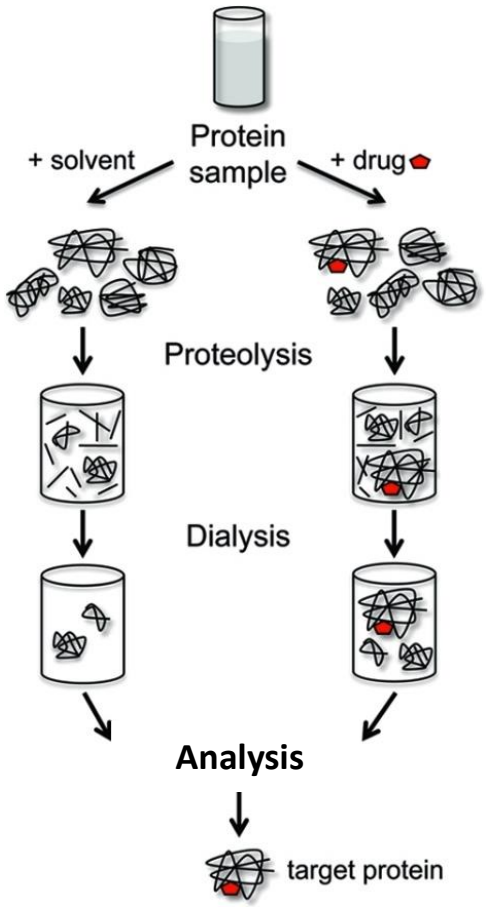


Figure 65 The basic strategy of DARTS.

Wild-type *M. tuberculosis* ClpC1 was found to be protected against pronase digestion by ecumicin treatment, and the protective effect positively correlated with ecumicin concentration (Figure 67). The protected protein band was excised and identified as ClpC1 by mass spectrometry. Such a protective effect was not observed for any of the four mutated ClpC1. This suggested ClpC1 being at least one of the molecular targets of ecumicin.

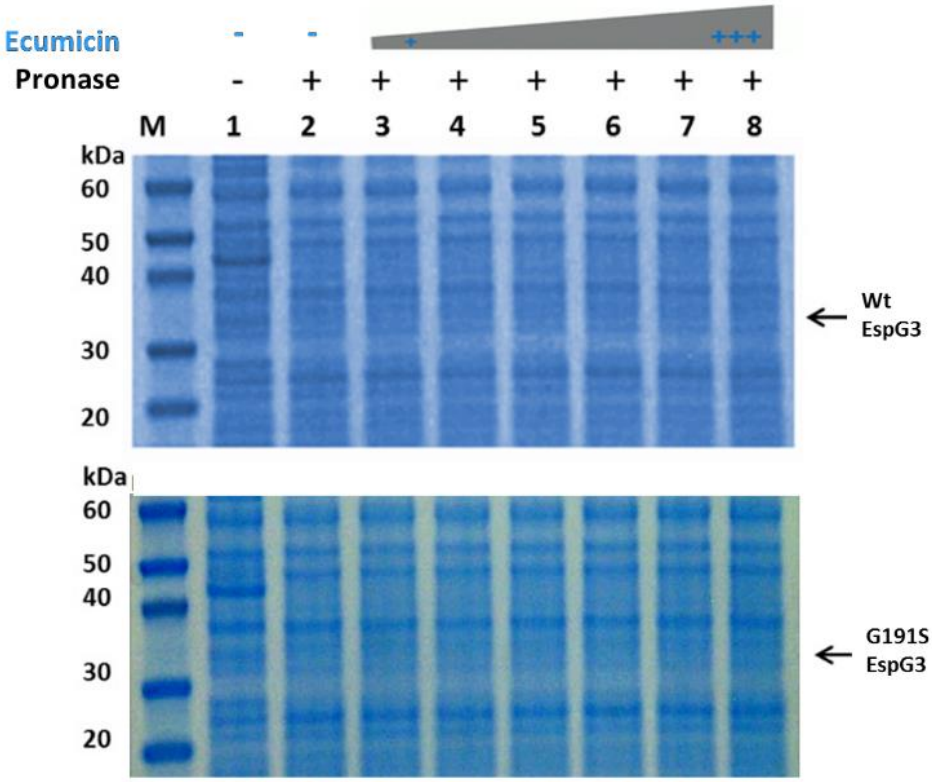


Figure 66. Ecumicin does not protect either wild-type or mutated *M. tuberculosis* EspG3. Recombinant *E. coli* BL21 over-expressing recombinant wild type or mutated *M. tuberculosis* EspG3 were lysed, treated with ecumicin at different concentrations, subjected to pronase digestion, and analyzed by SDS-PAGE. M, SeeBlue pre-stained standard; 1, whole cell lysate without any treatment; 2, whole cell lysate digested by pronase; 3-8, whole cell lysates treated with ecumicin at increasing concentrations (0.004,0.04, 0.4, 4, 40, and 80 µg/ml), and subjected to pronase digestion.

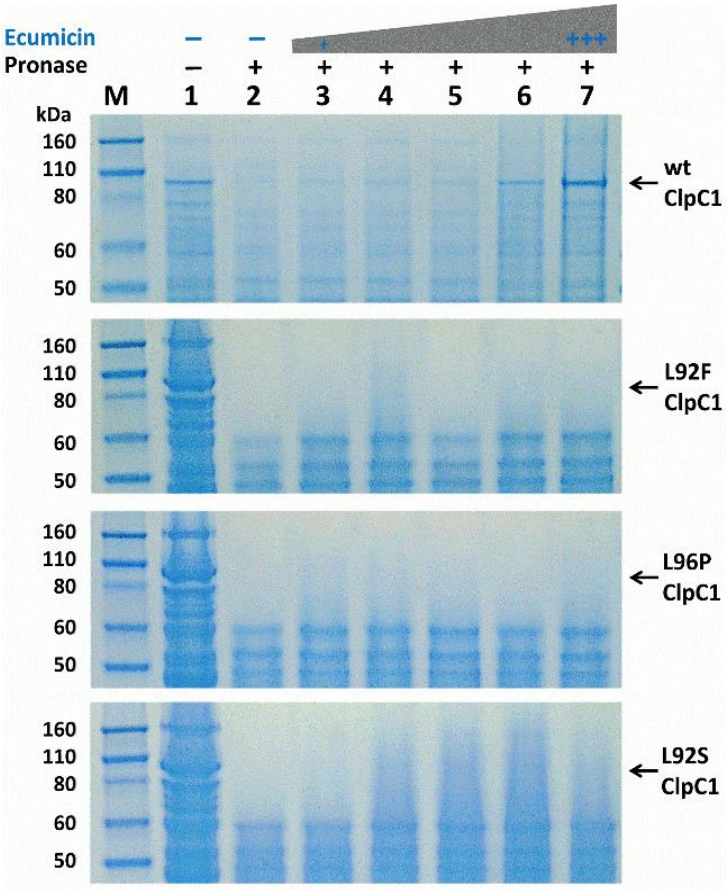


Figure 67. Ecumicin protects wild-type but not mutated *M. tuberculosis* ClpC1. Recombinant *E. coli* BL21 over-expressing recombinant wild type or mutated *M. tuberculosis* ClpC1 were lysed, treated with ecumicin at different concentrations, subjected to pronase digestion, and analyzed by SDS-PAGE. M, SeeBlue pre-stained standard; 1, whole cell lysate without any treatment; 2, whole cell lysate digested by pronase; 3-7, whole cell lysates treated with ecumicin at increasing concentrations (0.04, 0.4, 4, 40, and 80 µg/ml), and subjected to pronase digestion.

8.3 Biochemical studies confirmed ClpC1 as the target

ClpC1 (Figure 68) is a hexameric ATPase belonging to the large AAA family of ATPases (Hanson and Whiteheart 2005, Erzberger and Berger 2006), and in *M. tuberculosis* is an essential protein (Rengarajan, et al. 2005). ClpC1 associates with and supports ATP-dependent protein degradation by ClpP, a compartmentalized protease complex found in many bacteria, mitochondria, and chloroplasts (Lupas, et al. 1997, Yu and Houry 2007). In this process, ClpC1 binds certain cell proteins, unfolds, and translocates them into ClpP for degradation.

To determine whether ClpC1 is indeed the target of ecumicin in *M. tuberculosis*, and to clarify its mode of action, we tested if ecumicin directly affected the ATPase activity of ClpC1 purified from *M. tuberculosis*, as described recently (Akopian, et al. 2012). Surprisingly, ecumicin did not inhibit this activity, but instead stimulated the hydrolysis of ATP by several fold (Figure 69A). Addition of ecumicin did not change the specificity of ClpC1 as it could hydrolyze only ATP, but not CTP, GTP or UTP (data not shown).This activation occurs at low micromolar concentration (K_0 = 0.6 μM) and functions in a cooperative manner (Hill Coefficient = 1.7; Figure 69B). When mutated forms of ClpC1 from several ecumicin-resistant *M. tuberculosis* strains were cloned and expressed in *E. coli*, they showed similar ATPase activity to that of the wild-type enzyme, but very reduced stimulation by ecumicin (Figure 70A). These observations confirm that ClpC1 is the target of ecumicin in *M. tuberculosis* and that the changes in ClpC1 function are responsible for ecumicin's bactericidal action.

Using the same assay, cyclomarin, a smaller anti-*M. tuberculosis* peptide previously reported to target *M. tuberculosis* ClpC1 (Schmitt, et al. 2011), had no effect.

In mycobacteria, ClpC1 functions with ClpP1P2, a novel member of ClpP family found only in mycobacteria, where it is essential for viability (Akopian, et al. 2012). Therefore, ClpC1's ability to stimulate ATP-dependent degradation of the model substrate, FITC-casein, by ClpP1P2 was also analyzed in the presence of ecumicin. Surprisingly, even though ecumicin stimulated ATP hydrolysis, it caused a strong inhibition of ClpC1-dependent degradation of casein (Figure 71). Thus, the antibiotic uncouples ATP hydrolysis from protein degradation.

This unique target and mechanism predicts no cross-resistance with existing TB drugs, which is consistent with the observed data (TABLE XV). Interestingly, ecumicin did not affect the activity of a variety of purified ATPases (e.g. GroEL), including ClpX from *M. tuberculosis*, which also functions with ClpP1P2, and homologous AAA ATPases from *E. coli* (ClpA), archaea (PAN), and mammals (26S proteasome) (Figure 70B). This specificity and the fact that ClpC1 is essential only in mycobacteria can account for ecumicin's selective toxicity.

Figure 68. (A) Crystal structure of ClpC1 from *M. tuberculosis*. (B) Cyclomarin docked in ClpC1 from *M. tuberculosis* (Vasudevan, 2013).

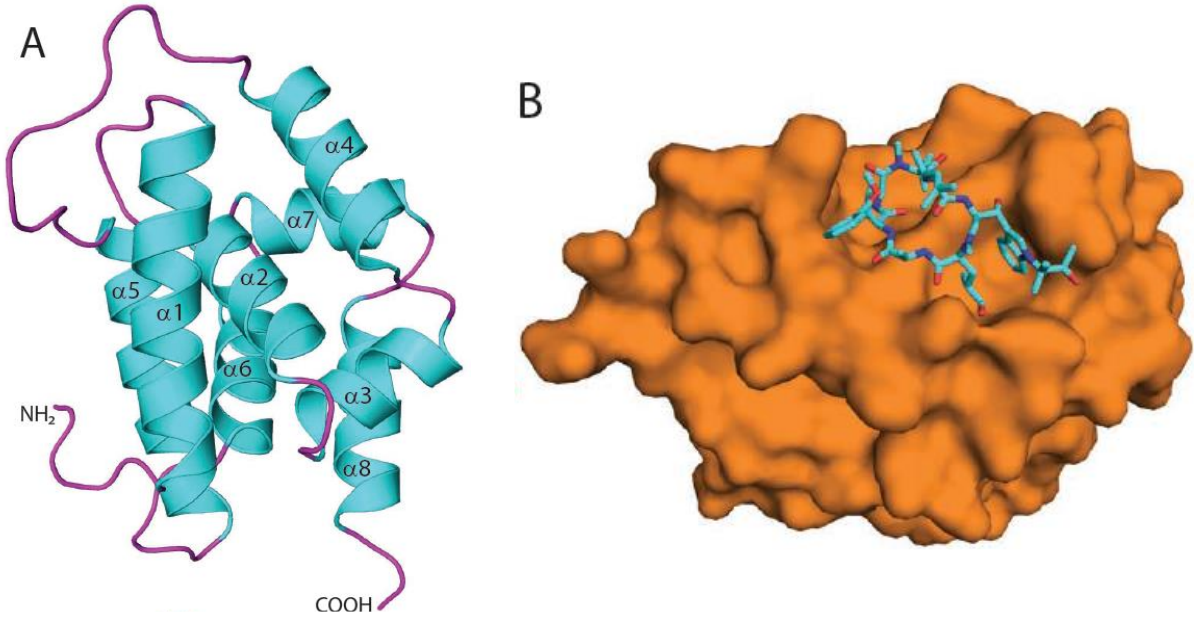
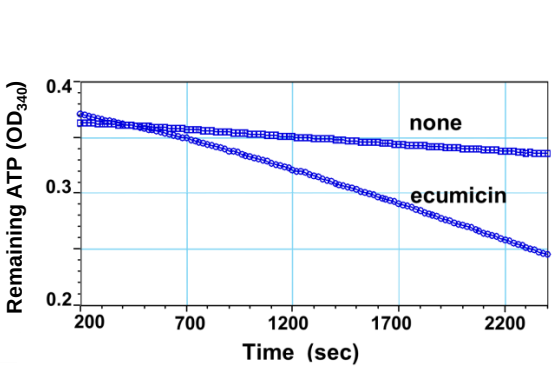
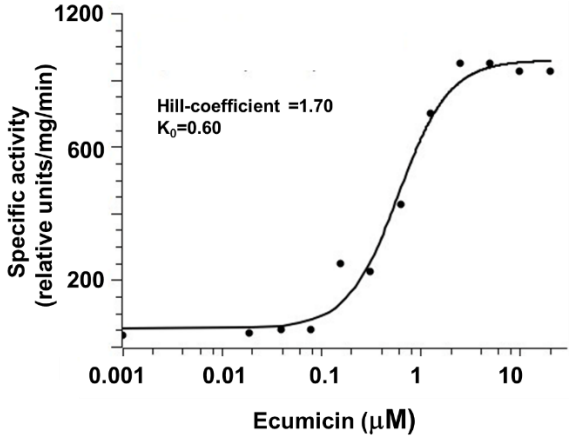


Figure 69. (A) Ecumicin enhances ATPase activity of wild-type ClpC1 derived from *M. tuberculosis*. Open circle, ecumicin 10 µM; open square, no ecumicin treatment. 2 µg of pure ClpC1 was mixed with 100µl of the assay buffer (50 mM TrisHCl pH 7.8; 100 mM KCl; 10% glycerol; 1 mM phosphoenolpyruvate; 1 mM NADH; 2 ml pyruvate kinase/lactic dehydrogenase (Sigma); 1 mM ATP) and the ATPase activity of ClpC1 was followed spectrometrically by NADH coupled assay at 340 nm. Similar results were obtained when the ATPase activity was measured with the Malachite Green method. (B) Hill Coefficient for Activation of ClpC1 by ecumicin. The K_0 and Hill-coefficient for ecumicin activation of wild-type ClpC1 ATPase were determined using curve fitting with classic Hill-kinetic through a Scaled Levenberg-Marquardt algorithm; tolerance 0.0001.



(A)



(B)

Figure 70. Ecumicin selectively activates wild-type ClpC1 derived from *M. tuberculosis.* (A) Ecumicin activates wild-type but not mutated ClpC1 from ecumicin-resistant strains. The ATPase activity of wild-type ClpC1 and mutant proteins isolated from ecumicin-resistant strains were measured as described in the absence and presence of 10µM ecumicin. The ATPase activity of each version of ClpC1 in the absence of ecumicin was taken as 100%. (B) Ecumicin activates *M. tuberculosis* ClpC1 but not several homologous AAA ATPases. The activities of purified AAA ATPases from several bacteria (*M. tuberculosis* ClpX; *E. coli* ClpA, and ClpB), archaea (PAN) and mouse (26S proteasome), as well as the activity of *E. coli* molecular chaperone GroEL were measured in the presence and absence of ecumicin (10 µM). ATPase activity of each ATPase in the absence of ecumicin was taken as 100%.

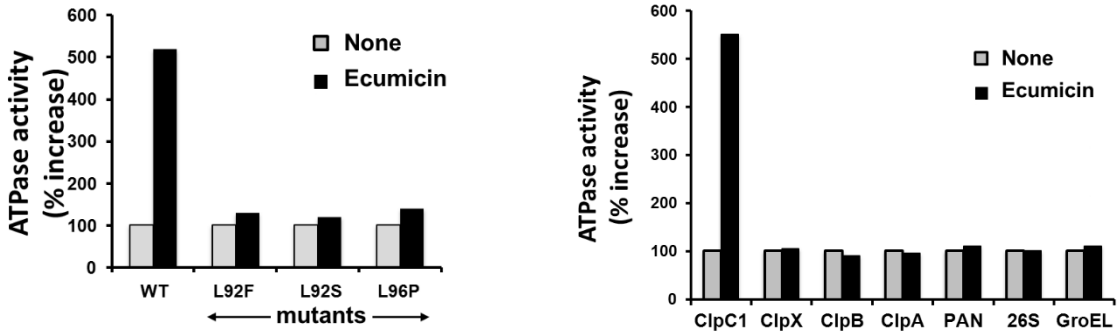
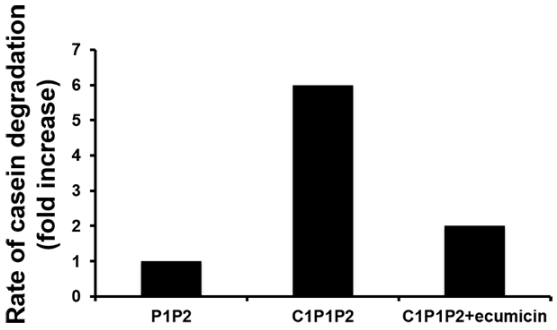


Figure 71. ClpC1 does not activate degradation of casein by ClpP1P2 in the presence of ecumicin. ClpP1P2 (100 nM) and ClpC1 (100 nM) were mixed in 80 µl of reaction buffer containing 50 mM potassium phosphate pH 7.6, 100 mM KCl, 8 mM MgCl2, 5% glycerol, 2mM ATP, 5mM Z-Leu-Leu. Protein degradation was measured fluorometrically using FITC-casein as a substrate in the presence or absence of 10 µM of ecumicin. Each result is the average of three independent experiments.



8.4 Discussion

Evidence from whole genome sequencing of ecumicin-resistant *M. tuberculosis*, DARTS analysis and biochemical studies all indicated that *M. tuberculosis* ClpC1 is the molecular target of ecumicin. Whole genome sequencing of these isolates also revealed common mutations in ppsC and espG3. The gene ppsC encodes the phthiocerol synthesis polyketide synthase type I PpsC, which is involved in the elongation of either C22-24 fatty acids by the addition of malonyl-CoA and methylmalonyl-CoA extender units to yield phthiocerol derivatives (Camacho, et. al. 2001). That ppsC is a non-essential (Lamichhane, et al. 2003, Rengarajan, et al. 2005, Griffin, et al. 2011) gene and that M. tuberculosis CDC1551 ppsC transposon mutant was found to be fully sensitive to ecumicin, suggest that PpsC is unlikely the target. The gene espG3 encodes the ESX-3 secretion-associated protein EspG3, and is essential for viability and infectivity of H37Rv (Brodin, et al. 2006, Raju, et al. 2012, Raju, et al. 2012). While its function remains unknown, the analogous protein EspG3 in *M. smegmatis* is found to be one of the core Esx-3 components that is required for both mycobactin-mediated iron acquisition and EsxG and EsxH export (Siegrist, et. al. 2014). As ecumicin failed to protect either the wild-type or mutant EspG3, we conclude that it is unlikely that EspG3 is the target.

Studies on ClpC1 paralogs in *E. coli* (ClpA and ClpX) have suggested that these chaperone proteins recognize protein substrates, bind to them, unfold them, and translocate them into the proteolytic chamber composed of ClpP proteins (Figure 72). Unfolding and translocating protein substrate by ClpA or ClpX require ATP binding and hydrolysis (Yu and Houry 2007). Ecumicin is able to uncouple ClpC1's ATP hydrolysis from protein degradation. Presumably, the depletion of ATP and the failure to carry out the selective ATP-dependent degradation of key cell proteins

account for ecumicin's cytotoxic action. This mechanism of action is quite novel and distinct from that of existing anti-*M. tuberculosis* agents.

Since all ecumicin-resistant *M. tuberculosis* had mutations in the N-terminal Repeat I of *clpC1* (proline for leucine 96, serine or phenylalanine for leucine 92, or proline for alanine 95), it is possible that ecumicin has strong interaction with the N-terminal domain of ClpC1.

A recent publication (Vasudevan, et al. 2013) suggested that cyclomarin A (Figure 73) exerts anti-*M. tuberculosis* activity through binding to the *N*-terminal domain of *M. tuberculosis* ClpC1 and causing uncontrolled proteolysis by associated ClpP protease (Figure 68B). Although only subtle conformational changes of ClpC1 were observed, cyclomarin A binding stabilizes the *N*-terminal domain structure. It was proposed that such interaction reduces the flexibility of the linker between the two *N*-terminal repeats and leaves the ClpC1 tunnel open, which allows free access for larger proteins into the unfolding and proteolytic core of the Clp machinery. This process may eventually lead to cell death due to indiscriminate digestion of cellular proteins.

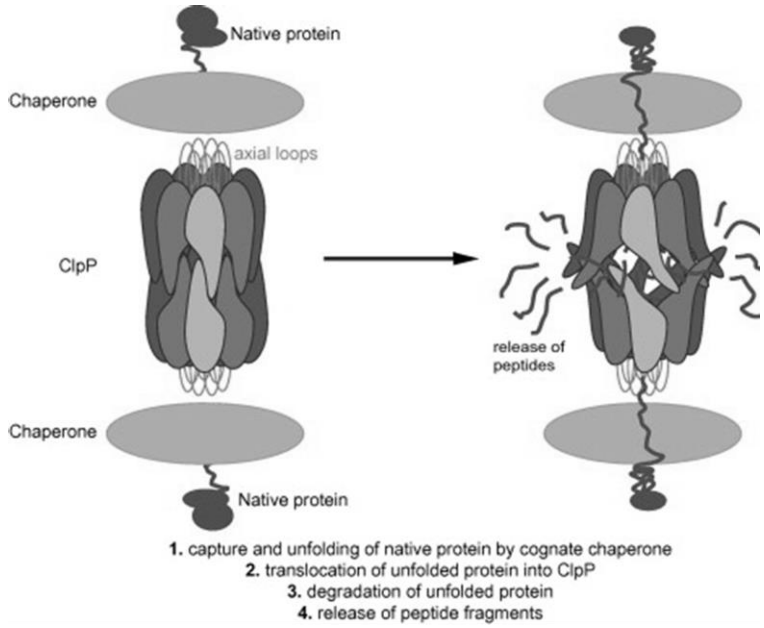
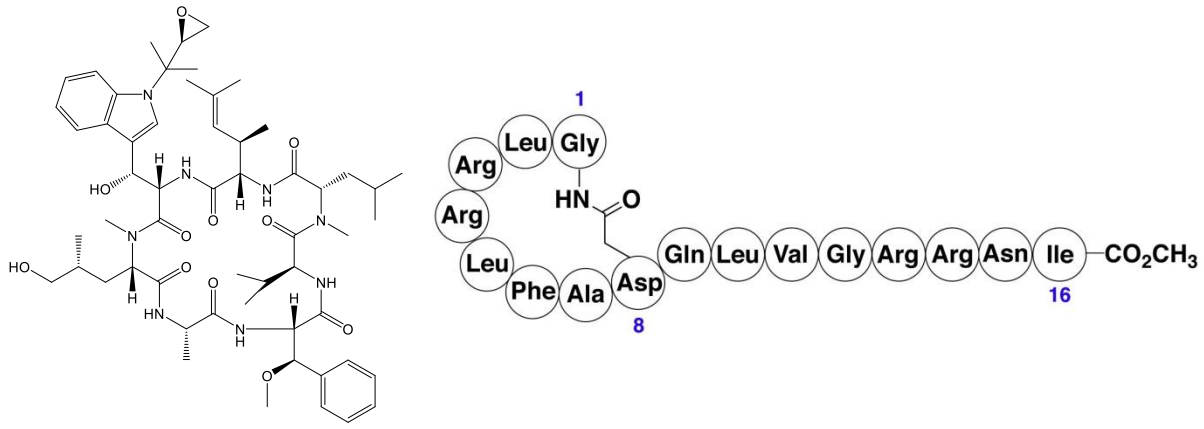


Figure 72 Model of ClpP mechanism of function. Shown is a cartoon model of the ClpP tetradecamer with the axial loops indicated. For simplicity, the chaperones bound to ClpP are drawn as simple ellipses. In the proposed model, substrate proteins are unfolded and then translocated into the ClpP cylinder by the bound chaperone. Unfolded polypeptides enter the ClpP proteolytic chamber through the axial pores which are lined by the axial loops. The polypeptide chains are then degraded into small peptides. The peptides are proposed to be released through axial pores that are transiently formed as a result of the dynamics in the handle region of the ClpP subunits. (Yu and Houry 2007)



Cyclomarin A Lassomycin

Figure 73 Structures of cyclomarin A and lassomycin.

Several pieces of evidence led us to propose that although ecumicin and cyclomarin A share the same target protein – mycobacteria ClpC1, they may bind to different binding pockets. While the key residues for cyclomarin binding are Phe^{2}, Phe^{80}, and Glu^{89}, key residues for ecumicin's activity include Leu^{92}, Ala^{95}, and Leu^{96}; while ecumicin promotes ClpC1's ATPase activity but inhibits the ClpC1P1P2 complex's proteolytic activity, cyclomarin A causes uncontrolled proteolysis by associated ClpP protease.

Another recently reported anti-*M. tuberculosis* cyclic peptide, lassomycin (Figure 73), also targets ClpC1 and acts by decoupling of ATPase activity and proteolytic activity (Gavrish, et al. 2014). Whereas ecumicin is a non-ribosomally encoded peptide with mostly non-polar amino acids, *N*-methylated amide bonds and a short three amino acid straight chain, lassomycin is synthesized ribosomally with many charged amino acids, no *N*-methylation amides and a long eight amino acid "spoke". Despite the pronounced differences in their structures, both peptides have similar mode of action. However, due to the differences in their structures, it is questionable if both peptides bind to ClpC1 at the same site.

Although lassomycin has demonstrated anti-*M. tuberculosis* activity in vitro, it might be difficult to prove its activity in vivo, as the eight amino acid "spoke" might be vulnerable to enzyme degradation, which is another distinguishing feature compared to ecumicin.

Considering the results of our mice efficacy study, ClpC1 appears to be an effective *M. tuberculosis* drug target in vitro and in vivo, and ecumicin may be a promising lead compound

8.5 Material and methods

Portions of this section were previously published under Antimicrobial Agents and Chemotherapy (Gao, 2014).

Selection of ecumicin-resistant strains of *M. tuberculosis*

Agar plates containing 1×, 2×, 4×, and 8× MIC against *M. tuberculosis* of ecumicin were prepared by adding an appropriate amount of compound to molten 7H11 agar media. *M. tuberculosis* $H_{37}Rv$, 10^9 colony forming units (cfu), was plated onto 1× MIC ecumicin containing 7H11 agar plates and incubated at 37°C for 3-4 weeks. Colonies that appeared on selection plates were phenotypically characterized, and representatives were re-streaked for isolated colonies onto 7H11 agar plates containing a 2-fold higher concentration of ecumicin. The process was repeated until no colonies appeared on selection plates. Resistance frequencies were determined by calculating the number of colonies arising on selective plates divided by the total CFU plated. Cells that grew upon 7H11 agar media with the highest ecumicin concentration (4× MIC) were inoculated into 7H9 liquid media and incubated at 37°C for 1-2 weeks. Harvested cells were washed with PBS and kept at -80°C.

Genomic DNA isolation and sequencing

Genomic DNAs of ecumicin-resistant *M. tuberculosis* strains ITR6, ITR7, ITR12, and ITR13 were isolated as described previously (Belisle, et al. 2009). Genomic DNA extracted from each of these *M. tuberculosis* strains and wild type H37Rv was prepared for sequencing on an Illumina HiSeq2000 instrument (Illumina, San Diego, CA). Initially, genomic DNA was sheared using a Covaris S2 focused ultrasonicator (Covaris, Woburn, MA) to a target peak size of 300 bp (intensity setting = 4, duty cycle = 10%, cycles per burst = 200, treatment time = 80 s, and temp = 7°C).

Subsequently, the sheared DNA was used to generate an Illumina library using the Apollo 324 NGS Library Prep System (Integenex, Pleasanton, CA) with the PrepX DNA kit. The system performs end repair, A-tailing, adapter ligation (with barcodes), and size selection. The final size distribution of the output library was 255-405 bp. The barcoded adapters were synthesized by BioO (NEXTflex DNA barcodes; BioO Scientific Corporation, Austin, TX). Individual libraries were quantified using the qPCR (Library Quantification Kit – Illumina, KAPA Biosystems, Woburn, MA) and pooled in equimolar amounts. Samples were purified using Agencourt AMPure magnetic beads (Beckman Coulter, Brea, CA) and re-quantified as above. The resulting pooled sample was sequenced on a single lane of a HiSeq2000 for 100 cycles from each end using a TruSeq SBS sequencing kit (V3) and analyzed with Casava1.8.2 (pipeline 1.9). The estimated error rate was 0.5 and 0.56% for the forward and reverse reads respectively. The raw sequence data were imported into the software package CLC Genomics Workbench (v5.5) as paired reads. Stringent trimming was performed (0.01 quality trimming threshold, no degeneracies allowed, and all sequences shorter than 100 bases after trimming were discarded). After trimming, approximately 5 to 11.5M reads were recovered from each sample. These reads were mapped to the reference genome of *M. tuberculosis* H37Rv (GenBank accession# NC_000962) using default assembly parameters (0.5 length fraction, and 0.8 similarity fraction) implemented within the CLC genomics workbench. Variants relative to the reference genome, including single nucleotide variants as well as insertions and deletions, were detected using the probabilistic variant detection routine within CLC genomics workbench. Parameters used included a minimum coverage of 50× and a minimum variant probability of 50%.

Drug affinity response target stability test

E. coli BL21-Gold(DE3) cells (Agilent Technologies), transformed with the plasmids containing DNA encoding *M. tuberculosis* ClpC1 or EspG3 (wild type and mutants) were grown in 1 ml LB media with 50 µg/ml kanamycin overnight (16 hours) at 37°C with shaking at 230 rpm. A new 1 ml LB culture (no drug) was inoculated from the overnight culture the next day. Cultures grew for 2 hours at 37°C with shaking at 230 rpm. Cultures were induced with 1 mM IPTG for 2 hours. After the induction period, cultures were placed on ice and mixed with NuPAGE 4× LDS Sample Buffer (Life Technologies). Samples were denatured at 95°C for 5 min and then electrophoresed on NuPAGE 4-12 % Bis-Tris gels in 1× MES SDS Running Buffer (Life Technologies). Gels were stained separately for both total protein with SimplyBlue SafeStain and His-tag specific protein with InVision His-tag In-Gel Stain according to the manufacturers protocols (Life Technologies). Protein size on the gel was estimated using the Novex Sharp Pre-stained or BenchMark His-tagged Protein Standard (Life Technologies). The expected size of the recombinant His-tagged proteins was approximately 95 kDa.

Each recombinant *E. coli* was lysed, treated with ecumicin at different concentrations, subjected to pronase digestion and analyzed by SDS-PAGE gel.

9. Ecumicin analogs from strain MJM5123

9.1 Introduction

9.1.1 Isolation of ecumicin analogs

The ecumicin-producing strain *Nonomuraea* MJM5123 also produces a number of ecumicin analogs, which are presumably synthesized by the same non-ribosomal peptide synthetase (NRPS). A preliminary HPLC analysis coupled with mass spectrometry suggested the existence of at least six such analogs (as indicated in Figure 74), all of which have similar activity to that of ecumicin (TABLE XXI).

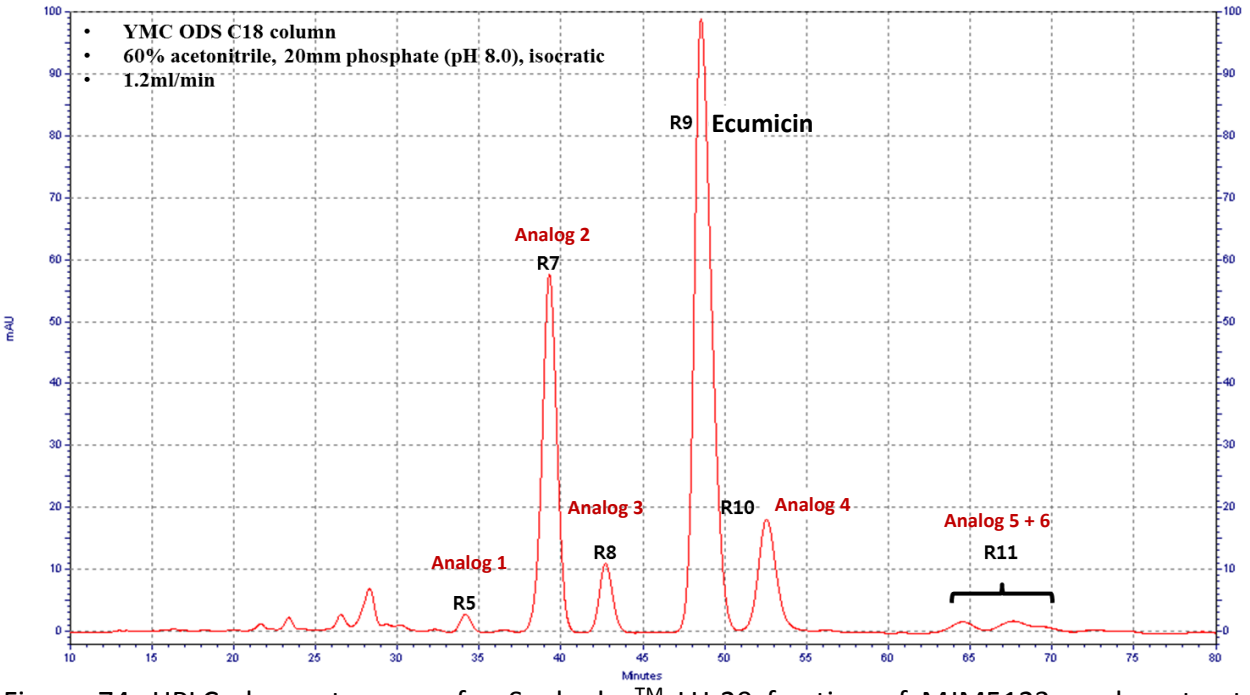


Figure 74. HPLC chromatogram of a Sephadex™ LH-20 fraction of MJM5123 crude extract. Column – YMC ODS-AQ (2.5µm, 10 × 250mm). Corresponding single charged pseudo molecular ions are R5 1584.9 (m/z), R7 1585.6 (m/z), R8 1569.1 (m/z), R9 (ecumicin) 1599.7 (m/z), R10 1583.1 (m/z) and R11 1613.8 (m/z).

TABLE XXI. SUMMARY OF ECUMICIN CONGENERS.

HPLC peak ID (from Figure 74)		**R5**	**R7**	**R8**	**R9**	**R10**	**R11**		
CCC fraction ID		H11	H12	H13	H14	H16	H17	H18	H20
W. W.		1585	1585	1569	1599	1583	1613		
Name		-	Norecumicin	Nordeoxyecumicin	Ecumicin	Deoxyecumicin	Homoecumicin-11I	Homoecumicin-13I	Homoecumicin-6I
MIC (μg/ml) vs. *M. tuberculosis*		<0.039	0.15	0.55	0.26-0.54	0.13	0.26		
AA sequence (*N*-terminus to *C*-terminus)	1	-	*N,N*-dimethyl-L-valine (*N,N*-Me_2-Val)						
	2	-	L-valine (Val^1)						
	3	-	*N*-methyl-L-valine (*N*-Me-Val^1)		*N*-methyl-L-allo-isoleucine (*N*-Me-Ile)				
	4	-	*N*-methyl-L-threonine (*N*-Me-Thr)						
	5	-	Threonine (Thr)						
	6	-	L-valine (Val^2)						L-isoleucine (Ile)
	7	-	*N*-methyl-L-leucine (*N*-Me-Leu)						
	8	-	L-valine (Val^3)						
	9	-	*N*-methyl-L-valine [*N*-Me-$Val^{(2)}$]						
	10	-	*N*-methyl-4-methoxy-tryptophan (*N*-Me-4-OMe-Trp)						
	11	-	L-valine (Val^4)					L-isoleucine (Ile)	L-valine (Val^4)
	12	-	Phenyl-L-serine (Ph-Ser)	L-phenylalanine (Phe)	Phenyl-L-serin (Ph-Ser)	L-phenylalanine (Phe)	Phenyl-L-serine (Ph-Ser)		
	13	-	L-valine (Val^5)				L-isoleucine (Ile)	L-valine (Val^5)	

By applying the ecumicin isolation protocol mentioned in Chapter 4 and including an additional preparative HPLC step, six ecumicin analogs were isolated and identified (Figure 75): norecumicin (peak R7 in Figure 74), nordeoxyecumicin (peak R8), deoxyecumicin (peak R10), homoecumicin-6I, homoecumicin-11I and homoecumicin-13I. The later three were components of peak R11 in Figure 74, and low in abundance – only sub-milligram amounts of samples were available from 110 L of optimized MJM5123 fermemtation. The structure elucidation of homoecumicin-13I, homoecumicin-11I and homoecumicin-13I was achieved with assistance from the group of Dr. Tobias Karakach at INB/NRC in Halifax (Canada), who host a Bruker 700 MHz NMR instrument equipped with a 1.7 mm cryoprobe.

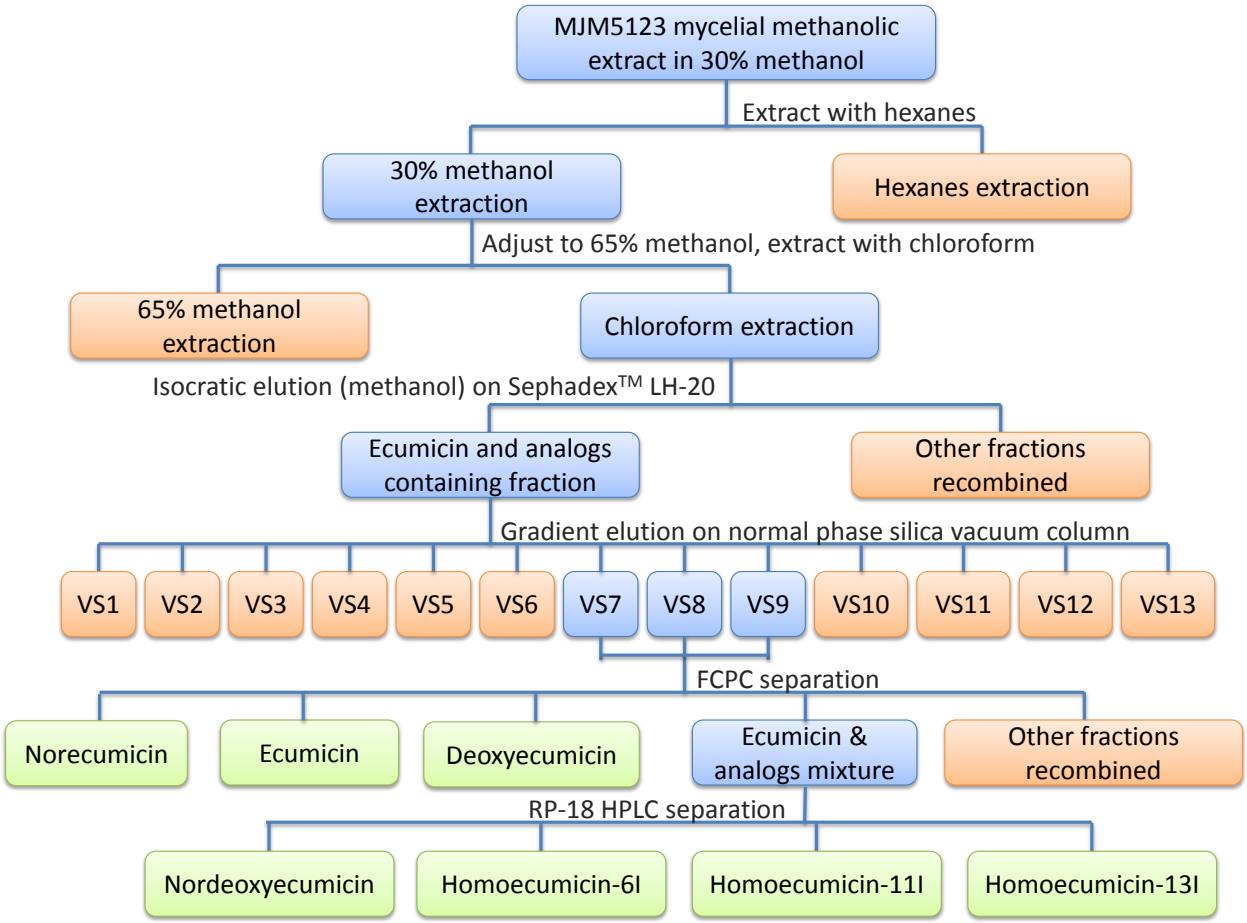


Figure 75. Separation scheme of ecumicin and its analogs.

9.1.2 NMR structure sequencing

Based on the assumption that the ecumicin congeners are synthesized by the same organism and presumably the same NRPS, and the small mass differences between them (14 amu and/or 16 amu), it is reasonable to assume that these peptides are structurally very similar to each other and exhibit only small structural differences, e.g. a methylene group (14 amu) or a hydroxyl group (16 amu). This was supported by the high level of similarity in the 1D- and 2D-NMR spectra of the compounds.

With the comprehensive knowledge on ecumicin's structure, and the availability of its HiFSA profile which provides a complete list of accurate proton chemical shifts (δ_H) and ^{1}H,^{1}H-coupling constants ($J_{H,H}$), we elucidated the structures of its analogs using a new method – NMR structure sequencing. This method analyzes each new peptide as a mixture of individual amino acid residues.

In peptide, each amino acid is separated by the amide bond, and, as a result, composed of one or more spin systems (Figure 76). As a result, 2D-TOCSY has been one of the most commonly used NMR experiments in peptide analysis. The ^{1}H NMR experiment, though usually yield highly complex ^{1}H spectrum with a peptide sample, has the advantage of being the most sensitive NMR experiment and easy to acquire. Without any ^{1}H,^{1}H-coupling between different amino acids, it is possible to study the ^{1}H sub-spectrum of individual amino acid residue without affecting the rest of the molecule. Study of ecumicin's HiFSA profile (see Chapter 5.4) suggests that the mathematical sum of all amino acid residues' sub-spectra would give rise to the ^{1}H

spectrum of the peptide, and therefore, further supports a possibility to study peptides as mixtures of individual amino acid residues.

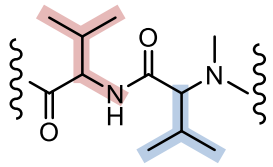


Figure 76. Each amino acid has its own spin system(s). Because of the amide bond, no $^{1}H,^{1}H$-coupling exists between different amino acids.

As all ecumicin congeners are structurally very similar peptides, subtraction of ^{1}H sub-spectra that correspond to mutual amino acid residues, would yield the ^{1}H sub-spectrum of the amino acid of difference. The characteristic pattern of this sub-spectrum would then lead to the identification of the amino acid of difference.

The position of the different amino acid can be determined by the 2D semi-selective HMBC experiment (see Chapter 5.2), or deduced by combining information from the NRPS gene (see Chapter 5.3) and ^{1}H NMR spectrum. The sequence and specificity of adenylation domains in the NRPS preclude the possibility of random connection of amino acids in ecumicin analogs. In addition, the ^{1}H sub-spectra of a certain type of amino acid residue usually share a same pattern, with variations on chemical shift values, which reflect the differences in each amino acid's surrounding chemical environment. The coupling constants are determined only by the spin

system, and would remain constant. As a result, the high level of similarity in the 1D-NMR spectra of all compounds suggests negligible variations in the chemical shifts of mutual amino acids, and, therefore, indicates minimal changes in their surrounding chemical environment, leading to the conclusion that the position of mutual amino acids remain unchanged in different peptides.

Briefly, the NMR structure sequencing method involves five sequential steps. First, ecumicin's HiFSA profile is used to match the experimental spectrum. Second, the whole spin system containing the "outlier" signals is removed from ecumicin's HiFSA profile, leading to a new HiFSA profile of only common amino acids. Next, subtraction of the HiFSA profile of only common amino acids from the experimental spectra would result in a ^{1}H sub-spectrum containing information about only the "different" amino acid, which leads to the structure elucidation of the "different" amino acid. Then, the location of the subtracted amino acid in ecumicin would predict the location of the "different" amino acid in new peptide. Finally, 2D-NMR spectra are analyzed to confirm the proposed structure.

This method was successfully applied in the cases of deoxyecumicin, norecumicin and nordeoxyecumicin (Chapter 9.1.2, 9.2.2 and 9.3.2). Although the ^{1}H NMR spectra of homoecumicin-11I and -13I were not as clear, their structures were elucidated with the help of early stage HiFSA calculations (Chapter 9.4.2 and 9.5.2). Homoecumicin-6I was an exception, as it was identified from a sample that contains at least four ecumicin-related peptides (Chapter 9.7.2). The high complexity of the ^{1}H NMR spectrum made it difficult to implement the NMR structure sequencing approach. However, the structure elucidation of homoecumicin-6I was based on the same basic ideas of this NMR sequencing method. Its 1D- and 2D-NMR spectra were

compared with corresponding spectra of other ecumicin-related peptides; attention was paid to the differences to construct the structure of the “different” amino acid and to identify its location in the peptide.

9.2 Deoxyecumicin

9.2.1 Isolation of deoxyecumicin (R10)

Deoxyecumicin (Figure 78) is one minor component of the anti-TB peptides produced by MJM5123. It was first isolated following the ecumicin isolation schemes as shown in Chapter 4 (also see Figure 75). The impurities in the sample were also ecumicin analogs, as identified by HR-MS and ^{1}H NMR experiments. The molecular weight of deoxyecumicin suggested that it corresponds to peak R10 in Figure 74.

The ^{1}H NMR spectrum of the deoxyecumicin sample (600 MHz, CD_3OD, **Figure 77**) was acquired under quantitative conditions (90 degree excitation pulse, acquisition time 5.4 s, relaxation delay 60.0 s) using a Bruker Avance 600 instrument. Processing used zero filling (2x), Lorentzian-Gaussian apodization (LB=-0.3, GB =0.05), and polynomial baseline correction.

The deoxyecumicin methyl doublet (δ_H 0.322 ppm) was isolated from an overlapping doublet (δ_H 0.332 ppm) by MNova using the line-fitting option. The de-convoluted methyl signal (δ_H 0.322 ppm) was selected as the most pure signal, and used to quantitate deoxyecumicin by applying the following integral-based 100% qHNMR method. The integral of the singlet was set to 3.000, representing the integral of three proton (3Hs). All other proton signals between δ_H 0.0 to 7.5 ppm in the spectrum, except for the solvent signals (HOD and CHD_2OD), were integrated, and the sum of these integrals was determined to be 217.7.

Assuming that deoxyecumicin has the same structure as ecumicin, it would contain a total of 125 non-exchangeable protons. Considering that all resonances not belonging to this molecule (i.e., the impurity signals) were typical peptide resonances, and assuming that they have the

same molecular weight as deoxyecumicin (i.e., isomeric impurities), the purity of this NMR sample was calculated as: Purity = 125×(3.00/3)/217.7×100 % = 57.4 %

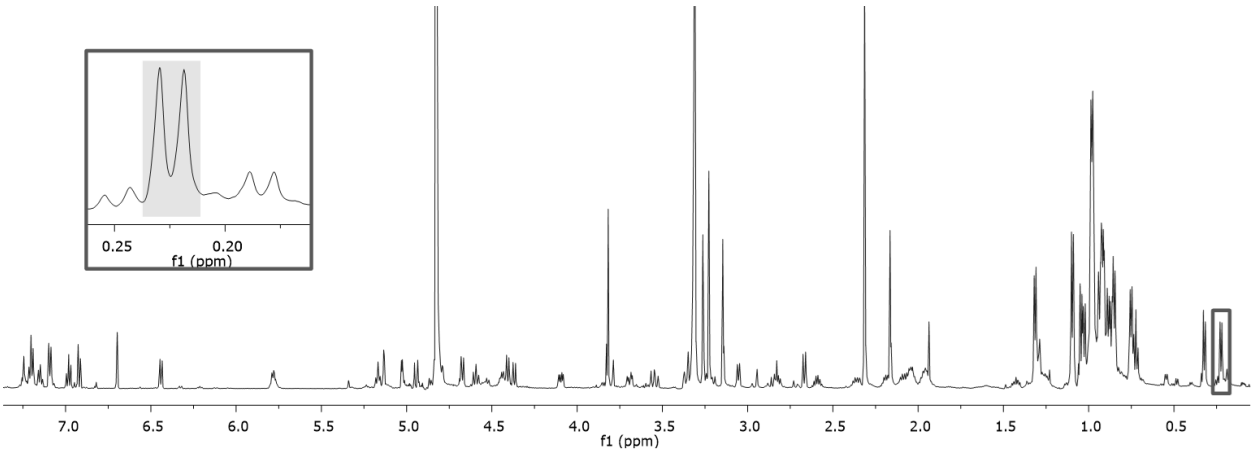


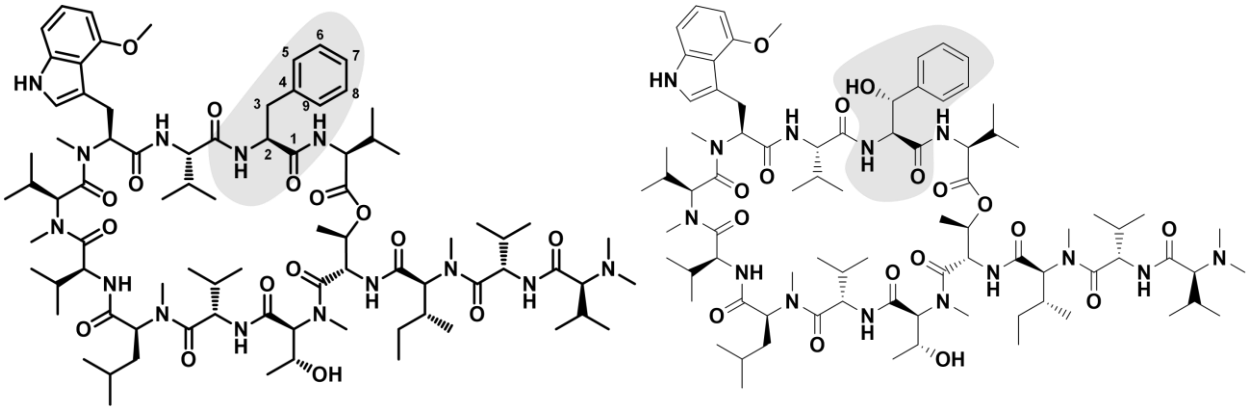
Figure 77. relative qHNMR analysis of deoxyecumicin sample.

Although the purity of this sample was low, the ^{1}H NMR signals were well dispersed. Structure elucidate was attempted on this sample without further purification.

9.2.2 Structure elucidation of deoxyecumicin by HiFSA-assisted approach

Deoxyecumicin (Figure 78) was isolated as a pale yellow powder. TABLE XXII summarizes the ^{13}C chemical shifts (δ_C), ^{1}H chemical shifts (δ_H) and $^{1}H,^{1}H$ scalar coupling constants (J_{HH}) of deoxyecumicin. Interpretation of ^{1}H NMR was done by ^{1}H iterative Full Spin Analysis, which led to the determination of accurate δ_H and J_{HH} values. As a result, all δ_H were reported with five decimals and all J_{HH} were reported with two decimals. High resolution mass spectrometry (Figure

79) revealed that deoxyecumicin has an exact mass of 1583.0055 amu, which is 16 amu less than that of ecumicin, indicating a possible structural difference of an oxygen atom.



(A) Deoxyecumicin (B) Ecumicin

Figure 78. (A) Proposed structure of deoxyecumicin. The molecular formula is $C_{83}H_{134}N_{14}O_{16}$. (B) Structure of ecumicin.

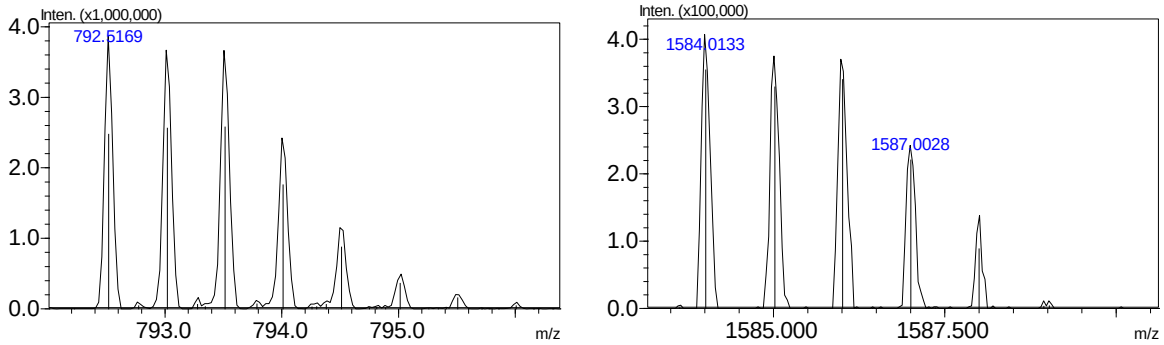


Figure 79. High-resolution MS spectrum of deoxyecumicin. $[M+2H]^{2+}$ 792.5169 (m/z), $[M+H]^{+}$ 1584.0133 (m/z). The exact mass of deoxyecumicin was calculated as 1583.0055 amu.

TABLE XXII ^{1}H AND ^{13}C NMR DATA OF DEOXYECUMICIN IN CD_3OD (600, 400 MHZ). INTERPRETATION OF ^{1}H NMR WAS DONE BY ^{1}H ITERATIVE FULL SPIN ANALYSIS.

Amino Acid		^{1}H δ in ppm(mult, J in Hz)	^{13}C δ in ppm
N,N-Me_2-V	1	-	173.35
	2	2.66806 (d, 9.03)	75.78
	3	2.07249 (dqq, 9.03, 7.33, 6.66)	28.49
	4,5	2.31402 (s)	42.4
	6	0.98065 (d, 7.33)	20.16
	7	0.85096 (d, 6.66)	19.4
l-V[1]	1	-	174.96
	2	4.67351 (d, 8.37)	55.76
	3	2.07249 (dqq, 8.37, 6.49, 6.58)	31.57
	4	1.04503 (d, 6.49)	19.48
	5	1.02684 (d, 6.58)	19.69
N-Me-l-*allo*-I	1	-	172.86
	2	4.94463 (d, 11.32)	61.6
	3	1.94906 (dddq, 11.32, 2.21, 7.00, 6.30)	34.42
	4	1.00008 (ddq, 2.21, -14.81, 7.10)	26.36
		1.26697 (ddq, 7.00, -14.81, 7.74)	
	5	0.75221 (d, 6.30)	19.36
	6	0.72352 (dd, 7.10, 7.74)	15.19
	7	3.22793 (s)	31.52
l-T	1	-	171.92
	2	5.13376 (d, 2.12)	53.37
	3	5.78360 (dq, 2.12, 6.54)	70.8
	4	1.31457 (d, 6.54)	17.8
N-Me-l-T	1	-	171.42
	2	5.02781 (d, 3.63)	63.92
	3	4.43548 (dq, 3.63, 7.13)	67.83
	4	0.88597 (d, 7.13)	19.89
	5	3.32014 (s)	35.28
l-V[2]	1	-	174.93
	2	4.82 (d, 9.22)	56.87
	3	2.35658 (dqq, 9.22, 6.60, 6.50)	31.84
	4	1.09561 (d, 6.60)	19.64
	5	0.98065 (d, 6.50)	19.7
N-Me-l-L	1	-	173.54
	2	5.16832 (dd, 7.43, 7.42)	56.8
	3	1.29169 (ddd, 7.43, -14.05, 1.87)	40.5

Amino Acid		^{1}H δ in ppm(mult, J in Hz)	^{13}C δ in ppm
		1.42565 (ddd, 7.42, -14.05, 5.78)	
	4	0.99420 (ddqq, 1.87, 5.78, 6.64, 6.64)	26.52
	5	0.224120 (d, 6.64)	21.96
	6	0.32176 (d, 6.64)	23.54
	7	3.26320 (s)	31.63
l-V[3]	1	-	173.63
	2	4.60155 (d, 9.22)	55.59
	3	2.038317 (dqq, 9.22, 6.41, 6.20)	32.74
	4	0.91467 (d, 6.41)	19.3
	5	0.86768 (d, 6.20)	19.48
N-Me-l-V	1	-	171.09
	2	3.05431 (d, 7.60)	71.6
	3	2.58779 (dqq, 7.60, 6.97, 6.51)	31.57
	4	0.98065 (d, 6.97)	19.75
	5	1.09561 (d, 6.51)	22.04
	6	3.14643 (s)	40.51
N-Me-4-OMe-l-Y	1	-	171.57
	2	4.09495 (dd, 11.17, 4.49)	71.09
	3	3.54716 (dd, 11.17, -13.59)	22.87
		3.69112 (dd, 4.49, -13.59)	
	4	-	113.3
	5	6.69763 (d, 0.87)	124.9
	6	-	156
	7	6.92071 (ddd, 0.87, 8.23, 0.90)	107
	8	6.98154 (dd, 8.23, 7.80)	124.3
	9	6.44080 (dd, 0.90, 7.80)	100.8
	10	-	140.9
	11	-	118.9
	12	3.81826 (s)	55.74
	13	2.16528 (s)	41.92
l-V[4]	1	-	174.11
	2	4.40704 (d, 8.33)	59.17
	3	2.18962 (dqq, 8.33, 6.03, 7.96)	33.62
	4	0.98065 (d, 6.03)	20.16
	5	0.98065 (d, 7.96)	19.79
	NH	-	-
l-F	1	-	174.29
	2	4.78000 (dd, 12.15, 10.60)	58.25

Amino Acid		^{1}H δ in ppm(mult, J in Hz)	^{13}C δ in ppm
	3	3.35000 (dd, 12.15, -14.13)	38.2
		2.84122 (dd, 10.60, -14.13)	
	4	-	140.9
	5,9*	7.09274 (dddd, 7.89, 1.29, 0.38, 1.86)	131.22
	6,8*	7.20245 (dddd, 7.89, 7.38, 1.98, 0.38)	130.47
	7*	7.14951 (dd, 1.29, 7.38)	128.3
l-V[5]	1	-	175.45
	2	4.36895 (d, 8.95)	59.36
	3	1.96594 (dqq, 8.95, 7.27, 6.83)	33.62
	4	0.93674 (d, 7.27)	19.54
	5	0.91992 (d, 6.83)	19.78

* Signals observed from an AA'MM'X spin system.

To maximize the amount of information obtained from the ^{1}H NMR spectrum of a new peptide before proposing a structure, the NMR structure sequencing method was applied. The resolution-enhanced ^{1}H NMR spectrum of deoxyecumicin, the X-ray crystal structure of ecumicin (CCDC ID 940680), and ecumicin's PERCH PMS text file was imported into the PERCH shell software. The ecumicin data was used as the predicted NMR parameters of deoxyecumicin. Only six δ_H values needed adjustment against the observed deoxyecumicin spectrum. Five were done manually by matching the splitting patterns; one (5.34 ppm, doublet) failed to match any resonances in the ^{1}H NMR spectrum and was left untouched. Iterative optimization was performed until a good agreement between the experimental and calculated spectrum was reached. This optimized ecumicin PMS text file will be referred to as deoxyecumicin's pseudo HiFSA profile.

As expected, the result (Figure 80) showed that β-proton signal of ecumicin's phenyl-serine unit (5.34 ppm, doublet) was missing from the ^{1}H NMR spectrum of deoxyecumicin. Although a doublet was found in deoxyecumicin's ^{1}H NMR spectrum at 5.34 ppm, its small integration (0.21 H, when deoxyecumicin's methyl signal at 0.22 ppm was set to 3 Hs) was a clear indication that this is a impurity signal. This "missing signal" led to the assumption that phenyl-serine unit does not exist in deoxyecumicin.

Additionally, three resonances (7.25, 3.35 and 2.84 ppm) that integrated for a little more than one proton each were only observed in deoxyecumicin's ^{1}H NMR spectrum, but not in the calculated spectrum. While resonances at 3.35 ppm and 2.84 ppm may belong to deoxyecumicin molecule, signal at 7.25 ppm is likely to belong to another ecumicin congener (as impurity) in the sample. The broad asymmetric singlet at 7.25 ppm resembles the overlapped phenylalanine proton resonances in ecumicin.

To remove the impact of the major impurity on analyzing the spectrum, HiFSA was performed again using the PERCH NMR software. This time, the ecumicin PMS text file was used as the predicted basic NMR values for both deoxyecumicin and the major impurity in the sample. As the ecumicin analogs were all postulated to have similar structures, the use of ecumicin to mimic the major analog impurity should be effective. Five δ_H values were manually adjusted for deoxyecumicin. For the impurity, δ_H values were manually adjusted as needed. Iterative optimization was performed until a good agreement between the experimental and calculated spectra was reached. This PMS text file will be referred to as deoxyecumicin's improved pseudo HiFSA profile.

As expected, the resonance at 7.25 ppm belonged to the impurity molecule. The new fingerprint file was able to find a good match for it.

Theoretically, subtraction of the spectra of common amino acids from deoxyecumicin's ^{1}H NMR spectrum would result in a clear sub-spectrum of the "different" amino acid unit in deoxyecumicin. However, as shown in Figure 82a, in real life, the subtraction resulted in a very noisy sub-spectrum. Considering that the deoxyecumicin sample was not pure, the noisiness of the subtraction was quite understandable. By the 100% qHNMR method, this sample contained approximately 5% non-peptidic impurities; the ratio of deoxyecumicin and the three closely related analogs was 100:35:18:14. Even though the major impurity was considered during the HiFSA process, singlet methyl signals of the minor ecumicin-related impurity could easily mask a one proton double of doublet (dd) signal of deoxyecumicin. A one-proton dd signal has four lines, so each line has the integration of approximately 0.25 H. A methyl singlet from the impurity that is only 18% of main compound would have the integration of 0.54 H. When the signals have similar line width, the methyl singlet from the minor impurity would create a background noise that is higher than a one-proton dd signal. Additionally, a tiny shift of the spectrum window that corresponds to only a few data points is possible when generating the 256k ^{1}H spectrum from a PMS text file. Such a tiny change will not be visible, but when doing a point by point subtraction of two 256k ^{1}H NMR spectra, it may create noise that is big enough to mask a double doublet signal.

As an alternative means of extracting the hidden information from the experimental ^{1}H NMR spectrum and determine the different amino acid, while avoiding the noise created by

spectral subtraction, we overlaid the spectra of common amino acids and deoxyecumicin's ^{1}H NMR spectrum (Figure 82b). This clearly revealed ^{1}H NMR profile of the "different" amino acid, as shown in expansion in Figure 82b. This amino acid unit has five aromatic protons (7.05 - 7.25 ppm), an α-proton (4.80 ppm, overlapped with an HOD peak), one signal at 2.84 ppm integrating for 1.5 proton and another at 3.35 ppm integrating for 1.8 proton. The latter two may serve as β-protons signals, but were overlapped with impurities' signals. This ^{1}H NMR profile suggested that deoxyecumicin has a phenylalanine where ecumicin has a phenyl-serine, and explained the 16 amu mass difference as the structural difference of a hydroxyl group.

The conclusion from NMR structure sequencing was supported by the DEPT-135 and ^{13}C NMR spectra of deoxyecumicin (Figure 83 and Figure **84**). The β-carbon signal of ecumicin showed up as a tertiary one at 72.97 ppm, while that of deoxyecumicin showed up as a secondary carbon at 38.20 ppm.

The proposed structure was further supported by COSY, HSQC, and HMBC NMR experiments. For fast structure elucidation, deoxyecumicin's 2D-NMR spectra were overlaid and compared with ecumicin's, as shown in Figure 85 to Figure **87**. COSY spectra comparison revealed the geminal coupling of deoxyecumicin phenylalanine's two β-protons, as well as the vicinal couplings between the α- and β-protons. The HSQC and HMBC comparisons confirmed the existence of all twelve common amino acids in deoxyecumicin and ecumicin, and supported the proposal that deoxyecumicin has a phenylalanine while ecumicin has a phenyl-serine.

Figure 80. Overlay of deoxyecumicin's pseudo HiFSA profile (blue) and experiemntal ^{1}H NMR spectrum of deoxyecumicin (red, 600 MHz, Bruker Avance 600).

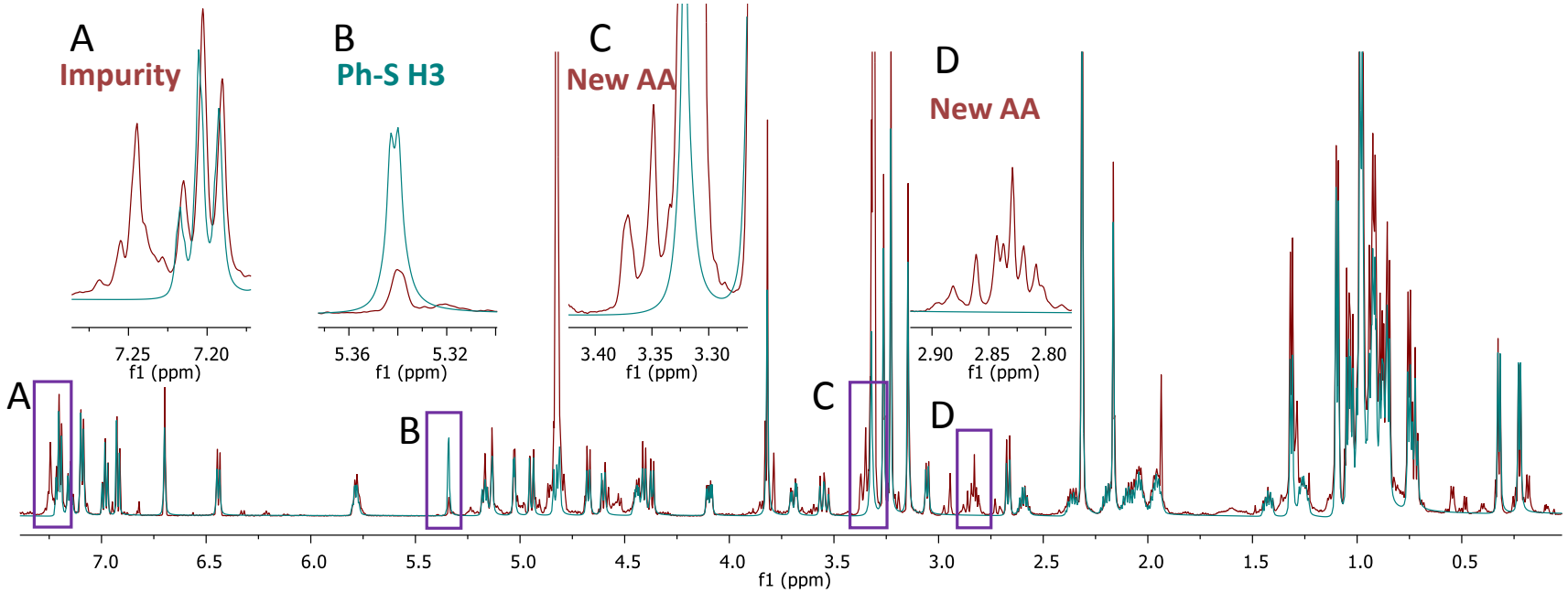


Figure 81. Overlay of the deoxyecumicin's improved pseudo HiFSA profile (blue) and 1H NMR spectrum of deoxyecumicin (red).

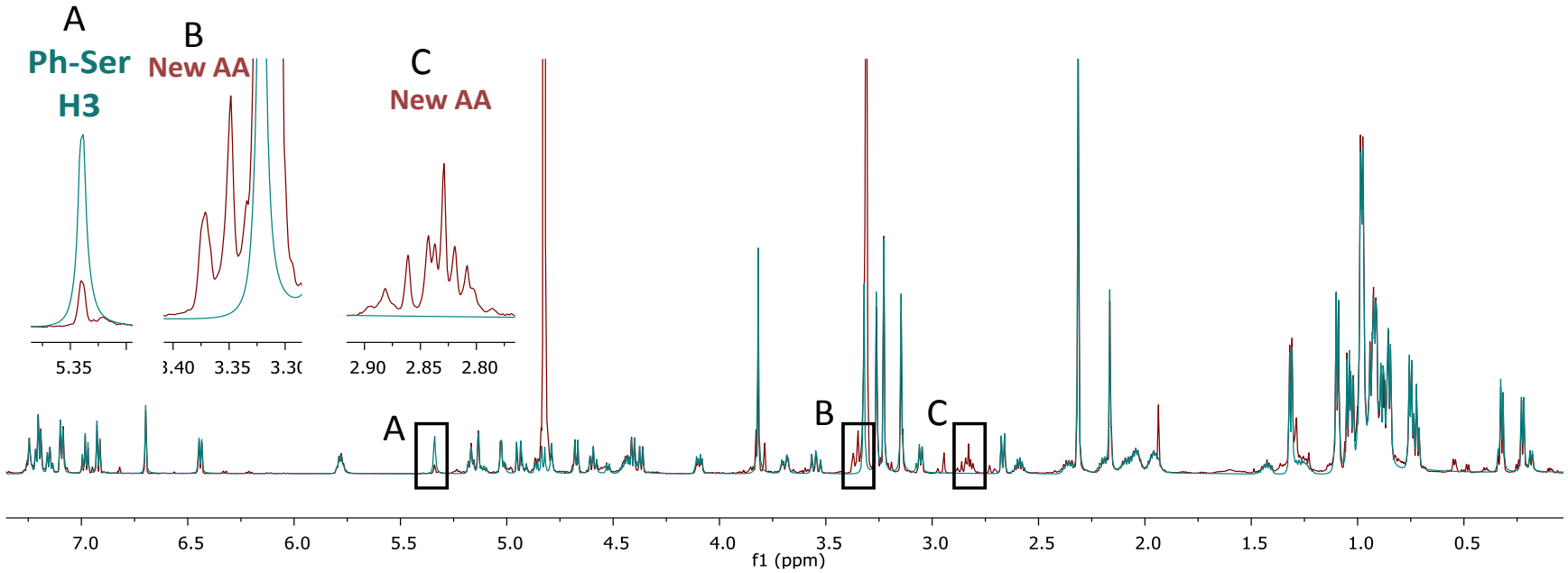


Figure 82. ^{1}H profile of the different amino acid in deoxyecumicin was presented as (a) subtraction of the spectrum of common amino acids from deoxyecumicin's ^{1}H NMR spectrum, and (b) overlay of the spectrum of common amino acids (blue) and deoxyecumicin's ^{1}H NMR spectrum (red).

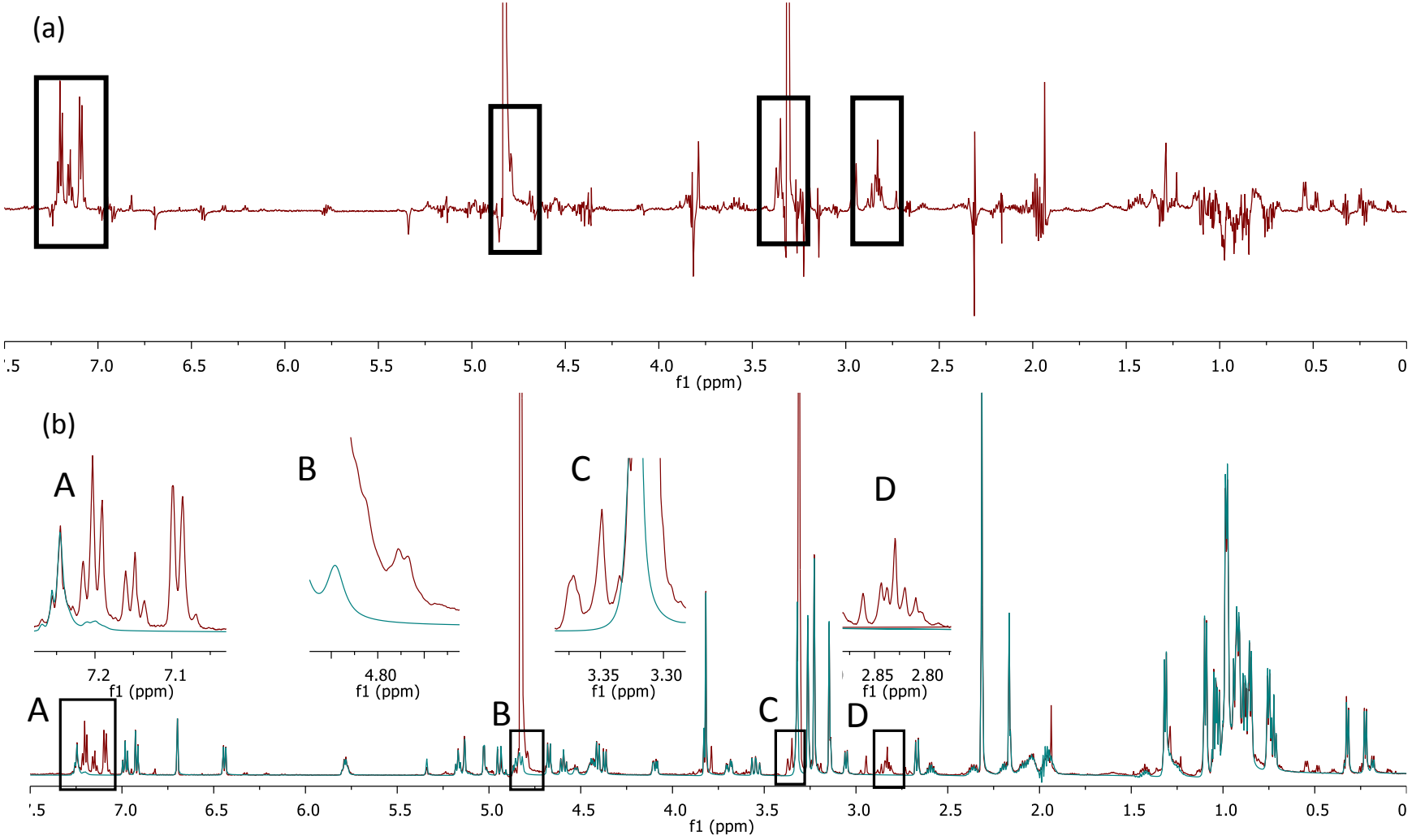


Figure 83. ^{13}C spectra of deoxyecumicin (blue) and ecumicin (red) with expansions.

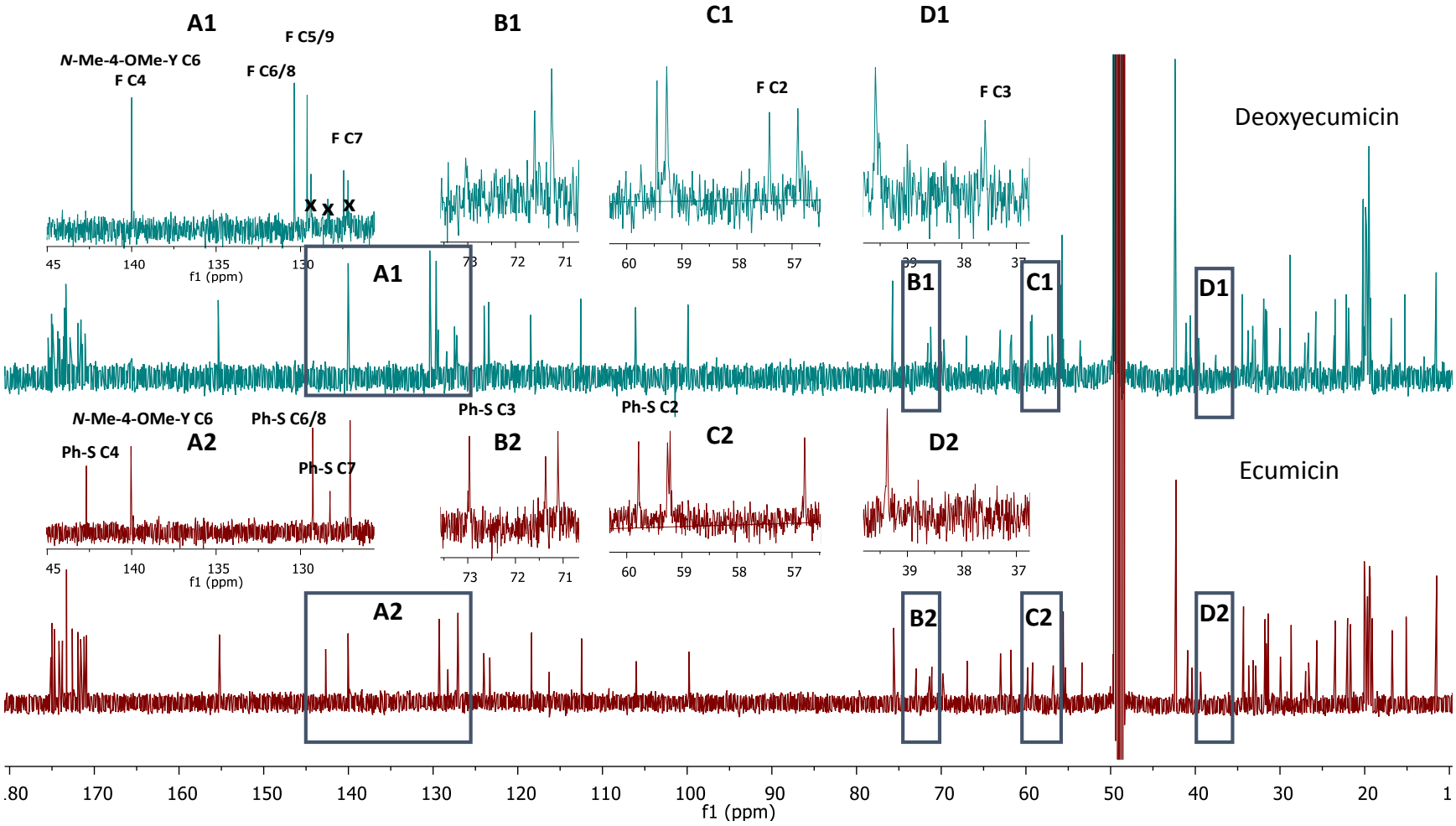


Figure 84. DEPT-135 spectra of deoxyecumicin (blue) and ecumicin (red) with expansions.

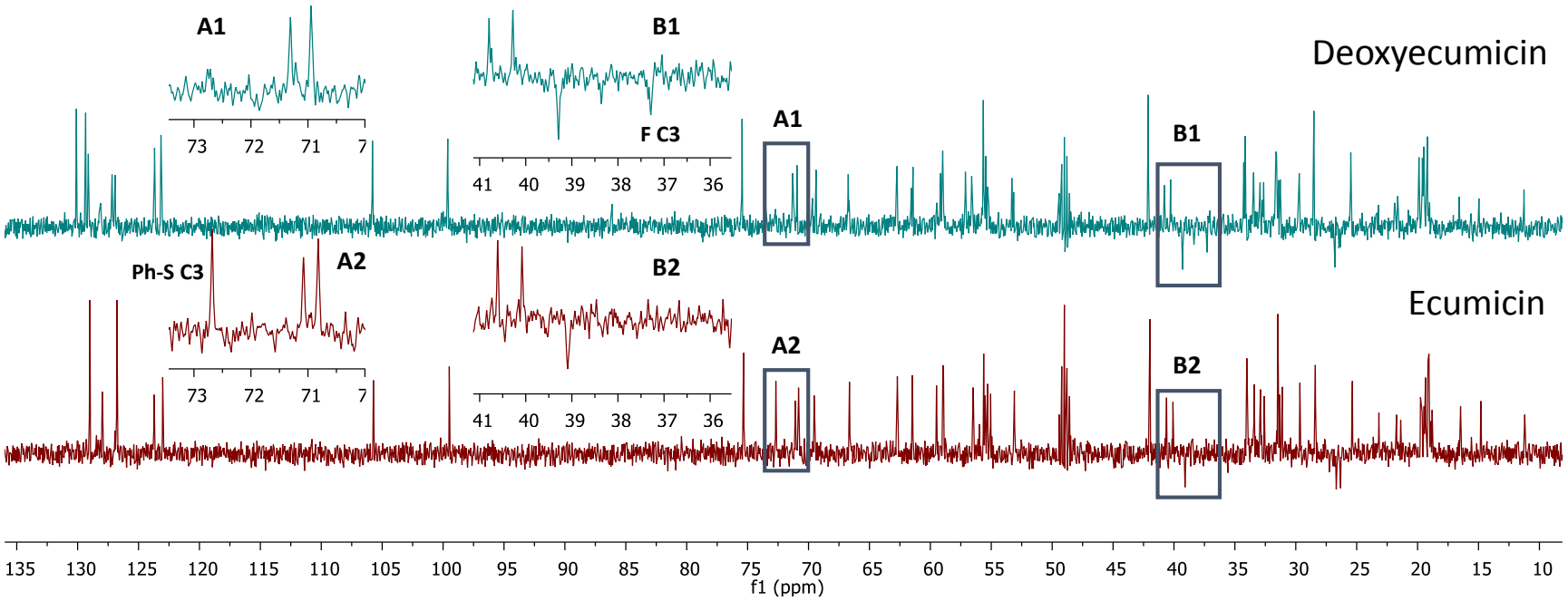


Figure 85. Comparison of COSY spectra of deoxyecumicin (grey) and ecumicin (yellow).

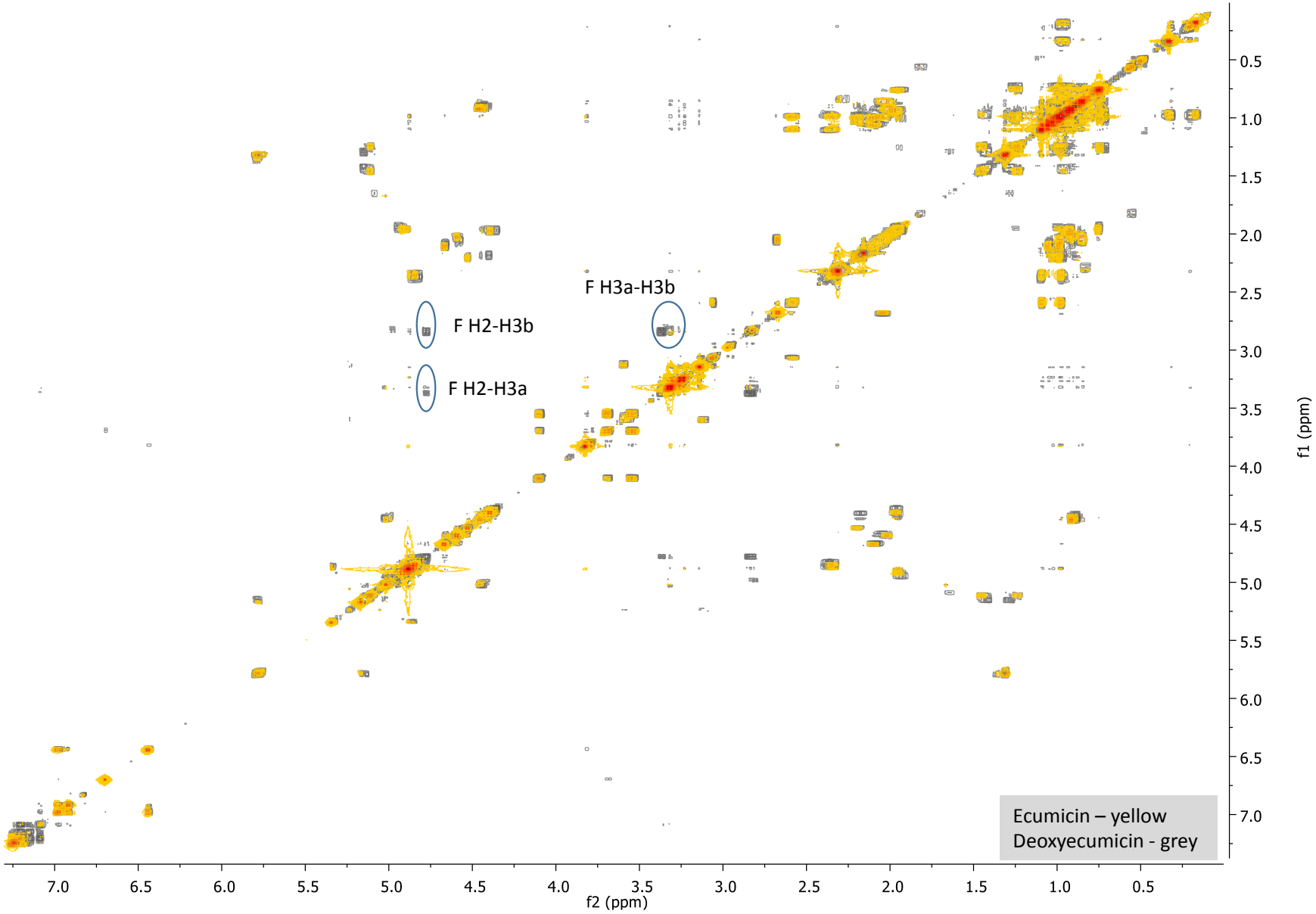


Figure 86. Comparison of HSQC spectra of deoxyecumicin (grey) and ecumicin (Red) with expansions.

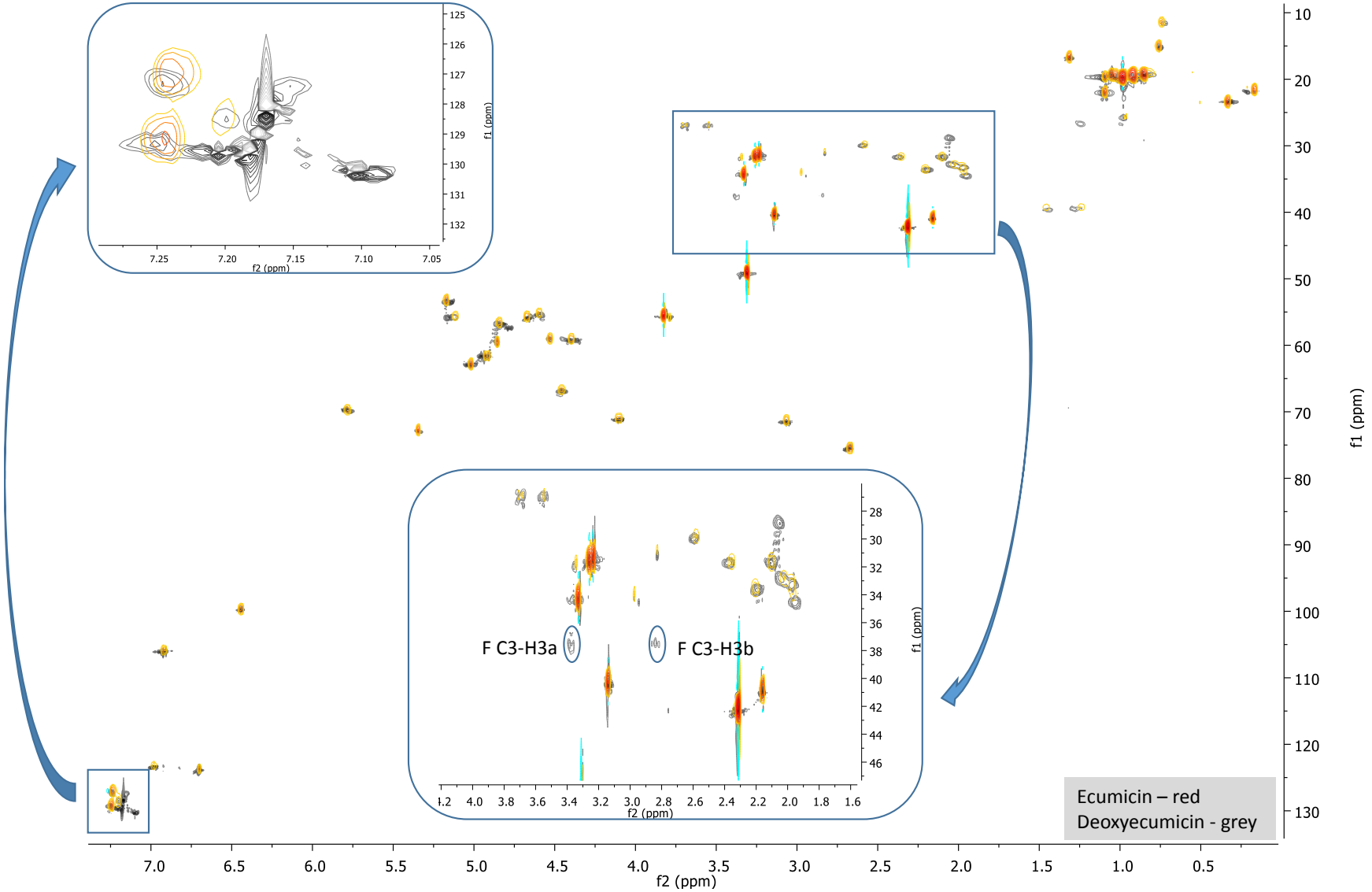
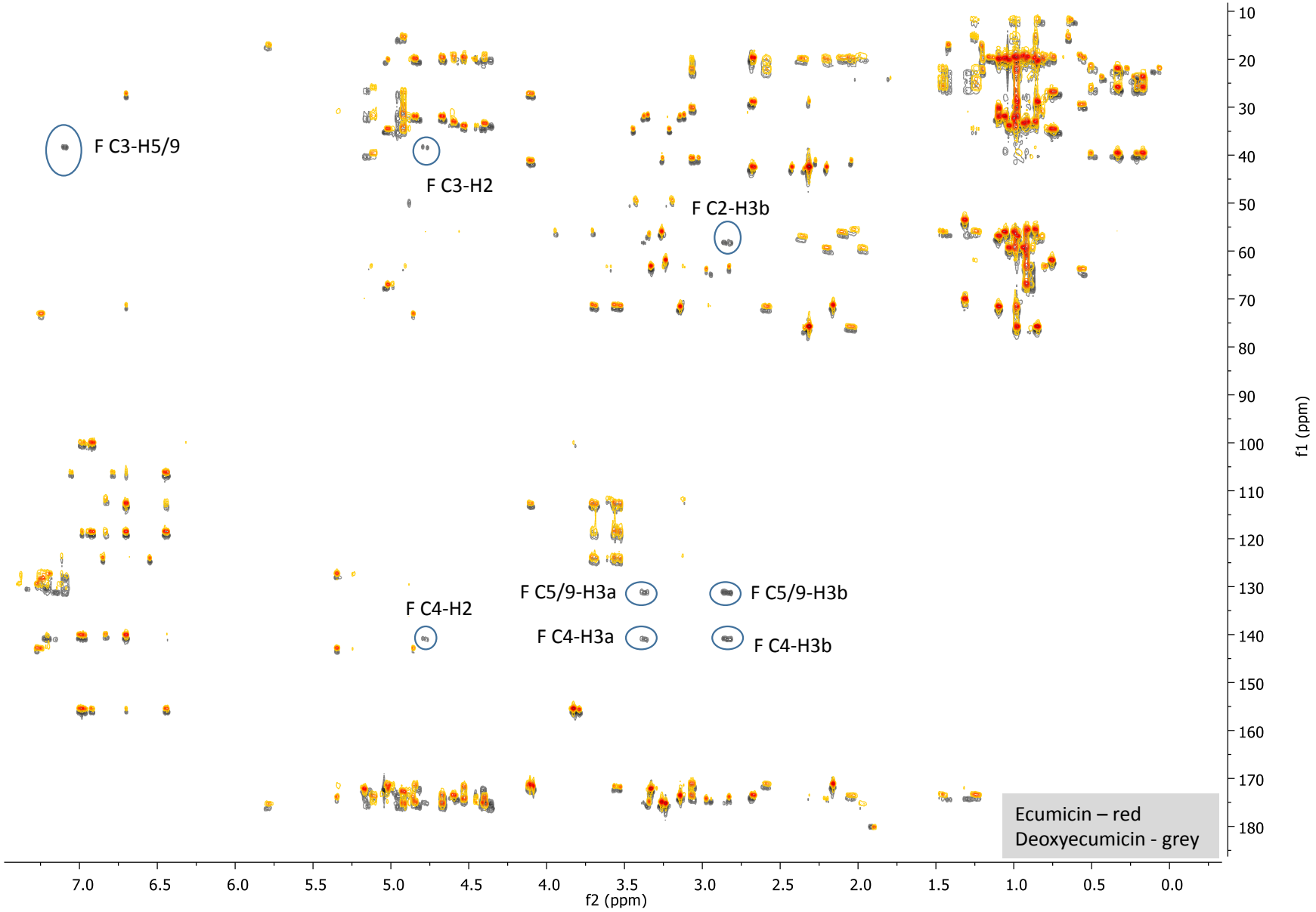


Figure 87. Comparison of the HMBC spectra of deoxyecumicin (grey) and ecumicin (Red).



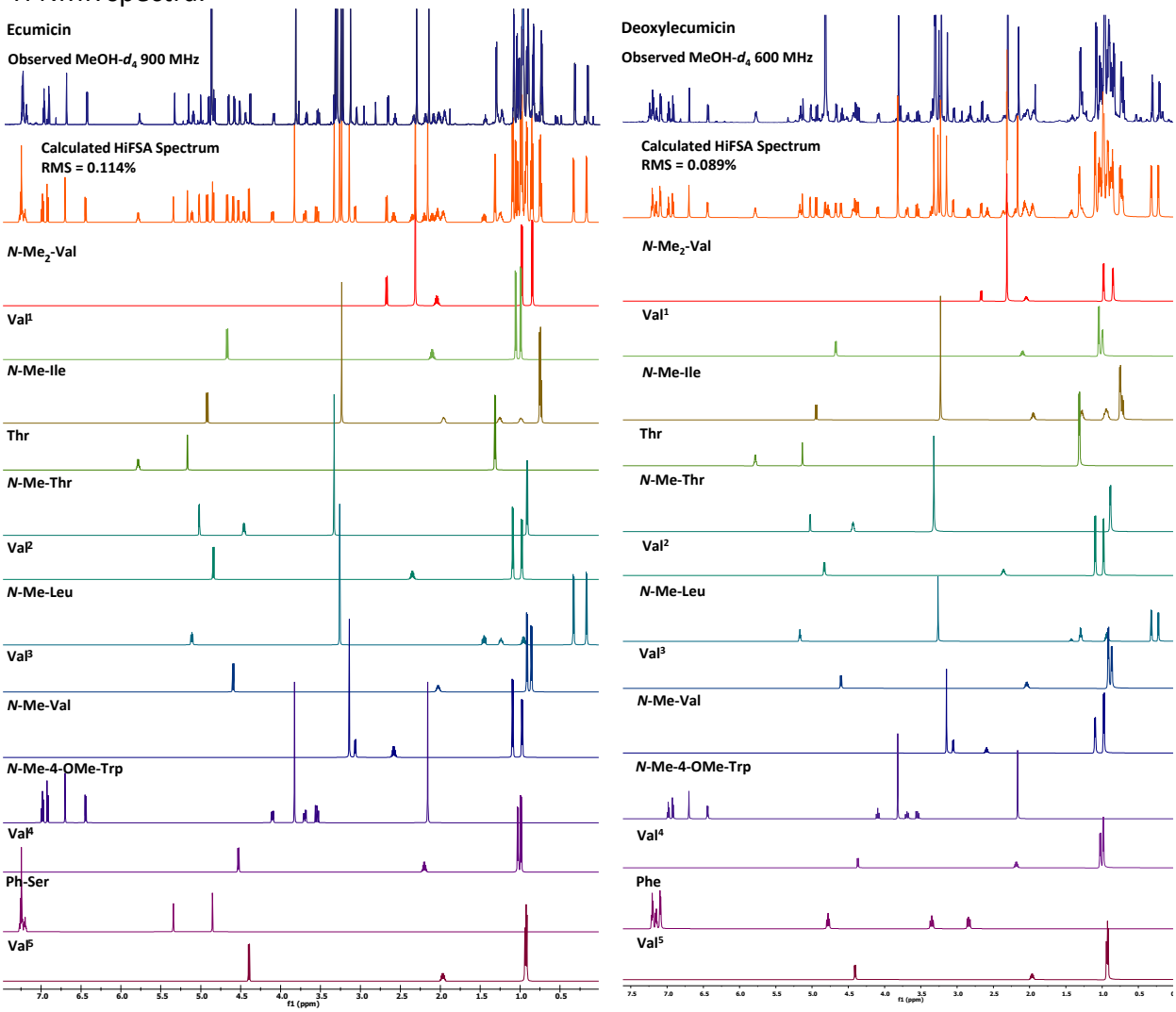
9.2.3 HiFSA fingerprint of deoxyecumicin.

Finally, the HiFSA fingerprint of deoxyecumicin was generated using the PERCH software tool. Briefly, the resolution-enhanced ^{1}H NMR spectrum (a JCAMP-DX file) of deoxyecumicin was imported into the PERCH shell and subjected to baseline correction, peak picking, and integration in the PAC module. The X-ray crystal structure of ecumicin was modified and used to build a molecular model of deoxyecumicin. Detailed analysis was carried out as described in previous publication (Napolitano, et al. 2012).

The iterative full spin analysis was able to resolve the visually observed overlapping multiplets, thereby allowing a precise interpretation of the δ_H and J_{HH} values for all signals (Figure 88B). As the computational study takes into consideration “both the structural analysis of the molecule of interest and the total line shape analysis of the ^{1}H NMR spectrum”, HiFSA is able to predict signal distortion in higher order coupled spin networks, (Napolitano, et al. 2012) e.g. the AA’MM’X spin system of the phenylalanine residue, and reproduce complex signal patterns (Figure 88A and B).

As a peptide is composed of amino acids that give rise to individual spin systems, HiFSA allows the extraction of individual amino acids’ sub-spectra. As shown in Figure 88, it is much easier to spot the structural difference by comparing the ^{1}H sub-spectrum of each pair of amino acids from the two peptides.

Figure 88 The ^{1}H iterative full spin analysis of (A) ecumicin and (B) deoxyecumicin. The figure includes individual, as well as stacked plot of the simulated amino acid sub-spectra, and observed ^{1}H NMR spectra.



9.3 Norecumicin

9.3.1 Isolation of norecumicin (R7)

Norecumicin (Figure 89), represented by peak R7 in Figure 74, is another major component of the ecumicin peptide family produced by *Nonomuraea sp.* MJM5123. Norecumicin was first isolated following the ecumicin isolation protocol as shown in Chapter 4 (also see Figure 75).

Purity of the norecumicin sample was determined by 100% NMR method as described in 9.2.1, with modifications. The ^{1}H NMR spectrum of the norecumicin sample (600 MHz, CD_3OD) was acquired under quantitative conditions (90 degree excitation pulse, acquisition time 6.0 s, relaxation delay 60.0 s) using a Bruker Avance 600 instrument.

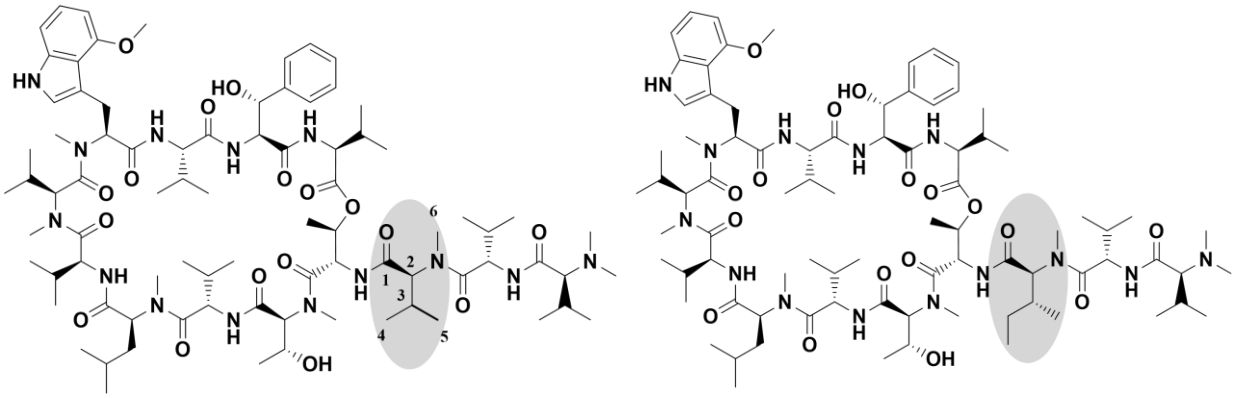
The methyl doublet (δ_H 0.148 ppm) was selected as the most pure signal, and the integral was set to 3.000, representing the integral of three protons (3H). All other proton signals between δ_H 0.0 to 7.5 ppm in the spectrum, except for the solvent signals (HOD and CHD_2OD), were integrated, and the sum of these integrals was determined to be 168.71.

Assuming norecumicin have the same molecular formula as ecumicin, a total of 125 non-exchangeable protons would be present in norecumicin. Assuming that impurities all have the same molecular weight as norecumicin, the purity of norecumicin (by non-exchangeable proton signal) was calculated as:

Purity = 125×(3.00/3)/168.71×100 % = 74.1 %

9.3.2 Structure elucidation of norecumicin using the NMR structure sequencing approach

Norecumicin (Figure 89) was isolated as a pale yellow powder. TABLE XXIII summarizes all the ^{13}C chemical shifts (δ_C), ^{1}H chemical shifts (δ_H) and $^{1}H,^{1}H$ scalar coupling constants (J_{HH}) of norecumicin. Interpretation of ^{1}H NMR spectrum was performed by ^{1}H iterative Full Spin Analysis. High resolution mass spectrometry (Figure 90) revealed that norecumicin has an exact mass of 1584.9980 amu, which is 14 amu less than that of ecumicin, indicating a possible structural difference of a methylene group.



(A) Norecumicin (B) Ecumicin

Figure 89 (A) Proposed structure of norecumicin. (B) Structure of ecumicin.

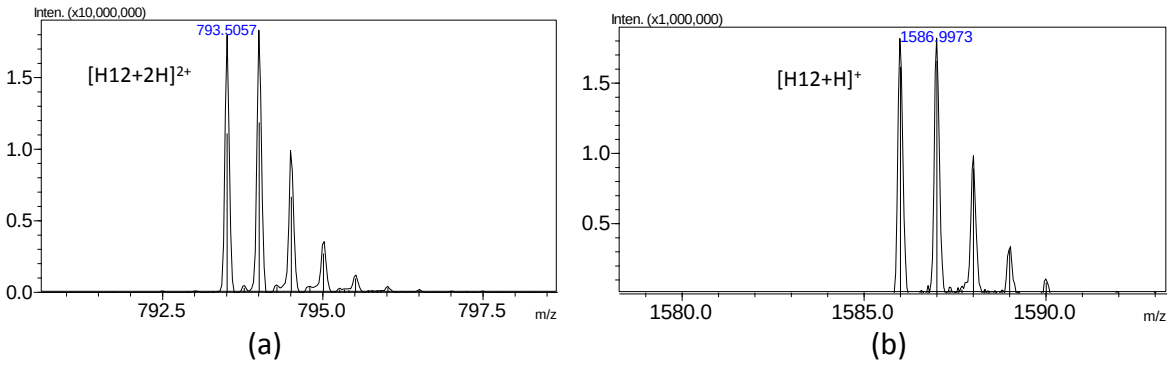


Figure 90 High resolution MS data of norecumicin. $[M+2H]^{2+}$ = 793.5057; $[M+H]^{+}$ = 1585.9958. So the exact mass for norecumicin was calculated to be 1584.9980.

TABLE XXIII. ^{1}H (900 MHZ, BRUKER AVANCE II 900) AND ^{13}C (100 MHZ, BRUKER DPX 400) NMR DATA OF NORECUMICIN IN CD_3OD. INTERPRETATION OF ^{1}H NMR WAS DONE BY ^{1}H ITERATIVE FULL SPIN ANALYSIS.

Amino Acid		**^{1}H δ in ppm(mult, *J* in Hz)**	**^{13}C δ in ppm**
N,N-Me_2-V	1	-	173.4
	2	2.67539 (d, 9.19)	75.75
	3	2.04262 (dqq, 9.19, 6.75, 6.46)	28.81
	4,5	2.31527 (s)	42.38
	6	1.09251 (d, 6.75)	19.83
	7	0.84589 (d, 6.46)	19.89
L-V[1]	1	-	175.11
	2	4.67201 (d, 8.76)	55.94
	3	2.10282 (dqq, 8.76, 6.78, 6.69)	31.78
	4	0.97722 (d, 6.78)	20.11
	5	1.05576 (d, 6.69)	19.34
N-Me-L-V[1]	1	-	172.66
	2	4.83401 (d, 11.07)	63.10
	3	2.17565 (dqq, 11.07, 6.42, 6.61)	28.04
	4	0.80988 (d, 6.42)	22.15
		0.79383 (d, 6.61)	19.48
	5	3.24864 (s)	31.56
L-T	1	-	172.01
	2	5.17398 (d, 2.29)	53.37
	3	5.78594 (dd, 2.29, 6.51)	70.06
	4	1.31305 (d, 6.51)	16.89
N-Me-L-T	1	-	171.20
	2	5.00850 (d, 4.01)	63.15

Amino Acid		^{1}H δ in ppm(mult, *J* in Hz)	^{13}C δ in ppm
	3	4.42627 (dd, 4.01, 6.61)	66.84
	4	0.91968 (d, 6.61)	20.17
	5	3.32324 (s)	34.34
L-V^{2}	1	-	174.83
	2	4.85329 (d, 8.92)	56.78
	3	2.35144 (dqq, 8.92, 7.23, 6.84)	31.92
	4	1.09380 (d, 7.23)	19.50
	5	0.97804 (d, 6.84)	19.36
N-Me-L-L	1	-	173.32
	2	5.08441 (dd, 6.77, 8.59)	55.88
	3	1.21889 (ddd, 6.77, -13.57, 6.30)	39.50
		1.46595 (ddd, 8.59, -13.57, 6.73)	
	4	0.99183 (ddqq, 6.30, 6.73, 6.62, 6.57)	25.76
	5	0.14802 (d, 6.62)	21.73
	6	0.33571 (d, 6.57)	23.62
	7	3.26027 (s)	31.83
L-V^{3}	1	-	173.46
	2	4.59574 (d, 8.91)	55.38
	3	2.02723 (dqq, 8.91, 6.83, 6.82)	33.04
	4	0.91243 (d, 6.83)	19.51
	5	0.85921 (d, 6.82)	19.58
N-Me-L-V^{2}	1	-	171.06
	2	3.06393 (d, 7.58)	71.49
	3	2.58188 (dqq, 7.58, 7.16, 6.12)	30.08
	4	0.98015 (d, 7.16)	19.79
	5	1.09389 (d, 6.12)	19.76
	6	3.13778 (s)	40.50
N-Me-4-OMe-L-Y	1	-	171.65
	2	4.10426 (dd, 11.17, 4.67)	71.23
	3	3.54493 (dd, 11,17, -13.72)	27.10
		3.69340 (dd, 4.67, -13.72)	
	4	-	112.53
	5	6.69818 (d, 0.81)	123.95
	6	-	155.35
	7	6.91749 (ddd, 0.81, 8.17, 0.57)	106.08
	8	6.98164 (dd, 8.17, 7.75)	123.44
	9	6.44215 (dd, 0.57, 7.75)	99.87
	10	-	140.01
	11	-	118.45
	12	3.82691 (s)	55.71
	13	2.15642 (s)	41.05
L-V^{4}	1	-	174.16
	2	4.53629 (d, 7.86)	59.20

Amino Acid		^{1}H δ in ppm(mult, *J* in Hz)	^{13}C δ in ppm
	3	2.19058 (dqq, 7.86, 6.81, 6.66)	33.78
	4	1.02676 (d, 6.81)	19.53
	5	0.99326 (d, 6.66)	20.12
Ph-L-THREO-S	1	-	173.80
	2	4.88388 (d, 1.59)	59.74
	3	5.32596 (d, 1.59)	73.04
	4	-	142.80
	5, 9*	7.22918 (dddd, 7.72, 1.00, 0.78, 0.70)	127.19
	6, 8*	7.25224 (dddd, 7.72, 7.50, 0.20, 0.78)	129.43
	7*	7.19840 (dd, 1.00, 7.50)	128.41
L-V[5]	1	-	175.27
	2	4.40221 (d, 8.83)	59.24
	3	1.96334 (dqq, 8.83, 6.73, 6.79)	33.02
	4	0.93700 (d, 6.73)	19.58
	5	0.92241 (d, 6.79)	19.25

* Signals observed from an AA'BB'C spin system.

The ^{1}H NMR spectrum of norecumicin was analyzed by the NMR structure sequencing method as described in Chapter 9.2.2.

A ^{1}H NMR spectrum generated from the pseudo HiFSA profile was superimposed on norecumicin's ^{1}H NMR spectrum (Figure 91). The two spectra matched well, with only four major differences noticed: (1) The signal(s) at 2.19 ppm integrated for two protons in the experimental spectrum, but it was only accounted for one proton in the calculated spectrum. (2) The signals at 1.96 ppm integrated for only two protons in the experimental spectrum, but in the calculated spectrum they were three belonging to one *N*-methyl-isoleucine and two valine units in ecumicin. (3) While signal at 1.23 ppm integrated for only one proton in the experimental spectrum, in the calculated spectrum it represented two protons belonging to *N*-methyl-isoleucine and *N*-methyl-leucine in ecumicin. (4) The methyl signal at 0.81 ppm represented as a doublet in the

experimental spectrum, but was a triplet in the calculated spectrum. In ecumicin, this methyl signal belongs to the *N*-methyl-isoleucine unit. Together these mismatches indicated that the structural difference(s) between ecumicin and norecumicin was related to the *N*-methyl-isoleucine unit of ecumicin.

Comparing of the spectra of common amino acids and norecumicin-3V's ^{1}H NMR spectrum (Figure 92) clearly revealed the ^{1}H NMR profile of the different amino acid, as shown in the expansions. This amino acid unit has one presumable α-proton signal at 4.88 ppm, half masked by the broad residual HOD peak, one *N*-methyl singlet at 3.24ppm, one presumable β-proton signal at 2.18 ppm, and two presumable methyl doublets at 0.81 and 0.79 ppm. This ^{1}H NMR profile suggested that norecumicin has an *N*-methyl-valine unit, whereas ecumicin has an *N*-methyl-isoleucine unit, which also explans the 14 amu mass difference.

The conclusion from the NMR structure sequencing was fully supported by the DEPT-135 and ^{13}C NMR spectra of norecumicin (Figure 93 andFigure **94**). The γ-carbon signal of *N*-methyl-isoleucine in ecumicin [a secondary carbon (CH_2) signal at 26.60 ppm] was missing from the spectrum of norecumicin.

The proposed structure was finally supported by COSY, HSQC, and HMBC NMR experiments. The 2D-NMR spectra of norecumicin were overlaid and compared with ecumicin's. As shown in Figure 95 to Figure **99** The comparison confirmed the existence of all twelve common amino acids in both peptides, and supported that norecumicin has an *N*-methyl-valine whereas ecumicin has an *N*-methyl-isoleucine.

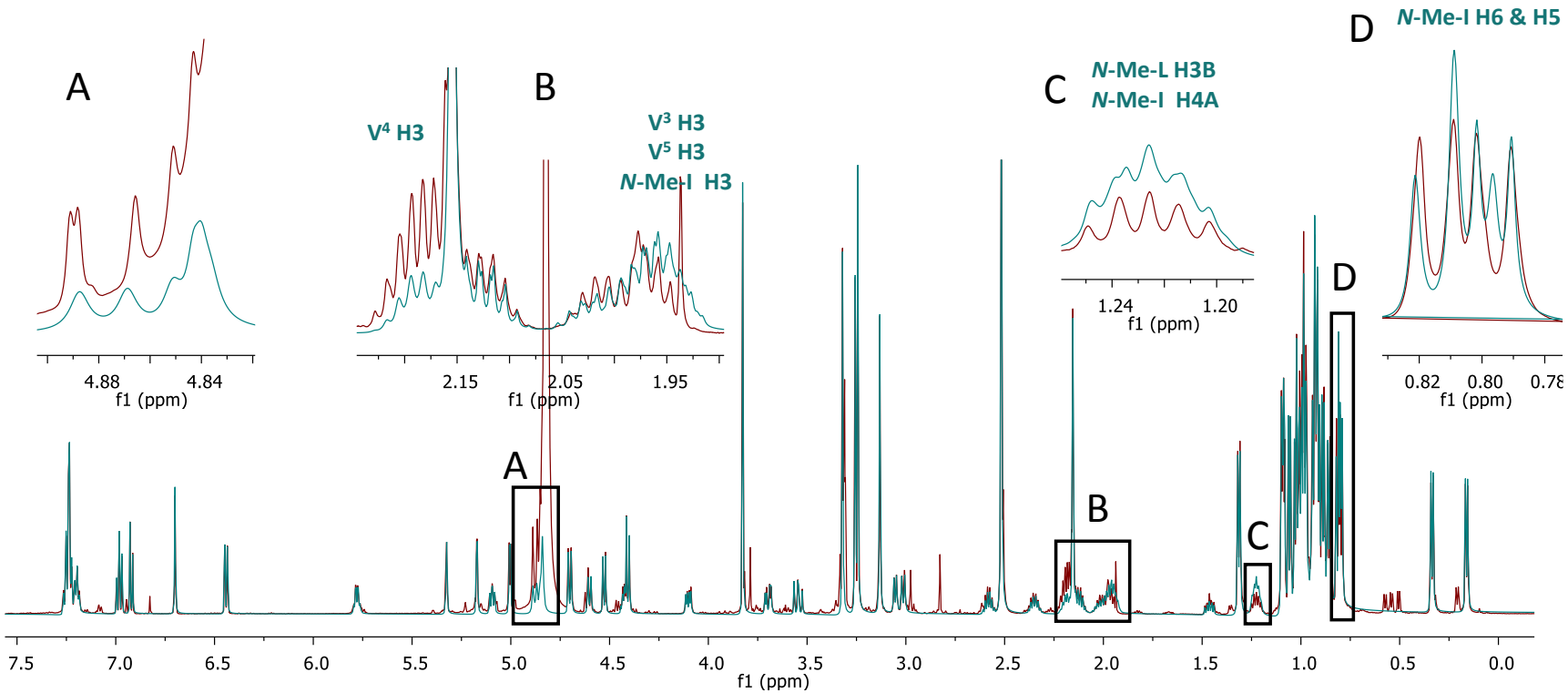


Figure 91. Overlay of norecumicin's pseudo HiFSA profile (blue) and ^{1}H NMR spectrum (red) indicates norecumicin does not contain *N*-methyl-isoleucine.

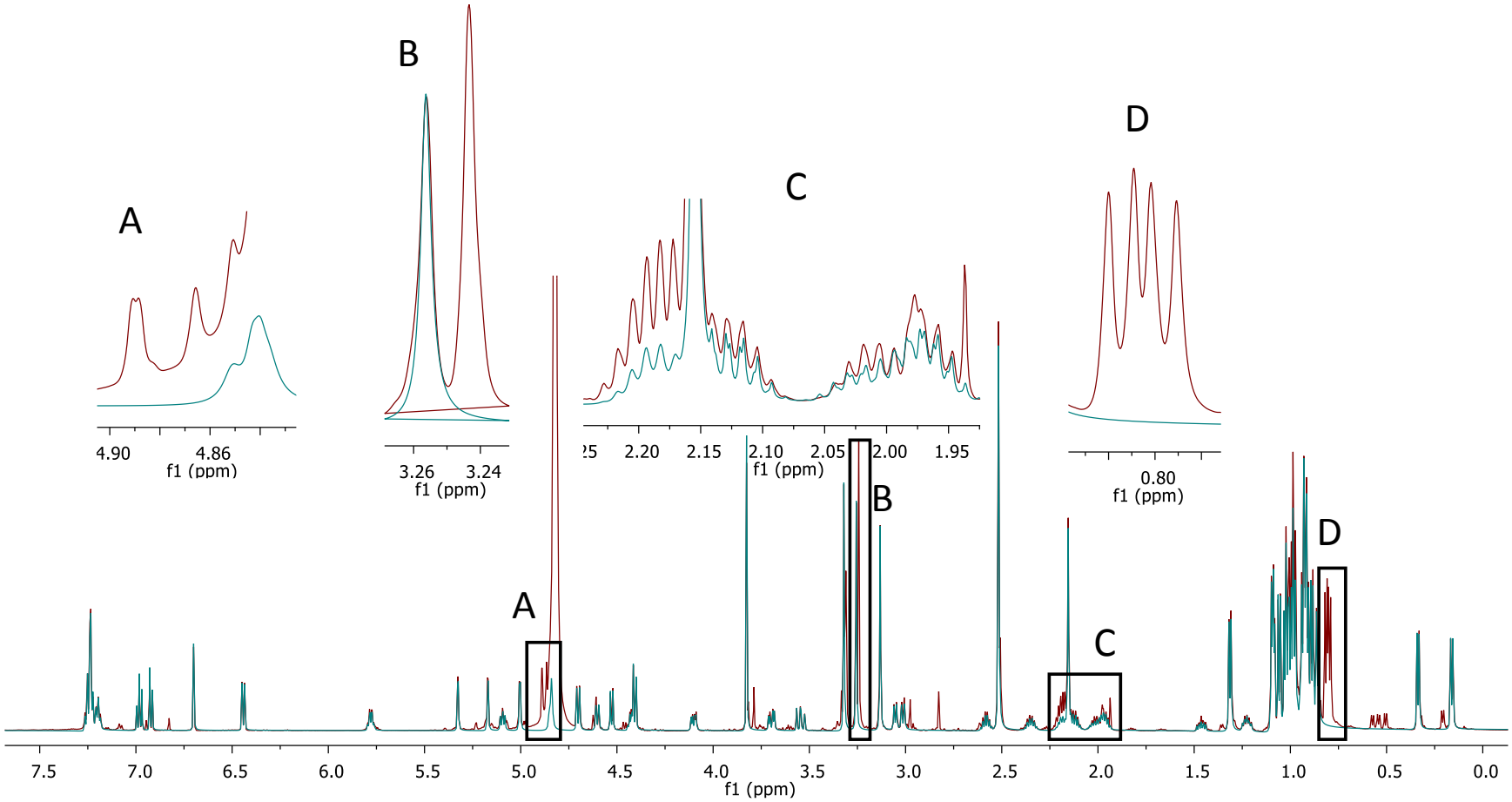


Figure 92 The spectrum of the different amino acid in norecumicin (in expansion) revealed by comparing ^{1}H NMR spectrum of norecumicin (red) and spectrum of those amino acids commonly observed in norecumicin and ecumicin (blue).

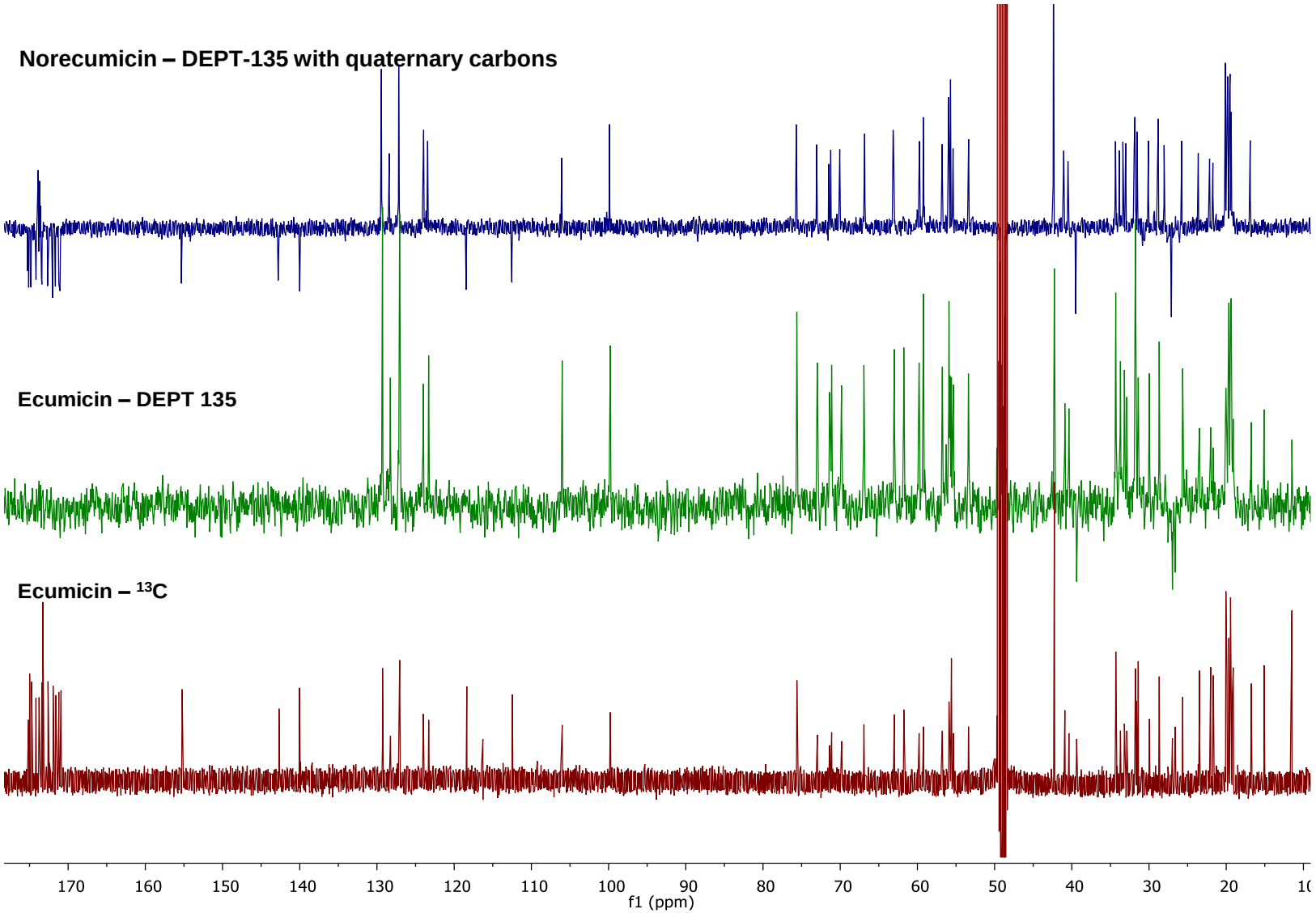


Figure 93. DEPTQ-135 spectrum of norecumicin (blue) compared with DEPT-135 (green) and ^{13}C (red) spectra of ecumicin.

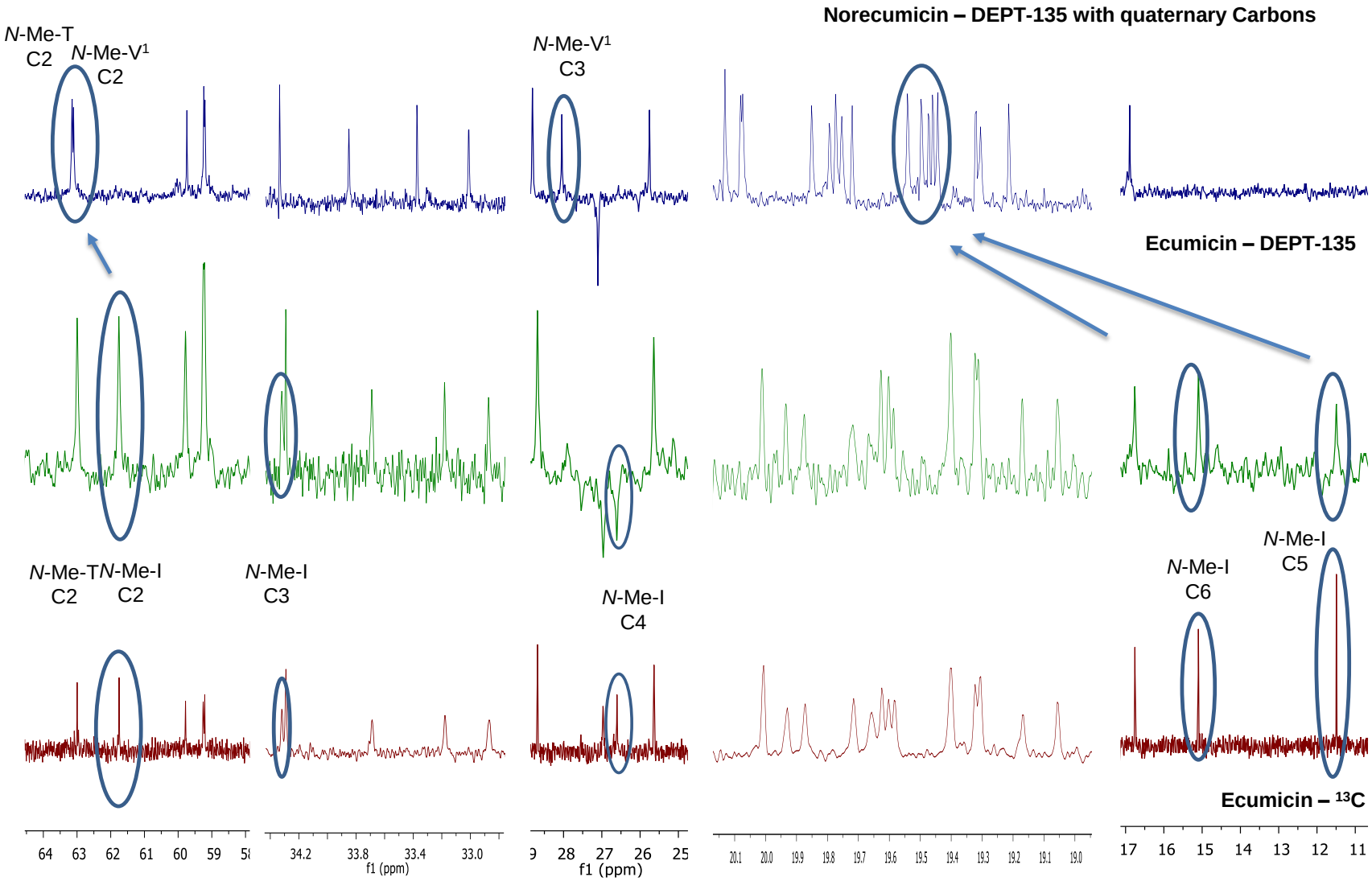


Figure 94. Expansions of DEPTQ-135 spectrum of norecumicin (blue) compared with DEPT-135 (green) and ^{13}C (red) spectra.

Figure 95 Comparison of COSY spectra of norecumicin (grey) and ecumicin (yellow).

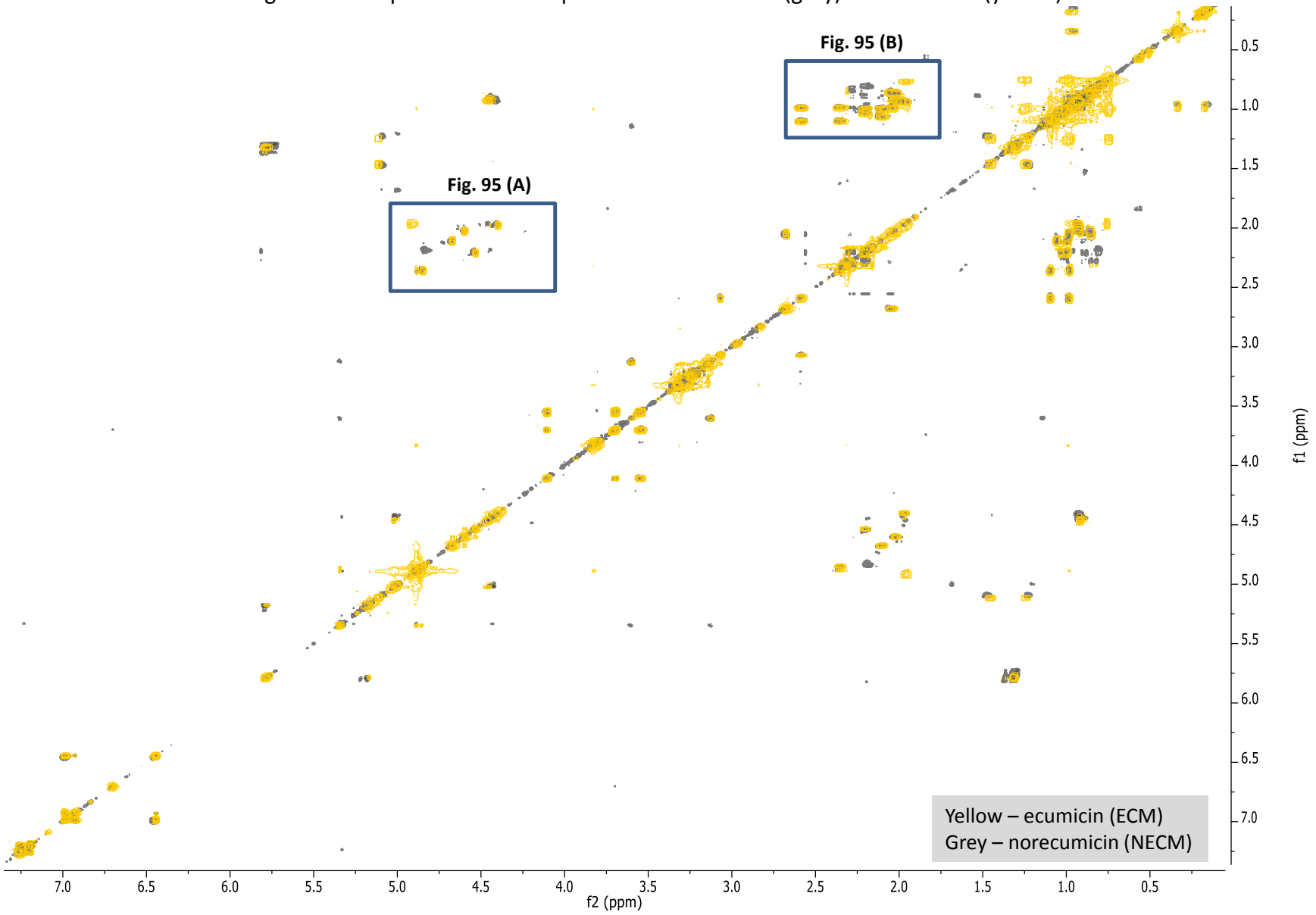


Figure 96 expansions on comparison of COSY spectra of norecumicin (NECM, grey) and ecumicin (ECM, yellow).

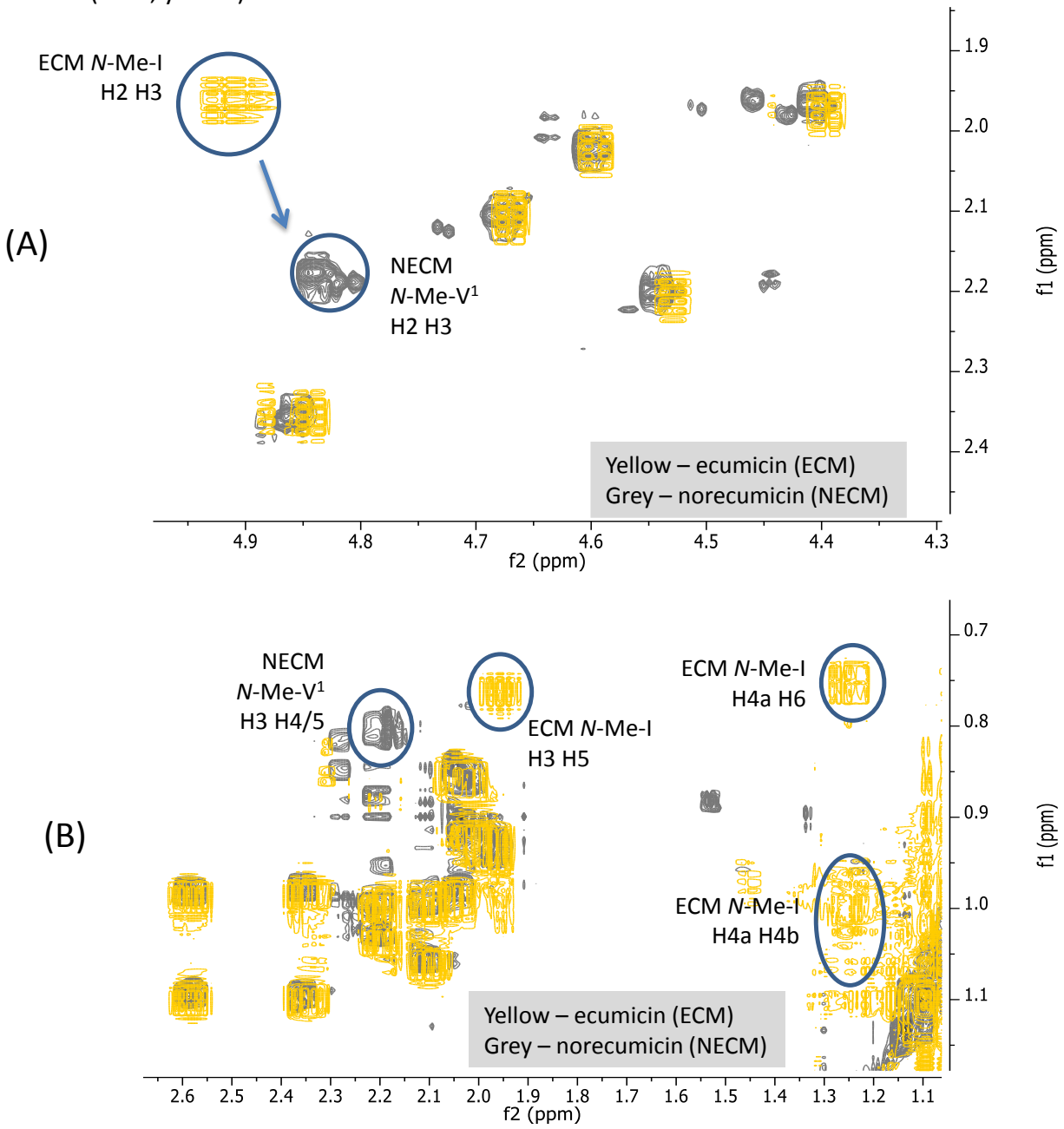


Figure 97 Comparison of HSQC spectra of norecumicin (NECM, red) and ecumicin (ECM, grey) with expansions.

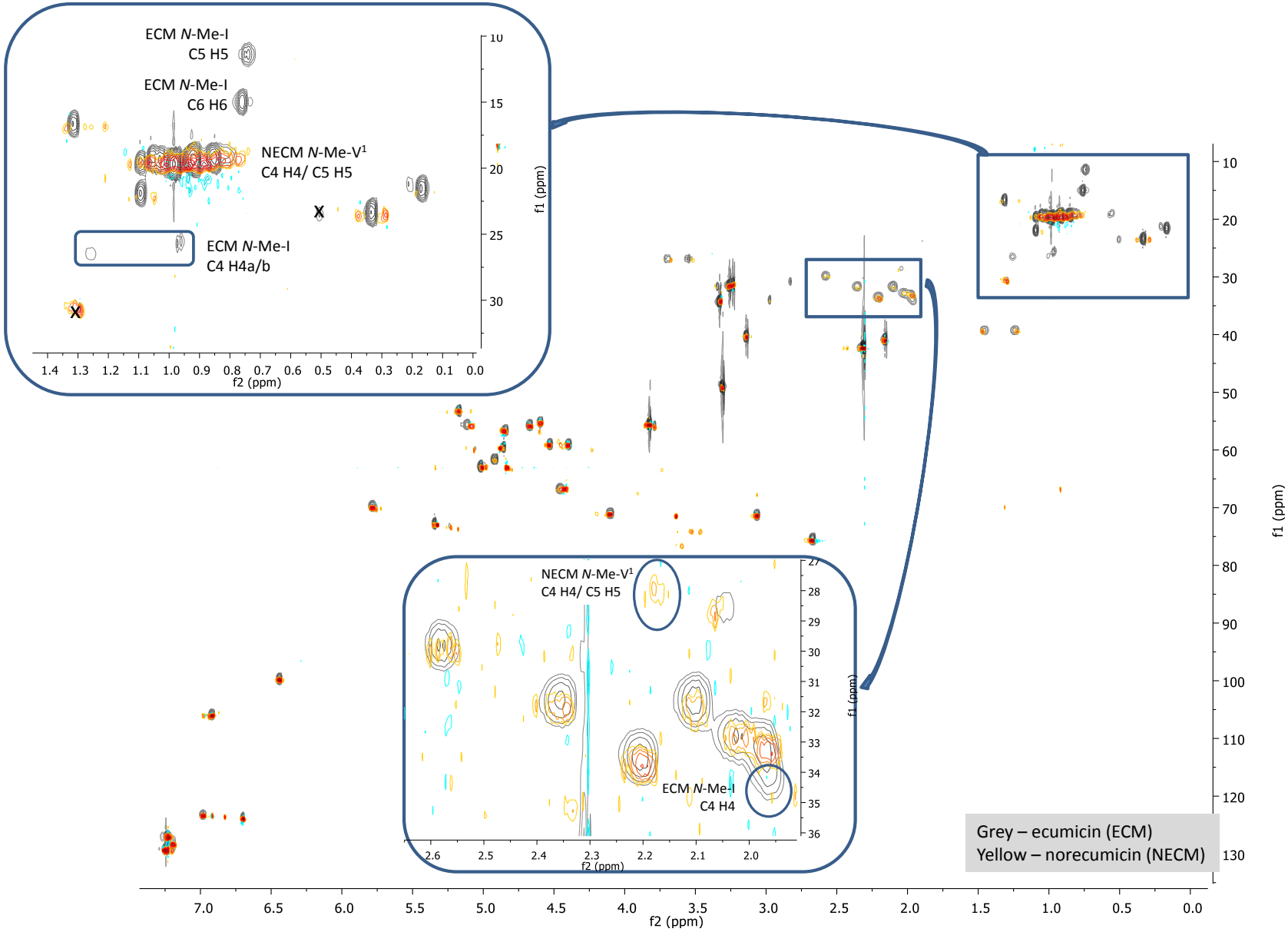


Figure 98 Comparison of HMBC spectra of norecumicin (NECM, yellow) and ecumicin (ECM, grey).

To be analyzed by semi-selective HMBC (Figure 99)

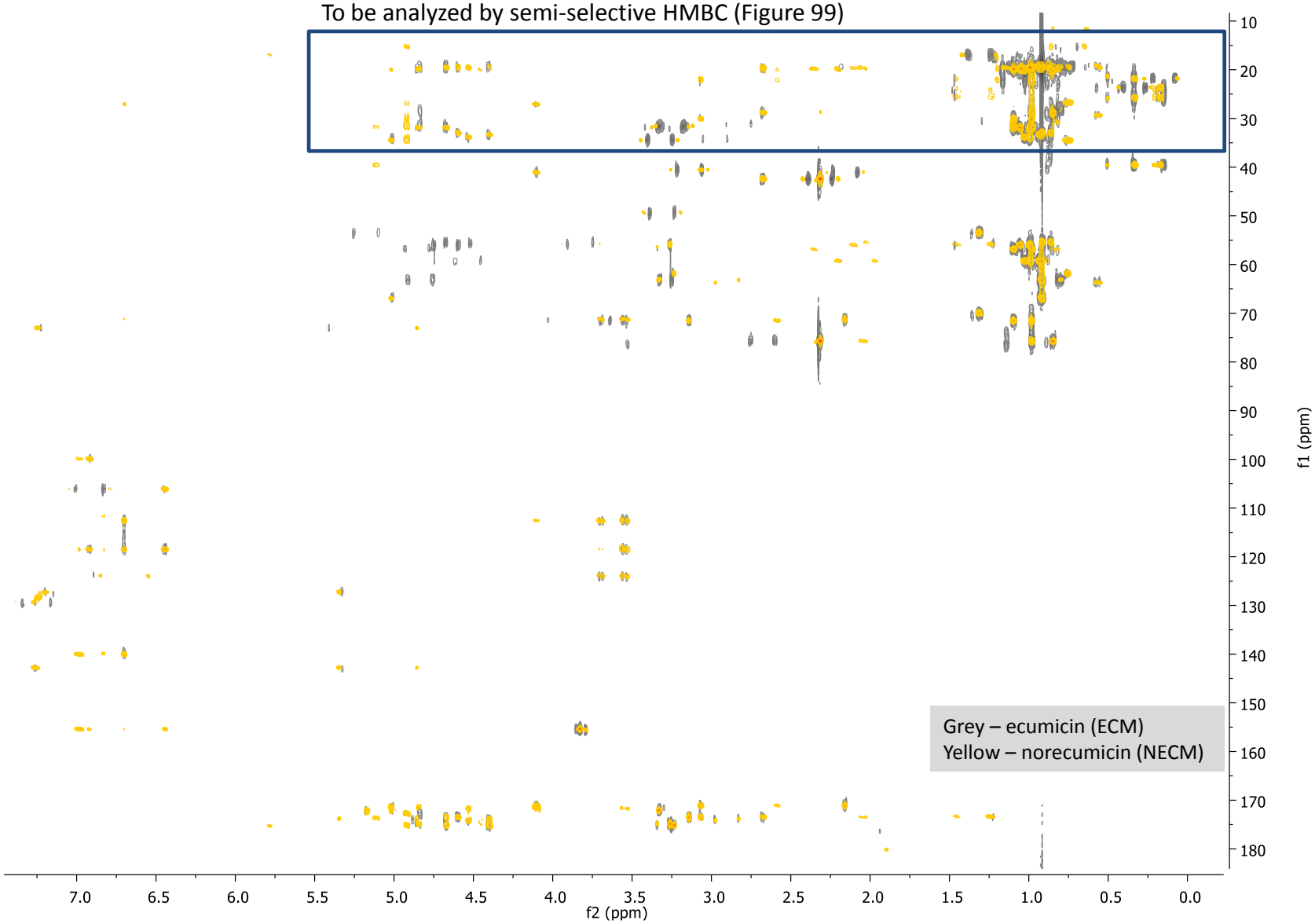
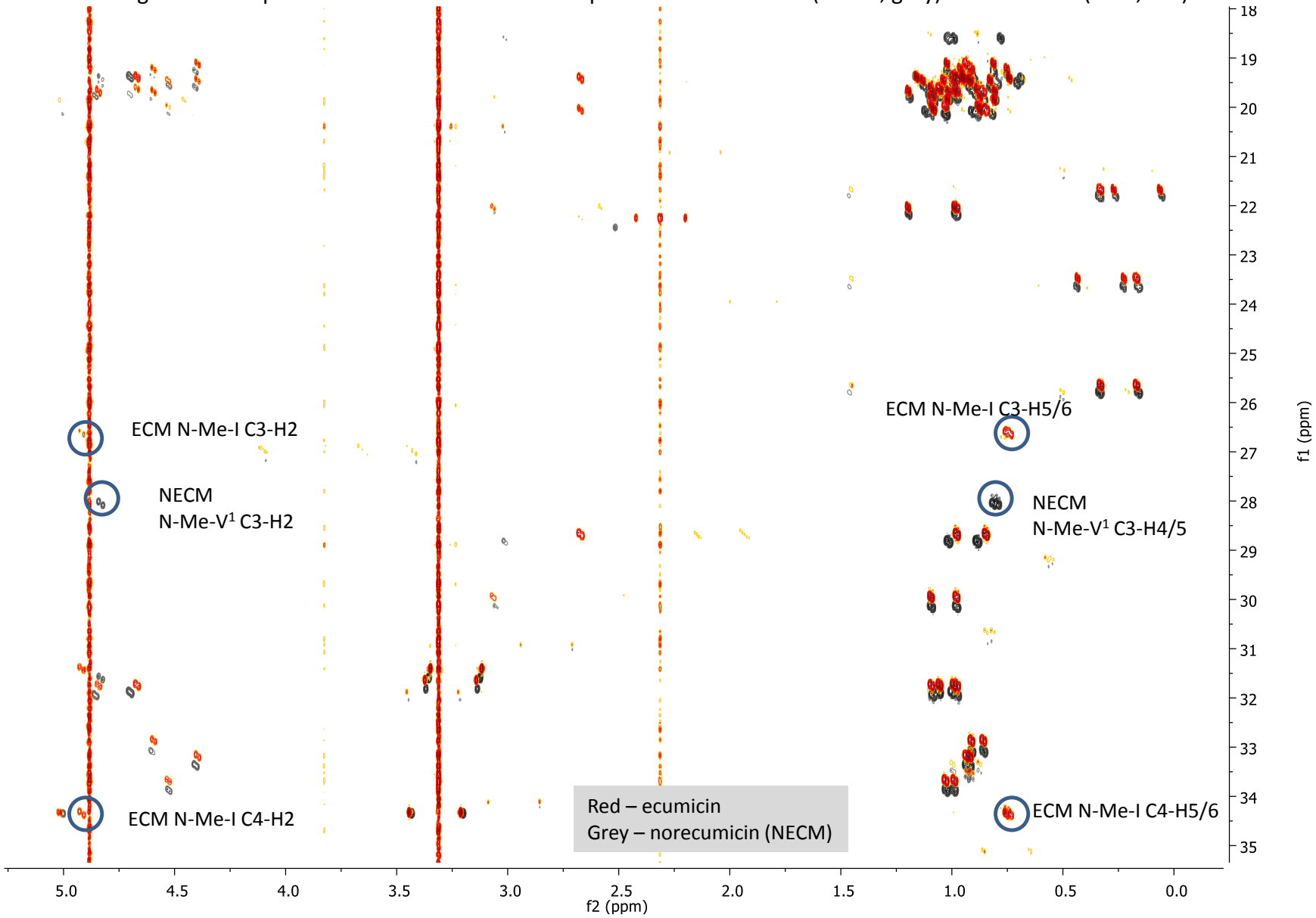


Figure 99 Comparison of semi-selective HMBC spectra of norecumicin (NECM, grey) and ecumicin (ECM, red).



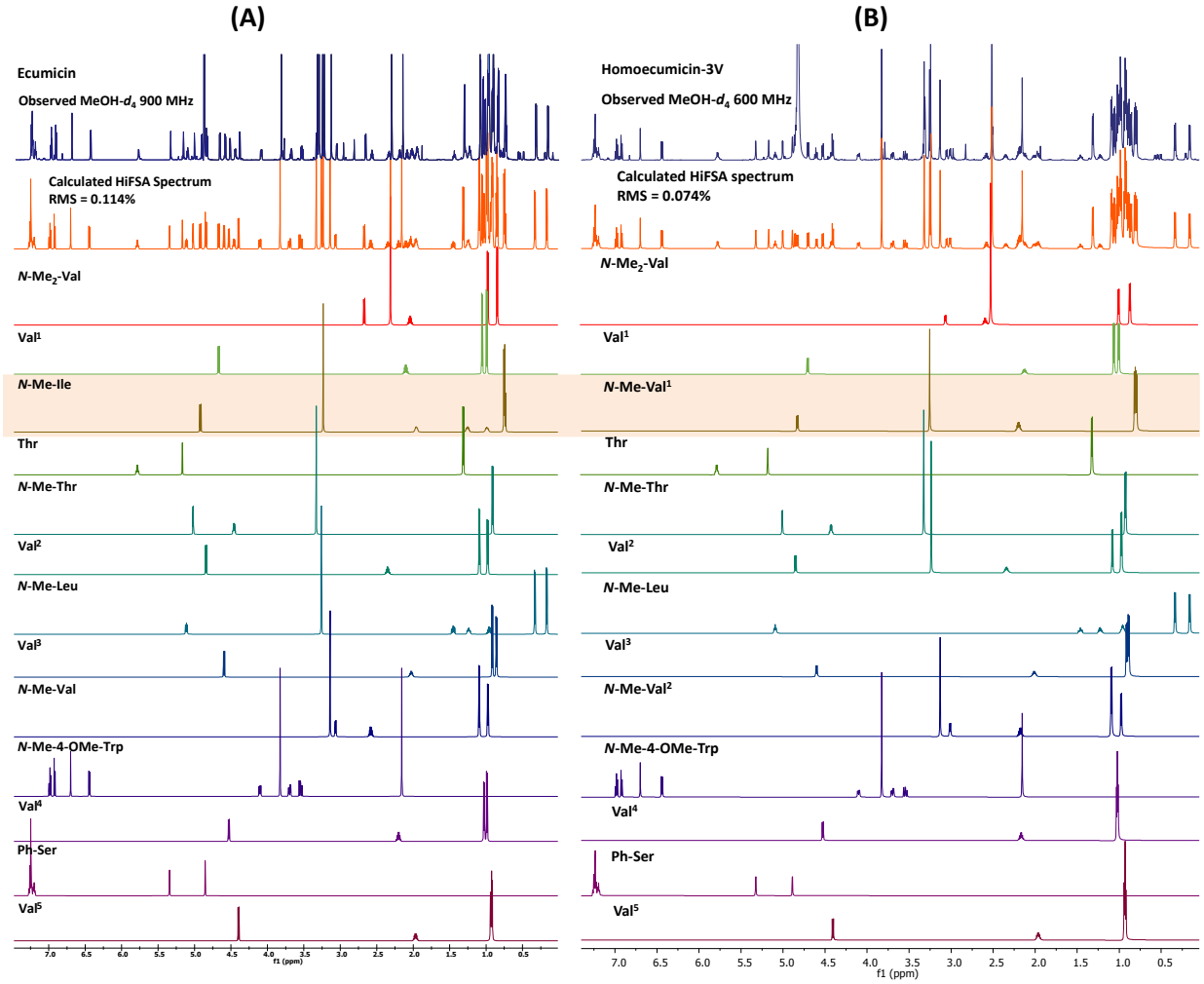
9.3.3 HiFSA fingerprint of norecumicin.

A HiFSA fingerprint was generated for norecumicin as described in Chapter 9.2.3. The iterative full spin analysis allowed the precise determination of the δ_H and J_{HH} values for all signals (Figure 100B), as summarized in TABLE XXIII.

As expected, HiFSA is able to "analyze signal distortion in higher order coupled spin networks and reproduce complex signal patterns" (Napolitano, 2012) (Figure 100A and B), e.g. the AA'BB'C spin system of phenyl-serine unit. Furthermore, as δ_H and J_{HH} are field-independent parameters, they can be efficiently used to simulate ^{1}H NMR data at different field strengths. For example, the HiFSA profile of ecumicin at 900 MHz has been used to simulate ^{1}H NMR data at 600 MHz, for the NMR structure sequencing of deoxyecumicin and norecumicin.

In addition, comparing the ^{1}H NMR sub-spectra of individual amino acids of ecumicin and norecumicin clearly indicated that their structure difference was harbored in the third amino acid from the *N*-terminus (highlighted in Figure 100). Ecumicin has an *N*-methyl-isoleucine at the position, whereas norecumicin has an *N*-methyl-valine.

Figure 100. The ^{1}H iterative full spin analysis of (A) ecumicin and (B) norecumicin, including the simulated amino acid sub-spectra, their mathematical sum, and observed ^{1}H NMR spectrum.



9.4 Nordeoxyecumicin

9.4.1 Isolation of nordeoxyecumicin (R8)

Nordeoxyecumicin (Figure 101), represented by peak R8 in Figure 74, is one minor component of the ecumicin peptide family produced by *Nonomuraea sp.* MJM5123. Nordeoxyecumicin was isolated by adding an HPLC separation step to the ecumicin isolation protocol. The overall separation scheme was as shown in Figure 75.

Purity of the nordeoxyecumicin sample was determined by 100% NMR method as described in 9.2.1, with modifications. The ^{1}H NMR spectrum of the nordeoxyecumicin sample (900 MHz, CD_3OD) was acquired under quantitative conditions (90 degree excitation pulse, acquisition time 4.0 s, relaxation delay 60.0 s) using a Bruker Avance II 900 instrument.

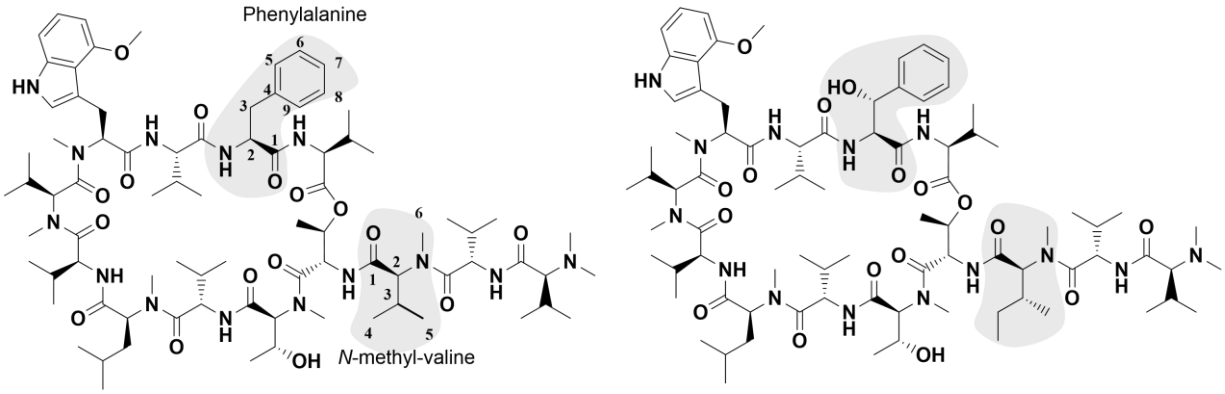
The upfield methyl doublet (δ_H 0.318 ppm) was selected as the most pure signal, and the integral was set to 3.000. All other proton signals between δ_H 0.0 to 7.5 ppm in the spectrum, except for the solvent signals (HOD and CHD_2OD), were integrated, and the sum of these integrals was determined to be 304.01.

Assuming nordeoxyecumicin have the same molecular formula as ecumicin, there would be a total of 125 non-exchangeable protons present in nordeoxyecumicin. Assuming that impurities all have the same molecular weight as nordeoxyecumicin, the purity was calculated as:

Purity = 125×(3.00/3)/304.01×100 % = 41.1 %

9.4.2 Structure elucidation of nordeoxyecumicin by HiFSA-assisted approach

Nordeoxyecumicin (Figure 101A) was isolated as a pale yellow powder. TABLE XXIV summarizes the ^{13}C chemical shifts (δ_C), ^{1}H chemical shifts (δ_H) and $^{1}H,^{1}H$ scalar coupling constants (J_{HH}) of nordeoxyecumicin. Interpretation of ^{1}H NMR was done by ^{1}H iterative Full Spin Analysis, by using the PERCH iterator. High resolution mass spectrometry (Figure 102) revealed that nordeoxyecumicin has an exact mass of 1568.9934 amu, which is 30 amu less than that of ecumicin, indicating a possible structural difference of a methylene group (14 amu) and a hydroxyl group (16 amu).



(A) Nordeoxyecumicin (B) Ecumicin

Figure 101. (A) Proposed structure of nordeoxyecumicin. (B) Structure of ecumicin.

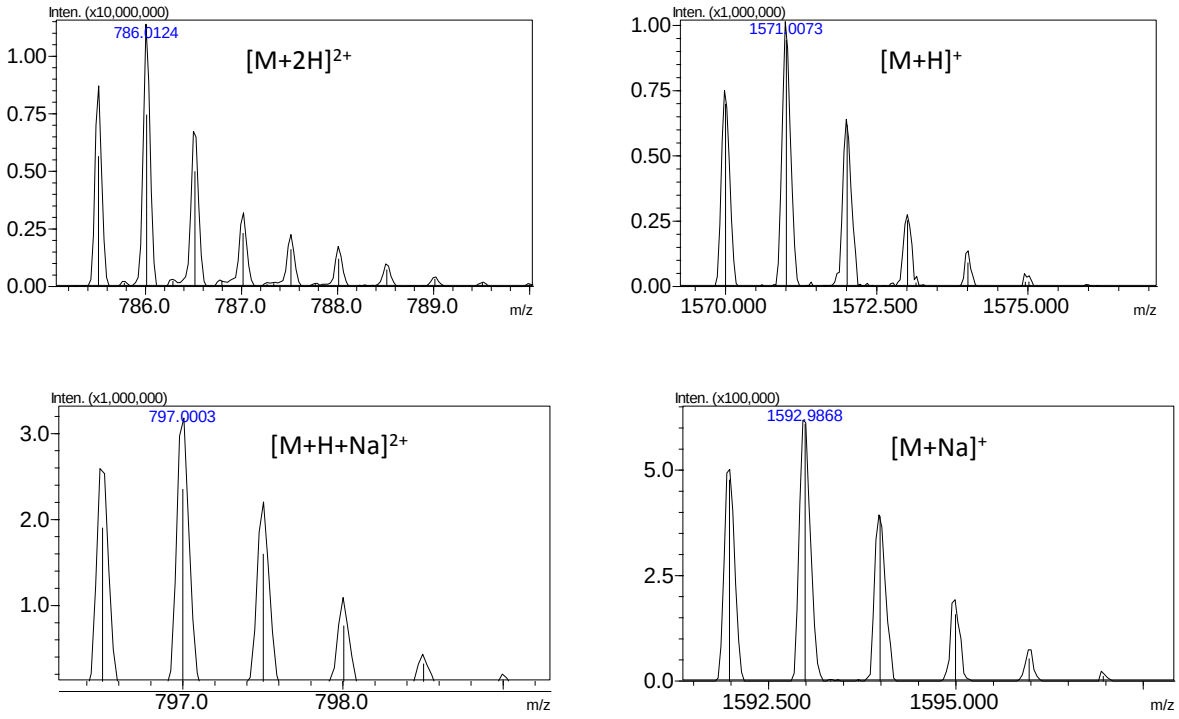


Figure 102 High resolution MS data of nordeoxyecumicin. $[M+2H]^{2+}$= 785.5098; $[M+H+Na]^{2+}$ = 796.4999; $[M+H]^{+}$ = 1570.0012; $[M+Na]^{+}$ = 1591.9786. The exact mass of nordeoxyecumicin was calculated to be 1568.9934.

TABLE XXIV ^{1}H (900 MHZ, BRUKER AVANCE II 900) AND ^{13}C (100 MHZ, BRUKER DPX 400) NMR DATA OF NORDEOXYECUMICIN IN CD_3OD. INTERPRETATION OF ^{1}H NMR WAS PERFORMED BY ^{1}H ITERATIVE FULL SPIN ANALYSIS.

Amino Acid		^{1}H δ in ppm(mult, J in Hz)	^{13}C δ in ppm
N,N-Me_2-V	1	-	173.41
	2	2.79000 (d, 8.77)	75.50
	3	2.08564 (dqq, 8.77, 6.72, 7.02)	28.80
	4,5	2.38198 (S)	42.38
	6	1.04849 (d, 6.72)	19.45
	7	0.98373 (d, 7.02)	20.13
L-V[1]	1	-	174.95
	2	4.67044 (d, 8.73)	56.02
	3	2.09118 (dqq, 8.73, 6.57, 7.14)	31.60
	4	0.85808 (d, 6.57)	19.18
	5	0.98918 (d, 7.14)	20.04
	NH	-	
N-Me-L-V[1]	1	-	172.83

Amino Acid		^{1}H δ in ppm(mult, J in Hz)	^{13}C δ in ppm
	2	4.85693 (d, 11.03)	63.04
	3	2.16055 (dqq, 11.03, 6.60, 6.58)	28.16
	4	0.79969 (d,6.60)	19.45
		0.79243 (d, 6.58)	19.43
	5	3.24856 (s)	31.71
L-T	1	-	171.86
	2	5.15236 (d, 2.33)	53.46
	3	5.790964 (dq, 2.33, 6.35)	69.82
	4	1.310021 (d, 6.35)	16.86
N-Me-L-T	1	-	171.31
	2	5.01601 (d, 3.85)	63.03
	3	4.40755 (dq, 3.85, 6.46)	66.91
	4	0.88552 (d, 6.46)	19.79
	5	3.31596 (s)	34.35
L-V^{2}	1	-	174.90
	2	4.83600 (d, 9.05)	56.84
	3	2.36320 (dqq, 9.05, 6.67, 6.97)	31.87
	4	1.09831 (d, 6.67)	19.83
	5	0.97478 (d, 6.97)	19.90
N-Me-L-L	1	-	173.57
	2	5.13209 (dd, 7.92, 7.14)	55.90
	3	1.43922 (ddd, 7.92, -12.12, 4.16)	39.55
		1.28085 (ddd, 7.14, -12.12, 5.74)	
	4	0.95726 (ddqq, 4.16, 5.74, 6.54, 6.59)	25.74
	5	0.31782 (d, 6.54)	23.51
	6	0.19318 (d, 6.59)	21.84
	7	3.264461 (s)	31.89
L-V^{3}	1	-	173.61
	2	4.58107 (d, 9.17)	55.50
	3	2.04477 (dqq, 9.17, 6.77, 6.74)	32.92
	4	0.91447 (d, 6.77)	19.67
	5	0.86711 (d, 6.74)	19.40
N-Me-L-V^{2}	1	-	171.14
	2	3.06194 (d, 7.74)	71.57
	3	2.59114 (dqq, 7.74, 6.61, 6.84)	29.99
	4	1.09378 (d, 6.61)	22.18
	5	0.97884 (d, 6.84)	19.77
	6	3.14583 (s)	40.56
N-Me-4-OMe-L-Y	1	-	171.58
	2	4.09584 (dd, 4.73, 11.18)	71.24
	3	3.68757 (dd, 4.73, -13.72)	27.06
		3.54366 (dd, 11.18, -13.72)	

Amino Acid		^{1}H δ in ppm(mult, J in Hz)	^{13}C δ in ppm
	4	-	112.52
	5	6.69509 (d, 0.81)	123.96
	6	-	155.35
	7	6.91766 (ddd, 0.81, 8.17, 0.33)	106.09
	8	6.98005 (dd, 8.17, 7.80)	123.44
	9	6.43806 (dd, 0.33, 7.80)	99.87
	10	-	140.01
	11	-	118.44
	12	3.815812 (s)	55.71
	13	2.162198 (s)	41.10
L-V[4]	1	-	174.05
	2	4.40599 (d, 8.47)	59.42
	3	2.175678 (dqq, 8.47, 6.72, 7.18)	33.80
	4	1.02549 (d, 6.72)	19.72
	5	0.98186 (d, 7.18)	20.21
L-F	1	-	174.30
	2	4.80209 (dd, 10.84, 2.65)	57.40
	3	2.83326 (dd, 10.84, -14.34)	37.58
		3.32008 (dd, 2.65, -14.34)	
	4	-	140.01
	5,9*	7.07722 (ddd, 6.77, 1.31, 1.13)	130.38
	6,8*	7.20103 (ddd, 6.77, 7.55, 0.80)	129.64
	7*	7.14970 (dd, 1.31, 7.55)	127.47
L-V[5]	1	-	175.47
	2	4.36438 (d, 9.07)	59.24
	3	1.95987 (dqq, 9.07, 6.85, 6.68)	33.29
	4	0.92244 (d, 6.85)	19.31
	5	0.93826 (d, 6.68)	19.54

* Signals observed from an AA'XX'M spin system.

In order to perform an in-depth analysis of the ^{1}H NMR spectrum of nordeoxyecumicin before its structure was proposed, NMR structure sequencing was applied as described in Chapter 9.2.2. The spectrum generated from the pseudo HiFSA profile was superimposed on nordeoxyecumicin's ^{1}H NMR spectrum (Figure 103). The two matched well with only a few differences noticed. The β-proton signal of ecumicin's phenyl-serine unit (5.34 ppm, doublet) was

missing from the spectrum of nordeoxyecumicin, while the α-proton signal of this unit (4.80 ppm, doublet) was found to be a double of doublet in the experimental spectrum. This led to the assumption that the new peptide does not contain a phenyl-serine unit.

In contrast, two resonances at 3.35 ppm and 2.84 ppm that integrated for a little more than one proton each, were only observed in the nordeoxyecumicin's ^{1}H NMR spectrum. The signal(s) at 2.19 ppm integrated for two protons in the experimental spectrum, but it only accounted for one proton in the calculated one. Conversely, the signal at 1.97 ppm integrated for only one proton in the experimental spectrum, but in the calculated one it integrated for two protons that belong to the *N*-methyl-isoleucine and a valine. While signal at 1.23 ppm integrated for only one proton in the experimental spectrum, in the calculated pseudo spectrum it represented two protons that belong to *N*-methyl-isoleucine and *N*-methyl-leucine. Additionally, the methyl signal at 0.87 ppm resonated as a doublet in experimental spectrum, whereas in the calculated spectrum it was a triplet belonging to the *N*-methyl-isoleucine unit. These mismatches indicated that nordeoxyecumicin does not contain the *N*-methyl-isoleucine unit corresponding to that of ecumicin, either.

When superimposing nordeoxyecumicin's ^{1}H NMR spectrum with the spectrum generated from the HiFSA profile of 11 amino acids that are common to both peptides (Figure 104), resonances belonging to the amino acids in question should not overlap with anything from the calculated spectrum. As shown in the expansions, seven resonances fulfilled such criteria. Leaving out the signal at 2.19 ppm, the remaining six resonances (marked in grey in Figure 104)

would match well with the ^{1}H NMR pattern of a phenylalanine. The COSY spectrum (Figure 107) confirmed the connectivity in between the six resonances as belonging to two spin systems.

Knowing that nordeoxyecumicin has a phenylalanine in place of the phenyl-serine unit, we manually added the spin systems of phenylalanine to the second PMS file, and optimized it against nordeoxyecumicin's experimental ^{1}H NMR spectrum using the PERCH software. To gain information on the second unknown amino acid that replaces *N*-methyl-isoleucine, we then deleted all information on this amino acid to generate a third PMS file for further analysis.

To extract information on the second unknown amino acid, we overlaid the spectrum generated from the third PMS file and ^{1}H NMR spectrum of nordeoxyecumicin (Figure 105). As shown in the expansions, this amino acid unit has one presumably α-proton signal at 4.86 ppm, one *N*-methyl singlet at 3.25 ppm, one presumably β-proton signal at 2.19 ppm, and two presumably methyl doublets at 0.88 and 0.87 ppm. This suggests that nordeoxyecumicin's second unknown amino acid is an *N*-methyl-valine. The COSY spectrum (Figure 107) confirmed connectivity within this amino acid. This ^{1}H NMR profile suggested that nordeoxyecumicin has an *N*-methyl-valine instead of the *N*-methyl-isoleucine unit, which explains the remaining 14 amu mass difference equivalent to the structural difference of a methylene group.

The conclusions from HiFSA-assisted structural elucidation were fully supported by the DEPT-135 and ^{13}C NMR spectra (Figure 106). The β-carbon signal of phenyl-serine in ecumicin showed up as a tertiary one at 72.97 ppm, whereas that of phenylalanine (in nordeoxyecumicin) showed up as a secondary carbon at 38.20 ppm. Additionally, the lack of an *N*-methyl-isoleucine's

χ-carbon (C4) signal (26.56 ppm, secondary) was a clear indication that nordeoxyecumicin contains an *N*-methyl-valine unit instead of the *N*-methyl-isoleucine in ecumicin.

The proposed structure was further supported by the HSQC and HMBC experiments. Nordeoxyecumicin's 2D-NMR spectra were overlaid and compared with ecumicin's, as shown in Figure 108 and **Figure 109**. These comparisons further confirmed the presence of all eleven common amino acids in both peptides, and the shared difference between nordeoxyecumicin having an *N*-methyl-valine in place of the *N*-methyl-isoleucine in ecumicin.

Figure 103. Overlay of nordeoxyecumicin's pseudo HiFSA profile (blue) and the ^{1}H NMR spectrum (red) indicated that nordeoxyecumicin does not contain *N*-methyl-isoleucine or phenylserine.

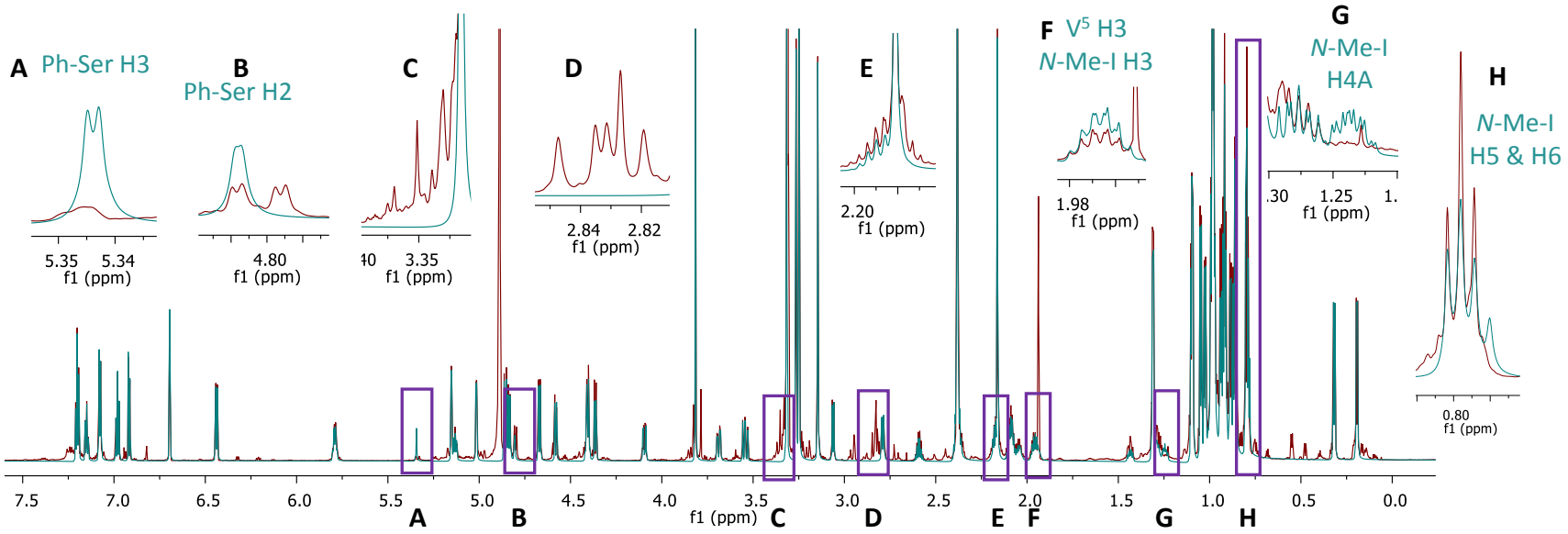


Figure 104. The overlay of the second ecumicin-based HiFSA profile (blue) and the ^{1}H NMR spectrum of nordeoxyecumicin (red) indicated that nordeoxyecumicin contains a phenylalanine (expansion in shadow) and a second unknown amino acid residue.

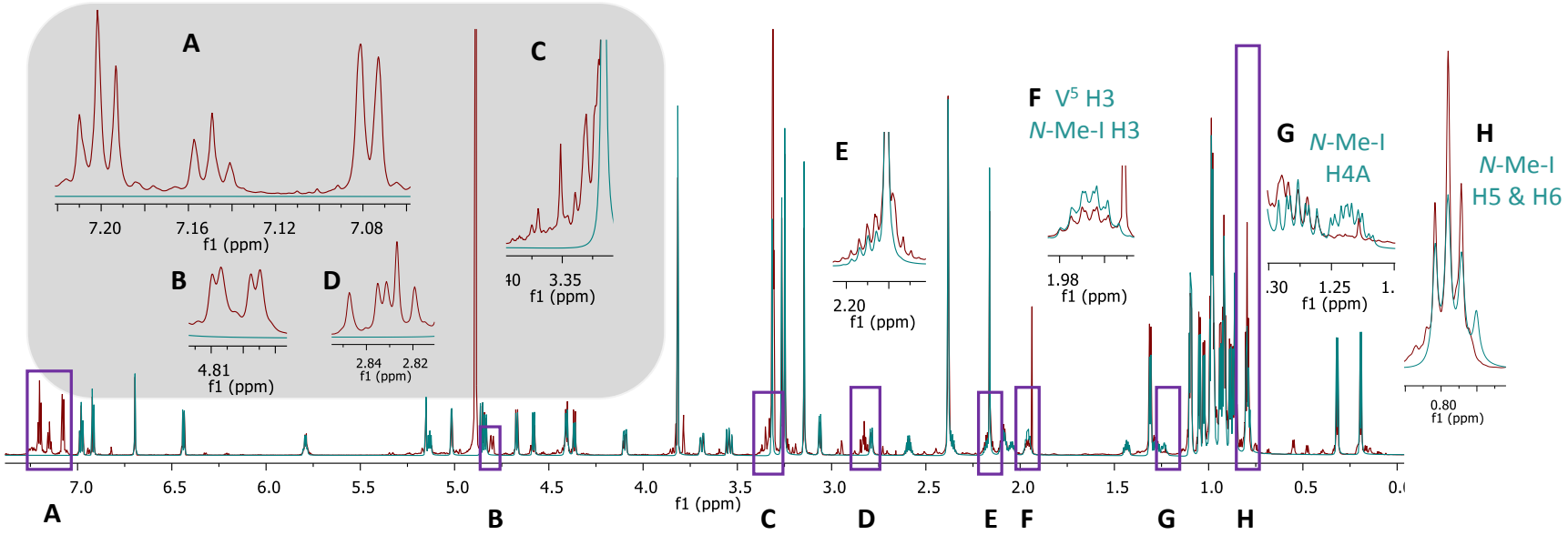


Figure 105. The overlay of the third ecumicin-based HiFSA profile (blue) and the ^{1}H NMR spectrum of nordeoxyecumicin (red) indicates nordeoxyecumicin contains a phenylalanine (expansion in shadow) instead of phenylserine, and an *N*-methyl-valine instead of *N*-methyl-isoleucine.

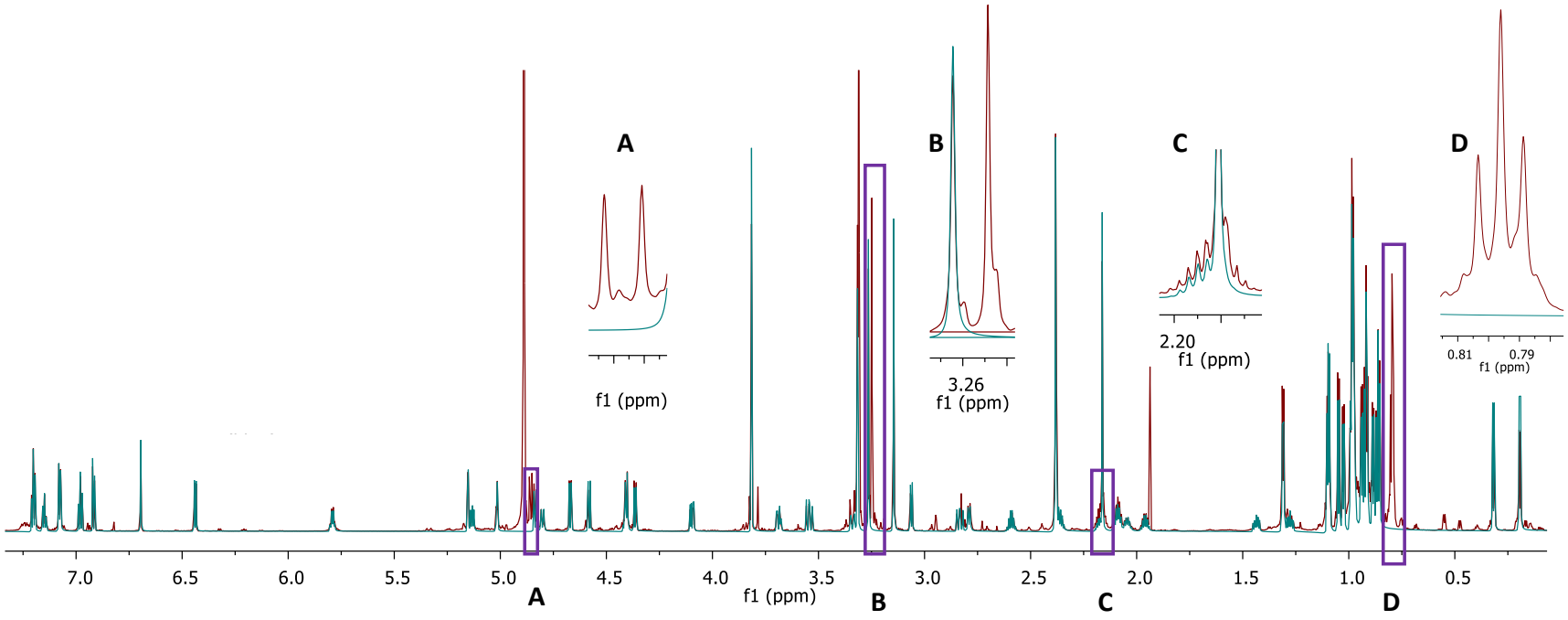


Figure 106. (A) DEPTQ-135 spectrum of nordeoxyecumicin (NDECM, blue), compared with DEPT-135 (ECM, green) and ^{13}C (red) spectra of ecumicin. (B) Expansions of DEPTQ-135 spectrum of NDECM (blue), compared with DEPT-135 (green).

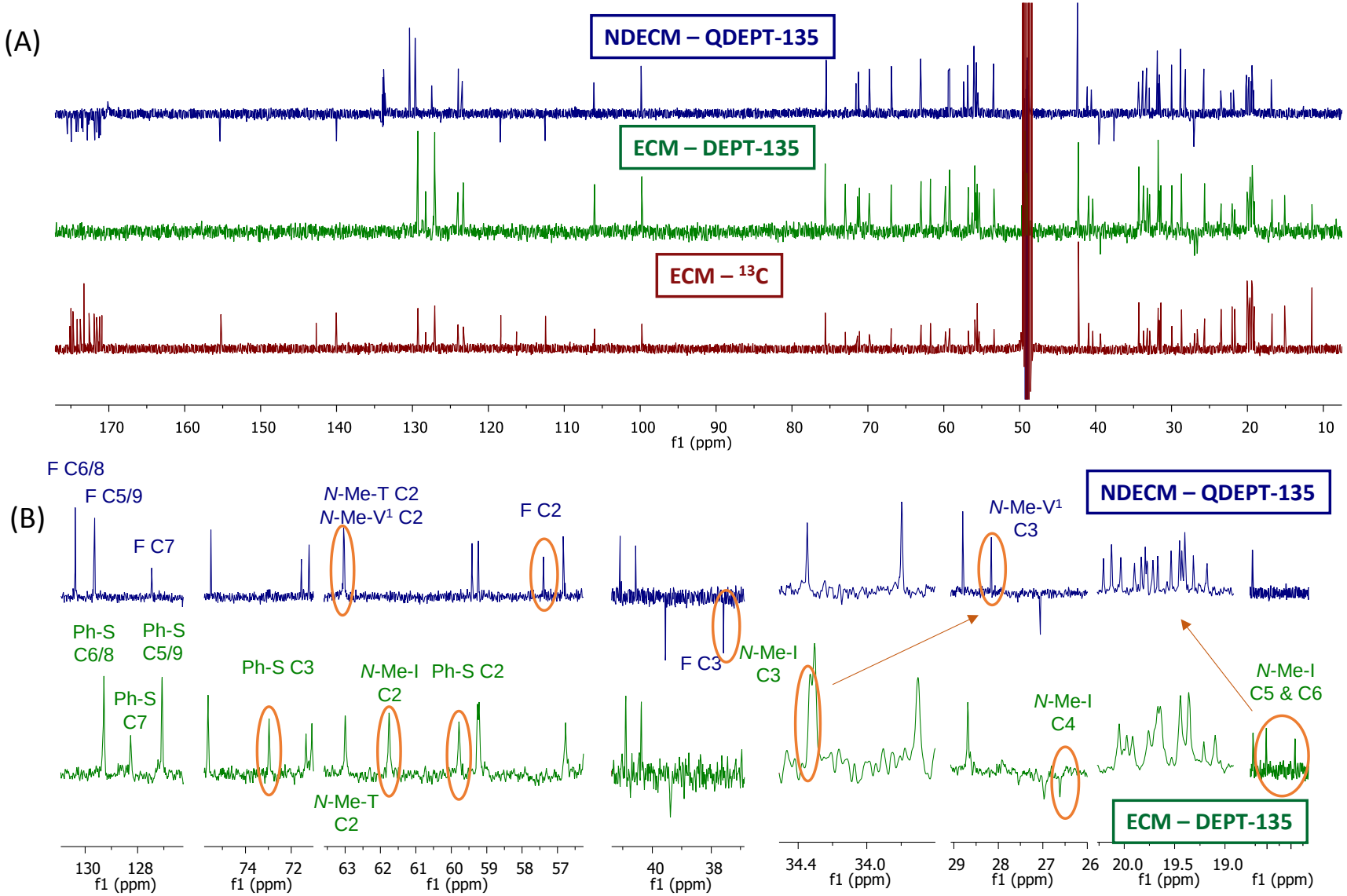


Figure 107. Comparison of the COSY spectra of nordeoxyecumicin (grey) and ecumicin (yellow).

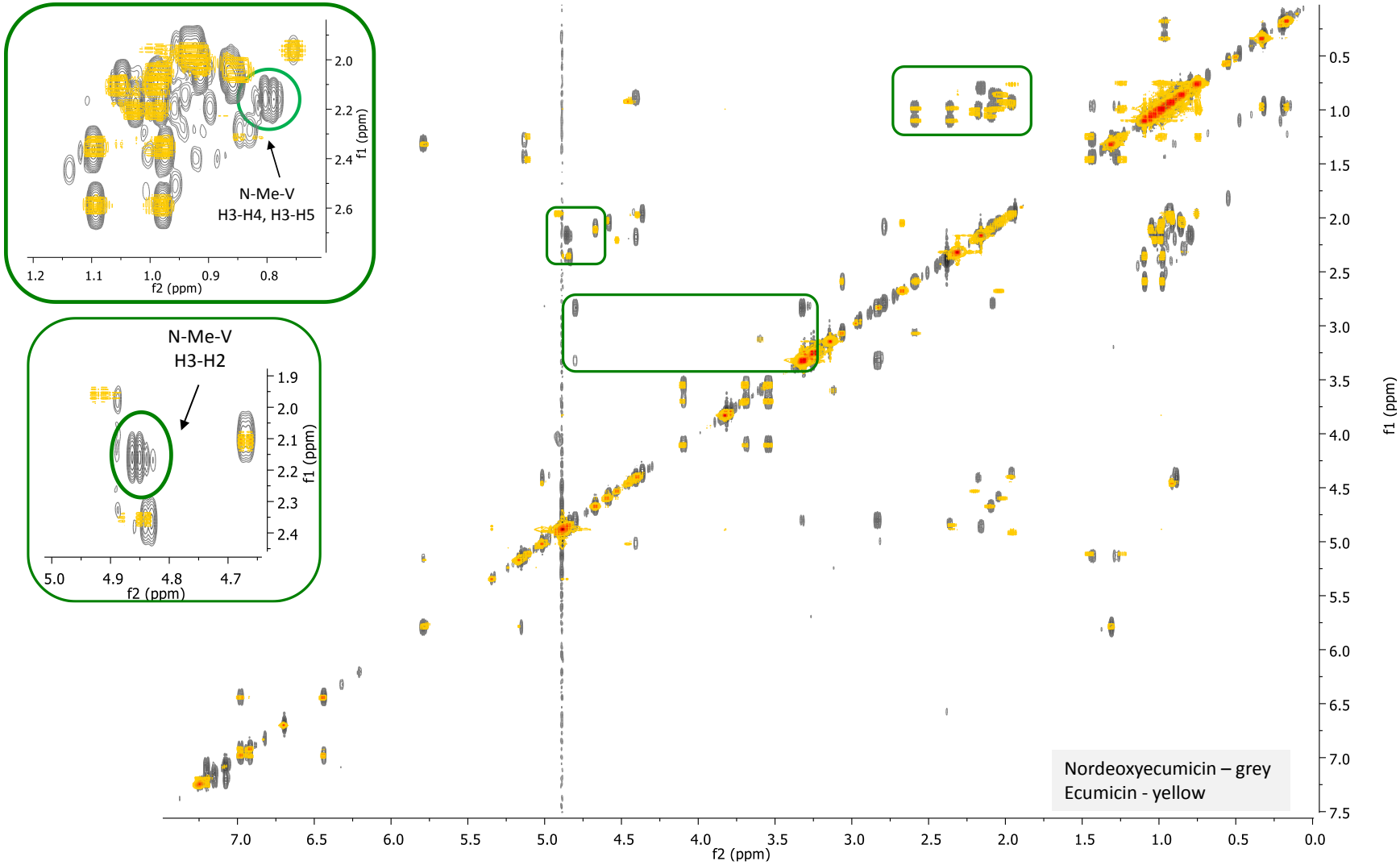


Figure 108. Comparison of the HSQC spectra of nordeoxyecumicin (grey) and ecumicin (red) with expansions.

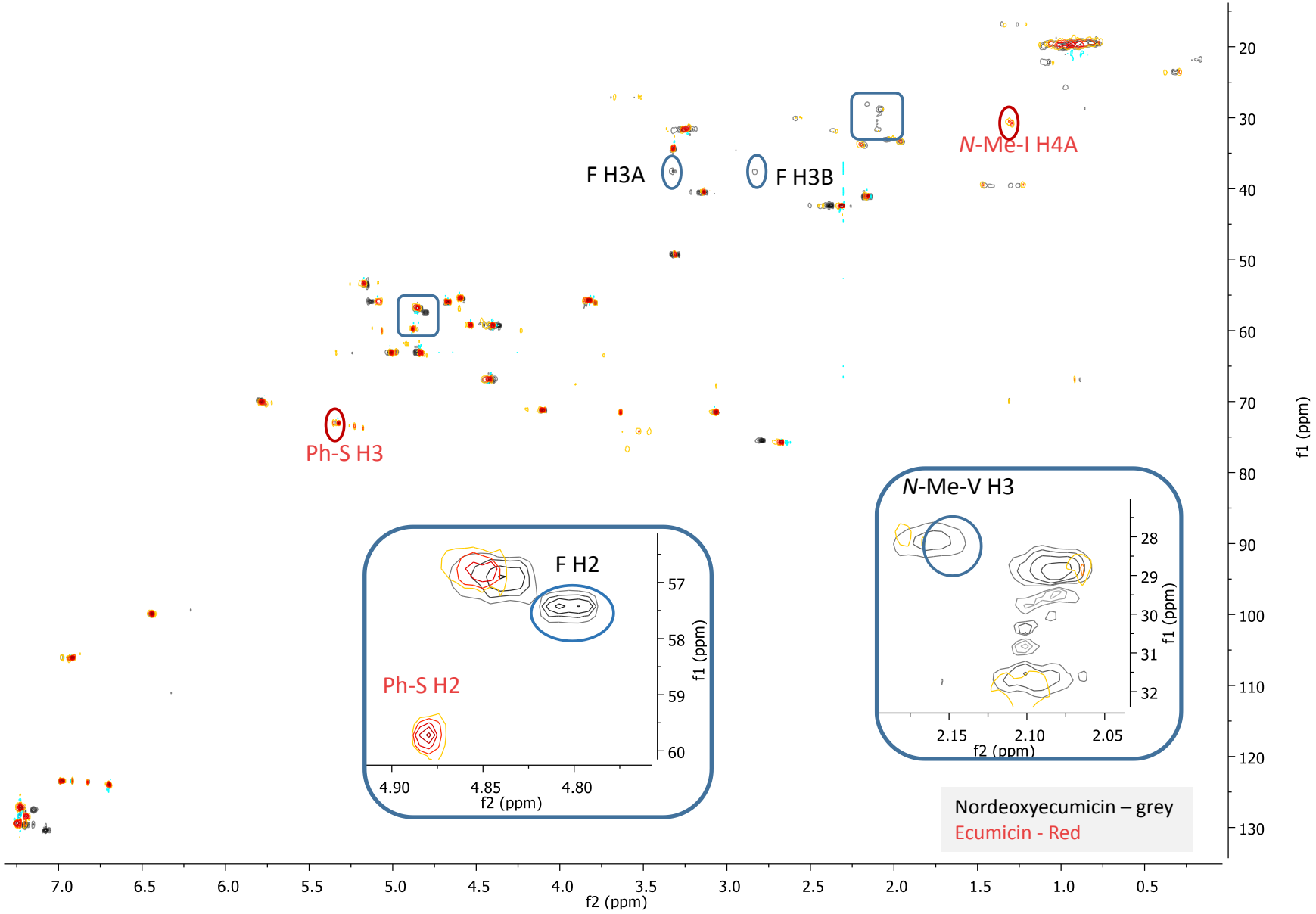
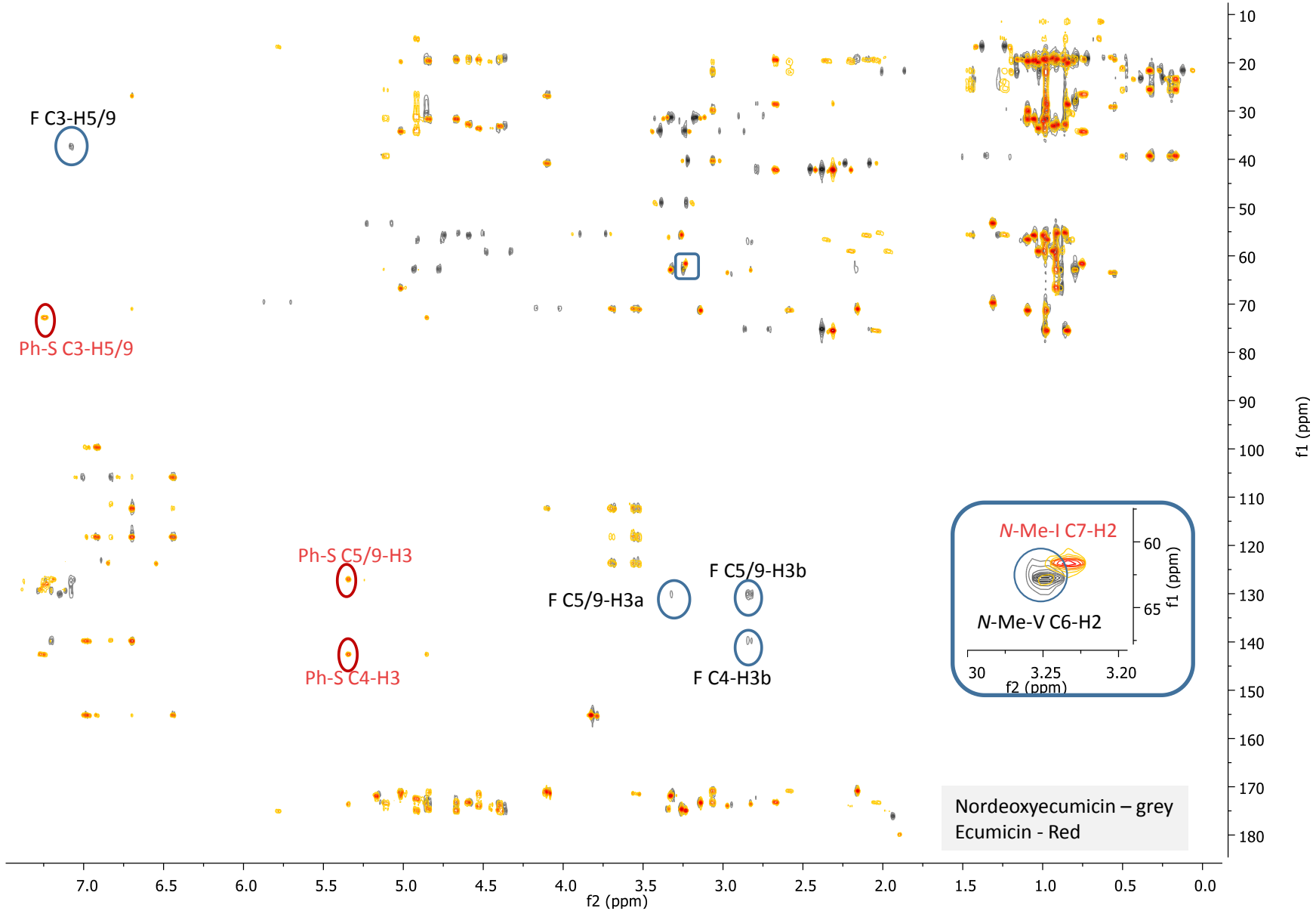


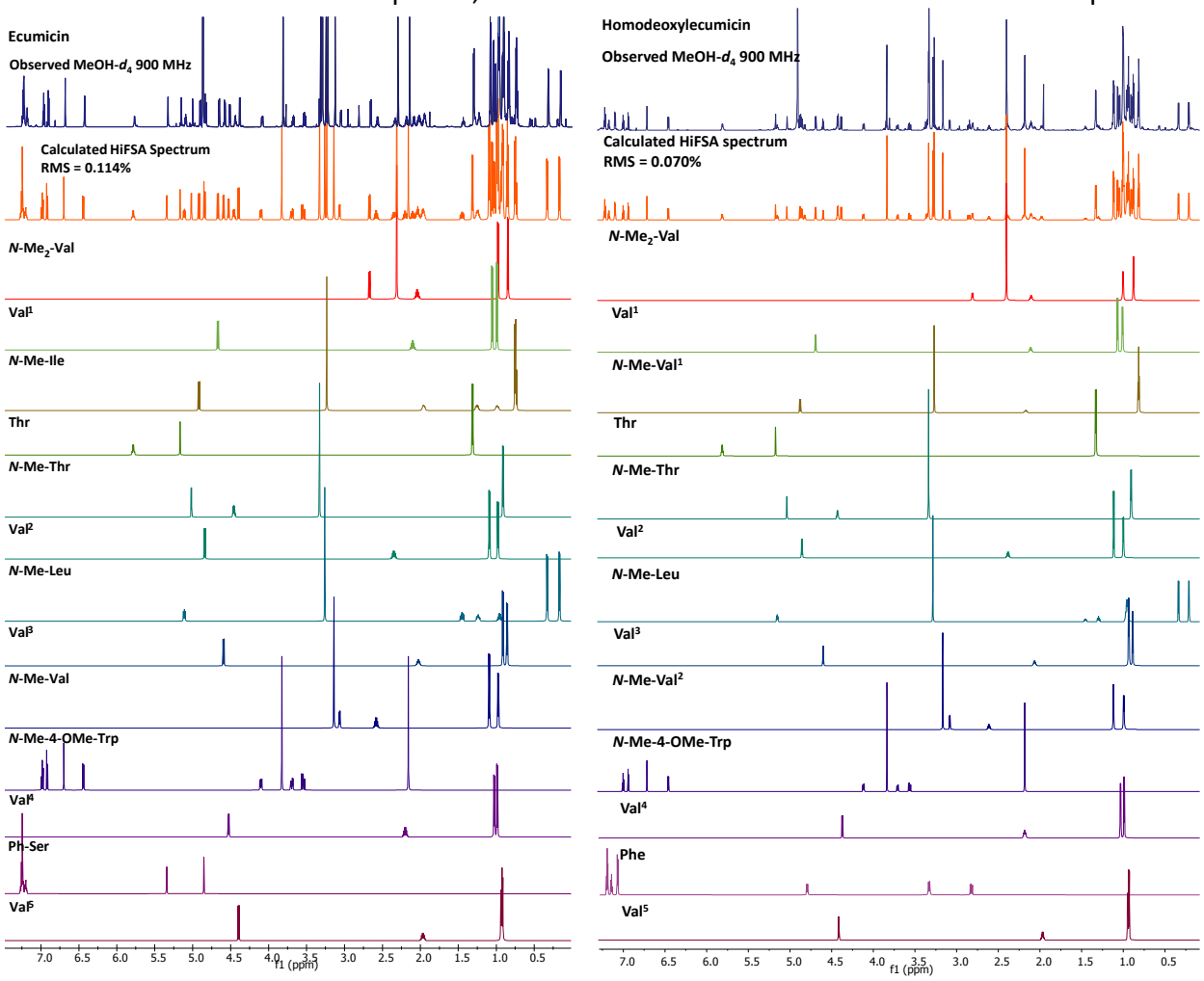
Figure 109. Comparison of the HMBC spectra of nordeoxyecumicin (grey) and ecumicin (red) with expansions.



9.4.3 HiFSA fingerprint of nordeoxyecumicin.

The HiFSA profile of nordeoxyecumicin was generated using the PERCH software tool, as described previously (Chapter 9.2.3). As a result, the observed overlapping multiplets were decipered, thereby allowing a thorough interpretation of the δ_H and J_{HH} values for all signals (TABLE XXIV). The comparison of individual spin systems corresponding to each amino acid (Figure 110) clearly presented the structural differences between nordeoxyecumicin and ecumicin. As the HiFSA study is able to predict "signal distortion in higher order coupled spin networks and reproduce complex signal patterns" (Napolitano, et al. 2012), it allows the re-generate of the AA'BB'C spin system (Figure 110A) and the AA'XX'M spin system (Figure 110B). Furthermore, because the HiFSA-generated ^{1}H NMR profiles consist of field-independent parameters, δ_H and J_{HH}, these high-resolution ^{1}H fingerprints can be efficiently used to simulate ^{1}H NMR data acquired at different field strengths. The HiFSA profile of nordeoxyecumicin is versatile, and can be used for chemical dereplication, qHNMR analysis, etc.

Figure 110. The ^{1}H iterative full spin analysis of (A) ecumicin and (B) nordeoxyecumicin, including the simulated amino acid sub-spectra, their mathematical sum and observed ^{1}H NMR spectrum.



9.5 Homoecumicin-11I

9.5.1 Isolation of homoecumicin-11I

Homoecumicin-11I (Figure 111), one component of R11 (Figure 74), is another member of the ecumicin peptide family produced by *Nonomuraea sp.* MJM5123. A very small amount of homoecumicin-11I (0.41 mg) was isolated by applying an additional HPLC separation step to the ecumicin isolation protocol discussed in Chapter 4. The overall separation scheme was as shown in Figure 75.

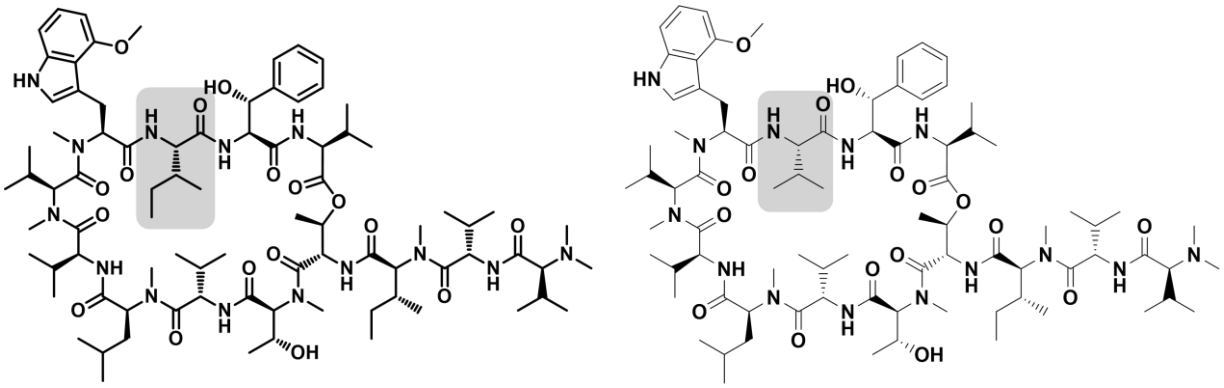
Purity of the homoecumicin-11I sample was estimated by the 100% NMR method as described in 9.2.1, with modifications. The ^{1}H NMR spectrum of the homoecumicin-11I sample (700 MHz, CD_3OD) was acquired under standard conditions (90 degree excitation pulse, acquisition time 3.8 s, relaxation delay 5.0 s) using a Bruker Avance III 700 instrument. Processing involved zero filling (2x), Lorentzian-Gaussian apodization (LB=-0.3, GB =0.02), and polynomial baseline correction.

The methyl doublet (δ_H 0.364 ppm) was selected as the most pure signal, and the integral was set to 3.000, representing the integral of three protons (3H). All other proton signals between δ_H 0.0 to 7.5 ppm in the spectrum, except for the solvent signals (HOD and CHD_2OD), were integrated, and the sum of these integrals was determined to be 330.5.

Assuming the molecular formula of homoecumicin-11I is identical to that of ecumicin, there would be a total of 125 non-exchangeable protons present in homoecumicin-11I. Assuming that impurities all have the same molecular weight as homoecumicin-11I, the purity was calculated as: Purity = 125×(3.00/3)/330.5×100 % = 37.8 %

9.5.2 Structure elucidation of homoecumicin-11I by HiFSA-assisted approach

Homoecumicin-11I (Figure 111) was isolated as a slightly yellow-colored powder. TABLE XXV summarizes the ^{13}C chemical shifts (δ_C), ^{1}H chemical shifts (δ_H) and $^{1}H,^{1}H$ scalar coupling constants (J_{HH}) of homoecumicin-11I. Interpretation of ^{1}H NMR was done by ^{1}H iterative Full Spin Analysis, and ^{13}C NMR data were obtained from interpration of the HSQC and HMBC spectrum. High resolution mass spectrometry (Figure 112) revealed that homoecumicin-11I has an exact mass of 1613.0140 amu, which is 14 amu more than that of ecumicin, indicating a possible structural difference of an additional methyl (RH to R-CH_3) or methylene group.



(A) Homoecumicin-11I (B) Ecumicin

Figure 111. (A) Proposed structure of homoecumicin-11I. (B) Structure of ecumicin.

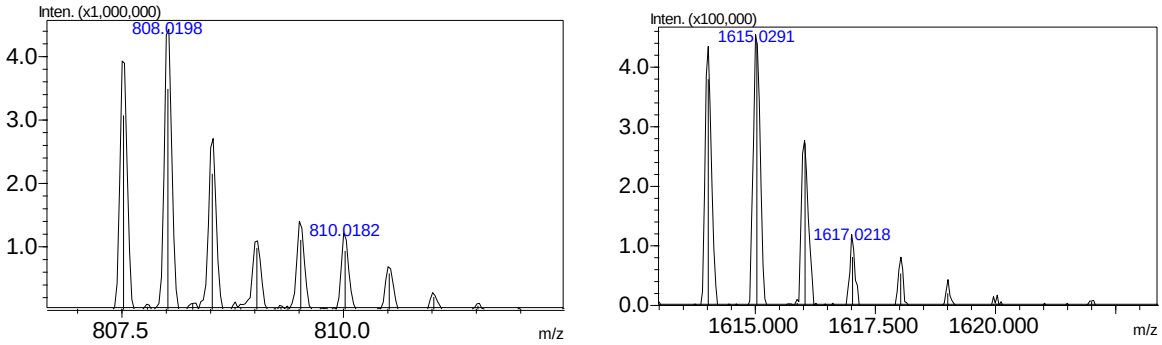


Figure 112. High resolution MS data of homoecumicin-11I. $[M+2H]^{2+}$= 807.5185 and $[M+H]^{+}$ = 1614.0213, so the exact mass of H13 was calculated to be 1613.0140.

TABLE XXV. ^{1}H AND ^{13}C NMR DATA OF HOMOECUMICIN-11I IN CD_3OD. INTERPRETATION OF ^{1}H NMR (700 MHZ) WAS DONE BY ^{1}H ITERATIVE FULL SPIN ANALYSIS; DUE TO HIGH LEVEL OF IMPURITIES IN THE SAMPLE, CHEMICAL SHIFTS FOR METHYL SIGNALS (0.84-1.10 PPM) WERE APPROXIMATE VALUES. ^{13}C NMR DATA WERE OBTAINED FROM INTERPRATION OF THE HSQC AND HMBC SPECTRUM. RESONANCES OF THE CARBONYL CARBONS AND METHYL CARBONS (19-20 PPM) WERE APPROXIMATE VALUES DUE TO SIGNAL OVERLAPPING IN BOTH 2D SPECTRA.

Amino Acid		^{1}H δ in ppm(mult, *J* in Hz)	^{13}C δ in ppm
N,N-Me_2-V	1	-	173
	2	2.70529 (d, 9.03)	75.61
	3	2.05355 (dqq, 9.03, 7.33, 6.66)	28.68
	4,5	2.33147 (s)	42.26
	6	0.98 (d, 7.33)	19.4
	7	0.85 (d, 6.66)	20.0
L-V[1]	1	-	174
	2	4.67025 (d, 8.37)	55.91
	3	2.10851 (dqq, 8.37, 6.49, 6.58)	31.62
	4	1.06 (d, 6.49)	19.6
	5	1.00 (d, 6.58)	19.5
N-Me-L-*allo*-I	1	-	173
	2	4.91421 (d, 11.32)	61.76
	3	1.95424 (dddq, 11.32, 2.21, 7.00, 6.30)	34.33
	4	0.99712 (ddq, 2.21, -14.81, 7.10)	26.61
		1.29080 (ddq, 7.00, -14.81, 7.74)	
	5	0.76 (d, 6.30)	11.5
	6	0.76 (dd, 7.10, 7.74)	15.1
	7	3.23554 (s)	31.4
L-T	1	-	172

Amino Acid		^{1}H δ in ppm(mult, *J* in Hz)	^{13}C δ in ppm
	2	5.16878 (d, 2.12)	53.39
	3	5.77581 (dq, 2.12, 6.54)	69.82
	4	1.31 (d, 6.54)	16.76
N-Me-L-T	1	-	171
	2	4.99943 (d, 3.63)	63.00
	3	4.44661 (dq, 3.63, 7.13)	66.93
	4	0.91 (d, 7.13)	19.9
	5	3.32548 (s)	34.30
L-V[2]	1	-	174
	2	4.86387 (d, 9.22)	56.77
	3	2.36565 (dqq, 9.22, 6.60, 6.50)	31.76
	4	1.09 (d, 6.60)	19.6
	5	0.98 (d, 6.50)	19.7
N-Me-L-L	1	-	173
	2	5.13179 (dd, 7.43, 7.42)	55.59
	3	1.23275 (ddd, 7.43, -14.05, 1.87)	39.37
		1.47750 (ddd, 7.42, -14.05, 5.78)	
	4	0.94883 (ddqq, 1.87, 5.78, 6.64, 6.64)	25.64
	5	0.18055 (d, 6.64)	21.67
	6	0.36399 (d, 6.64)	23.47
	7	3.26445 (s)	31.63
L-V[3]	1	-	173
	2	4.60962 (d, 9.22)	55.34
	3	2.00818 (dqq, 9.22, 6.41, 6.20)	32.88
	4	0.92 (d, 6.41)	19.7
	5	0.86 (d, 6.20)	19.7
N-Me-L-V	1	-	171
	2	3.07589 (d, 7.60)	71.37
	3	2.57597 (dqq, 7.60, 6.97, 6.51)	29.94
	4	0.96 (d, 6.97)	19.8
	5	1.10 (d, 6.51)	22.0
	6	3.13597 (s)	40.37
N-Me-4-OMe-L-Y	1	-	172
	2	4.118278 (dd, 11.17, 4.49)	71.11
	3	3.56446 (dd, 11.17, -13.59)	26.97
		3.69128 (dd, 4.49, -13.59)	
	4	-	112.47
	5	6.70184 (d, 0.87)	124
	6	-	140.04
	7	6.91948 (ddd, 0.87, 8.23, 0.90)	106.01
	8	6.98266 (dd, 8.23, 7.80)	123.3
	9	6.44345 (dd, 0.90, 7.80)	99.77
	10	-	155.23

Amino Acid		^{1}H δ in ppm(mult, *J* in Hz)	^{13}C δ in ppm
	11	-	118.36
	12	3.83015 (s)	55.59
	13	2.15773 (s)	40.9
L-I	1	-	174
	2	4.64593 (d, 7.18)	58.28
	3	1.96307 (dddq, 7.18, 11.65, 8.65, 6.80)	40.40
	4	1.57714 (ddq, 11.64, -15.20, 6.51)	20.07
		1.22206 (ddq, 8.65, -15.20, 6.81)	
	5	1.03 (d, 6.80)	19.7
	6	0.95 (dd, 6.51, 6.81)	19.7
Ph-L-*threo*-S	1	-	173
	2	4.91963 (d, 1.96)	59.78
	3	5.31912 (d, 1.96)	72.97
	4	-	142.68
	5,9*	7.22892 (dddd, 7.89, 1.29, 0.38, 1.86)	127.06
	6,8*	7.24918 (dddd, 7.89, 7.38, 1.98, 0.38)	129.28
	7*	7.19617 (dd, 1.29, 7.38)	128.25
L-V[5]	1	-	175
	2	4.40864 (d, 8.95)	59.26
	3	1.96736 (dqq, 8.95, 7.27, 6.83)	33.19
	4	0.93 (d, 7.27)	19.1
	5	0.92 (d, 6.83)	19.4

* Signals observed from an AA'BB'C spin system.

Due to the limited amount of sample, homoecumicin-11I was dissolved in 40 µl methanol-d_4 and NMR experiments including ^{1}H, COSY, HSQC, HMBC and semi-selective HMBC were acquired with a 700 MHz instrument equipped with a 1.7mm cryoprobe.

The presence of relatively large amount of other ecumicin analogs, the ^{1}H spectrum was complex. However, to acquire as much information as possible from the ^{1}H NMR spectrum of homoecumicin-11I, an attempt has been made to use the NMR structure sequencing method on the data.

The spectrum generated from the pseudo HiFSA profile was superimposed on homoecumicin-11I's ^{1}H NMR spectrum (Figure 113), several obvious differences were observed. However, due to the residual complexity, whether these differences all reflect the structural difference(s) between ecumicin and homoecumicin-11I is questionable. As shown in expansions, one sharp singlet was observed at 3.35 ppm, which integrated for approximately three protons. This suggested a possible additional *N*-methylation or *O*-methylation in homoecumicin-11I, which would explain the 14 amu difference. Alternatively, it could be the signal from residual nondeuterated methanol in the sample (Gottlieb, et al. 1997). However, the additional multiplet integrating for one proton was observed at 1.57 ppm, which might be part of an additional methylene group, would also explain the 14 amu mass difference. Another difference observed was that the β-signal of one of ecumicin's valines (V^4, 2.20 ppm) was potentially shifted to 1.95 ppm.

With two possible explanations for the 14 amu mass difference, information from the ^{1}H spectrum alone was inconclusive. To solve this problem, the 2D COSY (Figure 114), HSQC (Figure 115) and HMBC (Figure 116) spectra of homoecumicin-11I were studied.

In the homoecumicin-11I's HMBC spectrum (Figure 116), the proton signal at 3.35 ppm showed no correlation with any carbon signal, indicating that it is not a part of the homoecumicin-11I spectrum. On the other hand, the COSY spectrum (Figure 114) clearly linked the 1.57 ppm and 1.95 ppm signals, indicating the presence of an isoleucine unit. Comparison of the COSY spectra of homoecumicin-11I and ecumicin further confirmed that homoecumicin-11I has an isoleucine unit in place of a valine moiety in ecumicin.

The overlaid 2D-NMR spectra, as shown in Figure 114 to Figure **116**, confirmed the common presence of all the other twelve amino acids in both peptides.

The small amount and complex nature of the sample precludes our acquisition of a clear ^{13}C NMR spectrum for the structure elucidation of homoecumicin-11I..

Although attempts were made to acquire a semi-selective HMBC experiment with F1 focused on the carbonyl carbon region, the resultant spectrum (data not shown) exhibited a very low S/N ratio, and therefore insufficient in solving the exact location of the "new" amino acid unit. However, when comparing the first PMS file to the original ecumicin PMS text file, it was interesting to note that the chemical shifts of most signals remained essentially unchanged ($\Delta\delta < 0.05$ ppm), and the major differences were related to V^4 (the fourth valine unit, or the eleventh amino acid from the *N*-terminus of the peptide). Based on this observation, we concluded that the "new" isoleucine takes the place of the eleventh amino acid counting from the *N*-terminus of the peptide, in analogy to ecumicin.

Figure 113. Overlay of the psudo HiFSA profile (blue) and ^{1}H NMR spectrum of homoecumicin-11I (red) led to two possible explanations for their structural difference.

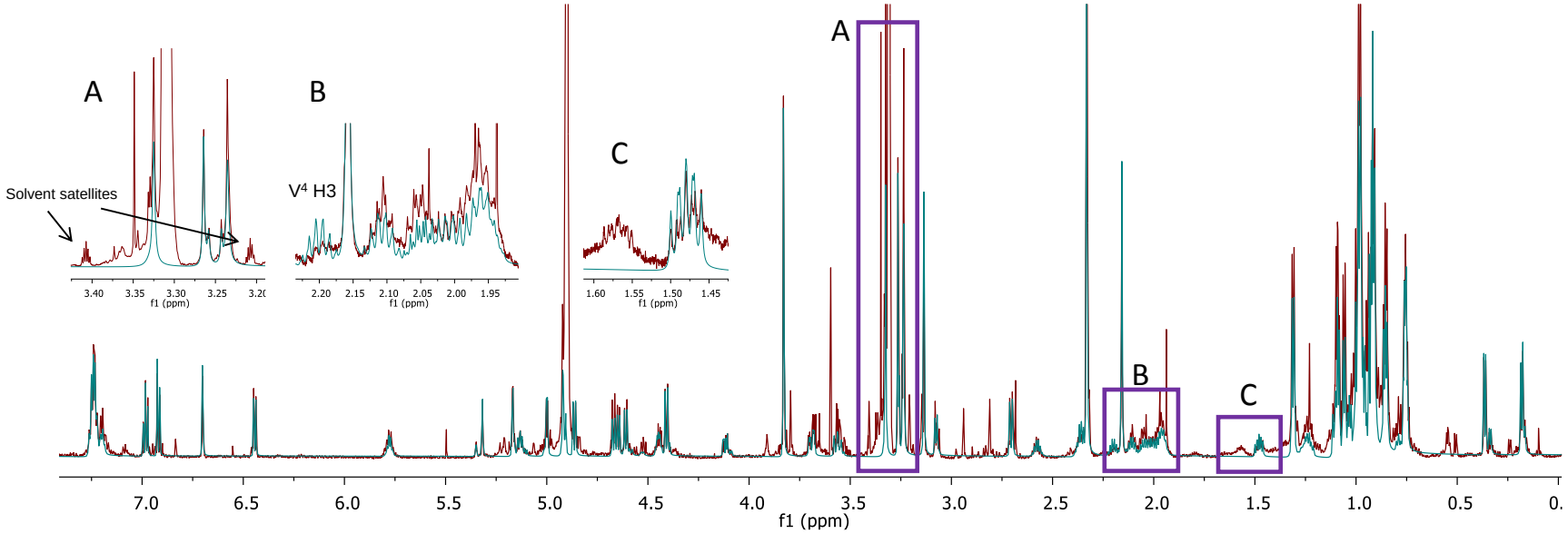


Figure 114. Comparison of the COSY spectra of homoecumicin-11I (grey) and ecumicin (yellow) with expansions.

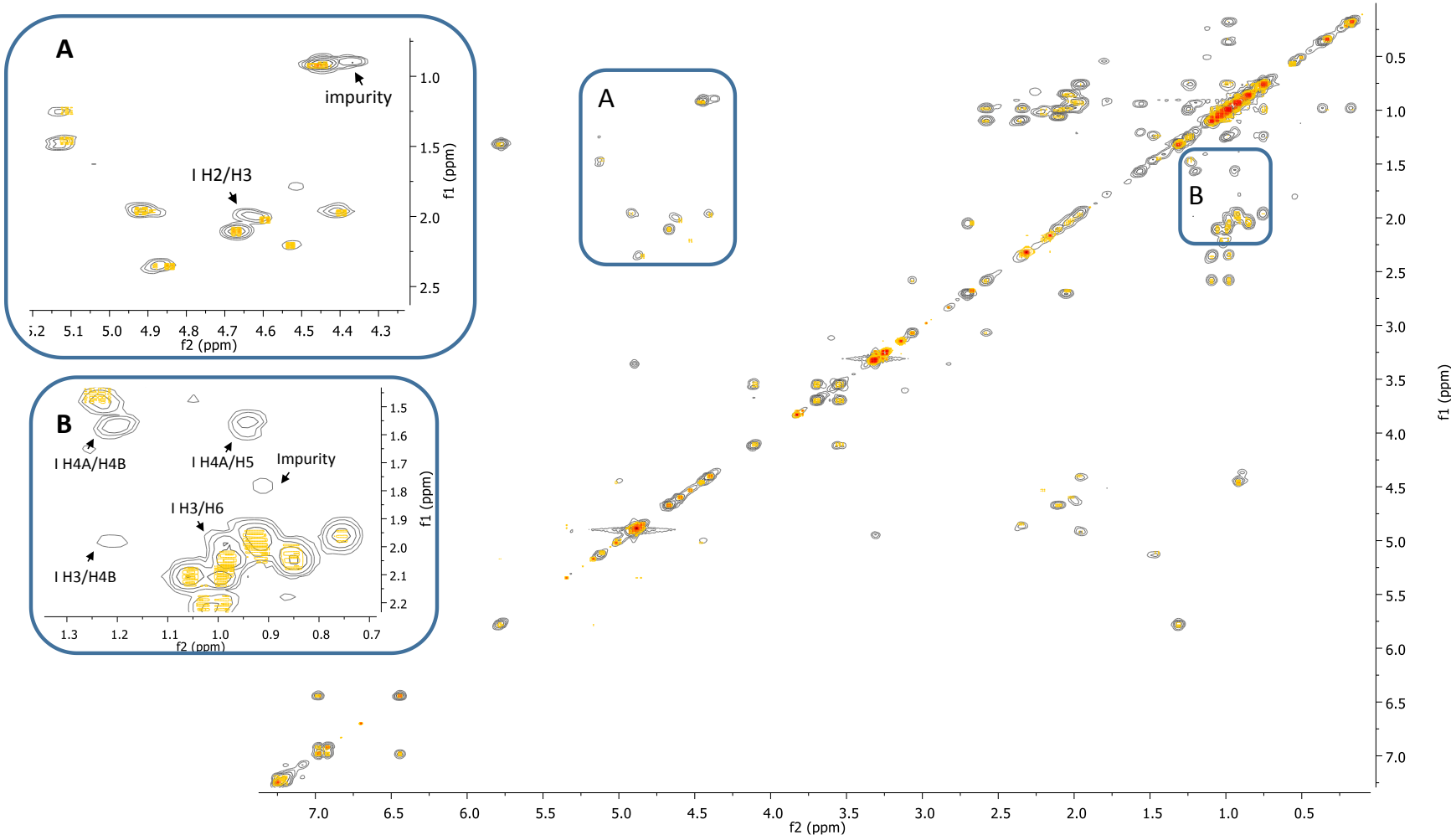


Figure 115. Comparison of the HMBC spectra of homoecumicin-11I (grey) and ecumicin (yellow) with one expansion.

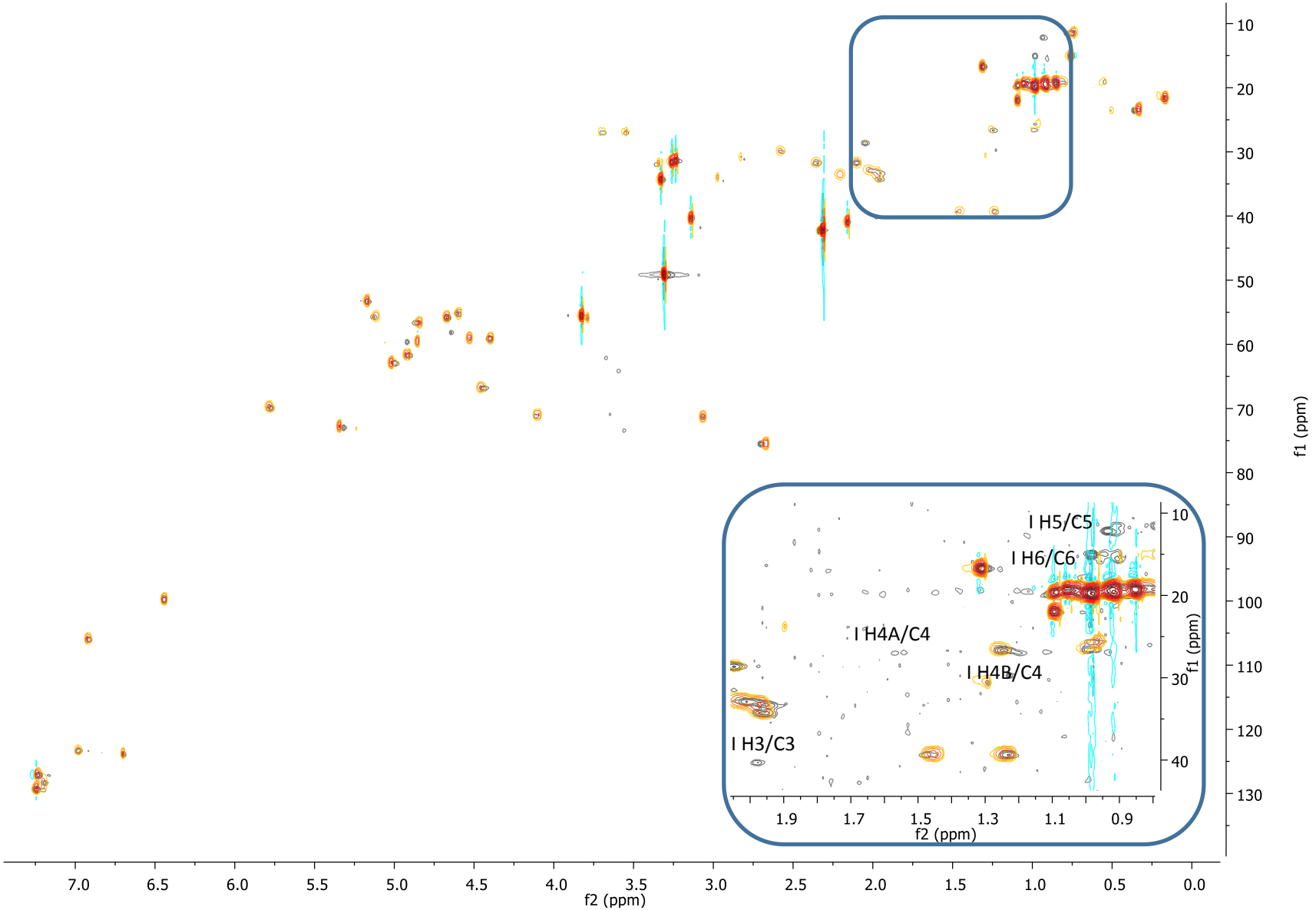
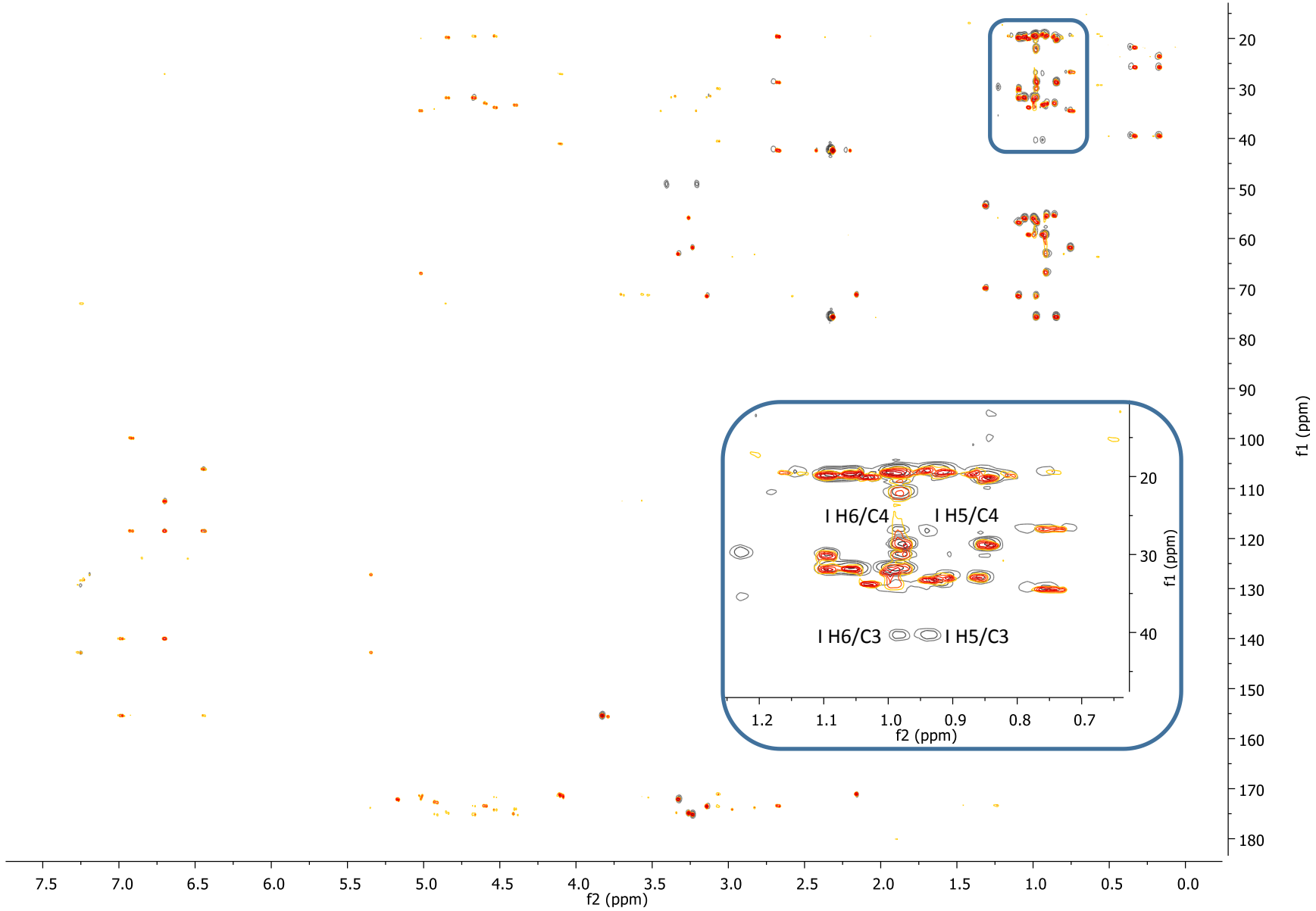


Figure 116. Comparison of the HMBC spectra of homoecumicin-11l (grey) and ecumicin (yellow) with one expansion.



9.5.3 HIFSA finger print of homoecumicin-11I

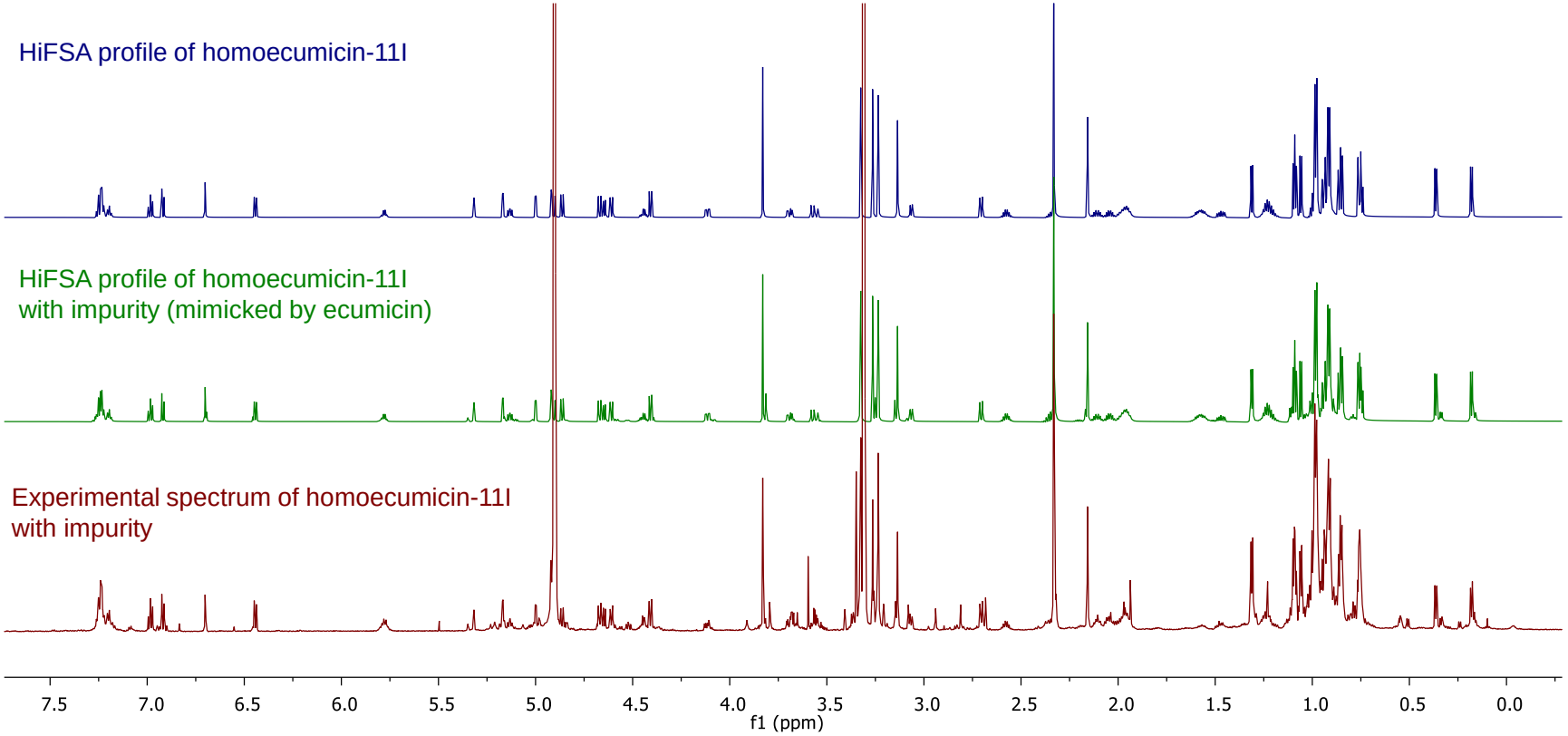
Several attempts were to generate HiFSA fingerprint for homoecumicin-11I, but none was unsuccessful.

In the first attempt, detailed analysis was carried out as describe in a previous publication (Napolitano, et al. 2012). The low purity of this sample presented a major challenge to the calculation in the Total-Line Fitting mode. The large amount of ecumicin-related impurities have caused a significant increase in integration of the overlapped regions, especially the terminal methyl region. During the iteration process, the PERCH iterator attempted to overcome this difficulty by modifying the “RESP(Y)” values of some signals. This led to the generation of a PMS file that would match the experimental spectrum well (RMS = 0.160 %), but exhibited a quantitative deviation in the exact shape of each signal. For example, the software assigned one methyl doublet with RESP(Y) = 0.6889, while another methyl doublet was given RESP(Y) = 0.1353. The ratio of the resultant integrals in the simulated spectrum would be approximately 5:1, which is not in line with the structure as both signals represent one methyl group in a same molecule.

As a result, a second attempt was made to generate the HiFSA profile of homoecumicin-11I, by having the PERCH iterator to perform the calculation based on the assumption that there are two major molecules in the sample, homoecumicin-11I and ecumicin. The later was used to mimic the major but yet unknown impurity, as the major impurities in the sample are ecumicin analogs. In order to avoid iteration of the “RESP(Y)” values, only Integral-Transform Fitting was performed. Using this approach, the resultant HiFSA profile fitted well with the experimental spectrum, with an RMS of 0.269 % (Figure 117).

Even though a good RMS and spectral agreement was achieved between the experimental and calculated spectra, the inclusion of a large number of variables in the heavily overlapped methyl region (0.80 – 1.10 ppm) and the existence of unidentified impurities, limited the reliability of the iterated chemical shifts of the methyl groups of homoecumicin-11I. Accordingly, the chemical shifts of these resonances are reported as estimated values with only two decimals in TABLE XXV. While a more pure sample of homoecumicin-11I would allow for a definite HiFSA profiling, this might be difficult to achieve due to its low abundance and the very close chromatographic similarity of this compound with its congeners.

Figure 117. ^{1}H NMR spectrum (700 MHz, methanol-d_4) and HiFSA profile of homoecumicin-11I with or without simulated impurity.



9.6 Homoecumicin-13I

9.6.1 Isolation of homoecumicin-13I

Homoecumicin-13I (Figure 118) representing another component of the R11 fraction in Figure 74, is another member of the ecumicin peptide family produced by *Nonomuraea sp.* MJM5123. A very small amount of homoecumicin-13I (0.27 mg) was isolated by applying an additional HPLC separation step to the ecumicin isolation protocol. The overall separation scheme was as shown in Figure 75.

Purity of the homoecumicin-13I sample was estimated by the 100% NMR method as described in 9.5.1, with modifications. Acquisition and processing of the ^{1}H NMR spectrum of the homoecumicin-13I sample were performed as described in 9.5.1.

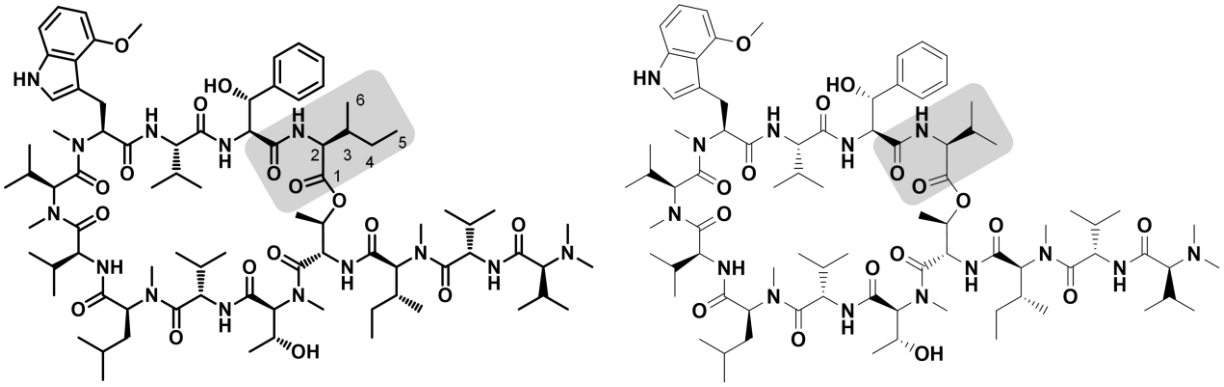
The methyl doublet (δ_H 0.337 ppm) was isolated from an overlapping doublet (δ_H 0.325) by Mnova using the line-fitting option. The de-convoluted methyl signal (δ_H 0.337) was selected as the most pure signal, and the integral was set to 3.000, representing the integral of three protons (3H). All other proton signals between δ_H 0.0 to 7.5 ppm in the spectrum, except for the solvent signals (HOD and CHD_2OD), were integrated, and the sum of these integrals was determined to be 341.5.

Assuming the molecular formula of homoecumicin-13I is the same as that of ecumicin, a total of 125 non-exchangeable protons present in homoecumicin-13I. Assuming that impurities all have the same molecular weight as homoecumicin-13I, the purity was calculated as:

Purity = 125×(3.00/3)/341.5×100 % = 36.6 %

9.6.2 Structure elucidation of homoecumicin-13I by HiFSA-assisted approach

Homoecumicin-13I (Figure 118) was isolated as a pale yellow powder. TABLE XXVI summarizes the ^{1}H chemical shifts (δ_H), $^{1}H,^{1}H$ scalar coupling constants (J_{HH}) and most ^{13}C chemical shifts (δ_C), of homoecumicin-13I. Interpretation of ^{1}H NMR was done by ^{1}H iterative Full Spin Analysis, and ^{13}C NMR data were obtained from interpration of the HSQC and HMBC spectrum. The ^{13}C NMR spectrum was not acquired due to the small sample size (0.27 mg). High resolution mass spectrometry (Figure 119) revealed that homoecumicin-13I has an exact mass of 1613.0174 amu, which is very close to that of homoecumicin-11I (Δ exact mass = 0.0034 amu). The +14 amu difference from the exact mass of ecumicin, indicated a possible structural difference of an additional methylene group.



(A) Homoecumicin-13I (B) Ecumicin

Figure 118 (A) Proposed structure of homoecumicin-13I. (B) Structure of ecumicin.

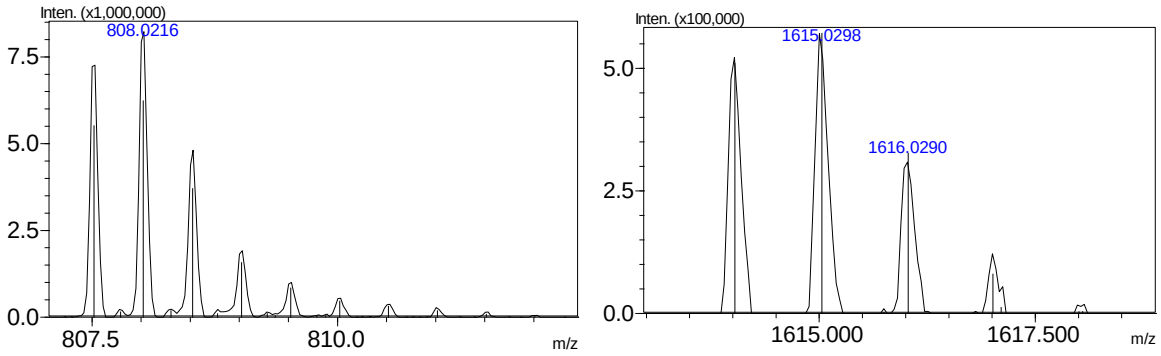


Figure 119. High resolution MS data of homoecumicin-13I. $[M+2H]^{2+}$= 807.5194 and $[M+H]^{+}$ = 1614.0247, so the exact mass of H13 was calculated to be 1613.0174.

TABLE XXVI. ^{1}H AND ^{13}C NMR DATA OF HOMOECUMICIN-13I IN CD_3OD. INTERPRETATION OF THE ^{1}H NMR (700 MHZ) WAS DONE BY ^{1}H ITERATIVE FULL SPIN ANALYSIS; DUE TO THE RESIDUE COMPLEXITY OF THE SAMPLE, CHEMICAL SHIFTS FOR METHYL SIGNALS (0.84 - 1.10 PPM) WERE APPROXIMATE VALUES. ^{13}C NMR DATA WERE OBTAINED VIA INTERPRATING THE HSQC AND HMBC SPECTRA; RESONANCES OF THE CARBONYL CARBONS AND METHYL CARBONS (19-20 PPM) WERE APPROXIMATE VALUES DUE TO SEVERE SIGNAL OVERLAPPING.

Amino Acid		^{1}H δ in ppm (mult, *J* in Hz)	^{13}C δ in ppm
N,N-Me_2-V	1	-	
	2	2.69022 (d, 9.03)	75.61
	3	2.05355 (dqq, 9.03, 7.33, 6.66)	28.68
	4,5	2.32549 (s)	42.26
	6	0.98 (d, 7.33)	19.4
	7	0.85 (d, 6.66)	20.0
L-V[1]	1	-	
	2	4.66507 (d, 8.37)	55.91
	3	2.09976 (dqq, 8.37, 6.49, 6.58)	31.62
	4	1.06 (d, 6.49)	19.6
	5	1.00 (d, 6.58)	19.5
N-Me-L-*allo*-I	1	-	
	2	4.91107 (d, 11.32)	61.76
	3	1.94974 (dddq, 11.32, 2.21, 7.00, 6.30)	34.33
	4	0.955039 (ddq, 2.21, -14.81, 7.10)	26.61
		1.29676 (ddq, 7.00, -14.81, 7.74)	
	5	0.76 (d, 6.30)	11.5
	6	0.75 (dd, 7.10, 7.74)	15.1
	7	3.23399 (s)	31.4
L-T	1	-	
	2	5.16103 (d, 2.12)	53.39

Amino Acid		^{1}H δ in ppm (mult, *J* in Hz)	^{13}C δ in ppm
	3	5.77264 (dq, 2.12, 6.54)	69.82
	4	1.31050 (d, 6.54)	16.76
N-Me-L-T	1	-	
	2	5.00806 (d, 3.63)	63.00
	3	4.44661 (dq, 3.63, 7.13)	66.93
	4	0.91 (d, 7.13)	19.9
	5	3.32909 (s)	34.30
L-V^{2}	1	-	
	2	4.51469 (d, 8.95)	59.26
	3	1.96467 (dqq, 8.95, 7.27, 6.83)	33.19
	4	0.93 (d, 7.27)	19.1
	5	0.92 (d, 6.83)	19.4
N-Me-L-L	1	-	
	2	5.11610 (dd, 7.43, 7.42)	55.59
	3	1.23757 (ddd, 7.43, -14.05, 1.87)	39.37
		1.45819 (ddd, 7.42, -14.05, 5.78)	
	4	0.94881 (ddqq, 1.87, 5.78, 6.64, 6.64)	25.64
	5	0.16898 (d, 6.64)	21.67
	6	0.33659 (d, 6.64)	23.47
	7	3.26059 (s)	31.63
L-V^{3}	1	-	
	2	4.60860 (d, 9.22)	55.34
	3	2.02620 (dqq, 9.22, 6.41, 6.20)	32.88
	4	0.92 (d, 6.41)	19.7
	5	0.86 (d, 6.20)	19.7
N-Me-L-V	1	-	
	2	3.07491 (d, 7.60)	71.37
	3	2.58434 (dqq, 7.60, 6.97, 6.51)	29.94
	4	0.98 (d, 6.97)	19.8
	5	1.10 (d, 6.51)	22.0
	6	3.14550 (s)	40.37
N-Me-4-OMe-L-Y	1	-	
	2	4.10158 (dd, 11.17, 4.49)	71.11
	3	3.56044 (dd, 11.17, -13.59)	26.97
		3.69094 (dd, 4.49, -13.59)	
	4	-	
	5	6.69838 (d, 0.87)	124
	6	-	
	7	6.91883 (ddd, 0.87, 8.23, 0.90)	106.01
	8	6.98233 (dd, 8.23, 7.80)	123.3
	9	6.44245 (dd, 0.90, 7.80)	99.77
	10	-	

Amino Acid		^{1}H δ in ppm (mult, *J* in Hz)	^{13}C δ in ppm
	11	-	
	12	3.83015 (s)	55.59
	13	2.15773 (s)	40.9
L-V[4]	1	-	
	2	4.52490 (d, 7.90)	59.21
	3	2.19963 (dqq,7.90, 6.75, 6.81)	33.7
	4	1.03 (d, 6.75)	19.7
	5	0.99 (d, 6.81)	19.7
Ph-L-*threo*-S	1	-	
	2	4.83911 (d, 1.96)	59.78
	3	5.31912 (d, 1.96)	72.97
		-	
	4	-	
	5,9*	7.23832 (dddd, 7.89, 1.29, 0.38, 1.86)	127.06
	6,8*	7.25511 (dddd, 7.89, 7.38, 1.98, 0.38)	129.28
	7*	7.20220 (dd, 1.29, 7.38)	128.25
L-I	1	-	
	2	4.83994 (d, 8.92)	59.65
	3	1.78519 (dddq, 8.92, 6.69, 7.03, 7.03)	39.33
	4	1.40045 (ddq, 6.69, -14.00, 7.03)	26.97
		1.12045 (ddq, 7.03, -14.00, 7.03)	
	5	0.91 (d, 7.03)	12.50
	6	0.91 (dd, 7.03, 7.03)	15.69

* Signals observed from an AA'BB'C spin system.

The entire 0.27 mg homoecumicin-13I sample was dissolved in 40 µl methanol-d_4 and placed in a 1.7 mm NMR tube. NMR spectra including ^{1}H, COSY, HSQC, HMBC and semi-selective HMBC were acquired using a 700 MHz instrument equipped with a 1.7 mm cryoprobe.

Because of the small sample size and presence of relatively large amount of other ecumicin analogs, the ^{1}H spectrum was rather complex. However, in an attempt to acquire as much information as possible from the ^{1}H NMR spectrum, NMR structure sequencing was applied.

As shown in Figure 120, the impurities' contribution to the signal intensities in ^{1}H spectrum of homoecumicin-13I was significant. As a result, it was quite difficult to find the difference between the spectrum generated from pseudo HiFSA profile and the experimental one. The presence of a signal in multiplet around 1.60 ppm together with the chemical shifts of upfield impurity signals at 0.18 and 0.36 ppm, indicated homoecumicin-11I being the major impurity. Accordingly, a second pseudo HiFSA profile was generated by including homoecumicin-11I into the calculation.

As shown in Figure 121, protons resonances at 2.36, 1.79, 1.40 and 1.12 ppm were observed in the experimental spectrum but missing from the simulated one. This supported the assumption of an additional methylene group in homoecumicin-13I compared to ecumicin. However, to locate this additional methylene group in the new molecule required more information.

The 2D-COSY spectrum revealed that the additional methylene group gave rise to the signals at 1.40 and 1.12 ppm., and it was located in a new isoleucine unit. The coupling pathway of this amino acid unit is marked in Figure 122.

The overlaid COSY, and HSQC spectra of ecumicin and homoecumicin-13I, as shown in Figure 122 and **Figure 123**, confirmed presence of all the other twelve amino acids common to both molecules. Due to the limited sample amount, the HMBC (Figure 124) and semi-selective HMBC (data not shown) spectra of homoecumicin-13I exhibited only low signal to noise ratios, and therefore, did not provide additional information about the amino acid connectivity. However, when comparing the HiFSA profiles of 12 common amino acids shared by the two

peptides relative to the original one of ecumicin, it was noted that the chemical shifts of most signals have remained relatively unchanged ($\Delta\delta < 0.05$ ppm), and the major differences were related to V^5, which is the fifth valine unit, or the thirteenth amino acid from the *N*-terminus of the peptide. Based on this observation, and the assumption that the peptide was synthesized by the NRPS that mainly produces ecumicin, we concluded that the "new" isoleucine is the thirteenth amino acid counting from the *N*-terminus of the peptide, and thus named it homoecumicin-13I.

Figure 120. Comparison of homoecumicin-13I's experimental ^{1}H spectrum (red) with the spectrum generated from the pseudo HiFSA profile (blue). The residual complexity limited the identification of the meaningful difference between the two spectra.

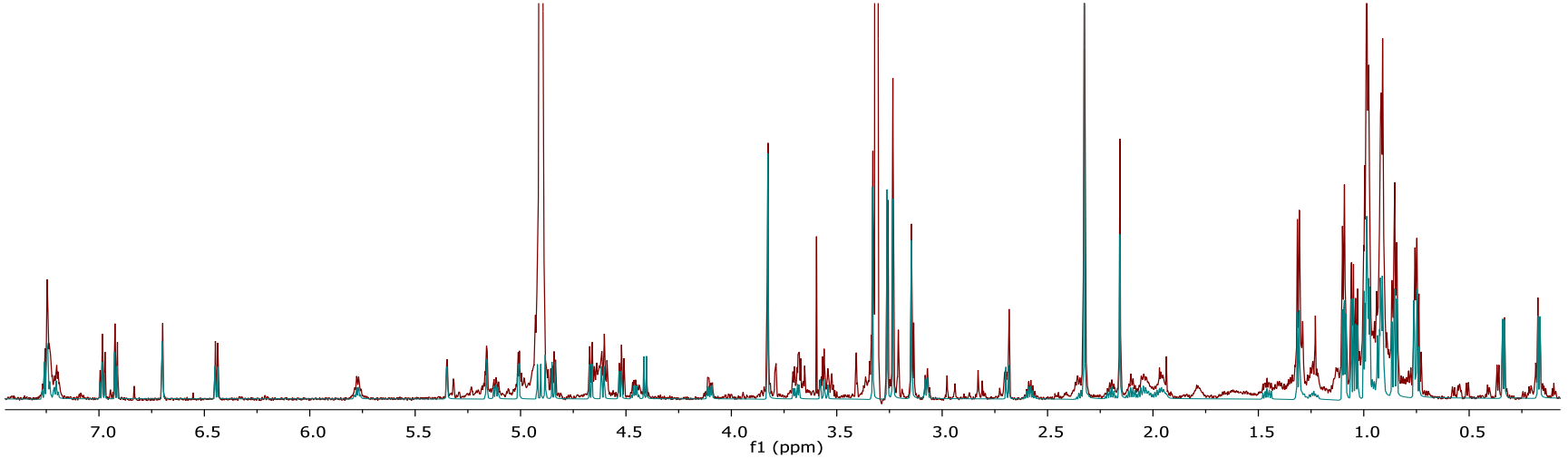


Figure 121. Comparison of homoecumicin-13I's experimental 1H spectrum (red) and the spectrum generated from the second pseudo HiFSA profile (blue). Inclusion of homoecumicin-11I as the major impurity in the calculation (blue) was critical for the identification of the meaningful differences between the two spectra.

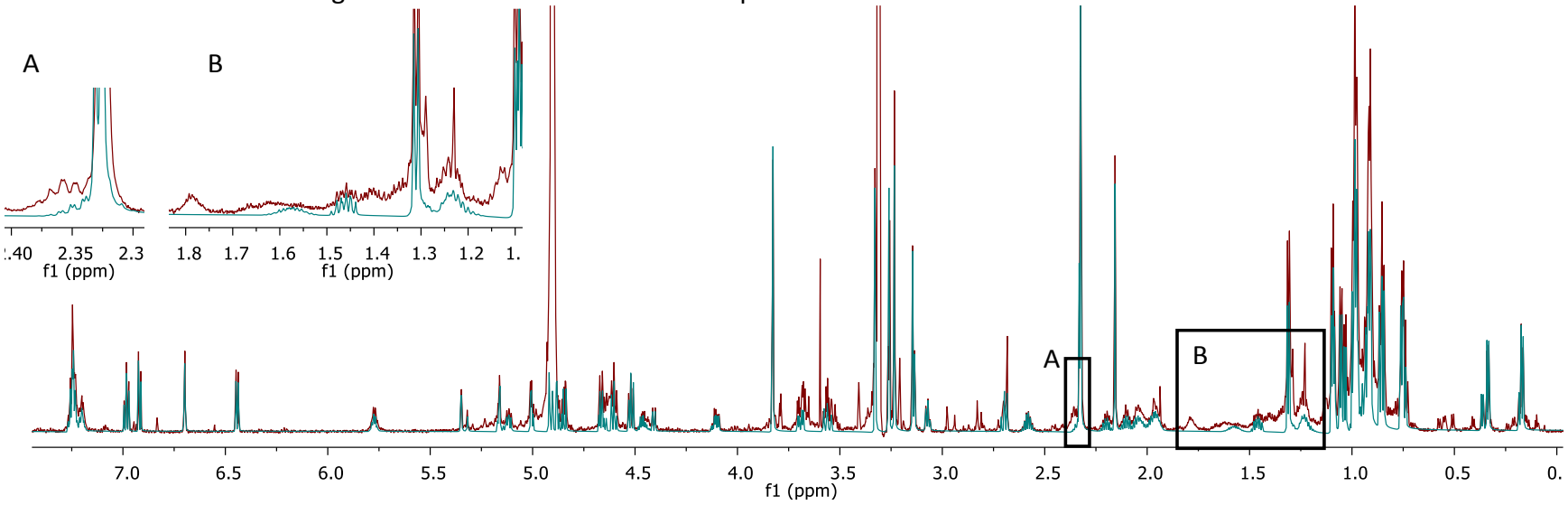


Figure 122. Comparison of the COSY spectra of homoecumicin-13I (grey) and ecumicin (yellow) with expansion pf one region.

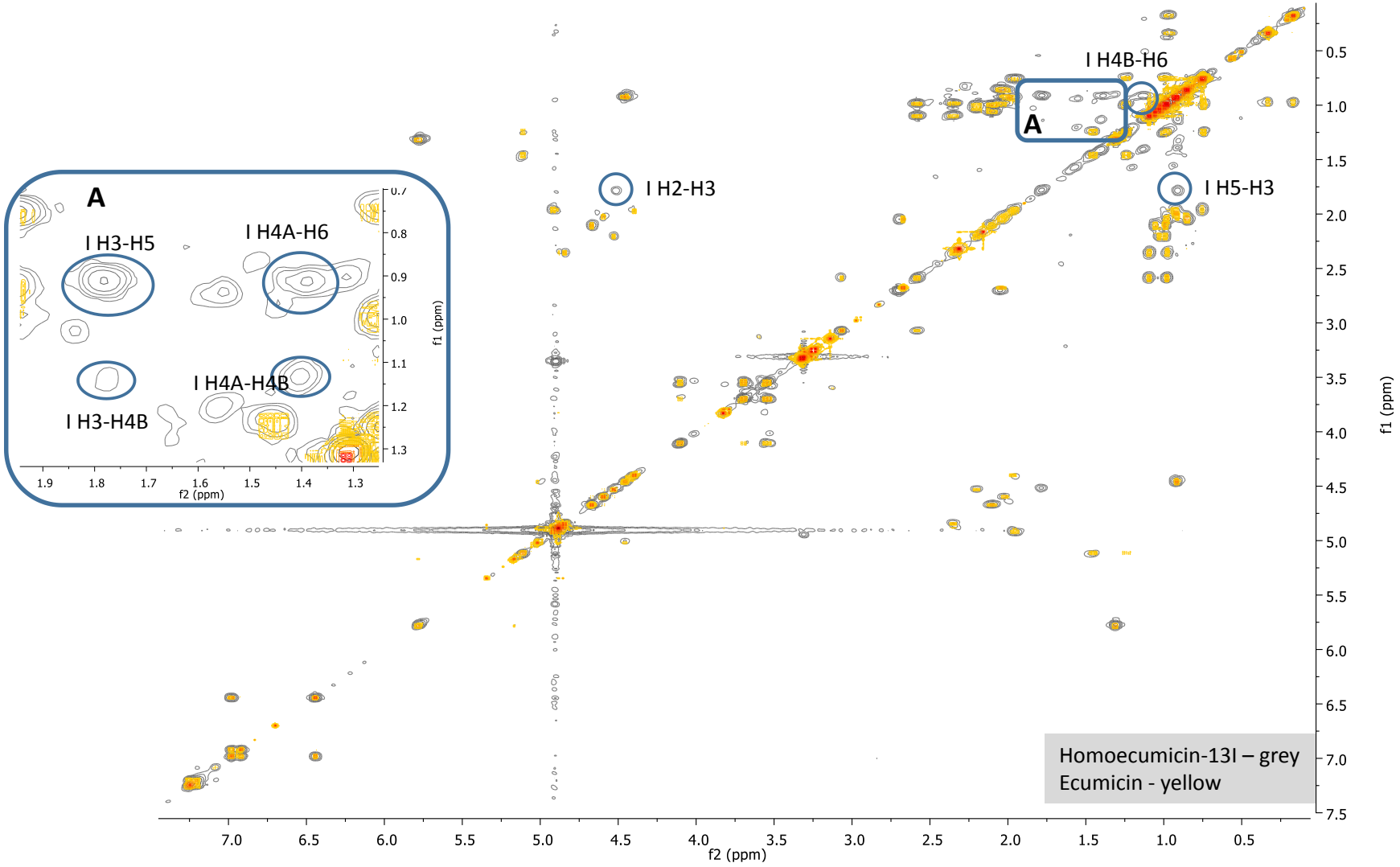


Figure 123. Comparison of HSQC spectra of homoecumicin-13I (grey) and ecumicin (yellow) with expansions

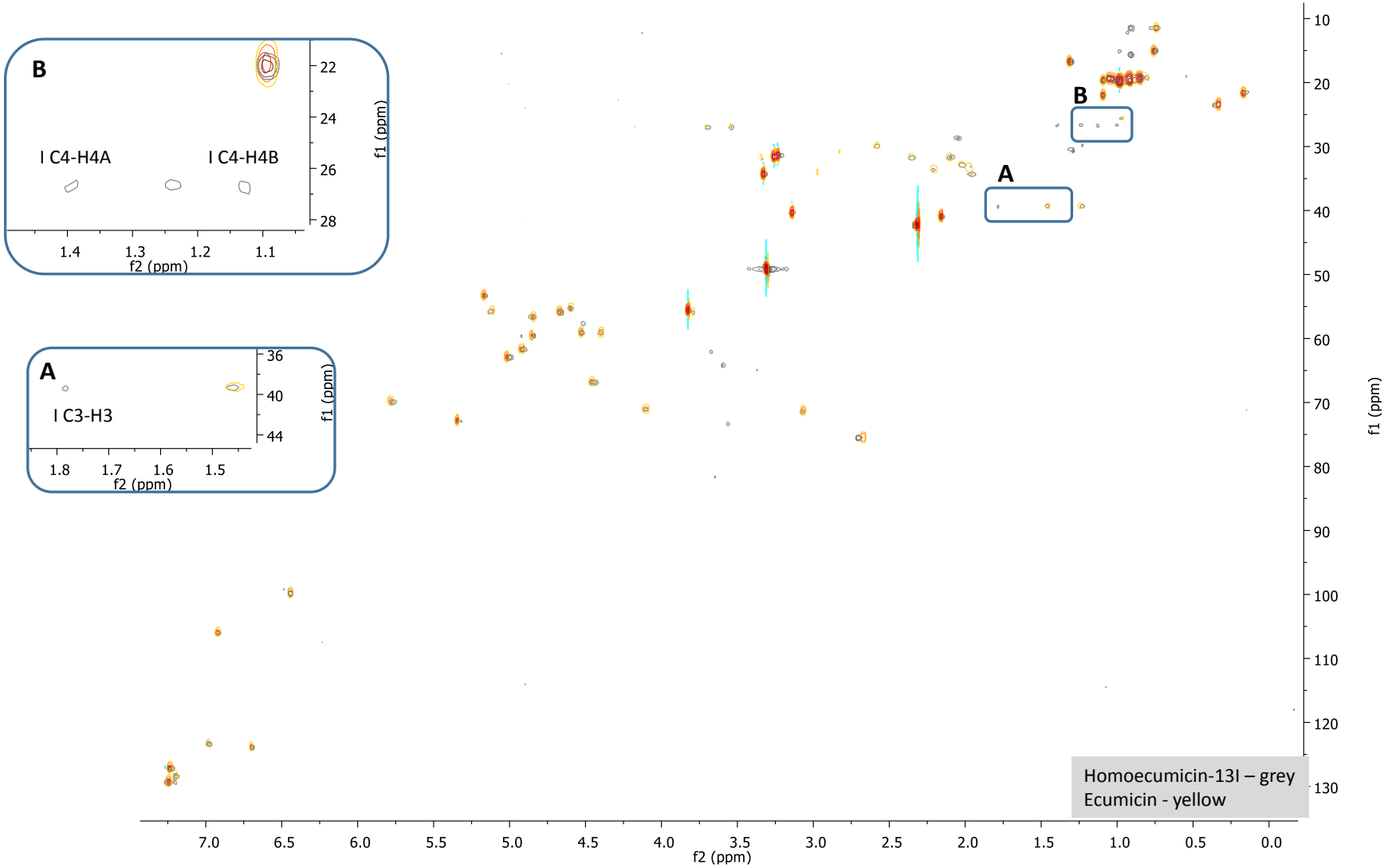
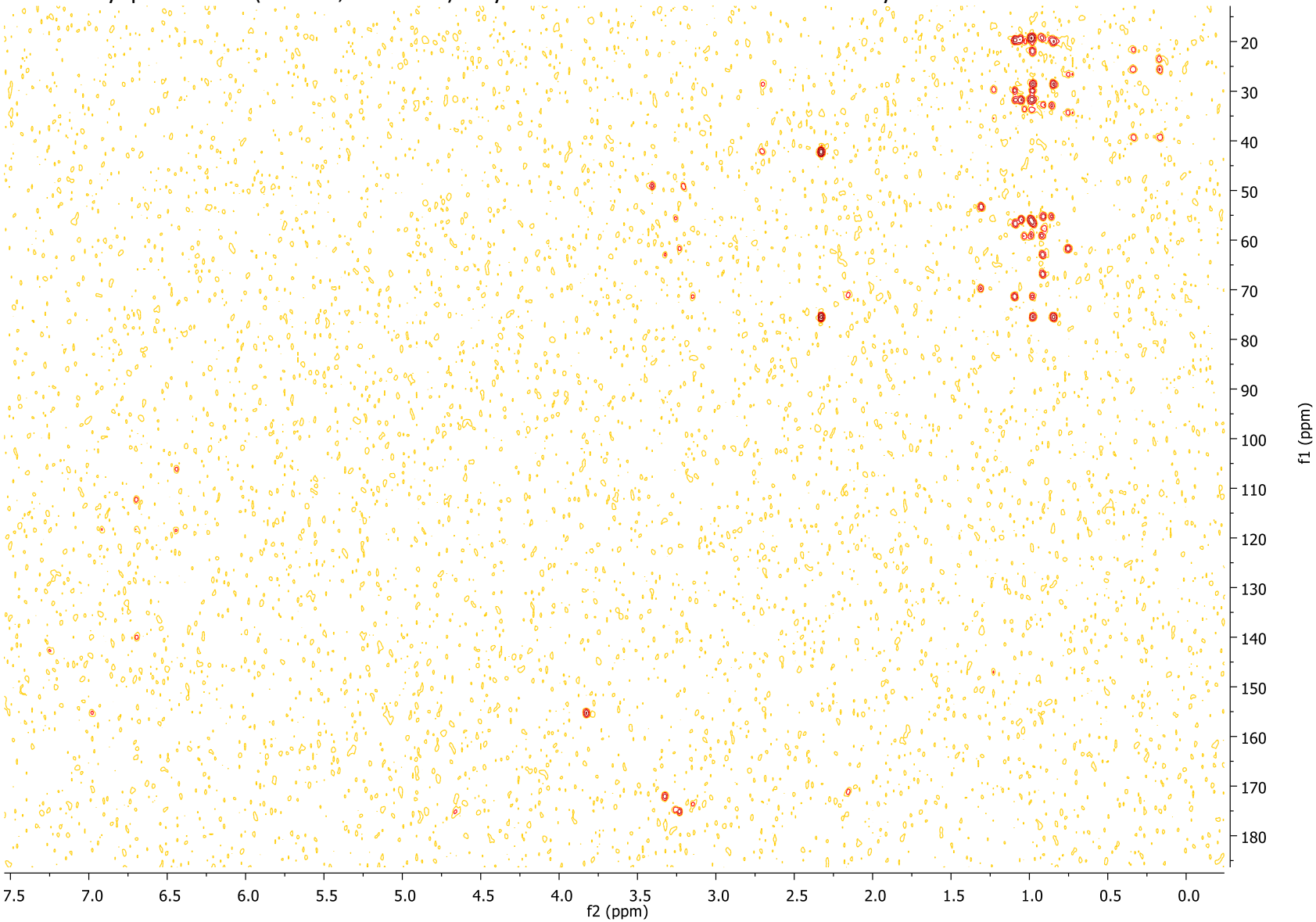


Figure 124. Due to the limited amount of sample (0.27 mg) of sample, the HMBC spectrum of homoecumicin-13I using a 700 MHz 1.7 mm cryoprobe NMR (NS = 64, TD1= 300) only showed the correlations of the methyl and a few select ^{1}H resonances.



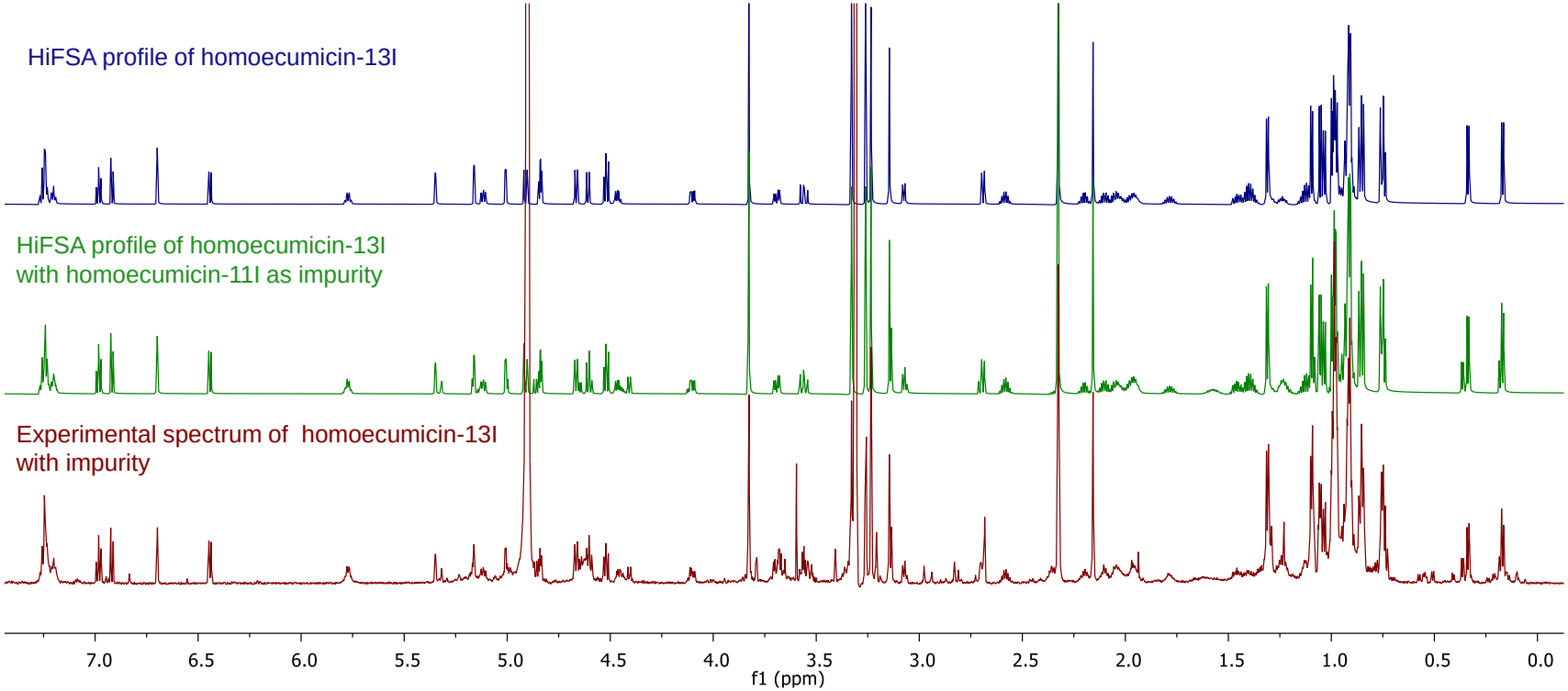
9.6.3 HIFSA fingerprint of homoecumicin-13I

Similar to the case of homoecumicin-11I, the small amount of the homoecumicin-13I sample, as well as its low purity, resulted in a rather complex ^{1}H spectrum. However, it was still possible to generate the HiFSA profile of homoecumicin-13I, by having the Perch iterator to perform calculation based on the assumption that there are two major components in the sample, homoecumicin-13I and homoecumicin-11I. In order to eliminating scaling of the "RESP(Y)" values as discussed in Chapter 9.5.3, only Integral-Transform Fitting was performed. The final calculated HiFSA profile fitted well with the experimental spectrum, with an RMS = 0.287 % (Figure 125).

Although a good agreement was achieved between the experimental and calculated spectrum, the existence of a large number of yet uncharacterized variables for signals associated with other smaller impurities, especially in the heavily overlapped methyl region (0.80 – 1.10 ppm), has reduced the reliability of iterated chemical shifts of homoecumicin-13I's methyl groups. So they were reported as approximate values with only two decimals.

Although a more pure sample of homoecumicin-13I would lead to a definite HiFSA profiling, this might be difficult to achieve. Together with its low yield (approximately 9 ng per liter fermentation), that the major impurities are homoecumicin-13I's congeners poses a challenge in the isolation of this compound, as they have very similar chromatographic behaviors.

Figure 125. ^{1}H NMR spectrum (700 MHz, methanol-d_4) and HiFSA profile of homoecumicin-13I with or without simulated impurity.



9.7 Homoecumicin-6I

9.7.1 Isolation of homoecumicin-6I

Homoecumicin-6I (Figure 126), which represents a third major component of R11 (Figure 74), is yet another member of the ecumicin peptide family produced by *Nonomuraea sp.* MJM5123. A small amount of homoecumicin-6I (0.31 mg) was isolated by applying an additional HPLC separation step to the ecumicin isolation protocol that was described in Chapter 4. The overall separation scheme is as shown in Figure 75.

Purity of the homoecumicin-6I sample was estimated by the 100% NMR method as described in 9.5.1, with modifications.

The methyl doublet (δ_H 0.197 ppm, labeled as **3** in Figure 128) was isolated from neighboring overlapping doublets (δ_H 0.211 and 0.212) using the line fitting method as implemented in the Mnova NMR software. The de-convoluted methyl signal (δ_H 0.197) was selected as the most pure signal, and the integral was set to 3.000, representing the integral of three protons (3H). All other proton signals between δ_H 0.0 to 7.5 ppm in the spectrum, except for the solvent signals (HOD and CHD_2OD), were integrated, and the sum of these integrals was determined to be 482.3.

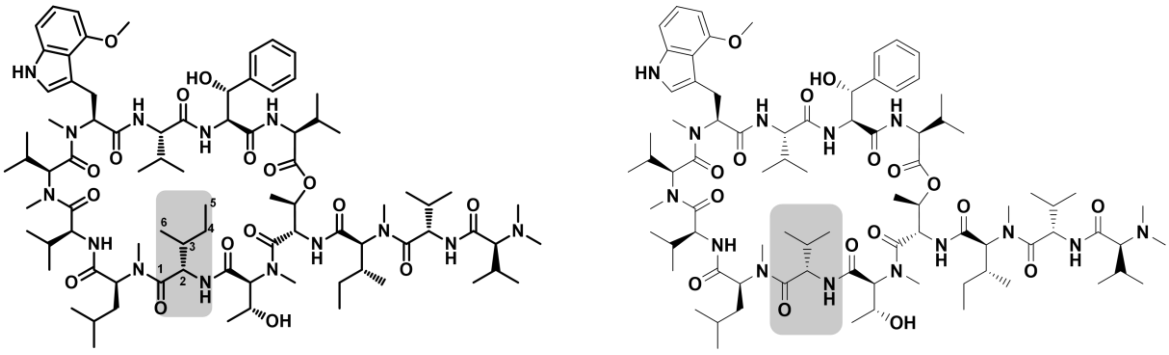
Assuming the molecular formula of homoecumicin-6I is the same as that of ecumicin, a total of 125 non-exchangeable protons present in homoecumicin-6I. Assuming that impurities all have the same molecular weight as homoecumicin-6I, the purity was calculated as:

Purity = 125×(3.00/3)/482.3×100 % = 25.9%

The purities of four other presumably ecumicin congeners (labeled as **1**, **2**, **4** and **5** in Figure 128) in this sample were analyzed to be 16.1 % (**1**), 3.32 % (**2**), 12.1 % (**4**) and 13.2 % (**5**). Together these five ecumicin congeners composed approximately 70.6% of the NMR sample.

9.7.2 Structure elucidation of homoecumicin-6I

Homoecumicin-6I (Figure 126) was isolated as a pale yellow powder. The ^{1}H chemical shifts (δ_H) and some ^{13}C chemical shifts (δ_C) of homoecumicin-6I were summarized in TABLE XXIII. ^{13}C NMR data were obtained via interprating the HSQC and HMBC spectra; resonances of the carbonyl carbons and methyl carbons (19-20 ppm) were approximate values due to severe signal overlapping. High resolution mass spectrometry (Figure 127) revealed that homoecumicin-6I has an exact mass of 1613.0140 amu, which is identical to that of homoecumicin-11I. The additional 14 amu, when compared to ecumicin, indicated a possible structural difference of an additional methyl or methylene group.



(A) Homoecumicin-6I (B) Ecumicin

Figure 126 (A) Proposed structure of homoecumicin-6I. (B) Structure of ecumicin.

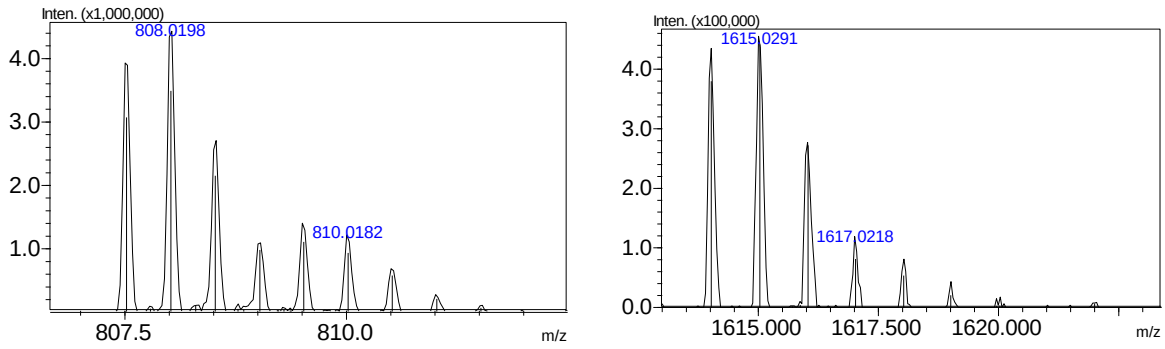


Figure 127 High resolution MS data of homoecumicin-6I. $[M+2H]^{2+}$= 807.5185 and $[M+H]^{+}$ = 1614.0213, so the exact mass of H13 was calculated to be 1613.0140.

Homoecumicin-6I was dissolved in 40 µl methanol-d_4 and NMR experiments including ^{1}H, COSY, HSQC, HMBC and semi-selective HMBC were acquired on a 700 MHz instrument equipped with a 1.7 mm cryoprobe.

The upfield signals are shown in expansions in Figure 128, and revealed that there are at least five ecumicin-related species in the sample. The high-resolution mass spectrum suggested all species had the same molecular weight. In addition, signals between 1.5 ppm and 2.0 ppm suggested the presence of homoecumicin-11I and homoecumicin-13I in this sample. The identities of the other two isomers were unknown.

The closeness in relative abundance of the four ecumicin-related isomeric compounds in the sample, together with the fact that two of them were unknown, made it an unsuitable case for the NMR structure sequencing approach.

In an attempt to gain structural information on the two unknowns, the 1D- and 2D-NMR spectra of this sample were compared with that of known ecumicin-related peptides. Here all spectra of homoecumicin-6I were shown in overlay with the spectra of ecumicin.

The existence of four ecumicin-related species made the ^{1}H NMR spectrum (Figure 128) of the sample especially difficult to interpret. Therefore, the structure elucidation started with interpretation of the 2D-COSY spectrum. Comparison of the new sample's 2D-COSY spectrum with that of known peptides revealed a coupling pathway of an amino acid that was not observed previously in the known species. As marked in Figure 129, this coupling pathway corresponds to an isoleucine unit.

The cases of both homoecumicin-11I and homoecumicn-13I had shown that the replacement of a valine residue by an isoleucine unit was responsible for the 14 amu difference observed in high resolution mass analyses. The observation of a new isoleucine coupling pathway in the present sample suggested that presumably the more abundant one of the two unknowns also had an isoleucine unit in place of the valine unit in ecumicin.

The overlaid 2D-NMR spectra (COSY, and HSQC) of ecumicin and of the present sample, is shown in Figure 129 and Figure **130**. They confirmed presence of all other twelve common amino acids.

Unfortunately, the low signal to noise ratio in the HMBC (Figure 131) and semi-selective HMBC spectra (data not shown) of this sample hampered the provision of additional information on the connectivity of amino acids in the new peptide(s).

At this point, the ^{1}H NMR spectrum of the new sample was carefully re-examined. Although the presence of four ecumicin-related species made the already heavily overlapped β-proton region and the terminal methyl proton region highly complicated, the α-proton region remained relatively clear. As shown in the comparative Figure 128, the intensities of the ecumicin signals could be adjusted to a level close to the most abundant species in the new sample according to the upfield signals (0.17 – 0.34 ppm). This revealed that most α-protons in both spectra have similar chemical shifts and similar intensities, except the one of ecumicin's V^2, i.e. the second valine, or the sixth amino acid of ecumicin counting from the *N*-terminus. While ecumicin's V^2 α-proton was observed as a doublet at 4.84 ppm, in the spectrum of the present sample, there was only a small hump at 4.84 ppm, whereas the new isoleucine's α-proton gives a signal at 4.97 ppm. Assuming that the change of one valine unit to an isoleucine unit do not have a significant impact on the peptide's backbone conformation, the chemical shifts of all common amino acids α-protons would remain relatively unchanged. This assumption is in congruent with the observation. Based on this reasoning, the new isoleucine in one of the two major peptides should be the sixth amino acid counting from the *N*-terminus. Therefore, this new peptide was named homoecumicin-6I.

Due to the existence of four ecumicin-related species in this sample, one of them still unknown, it was not feasible to deduce the accurate chemical shifts and coupling constants of the homoecumicin-6I proton signals; the low signal to noise ratio of HMBC spectrum precluded the assignment of all carbon signals. TABLE XXVII summarizes the approximate chemical shifts of homoecumicin-6I proton signals, and the chemical shifts of some carbon signals which were retrieved from the HSQC spectrum.

Figure 128. Comparison of the ^{1}H spectra of homoecumicin-6I (red) and ecumicin (blue). As shown in the expansion B, there were at least four ecumicin-related peptides present in the homoecumicin-6I sample.

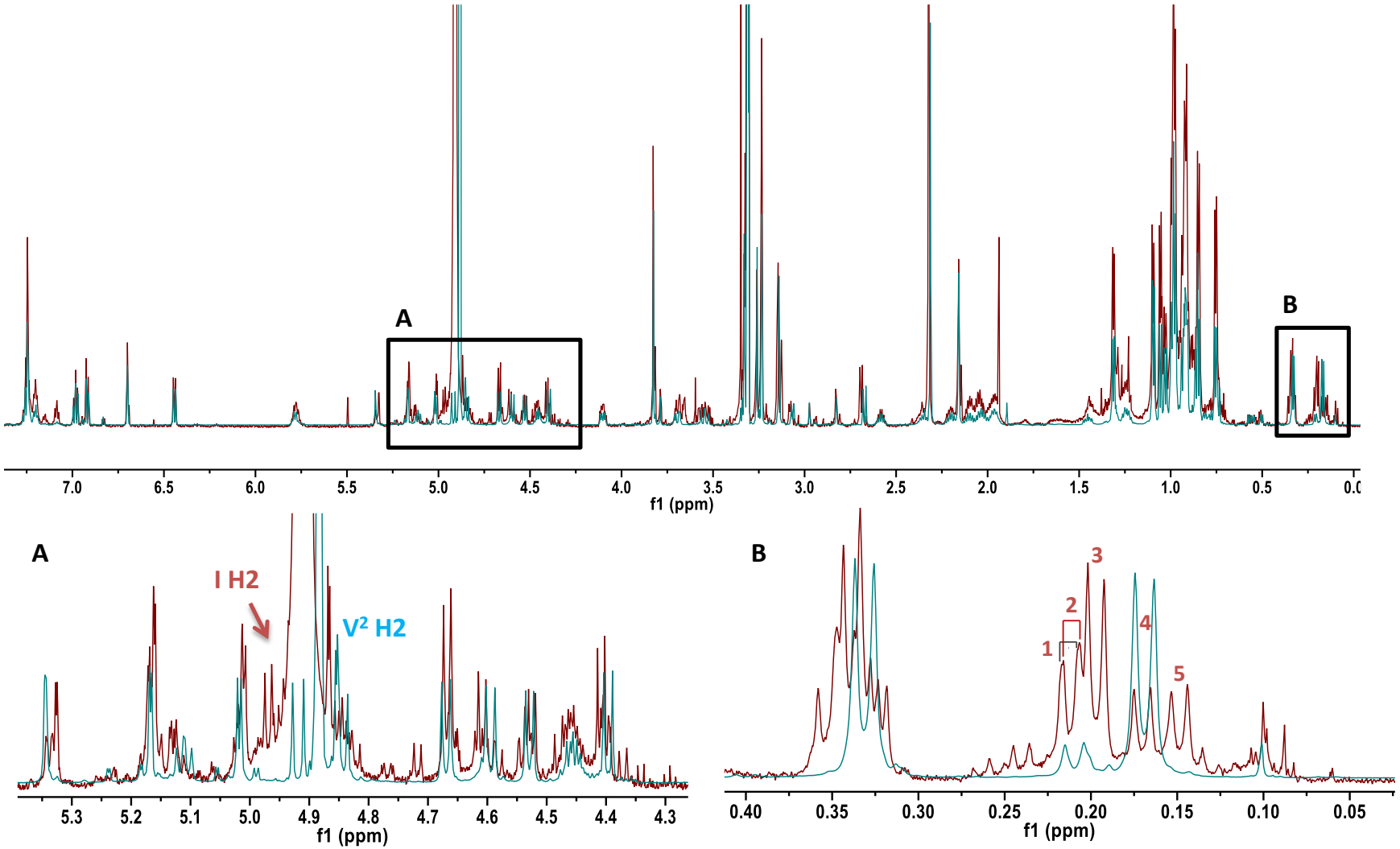


Figure 129. Comparison of the COSY spectra between homoecumicin-6I (grey) and ecumicin (yellow) revealed an additional isoleucine coupling pathway.

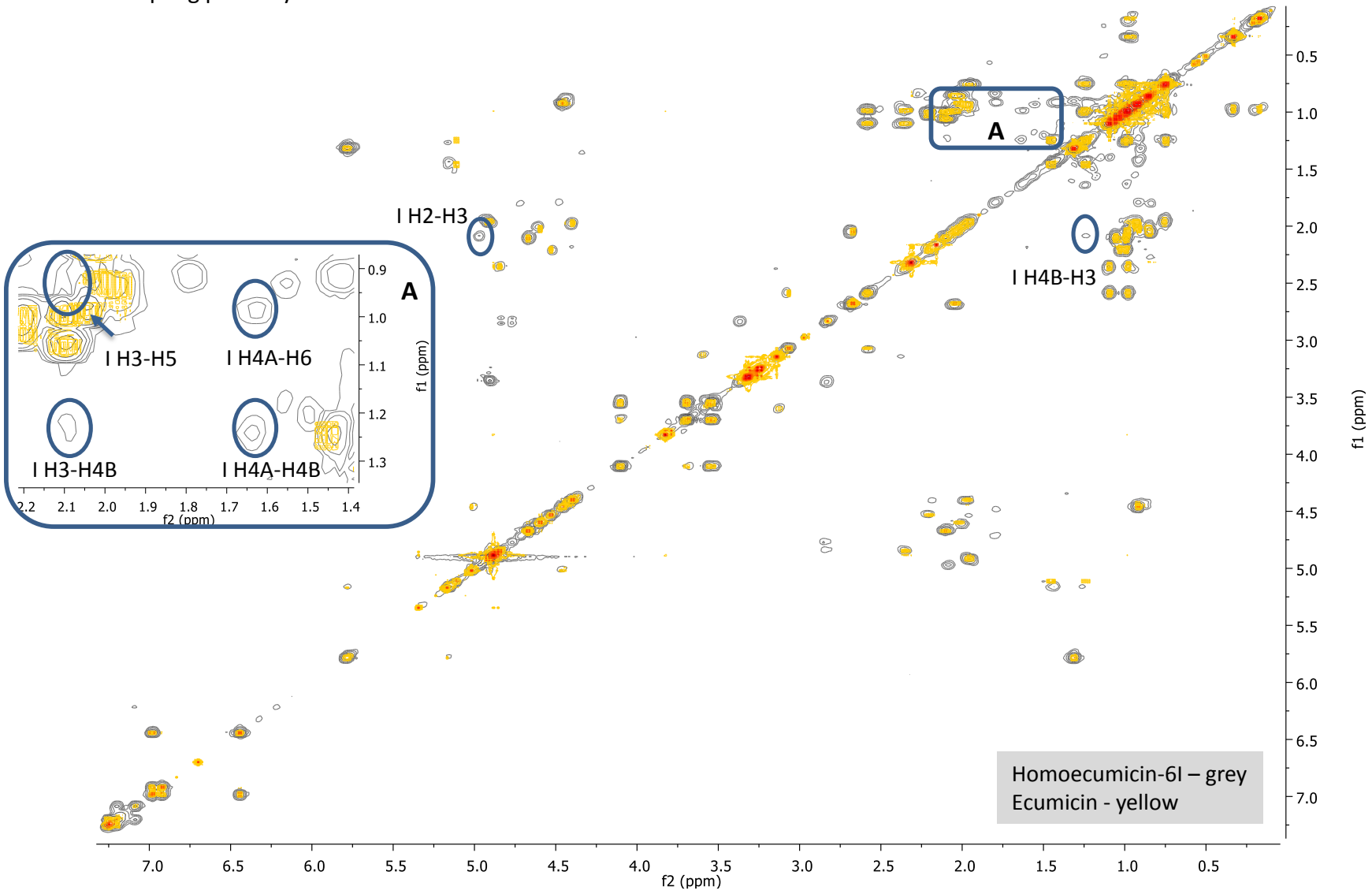


Figure 130. Comparison of the HSQC spectra of ecumicin (red) and homoecumicin-6I (grey).

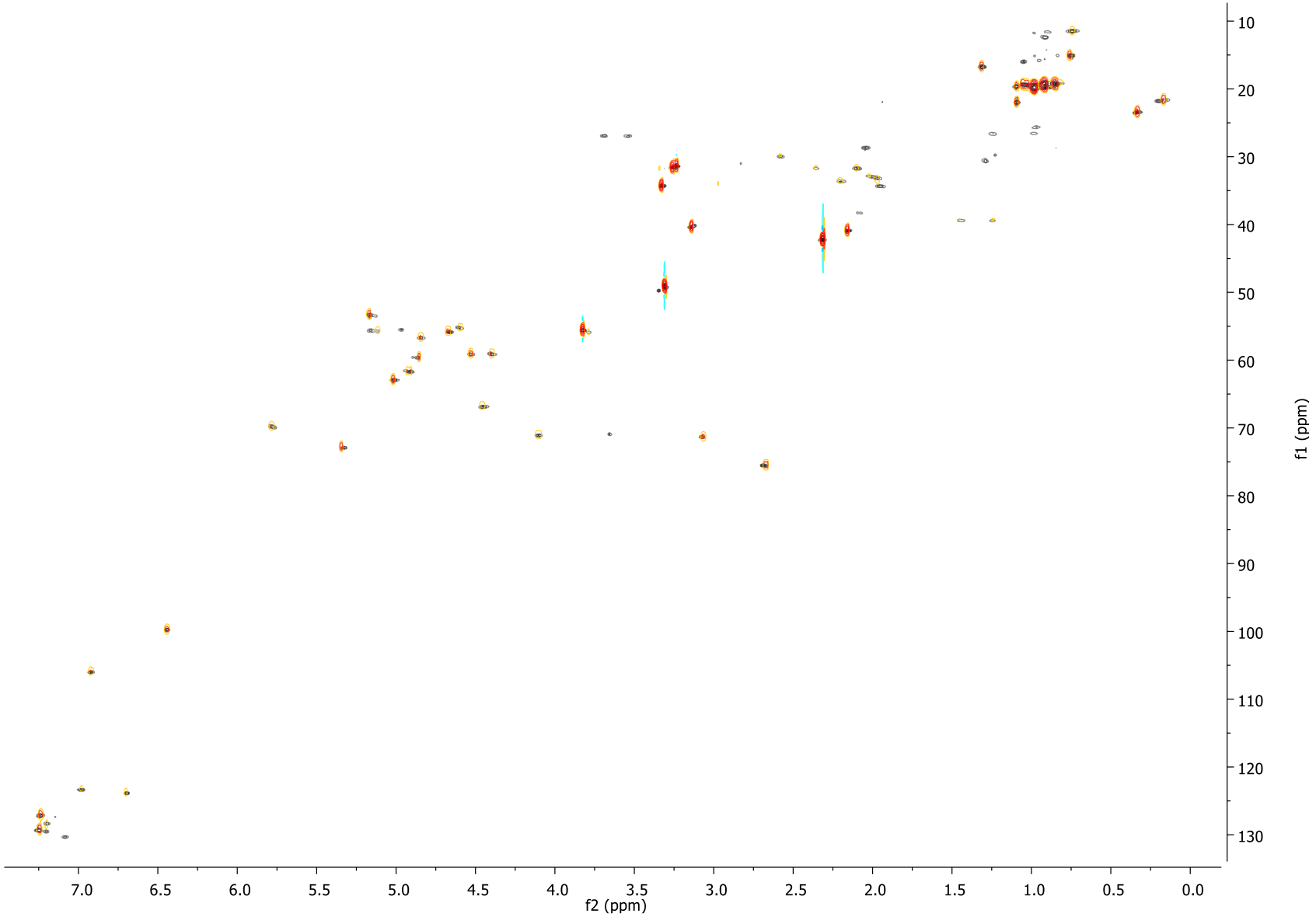


Figure 131. The HMBC spectrum of homoecumicin-13I using a 700 MHz 1.7 mm cryoprobe NMR (NS = 64, TD1= 300) only showed the correlations of the methyl and a few select ^{1}H resonances.

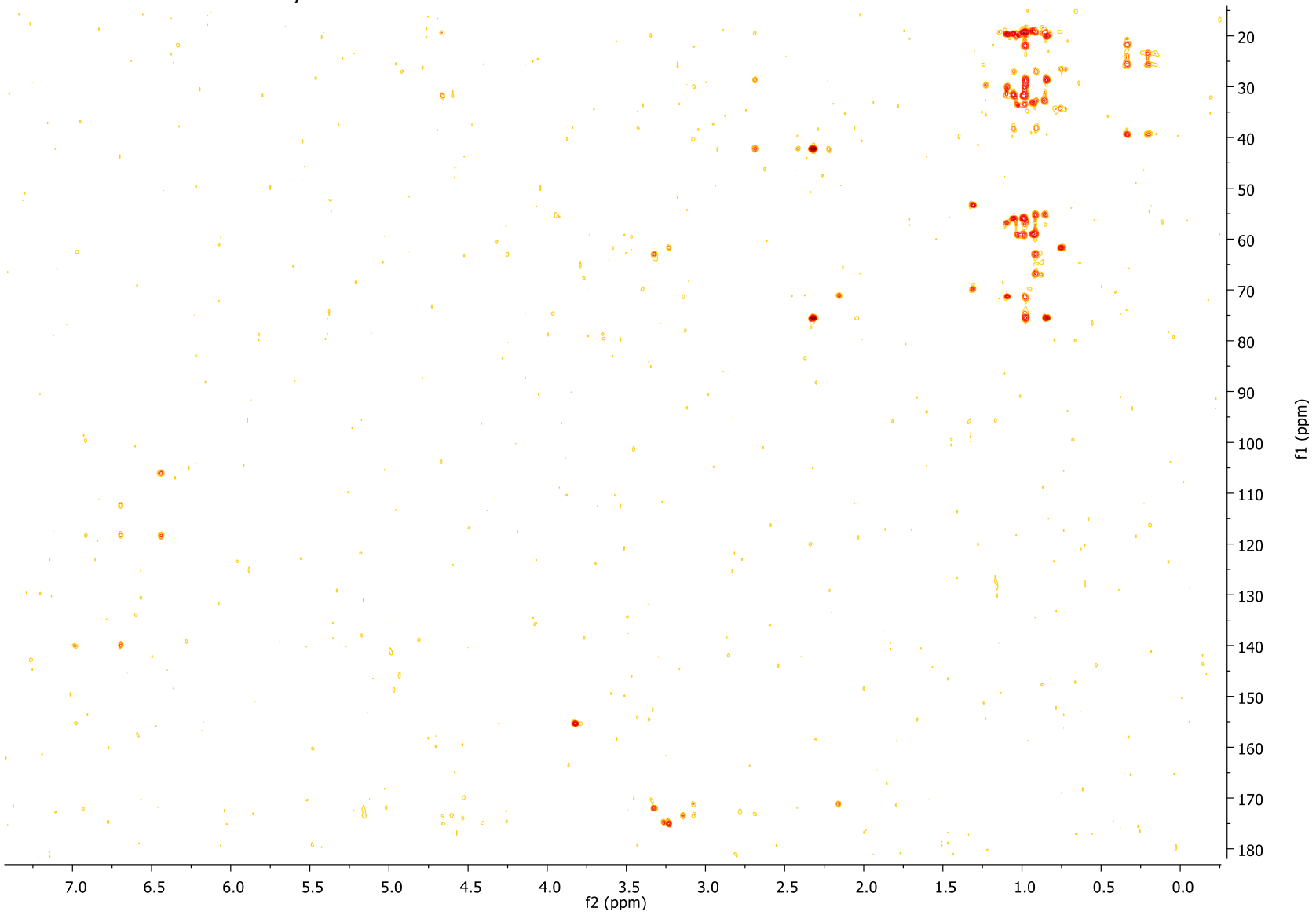


TABLE XXVII. AVAILABLE ^{1}H AND ^{13}C NMR DATA OF HOMOECUMICIN-6I IN CD_3OD. ^{1}H NMR DATA WERE EXTRACTED FROM 700 MHZ 1D ^{1}H AND 2D COSY SPECTRA, AND THE ^{13}C NMR DATA (175 MHZ) WERE OBTAINED FROM INTERPRATION OF HSQC AND HMBC SPECTRA.

Amino Acid		^{1}H δ in ppm (mult, J in Hz)	^{13}C δ in ppm
N,N-Me_2-V	1	-	N.A.
	2	2.69 (d, 8.93)	75.61
	3	2.05 (m)	28.68
	4,5	2.32 (s)	42.26
	6	0.98 (d)	19.4
	7	0.85 (d)	20.0
L-V[1]	1	-	N.A.
	2	4.67 (d, 8.37)	55.91
	3	2.10 (m)	31.62
	4	1.06 (d)	19.6
	5	1.00 (d)	19.5
N-Me-L-*allo*-I	1	-	N.A.
	2	4.92 (d)	61.76
	3	1.95 (m)	34.33
	4	0.96 (m)	26.61
		1.25 (m)	
	5	0.76 (d)	11.5
	6	0.75 (dd)	15.1
	7	3.23 (s)	31.4
L-T	1	-	N.A.
	2	5.16 (d)	53.39
	3	5.78 (dd)	69.82
	4	1.31 (d)	16.76
N-Me-L-T	1	-	N.A.
	2	5.01 (d)	63.00
	3	4.46 (dd)	66.93
	4	0.91 (d)	19.9
	5	3.33 (s)	34.30
L-I	1	-	N.A.
	2	4.97 (d)	59.10
	3	1.96 (m)	36.25
	4	1.62 (m)	29.69
		1.24 (m)	
	5	0.92	12.44
	6	0.99	14.98
N-Me-L-L	1	-	N.A.
	2	5.13 (dd)	55.59
	4	0.92 (d)	19.7
	5	0.86 (d)	19.7
N-Me-L-V	1	-	N.A.
	2	3.08 (d)	71.37
	3	2.58 (m)	29.94
	4	0.98 (d)	19.8
	5	1.10 (d)	22.0
	6	3.15 (s)	40.37
N-Me-4-OMe-L-Y	1	-	N.A.
	2	4.10 (dd)	71.11
	3	3.54 (dd)	26.97
		3.67 (dd)	
	4	-	-
	5	6.70 (s)	124
	6	-	N.A.
	7	6.92 (d, 8.23)	106.01
	8	6.98 (dd, 8.23, 7.80)	123.3
	9	6.44 (d, 7.80)	99.77
	10	-	N.A.
	11	-	N.A.
	12	3.83 (s)	55.59
	13	2.16 (s)	40.9
L-V[3]	1	-	N.A.
	2	4.52 (d, 7.90)	59.21
	3	2.20 (m)	33.7
	4	1.03 (d)	19.7
	5	0.99 (d)	19.7
	NH	-	
Ph-L-*threo*-S	1	-	N.A.
	2	4.87 (d)	59.78
	3	5.33 (d)	72.97
		-	
	4	-	
	5,9*	7.24 (m)	127.06
	6,8*	7.25 (m)	129.28
	7*	7.20 (m)	128.25
L-V[4]	1	-	N.A.

Amino Acid		^{1}H δ in ppm (mult, J in Hz)	^{13}C δ in ppm	Amino Acid		^{1}H δ in ppm (mult, J in Hz)	^{13}C δ in ppm
	3	1.24 (m)	39.37		2	4.41 (d, 7.62)	59.65
		1.46 (m)			3	1.97 (m)	39.33
	4	0.95 (m)	25.64		4	0.92 (d)	26.97
	5	0.20 (d, 6.71)	21.67		5	0.93 (d)	
	6	0.34 (d, 6.71)	23.47				
	7	3.26 (s)	31.63				
L-V[2]	1	-	N.A.				
	2	4.61 (d, 8.88)	55.34				
	3	2.03 (m)	32.88				

* Signals observed from an AA'BB'C spin system.

9.8 R5

A total of 0.40 mg R5 was collected from HPLC separation, and it was dissolved in 40 µl of methanol-d_4 and transferred to a 1.7 mm NMR tube. Several 1D- and 2D-NMR data were acquired from a Bruker 700 MHz instrument equipped with a 1.7 mm cryoprobe at Halifax, Canada.

Purity of the R5 sample was estimated by the 100% NMR method as described in 9.5.1, with modifications.

The methyl doublet (δ_H 0.140 ppm) was selected as the most pure signal, and the integral was set to 3.000, representing the integral of three protons (3H). All other proton signals between δ_H 0.0 to 7.5 ppm in the spectrum, except for the solvent signals (HOD and CHD_2OD), were integrated, and the sum of these integrals was determined to be 1003.1.

Assuming the molecular formula of the ecumicin congener in fraction R5 is the same as that of ecumicin, a total of 125 non-exchangeable protons present in this molecule. Assuming that impurities all have the same molecular weight as this peptide, the purity was calculated as:

Purity = 125×(3.00/3)/1003.1×100 % = 25.9%

Although the HR-MS spectrum of R5 showed a strong signal of an ecumicin analog (Figure 132), the ^{1}H NMR spectrum revealed that this peptide was only one component in the sample (Figure 133). The strong anti-TB activity of this fraction (MIC < 0.039 µg/ml) make it likely that the active principle belongs to another yet unidentified component(s) of the fraction.

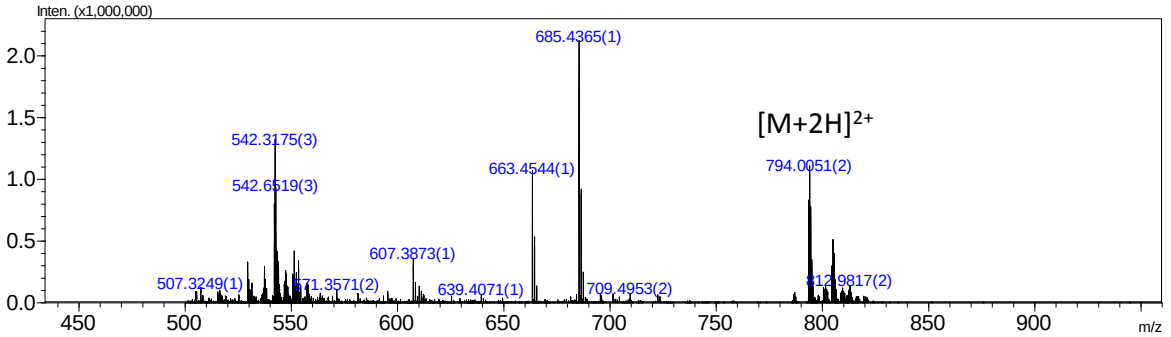


Figure 132. HR-MS spectrum of R5. The ecumicin analog signal $[M+2H]^{2+}$ = 793.5032, indicated an exact mass of 1584.9918.

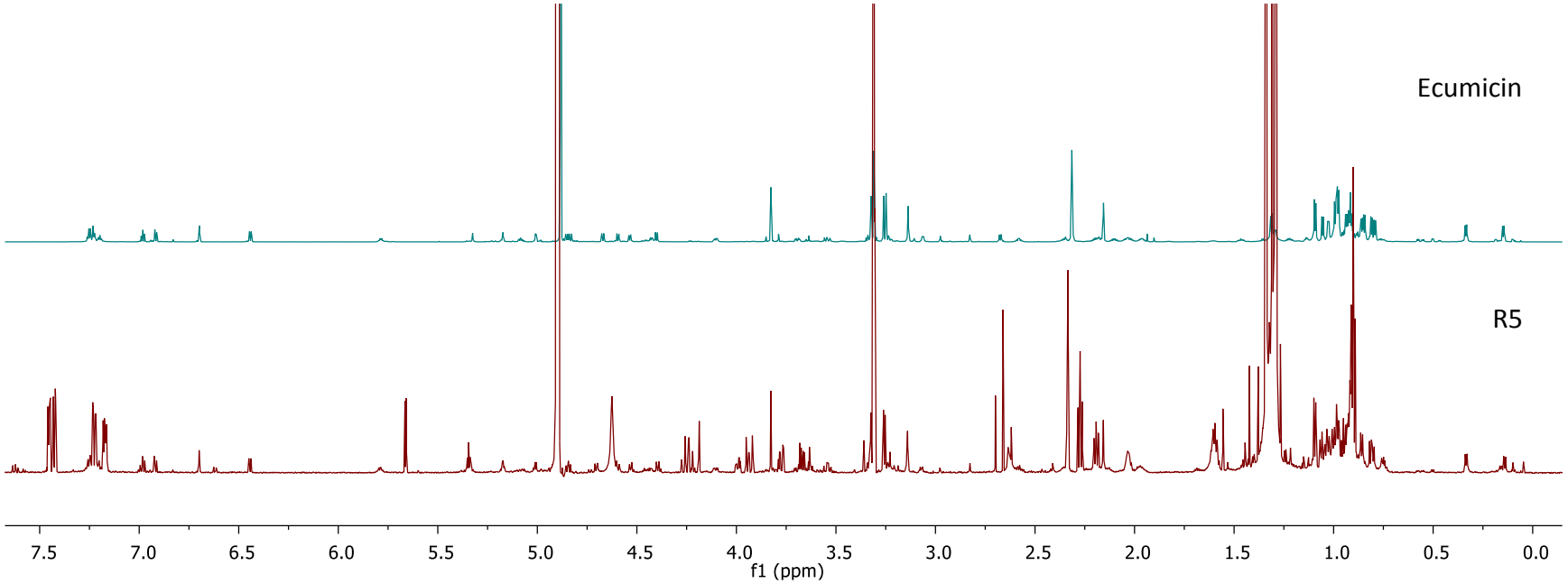


Figure 133. Comparison of the ^{1}H NMR spectrum of ecumicin (blue) and R5 (red) revealed an ecumicin analog that is only one component of R5.

9.9 Discussion

9.9.1 Using the upfield methyl signals to probe ecumicin congeners.

In this chapter, the purities of these samples were determined by the 100% qHNMR method using the very upfield signals (δ_H 0.10 – 0.40 ppm) of the molecules. These signals correspond to the terminal methyl groups (H-5 and H-6) of the *N*-methyl-leucine residue in all ecumicin congeners. As shown in Figure 134 (also Figure 47), in ecumicin, the methyl groups reside in the center of two de-shielding cones, above the two aromatic rings – the phenyl-serine and *N*-methyl-4-methoxy-tryptophan units. The similarity of the ^{1}H NMR spectra of all ecumicin congeners suggests that a small change in the peptides' structure, e.g., the addition or removal of a methylene group in the side chain of one amino acid residue, would not have a major effect on the overall conformation. However, the two upfield methyl signals are predicted to still be sensitive to small structural/conformational changes, as a slight change in their positions relative to the aromatic shielding cones would result in a pronounced change in their chemical shift values. The difference in the substituents of the aromatic systems (phenylalanine vs. phenyl-serine) would affect the aromatic stacking interactions (Hwang, 2014), and in turn affect the chemical shifts of the two upfield methyl signals. As a result, these highly sensitive upfield signals were selected to quantitate the corresponding ecumicin analogs.

When re-calculating the purity of ecumicin in fraction H14 (Figure 17) by the 100% qHNMR method using the upfield methyl resonance (δ_H 0.168 ppm), the purity was found to be 76.3 %. When setting the integral of this upfield signal to 3.00, representing three protons, all proton signals between δ_H 0 - 7.5 ppm were found to be 163.82. As ecumicin contains 125 non-exchangeable protons, the purity was thus calculated as: Purity % = 125/163.82×100% = 76.3%.

The major impurity in H14 was analyzed using the upfield signal (δ_H 0.210 ppm, $\Delta\delta_H$ = 42 ppb), and its amount was determined to be 14.4 % according to the 100% qHNMR method.

In contrast, when the purity of ecumicin in the fraction called "H14" was calculated to be 91.0 % in Chapter 4, the aromatic singlet (δ_H 6.698 ppm) was used for calculation. As the aromatic singlet is present in the ^{1}H spectra of both ecumicin and its congeners, with a $\Delta\delta_H$ of <1 ppb, this 91.0 % purity represented the amount of ecumicin and its analogue(s) in the fraction. Indeed this number is in congruent with the sum of the amount of ecumicin (δ_H 0.210 ppm, 76.3 %) and the analogue(s) (δ_H 0.224 ppm, 14.4 %), which is 90.7 %.

In conclusion, although in many cases, e.g. homoecumicin-13I and homoecumicin-6I, the upfield signals are overlapped, the distinguishable $\Delta\delta_H$ of these signals from different peptide species makes them ideal probe for qualitative and quantitative analyses. Signal overlap can be solved by either the de-convolution module(s) offered by modern NMR analysis software, such as the line fitting option in MNova or by via the HiFSA analysis using the PERCH iterator.

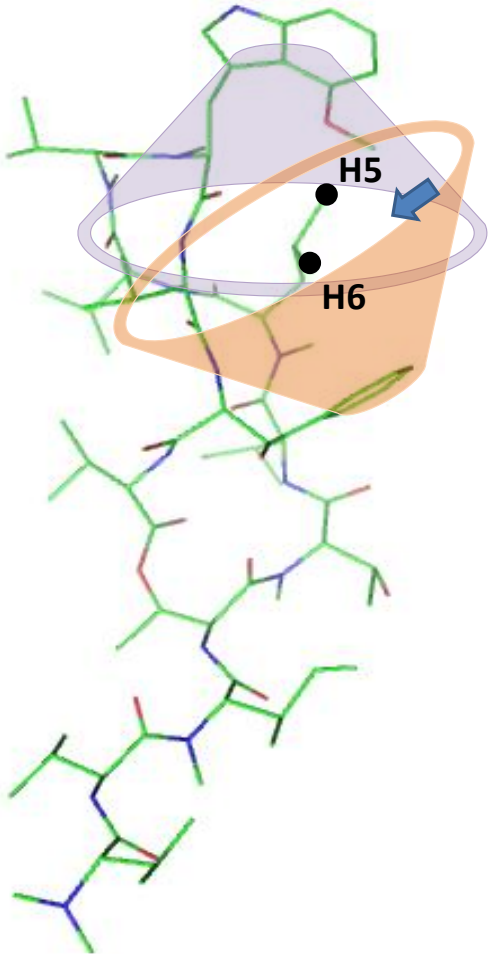


Figure 134. The crystal structure of ecumicin is suitable to explain how the shielding aromatic cones give rise to the two up field proton resonances in NMR spectra at 0.16824 ppm (H-5 of the *N*-Me-L residue) and 0.33065 ppm(H-6 of the *N*-Me-L residue).

9.9.2 Sample purity and presumably conformational isomer(s).

The structures of the peptides presented in this dissertation were all elucidated with samples of relatively low purity, ranging from 25.9 % to 76.3% (TABLE XXVIII) using the upfield methyl signal as probe in the 100% qHNMR analysis. While this may appear to be surprising at the lower end of the purity scale, it is consistent with the general observation that major constituents of a purified fraction ("compound") dominate the spectroscopic data and often produce highly consistent data sets for the purpose of structure elucidation. However, their HR-MS spectra suggested higher purities.

TABLE XXVIII. SUMMARY OF THE NMR ANALYSES OF THE ECUMICIN CONGENERS. THE PURITIES WERE DETERMINED BY THE 100% QHNMR METHOD AS DESCRIBED INDIVIDUALLY IN CHAPTERS 4 AND 9.

Compound ID	Sample size (mg)	Volume (µl)	Purity (%) by qHNMR	Adjusted purity (%)	Major impurities	Structure elucidation	HiFSA profile
Ecumicin	4.00	150	76.3	91.0	Other compounds	Yes	Yes
Deoxyecumicin	1.15	200	55.8	66.5	Ecumicin	Yes	Yes
Norecumicin	2.00	150	74.1	88.3	Deoxyecumicin	Yes	Yes
Nordeoxyecumicin	1.10	130	41.1	49.0	Ecumicin congeners	Yes	Yes
Homoecumicin-11I	0.41	40	37.8	45.1	Homoecumicin-13I	Yes	Yes
Homoecumicin-13I	0.27	40	36.6	43.6	Homoecumicin-11I	Yes	Yes
Homoecumicin-6I	0.31	40	25.9	30.9	Ecumicin congeners	Yes	No
R5	0.20	40	12.5	14.9	Other compounds	No	No

In the case of ecumicin's ^{1}H NMR spectrum, the impurities were composed of one closely related analog, presumably an ecumicin congener (δ_H 0.224 ppm, 14.4 %), and (an) unknown compound(s) (9.0 %). Due to signal overlapp, only a few signals corresponding to the impurities could be clearly identified. Three doublet signals with approximately the same integral as the doublet at 0.224 ppm were observed in ^{1}H NMR spectrum around 0.5 ppm. The 2D-NMR spectra (COSY, HSQC, TOCSY, HMBC) suggested that two of the doublet signals (δ_H 0.55 and 0.57 ppm) belong presumably to a valine residue [δ_H 3.74 (α), 1.82 (β), 0.55 (χ) and 0.57 (χ) ppm;δ_c 63.34 (α), 29.02 (β), 19.27 (χ) and 18.80 (χ) ppm]. The chemical shifts of the α-proton and α-carbon signals suggested that this valine might be a N-terminal amino acid residue or a free amino acid. The third doublet signal (δ_H 0.50 ppm) belonged xpresumably to a leucine residue [δ_H 5.03 (α), 1.67 (β), 1.25 (β), 1.11 (χ), 0.50 (δ) and 0.21 (δ) ppm; δ_c 56.50 (α), 39.25 (β),25.24 (χ), 23.76 (δ), and 20.96 (δ) ppm]. The unusual upfield proton chemical shifts of these methyl doublet signals (δ_H 0.21 – 0.57 ppm) implied that they are in a shielded chemical environment. If the two amino acid residues belonged to an ecumicin congener, these methyl groups would be located inside the aromatic shielding cone(s). As a result, the valine containing molecule (approximately 14.4 % purity by the 100% qHNMR method) would be in a conformation that is different from the one observed in X-ray crystallography study (Figure 134), but in congruence with ecumicin's ROESY data (**Figure 46**) – having the three amino acid side chain folding back towards the macrocycle or forming dimers. The clean HR-MS spectrum of the ecumicin sample (fraction H14, Figure 135), and the knowledge that ecumicin is a non-ribosomal peptide, suggested that this new peptide molecule is likely a conformational isomer of ecumicin, or a dimeric form. The ratio of the two isomers in methanol solution at 298K is approximately 5.2:1 by 100% qHNMR analysis.

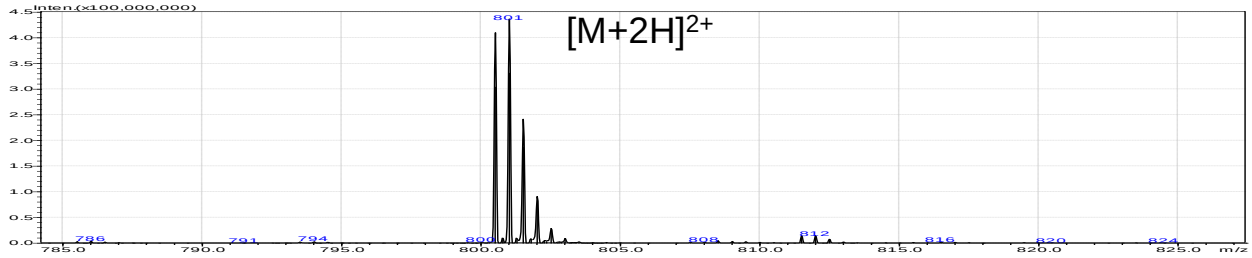


Figure 135. HR-MS spectrum of fraction H14 suggests the presence of only ecumicin and its isomer(s).

Notably, similar proton doublet resonances (δ_H 0.45 - 0.60 ppm) have been observed in all the ^{1}H NMR spectra of ecumicin congeners'. 2D NMR analyses revealed that these resonances belong to the same alleged leucine and valine residues. This observation implies that conformational isomers are very likely to exist in all ecumicin congers. As most ecumicin congeners samples contain considerable amounts of ecumicin analogue(s) as impurity, the determination of the exact ratio between impurities and conformers was difficult. The norecumicin sample was an exception, and a ratio of 5.35:1 between the presumably major and minor isomers was determined according to the 100% qHNMR method. Considering the near 4-fold concentration difference between ecumicin and norecumicin samples, it is more likely that the isomeric "impurities" are actual due to conformational species of the main molecule. As the dimerization reaction is usually a second order reaction, the equilibrium concentration is usually influenced by the initial concentration of the monomer. With an almost 4-fold concentration

difference, the equilibrated ratios of monomers and dimers of the two samples would not be so similar.

Assuming that the ratio of the two isomers is 5.2:1 for all analogs, the purity of each sample was adjusted. The new values range from 30.9 % to 91.0 % for the elucidated peptides (TABLE XXVIII).

9.9.3 The effect of sample purity and abundance on structure elucidation of new compounds.

The structures of all ecumicin congeners (including ecumicin) were elucidated from the NMR data of their major conformers. This means that only 83.9 % of a peptide in the NMR sample gives rise to signals that are acutally interpreted, while the remaining 16.1 % of the identical peptide are considered “impurity” signals while representing conformers. Accordingly, the effective purity in NMR-based structure elucidation would be only 83.9 % of the sample’s real purity with respect to single constitutional species (including stereochemistry, and excluding conformers).

Ecumicin congeners are complex molecules that have molecular weights around 1600 amu, which translates to approximately 130 protons and 83 carbons. It was believed that a pure and abundant sample is necessary to lead to unambiguous structure elucidation of molecules with this level of complexity. Surprisingly, the structures of all peptides presented in this dissertation were all elucidated with samples of modest to low effective purities (25.9 % to 76.3%, TABLE XXVIII). Furthermore, the structures of the three homoecumicins were analyzed with sub-milligrams of impure samples (< 40 %) using 1.7mm cryoprobe 750 MHz NMR technology. The large dynamic range in these size (amount of material) and purity of these NMR samples and the closeness in the major compounds’ structures provided a good example to explore the limits of the NMR-based natural product structure elucidation workflow.

The success in elucidating complex peptidic structures from relatively impure and very mass limited samples resulted mainly from the availability of the complete information on a

portal molecule, ecumicin, including the achievement of the full ^{1}H NMR spin analysis of the molecule which is the largest molecule for which this type of analysis has been achieved to date. The assumption that all congeners were synthesized by the same non-ribosomal peptide synthetase has restricted the analogues' structures to only a few possibilities. The NMR instrument with 1.7 mm microcryoprobe allowed analyzing sub-mg samples (< 0.5 mg) of ~1600 amu molecules. Even though not all 2D spectra of the small sized samples have good S/N, the ability to study the ^{1}H NMR sub-spectrum of individual amino acid enabled structure elucidation of even a 0.31 mg sample of homoecumicin-6I with only 25.9 % purity. However, the case of R5 suggests that sufficient purity is still desired for structure elucidation, even with full knowledge of a portal molecule, state-of-art NMR facilities, and advanced strategies in structural analysis. For the ecumicin congeners, 25% effective purity (by 100% qHNMR) seems to be the limit for structure elucidation without the need for further purification.

With the availability of the 1.7 mm micro cryoprobe technology at very high fields (750 MHz in the present case), the sample size seemingly should no longer be a limiting factor in the NMR-based structure elucidation. However, the cases of the (homo)ecumicins have suggested that near 100 µg quantities of a peptide [310 µg × 30.9 % purity] is still too little to achieve a good S/N in some 2D NMR experiments, especially the HMBC experiment. Moreover, with only sub-milligram of sample, it would be challenging to perform further purification, when a sample is found to be impure. As in the case of R5, although the purity is too low for full structure elucidation, it was not further fractionated. Even with a 100% recovery rate, only an estimated 30 µg ecumicin analog would be isolated, which is still too little for the NMR instrument available to us.

The generation of a HiFSA profile also relies in part on sample purity. As ^{1}H NMR is the most sensitive NMR experiment, usually a sample that leads to full structure elucidation would yield high enough S/N for HiFSA analysis. In the cases of ecumicin congeners, HiFSA profiles were generated for samples with > 40 % effective purity, by using the Total-Line Fitting mode of PERCH iterator to calculate for a precise fit. HiFSA profiles for samples with 35 % to 40 % purities were generated by using only the Integral-Transform Fitting mode, and resulted in a less accurate fit. For homoecumicin-6I, the co-existence of several analog peptides, two of which are unknown, resulted in a heavily overlapped ^{1}H NMR spectrum, which causes difficulties for the iterator with respect to locating the correct peaks for the calculations involved. As a result, at 25.9 % effective purity, it was not feasible to perform a HiFSA profiling for homoecumicin-6I.

9.9.4 The effect of pH on the ^{1}H NMR spectra of ecumicin and its analogs.

Ecumicin analogs are cyclic peptides with their C-terminal carboxylic acid neutralized by intramolecular an ester-bond formation and the N-terminus being a free tertiary amine. This makes these molecules slightly basic. As a result, the ^{1}H NMR spectral patterns of ecumicin and its analogs are sensitive to even residual quantities of acid which may remain in the sample. And examples of this behavior was observed in the case of norecumicin and deoxyecumicin.

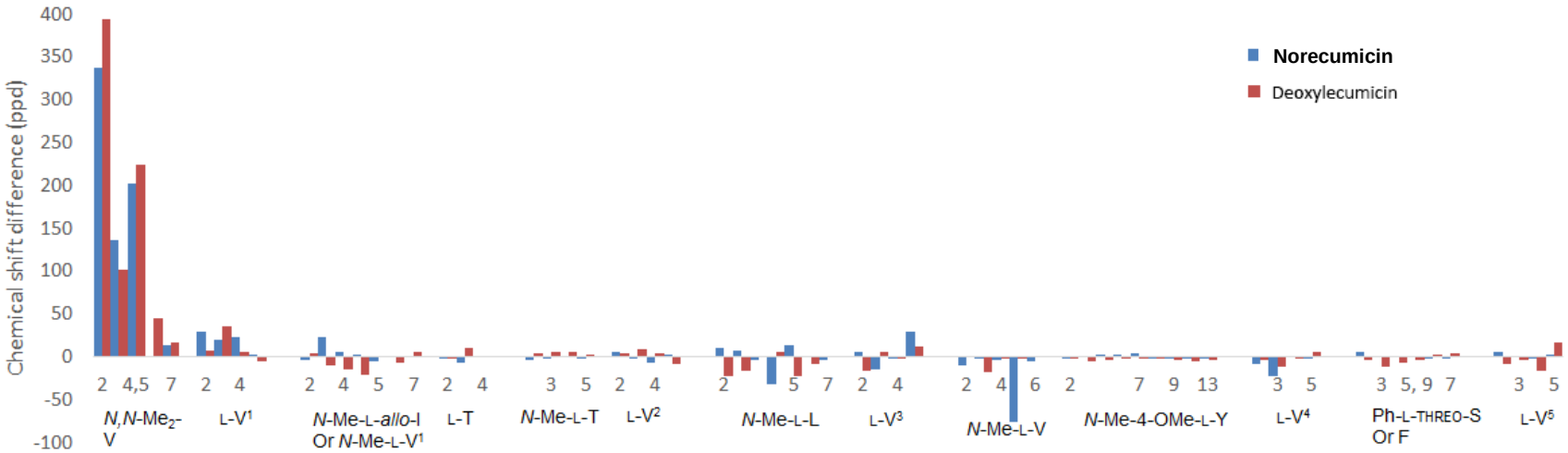
The HiFSA-generated ^{1}H NMR fingerprints proved a solid foundation for establishing chemical shift differences (Δδ) between a neutral sample and a sample with residual acid. As shown in TABLE XXIX and Figure 136, significant changes in chemical shifts (Δδ > 0.05 ppm or 50 ppb) were observed within the *N*-terminal amino acid (*N,N*-Me_2-V) residue, which harbors the basic functional group – the tertiary amine. In the presence of acid, the proton signals around the nitrogen atom of the tertiary amine moved downfield, as they were de-shielded by the addition of a proton to the nitrogen atom, creating a charged species. As shown in Figure 136, in the cases of both norecumicin and deoxyecumicin, the greatest changes in chemical shift upon formation of the protonated species were associated with protons around (up to two bonds away from) the nitrogen atom of the tertiary amine, exhibiting Δδ values between 200 and 400 ppb (0.200 to 0.400 ppm). Such chemical shift changes faded quickly as the distance between the protons and the tertiary nitrogen atom increased. For protons that were four bonds away from this nitrogen atom, Δδ values quickly fell below 50 ppb (0.05 ppm). These observations provided complementary structural information that was consistent with the NMR assignments.

When using ^{1}H NMR fingerprints for the identification of ecumicin and/or its analogs, special attention should be paid to variations in the chemical shifts of the *N,N*-Me_2-Val residue. While variations can be caused by any residual amount of acid in the sample, it may also be the indication of a new analog of the peptide family. Besides, the PERCH iterator would not be able to automatically adjust the chemical shifts of these signals, as the $\Delta\delta_H$ is too large, so manual adjustment of these signals is necessary.

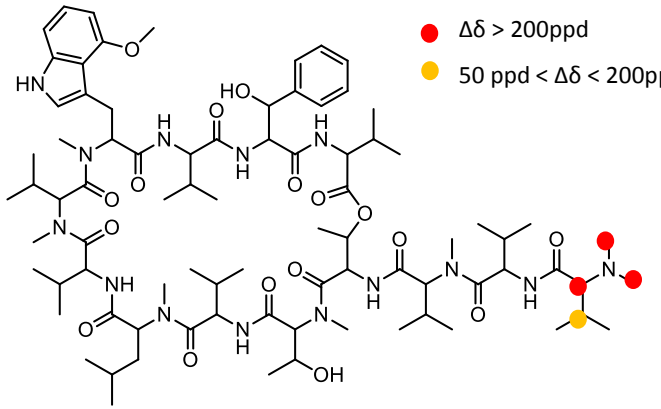
As the upfield methyl signals were selected for quantitative analysis of the major peptide species in an NMR sample, the effect of pH on these methyl protons' chemical shift was analyzed. Surprisingly, $\Delta\delta_H$s from -22.08 to 13.62 ppb were observed, suggesting that protonation of the *N*-terminal *N,N*-dimethyl-valine residue has an slight effect on the overall conformation of the molecule, which caused significant change in the chemical environment of the two methyl groups. As a result, although the upfield methyl signals are ideal for quantitative analysis, they were not suitable for the qualitative analysis across different samples at different pH. However, the PERCH iterator would be able to automatically adjust the HiFSA profile in such small scale, making the HiFSA profile of a peptide still useful for quantitative and qualitative analysis.

Figure 136. Differential chemical shifts (Δδ) of the ecumicin analogs norecumicin and deoxyecumicin, caused by residual acid (calculated from TABLE XXIX), represented by (a) bar chart, and (b) heat maps.

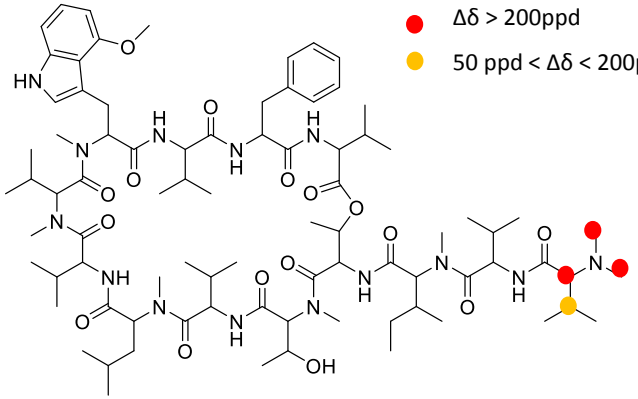
(A)



(B)



Norecumicin



Deoxyecumicin

TABLE XXIX. (A) RESIDUAL ACID AFFECTS THE ^{1}H NMR SPECTRA (METHANOL-D_4) OF NORECUMICIN. INTERPRETATION WAS MADE BY ^{1}H ITERATIVE FULL SPIN ANALYSIS.

		Norecumicin (600MHz, CD_3OD with residual acid)	Norecumcin (900MHz, with neutral pH)
Amino Acid		^{1}H δ in ppm(mult, *J* in Hz)	^{1}H δ in ppm(mult, *J* in Hz)
N,N-Me_2-V	1	-	-
	2	3.01324 (d, 7.78)	2.67539 (d, 9.19)
	3	2.17799 (ddd, 7.78, 6.78, 6.51)	2.04262 (ddd, 9.19, 6.75, 6.46)
	4,5	2.51667 (s)	2.31527 (s)
	6	1.09340 (d, 6.51)	1.09251 (d, 6.75)
	7	0.85865 (d, 6.78)	0.84589 (d, 6.46)
L-V[1]	1	-	-
	2	4.70170 (d, 8.60)	4.67201 (d, 8.76)
	3	2.12219 (ddd, 8.60, 6.80, 6.61)	2.10282 (ddd, 8.76, 6.78, 6.69)
	4	1.00029 (d, 6.80)	0.977216 (d, 6.78)
	5	1.05806 (d, 6.61)	1.055758 (d, 6.69)
	NH	-	-
N-Me-L-V[1]	1	-	-
	2	4.83000 (d, 8.07)	4.834013 (d, 11.07)
	3	2.19843 (ddd, 8.07, 6.51, 6.55)	2.175649 (ddd, 11.07, 6.42, 6.61)
	4	0.81478 (d, 6.51)	0.809878 (d, 6.42)
		0.79618 (d, 6.55)	0.793833 (d, 6.61)
	5	3.24336 (s)	3.248635 (s)
L-T	1	-	-
	2	5.17146 (d, 2.19)	5.173976 (d, 2.29)
	3	5.77937 (dd, 2.19, 6.41)	5.785936 (dd, 2.29, 6.51)
	4	1.31412 (d, 6.41)	1.313048 (d, 6.51)
	NH	-	-
N-Me-L-T	1	-	-
	2	5.00469 (d, 4.10)	5.00850 (d, 4.01)
	3	4.42422 (dd, 4.10, 6.60)	4.426267 (dd, 4.01, 6.61)
	4	0.92049 (d, 6.60)	0.919684 (d, 6.61)
	5	3.32064 (s)	3.323236 (s)
L-V[2]	1	-	-
	2	4.85855 (d, 8.88)	4.853292 (d, 8.92)
	3	2.34892 (ddd, 8.88, 6.66, 6.92)	2.351437 (ddd, 8.92, 7.23, 6.84)
	4	1.08741 (d, 6.66)	1.093803 (d, 7.23)
	5	0.98043 (d, 6.92)	0.978045 (d, 6.84)
N-Me-L-L	1	-	-
	2	5.09433 (dd, 7.26, 8.46)	5.08441 (dd, 6.77, 8.59)
	3	1.22635 (ddd, 7.26, -13.57, 6.30)	1.21889 (ddd, 6.77, -13.57, 6.30)

		Norecumicin (600MHz, CD_3OD with residual acid)	Norecumcin (900MHz, with neutral pH)
Amino Acid		^1H δ in ppm(mult, *J* in Hz)	^1H δ in ppm(mult, *J* in Hz)
		1.46286 (ddd, 8.46, -13.57, 5.09)	1.46595 (ddd, 8.59, -13.57, 6.73)
	4	0.95917 (dddd, 6.30, 5.09. 6.57, 6.62)	0.99183 (dddd, 6.30, 6.73, 6.62, 6.57)
	5	0.16164 (d, 6.57)	0.14802 (d, 6.62)
	6	0.33632 (d, 6.62)	0.33571 (d, 6.57)
	7	3.25635 (s)	3.26027 (s)
L-V[3]	1	-	-
	2	4.60181 (d, 8.74)	4.59574 (d, 8.91)
	3	2.01234 (ddd, 8.74, 6.82, 6.63)	2.02723 (ddd, 8.91, 6.83, 6.82)
	4	0.91169 (d, 6.82)	0.91243 (d, 6.83)
	5	0.88814 (d, 6.69)	0.85921 (d, 6.82)
N-Me-L-V	1	-	-
	2	3.05373 (d, 7.53)	3.063932 (d, 7.58)
	3	2.58079 (ddd, 7.52, 6.60, 6.81)	2.581881 (ddd, 7.58, 7.16, 6.12)
	4	1.01784 (d, 6.60)	0.980146 (d, 7.16)
	5	0.97672 (d, 6.81)	1.093888 (d, 6.12)
	6	3.13191 (s)	3.137783 (s)
N-Me-4-OMe-L-Y	1	-	-
	2	4.10142 (dd, 11.17, 4.59)	4.10426 (dd, 11.17, 4.67)
	3	3.54603 (dd, 11.17, -13.68)	3.54493 (dd, 11,17, -13.72)
		3.69647 (dd, 4.59, -13.68)	3.69340 (dd, 4.67, -13.72)
	5	6.70011 (d, 0.88)	6.69818 (d, 0.81)
	7	6.92224 (ddd, 0.53, 0.88, 8.23)	6.91749 (ddd, 0.81, 8.17, 0.57)
	8	6.98161 (dd, 8.23, 7.79)	6.98164 (dd, 8.17, 7.75)
	9	6.44190 (dd, 0.53, 7.79)	6.44215 (dd, 0.57, 7.75)
	12	3.82647 (s)	3.82691 (s)
	13	2.15483 (s)	2.15642 (s)
	NH	-	-
L-V[4]	1	-	-
	2	4.52754 (d, 7.65)	4.53629 (d, 7.86)
	3	2.16809 (ddd, 7.65, 6.84, 6.80)	2.19058 (ddd, 7.86, 6.81, 6.66)
	4	1.02723 (d, 6.84)	1.026756 (d, 6.81)
	5	0.99273 (d, 6.80)	0.993264 (d, 6.66)
	NH	-	-
Ph-L-THREO-S	1	-	-
	2	4.88974 (d, 1.84)	4.88388 (d, 1.59)
	3	5.32611 (d, 1.84)	5.32596 (d, 1.59)
	5, 9	7.23067 (dddd, 7.89, 1.38, 1.21, 0.44)	7.22918 (dddd, 7.72, 1.00, 0.78, 0.70)

		Norecumicin (600MHz, CD_3OD with residual acid)	Norecumcin (900MHz, with neutral pH)
Amino Acid		^{1}H δ in ppm(mult, *J* in Hz)	^{1}H δ in ppm(mult, *J* in Hz)
	6, 8, 7	7.25003 (dddd, 0.76, 1.21, 7.89, 7.40) 7.19683 (dd, 1.38, 7.40)	7.25224 (dddd, 7.72, 7.50, 0.20, 0.78) 7.198397 (dd, 1.00, 7.50)
	NH	-	-
L-V^5	1	-	-
	2	4.40752 (d, 8.71)	4.40221 (d, 8.83)
	3	1.96490 (ddd, 8.71, 6.38, 6.10)	1.96334 (ddd, 8.83, 6.73, 6.79)
	4	0.93602 (d, 6.38)	0.93700 (d, 6.73)
	5	0.92487 (d, 6.10)	0.92241 (d, 6.79)
	NH	-	-

(B) RESIDUAL ACID AFFECTS ^{1}H NMR SPECTRUM (METHANOL-D_4) OF DEOXYECUMICIN. INTERPRETATION OF ^{1}H NMR WAS DONE BY ^{1}H ITERATIVE FULL SPIN ANALYSIS.

		Deoxyecumicin (600MHz, CD_3OD with residual acid)	Deoxyecumicin (600MHz, CD_3OD at neutral pH)
Amino Acid		1H δ in ppm(mult, J in Hz)	1H δ in ppm(mult, J in Hz)
N,N-Me$_2$-V	1	-	-
	2	3.06282 (d, 7.81)	2.66806 (d, 9.03)
	3	2.17472 (ddd, 7.81, 8.57, 6.61)	2.07249 (ddd, 9.03, 7.33, 6.66)
	4,5	2.53796 (s)	2.31402 (s)
	6	0.86799 (d, 8.57)	0.98065 (d, 7.33)
	7	1.02491 (d, 6.61)	0.85096 (d, 6.66)
L-V^1	1	-	-
	2	4.68063 (d, 8.73)	4.67351 (d, 8.37)
	3	2.10730 (ddd, 8.73, 6.60, 6.69)	2.07249 (ddd, 8.37, 6.49, 6.58)
	4	1.05132 (d, 6.60)	1.04503 (d, 6.49)
	5	1.02085 (d, 6.69)	1.02684 (d, 6.58)
	NH	-	-
N-Me-L-*allo*-I	1	-	-
	2	4.94831 (d, 11.27)	4.94463 (d, 11.32)
	3	1.93951 (dddd, 11.27, 1.997, 9.21, 6.56)	1.94906 (dddd, 11.32, 2.21, 7.00, 6.30)
	4	0.98568 (ddd, 1.997, -13.95, 7.62) 1.24598 (ddd, 9.21, -13.95, 7.23)	1.00008 (ddd, 2.21, -14.81, 7.10) 1.26697 (ddd, 7.00, -14.81, 7.74)
	5	0.75324 (d, 6.56)	0.75221 (d, 6.30)
	6	0.71644 (dd, 7.62, 7.23)	0.72352 (dd, 7.10, 7.74)
	7	3.23331 (s)	3.22793 (s)

		Deoxyecumicin (600MHz, CD_3OD with residual acid)	Deoxyecumicin (600MHz, CD_3OD at neutral pH)
Amino Acid		1H δ in ppm(mult, J in Hz)	1H δ in ppm(mult, J in Hz)
L-T	1	-	-
	2	5.13079 (d, 2.24)	5.13376 (d, 2.12)
	3	5.79431 (dd, 2.24, 6.42)	5.78360 (dd, 2.12, 6.54)
	4	1.31460 (d, 6.42)	1.31457 (d, 6.54)
	NH	-	-
N-Me-L-T	1	8.478019 (OH)	-
	2	5.03163 (d, 3.58)	5.02781 (d, 3.63)
	3	4.44188 (dd, 3.58, 6.48)	4.43548 (dd, 3.63, 7.13)
	4	0.89152 (d, 6.48)	0.88597 (d, 7.13)
	5	3.26488 (s)	3.32014 (s)
L-V[2]	1	-	-
	2	4.82465 (d, 9.18)	4.82 (d, 9.22)
	3	2.36479 (ddd, 9.18, 7.06, 6.57)	2.35658 (ddd, 9.22, 6.60, 6.50)
	4	0.97173 (d, 7.06)	1.09561 (d, 6.60)
	5	1.09979 (d, 6.57)	0.98065 (d, 6.50)
	NH	-	-
N-Me-L-L	1	-	-
	2	5.14539 (dd, 7.76, 6.09)	5.16832 (dd, 7.43, 7.42)
	3	1.27594 (ddd, 7.76, -13.86, 6.63)	1.29169 (ddd, 7.43, -14.05, 1.87)
		1.42733 (ddd, 6.09, -13.86, 8.53)	1.42565 (ddd, 7.42, -14.05, 5.78)
	4	1.00015 (dddd, 6.63, 8.53, 6.75, 6.54)	0.99420 (dddd, 1.87, 5.78, 6.64, 6.64)
	5	0.20204 (d, 6.75)	0.22412 (d, 6.64)
	6	0.31392 (d, 6.54)	0.32176 (d, 6.64)
	7	3.32323 (s)	3.26320 (s)
L-V[3]	1	-	-
	2	4.58468 (d, 9.05)	4.60155 (d, 9.22)
	3	2.04318 (ddd, 9.05, 6.71, 8.25)	2.038317 (ddd, 9.22, 6.41, 6.20)
	4	0.91397 (d, 6.71)	0.91467 (d, 6.41)
	5	0.87899 (d, 6.50)	0.86768 (d, 6.20)
	NH	-	-
N-Me-L-V	1	-	-
	2	3.05526 (d, 7.87)	3.05431 (d, 7.60)
	3	2.56999 (ddd, 7.87, 6.61, 6.63)	2.58779 (ddd, 7.60, 6.97, 6.51)
	4	0.97893 (d, 6.61)	0.98065 (d, 6.97)
	5	1.09301 (d, 6.63)	1.09561 (d, 6.51)
	6	3.14711 (s)	3.14643 (s)

		Deoxyecumicin (600MHz, CD_3OD with residual acid)	Deoxyecumicin (600MHz, CD_3OD at neutral pH)
Amino Acid		1H δ in ppm(mult, J in Hz)	1H δ in ppm(mult, J in Hz)
N-Me-4-OMe-L-Y	1	-	-
	2	4.09232 (dd, 11.15, 4.65)	4.09495 (dd, 11.17, 4.49)
	3	3.54210 (dd, 11.15, -13.73)	3.54716 (dd, 11.17, -13.59)
		3.68765 (dd, 4.65, -13.73)	3.69112 (dd, 4.49, -13.59)
	5	6.69559 (d, 0.86)	6.69763 (d, 0.87)
	7	6.919234 (ddd, 0.86, 8.17, 0.61)	6.92071 (ddd, 0.87, 8.23, 0.90)
	8	6.98023 (dd, 8.17, 7.82)	6.98154 (dd, 8.23, 7.80)
	9	6.43746 (dd, .61, 7.82)	6.44080 (dd, 0.90, 7.80)
	12	3.81340 (s)	3.81826 (s)
	13	2.16169 (s)	2.16528 (s)
	NH	-	-
L-V^4	1	-	-
	2	4.40250 (d, 8.40)	4.40704 (d, 8.33)
	3	2.17843 (ddd, 8.40, 7.00, 6.81)	2.18962 (ddd, 8.33, 6.03, 7.96)
	4	0.97833 (d, 7.00)	0.98065 (d, 6.03)
	5	0.98567 (d, 6.81)	0.98065 (d, 7.96)
	NH	-	-
L-F	1	-	-
	2	4.77581 (dd, 3.55, 10.64)	4.78000 (dd, 12.15, 10.60)
	3	3.33877 (dd, 3.55, -15.01)	3.35000 (dd, 12.15, -14.13)
		2.83462 (dd, 10.64, -15.01)	2.84122 (dd, 10.60, -14.13)
	5, 9	7.08838 (dddd, 7.65, 1.24, 0.34, 1.33)	7.09274 (dddd, 7.89, 1.29, 0.38, 1.86)
	6, 8	7.20515 (dddd, 7.65, 7.39, 1.20, 0.34)	7.20245 (dddd, 7.89, 7.38, 1.98, 0.38)
	7	7.15283 (dd, 1.24, 7.39)	7.14951 (dd, 1.29, 7.38)
	NH	-	-
L-V^5	1	-	-
	2	4.35996 (d, 9.21)	4.36895 (d, 8.95)
	3	1.96233 (ddd, 9.21, 6.66, 6.62)	1.96594 (ddd, 8.95, 7.27, 6.83)
	4	0.92021 (d, 6.66)	0.93674 (d, 7.27)
	5	0.93622 (d, 6.62)	0.91992 (d, 6.83)
	NH	-	-

9.9.5 Comparison of the ^{1}H NMR fingerprints of the ecumicin congeners.

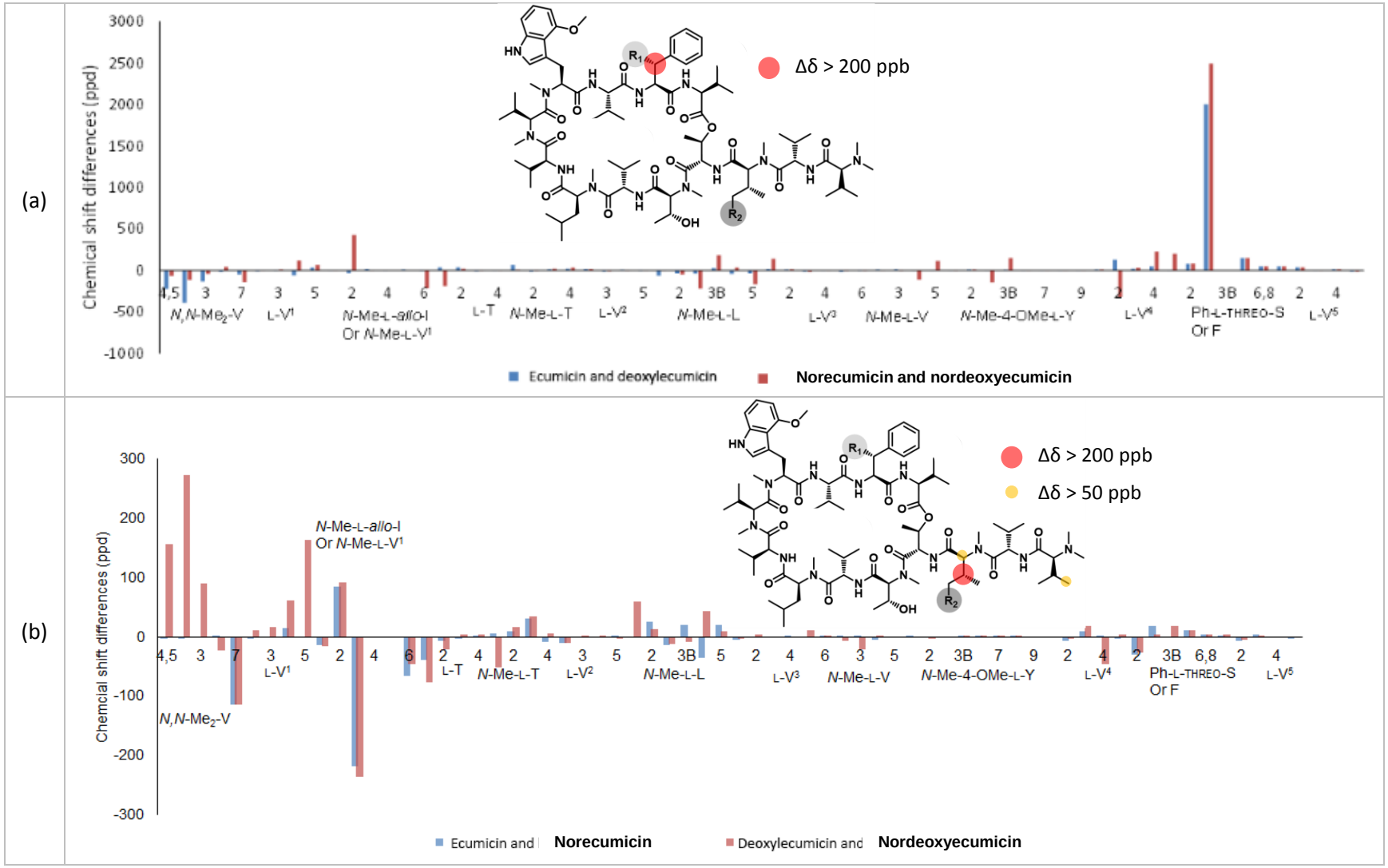
The HiFSA-generated ^{1}H NMR fingerprints proved to be a solid foundation for establishing chemical shift differences (Δ*δ*) between norecumicin, nordeoxyecumicin, ecumicin and deoxyecumicin. Taking into consideration the digital resolution of high-/ultrahigh-field NMR spectra (0.00015 ppm/pt at 600 MHz and 0.000029 ppm/pt at 900 MHz for ^{1}H), here we expressed the Δδ values in parts per billion (ppb, 1000 ppb = 1 ppm). (Napolitano, 2013) In general, the chemical shift differences (Δδ) between the four compounds were less than 300 ppb (0.300 ppm) when the chemical shift differences caused by residual acid and major structure differences were not included.

In case of the structural difference of a hydroxyl group (Ph-L-THREO-S and L-F), as seen in the pairs of ecumicin and deoxyecumicin, norecumicin-3V and nordeoxyecumicin, the greatest Δ*δ* was observed in H3 (β-proton) of the amino acid, with an upfield shift of over 2000 ppb (2.00 ppm). As in both cases the signals of H3 in Ph-L-THREO-S were located in a clear region of the ^{1}H NMR spectra, they were the most suitable for rapid discrimination of Ph-L-THREO-S and L-F.

In case of the structural differences associated with a methylene group (*N*-Me-L-ALLO-L and *N*-Me-L-V), as seen in the pairs of ecumicin and norecumicin-3V, nordeoxyecumicin and deoxyecumicin (Figure 137), the greatest Δ*δ* was observed in H3 (β-proton) of the amino acids, with a downfield shift of over 200 ppb (0.200 ppm). These signals were not located in a clear region of the ^{1}H NMR spectra, so a marker was still needed for rapid discrimination of *N*-Me-L-ALLO-L and *N*-Me-L-V. Fortunately, H2 (α-proton), H4/6 and H5/7 of the amino acids were located in clear regions. Significant changes in chemical shifts were observed in the signals corresponding

to them, though not as big as for H3. The Δδ observed for H2 (α-proton) was an upfield shift of approximately 100 ppb (0.100 ppm), while the Δδ observed in H4/6 and H5/7 ware downfield shifts of approximately 50 ppb (0.050 ppm). These substituent chemical shifts can be used together for rapid discrimination of the structural difference of a methylene group (*N*-Me-L-ALLO-L and *N*-Me-L-V).

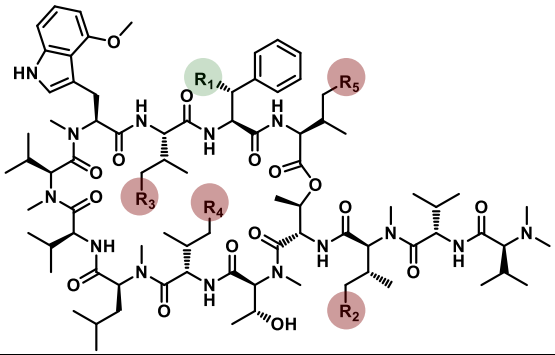
Figure 137. Differences in the chemical shifts of ecumicin and its analogs that reflect their structural differences. (a) The one hydroxyl group difference between Ph-L-THREO-S and L-F, and (b) the one methylene group difference between *N*-Me-L-ALLO-L and *N*-Me-L-V.



9.9.6 Structural-activity relationship concluded from ecumicin and its analogs.

The naturally occurring ecumicin analogs provided a starting point to understand the structural-activity relationship of this class of peptides, which will eventually benefit the lead optimization process. TABLE XXX summarizes the structures and activities of ecumicin and its analogs. These compounds differ from each other by only a hydroxyl group and/or a methylene group. Considering the limitation of the experimental precision of the MABA assay and the purity of some of the analogs isolated, there was no significant difference in the anti-TB activity of these compounds, suggesting that the altered moieties of the congeners were not essential for the anti-TB activity.

TABLE XXX. BRIEF SUMMARY OF ECUMICIN AND ITS ANALOGS PRODUCED BY *NONOMURAEA* MJM5123, AND THEIR ANTI-TB ACTIVITY.

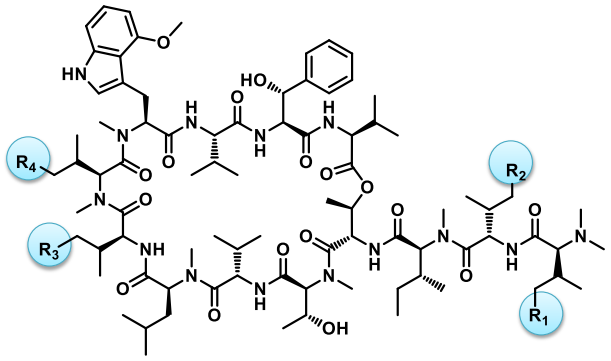


	MIC vs *M. tuberculosis* (μg/ml)	Molecular weight	Structure				
			R_1	R_2	R_3	R_4	R_5
Ecumicin	0.26	1599	OH	CH3	H	H	H
Deoxyecumicin	0.13	1583	H	CH3	H	H	H
Nordeoxyecumicin	0.55	1569	H	H	H	H	H
Norecumicin-3V	0.15	1585	OH	H	H	H	H
Homoecumicin-11I	0.26	1613	OH	CH3	CH3	H	H
Homoecumicin-13I	0.26	1613	OH	CH3	H	H	CH3
Homoecumicin-6I	0.26	1613	OH	CH3	H	CH3	H

9.9.7 Possible structures of other ecumicin analogs produced by *Nonomuraea* MJM5123.

Combining information from Chapter 6, the occurrence of deoxyecumicin is likely due to either incorporation of natural phenylalanine or failure to oxidize this amino acid after its incorporation into the peptide. Homoecumicins are likely to be produced due to errors in adenylation domains recognition for L-valine and isoleucine residues. An ATP-ppi exchange assay (Fersht 1985) has been developed to study the substrate specificity of NRPS adenylation domains. This assay measures the reversible formation of the aminoacyl-AMP derivative, and thus determines amino acid selectivity. The substrate specificity of L-allo-isoleucine adenylation domain (Couch, et al. 2004) and L-valine adenylation domain (Wilson, et al. 2013) has been analyzed by this assay. It was found that the L-allo-isoleucine adenylation domain has a relatively high chance to recognize a valine, and vice versa.

In spite of the fact that ecumicin has five valines, one *N*-methyl-valines and one *N,N*-dimethyl-valine, only three analogs have been identified with a valine to isoleucine change. The fact that the sample which contains homoecumicin-6I also contains another unknown peptide with molecular weight of 1613 amu, and the observation that HPLC chromatography of homoecumicin-11I, -13I and -6I (Figure 140) exhibits a few more unexploited peaks (due to their complex nature), altogether implies the possibility that *Nonomuraea* MJM5123 produces several other close ecumicin congeners. Among the possible ecumicin analogs are homoecumicin-1I, -2I, -8I, and -9I (Figure 138). However, as seen in the case of homoecumicin-11I, -13I and -6I, these analogs are not likely to have significantly different anti-M. tuberculosis activity compared to other known members in the ecumicin peptide family.



Homoecumicin-1I	R_1= CH_3	R_2= H	R_3= H	R_4= H
Homoecumicin-2I	R_1= H	R_2= CH_3	R_3= H	R_4= H
Homoecumicin-8I	R_1= H	R_2= H	R_3= CH_3	R_4= H
Homoecumicin-9I	R_1= H	R_2= H	R_3= H	R_4= CH_3

Figure 138. Other possible ecumicin analogs.

9.10 Material and methods

Semi-preparative HPLC separation of ecumicin analogs.

Semi-preparative HPLC experiments were performed on a Waters Delta® 600 system with a Waters 996 photodoide array detector.

HPLC separation of nordeoxyecumicin

Semi-preparative HPLC on an RP column (YMC ODS-AQ 2.5µm, 10 × 250mm) using a bi-phase linear gradient was applied as the final purification step. The flow rate was kept at 3 ml/min. After sample injection, mobile phase was kept at 49% acetonitrile (1% formic acid) for two minutes, then in 15 minutes, ramped up to 67% acetonitrile (1% formic acid), washed with 95% acetonitrile (1% formic acid) for 5 minutes and finally re-equilibrated with 49% acetonitrile (1% formic acid) for 5 minutes. Nordeoxyecumicin eluted at 15.195 min.

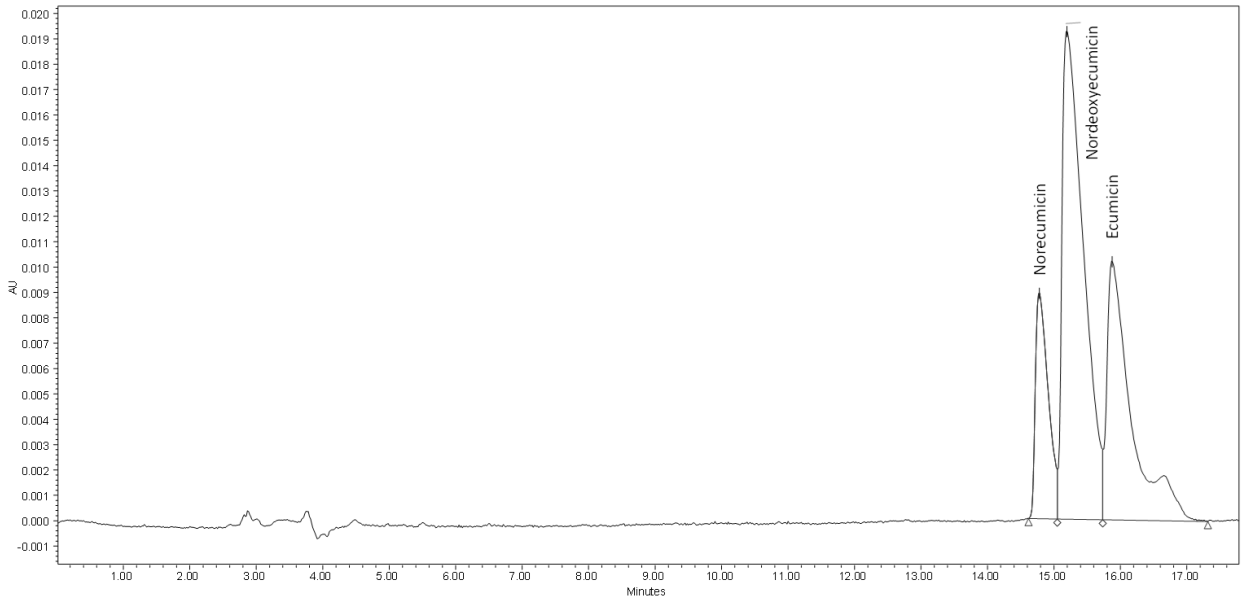


Figure 139. Semi-preparative HPLC separation of norecumicin-3V, nordeoxyecumicin and ecumicin.

HPLC separation of nordeoxyecumicin

Semi-preparative HPLC on an RP column (YMC ODS-AQ 2.5µm, 10 × 250mm) using an isocratic elution (51% acetonitrile, and 1% formic acid) was applied as the final purification step. After sample injection, the flow rate of mobile phase was kept at 3 ml/min. Homoecumicin-11I, homoecumicin-13I and homoecumicin-6I eluted at 20.28 min, 21.06 min and 22.50 min, respectively.

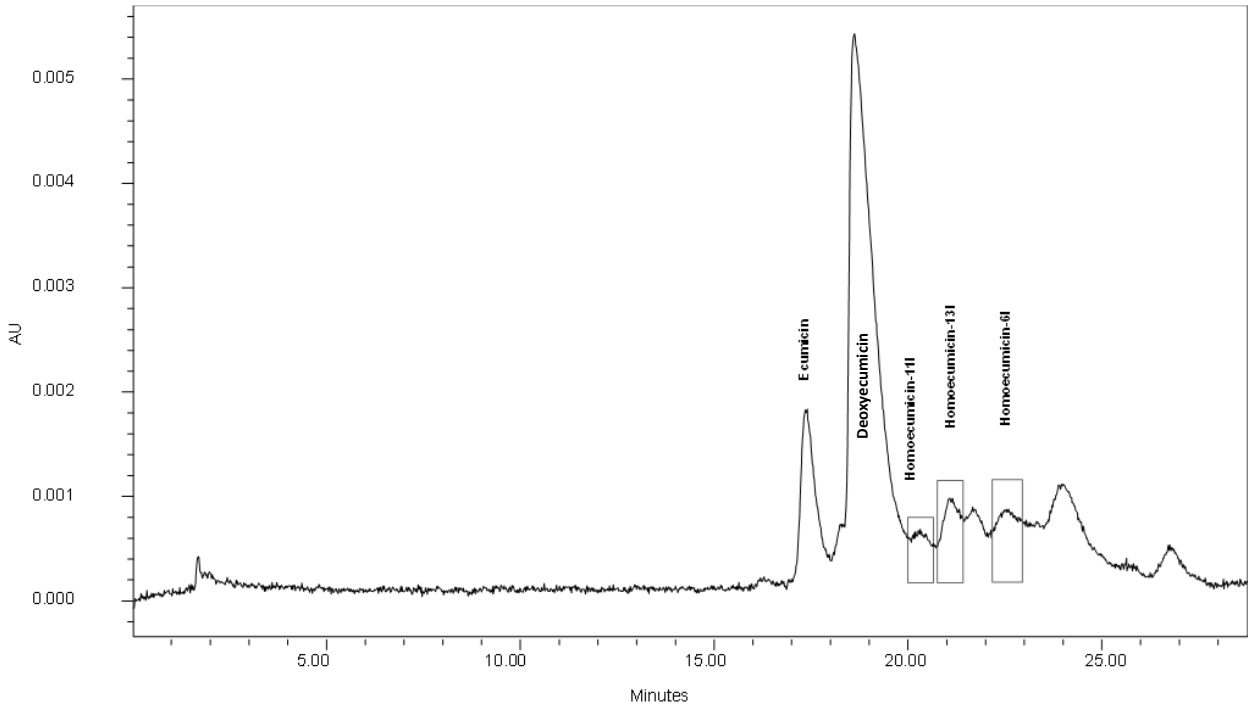


Figure 140. Semi-preparative HPLC separation of ecumicin, deoxyecumicin, homoecumicin-11I, homoecumicin-13I and homoecumicin-6I.

NMR experiments

Norecumicin, nordeoxyecumicin, and deoxyecumicin were prepared in 3 mm NMR tubes with 99.8% methanol-d_4; all NMR experiments were aquired at 600 or 900 MHz, with Bruker Avance 600 or Bruker Avance II 900 instruments, respectively, equipped with cryogenic sensitivity-enhanced triple-resonance 5 mm inverse TCI cryoprobes. H11, H17, H18 and H20 were prepared in 1.7 mm NMR tubes with 99.96% methanol-d_4; all NMR data were obtained at 700 MHz, with a Bruker Avance III 700 instrument equipped with a cryogenic sensitivity-enhanced triple-resonance 1.7 mm inverse TCI cryoprobe. All NMR experiments were performed using standard Bruker pulse sequences.

All NMR spectra were processed with MNova. The ^{1}H full spin analyses were performed with PERCH NMR software (v.2012.1, PERCH Solutions Ltd., Kuopio, Finland).

MS experiments

High-resolution mass spectra were obtained with a Shimadzu IT-TOF LC mass spectrometer.

In vitro biological activity

In vitro biological activity of ecumicin analogs were assessed as described in Chapter 7 (7.1.4).

10. Conclusion

The discovery of ecumicin and its analogs demonstrates that it is possible to find new potent, narrow-spectrum anti- *M. tuberculosis* secondary metabolites from actinomycetes by direct whole-cell based high-throughput screening, and to both biologically dereplicate and profile them prior to their isolation as the active principle of the lead extracts. Inclusion of a panel of *M. tuberculosis* isolates resistant to actinomycete-derived drugs and organisms such as *E. coli* and *S. aureus* , as has been used in previous screening campaigns, minimized the chance of re-discovering known compounds. Toxicity of an extract/fraction to a mammalian cell line, while conceivably due to a compound(s) other than that responsible for inhibition of *M. tuberculosis*, was nonetheless used in the prioritization process and can reduce the probability of isolating non-selective compounds at the end of the bioassay-guided isolation process.

The present success in the bio-assay guided isolation of a highly active compound was also partially due to the presence of distinct active compounds in the actinomycete extract, and partially due to the availability of the quantitative and reproducible assays (MABA, LORA, and VERO cells IC_{50} assays).

Structure elucidation of the major active component, ecumicin, involved a wide range of spectroscopic techniques, including NMR, LC-HR-MS, LC-MS^2, X-ray crystallography, UV, CD, and IR, as well as chemical derivatization – the Marfey's analysis. The structure of ecumicin indicated that it is a non-ribosomal peptide (NRP), which was confirmed by the identification of corresponding NRPS gene from the *Nonomuraea sp*. The identified NRPS gene in turn confirmed the structure of ecumicin, and provided clues on possible congeners.

The ^{1}H NMR spectrum of ecumicin was registered in the form of a ^{1}H iterative Full Spin Analysis (HiFSA) profile, which allowed a complete and precise determination of the field independent parameters, δ_H and $J_{H,H}$. These parameters can be used for the re-generation of the ^{1}H NMR spectrum of ecumicin at any field strength, which can be used for the quantitative and/or qualitative analyses including unambiguous dereplication of the molecule.

The presence of distinct amino acid residues in peptides, and in particular their separation by amide bonds, makes it possible to study the individual ^{1}H sub-spectra of each amino acid without affecting the rest of the molecule. With the availability of ecumicin's HiFSA profile, sub-spectra of all amino acids were generated. This also led to the development of a new approach in the structure elucidation of ecumicin analogs and peptides in general, i.e., the NMR structure sequencing method. This method was established based on the assumption that all ecumicin congeners are structurally very similar, such that subtraction of ^{1}H sub-spectra that correspond to corresponding amino acid residues would yield the ^{1}H sub-spectrum of the amino acid of difference. By applying this method, even the structures of minor ecumicin analogs (< 0.5 mg each) contained in complex samples (purity < 40 % by the 100% qHNMR) could be elucidated successfully.

As all ecumicin congeners have similar anti-*M. tuberculosis* activity, and ecumicin is the most abundant chemical species, it was selected for intensive in vitro analysis. Its potency, selective bactericidal activity, and ability to taregt even XDR strains makes ecumicin and interesting new molecule to study for its in vivo activity.

Genome sequencing of spontaneous ecumicin-resistant clones as well as binding assays (DARTS test) implicated ClpC1 being the primary molecular target of ecumicin. ClpP1P2, as well as its regulatory factors, ClpC1 and ClpX, are essential in *M. tuberculosis*, presumably to eliminate critical proteins whose accumulation is toxic. Biochemical studies suggest that ecumicin stimulates ClpC1's ATPase activity, while inhibiting the ClpC1-dependent protein degradation. Presumably the accumulation of critical proteins and depletion of ATP lead to selective mycobacterial cell death.

After several failed attempt in oral administration of ecumicin, a proof-of-concept study has been performed focusing on parental administration of the molecule. Formulation development focus on improving solubility, and as a result, a nano micelle formulation was developed. With this formulation, we have demonstrated for the first time that ClpC1 is a druggable target in *M. tuberculosis* bacteria which reside in both cellular (macrophage) and mouse hosts. While bactericidal in vitro, the static activity observed for ecumicin in vivo may have been due to the limited dosage and treatment duration which in turn was dictated by limited micellar loading and compound availability, respectively. As the bactericidal activity is both time and concentration dependent in vitro, future experiment with higher dosage and elongated treatment duration will hopefully lead to in vivo bactericidal activity.

REFERENCES

Akopian, T., O. Kandror, R. M. Raju, M. Unnikrishnan, E. J. Rubin and A. L. Goldberg (2012). "The active ClpP protease from M. tuberculosis is a complex composed of a heptameric ClpP1 and a ClpP2 ring." EMBO J **31**(6): 1529-1541.

Al-Balas, Q., N. G. Anthony, B. Al-Jaidi, A. Alnimr, G. Abbott, A. K. Brown, R. C. Taylor, G. S. Besra, T. D. McHugh, S. H. Gillespie, B. F. Johnston, S. P. Mackay and G. D. Coxon (2009). "Identification of 2-aminothiazole-4-carboxylate derivatives active against Mycobacterium tuberculosis H37Rv and the beta-ketoacyl-ACP synthase mtFabH." PLoS One **4**(5): e5617.

Ananthan, S., E. R. Faaleolea, R. C. Goldman, J. V. Hobrath, C. D. Kwong, B. E. Laughon, J. A. Maddry, A. Mehta, L. Rasmussen, R. C. Reynolds, J. A. Secrist, 3rd, N. Shindo, D. N. Showe, M. I. Sosa, W. J. Suling and E. L. White (2009). "High-throughput screening for inhibitors of Mycobacterium tuberculosis H37Rv." Tuberculosis (Edinb) **89**(5): 334-353.

Andries, K., P. Verhasselt, J. Guillemont, H. W. Gohlmann, J. M. Neefs, H. Winkler, J. Van Gestel, P. Timmerman, M. Zhu, E. Lee, P. Williams, D. de Chaffoy, E. Huitric, S. Hoffner, E. Cambau, C. Truffot-Pernot, N. Lounis and V. Jarlier (2005). "A diarylquinoline drug active on the ATP synthase of Mycobacterium tuberculosis." Science **307**(5707): 223-227.

Anand, S., M. V. Prasad, G. Yadav, N. Kumar, J. Shehara, M. Z. Ansari and D. Mohanty (2010). "SBSPKS: structure based sequence analysis of polyketide synthases." Nucleic acids research **38**(Web Server issue): W487-496.

Ananthan, S., E. R. Faaleolea, R. C. Goldman, J. V. Hobrath, C. D. Kwong, B. E. Laughon, J. A. Maddry, A. Mehta, L. Rasmussen, R. C. Reynolds, J. A. Secrist, 3rd, N. Shindo, D. N. Showe, M. I. Sosa, W. J. Suling and E. L. White (2009). "High-throughput screening for inhibitors of Mycobacterium tuberculosis H37Rv." Tuberculosis (Edinb) **89**(5): 334-353.

Bartlett, G. J., A. Choudhary, R. T. Raines and D. N. Woolfson (2010). "n-->pi* interactions in proteins." Nat Chem Biol **6**(8): 615-620.

Bartlett, G. J., R. W. Newberry, B. Vanveller, R. T. Raines and D. N. Woolfson (2013). "Interplay of Hydrogen Bonds and n-->pi* Interactions in Proteins." J Am Chem Soc **135**(49): 18682-18688.

Becker, B., M. P. Lechevalier, R. E. Gordon and H. A. Lechevalier (1964). "Rapid Differentiation between Nocardia and Streptomyces by Paper Chromatography of Whole-Cell Hydrolysates." Applied microbiology **12**: 421-423.

Belisle, J., S. Mahaffey and P. Hill (2009). Isolation of Mycobacterium Species Genomic DNA. Mycobacteria Protocols. T. Parish and A. C. Brown, Humana Press. **465:** 1-12.

Benson, D. A., I. Karsch-Mizrachi, D. J. Lipman, J. Ostell and D. L. Wheeler (2008). "GenBank." Nucleic acids research **36**(Database issue): D25-30.

Berdy, J. (2005). "Bioactive microbial metabolites." J Antibiot **58**(1): 1-26.

Bhushan, R. and H. Bruckner (2011). "Use of Marfey's reagent and analogs for chiral amino acid analysis: assessment and applications to natural products and biological systems." Journal of chromatography. B, Analytical technologies in the biomedical and life sciences **879**(29): 3148-3161.

Brigden, G., B. T. Nyang'wa, P. du Cros, F. Varaine, J. Hughes, M. Rich, C. R. Horsburgh, Jr., C. D. Mitnick, E. Nuermberger, H. McIlleron, P. P. Phillips and M. Balasegaram (2014). "Principles for designing future regimens for multidrug-resistant tuberculosis." Bull World Health Organ **92**(1): 68-74.

Brodin, P., L. Majlessi, L. Marsollier, M. I. de Jonge, D. Bottai, C. Demangel, J. Hinds, O. Neyrolles, P. D. Butcher, C. Leclerc, S. T. Cole and R. Brosch (2006). "Dissection of ESAT-6 system 1 of Mycobacterium tuberculosis and impact on immunogenicity and virulence." Infect Immun **74**(1): 88-98.

Camacho LR, Constant P, Raynaud C, Laneelle MA, Triccas JA, Gicquel B, Daffe M, Guilhot C. (2001). "Analysis of the phthiocerol dimycocerosate locus of Mycobacterium tuberculosis. Evidence that this lipid is involved in the cell wall permeability barrier." The Journal of biological chemistry **276:**19845-19854.

Campbell, J. B. (2010). "Improving lead generation success through integrated methods: transcending 'drug discovery by numbers'." IDrugs **13**(12): 874-879.

Cantrell, C. L., T. Lu, F. R. Fronczek, N. H. Fischer, L. B. Adams and S. G. Franzblau (1996). "Antimycobacterial cycloartanes from Borrichia frutescens." Journal of Natural Products **59**(12): 1131-1136.

Cho, S. H., S. Warit, B. Wan, C. H. Hwang, G. F. Pauli and S. G. Franzblau (2007). "Low-oxygen-recovery assay for high-throughput screening of compounds against nonreplicating Mycobacterium tuberculosis." Antimicrob Agents Chemother **51**(4): 1380-1385.

Claridge, T. D. and I. Perez-Victoria (2003). "Enhanced 13C resolution in semi-selective HMbC: a band-selective, constant-time HMBC for complex organic structure elucidation by NMR." Org Biomol Chem **1**(21): 3632-3634.

Collins, L. and S. G. Franzblau (1997). "Microplate alamar blue assay versus BACTEC 460 system for high-throughput screening of compounds against Mycobacterium tuberculosis and Mycobacterium avium." Antimicrob Agents Chemother **41**(5): 1004-1009.

Cooper, C. B. (2013). "Development of Mycobacterium tuberculosis Whole Cell Screening Hits as Potential Antituberculosis Agents." J Med Chem.

Corbett, E. L., C. J. Watt, N. Walker, D. Maher, B. G. Williams, M. C. Raviglione and C. Dye (2003). "The growing burden of tuberculosis: global trends and interactions with the HIV epidemic." Arch Intern Med **163**(9): 1009-1021.

Croy S. R., Kwon G. S. (2006) "Polymeric micelles for drug delivery." Curr Pharm Des. **12**(36):4669-84.

Couch, R., S. E. O'Connor, H. Seidle, C. T. Walsh and R. Parry (2004). "Characterization of CmaA, an adenylation-thiolation didomain enzyme involved in the biosynthesis of coronatine." J Bacteriol **186**(1): 35-42.

Delcher, A. L., K. A. Bratke, E. C. Powers and S. L. Salzberg (2007). "Identifying bacterial genes and endosymbiont DNA with Glimmer." Bioinformatics **23**(6): 673-679.

Diacon, A. H., P. R. Donald, A. Pym, M. Grobusch, R. F. Patientia, R. Mahanyele, N. Bantubani, R. Narasimooloo, T. De Marez, R. van Heeswijk, N. Lounis, P. Meyvisch, K. Andries and D. F. McNeeley (2012). "Randomized pilot trial of eight weeks of bedaquiline (TMC207) treatment for multidrug-resistant tuberculosis: long-term outcome, tolerability, and effect on emergence of drug resistance." Antimicrob Agents Chemother **56**(6): 3271-3276.

Drewry, D. H. and R. Macarron (2010). "Enhancements of screening collections to address areas of unmet medical need: an industry perspective." Curr Opin Chem Biol **14**(3): 289-298.

Erzberger, J. P. and J. M. Berger (2006). "Evolutionary relationships and structural mechanisms of AAA+ proteins." Annu Rev Biophys Biomol Struct **35**: 93-114.

Felsenstein, J. (Jul, 1985). "Confidence limits on phylogenies: an approach using the bootstrap." Evolution **39**(4): 783-791.

Fersht, A. (1985). Enzyme structure and mechanism.

Filliol, I., A. S. Motiwala, M. Cavatore, W. Qi, M. H. Hazbon, M. Bobadilla del Valle, J. Fyfe, L. Garcia-Garcia, N. Rastogi, C. Sola, T. Zozio, M. I. Guerrero, C. I. Leon, J. Crabtree, S. Angiuoli, K. D. Eisenach, R. Durmaz, M. L. Joloba, A. Rendon, J. Sifuentes-Osornio, A. Ponce de Leon, M. D. Cave, R. Fleischmann, T. S. Whittam and D. Alland (2006). "Global phylogeny of Mycobacterium tuberculosis based on single nucleotide polymorphism (SNP) analysis: insights into tuberculosis evolution, phylogenetic accuracy of other DNA fingerprinting systems, and recommendations for a minimal standard SNP set." Journal of bacteriology **188**(2): 759-772.

Fischer, B., P. Heffeter, K. Kryeziu, L. Gille, S. M. Meier, W. Berger, C. R. Kowol and B. K. Keppler (2013). "Poly(lactic acid) nanoparticles of the lead anticancer ruthenium compound KP1019 and its surfactant-mediated activation." Dalton Transactions.

Friesen, J. B. and G. F. Pauli (2008). "Performance characteristics of countercurrent separation in analysis of natural products of agricultural significance." Journal of agricultural and food chemistry **56**(1): 19-28.

Gandhi, N. R., A. Moll, A. W. Sturm, R. Pawinski, T. Govender, U. Lalloo, K. Zeller, J. Andrews and G. Friedland (2006). "Extensively drug-resistant tuberculosis as a cause of death in patients co-infected with tuberculosis and HIV in a rural area of South Africa." Lancet **368**(9547): 1575-1580.

Gavrish, E., C. S. Sit, S. Cao, O. Kandror, A. Spoering, A. Peoples, L. Ling, A. Fetterman, D. Hughes, A. Bissell, H. Torrey, T. Akopian, A. Mueller, S. Epstein, A. Goldberg, J. Clardy and K. Lewis (2014). "Lassomycin, a Ribosomally Synthesized Cyclic Peptide, Kills Mycobacterium tuberculosis by Targeting the ATP-Dependent Protease ClpC1P1P2." Chem Biol **21**(4): 509-518.

Cai, G. J. G. Napolitano, J.B. McAlpine, Y. Wang, B. U. Jaki, J. Suh, S. H. Yang, I. Lee, S. G. Franzblau, G. F. Pauli, and S. Cho (2013) "Hytramycins V and I, Anti-Mycobacterium tuberculosis Hexapeptides from a Streptomyces hygroscopicus Strain" J. Nat. Prod., 76 (11), pp 2009–2018

Gill, S.K., H. Xu, P. D. Kirchhoff, T. Cierpicki, A. J. Turbiak, B. Wan, N. Zhang, K. Peng, S. G. Franzblau, G. A. Garcia, and H. D. Hollis Showalter. " Structure-Based Design of Novel Benzoxazinorifamycins with Potent Binding Affinity to Wild-Type and Rifampin-Resistant Mutant Mycobacterium tuberculosis RNA Polymerases" J. Med. Chem., 55 (8), pp 3814–3826

Godfrey, K. (1985). "Statistics in practice. Comparing the means of several groups." N Engl J Med **313**(23): 1450-1456.

Goldman, R. C. and B. E. Laughon (2009). "Discovery and validation of new antitubercular compounds as potential drug leads and probes." Tuberculosis (Edinb) **89**(5): 331-333.

Gottlieb, H. E., V. Kotlyar and A. Nudelman (1997). "NMR Chemical Shifts of Common Laboratory Solvents as Trace Impurities." J Org Chem **62**(21): 7512-7515.

Griffin, J. E., J. D. Gawronski, M. A. Dejesus, T. R. Ioerger, B. J. Akerley and C. M. Sassetti (2011). "High-resolution phenotypic profiling defines genes essential for mycobacterial growth and cholesterol catabolism." PLoS Pathog **7**(9): e1002251.

Hanson, P. I. and S. W. Whiteheart (2005). "AAA+ proteins: have engine, will work." Nat Rev Mol Cell Biol **6**(7): 519-529.

Henrich, C. J. and J. A. Beutler (2013). "Matching the power of high throughput screening to the chemical diversity of natural products." Nat Prod Rep **30**(10): 1284-1298.

Humnabadkar, V., R. K. Jha, N. Ghatnekar and S. M. De Sousa (2011). "A high-throughput screening assay for simultaneous selection of inhibitors of *Mycobacterium tuberculosis* 1-deoxy-D-xylulose-5-phosphate synthase (Dxs) or 1-deoxy-D-xylulose 5-phosphate reductoisomerase (Dxr)." J Biomol Screen **16**(3): 303-312.

Hwang, J., P. Li , W. R. Carroll , P. J. Pellechia , and K. D. Shimizu (2014). "Additivity of substituent effects in aromatic stacking interactions." J Am Chem Soc Just Accepted Manuscript.

Igarashi, M., N. Nakagawa, N. Doi, S. Hattori, H. Naganawa and M. Hamada (2003). "Caprazamycin B, a novel anti-tuberculosis antibiotic, from Streptomyces sp." J Antibiot **56**(6): 580-583.

Jaki, U.B., O. Zerbe, J. Heilmann and O. Sticher. "Two Novel Cyclic Peptides with Antifungal Activity from the Cyanobacterium Tolypothrix byssoidea (EAWAG 195)" *J. Nat. Prod.*, *64* (2), pp 154–158

Jean Kumar, V. U., O. Poyraz, S. Saxena, R. Schnell, P. Yogeeswari, G. Schneider and D. Sriram (2013). "Discovery of novel inhibitors targeting the Mycobacterium tuberculosis O-acetylserine sulfhydrylase (CysK1) using virtual high-throughput screening." Bioorg Med Chem Lett **23**(5): 1182-1186.

Kaufmann, S. H. (2010). "Future vaccination strategies against tuberculosis: thinking outside the box." Immunity **33**(4): 567-577.

Kaufmann, S. H. and S. K. Parida (2007). "Changing funding patterns in tuberculosis." Nat Med **13**(3): 299-303.

Kulanthaivel Palaniappan, V. V. (2000). Rufomycins and derivatives thereof useful as inhibitors of multi-drug resistance associated protein-1 (mrp-1). E. L. a. Company. **WO2000078795 A2**.

Kafatos, F. C., C. W. Jones and A. Efstratiadis (1979). "Determination of nucleic acid sequence homologies and relative concentrations by a dot hybridization procedure." Nucleic acids research **7**(6): 1541-1552.

Kanehisa, M., M. Araki, S. Goto, M. Hattori, M. Hirakawa, M. Itoh, T. Katayama, S. Kawashima, S. Okuda, T. Tokimatsu and Y. Yamanishi (2008). "KEGG for linking genomes to life and the environment." Nucleic acids research **36**(Database issue): D480-484.

Kar, N. P., D. Sikriwal, P. Rath, R. K. Choudhary and J. K. Batra (2008). "Mycobacterium tuberculosis ClpC1: characterization and role of the N-terminal domain in its function." FEBS J **275**(24): 6149-6158.

Kumar, K. S., P. S. Kumar and S. Vijayalakshmi (2011). "Anticancer studies of drug encapsulated polyethylene terephthalate-Co-polylactic acid nanocapsules." J Pharm Bioallied Sci **3**(2): 286-293.

Kwon, G. S., M. Naito, M. Yokoyama, T. Okano, Y. Sakurai and K. Kataoka (1995). "Physical entrapment of adriamycin in AB block copolymer micelles." Pharm Res **12**(2): 192-195.

Laatikainen, R., M. Tiainen, S.-P. Korhonen and M. Niemitz (2007). Computerized Analysis of High-resolution Solution-state Spectra. eMagRes, John Wiley & Sons, Ltd.

Lagesen, K., P. Hallin, E. A. Rodland, H. H. Staerfeldt, T. Rognes and D. W. Ussery (2007). "RNAmmer: consistent and rapid annotation of ribosomal RNA genes." Nucleic acids research **35**(9): 3100-3108.

Lamichhane, G., M. Zignol, N. J. Blades, D. E. Geiman, A. Dougherty, J. Grosset, K. W. Broman and W. R. Bishai (2003). "A postgenomic method for predicting essential genes at subsaturation levels of mutagenesis: application to Mycobacterium tuberculosis." Proc Natl Acad Sci U S A **100**(12): 7213-7218.

Lawrence, M. J. and G. D. Rees (2000). "Microemulsion-based media as novel drug delivery systems." Adv Drug Deliv Rev **45**(1): 89-121.

Le Garrec, D., S. Gori, L. Luo, D. Lessard, D. C. Smith, M. A. Yessine, M. Ranger and J. C. Leroux (2004). "Poly(N-vinylpyrrolidone)-block-poly(D,L-lactide) as a new polymeric solubilizer for hydrophobic anticancer drugs: in vitro and in vivo evaluation." J Control Release **99**(1): 83-101.

Lomenick, B., R. Hao, N. Jonai, R. M. Chin, M. Aghajan, S. Warburton, J. Wang, R. P. Wu, F. Gomez, J. A. Loo, J. A. Wohlschlegel, T. M. Vondriska, J. Pelletier, H. R. Herschman, J. Clardy, C. F. Clarke and J. Huang (2009). "Target identification using drug affinity responsive target stability (DARTS)." Proceedings of the National Academy of Sciences of the United States of America **106**(51): 21984-21989.

Lowe, T. M. and S. R. Eddy (1997). "tRNAscan-SE: a program for improved detection of transfer RNA genes in genomic sequence." Nucleic acids research **25**(5): 955-964.

Lucke, A., J. Tessmar, E. Schnell, G. Schmeer and A. Gopferich (2000). "Biodegradable poly(D,L-lactic acid)-poly(ethylene glycol)-monomethyl ether diblock copolymers: structures and surface properties relevant to their use as biomaterials." Biomaterials **21**(23): 2361-2370.

Lupas, A., J. M. Flanagan, T. Tamura and W. Baumeister (1997). "Self-compartmentalizing proteases." Trends Biochem Sci **22**(10): 399-404.

Maddry, J. A., S. Ananthan, R. C. Goldman, J. V. Hobrath, C. D. Kwong, C. Maddox, L. Rasmussen, R. C. Reynolds, J. A. Secrist, 3rd, M. I. Sosa, E. L. White and W. Zhang (2009). "Antituberculosis activity of the molecular libraries screening center network library." Tuberculosis (Edinb) **89**(5): 354-363.

Makarov, V., G. Manina, K. Mikusova, U. Mollmann, O. Ryabova, B. Saint-Joanis, N. Dhar, M. R. Pasca, S. Buroni, A. P. Lucarelli, A. Milano, E. De Rossi, M. Belanova, A. Bobovska, P. Dianiskova, J. Kordulakova, C. Sala, E. Fullam, P. Schneider, J. D. McKinney, P. Brodin, T. Christophe, S. Waddell, P. Butcher, J. Albrethsen, I. Rosenkrands, R. Brosch, V. Nandi, S. Bharath, S. Gaonkar, R. K. Shandil, V. Balasubramanian, T. Balganesh, S. Tyagi, J. Grosset, G. Riccardi and S. T. Cole (2009). "Benzothiazinones kill Mycobacterium tuberculosis by blocking arabinan synthesis." Science **324**(5928): 801-804.

Mangalindan, G. C., M. T. Talaue, L. J. Cruz, S. G. Franzblau, L. B. Adams, A. D. Richardson, C. M. Ireland and G. P. Concepcion (2000). "Agelasine F from a Philippine Agelas sp. sponge exhibits in vitro antituberculosis activity." Planta medica **66**(4): 364-365.

Manger, M., M. Scheck, H. Prinz, J. P. von Kries, T. Langer, K. Saxena, H. Schwalbe, A. Furstner, J. Rademann and H. Waldmann (2005). "Discovery of Mycobacterium tuberculosis protein tyrosine phosphatase A (MptpA) inhibitors based on natural products and a fragment-based approach." Chembiochem **6**(10): 1749-1753.

Matsumoto, M., H. Hashizume, T. Tomishige, M. Kawasaki, H. Tsubouchi, H. Sasaki, Y. Shimokawa and M. Komatsu (2006). "OPC-67683, a nitro-dihydro-imidazooxazole derivative with promising action against tuberculosis in vitro and in mice." PLoS Med **3**(11): e466.

Mitchison, D. A. (1985). "The action of antituberculosis drugs in short-course chemotherapy." Tubercle **66**(3): 219-225.

D.E. Minnikin, a., A.G. O'Donnella, b, M. Goodfellowb, G. Aldersonb, M. Athalyeb, A. Schaala, J.H. Parletta (1984). "An integrated procedure for the extraction of bacterial isoprenoid quinones and polar lipids." Journal of microbiological methods **2**(5): 233-241.

Mitchison, D. A. (1985). "The action of antituberculosis drugs in short-course chemotherapy." Tubercle **66**(3): 219-225.

Mitchison, D. A. (1985). "The action of antituberculosis drugs in short-course chemotherapy." Tubercle **66**(3): 219-225.

Napolitano, J. G., T. Godecke, M. F. Rodriguez-Brasco, B. U. Jaki, S. N. Chen, D. C. Lankin and G. F. Pauli (2012). "The tandem of full spin analysis and qHNMR for the quality control of botanicals exemplified with Ginkgo biloba." J Nat Prod **75**(2): 238-248.

Napolitano, D. C. Lankin, T. N. Graf, J. B. Friesen, S. N. Chen, J. B. McAlpine, N. H. Oberlies and G. F. Pauli (2013) " HiFSA fingerprinting applied to isomers with near-identical NMR spectra: the silybin/isosilybin case." J Org Chem. 78(7):2827-39.

NCCLS (1990). Methods for Dilution Antimicrobial Susceptibility Tests for Bacteria That Grow Aerobically. Villanova, PA, Clinical and Laboratory Standards Institute.

NCCLS (1991). Performance Standards for Antimicrobial Susceptibility Testing. Villanova, PA, Clinical and Laboratory Standards Institute.

Oerlemans, C., Bult, W., Bos, M., Storm, G., Nijsen J. F. W., and Hennink W. E. " Polymeric Micelles in Anticancer Therapy: Targeting, Imaging and Triggered Release." (2010) Pharm Res. **27**(12): 2569–2589.

Ottenhoff, T. H. (2009). "Overcoming the global crisis: "yes, we can", but also for TB ... ?" Eur J Immunol **39**(8): 2014-2020.

Ottenhoff, T. H., T. M. Doherty, J. T. van Dissel, P. Bang, K. Lingnau, I. Kromann and P. Andersen (2010). "First in humans: a new molecularly defined vaccine shows excellent safety and strong induction of long-lived Mycobacterium tuberculosis-specific Th1-cell like responses." Hum Vaccin **6**(12): 1007-1015.

Ottenhoff, T. H. and S. H. Kaufmann (2012). "Vaccines against tuberculosis: where are we and where do we need to go?" PLoS Pathog **8**(5): e1002607.

Parternership, S. T. (2013). "Working Group on New TB Drugs - Drug Pipeline." from http://www.newtbdrugs.org/pipeline.php.

Paternership, S. T. (2013). "Global TB Vaccine Pipeline." from http://www.stoptb.org/wg/new_vaccines/documents.asp.

Pauli, G. F., T. Godecke, B. U. Jaki and D. C. Lankin (2012). "Quantitative 1H NMR. Development and potential of an analytical method: an update." Journal of Natural Products **75**(4): 834-851.

Pauli, G. F., R. J. Casea, T. Inuia, Y. Wang, S. Cho, N. H. Fischerc, S. G. Franzblau (2005). " New perspectives on natural products in TB drug research" Life Sciences 78(5):pp 485–494.

Peer, D., J. M. Karp, S. Hong, O. C. Farokhzad, R. Margalit and R. Langer (2007). "Nanocarriers as an emerging platform for cancer therapy." Nat Nanotechnol **2**(12): 751-760.

Pethe K, Bifani P, Jang J, Kang S, Park S, Ahn S, Jiricek J, Jung J, Jeon HK, Cechetto J, Christophe T, Lee H, Kempf M, Jackson M, Lenaerts AJ, Pham H, Jones V, Seo MJ, Kim YM, Seo M, Seo JJ, Park D, Ko Y, Choi I, Kim R, Kim SY, Lim S, Yim SA, Nam J, Kang H, Kwon H, Oh CT, Cho Y, Jang Y, Kim J, Chua A, Tan BH, Nanjundappa MB, Rao SP, Barnes WS, Wintjens R, Walker JR, Alonso S, Lee S, Kim J, Oh S, Oh T, Nehrbass U, Han SJ, No Z, Lee J, Brodin P, Cho SN, Nam K, Kim J. (2013). " Discovery of Q203, a potent clinical candidate for the treatment of tuberculosis." Nat Med. 19(9):1157-60.

Pospiech, A. and B. Neumann (1995). "A versatile quick-prep of genomic DNA from gram-positive bacteria." Trends in genetics **11**(6): 217-218.

Protopopova, M., C. Hanrahan, B. Nikonenko, R. Samala, P. Chen, J. Gearhart, L. Einck and C. A. Nacy (2005). "Identification of a new antitubercular drug candidate, SQ109, from a combinatorial library of 1,2-ethylenediamines." J Antimicrob Chemother **56**(5): 968-974.

Qiu, Y. (2008). Developing Solid Oral Dosage Forms. US, Academic Press.

Raju, R. M., A. L. Goldberg and E. J. Rubin (2012). "Bacterial proteolytic complexes as therapeutic targets." Nat Rev Drug Discov **11**(10): 777-789.

Raju, R. M., M. Unnikrishnan, D. H. Rubin, V. Krishnamoorthy, O. Kandror, T. N. Akopian, A. L. Goldberg and E. J. Rubin (2012). "Mycobacterium tuberculosis ClpP1 and ClpP2 function together in protein degradation and are required for viability in vitro and during infection." PLoS Pathog **8**(2): e1002511.

Rausch, C., T. Weber, O. Kohlbacher, W. Wohlleben and D. H. Huson (2005). "Specificity prediction of adenylation domains in nonribosomal peptide synthetases (NRPS) using transductive support vector machines (TSVMs)." Nucleic Acids Res **33**(18): 5799-5808.

Rawls, K. A., C. Grundner and J. A. Ellman (2010). "Design and synthesis of nonpeptidic, small molecule inhibitors for the Mycobacterium tuberculosis protein tyrosine phosphatase PtpB." Org Biomol Chem **8**(18): 4066-4070.

Rawls, K. A., P. T. Lang, J. Takeuchi, S. Imamura, T. D. Baguley, C. Grundner, T. Alber and J. A. Ellman (2009). "Fragment-based discovery of selective inhibitors of the Mycobacterium tuberculosis protein tyrosine phosphatase PtpA." Bioorg Med Chem Lett **19**(24): 6851-6854.

Reddy, V. M., L. Einck and C. A. Nacy (2008). "In vitro antimycobacterial activities of capuramycin analogues." Antimicrob Agents Chemother **52**(2): 719-721.

Rengarajan, J., B. R. Bloom and E. J. Rubin (2005). "Genome-wide requirements for Mycobacterium tuberculosis adaptation and survival in macrophages." Proc Natl Acad Sci U S A **102**(23): 8327-8332.

Rottig, M., M. H. Medema, K. Blin, T. Weber, C. Rausch and O. Kohlbacher (2011). "NRPSpredictor2--a web server for predicting NRPS adenylation domain specificity." Nucleic Acids Res **39**(Web Server issue): W362-367.

Rottig, M., M. H. Medema, K. Blin, T. Weber, C. Rausch and O. Kohlbacher (2011). "NRPSpredictor2--a web server for predicting NRPS adenylation domain specificity." Nucleic acids research **39**(Web Server issue): W362-367.

Saitou, N. and M. Nei (1987). "The neighbor-joining method: a new method for reconstructing phylogenetic trees." Molecular biology and evolution **4**(4): 406-425.

Sasser, M. (1990). Bacterial Identification by Gas Chromatographic Analysis of Fatty Acids Methyl Esters (GC-FAME). MIDI technical note. M. t. note. Newark, MIDI Inc. **MIDI technical note 101**.

Schmitt, E. K., M. Riwanto, V. Sambandamurthy, S. Roggo, C. Miault, C. Zwingelstein, P. Krastel, C. Noble, D. Beer, S. P. Rao, M. Au, P. Niyomrattanakit, V. Lim, J. Zheng, D. Jeffery, K. Pethe and L. R. Camacho (2011). "The natural product cyclomarin kills Mycobacterium tuberculosis by targeting the ClpC1 subunit of the caseinolytic protease." Angewandte Chemie International Edition **50**(26): 5889-5891.

Schmitz, R. Y. and F. Skoog (1970). "The use of dimethylsulfoxide as a solvent in the tobacco bioassay for cytokinins." Plant Physiol **45**(4): 537-538.

Shirling, E. B. and D. Gottlieb (1966). "Methods for characterization of Streptomyces species." International Journal of Systematic and Evolutionary Microbiology **16**(3): 313-340.

Siegrist MS, Steigedal M, Ahmad R, Mehra A, Dragset MS, Schuster BM, Philips JA, Carr SA, Rubin EJ (2014). "Mycobacterial Esx-3 requires multiple components for iron acquisition." mBio **5:**e01073-01014.

Singh, S. B. and J. F. Barrett (2006). "Empirical antibacterial drug discovery--foundation in natural products." Biochem Pharmacol **71**(7): 1006-1015.

Singh, S. B., K. Young and L. Miesel (2011). "Screening strategies for discovery of antibacterial natural products." Expert Rev Anti Infect Ther **9**(8): 589-613.

Sivendran, S., V. Jones, D. Sun, Y. Wang, A. E. Grzegorzewicz, M. S. Scherman, A. D. Napper, J. A. McCammon, R. E. Lee, S. L. Diamond and M. McNeil (2010). "Identification of triazinoindol-benzimidazolones as nanomolar inhibitors of the Mycobacterium tuberculosis enzyme TDP-6-deoxy-d-xylo-4-hexopyranosid-4-ulose 3,5-epimerase (RmlC)." Bioorg Med Chem **18**(2): 896-908.

Soellner, M. B., K. A. Rawls, C. Grundner, T. Alber and J. A. Ellman (2007). "Fragment-based substrate activity screening method for the identification of potent inhibitors of the Mycobacterium tuberculosis phosphatase PtpB." J Am Chem Soc **129**(31): 9613-9615.

Stanley, S. A., S. S. Grant, T. Kawate, N. Iwase, M. Shimizu, C. Wivagg, M. Silvis, E. Kazyanskaya, J. Aquadro, A. Golas, M. Fitzgerald, H. Dai, L. Zhang and D. T. Hung (2012). "Identification of novel inhibitors of M. tuberculosis growth using whole cell based high-throughput screening." ACS Chem Biol **7**(8): 1377-1384.

Stansly, P. G. (1946). "The Presumptive Identification of Antibiotics." Science **103**(2674): 402-403.

Stapley, E. O. (1958). "Cross-resistance studies and antibiotic identification." Appl Microbiol **6**(6): 392-398.

Stover, C. K., P. Warrener, D. R. VanDevanter, D. R. Sherman, T. M. Arain, M. H. Langhorne, S. W. Anderson, J. A. Towell, Y. Yuan, D. N. McMurray, B. N. Kreiswirth, C. E. Barry and W. R. Baker (2000). "A small-molecule nitroimidazopyran drug candidate for the treatment of tuberculosis." Nature **405**(6789): 962-966.

Suzek, B. E., H. Huang, P. McGarvey, R. Mazumder and C. H. Wu (2007). "UniRef: comprehensive and non-redundant UniProt reference clusters." Bioinformatics **23**(10): 1282-1288.

Takahashi, Y., M. Igarashi, T. Miyake, H. Soutome, K. Ishikawa, Y. Komatsuki, Y. Koyama, N. Nakagawa, S. Hattori, K. Inoue, N. Doi and Y. Akamatsu (2013). "Novel semisynthetic antibiotics from caprazamycins A-G: caprazene derivatives and their antibacterial activity." J Antibiot **66**(3): 171-178.

Tamaoka, J. (1986). "Analysis of bacterial menaquinone mixtures by reverse-phase high-performance liquid chromatography." Methods in enzymology **123**: 251-256.

Tamura, K., J. Dudley, M. Nei and S. Kumar (2007). "MEGA4: Molecular Evolutionary Genetics Analysis (MEGA) software version 4.0." Molecular biology and evolution **24**(8): 1596-1599.

Tatusov, R. L., E. V. Koonin and D. J. Lipman (1997). "A genomic perspective on protein families." Science **278**(5338): 631-637.

Thompson, J. D., T. J. Gibson, F. Plewniak, F. Jeanmougin and D. G. Higgins (1997). "The CLUSTAL_X windows interface: flexible strategies for multiple sequence alignment aided by quality analysis tools." Nucleic acids research **25**(24): 4876-4882.

Torchilin, V. P. (2008). Multifunctional Pharmaceutical Nanocarriers.

Vasan, M., J. Neres, J. Williams, D. J. Wilson, A. M. Teitelbaum, R. P. Remmel and C. C. Aldrich (2010). "Inhibitors of the salicylate synthase (MbtI) from Mycobacterium tuberculosis discovered by high-throughput screening." ChemMedChem **5**(12): 2079-2087.

Vasudevan, D., S. P. Rao and C. G. Noble (2013). "Structural basis of mycobacterial inhibition by cyclomarin A." J Biol Chem **288**(43): 30883-30891.

Wang, J., Qie, Y., Liu, W. and Wang H. (2012) " Protective efficacy of a recombinant BCG secreting antigen 85B/Rv3425 fusion protein against Mycobacterium tuberculosis infection in mice." Hum Vaccin Immunother. 8(12): 1869–1874.

White, R.J. (2012) "The early history of antibiotic discovery: the emperism ruled" Antibiotic Discovery and Development

WHO. (2012). "Global tuberculosis control 2012."

WHO. http://www.who.int/immunization/research/development/tuberculosis/en/

Wilson, D. J., C. Shi, A. M. Teitelbaum, A. M. Gulick and C. C. Aldrich (2013). "Characterization of AusA: a dimodular nonribosomal peptide synthetase responsible for the production of aureusimine pyrazinones." Biochemistry **52**(5): 926-937.

Yamaguchi, H., S. Sato, S. Yoshida, K. Takada, M. Itoh, H. Seto and N. Otake (1986). "Capuramycin, a new nucleoside antibiotic. Taxonomy, fermentation, isolation and characterization." J Antibiot **39**(8): 1047-1053.

Yoon, T. M., J. W. Kim, J. G. Kim, W. G. Kim and J. W. Suh (2006). "Talosins A and B: new isoflavonol glycosides with potent antifungal activity from Kitasatospora kifunensis MJM341. I. Taxonomy, fermentation, isolation, and biological activities." The Journal of antibiotics **59**(10): 633-639.

Yu, A. Y. and W. A. Houry (2007). "ClpP: a distinctive family of cylindrical energy-dependent serine proteases." FEBS Lett **581**(19): 3749-3757.

Zhang, Y. (2011) "Drug Resistant and Persistent Tuberculosis: Mechanisms and Drug Development" Antibiotic Discovery and Development, pp 719-749

Zhou B, He Y, Zhang X, Xu J, Luo Y, Wang Y, Franzblau SG, Yang Z, Chan RJ, Liu Y, Zheng J, Zhang ZY. (2010). "Targeting mycobacterium protein tyrosine phosphatase B for antituberculosis agents." Proc Natl Acad Sci U S A **107:**4573-4578.

Zumla, A., P. Nahid and S. T. Cole (2013). "Advances in the development of new tuberculosis drugs and treatment regimens." Nat Rev Drug Discov **12**(5): 388-404.

APPENDICES

Appendix A. Author contributions*

Dr. Scott G. Franzblau supervised the project.

Dr. Joo-Won Suh's team at Myongji University collected and maintained actinomycete extract library; .they also identified and cultured strain MJM5123. Drs. Sang-Hyun Cho, Yuehong Wang, Wei Gao, Guido F. Pauli and Scott G. Franzblau designed and performed the in vitro high throughput screen, growth inhibition, and bactericidal experiments. Dr. Wei Gao, designed and performed purification experiments and determined structure of ecumicin, under the supervision of Drs. Guido F. Pauli and Brent J. Friesen. Crystallographic data of ecumicin was provided by Dr. Joo-Won Suh's group at Myongji University. Dr. Joo-Won Suh's group at Myongji University, Drs. Wei Gao and James B. McAlpine analyzed the ecumcin-synthesizing NRPS. Drs. Seungpyo Hong's team designed and prepared the micelle formulation. Dr. Wei Gao and analyzed the sample for in vivo (mouse) PK experiments. Drs. Wei Gao, Yuehong Wang and Scott G. Franzblau designed and performed in vivo (mouse) efficacy experiment; Drs. Wei Gao and Sang-Hyun Cho prepared ecumicin-resistant *M. tuberculosis* strains and isolated the genomic DNAs; Jeffery R. Anderson and Dr. Sang-Hyun Cho designed and performed IPTG-induced expression of *M. tuberculosis* clpC1 in *E. coli*; Surafel Mulugeta, Jeffery R. Anderson and Dr. Sang-Hyun Cho designed and performed DARTS experiment; Drs Alfred L. Goldberg, Tatos Akopian, and Olga Kandror (Harvard University) designed and performed biochemical experiment on ecumicin binding and activation of wild-type ClpC1.

* Authors are from University of Illinois at Chicago unless otherwise noted.

Appendix B. Composition of media used in generating Actinomycetes library.

<1> G.S.S. medium	**<2> Bennett's medium**	**<3> DYC medium**
Soluble starch 10g	Glucose 10g	Dextrine 25g
Glucose 20g	Yeast extract 1g	Dry yeast 12g
Soybean meal 25g	Bacto-peptone 2g	CSL 20g
Beef extract 1g	Beef extract 1g	NaBr 1g
Yeast extract 4g	D.I. Water 1L	$CoCl_2$ 1g
NaCl 2g	pH 7.2	D.I. Water 1L
K_2HPO_4 0.25g		pH 7.0
$CaCO_3$ 2g		
D.I. Water 1L		
pH 7.2		

Appendix C. Biological profile of initial hits.

ID	Media	Extraction	% inhib at 10 µl/ml (MABA)	MICs v.s. replicating *M. tuberculosis* in µl/ml (%, at 10 µl/ml)				VERO IC_{50}
				Rv	rKM	rRMP	rSM	
76	GSS	W	**91.82%**	**4.83**	85%	9.66	9.97	**> 10**
162	GSS	W	**95.35%**	**8.74**	87%	85%	76%	**> 10**
187	GSS	E	**95.31%**	**53%**	88%	55%	9.94	**> 10**
203	GSS	E	**94.85%**	**36%**	24%	78%	66%	**> 10**
212	GSS	E	**99.49%**	**21%**	0%	10%	16%	**> 10**
239	GSS	E	**93.73%**	**63%**	39%	9.81	77%	**> 10**
242	GSS	M	**91.53%**	**30%**	0%	0%	13%	**> 10**
302	BN	E	**99.20%**	**4.78**	9.77	89%	30%	**2.35**
352	GSS	E	**99.24%**	**8.87**	9.93	6.87	8.88	**> 10**
379	BN	E	**97.60%**	**8.82**	9.43	9.91	9.99	**> 10**
379	BN	W	**99.31%**	**2.30**	2.29	2.73	2.29	**7.51**
387	BN	W	**96.24%**	**8.89**	9.39	9.54	9.64	**> 10**
466	BN	E	**93.44%**	**31%**	9.98	48%	9.93	**> 10**
1080	BN	E	**99.27%**	**4.57**	8.35	9.46	9.61	**1.42**
1289	GSS	E	**94.07%**	**29%**	0%	17%	7%	**> 10**
1289	BN	M	**99.23%**	**4.66**	4.83	2.37	6.82	**> 10**
1300	GSS	E	**98.71%**	**9.09**	8.83	87%	84%	**1.04**
1310	GSS	E	**95.35%**	**80%**	88%	87%	8.65	**1.56**
1357	BN	E	**99.51%**	**4.85**	9.86	9.36	70%	**<0.625**
1357	BN	W	**99.16%**	**1.97**	2.50	2.43	4.57	**0.73**
1360	BN	M	**99.25%**	**4.16**	4.79	4.79	9.37	**0.75**
1372	BN	E	**99.26%**	**4.70**	4.88	4.94	89%	**0.73**
1372	GSS	E	**99.16%**	**4.90**	9.87	9.56	54%	**2.40**
1382	BN	M	**98.99%**	**4.64**	9.67	8.98	89%	**1.07**
1389	BN	E	**99.65%**	**4.51**	87%	9.53	40%	**1.05**
1389	BN	W	**99.40%**	**4.69**	9.84	9.42	88%	**1.59**
1393	BN	E	**99.45%**	**4.73**	4.95	9.36	82%	**1.41**
1393	BN	W	**99.39%**	**2.37**	3.55	4.61	9.09	**0.71**
1401	GSS	E	**99.33%**	**4.66**	4.88	4.46	4.68	**> 10**
1401	BN	W	**99.44%**	**1.19**	1.24	1.63	1.20	**6.62**
1430	BN	M	**99.12%**	**4.57**	6.40	4.79	4.77	**> 10**
1442	DSC	E	**98.72%**	**4.75**	7.82	5.11	8.83	**1.67**
1442	BN	M	**99.06%**	**2.37**	2.75	3.90	4.93	**0.68**
1442	GSS	W	**98.78%**	**1.20**	2.07	1.90	2.65	**< 0.625**
1483	GSS	E	**99.77%**	**2.37**	2.99	2.63	4.46	**0.72**

Appendix C (continued)

ID	Media	Extraction	% inhib at 10 µl/ml (MABA)	MICs v.s. replicating *M. tuberculosis* in µl/ml (%, at 10 µl/ml)				VERO IC_{50}
				Rv	rKM	rRMP	rSM	
1484	GSS	E	**99.38%**	**1.15**	1.67	1.24	2.20	**< 0.625**
1503	BN	E	**99.49%**	**2.42**	2.44	2.36	2.28	**6.64**
1503	BN	M	**99.60%**	**4.16**	3.99	2.48	3.47	**6.83**
1520	GSS	E	**99.30%**	**4.53**	4.96	4.82	9.42	**1.32**
1520	BN	M	**99.08%**	**0.60**	2.13	1.30	2.46	**< 0.625**
1522	BN	M	**99.38%**	**4.39**	4.83	4.76	4.86	**> 10**
1526	GSS	E	**99.18%**	**1.66**	2.35	2.16	2.36	**> 10**
1526	DSC	E	**99.24%**	**4.68**	9.70	9.58	9.97	**> 10**
1543	BN	E	**99.25%**	**1.20**	2.38	2.19	2.32	**> 10**
1543	GSS	E	**99.49%**	**2.24**	3.95	2.36	3.03	**> 10**
1543	BN	M	**94.78%**	**8.99**	87%	9.67	56%	**> 10**
1556	BN	E	**99.25%**	**1.19**	0%	0%	3.77	**> 10**
1556	GSS	E	**99.00%**	**4.53**	9.70	8.10	9.61	**> 10**
1556	BN	M	**99.29%**	**1.70**	2.29	9.65	2.35	**> 10**
1562	BN	E	**98.94%**	**8.23**	9.38	9.73	9.52	**3.86**
1562	GSS	E	**99.19%**	**4.53**	4.67	4.73	4.69	**< 0.625**
2479	BN	M	**97.48%**	**3.91**	4.46	4.73	2.19	**> 10**
2486	BN	E	**98.77%**	**4.78**	4.71	4.69	4.16	**> 10**
2486	GSS	E	**99.69%**	**5.00**	4.98	4.79	4.48	**> 10**
2490	GSS	E	**99.75%**	**6.28**	6.15	4.96	4.47	**> 10**
2513	BN	E	**99.42%**	**3.44**	1.02	4.13	3.31	**> 10**
2523	GSS	E	**99.21%**	**4.45**	2.97	4.50	2.49	**> 10**
2526	BN	E	**99.41%**	**1.44**	2.06	1.38	1.08	**> 10**
2526	GSS	E	**98.15%**	**8.70**	7.04	7.56	5.47	**> 10**
2526	BN	M	**99.33%**	**1.66**	1.58	1.23	1.11	**6.323**
2530	BN	M	**99.28%**	**4.47**	2.42	4.59	2.39	**> 10**
2558	GSS	E	**99.10%**	**1.22**	1.23	2.01	2.31	**0.628**
2581	GSS	E	**107.14%**	**4%**	29%	10%	17%	**> 10**
2582	BN	E	**93.25%**	**1.98**	**0.91**	3.12	2.43	**< 0.625**
2612	BN	E	**91.43%**	**1.72**	1.57	3.22	3.85	**0.709**
3806	GSS	E	**99.28%**	**2.33**	4.98	4.56	4.95	**1.297**
3806	GSS	M	**97.78%**	**4.74**	7.83	5.55	9.89	**1.561**
3931	DYC	W	**107.70%**	**36%**	0%	13%	25%	**> 10**
4118	DYC	E	**98.19%**	**2.26**	4.30	7.89	1.73	**> 10**

Appendix C (continued)

ID	Media	Extraction	% inhib at 10 µl/ml (MABA)	MICs v.s. replicating *M. tuberculosis* in µl/ml (%, at 10 µl/ml)				VERO IC_{50}
				Rv	rKM	rRMP	rSM	
4135	DYC	E	**95.06%**	**3.70**	4.93	8.87	2.27	**> 10**
4138	GSS	E	**96.50%**	**1.80**	**0.88**	3.93	3.83	**< 0.625**
4139	DYC	E	**97.53%**	**2.40**	7.20	87%	9.95	**> 10**
4149	BN	E	**98.25%**	**1.72**	**0.58**	2.51	3.63	**< 0.625**
4178	BN	E	**91.72%**	**4.35**	2.14	4.60	4.64	**6.385**
4259	BN	E	**98.67%**	**4.50**	5.53	9.79	78%	**> 10**
4259	DYC	E	**97.27%**	**4.78**	9.95	83%	9.45	**> 10**
4263	GSS	E	**99.29%**	**2.37**	3.07	5.80	8.56	**> 10**
4263	GSS	W	**97.70%**	**4.82**	9.69	88%	9.57	**> 10**
4295	BN	M	**99.28%**	**4.73**	4.59	4.78	7.86	**1.406**
4296	GSS	E	**91.82%**	**6.88**	9.53	9.41	85%	**2.283**
4296	BN	M	**99.15%**	**1.09**	**0.77**	1.20	1.53	**< 0.625**
4296	GSS	M	**99.27%**	**2.34**	3.73	4.53	4.73	**0.913**
4296	DYC	M	**98.64%**	**4.75**	7.51	4.80	8.67	**1.612**
4302	GSS	M	**98.91%**	**4.76**	4.84	4.90	4.44	**> 10**
4302	BN	M	**99.44%**	**1.94**	1.14	2.27	1.34	**5.409**
4318	GSS	E	**99.63%**	**4.84**	6.64	7.87	4.75	**> 10**
4318	BN	M	**99.50%**	**2.48**	3.32	3.44	2.39	**7.285**
4318	GSS	M	**99.05%**	**2.38**	2.32	3.90	2.18	**9.969**
4319	GSS	E	**99.43%**	**4.40**	4.52	4.67	4.05	**> 10**
4320	BN	E	**99.68%**	**4.70**	4.82	4.68	4.50	**4.982**
4325	GSS	E	**99.19%**	**4.68**	4.78	4.89	3.61	**> 10**
4413	GSS	E	**99.77%**	**4.18**	3.54	4.49	3.67	**> 10**
4413	BN	E	**99.43%**	**4.87**	4.90	8.30	5.20	**> 10**
4413	BN	M	**98.27%**	**2.49**	2.52	4.36	2.24	**> 10**
4414	GSS	E	**97.75%**	**7.58**	6.86	9.21	6.02	**> 10**
4414	BN	M	**95.69%**	**7.36**	9.61	9.16	6.86	**> 10**
4424	GSS	E	**91.16%**	**8.14**	9.43	9.29	8.22	**> 10**
4424	BN	M	**99.60%**	**4.59**	4.68	4.73	4.60	**> 10**
4426	GSS	W	**97.34%**	**6.69**	35%	7.86	5.00	**> 10**
4447	GSS	E	**99.48%**	**4.91**	**0.20**	4.79	4.82	**7.366**
4481	GSS	E	**99.06%**	**4.75**	49%	8.41	8.31	**1.724**
4510	BN	E	**99.88%**	**8.50**	2.36	9.43	7.83	**> 10**
4510	GSS	E	**99.28%**	**8.55**	88%	6.15	9.86	**> 10**

Appendix C (continued)

ID	Media	Extraction	% inhib at 10 µl/ml (MABA)	MICs v.s. replicating *M. tuberculosis* in µl/ml (%, at 10 µl/ml)				VERO IC_{50}
				Rv	rKM	rRMP	rSM	
4510	BN	M	**98.99%**	**4.75**	1.09	4.70	4.16	**> 10**
4537	GSS	W	**95.99%**	**8.58**	9.23	8.16	8.49	**> 10**
4611	BN	E	**98.18%**	**1.84**	**0.75**	3.61	3.60	**< 0.625**
4642	GSS	W	**95.40%**	**4.36**	88%	5.92	15%	**> 10**
4653	BN	M	**96.80%**	**3.81**	4.08	4.88	3.29	**> 10**
4715	GSS	E	**95.10%**	**5.43**	4.34	4.67	4.61	**> 10**
4719	BN	E	**99.58%**	**4.66**	4.51	4.82	4.59	**> 10**
4721	GSS	E	**99.12%**	**6.69**	5.88	8.01	4.92	**> 10**
4721	BN	E	**98.44%**	**2.28**	2.45	3.50	2.27	**7.034**
4721	BN	M	**98.45%**	**4.94**	4.73	6.81	4.59	**> 10**
4777	GSS	M	**99.04%**	**6.42**	4.85	5.38	4.89	**> 10**
4789	BN	E	**99.84%**	**4.79**	4.43	4.79	4.16	**> 10**
4789	GSS	E	**99.38%**	**4.83**	4.64	4.93	4.85	**> 10**
4789	BN	M	**98.68%**	**9.52**	9.31	9.30	8.13	**> 10**
4796	GSS	E	**99.51%**	**4.77**	4.60	4.80	4.34	**> 10**
4824	GSS	E	**99.56%**	**4.85**	4.58	4.79	4.42	**> 10**
4824	BN	E	**95.07%**	**8.83**	7.93	8.30	4.85	**6.451**
4824	BN	M	**98.66%**	**2.34**	1.69	2.33	1.45	**> 10**
4828	GSS	E	**95.55%**	**9.14**	4.79	9.10	7.70	**> 10**
4887	BN	E	**99.65%**	**4.83**	5.94	4.82	4.66	**> 10**
4887	BN	M	**99.43%**	**2.22**	2.26	2.39	2.24	**9.429**
4899	GSS	E	**98.87%**	**4.43**	4.36	4.82	4.56	**1.022**
4901	BN	E	**98.53%**	**4.31**	2.33	3.15	3.16	**> 10**
4928	GSS	E	**93.44%**	**6.22**	8.41	8.67	7.63	**> 10**
4955	GSS	M	**99.87%**	**4.73**	4.60	5.72	4.42	**> 10**
4955	BN	M	**99.56%**	**1.14**	**0.75**	1.08	**0.94**	**3.456**
4977	BN	E	**99.49%**	**4.12**	4.26	4.01	2.81	**> 10**
4977	GSS	E	**93.33%**	**6.85**	7.63	4.85	3.21	**> 10**
4977	BN	M	**99.42%**	**2.42**	2.45	2.32	2.01	**> 10**
4999	GSS	E	**90.42%**	**18%**	8%	31%	4%	**> 10**
5007	GSS	E	**90.58%**	**32%**	3%	18%	7%	**> 10**
5007	GSS	M	**90.00%**	**24%**	26%	31%	5%	**> 10**
5123	GSS	M	**99.80%**	**0.51**	**0.31**	**0.89**	**0.84**	**> 10**
5132	BN	E	**92.56%**	**4.53**	4.82	4.19	4.45	**> 10**

Appendix C (continued)

ID	Media	Extraction	% inhib at 10 µl/ml (MABA)	MICs v.s. replicating *M. tuberculosis* in µl/ml (%, at 10 µl/ml)				VERO IC_{50}
				Rv	rKM	rRMP	rSM	
5154	BN	E	**98.97%**	**8.75**	4.98	8.44	9.50	**5.007**
5154	GSS	M	**99.51%**	**3.53**	1.32	3.20	4.36	**1.396**
5159	GSS	W	**97.08%**	**4.65**	4.86	7.97	4.81	**> 10**
5176	BN	E	**92.05%**	**7.37**	4.66	7.08	8.95	**6.519**
5188	GSS	E	**106.70%**	**81%**	49%	0%	29%	**> 10**
5204	GSS	E	**99.44%**	**1.17**	**0.20**	2.00	2.39	**< 0.625**
5204	DYC	M	**97.96%**	**1.49**	1.09	2.37	2.55	**< 0.625**
5222	GSS	M	**92.89%**	**7.75**	2.36	5.67	6.34	**1.891**
5249	GSS	E	**97.88%**	**8.31**	9.23	67%	8.59	**> 10**
5249	BN	E	**93.85%**	**9.48**	88%	24%	87%	**> 10**
5287	GSS	M	**93.67%**	**4.96**	3.60	4.34	4.32	**> 10**
5317	BN	E	**98.76%**	**1.51**	1.19	1.25	1.21	**4.100**
5317	BN	M	**93.98%**	**5.65**	4.22	4.83	4.75	**> 10**
5345	GSS	M	**99.33%**	**4.79**	4.78	4.74	4.45	**> 10**
5384	BN	E	**94.03%**	**6.72**	4.69	4.68	6.11	**> 10**
5384	GSS	M	**99.87%**	**4.38**	2.31	4.65	4.54	**1.737**
5424	BN	M	**99.87%**	**2.28**	2.40	2.34	2.16	**6.700**
5453	BN	M	**96.81%**	**3.84**	2.49	4.74	4.25	**1.621**
5456	GSS	M	**94.14%**	**6.32**	2.46	7.23	4.82	**2.812**
5492	GSS	E	**90.10%**	**7.30**	4.86	9.71	9.89	**7.231**
5509	BN	M	**96.99%**	**4.35**	2.30	4.89	4.48	**1.640**
5560	GSS	E	**99.12%**	**2.28**	2.29	3.66	1.90	**> 10**
5560	BN	E	**90.28%**	**7.00**	8.64	8.59	7.64	**> 10**
5560	BN	M	**97.42%**	**4.54**	4.27	4.02	4.94	**> 10**
5585	DYC	M	**93.74%**	**7.53**	4.11	8.07	6.18	**3.081**
5586	BN	M	**99.33%**	**4.57**	3.51	3.67	4.58	**3.448**
5609	BN	E	**91.72%**	**8.08**	5.19	6.99	6.01	**> 10**
5609	BN	M	**98.13%**	**7.11**	4.79	4.96	7.00	**> 10**
5618	BN	M	**91.72%**	**4.98**	4.34	4.69	8.10	**> 10**
5633	GSS	E	**91.37%**	**3.87**	**0.84**	4.66	4.10	**3.181**
5637	GSS	E	**95.22%**	**4.52**	4.08	4.51	4.43	**> 10**
5692	DYC	W	**106.09%**	**40%**	13%	1%	35%	**> 10**
5697	DYC	M	**97.59%**	**4.97**	4.94	7.64	4.99	**> 10**
5700	DYC	E	**91.39%**	**52%**	15%	37%	27%	**> 10**

Appendix C (continued)

ID	Media	Extraction	% inhib at 10 µl/ml (MABA)	MICs v.s. replicating *M. tuberculosis* in µl/ml (%, at 10 µl/ml)				VERO IC_{50}
				Rv	rKM	rRMP	rSM	
5716	DYC	E	**97.65%**	**0%**	21%	4%	24%	**> 10**
5738	GSS	W	**92.12%**	**48%**	47%	3%	26%	**> 10**
5745	GSS	M	**98.97%**	**6.08**	3.60	4.61	4.62	**> 10**
5763	GSS	M	**94.60%**	**6.71**	4.18	4.37	4.67	**> 10**
5763	BN	M	**99.47%**	**4.00**	1.24	3.06	2.95	**1.826**
5786	BN	E	**99.46%**	**1.03**	3.70	4.42	4.03	**3.748**
5786	BN	M	**99.55%**	**3.41**	2.82	4.18	2.86	**9.138**
5787	DYC	W	**94.10%**	**4.44**	33%	4.30	5.42	**> 10**
5893	GSS	M	**94.49%**	**8.96**	7.77	6.32	7.53	**> 10**
5893	GSS	W	**97.11%**	**8.13**	7.25	7.14	7.63	**> 10**
5960	DYC	E	**90.13%**	**2.20**	**0.63**	2.40	3.59	**> 10**
6005	GSS	M	**91.65%**	**6.61**	8.27	5.05	4.90	**> 10**
6083	DYC	E	**96.43%**	**7.37**	4.17	4.90	7.03	**> 10**
6089	BN	E	**99.10%**	**4.01**	2.43	2.38	4.50	**8.725**
6089	BN	M	**96.88%**	**5.64**	2.35	4.44	8.88	**> 10**
6171	GSS	E	**97.00%**	**6.71**	4.43	7.74	8.92	**8.253**
6174	GSS	E	**107.10%**	**38%**	36%	21%	17%	**> 10**
6275	GSS	E	**99.34%**	**8.54**	5.35	8.14	8.01	**> 10**
6342	GSS	E	**93.00%**	**7.63**	3.81	4.88	4.47	**> 10**
6342	GSS	M	**98.13%**	**4.32**	2.19	3.99	4.46	**4.123**
6392	GSS	E	**92.92%**	**4.31**	**0.50**	2.39	3.31	**0.767**
6477	GSS	M	**97.02%**	**8.37**	6.14	6.89	9.55	**> 10**
6477	DYC	W	**98.95%**	**2.57**	2.36	3.34	4.81	**> 10**
6477	BN	W	**98.11%**	**4.48**	3.60	4.15	7.57	**> 10**
6497	BN	E	**96.50%**	**9.31**	8.83	9.25	74%	**2.074**
6497	GSS	M	**94.21%**	**9.44**	9.18	9.40	53%	**0.793**
6497	BN	M	**100.18%**	**2.34**	2.43	2.43	4.91	**< 0.625**
6615	GSS	W	**94.24%**	**4.84**	79%	7.81	2.19	**> 10**
6637	GSS	E	**97.37%**	**8.14**	6.15	5.07	7.53	**> 10**
6646	DYC	M	**91.07%**	**5%**	0%	0%	0%	**> 10**
6648	DYC	W	**97.02%**	**85%**	9.90	85%	69%	**> 10**
6656	GSS	E	**98.78%**	**4.68**	3.78	3.48	4.59	**> 10**
6656	GSS	M	**99.55%**	**4.12**	2.38	2.37	4.07	**1.551**
6664	GSS	M	**95.12%**	**9.54**	4.27	8.85	84%	**0.768**

Appendix C (continued)

ID	Media	Extraction	% inhib at 10 µl/ml (MABA)	MICs v.s. replicating *M. tuberculosis* in µl/ml (%, at 10 µl/ml)				VERO IC_{50}
				Rv	rKM	rRMP	rSM	
6676	DYC	M	**98.01%**	**7.14**	2.45	5.87	9.38	**0.795**
6676	BN	M	**91.67%**	**9.20**	2.47	6.58	9.42	**6.220**
6765	GSS	W	**95.48%**	**8.80**	7.60	8.24	89%	**> 10**
6815	GSS	E	**90.92%**	**9.81**	9.59	9.47	9.52	**> 10**
6831	BN	E	**99.02%**	**2.43**	2.46	4.62	5.79	**0.755**
6831	GSS	E	**98.39%**	**2.19**	2.12	2.35	4.53	**< 0.625**
6831	BN	M	**99.01%**	**0.60**	**0.61**	**0.93**	1.24	**< 0.625**
6833	GSS	M	**97.61%**	**3.68**	9.20	3.22	0%	**> 10**
6833	DYC	W	**99.46%**	**5.45**	9.48	4.33	55%	**2.487**
6833	GSS	W	**98.37%**	**1.51**	3.60	1.16	0%	**> 10**
6857	GSS	M	**97.31%**	**4.30**	8.14	2.48	60%	**> 10**
6857	GSS	W	**98.34%**	**1.93**	4.49	2.02	7.09	**> 10**
6857	DYC	W	**97.45%**	**5.90**	87%	4.68	9.99	**> 10**
6872	DYC	W	**98.89%**	**4.62**	9.80	4.22	9.13	**> 10**
6886	BN	E	**99.04%**	**8.50**	7.71	4.79	9.39	**> 10**
6886	BN	M	**99.37%**	**4.63**	4.59	4.41	4.74	**> 10**
6890	BN	E	**98.80%**	**2.17**	2.36	2.27	2.34	**1.179**
6890	BN	M	**93.48%**	**2.17**	2.09	1.24	2.19	**1.171**
6895	GSS	W	**98.30%**	**7.14**	8.68	8.17	83%	**> 10**
6913	GSS	E	**97.91%**	**4.39**	1.53	8.98	6.76	**> 10**
6913	BN	E	**99.19%**	**4.55**	7.35	9.75	8.38	**> 10**
6913	GSS	W	**98.32%**	**1.23**	**Redo!**	3.49	8.63	**> 10**
7035	DYC	W	**95.33%**	**8.43**	41%	5.71	8.41	**> 10**
7049	GSS	E	**99.76%**	**8.99**	9.00	4.84	8.63	**> 10**
7049	BN	M	**99.74%**	**0.85**	**0.60**	**0.60**	**0.62**	**5.540**
7483	BN	E	**99.82%**	**1.55**	2.25	2.27	2.26	> 10
7483	BN	M	**99.70%**	**1.23**	2.12	1.97	1.24	**8.28**
7630	DYC	E	**93.32%**	**9.91**	9.65	39%	9.43	> 10
7739	GSS	E	**91.34%**	**6.57**	4.77	87%	8.29	**3.69**
7739	BN	E	**95.79%**	**4.95**	4.63	6.64	6.19	**4.71**
7767	GSS	E	**92.81%**	**8.33**	**0.31**	4.20	2.76	**2.03**
7924	GSS	W	**92.13%**	**51%**	8.71	5.69	4.50	> 10
7933	BN	M	**92.65%**	**64%**	8.39	9.65	67%	> 10
8016	GSS	E	**99.27%**	**4.70**	3.80	8.32	4.64	> 10

Appendix C (continued)

ID	Media	Extraction	% inhib at 10 µl/ml (MABA)	MICs v.s. replicating *M. tuberculosis* in µl/ml (%, at 10 µl/ml)				VERO IC_{50}
				Rv	rKM	rRMP	rSM	
8088	BN	M	**99.41%**	**4.73**	2.35	4.38	89%	> 10
8106	DYC	W	**99.01%**	**8.14**	2.42	**1.00**	2.26	> 10
8117	DYC	W	**97.94%**	**80%**	9.80	4.92	5.06	> 10
8124	GSS	E	**99.97%**	**4.72**	9.97	8.54	9.60	**1.26**
8178	GSS	E	**97.32%**	**4.36**	**0.31**	3.31	2.49	**0.95**
8252	BN	E	**100.13%**	**2.41**	3.64	4.78	8.19	**< 0.625**
8252	BN	M	**100.08%**	**4.34**	4.66	4.69	9.20	**< 0.625**
8412	GSS	E	**98.44%**	**2.86**	**0.30**	2.03	**0.58**	> 10
8427	GSS	E	**99.48%**	**4.76**	4.94	4.77	4.88	> 10
8427	BN	M	**99.41%**	**2.92**	2.60	2.40	4.02	> 10
8429	BN	M	**97.52%**	**0.51**	**0.47**	**0.56**	**0.58**	**2.96**
8454	GSS	E	**95.45%**	**6.97**	**0.51**	3.60	3.86	**0.92**
8490	GSS	E	**90.32%**	**21%**	9.52	9.23	8.91	> 10
8498	BN	M	**97.71%**	**4.77**	4.89	4.72	4.90	> 10
8511	GSS	E	**99.33%**	**4.92**	8.40	4.87	8.59	> 10
8533	GSS	E	**93.68%**	**35%**	8.26	88%	87%	> 10
8583	GSS	M	**99.24%**	**52%**	6.10	4.97	0%	> 10
8583	GSS	W	**99.35%**	**9.42**	4.78	3.67	0%	> 10
8602	GSS	E	**99.62%**	**4.72**	7.36	9.63	75%	**1.20**
8602	BN	E	**99.09%**	**4.88**	9.60	9.78	71%	**2.09**
8602	BN	M	**99.30%**	**1.19**	1.21	1.24	4.59	**< 0.625**
8699	GSS	W	**95.93%**	**43%**	86%	8.60	19%	> 10
8817	GSS	E	**99.55%**	**3.74**	4.48	4.56	4.63	> 10
8880	BN	E	**92.22%**	**86%**	9.68	9.97	32%	**8.40**
8880	DYC	M	**99.49%**	**3.90**	3.64	2.15	4.84	> 10
8880	BN	M	**99.39%**	**4.68**	3.56	2.35	4.71	> 10
8880	GSS	M	**98.46%**	**54%**	9.91	9.33	21%	> 10
8915	BN	E	**94.86%**	**9.53**	85%	9.88	86%	**8.83**
8915	BN	M	**99.25%**	**2.37**	3.74	3.48	3.87	> 10
8938	DYC	W	**107.81%**	**34%**	25%	10%	0%	**8.47**
8976	GSS	E	**98.84%**	**4.66**	4.91	4.86	4.76	> 10
8976	BN	E	**98.72%**	**4.84**	4.95	5.81	8.91	> 10
9023	GSS	E	**99.40%**	**7.78**	4.92	4.36	7.61	**3.44**
9023	DYC	E	**99.39%**	**6.21**	4.89	4.93	9.24	> 10

Appendix C (continued)

ID	Media	Extraction	% inhib at 10 µl/ml (MABA)	MICs v.s. replicating *M. tuberculosis* in µl/ml (%, at 10 µl/ml)				VERO IC_{50}
				Rv	rKM	rRMP	rSM	
9023	GSS	M	**99.40%**	**9.15**	7.51	4.74	9.11	**1.45**
9023	BN	M	**99.40%**	**1.96**	1.72	1.15	2.10	**5.13**
9027	BN	E	**99.11%**	**4.71**	4.95	4.85	4.79	**1.11**
9027	BN	M	**99.35%**	**1.17**	1.21	1.21	1.20	**3.77**
9030	GSS	E	**97.39%**	**65%**	61%	9.96	29%	> 10
9166	BN	M	**99.80%**	**0.59**	**0.62**	**0.60**	**0.92**	**3.23**
9257	DYC	W	**93.25%**	**60%**	9.92	6.73	5%	> 10
9293	BN	M	**99.54%**	**20%**	10%	3%	0%	> 10
9345	GSS	W	**97.35%**	**63%**	9.54	4.70	12%	> 10
9346	BN	E	**94.94%**	**70%**	68%	9.86	37%	**2.31**
9346	GSS	E	**100.22%**	**4.72**	4.92	4.82	4.78	> 10
9346	BN	M	**99.53%**	**9.17**	8.88	6.52	9.53	> 10
9364	GSS	E	**99.89%**	**9.20**	9.22	7.79	80%	> 10
9364	BN	M	**98.04%**	**9.84**	86%	9.56	68%	> 10
9407	GSS	E	**91.64%**	**8.18**	1.22	4.43	3.67	**1.86**
9421	DYC	W	**95.35%**	**58%**	8.43	5.42	3%	> 10
9422	GSS	W	**92.99%**	**73%**	9.65	3.11	11%	> 10
9431	GSS	E	**94.22%**	**6.77**	**0.61**	3.51	2.32	**0.58**
9431	DYC	E	**91.99%**	**7.75**	**0.57**	3.85	3.33	**0.98**
9459	GSS	W	**98.29%**	**81%**	5.88	2.94	28%	> 10
9469	DYC	E	**97.73%**	**3.68**	2.39	7.68	3.10	> 10
9469	GSS	E	**99.40%**	**5.68**	4.63	9.57	4.63	> 10
9469	DYC	M	**95.19%**	**9.41**	9.16	71%	8.95	> 10
9469	DYC	W	**96.88%**	**4.77**	4.82	89%	4.69	> 10
9538	GSS	E	**93.92%**	**3.19**	4.00	4.28	3.24	**> 10**
9564	GSS	E	**99.40%**	**4.33**	4.81	8.76	5.72	**> 10**
9564	BN	E	**97.70%**	**8.92**	9.65	83%	9.69	**> 10**
9580	BN	E	**99.33%**	**4.78**	4.74	4.76	4.76	**> 10**
9580	BN	M	**99.34%**	**1.16**	**0.80**	1.08	1.17	**0.896**
9598	GSS	E	**99.17%**	**7.38**	4.95	4.78	8.21	**> 10**
9615	BN	E	**100.00%**	**2.91**	**0.87**	2.05	2.24	**0.653**
9615	GSS	E	**99.45%**	**4.71**	4.16	4.53	4.59	**0.899**
9615	DYC	E	**99.46%**	**4.46**	1.83	3.92	4.47	**2.751**
9615	GSS	M	**98.11%**	**9.22**	7.81	8.57	8.96	**1.209**

Appendix C (continued)

ID	Media	Extraction	% inhib at 10 µl/ml (MABA)	MICs v.s. replicating *M. tuberculosis* in µl/ml (%, at 10 µl/ml)				VERO IC_{50}
				Rv	rKM	rRMP	rSM	
9662	BN	M	**99.97%**	**9.42**	7.15	7.74	8.71	**> 10**
/9676	GSS	E	**99.65%**	**4.66**	4.64	4.68	8.39	**1.229**
9676	BN	M	**98.77%**	**1.21**	1.17	1.19	2.34	**< 0.625**
9676	GSS	W	**98.82%**	**9.03**	7.85	9.25	9.79	**1.987**
9739	DYC	E	**93.95%**	**4.79**	**0.52**	2.42	3.54	**4.658**
9752	GSS	E	**99.23%**	**4.79**	4.90	4.77	4.98	**4.212**
9752	BN	E	**99.07%**	**8.58**	8.29	8.89	9.30	**> 10**
9752	BN	M	**99.52%**	**4.62**	4.25	4.60	4.57	**> 10**
9798	BN	W	**90.88%**	**32%**	7%	22%	0%	**> 10**

Appendix D. Biological profile of priority group 1-4.

Priority group	ID	Species	Media	Frac.	% inhib. at 10µl/ml (MABA)	MICs vs replicating *M. tuberculosis* (µl/ml)					IC_{50} (µl/ml)			MIC (µl/ml) vs				Activity vs non-replicating *M. tuberculosis*	
						Rv	rKM	rRMP	rSM	rCS	1	2	3	*E.coli*	*S. aureus*	*C. albicans*	*M. smeg*	% inhib at 10 µl/ml	MIC (µl/ml)
1	5123	*Nomomuraea sp.*	GSS	M	99.8%	0.51	0.31	0.89	0.84	2.49	> 10	> 20	> 40	0%	0%	64%	0%	17%	48%
1	7483	*Streptomyces sp.*	BN	E	99.8%	1.55	2.25	2.27	2.26	4.68	> 10	> 20	> 40	17%	4.34	8.03	0%	101%	0.48
1	8412	*Streptomyces atratus*	GSS	E	98.4%	2.86	0.30	2.03	0.58	0.25	> 10	> 20	> 40	0%	12%	0%	2.3	22%	55%
2	1526	*Streptomyces sp.*	GSS	E	99.2%	1.66	2.35	2.16	2.36	89%	> 10	> 20	> 40	23%	3.71	86%	0%	100%	1.68
2	1543	*Streptomyces sp.*	BN	E	99.2%	1.20	2.38	2.19	2.32	1.22	> 10	> 20	28.2	0%	2.94	7.22	0%	101%	0.11
2	2526	*Streptomyces sp.*	BN	E	99.4%	1.44	2.06	1.38	1.08	1.15	> 10	> 20	29.9	12%	1.78	4.27	0%	99%	0.08
2	4824	*Streptomyces sp.*	BN	M	98.7%	2.34	1.69	2.33	1.45	1.48	> 10	> 20	29.2	22%	2.01	4.26	56%	100%	4.23
2	4977	*Pending*	BN	M	99.4%	2.42	2.45	2.32	2.01	2.33	> 10	> 20	> 40	22%	2.14	4.84	44%	100%	0.04
2	5560	*Pending*	GSS	E	99.1%	2.28	2.29	3.66	1.90	3.74	> 10	16.0	> 40	0%	0.46	7.02	59%	99%	0.23
3	1401	*Streptomyces sp.*	GSS	E	99.3%	4.66	4.88	4.46	4.68	4.30	> 10		> 40	13%	4.48	65%	16%	101%	0.30
3	4302	*Streptomyces praecox*	GSS	M	98.9%	4.76	4.84	4.90	4.44	4.77	> 10		> 40	26%	8.02	4.97	11%	98%	0.45
3	4413	*Streptomyces sp.*	BN	M	98.3%	2.49	2.52	4.36	2.24	2.50	> 10	13.40	> 40	19%	3.02	85%	19%	101%	30%
3	4721	*Strep. floridae* or *puniceus*	BN	M	98.4%	4.94	4.73	6.81	4.59	4.66	> 10	> 20	> 40	15%	4.22	22%	16%	101%	8.85
3	4887	*Streptomyces sp.*	BN	E	99.6%	4.83	5.94	4.82	4.66	4.74	> 10		> 40	10%	4.82	6%	6%	101%	0%
3	5132	*Strep. Cellulosae* or *cyanews*	BN	E	92.6%	4.53	4.82	4.19	4.45	21%	> 10	> 10	> 40	1%	39%	0%	11%	58%	7.58
3	5960	*Streptomyces sp. 3490*	DYC	E	90.1%	2.20	0.63	2.40	3.59	0.96	> 10	<0.01	3.2	13%	0.22	64%	12%	14%	0.25
3	6477	*Pending*	DYC	W	98.9%	2.57	2.36	3.34	4.81	4.80	> 10	> 10	> 40	2%	35%	73%	87%	101%	0.24
3	6833	*Pending*	GSS	W	98.4%	1.51	3.60	1.16	0%	0%	> 10	>20	> 40	0%	26%	88%	24%	101%	0.15
3	7049	*Streptomyces sp.*	BN	M	99.7%	0.85	0.60	0.60	0.62	0.57	5.5		9.4	14%	0.90	1.88	77%	100%	0.58
3	8106	*Streptomyces sp.*	DYC	W	99.0%	8.14	2.42	1.00	2.26	2.92	> 10	>20	> 40	4.75	4.42	4.91	2.38	83%	0.26
3	8427	*Streptomyces BR57* or *N0077*	BN	M	99.4%	2.92	2.60	2.40	4.02	2.35	> 10		> 40	4%	3.17	88%	17%	100%	0.46

Appendix D (continued)

Priority group	ID	Species	Media	Frac.	% inhib. at 10µl/ml (MABA)	MICs vs replicating *M. tuberculosis* (µl/ml)					IC_{50} (µl/ml)			MIC (µl/ml) vs				Activity vs non-replicating *M. tuberculosis*	
						Rv	rKM	rRMP	rSM	rCS	1	2	3	*E.coli*	*S. aureus*	*C. albicans*	*M. smeg*	% inhib at 10 µl/ml	MIC (µl/ml)
3	8915	*Streptomyces praecox*	BN	M	99.2%	2.37	3.74	3.48	3.87	3.73	> 10	>10	> 40	2%	4.20	87%	8%	100%	0%
4	352		GSS	E	99.2%	8.87	9.93	6.87	8.88		> 10	>20	13.68	15%	3.57	7.73	0%	100%	
4	379		BN	E	97.60%	8.82	9.43	9.91	9.99		> 10								
4	387		BN	W	96.24%	8.89	9.39	9.54	9.64		> 10								
4	1289	*Streptomyces purpeofuscus*	BN	M	99.2%	4.66	4.83	2.37	6.82		> 10	>20	8.76	12%	84%	42%	0%	86%	
4	1430		BN	M	99.1%	4.57	6.40	4.79	4.77		> 10	>20	13.86	0%	3.61	7.22	10%	99%	
4	1522	*Streptomyces sp. BR57*	BN	M	99.4%	4.39	4.83	4.76	4.86		> 10	>20	13.43	13%	2.29	6.22	15%	99%	
4	1556		BN	M	99.3%	1.70	2.29	9.65	2.35		> 10		7.09	10%	1.00	2.74	84%	-44%	
4	2479		BN	M	97.5%	3.91	4.46	4.73	2.19		> 10		> 20	11%	0.47	4.61	4%	86%	
4	2486		BN	E	98.8%	4.78	4.71	4.69	4.16		> 10	>20	13.16	15%	3.21	9.77	15%	99%	
4	2490		GSS	E	99.7%	6.28	6.15	4.96	4.47		> 10	>20	13.92	17%	3.61	47%	9%	100%	
4	2513		BN	E	99.4%	3.44	1.02	4.13	3.31		> 10	>20	> 20	10%	4.04	39%	0%	100%	
4	2523		GSS	E	99.2%	4.45	2.97	4.50	2.49		> 10	14.62	6.93	12%	1.11	4.75	89%	100%	
4	2530		BN	M	99.3%	4.47	2.42	4.59	2.39		> 10		7.02	14%	1.58	5.00	81%	99%	
4	4118		DYC	E	98.2%	2.26	4.30	7.89	1.73		> 10	>20	> 20	2%	41%	0%	9%	-42%	
4	4135		DYC	E	95.1%	3.70	4.93	8.87	2.27		> 10	>20	> 20	7%	14%	0%	7%	-46%	
4	4263		GSS	E	99.3%	2.37	3.07	5.80	8.56		> 10	>20	> 20	8%	35%	0%	0%	23%	
4	4318		GSS	E	99.6%	4.84	6.64	7.87	4.75		> 10	>20	14.84	19%	3.82	84%	21%	99%	
4	4319		GSS	E	99.4%	4.40	4.52	4.67	4.05		> 10	>20	14.11	17%	2.22	7.70	22%	99%	
4	4325		GSS	E	99.2%	4.68	4.78	4.89	3.61		> 10	>20	14.19	20%	2.22	75%	17%	99%	
4	4414		BN	M	95.7%	7.36	9.61	9.16	6.86		> 10	>20	15.54	24%	3.93	63%	0%	100%	

Appendix D (continued)

Priority group	ID	Species	Media	Frac.	% inhib. at 10µl/ml (MABA)	MICs vs replicating *M. tuberculosis* (µl/ml)					IC_{50} (µl/ml)			MIC (µl/ml) vs				Activity vs non-replicating *M. tuberculosis*	
						Rv	rKM	rRMP	rSM	rCS	1	2	3	*E.coli*	*S. aureus*	*C. albicans*	*M. smeg*	% inhib at 10 µl/ml	MIC (µl/ml)
4	4424		BN	M	99.6%	4.59	4.68	4.73	4.60		> 10	>20	14.55	15%	3.87	9.67	12%	98%	
4	4510		BN	M	99.0%	4.75	1.09	4.70	4.16		> 10	>20	6.87	15%	1.71	2.99	85%	99%	
4	4537		GSS	W	96.0%	8.58	9.23	8.16	8.49		> 10	>20	> 20	4.71	4.41	88%	0%	27%	
4	4653		BN	M	96.8%	3.81	4.08	4.88	3.29		> 10	>20	18.80	6%	0.23	2.28	0%	94%	
4	4715		GSS	E	95.1%	5.43	4.34	4.67	4.61		> 10	>20	19.17	8%	0.29	4.50	0%	99%	
4	4719		BN	E	99.6%	4.66	4.51	4.82	4.59		> 10	>20	13.18	15%	2.73	4.97	15%	101%	
4	4777		GSS	M	99.0%	6.42	4.85	5.38	4.89		> 10	>20		18%	3.81	9%	7%	99%	
4	4789		BN	E	99.8%	4.79	4.43	4.79	4.16		> 10	>20		16%	0.25	4.81	49%	101%	
4	4796		GSS	E	99.5%	4.77	4.60	4.80	4.34		> 10	>20		11%	2.26	4.91	20%	101%	
4	4828		GSS	E	95.5%	9.14	4.79	9.10	7.70		> 10	>20		21%	4.60	29%	4%	99%	
4	4901		BN	E	98.5%	4.31	2.33	3.15	3.16		> 10	>20		8%	0.22	3.77	16%	99%	
4	4955		GSS	M	99.9%	4.73	4.60	5.72	4.42		> 10	>20		17%	3.01	65%	66%	100%	
4	5159		GSS	W	97.1%	4.65	4.86	7.97	4.81		> 10	>20		7%	5%	0%	0%	80%	
4	5287		GSS	M	93.7%	4.96	3.60	4.34	4.32		> 10	>20		15%	0.26	4.72	0%	96%	
4	5317		BN	M	94.0%	5.65	4.22	4.83	4.75		> 10			19%	0.28	4.74	0%	96%	
4	5345		GSS	M	99.3%	4.79	4.78	4.74	4.45		> 10			22%	4.27	59%	0%	100%	
4	5384		BN	E	94.0%	6.72	4.69	4.68	6.11		> 10			15%	0.54	89%	0%	95%	
4	5609		BN	M	98.1%	7.11	4.79	4.96	7.00		> 10			21%	0.99	8.50	19%	85%	
4	5618		BN	M	91.7%	4.98	4.34	4.69	8.10		> 10			7%	0.37	3.10	20%	96%	
4	5637		GSS	E	95.2%	4.52	4.08	4.51	4.43		> 10			8%	0.90	4.87	15%	97%	
4	5697		DYC	M	97.6%	4.97	4.94	7.64	4.99		> 10			11%	3.62	9.86	20%	100%	

Appendix D (continued)

Priority group	ID	Species	Media	Frac.	% inhib. at 10µl/ml (MABA)	MICs vs replicating *M. tuberculosis* (µl/ml)					IC_{50} (µl/ml)			MIC (µl/ml) vs				Activity vs non-replicating *M. tuberculosis*	
						Rv	rKM	rRMP	rSM	rCS	1	2	3	*E.coli*	*S. aureus*	*C. albicans*	*M. smeg*	% inhib at 10 µl/ml	MIC (µl/ml)
4	5745		GSS	M	99.0%	6.08	3.60	4.61	4.62		> 10			12%	0.27	2.39	3%	94%	
4	5763		GSS	M	94.6%	6.71	4.18	4.37	4.67		> 10			2%	0.47	2.45	6%	88%	
4	5893		GSS	W	97.1%	8.13	7.25	7.14	7.63		> 10			0%	6%	40%	46%	76%	
4	6005		GSS	M	91.6%	6.61	8.27	5.05	4.90		> 10			12%	0.27	4.78	2%	96%	
4	6083		DYC	E	96.4%	7.37	4.17	4.90	7.03		> 10			7%	0.45	4.94	0%	99%	
4	6089		BN	M	96.9%	5.64	2.35	4.44	8.88		> 10			9%	0.24	2.56	0%	92%	
4	6275		GSS	E	99.3%	8.54	5.35	8.14	8.01		> 10			21%	3.47	76%	0%	100%	
4	6342		GSS	E	93.0%	7.63	3.81	4.88	4.47		> 10			8%	0.28	2.79	0%	89%	
4	6637		GSS	E	97.4%	8.14	6.15	5.07	7.53		> 10			9%	0.51	88%	21%	101%	
4	6656		GSS	E	98.8%	4.68	3.78	3.48	4.59		> 10			7%	0.13	2.34	0%	101%	
4	6857		GSS	W	98.3%	1.93	4.49	2.02	7.09		> 10			2.39	4.50	4.31	1.16	100%	
4	6872		DYC	W	98.9%	4.62	9.80	4.22	9.13		> 10			9.72	68%	8.52	9.84	102%	
4	6886		BN	M	99.4%	4.63	4.59	4.41	4.74		> 10			12%	1.80	4.78	29%	101%	
4	6913		GSS	W	98.3%	1.23	Redo	3.49	8.63		> 10			0%	4%	38%	0%	100%	
4	8016		GSS	E	99.3%	4.70	3.80	8.32	4.64		> 10			12%	1.99	5.00	40%	99%	
4	8498		BN	M	97.7%	4.77	4.89	4.72	4.90		> 10			14%	2.28	86%	23%	100%	
4	8511		GSS	E	99.3%	4.92	8.40	4.87	8.59		> 10			15%	3.59	4.95	0%	100%	
4	8817		GSS	E	99.5%	3.74	4.48	4.56	4.63		> 10			12%	2.18	4.50	65%	98%	
4	8880		DYC	M	99.5%	3.90	3.64	2.15	4.84		> 10			0%	8.95	12%	36%	86%	
4	8976		GSS	E	98.8%	4.66	4.91	4.86	4.76		> 10			11%	1.91	4.52	42%	99%	
4	9023		DYC	E	99.4%	6.21	4.89	4.93	9.24		> 10			0%	9.25	16%	25%	54%	

Appendix D (continued)

Priority group	ID	Species	Media	Frac.	% inhib. at 10µl/ml (MABA)	MICs vs replicating *M. tuberculosis* (µl/ml)					IC_{50} (µl/ml)			MIC (µl/ml) vs				Activity vs non-replicating *M. tuberculosis*	
						Rv	rKM	rRMP	rSM	rCS	1	2	3	*E.coli*	*S. aureus*	*C. albicans*	*M. smeg*	% inhib at 10 µl/ml	MIC (µl/ml)
4	9346		GSS	E	100.2%	4.72	4.92	4.82	4.78		> 10			9%	2.46	8.15	0%	52%	
4	9346		BN	M	99.5%	9.17	8.88	6.52	9.53		> 10			20%	4.59	70%	0%	100%	
4	9469		DYC	E	97.7%	3.68	2.39	7.68	3.10		> 10			0%	27%	0%	9.78	30%	
4	9538		GSS	E	93.9%	3.19	4.00	4.28	3.24		> 10			0%	0%	76%	0%	102%	
4	9564		GSS	E	99.4%	4.33	4.81	8.76	5.72		> 10			0%	12%	0%	0%	101%	
4	9580		BN	E	99.3%	4.78	4.74	4.76	4.76		> 10			12%	8.95	0%	0%	102%	
4	9598		GSS	E	99.2%	7.38	4.95	4.78	8.21		> 10			16%	4.27	9.96	0%	100%	
4	9662		BN	M	100.0%	9.42	7.15	7.74	8.71		> 10			27%	4.40	35%	0%	101%	
4	9752		BN	M	99.5%	4.62	4.25	4.60	4.57		> 10			13%	2.43	7.97	0%	100%	

Appendix E Biological profiling of some top hits, and their chromatography fractions generated from. G, GSS; M, methanolic extract. rKM, kanamycin-resistant strain; rRMP, rifampin-resistant; rSM, streptomycin-resistant; rCS, cycloserine-resistant.

Sample	MIC vs M. tuberculosis (μg/ml)					IC50 vs VERO (μg/ml)	LORA (μg/ml)	Spectrum Activity (% inhibition at 100μg/ml)			
	Rv	rRMP	rSM	rKM	rCS			*E.coli*	*S. aureus*	*C. albican*	*M. smegmatis*
MJM5123 (G/M)	5.01	9.10	2.42	9.83	4.91	> 100	> 100	0%	12%	0%	33%
20% Methanol	25%	7%	6%	1%	7%	> 100	> 100	0%	5%	29%	12%
40% Methanol	13%	16%	0%	7%	12%	> 100	> 100	0%	3%	0%	18%
60% Methanol	17%	17%	0%	3%	0%	> 100	> 100	0%	5%	36%	10%
80% Methanol	8.48	9.34	2.46	9.42	4.80	> 100	> 100	0%	0%	0%	22%
100% Methanol	0.14	0.25	0.04	0.60	0.15	> 100	1.57	0%	1%	38%	9.72
Chloroform	0.19	0.51	0.08	0.40	0.15	> 100	6.70	0%	7%	71%	9.99

Sample	**MABA MIC (μg/ml)**	**IC50**				**LORA MIC (μg/ml)**	**Spectrum Activity (μg/ml)**			
		Vero	**Vero**	**Vero**	**HepG2**		***E.coli***	***S. aureus***	***C. albicans***	***M. smegmatis***
A-8412E	< 0.195	> 200	> 200	> 200	3.526	21.89	16%	0%	45%	0.38
20% Methanol	1.25	146	> 200	> 200	169.7	42.51	0%	0%	43%	4.15
40% Methanol	**0.26**	> 200	< 12.5	18.30	113.4	9.02	12.13	51%	65%	0.75
60% Methanol	0.75	129	19.93	19.10	26.75	30.85	0%	78%	80%	2.51
80% Methanol	**< 0.195**	< 12.5	> 200	>200	26.22	82%	0%	0%	56%	< 0.195
100% Methanol	< 0.195	< 12.5	< 12.5	<12.5	2.726	0.75	0%	0%	33%	< 0.195
Chloroform	2.49	< 12.5	> 200	181.20	64.04	18.70	0%	3%	0%	3.48

Appendix E (continued)

Sample	MABA MIC (µg/ml)	IC50				LORA MIC (µg/ml)	Spectrum Activity (µg/ml)			
		Vero	Vero	Vero	HepG2		*E.coli*	*S. aureus*	*C. albicans*	*M. smegmatis*
7483M										
20% Methanol	34%	> 200				85%	0%	0%	38%	15%
40% Methanol	2%	> 200				21.65	0%	0%	0%	13%
60% Methanol	21%	> 200				83%	0%	0%	0%	19%
80% Methanol	90%	161.80				5.84	0%	64%	0%	26%
100% Methanol	0.75	< 12.5				< 0.195	8%	1.41	49%	83%
Chloroform	24.14	87.08				3.52	0%	46.78	10%	0%
7483E										
20% Methanol	0.75	61.64				< 0.195	0%	2.03	2.37	43.60
40% Methanol	45.25	61.53				6.22	0%	68%	71%	8%
60% Methanol	42.48	32.47				5.70	0%	72%	48.07	6%
80% Methanol	2.88	17.07				0.35	0%	5.08	8.91	48.41
100% Methanol	0.27	< 12.5				< 0.195	0%	0.55	0.38	10.12
Chloroform	6.06	> 200				0.84	0%	19.11	48.49	10%

Sample	MABA MIC (µg/ml)	IC50 **(µg/ml)**				LORA MIC (µg/ml)	Spectrum Activity (µg/ml)			
		Vero	Vero	Vero	HepG2		*E.coli*	*S. aureus*	*C. albicans*	*M. smegmatis*
A-4977M	1.88	31.32	< 12.5	<12.5	3.4	< 0.195	5%	2.91	6.09	16.21
20% Methanol	23.93	19.25	161.80	142.00	11.7	8.53	6%	40.23	0%	12%
40% Methanol	23.77	71.71	152.20	70.00	9.6	3.52	5%	38.18	0%	15%
60% Methanol	24.22	71.76	154.80	150.00	10.9	3.66	4%	39.97	0%	8%
80% Methanol	1.44	39.09	< 12.5	< 12.5	6.5	< 0.195	9%	2.11	6.18	83%
100% Methanol	< 0.195	< 12.5	< 12.5	< 12.5	6.1	< 0.195	4%	0.66	1.55	5.60
Chloroform	2.54	> 200	< 12.5	< 12.5	5.8	< 0.195	11%	4.53	86%	23.53

Appendix E (continued)

Sample	MABA MIC (μg/ml)	IC50 (μg/ml) Vero	LORA MIC (μg/ml)	Spectrum Activity (μg/ml)			
				E.coli	*S. aureus*	*C. albicans*	*M. smegmatis*
A-1543E	0.22	< 12.5	< 0.195	11%	0.68	1.63	11.53
20% Methanol	0.75	< 12.5	< 0.195	9%	1.36	4.48	35.44
40% Methanol	49.27	191.70	11.06	0%	18%	35%	19%
60% Methanol	22.51	38.61	1.96	0%	71%	48.30	0%
80% Methanol	0.70	< 12.5	< 0.195	12%	2.37	8.60	33.93
100% Methanol	< 0.195	< 12.5	< 0.195	14%	0.61	1.47	7.62
Chloroform	2.93	21.36	0.22	12%	8.43	44%	0%

Sample	MABA MIC (μg/ml)	IC50 (μg/ml) Vero	LORA MIC (μg/ml)	Spectrum Activity (μg/ml)			
				E.coli	*S. aureus*	*C. albicans*	*M. smegmatis*
A-2526E	0.74	< 12.5	< 0.195	11%	1.40	3.00	12.16
20% Methanol	1.53	15.10	< 0.195	8%	3.63	5.63	43.65
40% Methanol	12.34	52.74	1.46	6%	23.39	66%	46%
60% Methanol	90%	> 200	17.63	0%	30%	37%	9%
80% Methanol	1.17	< 12.5	< 0.195	12%	4.89	21.07	46.62
100% Methanol	< 0.195	< 12.5	< 0.195	0%	0.29	0.74	16.29
Chloroform	3.01	< 12.5	0.33	13%	9.96	70%	20%

Sample	MABA MIC (μg/ml)	IC50 (μg/ml) Vero	LORA MIC (μg/ml)	Spectrum Activity (μg/ml)			
				E.coli	*S. aureus*	*C. albicans*	*M. smegmatis*
A-4824M	20.30	81.80	< 0.391	0%	8.40	87%	0%
20% Methanol	24.09	152				15%	0%
40% Methanol	49.71	>200				3%	0%
60% Methanol	0.37	< 12.5				2.67	5.98
80% Methanol	2.94	< 12.5				2.94	24.04
100% Methanol	< 0.195	< 12.5				0.77	1.54
Chloroform	1.49	< 12.5				9.02	85%

Appendix E (continued)

Sample	MABA MIC (μg/ml)	IC50 (μg/ml) Vero	LORA MIC (μg/ml)	Spectrum Activity (μg/ml)				Counter screening			
				E.coli	*S. aureus*	*C. albicans*	*M. smegmatis*	rRmp	rSm	rKm	rCs
A-5560E	3.03	< 12.5	15%	0%	54%	34%	8%	45%	0%	0%	18%
20% Methanol	1.01	< 12.5	29%	0%	10%	43%	0%	19%	0%	0%	0%
40% Methanol	5.48	19.1	26%	0%	21%	0%	6%	21%	14%	17%	0%
60% Methanol	6.10	14	3.48	0%	28%	0%	3%	71%	63%	73%	45%
80% Methanol	4.80	< 12.5	0.99	0%	85%	9.73	19%	7.50	7.42	4.68	9.49
100% Methanol	0.43	< 12.5	0.49	0%	0.90	4.83	18%	1.77	2.20	2.29	4.43
Chloroform	8.13	78.4				4%	6%				

Sample	MABA MIC (μg/ml)	IC50 (μg/ml) Vero	LORA MIC (μg/ml)	Spectrum Activity (μg/ml)				Counter screening			
				E.coli	*S. aureus*	*C. albicans*	*M. smegmatis*	rRmp	rSm	rKm	rCs
A-4302	7.77	< 12.5	4.27	0%	7%	37%	3%	33%	4%	0%	2%
20% Methanol	48%	< 12.5	57%	0%	4%	4%	11%	24%	0%	0%	0%
40% Methanol	0%	< 12.5	78%	0%	8%	0%	1%	29%	0%	0%	0%
60% Methanol	35%	< 12.5	61%	0%	0%	16%	9%	24%	0%	0%	0%
80% Methanol	24.98	42.3	1.16	0%	56%	9%	8%	8.30	8.85	9.71	9.29
100% Methanol	0.69	< 12.5	4.40	0%	15%	0%	19%	29%	7%	7%	3%
Chloroform	2.79	15.5				69%	88%				

Sample	MABA MIC (ug/ml)	IC50 (μg/ml) Vero	LORA MIC (μg/ml)	Spectrum Activity (μg/ml)				Counter screening			
				E.coli	*S. aureus*	*C. albicans*	*M. smegmatis*	rRmp	rSm	rKm	rCs
A-1401E	10.27	31.32	0.749	0%	24.66	79%	76%	10.90	8.77	5.73	11.36
20% Methanol	8.29	61.64	1.144	0%	70%	39%	19%	11.38	10.15	7.07	11.78
40% Methanol	75.13	61.53	24.333	0%	38%	37%	0%	73%	41%	80%	54%
60% Methanol	51.06	32.47	22.197	0%	11.79	59%	0%	85%	87%	47.21	82%
80% Methanol	5.52	17.07	1.059	0%	67%	0%	0%	5.83	5.81	4.99	8.87
100% Methanol	2.49	< 12.5	< 0.391	6%	2%	80%	38%	1.54	1.43	1.05	1.56
Chloroform	98.03	> 200	11.292	0%	35%	42%	0%	58%	41.09	82%	49%

Appendix E (continued)

Sample	MABA MIC (ug/ml)	IC50 (μg/ml) (Vero)	LORA MIC (μg/ml)	Spectrum Activity (μg/ml)				Counter screening			
				E.coli	*S. aureus*	*C. albicans*	*M. smegmatis*	rRmp	rSm	rKm	rCs
A-1526E-SE	72.69	> 200	19.361	0%	0%	16%	0%	69%	47.18	23.22	42.81
20% Methanol	4.03	19.25	0.507	0%	2.32	70%	80%	3.07	2.90	2.71	4.42
40% Methanol	47.53	71.71	22.344	0%	14%	72%	0%	74%	81%	88%	82%
60% Methanol	56.31	71.76	23.49	0%	24%	81%	0%	80%	83%	49.59	87%
80% Methanol	34.57	39.09	7.743	0%	55%	41%	16%	47.07	43.57	38.82	48.40
100% Methanol	1.44	< 12.5	< 0.391	0%	2.41	3.03	32%	2.42	1.99	1.44	2.78
Chloroform	50%	> 200	10.632	0%	88%	41%	0%	53%	72%	50%	13%

Sample	MABA MIC (ug/ml)	IC50 (ug/ml) (Vero)	LORA MIC (ug/ml)	Spectrum Activity (μg/ml)				Counter screening			
				E.coli	*S. aureus*	*C. albicans*	*M. smegmatis*	rRmp	rSm	rKm	rCs
A-4887E	< 0.391	< 12.5	< 0.391	0%	0.32	1.39	2.95	0.21	< 0.195	< 0.195	0.31
20% Methanol	22.73	146	4.633	0%	23.03	15%	0%	23.69	23.33	22.19	37.05
40% Methanol	42.37	> 200	7.937	0%	86%	38%	0%	46.02	39.01	42.93	48.35
60% Methanol	90.81	129.80	11.635	0%	68%	6%	0%	59%	80%	71%	13%
80% Methanol	0.60	< 12.5	< 0.391	0%	1.00	1.78	46.51	0.69	0.37	0.33	0.70
100% Methanol	< 0.391	< 12.5	< 0.391	0%	0.67	2.80	5.90	0.55	0.41	0.34	0.53
Chloroform											

Sample	MABA MIC (ug/ml)	IC50 (ug/ml) (Vero)	LORA MIC (ug/ml)	Spectrum Activity (μg/ml)				Counter screening			
				E.coli	*S. aureus*	*C. albicans*	*M. smegmatis*	rRmp	rSm	rKm	rCs
7193E	8%	> 20	> (10) 73%	0%	0%	0%	0%	N.A.	0%	0%	0%
7193E-C1	5%	> 1600	621.82	0%	0%	23%	30%	23%	0%	0%	4%
7193E-C2	3%	>160	> (80) 62%	0%	20%	0%	13%	65%	45%	66.69	66.12
7193E-C3	1%	67.11	> (80) 75%	0%	31.43	0%	4%	N.A.	N.A.	N.A.	N.A.
7193E-C4	10%	69.51	> (80) 52%	0%	75%	0%	21%	48%	7%	67%	88%
7193E-C5	18.94	N.A.	N.A.	N.A.	N.A.	N.A.	N.A.	N.A.	N.A.	N.A.	N.A.
7193E-C6	9.39	43.18	1.14	0%	6.35	0%	51%	4.88	4.36	4.76	4.90
7193E-C7	84%	123.10	8.69	0%	74	0%	29%	73.98	62.52	61.13	65.34

Appendix E (continued)

Strain	Sample	MABA MIC (μg/ml)	IC50 (Vero) (μg/ml)
A-4977E	A-4977E	1.35	9.44
	20% Methanol	7.7	32.92
	40% Methanol	24.78	27.49
	60% Methanol	41.48	> 100
	80% Methanol	6.14	7.11
	100% Methanol	0.34	< 6.25
	Chloroform	1.64	> 100
A-1543M	A-1543M	5.64	58.02
	20% Methanol	22%	> 100
	40% Methanol	43.44	> 100
	60% Methanol	13%	> 100
	80% Methanol	25%	> 100
	100% Methanol	0.52	< 6.25
	Chloroform	10	> 100
A-7049M-SE	A-7049M-SE	0.39	< 6.25
	20% Methanol	0.75	8.48
	40% Methanol	0.88	13.03
	60% Methanol	N/D	
	80% Methanol	0.76	< 6.25
	100% Methanol	< 0.195	< 6.25
	Chloroform	1.44	34.04
A-4413BM	A-4413BM	9.29	42.48
	20% Methanol	48.29	> 200
	40% Methanol	7%	> 200
	60% Methanol	3%	> 200
	80% Methanol	23.05	69.56
	100% Methanol	0.56	< 12.5
	Chloroform	11.67	38.47
A-4413BE	A-4413BE	3.03	17.45
	20% Methanol	23.25	99.34
	40% Methanol	47.61	> 200
	60% Methanol	34%	> 200
	80% Methanol	8.91	29.05
	100% Methanol	0.71	< 12.5
	Chloroform	10.47	39.41
A-4721BM	A-4721BM	24.49	137.1
	20% Methanol	47.82	> 200
	40% Methanol	48.61	> 200

Appendix E (continued)

Strain	Sample	MABA MIC (μg/ml)	IC50 (Vero) (μg/ml)
A-4721BM	60% Methanol	10%	> 200
	80% Methanol	7.58	28.76
	100% Methanol	0.76	< 12.5
	Chloroform	47.69	> 200
A-4721BE	A-4721BE	6.04	23.38
	20% Methanol	51%	> 200
	40% Methanol	1%	> 200
	60% Methanol	16%	> 200
	80% Methanol	29%	23.07
	100% Methanol	1.21	< 12.5
	Chloroform	5.27	16.97
A-6833GM	A-6833GM	6%	> 200
	20% Methanol	0%	> 200
	40% Methanol	5%	> 200
	60% Methanol	0%	> 200
	80% Methanol	2%	> 200
	100% Methanol	0%	> 200
	Chloroform	0%	> 200
A-8427BM	A-8427BM	1.02	< 12.5
	20% Methanol	5.94	29.53
	40% Methanol	47.97	> 200
	60% Methanol	49.47	> 200
	80% Methanol	0.72	< 12.5
	100% Methanol	0.38	< 12.5
	Chloroform	11.25	64.97
A-8915BM	A-8915BM	1.56	< 12.5
	20% Methanol	5.55	19.61
	40% Methanol	46.58	129.3
	60% Methanol	49.54	> 200
	80% Methanol	0.74	< 12.5
	100% Methanol	0.39	< 12.5
	Chloroform		

Appendix E (continued)

Strain	Sample	MABA MIC (μg/ml)	IC50 (Vero) (μg/ml)
1430BM	1430BM	27%	
	20% Methanol	12%	
	40% Methanol	17%	
	60% Methanol	18%	
	80% Methanol	55%	
1430BM	100% Methanol	24.62	
	Chloroform	48.67	
2479BE	2479BE	19.74	
	20% Methanol	18.26	
	40% Methanol	99.94	
	60% Methanol	7%	
	80% Methanol	46.7	
	100% Methanol	1.33	
	Chloroform	55.41	
2490GE	2490GE	24.88	
	20% Methanol	60.9	
	40% Methanol	0%	
	60% Methanol	84%	
	80% Methanol	88.03	
	100% Methanol	72%	
	Chloroform	75%	
2523	2523	51%	
	20% Methanol	50%	
	40% Methanol	43%	
	60% Methanol	65%	
	80% Methanol	91.58	
	100% Methanol	47.79	
	Chloroform	11.97	
2486BE	2486BE	44.35	
	20% Methanol	50	
	40% Methanol	69%	
	60% Methanol	76%	
	80% Methanol	3.04	
	100% Methanol	12.05	
	Chloroform	37.03	

Appendix E (continued)

Strain	Sample	MABA MIC (μg/ml)	IC50 (Vero) (μg/ml)
2523GE	2523GE	1.167	
2523GE	20% Methanol	9.593	
	40% Methanol	33.998	
	60% Methanol	38.491	
	80% Methanol	19.024	
	100% Methanol	24.571	
	Chloroform	40.985	
4510BE	4510BE	44.68	10.57
4510BE	20% Methanol	61.563	>100
	40% Methanol	73%	>100
	60% Methanol	43%	>100
	80% Methanol	40%	30.01
	100% Methanol	0.63	4.6
	Chloroform	5.65	10.7
2479BM	2479BM	25.22	
2479BM	20% Methanol	47.87	
	40% Methanol	0%	
	60% Methanol	65%	
	80% Methanol	12.02	
	100% Methanol	1.26	
	Chloroform	31.76	
1522BM	1522BM	22.32	
1522BM	20% Methanol	23.94	
	40% Methanol	67%	
	60% Methanol	49%	
	80% Methanol	94.77	
	100% Methanol	19.48	
	Chloroform	25.61	
4118DE	4118DE	33.14	
4118DE	20% Methanol	60.38	
	40% Methanol	8.46	
	60% Methanol	5.92	
	80% Methanol	44.59	
	100% Methanol	24.94	
	Chloroform	84%	

Appendix E (continued)

Strain	Sample	MABA MIC (μg/ml)	IC50 (Vero) (μg/ml)
2530BM	2530BM	24.38	
2530BM	20% Methanol	97.2	
2530BM	40% Methanol	12%	
	60% Methanol	14%	
2530BM	80% Methanol	6.976	
	100% Methanol	1.279	
	Chloroform	12.33	
4135DE	4135DE	85%	
4135DE	20% Methanol	87%	
	40% Methanol	84%	
	60% Methanol	47.15	
	80% Methanol	86%	
	100% Methanol	38.02	
	Chloroform	22.06	
4325GE	4325GE	1.04	
4325GE	20% Methanol	MISSING	
	40% Methanol	1.46	
	60% Methanol	86%	
	80% Methanol	23.94	
	100% Methanol	1.82	
	Chloroform	3.36	
4414BM	4414BM	3.74	32.8
4414BM	20% Methanol	0.89	66.68
	40% Methanol	11.8	>100
	60% Methanol	47.14	>100
	80% Methanol	12.07	13.4
	100% Methanol	1.51	11.69
	Chloroform	15.54	44.96
4325GE	4325GE	13.78	
4325GE	20% Methanol	1.58	
	40% Methanol	>100 (2%)	
	60% Methanol	98.54	
	80% Methanol	2.58	
	100% Methanol	99.35	
	Chloroform	98.32	

Appendix E (continued)

Strain	Sample	MABA MIC (μg/ml)	IC50 (Vero) (μg/ml)
4414BM	4414BM	3.55	
4414BM	20% Methanol	11.87	
4414BM	40% Methanol	12.34	
4414BM	60% Methanol	23.67	
	80% Methanol	1.52	
	100% Methanol	2.07	
	Chloroform	6.2	
4828GE	4828GE	94.06	
4828GE	20% Methanol	94.65	
	40% Methanol	>100 (2%)	
	60% Methanol	>100 (6%)	
	80% Methanol	>100 (27%)	
	100% Methanol	46.95	
	Chloroform	>100 (22%)	
4424BM	4424BM	1.11	
4424BM	20% Methanol	10.04	
	40% Methanol	49.56	
	60% Methanol	39.07	
	80% Methanol	1.92	
	100% Methanol	1.54	
	Chloroform	3.08	
2523GE	2523GE	>100 (11%)	>100
2523GE	20% Methanol	0.96	33.73
	40% Methanol	3.12	32.47
	60% Methanol	1.36	13.09
	80% Methanol	1.12	3.69
	100% Methanol	1.98	11.4
	Chloroform	>100 (90%)	
4777GM	4777GM	>100 (54%)	
4777GM	20% Methanol	>100 (0%)	
	40% Methanol	>100 (0%)	
	60% Methanol	>100 (0%)	
	80% Methanol	>100 (6%)	
	100% Methanol	36.33	
	Chloroform	93.84	

Appendix E (continued)

Strain	Sample	MABA MIC (μg/ml)	IC50 (Vero) (μg/ml)
4719BE	4719BE	EMPTY	
4719BE	20% Methanol	<0.391	10.52
4719BE	40% Methanol	>100 (88%)	>100
4719BE	60% Methanol	94.54	>100
	80% Methanol	3	11.08
	100% Methanol	<0.391	1.55
	Chloroform	0.76	11.13
4653BW	4653BW	>100 (11%)	
4653BW	20% Methanol	>100 (4%)	
	40% Methanol	>100 (7%)	
	60% Methanol	>100 (0%)	
	80% Methanol	>100 (13%)	
	100% Methanol	>100 (7%)	
	Chloroform	>100 (2%)	
2523GE	2523GE	>100 (0%)	
2523GE	20% Methanol	>100 (0%)	
	40% Methanol	>100 (0%)	
	60% Methanol	>100 (4%)	
	80% Methanol	90.59	
	100% Methanol	>100 (43%)	
	Chloroform	>100 (13%)	
4789BE	4789BE	1.09	
4789BE	20% Methanol	3.03	
	40% Methanol	>100 (8%)	
	60% Methanol	>100 (81%)	
	80% Methanol	4.24	
	100% Methanol	3.27	
	Chloroform	28.32	
4653BW	4653BW	>100 (0%)	
4653BW	20% Methanol	>100 (0%)	
	40% Methanol	>100 (5%)	
	60% Methanol	>100 (8%)	
	80% Methanol	>100 (0%)	
	100% Methanol	>100 (14%)	
	Chloroform	>100 (0%)	

Appendix E (continued)

Strain	Sample	MABA MIC (μg/ml)	IC50 (Vero) (μg/ml)
4715GE	4715GE	9.84	
4715GE	20% Methanol	12.04	
4715GE	40% Methanol	>100 (17%)	
4715GE	60% Methanol	>100 (12%)	
	80% Methanol	36.13	
	100% Methanol	9.11	
	Chloroform	23.4	
6833GW	6833GW	80.42	
6833GW	20% Methanol	>100 (32%)	
	40% Methanol	33.46	
	60% Methanol	74.94	
	80% Methanol	48.47	
	100% Methanol	>100 (90%)	
	Chloroform	>100 (0%)	

Appendix F. PMS file for ecumicin.

* NEW: the lines beginning by * are comment lines !
* To keep all the chemical shifts fixed during iteration
* replace "CHEMICAL SHIFTS(HZ):" by "..SHIFTS(HZ): fixed"
* The couplings can be fixed in the same way

NMR-data: C:\Users\jgnapo_2\Desktop\Wei_H14_XRays\H14_withoutGO
#$? Date 22. 2.2012; Time 18:15:36 perch.8th

CHEMICAL SHIFTS(PPM):
PROTON 2*SPIN= 1 SPECIES=1H POPULATION(Y)= 1.00000
10Trp_H8/ 1 6.981702 1*1*1 STAT=Y PRED= 7.318 RANGE= 0.199 WIDTH(Y)= 1.215 RESP(Y)= 0.2294 HSQC= C74
01ValH45/ 1 2.312749 1*1*6 STAT=Y PRED= 2.370 RANGE= 0.307 WIDTH(Y)= 1.536 RESP(Y)= 0.1971 HSQC= C1_2
01Val_H2/ 1 2.671561 1*1*1 STAT=Y PRED= 4.169 RANGE= 0.639 WIDTH(Y)= 1.557 RESP(Y)= 0.1955 HSQC= C4
01Val_H3/ 1 2.042384 1*1*1 STAT=Y PRED= 1.952 RANGE= 0.819 WIDTH(Y)= 1.561 RESP(Y)= 0.1582 HSQC= C5
01Val_H6/ 1 0.847135 1*1*3 STAT=Y PRED= 0.509 RANGE= 0.869 WIDTH(Y)= 1.598 RESP(Y)= 0.2195 HSQC= C6
01Val_H7/ 1 0.978236 1*1*3 STAT=Y PRED= 0.818 RANGE= 0.359 WIDTH(Y)= 1.688 RESP(Y)= 0.1917 HSQC= C7
02Val_H2/ 1 4.669057 1*1*1 STAT=Y PRED= 4.508 RANGE= 0.809 WIDTH(Y)= 1.467 RESP(Y)= 0.1935 HSQC= C10
02Val_H3/ 1 2.101399 1*1*1 STAT=Y PRED= 2.155 RANGE= 0.779 WIDTH(Y)= 1.561 RESP(Y)= 0.1880 HSQC= C12
02Val_H4/ 1 0.992199 1*1*3 STAT=Y PRED= 1.038 RANGE= 0.279 WIDTH(Y)= 1.468 RESP(Y)= 0.1493 HSQC= C13
02Val_H5/ 1 1.055401 1*1*3 STAT=Y PRED= 0.943 RANGE= 0.249 WIDTH(Y)= 1.538 RESP(Y)= 0.2055 HSQC= C14
03Ile_H7/ 1 3.233925 1*1*3 STAT=Y PRED= 3.196 RANGE= 0.369 WIDTH(Y)= 1.536 RESP(Y)= 0.2005 HSQC= C15
03Ile_H2/ 1 4.918283 1*1*1 STAT=Y PRED= 4.617 RANGE= 1.628 WIDTH(Y)= 1.466 RESP(Y)= 0.1936 HSQC= C17
03Ile_H3/ 1 1.957476 1*1*1 STAT=Y PRED= 2.032 RANGE= 0.706 WIDTH(Y)= 2.929 RESP(Y)= 0.1562 HSQC= C19
03IleH4A/ 1 0.989134 1*1*1 STAT=Y PRED= 1.465 RANGE= 0.699 WIDTH(Y)= 5.275 RESP(Y)= 1.0000 HSQC= C20
03IleH4B/ 1 1.255324 1*1*1 STAT=Y PRED= 1.175 RANGE= 0.589 WIDTH(Y)= 2.795 RESP(Y)= 0.1091 HSQC= C20
03Ile_H6/ 1 0.753945 1*1*3 STAT=Y PRED= 0.723 RANGE= 0.398 WIDTH(Y)= 1.613 RESP(Y)= 0.1953 HSQC= C21
03Ile_H5/ 1 0.743889 1*1*3 STAT=Y PRED= 0.880 RANGE= 0.219 WIDTH(Y)= 1.391 RESP(Y)= 0.1663 HSQC= C22
04Thr_H2/ 1 5.166937 1*1*1 STAT=Y PRED= 4.668 RANGE= 1.016 WIDTH(Y)= 1.377 RESP(Y)= 0.1774 HSQC= C24
04Thr_H3/ 1 5.783161 1*1*1 STAT=Y PRED= 4.010 RANGE= 0.479 WIDTH(Y)= 1.941 RESP(Y)= 0.1822 HSQC= C25
04Thr_H4/ 1 1.313144 1*1*3 STAT=Y PRED= 1.270 RANGE= 0.499 WIDTH(Y)= 1.818 RESP(Y)= 0.2026 HSQC= C27
05Thr_H5/ 1 3.329509 1*1*3 STAT=Y PRED= 3.257 RANGE= 0.399 WIDTH(Y)= 1.439 RESP(Y)= 0.1781 HSQC= C29
05Thr_H2/ 1 5.017583 1*1*1 STAT=Y PRED= 4.099 RANGE= 1.025 WIDTH(Y)= 1.500 RESP(Y)= 0.1944 HSQC= C31
05Thr_H3/ 1 4.457478 1*1*1 STAT=Y PRED= 4.345 RANGE= 0.719 WIDTH(Y)= 1.572 RESP(Y)= 0.1838 HSQC= C32
05Thr_H4/ 1 0.911837 1*1*3 STAT=Y PRED= 1.252 RANGE= 0.299 WIDTH(Y)= 1.939 RESP(Y)= 0.1922 HSQC= C34
06Val_H2/ 1 4.842224 1*1*1 STAT=Y PRED= 4.525 RANGE= 1.409 WIDTH(Y)= 1.382 RESP(Y)= 0.1523 HSQC= C37
06Val_H3/ 1 2.350353 1*1*1 STAT=Y PRED= 1.975 RANGE= 1.019 WIDTH(Y)= 1.789 RESP(Y)= 0.1830 HSQC= C38
06Val_H4/ 1 1.092268 1*1*3 STAT=Y PRED= 0.938 RANGE= 0.219 WIDTH(Y)= 1.894 RESP(Y)= 0.1902 HSQC= C39
06Val_H5/ 1 0.979285 1*1*3 STAT=Y PRED= 1.094 RANGE= 0.389 WIDTH(Y)= 2.275 RESP(Y)= 0.1940 HSQC= C40
07Leu_H7/ 1 3.258856 1*1*3 STAT=Y PRED= 3.110 RANGE= 0.376 WIDTH(Y)= 1.459 RESP(Y)= 0.1758 HSQC= C42
07Leu_H2/ 1 5.110377 1*1*1 STAT=Y PRED= 5.342 RANGE= 1.085 WIDTH(Y)= 2.240 RESP(Y)= 0.1736 HSQC= C44
07LeuH3A/ 1 1.452263 1*1*1 STAT=Y PRED= 1.444 RANGE= 0.429 WIDTH(Y)= 1.805 RESP(Y)= 0.1253 HSQC= C45
07LeuH3B/ 1 1.238825 1*1*1 STAT=Y PRED= 1.914 RANGE= 0.369 WIDTH(Y)= 3.321 RESP(Y)= 0.2550 HSQC= C45
07Leu_H4/ 1 0.957012 1*1*1 STAT=Y PRED= 1.630 RANGE= 0.627 WIDTH(Y)= 1.520 RESP(Y)= 0.1513 HSQC= C46
07Leu_H5/ 1 0.330648 1*1*3 STAT=Y PRED= 0.972 RANGE= 0.316 WIDTH(Y)= 1.961 RESP(Y)= 0.1633 HSQC= C47
07Leu_H6/ 1 0.168240 1*1*3 STAT=Y PRED= 0.972 RANGE= 0.149 WIDTH(Y)= 1.885 RESP(Y)= 0.1544 HSQC= C48
08Val_H2/ 1 4.594366 1*1*1 STAT=Y PRED= 4.489 RANGE= 0.899 WIDTH(Y)= 1.578 RESP(Y)= 0.1883 HSQC= C51
08Val_H3/ 1 2.026705 1*1*1 STAT=Y PRED= 1.995 RANGE= 0.486 WIDTH(Y)= 2.872 RESP(Y)= 0.1833 HSQC= C52
08Val_H4/ 1 0.915098 1*1*3 STAT=Y PRED= 1.060 RANGE= 0.237 WIDTH(Y)= 1.731 RESP(Y)= 0.1845 HSQC= C53
08Val_H5/ 1 0.858580 1*1*3 STAT=Y PRED= 0.999 RANGE= 0.229 WIDTH(Y)= 2.065 RESP(Y)= 0.1899 HSQC= C54
09Val_H6/ 1 3.139923 1*1*3 STAT=Y PRED= 3.169 RANGE= 0.466 WIDTH(Y)= 1.931 RESP(Y)= 0.1698 HSQC= C56

Appendix F (continued)

09Val_H2/ 1 3.065448 1*1*1 STAT=Y PRED= 5.153 RANGE= 0.719 WIDTH(Y)= 2.597 RESP(Y)= 0.1650 HSQC= C58
09Val_H3/ 1 2.582945 1*1*1 STAT=Y PRED= 2.524 RANGE= 0.407 WIDTH(Y)= 1.736 RESP(Y)= 0.1528 HSQC= C59
09Val_H4/ 1 1.093807 1*1*3 STAT=Y PRED= 1.319 RANGE= 0.227 WIDTH(Y)= 1.741 RESP(Y)= 0.1953 HSQC= C60
09Val_H5/ 1 0.975890 1*1*3 STAT=Y PRED= 1.075 RANGE= 0.239 WIDTH(Y)= 2.379 RESP(Y)= 0.1859 HSQC= C61
10TrpH13/ 1 2.157320 1*1*3 STAT=Y PRED= 2.936 RANGE= 0.895 WIDTH(Y)= 1.862 RESP(Y)= 0.1713 HSQC= C63
10Trp_H2/ 1 4.102017 1*1*1 STAT=Y PRED= 5.043 RANGE= 1.765 WIDTH(Y)= 2.064 RESP(Y)= 0.1681 HSQC= C65
10TrpH3A/ 1 3.544888 1*1*1 STAT=Y PRED= 3.613 RANGE= 0.469 WIDTH(Y)= 1.516 RESP(Y)= 0.1749 HSQC= C66
10TrpH3B/ 1 3.693826 1*1*1 STAT=Y PRED= 3.367 RANGE= 0.629 WIDTH(Y)= 2.118 RESP(Y)= 0.1765 HSQC= C66
10Trp_H5/ 1 6.698373 1*1*1 STAT=Y PRED= 6.772 RANGE= 0.276 WIDTH(Y)= 1.649 RESP(Y)= 0.2013 HSQC= C68
10Trp_H9/ 1 6.441824 1*1*1 STAT=Y PRED= 7.089 RANGE= 0.219 WIDTH(Y)= 1.143 RESP(Y)= 0.2128 HSQC= C73
10Trp_H7/ 1 6.918050 1*1*1 STAT=Y PRED= 7.333 RANGE= 0.309 WIDTH(Y)= 0.719 RESP(Y)= 0.1990 HSQC= C75
10TrpH12/ 1 3.825517 1*1*3 STAT=Y PRED= 4.072 RANGE= 0.249 WIDTH(Y)= 1.244 RESP(Y)= 0.1876 HSQC= C77
11Val_H2/ 1 4.528581 1*1*1 STAT=Y PRED= 4.303 RANGE= 1.449 WIDTH(Y)= 1.849 RESP(Y)= 0.1834 HSQC= C80
11Val_H3/ 1 2.200081 1*1*1 STAT=Y PRED= 2.094 RANGE= 0.589 WIDTH(Y)= 1.854 RESP(Y)= 0.1757 HSQC= C81
11Val_H4/ 1 1.028241 1*1*3 STAT=Y PRED= 1.094 RANGE= 0.249 WIDTH(Y)= 2.106 RESP(Y)= 0.1836 HSQC= C82
11Val_H5/ 1 0.989118 1*1*3 STAT=Y PRED= 1.080 RANGE= 0.299 WIDTH(Y)= 1.787 RESP(Y)= 0.1359 HSQC= C83
12Phe_H2/ 1 4.853691 1*1*1 STAT=Y PRED= 4.499 RANGE= 0.989 WIDTH(Y)= 1.261 RESP(Y)= 0.1673 HSQC= C86
12Phe_H3/ 1 5.343847 1*1*1 STAT=Y PRED= 5.208 RANGE= 0.489 WIDTH(Y)= 1.884 RESP(Y)= 0.1897 HSQC= C87
12Phe_H5/ 1 7.239588 1*2*1 STAT=Y PRED= 7.524 RANGE= 0.309 WIDTH(Y)= 2.042 RESP(Y)= 0.2024 HSQC= C89_93
12Phe_H6/ 1 7.255487 1*2*1 STAT=Y PRED= 7.372 RANGE= 0.579 WIDTH(Y)= 1.207 RESP(Y)= 0.2038 HSQC= C90_92
12Phe_H7/ 1 7.200632 1*1*1 STAT=Y PRED= 7.281 RANGE= 0.309 WIDTH(Y)= 1.557 RESP(Y)= 0.2174 HSQC= C91
13Val_H2/ 1 4.396080 1*1*1 STAT=Y PRED= 4.169 RANGE= 0.669 WIDTH(Y)= 1.205 RESP(Y)= 0.1804 HSQC= C97
13Val_H3/ 1 1.967817 1*1*1 STAT=Y PRED= 1.935 RANGE= 0.869 WIDTH(Y)= 1.973 RESP(Y)= 0.2062 HSQC= C99
13Val_H4/ 1 0.934963 1*1*3 STAT=Y PRED= 1.277 RANGE= 0.219 WIDTH(Y)= 2.666 RESP(Y)= 0.2386 HSQC= C100
13Val_H5/ 1 0.919356 1*1*3 STAT=Y PRED= 0.933 RANGE= 0.278 WIDTH(Y)= 2.083 RESP(Y)= 0.2256 HSQC= C101

COUPLING CONSTANTS(HZ):
J115_217 7.7969 J 10Trp_H8 10Trp_H9 STAT=Y PRED= 8.100 RANGE= 0.890
J115_218 8.1808 J 10Trp_H8 10Trp_H7 STAT=Y PRED= 7.850 RANGE= 0.800
J122_123 9.1737 J 01Val_H2 01Val_H3 STAT=Y PRED= 12.510 RANGE= 4.000
J123_124 6.5890 J 01Val_H3 01Val_H6 STAT=Y PRED= 6.640 RANGE= 0.200
J123_127 6.6205 J 01Val_H3 01Val_H7 STAT=Y PRED= 6.640 RANGE= 0.200
J131_132 8.7545 J 02Val_H2 02Val_H3 STAT=Y PRED= 12.600 RANGE= 6.000
J132_133 6.7841 J 02Val_H3 02Val_H4 STAT=Y PRED= 6.640 RANGE= 0.200
J132_136 6.7206 J 02Val_H3 02Val_H5 STAT=Y PRED= 6.640 RANGE= 0.200
J142_143 11.2297 J 03Ile_H2 03Ile_H3 STAT=Y PRED= 13.150 RANGE= 4.000
J143_144 0.4614 J 03Ile_H3 03IleH4A STAT=Y PRED= 1.950 RANGE= 3.000
J143_145 2.9276 J 03Ile_H3 03IleH4B STAT=Y PRED= 12.660 RANGE= 2.800
J143_146 6.6276 J 03Ile_H3 03Ile_H6 STAT=Y PRED= 6.640 RANGE= 0.200
J144_145 -12.2168 J 03IleH4A 03IleH4B STAT=Y PRED= -13.400 RANGE= 0.600
J144_149 7.2855 J 03IleH4A 03Ile_H5 STAT=Y PRED= 7.440 RANGE= 0.150
J145_149 7.6340 J 03IleH4B 03Ile_H5 STAT=Y PRED= 7.440 RANGE= 0.150
J153_154 2.3441 J 04Thr_H2 04Thr_H3 STAT=Y PRED= 2.690 RANGE= 6.600
J154_155 6.5134 J 04Thr_H3 04Thr_H4 STAT=Y PRED= 6.250 RANGE= 0.600
J161_162 3.7259 J 05Thr_H2 05Thr_H3 STAT=Y PRED= 2.440 RANGE= 4.400
J162_164 6.4691 J 05Thr_H3 05Thr_H4 STAT=Y PRED= 6.250 RANGE= 0.600
J168_169 8.9180 J 06Val_H2 06Val_H3 STAT=Y PRED= 2.980 RANGE= 6.600
J169_170 6.6944 J 06Val_H3 06Val_H4 STAT=Y PRED= 6.640 RANGE= 0.200
J169_173 7.0316 J 06Val_H3 06Val_H5 STAT=Y PRED= 6.640 RANGE= 0.200
J179_180 6.2437 J 07Leu_H2 07LeuH3A STAT=Y PRED= 3.040 RANGE= 6.000

Appendix F (continued)

```
J179_181    8.3839   J 07Leu_H2 07LeuH3B   STAT=Y  PRED= 13.950 RANGE= 4.000
J180_181  -13.3047   J 07LeuH3A 07LeuH3B   STAT=Y  PRED= -14.710 RANGE= 1.600
J180_182    8.2119   J 07LeuH3A 07Leu_H4   STAT=Y  PRED= 12.990 RANGE= 2.560
J181_182    5.7896   J 07LeuH3B 07Leu_H4   STAT=Y  PRED= 2.270 RANGE= 3.000
J182_183    6.5482   J 07Leu_H4 07Leu_H5   STAT=Y  PRED= 6.640 RANGE= 0.200
J182_186    6.5879   J 07Leu_H4 07Leu_H6   STAT=Y  PRED= 6.640 RANGE= 0.200
J190_191    8.8736   J 08Val_H2 08Val_H3   STAT=Y  PRED= 12.880 RANGE= 6.000
J191_192    6.5520   J 08Val_H3 08Val_H4   STAT=Y  PRED= 6.640 RANGE= 0.200
J191_195    6.7834   J 08Val_H3 08Val_H5   STAT=Y  PRED= 6.640 RANGE= 0.200
J201_202    7.6281   J 09Val_H2 09Val_H3   STAT=Y  PRED= 12.960 RANGE= 4.000
J202_203    6.4961   J 09Val_H3 09Val_H4   STAT=Y  PRED= 6.640 RANGE= 0.200
J202_206    6.7760   J 09Val_H3 09Val_H5   STAT=Y  PRED= 6.640 RANGE= 0.200
J212_213   11.1630   J 10Trp_H2 10TrpH3A   STAT=Y  PRED= 12.890 RANGE= 4.000
J212_214    4.7143   J 10Trp_H2 10TrpH3B   STAT=Y  PRED= 1.900 RANGE= 4.400
J213_214  -13.7295   J 10TrpH3A 10TrpH3B   STAT=Y  PRED= -16.760 RANGE= 2.560
J215_218    0.4880   J 10Trp_H5 10Trp_H7   STAT=Y  PRED= -0.300 RANGE= 0.500
J217_218    0.6708   J 10Trp_H9 10Trp_H7   STAT=Y  PRED= 1.020 RANGE= 1.200
J223_224    7.9094   J 11Val_H2 11Val_H3   STAT=Y  PRED= 3.450 RANGE= 9.000
J224_225    6.7483   J 11Val_H3 11Val_H4   STAT=Y  PRED= 6.640 RANGE= 0.200
J224_228    6.8064   J 11Val_H3 11Val_H5   STAT=Y  PRED= 6.640 RANGE= 0.200
J232_233    1.9005   J 12Phe_H2 12Phe_H3   STAT=Y  PRED= 1.900 RANGE= 6.600
J234_238    1.3335   J 12Phe_H5 12Phe_H5   STAT=Y  PRED= 1.980 RANGE= 1.200
J234_235    7.6508   J 12Phe_H5 12Phe_H6   STAT=Y  PRED= 7.660 RANGE= 0.340
J234_237    0.7769   J 12Phe_H6 12Phe_H5   STAT=Y  PRED= 0.550 RANGE= 0.750
J234_236    1.2760   J 12Phe_H5 12Phe_H7   STAT=Y  PRED= 1.260 RANGE= 1.200
J235_237    1.7027   J 12Phe_H6 12Phe_H6   STAT=Y  PRED= 1.480 RANGE= 1.200
J235_236    7.4760   J 12Phe_H6 12Phe_H7   STAT=Y  PRED= 7.400 RANGE= 0.240
J241_242    8.8924   J 13Val_H2 13Val_H3   STAT=Y  PRED= 12.320 RANGE= 6.000
J242_243    6.8372   J 13Val_H3 13Val_H4   STAT=Y  PRED= 6.640 RANGE= 0.200
J242_246    6.4162   J 13Val_H3 13Val_H5   STAT=Y  PRED= 6.640 RANGE= 0.200

CONTROL PARAMETERS:
      Solvent =  none (def. 99% enriched)
        1.000 =  Concentration (vol%, def=1.0%)
   0.00100000 =  Minimum line-intensity
   0.00100000 =  Diagonalization criterium (not in use)
  11.63298470 =  Left frequency (ppm)
  -4.33373638 =  Right frequency (ppm)
        0.000 =  Acquisition time (s, for QMTLS)
        0.715 =  Line-width (for modes D, P & T, 0=use defaults)
  0.103379714 =  Data-point resolution (Hz)
       28.306 =  GAUSSIAN (%, 0=use default from INF)
      -10.087 =  Dispersion contribution (%, 0=use default from INF)
   0.00000000 =  Decoupling frequency (for DORES)

CONSTRAINTS (in equations X0 = 1.0)...use no empty lines
 EQUAL 01Val_H2 = 13Val_H2
 EQUAL 06Val_H5 = 11Val_H4
 EQUAL 07Leu_H5 = 07Leu_H6
 IGNORE(HZ):   940.350 to   936.356
```

Appendix F (continued)

IGNORE(HZ): 2062.779 to 2027.293
IGNORE(HZ): 1175.285 to 1149.842
IGNORE(HZ): 1232.768 to 1209.210
IGNORE(HZ): 5188.061 to 5161.182
IGNORE(HZ): 4803.141 to 4787.420
IGNORE(HZ): 812.060 to 780.231

End of file

Appendix G. The pseudo HiFSA profile of deoxyecumicin.

* NEW: the lines beginning by * are comment lines !
* To keep all the chemical shifts fixed during iteration
* replace "CHEMICAL SHIFTS(HZ):" by "..SHIFTS(HZ): fixed"
* The couplings can be fixed in the same way

NMR-data: C:\Users\jgnapo_2\Desktop\Wei_H14_XRays\H14_withoutGO
#$œ Date 22. 2.2012; Time 18:15:36 perch.8th

CHEMICAL SHIFTS(PPM):
PROTON 2*SPIN= 1 SPECIES=1H POPULATION(Y)= 1.00000
10Trp_H8/ 1 6.981702 1*1*1 STAT=Y PRED= 7.318 RANGE= 0.199 WIDTH(Y)= 1.215 RESP(Y)= 0.2294 HSQC= C74
01ValH45/ 1 2.312749 1*1*6 STAT=Y PRED= 2.370 RANGE= 0.307 WIDTH(Y)= 1.536 RESP(Y)= 0.1971 HSQC= C1_2
01Val_H2/ 1 2.671561 1*1*1 STAT=Y PRED= 4.169 RANGE= 0.639 WIDTH(Y)= 1.557 RESP(Y)= 0.1955 HSQC= C4
01Val_H3/ 1 2.042384 1*1*1 STAT=Y PRED= 1.952 RANGE= 0.819 WIDTH(Y)= 1.561 RESP(Y)= 0.1582 HSQC= C5
01Val_H6/ 1 0.847135 1*1*3 STAT=Y PRED= 0.509 RANGE= 0.869 WIDTH(Y)= 1.598 RESP(Y)= 0.2195 HSQC= C6
01Val_H7/ 1 0.978236 1*1*3 STAT=Y PRED= 0.818 RANGE= 0.359 WIDTH(Y)= 1.688 RESP(Y)= 0.1917 HSQC= C7
02Val_H2/ 1 4.669057 1*1*1 STAT=Y PRED= 4.508 RANGE= 0.809 WIDTH(Y)= 1.467 RESP(Y)= 0.1935 HSQC= C10
02Val_H3/ 1 2.101399 1*1*1 STAT=Y PRED= 2.155 RANGE= 0.779 WIDTH(Y)= 1.561 RESP(Y)= 0.1880 HSQC= C12
02Val_H4/ 1 0.992199 1*1*3 STAT=Y PRED= 1.038 RANGE= 0.279 WIDTH(Y)= 1.468 RESP(Y)= 0.1493 HSQC= C13
02Val_H5/ 1 1.055401 1*1*3 STAT=Y PRED= 0.943 RANGE= 0.249 WIDTH(Y)= 1.538 RESP(Y)= 0.2055 HSQC= C14
03Ile_H7/ 1 3.233925 1*1*3 STAT=Y PRED= 3.196 RANGE= 0.369 WIDTH(Y)= 1.536 RESP(Y)= 0.2005 HSQC= C15
03Ile_H2/ 1 4.918283 1*1*1 STAT=Y PRED= 4.617 RANGE= 1.628 WIDTH(Y)= 1.466 RESP(Y)= 0.1936 HSQC= C17
03Ile_H3/ 1 1.957476 1*1*1 STAT=Y PRED= 2.032 RANGE= 0.706 WIDTH(Y)= 2.929 RESP(Y)= 0.1562 HSQC= C19
03IleH4A/ 1 0.989134 1*1*1 STAT=Y PRED= 1.465 RANGE= 0.699 WIDTH(Y)= 5.275 RESP(Y)= 1.0000 HSQC= C20
03IleH4B/ 1 1.255324 1*1*1 STAT=Y PRED= 1.175 RANGE= 0.589 WIDTH(Y)= 2.795 RESP(Y)= 0.1091 HSQC= C20
03Ile_H6/ 1 0.753945 1*1*3 STAT=Y PRED= 0.723 RANGE= 0.398 WIDTH(Y)= 1.613 RESP(Y)= 0.1953 HSQC= C21
03Ile_H5/ 1 0.743889 1*1*3 STAT=Y PRED= 0.880 RANGE= 0.219 WIDTH(Y)= 1.391 RESP(Y)= 0.1663 HSQC= C22
04Thr_H2/ 1 5.166937 1*1*1 STAT=Y PRED= 4.668 RANGE= 1.016 WIDTH(Y)= 1.377 RESP(Y)= 0.1774 HSQC= C24
04Thr_H3/ 1 5.783161 1*1*1 STAT=Y PRED= 4.010 RANGE= 0.479 WIDTH(Y)= 1.941 RESP(Y)= 0.1822 HSQC= C25
04Thr_H4/ 1 1.313144 1*1*3 STAT=Y PRED= 1.270 RANGE= 0.499 WIDTH(Y)= 1.818 RESP(Y)= 0.2026 HSQC= C27
05Thr_H5/ 1 3.329509 1*1*3 STAT=Y PRED= 3.257 RANGE= 0.399 WIDTH(Y)= 1.439 RESP(Y)= 0.1781 HSQC= C29
05Thr_H2/ 1 5.017583 1*1*1 STAT=Y PRED= 4.099 RANGE= 1.025 WIDTH(Y)= 1.500 RESP(Y)= 0.1944 HSQC= C31
05Thr_H3/ 1 4.457478 1*1*1 STAT=Y PRED= 4.345 RANGE= 0.719 WIDTH(Y)= 1.572 RESP(Y)= 0.1838 HSQC= C32
05Thr_H4/ 1 0.911837 1*1*3 STAT=Y PRED= 1.252 RANGE= 0.299 WIDTH(Y)= 1.939 RESP(Y)= 0.1922 HSQC= C34
06Val_H2/ 1 4.842224 1*1*1 STAT=Y PRED= 4.525 RANGE= 1.409 WIDTH(Y)= 1.382 RESP(Y)= 0.1523 HSQC= C37
06Val_H3/ 1 2.350353 1*1*1 STAT=Y PRED= 1.975 RANGE= 1.019 WIDTH(Y)= 1.789 RESP(Y)= 0.1830 HSQC= C38
06Val_H4/ 1 1.092268 1*1*3 STAT=Y PRED= 0.938 RANGE= 0.219 WIDTH(Y)= 1.894 RESP(Y)= 0.1902 HSQC= C39
06Val_H5/ 1 0.979285 1*1*3 STAT=Y PRED= 1.094 RANGE= 0.389 WIDTH(Y)= 2.275 RESP(Y)= 0.1940 HSQC= C40
07Leu_H7/ 1 3.258856 1*1*3 STAT=Y PRED= 3.110 RANGE= 0.376 WIDTH(Y)= 1.459 RESP(Y)= 0.1758 HSQC= C42
07Leu_H2/ 1 5.110377 1*1*1 STAT=Y PRED= 5.342 RANGE= 1.085 WIDTH(Y)= 2.240 RESP(Y)= 0.1736 HSQC= C44
07LeuH3A/ 1 1.452263 1*1*1 STAT=Y PRED= 1.444 RANGE= 0.429 WIDTH(Y)= 1.805 RESP(Y)= 0.1253 HSQC= C45
07LeuH3B/ 1 1.238825 1*1*1 STAT=Y PRED= 1.914 RANGE= 0.369 WIDTH(Y)= 3.321 RESP(Y)= 0.2550 HSQC= C45
07Leu_H4/ 1 0.957012 1*1*1 STAT=Y PRED= 1.630 RANGE= 0.627 WIDTH(Y)= 1.520 RESP(Y)= 0.1513 HSQC= C46
07Leu_H5/ 1 0.330648 1*1*3 STAT=Y PRED= 0.972 RANGE= 0.316 WIDTH(Y)= 1.961 RESP(Y)= 0.1633 HSQC= C47
07Leu_H6/ 1 0.168240 1*1*3 STAT=Y PRED= 0.972 RANGE= 0.149 WIDTH(Y)= 1.885 RESP(Y)= 0.1544 HSQC= C48
08Val_H2/ 1 4.594366 1*1*1 STAT=Y PRED= 4.489 RANGE= 0.899 WIDTH(Y)= 1.578 RESP(Y)= 0.1883 HSQC= C51
08Val_H3/ 1 2.026705 1*1*1 STAT=Y PRED= 1.995 RANGE= 0.486 WIDTH(Y)= 2.872 RESP(Y)= 0.1833 HSQC= C52
08Val_H4/ 1 0.915098 1*1*3 STAT=Y PRED= 1.060 RANGE= 0.237 WIDTH(Y)= 1.731 RESP(Y)= 0.1845 HSQC= C53
08Val_H5/ 1 0.858580 1*1*3 STAT=Y PRED= 0.999 RANGE= 0.229 WIDTH(Y)= 2.065 RESP(Y)= 0.1899 HSQC= C54
09Val_H6/ 1 3.139923 1*1*3 STAT=Y PRED= 3.169 RANGE= 0.466 WIDTH(Y)= 1.931 RESP(Y)= 0.1698 HSQC= C56

Appendix G (continued)

09Val_H2/ 1 3.065448 1*1*1 STAT=Y PRED= 5.153 RANGE= 0.719 WIDTH(Y)= 2.597 RESP(Y)= 0.1650 HSQC= C58
09Val_H3/ 1 2.582945 1*1*1 STAT=Y PRED= 2.524 RANGE= 0.407 WIDTH(Y)= 1.736 RESP(Y)= 0.1528 HSQC= C59
09Val_H4/ 1 1.093807 1*1*3 STAT=Y PRED= 1.319 RANGE= 0.227 WIDTH(Y)= 1.741 RESP(Y)= 0.1953 HSQC= C60
09Val_H5/ 1 0.975890 1*1*3 STAT=Y PRED= 1.075 RANGE= 0.239 WIDTH(Y)= 2.379 RESP(Y)= 0.1859 HSQC= C61
10TrpH13/ 1 2.157320 1*1*3 STAT=Y PRED= 2.936 RANGE= 0.895 WIDTH(Y)= 1.862 RESP(Y)= 0.1713 HSQC= C63
10Trp_H2/ 1 4.102017 1*1*1 STAT=Y PRED= 5.043 RANGE= 1.765 WIDTH(Y)= 2.064 RESP(Y)= 0.1681 HSQC= C65
10TrpH3A/ 1 3.544888 1*1*1 STAT=Y PRED= 3.613 RANGE= 0.469 WIDTH(Y)= 1.516 RESP(Y)= 0.1749 HSQC= C66
10TrpH3B/ 1 3.693826 1*1*1 STAT=Y PRED= 3.367 RANGE= 0.629 WIDTH(Y)= 2.118 RESP(Y)= 0.1765 HSQC= C66
10Trp_H5/ 1 6.698373 1*1*1 STAT=Y PRED= 6.772 RANGE= 0.276 WIDTH(Y)= 1.649 RESP(Y)= 0.2013 HSQC= C68
10Trp_H9/ 1 6.441824 1*1*1 STAT=Y PRED= 7.089 RANGE= 0.219 WIDTH(Y)= 1.143 RESP(Y)= 0.2128 HSQC= C73
10Trp_H7/ 1 6.918050 1*1*1 STAT=Y PRED= 7.333 RANGE= 0.309 WIDTH(Y)= 0.719 RESP(Y)= 0.1990 HSQC= C75
10TrpH12/ 1 3.825517 1*1*3 STAT=Y PRED= 4.072 RANGE= 0.249 WIDTH(Y)= 1.244 RESP(Y)= 0.1876 HSQC= C77
11Val_H2/ 1 4.528581 1*1*1 STAT=Y PRED= 4.303 RANGE= 1.449 WIDTH(Y)= 1.849 RESP(Y)= 0.1834 HSQC= C80
11Val_H3/ 1 2.200081 1*1*1 STAT=Y PRED= 2.094 RANGE= 0.589 WIDTH(Y)= 1.854 RESP(Y)= 0.1757 HSQC= C81
11Val_H4/ 1 1.028241 1*1*3 STAT=Y PRED= 1.094 RANGE= 0.249 WIDTH(Y)= 2.106 RESP(Y)= 0.1836 HSQC= C82
11Val_H5/ 1 0.989118 1*1*3 STAT=Y PRED= 1.080 RANGE= 0.299 WIDTH(Y)= 1.787 RESP(Y)= 0.1359 HSQC= C83
12Phe_H2/ 1 4.853691 1*1*1 STAT=Y PRED= 4.499 RANGE= 0.989 WIDTH(Y)= 1.261 RESP(Y)= 0.1673 HSQC= C86
12Phe_H3/ 1 5.343847 1*1*1 STAT=Y PRED= 5.208 RANGE= 0.489 WIDTH(Y)= 1.884 RESP(Y)= 0.1897 HSQC= C87
12Phe_H5/ 1 7.239588 1*2*1 STAT=Y PRED= 7.524 RANGE= 0.309 WIDTH(Y)= 2.042 RESP(Y)= 0.2024 HSQC= C89_93
12Phe_H6/ 1 7.255487 1*2*1 STAT=Y PRED= 7.372 RANGE= 0.579 WIDTH(Y)= 1.207 RESP(Y)= 0.2038 HSQC= C90_92
12Phe_H7/ 1 7.200632 1*1*1 STAT=Y PRED= 7.281 RANGE= 0.309 WIDTH(Y)= 1.557 RESP(Y)= 0.2174 HSQC= C91
13Val_H2/ 1 4.396080 1*1*1 STAT=Y PRED= 4.169 RANGE= 0.669 WIDTH(Y)= 1.205 RESP(Y)= 0.1804 HSQC= C97
13Val_H3/ 1 1.967817 1*1*1 STAT=Y PRED= 1.935 RANGE= 0.869 WIDTH(Y)= 1.973 RESP(Y)= 0.2062 HSQC= C99
13Val_H4/ 1 0.934963 1*1*3 STAT=Y PRED= 1.277 RANGE= 0.219 WIDTH(Y)= 2.666 RESP(Y)= 0.2386 HSQC= C100
13Val_H5/ 1 0.919356 1*1*3 STAT=Y PRED= 0.933 RANGE= 0.278 WIDTH(Y)= 2.083 RESP(Y)= 0.2256 HSQC= C101

COUPLING CONSTANTS(HZ):
J115_217 7.7969 J 10Trp_H8 10Trp_H9 STAT=Y PRED= 8.100 RANGE= 0.890
J115_218 8.1808 J 10Trp_H8 10Trp_H7 STAT=Y PRED= 7.850 RANGE= 0.800
J122_123 9.1737 J 01Val_H2 01Val_H3 STAT=Y PRED= 12.510 RANGE= 4.000
J123_124 6.5890 J 01Val_H3 01Val_H6 STAT=Y PRED= 6.640 RANGE= 0.200
J123_127 6.6205 J 01Val_H3 01Val_H7 STAT=Y PRED= 6.640 RANGE= 0.200
J131_132 8.7545 J 02Val_H2 02Val_H3 STAT=Y PRED= 12.600 RANGE= 6.000
J132_133 6.7841 J 02Val_H3 02Val_H4 STAT=Y PRED= 6.640 RANGE= 0.200
J132_136 6.7206 J 02Val_H3 02Val_H5 STAT=Y PRED= 6.640 RANGE= 0.200
J142_143 11.2297 J 03Ile_H2 03Ile_H3 STAT=Y PRED= 13.150 RANGE= 4.000
J143_144 0.4614 J 03Ile_H3 03IleH4A STAT=Y PRED= 1.950 RANGE= 3.000
J143_145 2.9276 J 03Ile_H3 03IleH4B STAT=Y PRED= 12.660 RANGE= 2.800
J143_146 6.6276 J 03Ile_H3 03Ile_H6 STAT=Y PRED= 6.640 RANGE= 0.200
J144_145 -12.2168 J 03IleH4A 03IleH4B STAT=Y PRED= -13.400 RANGE= 0.600
J144_149 7.2855 J 03IleH4A 03Ile_H5 STAT=Y PRED= 7.440 RANGE= 0.150
J145_149 7.6340 J 03IleH4B 03Ile_H5 STAT=Y PRED= 7.440 RANGE= 0.150
J153_154 2.3441 J 04Thr_H2 04Thr_H3 STAT=Y PRED= 2.690 RANGE= 6.600
J154_155 6.5134 J 04Thr_H3 04Thr_H4 STAT=Y PRED= 6.250 RANGE= 0.600
J161_162 3.7259 J 05Thr_H2 05Thr_H3 STAT=Y PRED= 2.440 RANGE= 4.400
J162_164 6.4691 J 05Thr_H3 05Thr_H4 STAT=Y PRED= 6.250 RANGE= 0.600
J168_169 8.9180 J 06Val_H2 06Val_H3 STAT=Y PRED= 2.980 RANGE= 6.600
J169_170 6.6944 J 06Val_H3 06Val_H4 STAT=Y PRED= 6.640 RANGE= 0.200
J169_173 7.0316 J 06Val_H3 06Val_H5 STAT=Y PRED= 6.640 RANGE= 0.200
J179_180 6.2437 J 07Leu_H2 07LeuH3A STAT=Y PRED= 3.040 RANGE= 6.000

Appendix G (continued)

```
 J179_181    8.3839   J 07Leu_H2 07LeuH3B   STAT=Y  PRED= 13.950 RANGE= 4.000
 J180_181  -13.3047   J 07LeuH3A 07LeuH3B   STAT=Y  PRED= -14.710 RANGE= 1.600
 J180_182    8.2119   J 07LeuH3A 07Leu_H4   STAT=Y  PRED= 12.990 RANGE= 2.560
 J181_182    5.7896   J 07LeuH3B 07Leu_H4   STAT=Y  PRED= 2.270 RANGE= 3.000
 J182_183    6.5482   J 07Leu_H4 07Leu_H5   STAT=Y  PRED= 6.640 RANGE= 0.200
 J182_186    6.5879   J 07Leu_H4 07Leu_H6   STAT=Y  PRED= 6.640 RANGE= 0.200
 J190_191    8.8736   J 08Val_H2 08Val_H3   STAT=Y  PRED= 12.880 RANGE= 6.000
 J191_192    6.5520   J 08Val_H3 08Val_H4   STAT=Y  PRED= 6.640 RANGE= 0.200
 J191_195    6.7834   J 08Val_H3 08Val_H5   STAT=Y  PRED= 6.640 RANGE= 0.200
 J201_202    7.6281   J 09Val_H2 09Val_H3   STAT=Y  PRED= 12.960 RANGE= 4.000
 J202_203    6.4961   J 09Val_H3 09Val_H4   STAT=Y  PRED= 6.640 RANGE= 0.200
 J202_206    6.7760   J 09Val_H3 09Val_H5   STAT=Y  PRED= 6.640 RANGE= 0.200
 J212_213   11.1630   J 10Trp_H2 10TrpH3A   STAT=Y  PRED= 12.890 RANGE= 4.000
 J212_214    4.7143   J 10Trp_H2 10TrpH3B   STAT=Y  PRED= 1.900 RANGE= 4.400
 J213_214  -13.7295   J 10TrpH3A 10TrpH3B   STAT=Y  PRED= -16.760 RANGE= 2.560
 J215_218    0.4880   J 10Trp_H5 10Trp_H7   STAT=Y  PRED= -0.300 RANGE= 0.500
 J217_218    0.6708   J 10Trp_H9 10Trp_H7   STAT=Y  PRED= 1.020 RANGE= 1.200
 J223_224    7.9094   J 11Val_H2 11Val_H3   STAT=Y  PRED= 3.450 RANGE= 9.000
 J224_225    6.7483   J 11Val_H3 11Val_H4   STAT=Y  PRED= 6.640 RANGE= 0.200
 J224_228    6.8064   J 11Val_H3 11Val_H5   STAT=Y  PRED= 6.640 RANGE= 0.200
 J232_233    1.9005   J 12Phe_H2 12Phe_H3   STAT=Y  PRED= 1.900 RANGE= 6.600
 J234_238    1.3335   J 12Phe_H5 12Phe_H5   STAT=Y  PRED= 1.980 RANGE= 1.200
 J234_235    7.6508   J 12Phe_H5 12Phe_H6   STAT=Y  PRED= 7.660 RANGE= 0.340
 J234_237    0.7769   J 12Phe_H6 12Phe_H5   STAT=Y  PRED= 0.550 RANGE= 0.750
 J234_236    1.2760   J 12Phe_H5 12Phe_H7   STAT=Y  PRED= 1.260 RANGE= 1.200
 J235_237    1.7027   J 12Phe_H6 12Phe_H6   STAT=Y  PRED= 1.480 RANGE= 1.200
 J235_236    7.4760   J 12Phe_H6 12Phe_H7   STAT=Y  PRED= 7.400 RANGE= 0.240
 J241_242    8.8924   J 13Val_H2 13Val_H3   STAT=Y  PRED= 12.320 RANGE= 6.000
 J242_243    6.8372   J 13Val_H3 13Val_H4   STAT=Y  PRED= 6.640 RANGE= 0.200
 J242_246    6.4162   J 13Val_H3 13Val_H5   STAT=Y  PRED= 6.640 RANGE= 0.200

CONTROL PARAMETERS:
      Solvent =  none (def. 99% enriched)
        1.000 =  Concentration (vol%, def=1.0%)
   0.00100000 =  Minimum line-intensity
   0.00100000 =  Diagonalization criterium (not in use)
  11.63298470 =  Left frequency (ppm)
  -4.33373638 =  Right frequency (ppm)
        0.000 =  Acquisition time (s, for QMTLS)
        0.715 =  Line-width (for modes D, P & T, 0=use defaults)
  0.103379714 =  Data-point resolution (Hz)
       28.306 =  GAUSSIAN (%, 0=use default from INF)
      -10.087 =  Dispersion contribution (%, 0=use default from INF)
   0.00000000 =  Decoupling frequency (for DORES)

CONSTRAINTS (in equations X0 = 1.0)...use no empty lines
 EQUAL 01Val_H2 = 13Val_H2
 EQUAL 06Val_H5 = 11Val_H4
 EQUAL 07Leu_H5 = 07Leu_H6
 IGNORE(HZ):   940.350 to   936.356
```

Appendix G (continued)

IGNORE(HZ): 2062.779 to 2027.293
IGNORE(HZ): 1175.285 to 1149.842
IGNORE(HZ): 1232.768 to 1209.210
IGNORE(HZ): 5188.061 to 5161.182
IGNORE(HZ): 4803.141 to 4787.420
IGNORE(HZ): 812.060 to 780.231

END of FILE

Appendix H. The improved pseudo HiFSA profile of deoxyecumicin.

* NEW: the lines beginning by * are comment lines !
* To keep all the chemical shifts fixed during iteration
* replace "CHEMICAL SHIFTS(HZ):" by "..SHIFTS(HZ): fixed"
* The couplings can be fixed in the same way

NMR-data: C:\Users\jgnapo_2\Desktop\Wei_H14_XRays\H14_withoutGO
#$œ Date 5. 3.2014; Time 5:32:40 perch.pms

CHEMICAL SHIFTS(PPM):
PROTON 2*SPIN= 1 SPECIES=1H POPULATION(Y)= 0.64679
10Trp_H8/ 1 6.983053 1*1*1 STAT=Y PRED= 7.318 RANGE= 0.197 WIDTH(Y)= 2.918 RESP(Y)= 0.0950 HSQC= C74
01ValH45/ 1 2.313729 1*1*6 STAT=Y PRED= 2.370 RANGE= 0.307 WIDTH(Y)= 2.374 RESP(Y)= 0.1269 HSQC= C1_2
01Val_H2/ 1 2.667577 1*1*1 STAT=Y PRED= 4.169 RANGE= 0.637 WIDTH(Y)= 2.140 RESP(Y)= 0.1182 HSQC= C4
01Val_H3/ 1 2.050022 1*1*1 STAT=Y PRED= 1.952 RANGE= 0.815 WIDTH(Y)= 2.950 RESP(Y)= 0.1124 HSQC= C5
01Val_H6/ 1 0.851269 1*1*3 STAT=Y PRED= 0.509 RANGE= 0.865 WIDTH(Y)= 3.418 RESP(Y)= 0.1182 HSQC= C6
01Val_H7/ 1 0.981248 1*1*3 STAT=Y PRED= 0.818 RANGE= 0.357 WIDTH(Y)= 2.537 RESP(Y)= 0.1144 HSQC= C7
02Val_H2/ 1 4.673890 1*1*1 STAT=Y PRED= 4.508 RANGE= 0.805 WIDTH(Y)= 4.074 RESP(Y)= 0.1462 HSQC= C10
02Val_H3/ 1 2.085055 1*1*1 STAT=Y PRED= 2.155 RANGE= 0.775 WIDTH(Y)= 2.449 RESP(Y)= 0.1053 HSQC= C12
02Val_H4/ 1 0.982708 1*1*3 STAT=Y PRED= 1.038 RANGE= 0.277 WIDTH(Y)= 2.759 RESP(Y)= 0.1228 HSQC= C13
02Val_H5/ 1 1.045184 1*1*3 STAT=Y PRED= 0.943 RANGE= 0.247 WIDTH(Y)= 2.640 RESP(Y)= 0.1342 HSQC= C14
03Ile_H7/ 1 3.227709 1*1*3 STAT=Y PRED= 3.196 RANGE= 0.367 WIDTH(Y)= 2.776 RESP(Y)= 0.1592 HSQC= C15
03Ile_H2/ 1 4.944549 1*1*1 STAT=Y PRED= 4.617 RANGE= 1.628 WIDTH(Y)= 1.993 RESP(Y)= 0.0997 HSQC= C17
03Ile_H3/ 1 1.938019 1*1*1 STAT=Y PRED= 2.032 RANGE= 0.705 WIDTH(Y)= 3.112 RESP(Y)= 0.1704 HSQC= C19
03IleH4A/ 1 0.924796 1*1*1 STAT=Y PRED= 1.465 RANGE= 0.697 WIDTH(Y)= 5.496 RESP(Y)= 0.9453 HSQC= C20
03IleH4B/ 1 1.301495 1*1*1 STAT=Y PRED= 1.175 RANGE= 0.587 WIDTH(Y)= 3.721 RESP(Y)= 0.3274 HSQC= C20
03Ile_H6/ 1 0.753003 1*1*3 STAT=Y PRED= 0.723 RANGE= 0.397 WIDTH(Y)= 3.460 RESP(Y)= 0.1267 HSQC= C21
03Ile_H5/ 1 0.723527 1*1*3 STAT=Y PRED= 0.880 RANGE= 0.217 WIDTH(Y)= 2.511 RESP(Y)= 0.1077 HSQC= C22
04Thr_H2/ 1 5.133407 1*1*1 STAT=Y PRED= 4.668 RANGE= 1.015 WIDTH(Y)= 2.338 RESP(Y)= 0.1201 HSQC= C24
04Thr_H3/ 1 5.783119 1*1*1 STAT=Y PRED= 4.010 RANGE= 0.477 WIDTH(Y)= 3.356 RESP(Y)= 0.0954 HSQC= C25
04Thr_H4/ 1 1.314106 1*1*3 STAT=Y PRED= 1.270 RANGE= 0.497 WIDTH(Y)= 2.339 RESP(Y)= 0.1237 HSQC= C27
05Thr_H5/ 1 3.320271 1*1*3 STAT=Y PRED= 3.257 RANGE= 0.397 WIDTH(Y)= 2.864 RESP(Y)= 0.1330 HSQC= C29
05Thr_H2/ 1 5.027764 1*1*1 STAT=Y PRED= 4.099 RANGE= 1.025 WIDTH(Y)= 2.437 RESP(Y)= 0.1146 HSQC= C31
05Thr_H3/ 1 4.434703 1*1*1 STAT=Y PRED= 4.345 RANGE= 0.717 WIDTH(Y)= 2.793 RESP(Y)= 0.1177 HSQC= C32
05Thr_H4/ 1 0.885803 1*1*3 STAT=Y PRED= 1.252 RANGE= 0.297 WIDTH(Y)= 3.099 RESP(Y)= 0.1331 HSQC= C34
06Val_H2/ 1 4.825834 1*1*1 STAT=Y PRED= 4.525 RANGE= 1.405 WIDTH(Y)= 5.324 RESP(Y)= 0.1511 HSQC= C37
06Val_H3/ 1 2.363811 1*1*1 STAT=Y PRED= 1.975 RANGE= 1.015 WIDTH(Y)= 3.643 RESP(Y)= 0.1139 HSQC= C38
06Val_H4/ 1 1.096438 1*1*3 STAT=Y PRED= 0.938 RANGE= 0.217 WIDTH(Y)= 3.235 RESP(Y)= 0.0950 HSQC= C39
06Val_H5/ 1 0.981084 1*1*3 STAT=Y PRED= 1.094 RANGE= 0.387 WIDTH(Y)= 3.327 RESP(Y)= 0.1145 HSQC= C40
07Leu_H7/ 1 3.263047 1*1*3 STAT=Y PRED= 3.110 RANGE= 0.375 WIDTH(Y)= 2.476 RESP(Y)= 0.1144 HSQC= C42
07Leu_H2/ 1 5.168766 1*1*1 STAT=Y PRED= 5.342 RANGE= 1.085 WIDTH(Y)= 2.976 RESP(Y)= 0.1164 HSQC= C44
07LeuH3A/ 1 1.426201 1*1*1 STAT=Y PRED= 1.444 RANGE= 0.427 WIDTH(Y)= 2.845 RESP(Y)= 0.0645 HSQC= C45
07LeuH3B/ 1 1.263367 1*1*1 STAT=Y PRED= 1.914 RANGE= 0.367 WIDTH(Y)= 3.300 RESP(Y)= 0.0250 HSQC= C45
07Leu_H4/ 1 0.929673 1*1*1 STAT=Y PRED= 1.630 RANGE= 0.627 WIDTH(Y)= 0.635 RESP(Y)= 0.0262 HSQC= C46
07Leu_H5/ 1 0.321895 1*1*3 STAT=Y PRED= 0.972 RANGE= 0.315 WIDTH(Y)= 2.804 RESP(Y)= 0.0994 HSQC= C47
07Leu_H6/ 1 0.224427 1*1*3 STAT=Y PRED= 0.972 RANGE= 0.147 WIDTH(Y)= 2.934 RESP(Y)= 0.1019 HSQC= C48
08Val_H2/ 1 4.601908 1*1*1 STAT=Y PRED= 4.489 RANGE= 0.895 WIDTH(Y)= 2.859 RESP(Y)= 0.0784 HSQC= C51
08Val_H3/ 1 2.035456 1*1*1 STAT=Y PRED= 1.995 RANGE= 0.485 WIDTH(Y)= 2.821 RESP(Y)= 0.0823 HSQC= C52
08Val_H4/ 1 0.905401 1*1*3 STAT=Y PRED= 1.060 RANGE= 0.237 WIDTH(Y)= 5.457 RESP(Y)= 0.0482 HSQC= C53
08Val_H5/ 1 0.867810 1*1*3 STAT=Y PRED= 0.999 RANGE= 0.227 WIDTH(Y)= 3.597 RESP(Y)= 0.1328 HSQC= C54

Appendix H (continued)

09Val_H6/ 1 3.146274 1*1*3 STAT=Y PRED= 3.169 RANGE= 0.465 WIDTH(Y)= 2.526 RESP(Y)= 0.1119 HSQC= C56
09Val_H2/ 1 3.054073 1*1*1 STAT=Y PRED= 5.153 RANGE= 0.717 WIDTH(Y)= 3.037 RESP(Y)= 0.1144 HSQC= C58
09Val_H3/ 1 2.593761 1*1*1 STAT=Y PRED= 2.524 RANGE= 0.407 WIDTH(Y)= 2.512 RESP(Y)= 0.0810 HSQC= C59
09Val_H4/ 1 1.097701 1*1*3 STAT=Y PRED= 1.319 RANGE= 0.227 WIDTH(Y)= 5.464 RESP(Y)= 0.0726 HSQC= C60
09Val_H5/ 1 0.976341 1*1*3 STAT=Y PRED= 1.075 RANGE= 0.237 WIDTH(Y)= 3.101 RESP(Y)= 0.0961 HSQC= C61
10TrpH13/ 1 2.165324 1*1*3 STAT=Y PRED= 2.936 RANGE= 0.895 WIDTH(Y)= 2.521 RESP(Y)= 0.1165 HSQC= C63
10Trp_H2/ 1 4.094748 1*1*1 STAT=Y PRED= 5.043 RANGE= 1.765 WIDTH(Y)= 2.790 RESP(Y)= 0.0653 HSQC= C65
10TrpH3A/ 1 3.545626 1*1*1 STAT=Y PRED= 3.613 RANGE= 0.467 WIDTH(Y)= 3.303 RESP(Y)= -0.0090 HSQC= C66
10TrpH3B/ 1 3.690903 1*1*1 STAT=Y PRED= 3.367 RANGE= 0.627 WIDTH(Y)= 2.655 RESP(Y)= 0.0939 HSQC= C66
10Trp_H5/ 1 6.699103 1*1*1 STAT=Y PRED= 6.772 RANGE= 0.275 WIDTH(Y)= 2.961 RESP(Y)= 0.0950 HSQC= C68
10Trp_H9/ 1 6.442889 1*1*1 STAT=Y PRED= 7.089 RANGE= 0.217 WIDTH(Y)= 3.286 RESP(Y)= 0.0964 HSQC= C73
10Trp_H7/ 1 6.921954 1*1*1 STAT=Y PRED= 7.333 RANGE= 0.307 WIDTH(Y)= 2.283 RESP(Y)= 0.0883 HSQC= C75
10TrpH12/ 1 3.818211 1*1*3 STAT=Y PRED= 4.072 RANGE= 0.247 WIDTH(Y)= 2.165 RESP(Y)= 0.1143 HSQC= C77
11Val_H2/ 1 4.368919 1*1*1 STAT=Y PRED= 4.303 RANGE= 1.445 WIDTH(Y)= 2.482 RESP(Y)= 0.0966 HSQC= C80
11Val_H3/ 1 2.195172 1*1*1 STAT=Y PRED= 2.094 RANGE= 0.587 WIDTH(Y)= 3.768 RESP(Y)= 0.1307 HSQC= C81
11Val_H4/ 1 1.026649 1*1*3 STAT=Y PRED= 1.094 RANGE= 0.247 WIDTH(Y)= 3.019 RESP(Y)= 0.1535 HSQC= C82
11Val_H5/ 1 0.984184 1*1*3 STAT=Y PRED= 1.080 RANGE= 0.297 WIDTH(Y)= 3.657 RESP(Y)= 0.1309 HSQC= C83
12Phe_H2/ 1 4.797430 1*1*1 STAT=Y PRED= 4.499 RANGE= 0.985 WIDTH(Y)= 8.795 RESP(Y)= 0.0137 HSQC= C86
12Phe_H3/ 1 5.339936 1*1*1 STAT=Y PRED= 5.208 RANGE= 0.487 WIDTH(Y)= 2.981 RESP(Y)= 0.1367 HSQC= C87
12Phe_H5/ 1 7.092651 1*2*1 STAT=Y PRED= 7.524 RANGE= 0.307 WIDTH(Y)= 2.752 RESP(Y)= 0.1357 HSQC= C89_93
12Phe_H6/ 1 7.202430 1*2*1 STAT=Y PRED= 7.372 RANGE= 0.577 WIDTH(Y)= 2.201 RESP(Y)= 0.1383 HSQC= C90_92
12Phe_H7/ 1 7.149465 1*1*1 STAT=Y PRED= 7.281 RANGE= 0.307 WIDTH(Y)= 2.457 RESP(Y)= 0.1310 HSQC= C91
13Val_H2/ 1 4.406966 1*1*1 STAT=Y PRED= 4.169 RANGE= 0.667 WIDTH(Y)= 3.030 RESP(Y)= 0.1506 HSQC= C97
13Val_H3/ 1 1.969060 1*1*1 STAT=Y PRED= 1.935 RANGE= 0.865 WIDTH(Y)= 3.185 RESP(Y)= 1.0000 HSQC= C99
13Val_H4/ 1 0.936791 1*1*3 STAT=Y PRED= 1.277 RANGE= 0.217 WIDTH(Y)= 4.983 RESP(Y)= 0.0408 HSQC= C100
13Val_H5/ 1 0.920725 1*1*3 STAT=Y PRED= 0.933 RANGE= 0.277 WIDTH(Y)= 2.396 RESP(Y)= 0.0898 HSQC= C101
PROTON 2*SPIN= 1 SPECIES=1H POPULATION(Y)= 0.35321
10Y_H8 / 2 6.981128 1*1*1 STAT=Y PRED= 7.318 RANGE= 0.197 WIDTH(Y)= 1.362 RESP(Y)= 0.1077 HSQC= 2C74
01VH45 / 2 2.316357 1*1*6 STAT=Y PRED= 2.370 RANGE= 0.307 WIDTH(Y)= 2.312 RESP(Y)= 0.0837 HSQC= 2C1_2
01V_H2 / 2 2.670690 1*1*1 STAT=Y PRED= 4.169 RANGE= 0.637 WIDTH(Y)= 2.428 RESP(Y)= 0.0649 HSQC= 2C4
01V_H3 / 2 2.042286 1*1*1 STAT=Y PRED= 1.952 RANGE= 0.815 WIDTH(Y)= 2.318 RESP(Y)= 0.1573 HSQC= 2C5
01V_H6 / 2 0.847521 1*1*3 STAT=Y PRED= 0.509 RANGE= 0.865 WIDTH(Y)= 4.120 RESP(Y)= 0.1144 HSQC= 2C6
01V_H7 / 2 0.979456 1*1*3 STAT=Y PRED= 0.818 RANGE= 0.357 WIDTH(Y)= 1.806 RESP(Y)= 0.0934 HSQC= 2C7
02V_H2 / 2 4.672940 1*1*1 STAT=Y PRED= 4.508 RANGE= 0.805 WIDTH(Y)= 1.704 RESP(Y)= 0.0590 HSQC= 2C10
02V_H3 / 2 2.102035 1*1*1 STAT=Y PRED= 2.155 RANGE= 0.775 WIDTH(Y)= 2.216 RESP(Y)= 0.0766 HSQC= 2C12
02V_H4 / 2 1.001765 1*1*3 STAT=Y PRED= 1.038 RANGE= 0.277 WIDTH(Y)= 4.785 RESP(Y)= 0.0968 HSQC= 2C13
02V_H5 / 2 1.054994 1*1*3 STAT=Y PRED= 0.943 RANGE= 0.247 WIDTH(Y)= 1.835 RESP(Y)= 0.0425 HSQC= 2C14
03I_H7 / 2 3.227585 1*1*3 STAT=Y PRED= 3.196 RANGE= 0.367 WIDTH(Y)= 4.020 RESP(Y)= 0.0410 HSQC= 2C15
03I_H2 / 2 4.917218 1*1*1 STAT=Y PRED= 4.617 RANGE= 1.628 WIDTH(Y)= 1.218 RESP(Y)= 0.0198 HSQC= 2C17
03I_H3 / 2 1.966822 1*1*1 STAT=Y PRED= 2.032 RANGE= 0.705 WIDTH(Y)= 3.820 RESP(Y)= 1.0000 HSQC= 2C19
03IH4A / 2 0.961339 1*1*1 STAT=Y PRED= 1.465 RANGE= 0.697 WIDTH(Y)= 5.241 RESP(Y)= 0.4654 HSQC= 2C20
03IH4B / 2 1.258661 1*1*1 STAT=Y PRED= 1.175 RANGE= 0.587 WIDTH(Y)= 2.889 RESP(Y)= 0.1943 HSQC= 2C20
03I_H6 / 2 0.750814 1*1*3 STAT=Y PRED= 0.723 RANGE= 0.397 WIDTH(Y)= 1.500 RESP(Y)= 0.0724 HSQC= 2C21
03I_H5 / 2 0.752205 1*1*3 STAT=Y PRED= 0.880 RANGE= 0.217 WIDTH(Y)= 4.341 RESP(Y)= 0.0972 HSQC= 2C22
04T_H2 / 2 5.166397 1*1*1 STAT=Y PRED= 4.668 RANGE= 1.015 WIDTH(Y)= 1.968 RESP(Y)= 0.0520 HSQC= 2C24
04T_H3 / 2 5.783803 1*1*1 STAT=Y PRED= 4.010 RANGE= 0.477 WIDTH(Y)= 3.202 RESP(Y)= 0.1104 HSQC= 2C25
04T_H4 / 2 1.316886 1*1*3 STAT=Y PRED= 1.270 RANGE= 0.497 WIDTH(Y)= 2.401 RESP(Y)= 0.0773 HSQC= 2C27
05T_H5 / 2 3.326836 1*1*3 STAT=Y PRED= 3.257 RANGE= 0.397 WIDTH(Y)= 5.251 RESP(Y)= 0.1276 HSQC= 2C29
05T_H2 / 2 5.011839 1*1*1 STAT=Y PRED= 4.099 RANGE= 1.025 WIDTH(Y)= 4.062 RESP(Y)= 0.0389 HSQC= 2C31
05T_H3 / 2 4.452619 1*1*1 STAT=Y PRED= 4.345 RANGE= 0.717 WIDTH(Y)= 3.220 RESP(Y)= 0.1222 HSQC= 2C32

Appendix H (continued)

```
05T_H4  / 2    0.915828  1*1*3  STAT=Y  PRED= 1.252 RANGE= 0.297 WIDTH(Y)= 2.010 RESP(Y)= 0.0685 HSQC= 2C34
06V_H2  / 2    4.847775  1*1*1  STAT=Y  PRED= 4.525 RANGE= 1.405 WIDTH(Y)= 5.287 RESP(Y)= 0.2609 HSQC= 2C37
06V_H3  / 2    2.348346  1*1*1  STAT=Y  PRED= 1.975 RANGE= 1.015 WIDTH(Y)= 2.039 RESP(Y)= 0.0383 HSQC= 2C38
06V_H4  / 2    1.094360  1*1*3  STAT=Y  PRED= 0.938 RANGE= 0.217 WIDTH(Y)= 1.431 RESP(Y)= 0.0937 HSQC= 2C39
06V_H5  / 2    0.975087  1*1*3  STAT=Y  PRED= 1.094 RANGE= 0.387 WIDTH(Y)= 2.216 RESP(Y)= 0.1134 HSQC= 2C40
07L_H7  / 2    3.256784  1*1*3  STAT=Y  PRED= 3.110 RANGE= 0.375 WIDTH(Y)= 2.112 RESP(Y)= 0.0273 HSQC= 2C42
07L_H2  / 2    5.107801  1*1*1  STAT=Y  PRED= 5.342 RANGE= 1.085 WIDTH(Y)= 2.095 RESP(Y)= 0.0187 HSQC= 2C44
07LH3A  / 2    1.453160  1*1*1  STAT=Y  PRED= 1.444 RANGE= 0.427 WIDTH(Y)= 1.776 RESP(Y)= -0.0322 HSQC= 2C45
07LH3B  / 2    1.233198  1*1*1  STAT=Y  PRED= 1.914 RANGE= 0.367 WIDTH(Y)= 3.329 RESP(Y)= 0.0476 HSQC= 2C45
07L_H4  / 2    0.959553  1*1*1  STAT=Y  PRED= 1.630 RANGE= 0.627 WIDTH(Y)= 1.082 RESP(Y)= 0.0916 HSQC= 2C46
07L_H5  / 2    0.333644  1*1*3  STAT=Y  PRED= 0.972 RANGE= 0.315 WIDTH(Y)= 3.344 RESP(Y)= 0.0304 HSQC= 2C47
07L_H6  / 2    0.183852  1*1*3  STAT=Y  PRED= 0.972 RANGE= 0.147 WIDTH(Y)= 3.257 RESP(Y)= 0.0424 HSQC= 2C48
08V_H2  / 2    4.585484  1*1*1  STAT=Y  PRED= 4.489 RANGE= 0.895 WIDTH(Y)= 2.825 RESP(Y)= 0.1093 HSQC= 2C51
08V_H3  / 2    2.027966  1*1*1  STAT=Y  PRED= 1.995 RANGE= 0.485 WIDTH(Y)= 2.883 RESP(Y)= 0.0132 HSQC= 2C52
08V_H4  / 2    0.914194  1*1*3  STAT=Y  PRED= 1.060 RANGE= 0.237 WIDTH(Y)= 1.405 RESP(Y)= 0.0548 HSQC= 2C53
08V_H5  / 2    0.850989  1*1*3  STAT=Y  PRED= 0.999 RANGE= 0.227 WIDTH(Y)= 2.119 RESP(Y)= 0.0754 HSQC= 2C54
09V_H6  / 2    3.139138  1*1*3  STAT=Y  PRED= 3.169 RANGE= 0.465 WIDTH(Y)= 2.316 RESP(Y)= 0.0307 HSQC= 2C56
09V_H2  / 2    3.069536  1*1*1  STAT=Y  PRED= 5.153 RANGE= 0.717 WIDTH(Y)= 2.567 RESP(Y)= 0.0053 HSQC= 2C58
09V_H3  / 2    2.583162  1*1*1  STAT=Y  PRED= 2.524 RANGE= 0.407 WIDTH(Y)= 1.843 RESP(Y)= 0.0169 HSQC= 2C59
09V_H4  / 2    1.095853  1*1*3  STAT=Y  PRED= 1.319 RANGE= 0.227 WIDTH(Y)= 1.796 RESP(Y)= 0.1107 HSQC= 2C60
09V_H5  / 2    0.977932  1*1*3  STAT=Y  PRED= 1.075 RANGE= 0.237 WIDTH(Y)= 1.536 RESP(Y)= 0.0873 HSQC= 2C61
10YH13  / 2    2.158367  1*1*3  STAT=Y  PRED= 2.936 RANGE= 0.895 WIDTH(Y)= 2.136 RESP(Y)= 0.0317 HSQC= 2C63
10Y_H2  / 2    4.095302  1*1*1  STAT=Y  PRED= 5.043 RANGE= 1.765 WIDTH(Y)= 2.597 RESP(Y)= 0.0913 HSQC= 2C65
10YH3A  / 2    3.547008  1*1*1  STAT=Y  PRED= 3.613 RANGE= 0.467 WIDTH(Y)= 2.191 RESP(Y)= 0.2121 HSQC= 2C66
10YH3B  / 2    3.696022  1*1*1  STAT=Y  PRED= 3.367 RANGE= 0.627 WIDTH(Y)= 2.734 RESP(Y)= 0.0558 HSQC= 2C66
10Y_H5  / 2    6.697081  1*1*1  STAT=Y  PRED= 6.772 RANGE= 0.275 WIDTH(Y)= 1.582 RESP(Y)= 0.0880 HSQC= 2C68
10Y_H9  / 2    6.439998  1*1*1  STAT=Y  PRED= 7.089 RANGE= 0.217 WIDTH(Y)= 1.251 RESP(Y)= 0.0951 HSQC= 2C73
10Y_H7  / 2    6.920387  1*1*1  STAT=Y  PRED= 7.333 RANGE= 0.307 WIDTH(Y)= 0.777 RESP(Y)= 0.0925 HSQC= 2C75
10YH12  / 2    3.828094  1*1*3  STAT=Y  PRED= 4.072 RANGE= 0.247 WIDTH(Y)= 2.057 RESP(Y)= 0.0490 HSQC= 2C77
11V_H2  / 2    4.526543  1*1*1  STAT=Y  PRED= 4.303 RANGE= 1.445 WIDTH(Y)= 6.717 RESP(Y)= 0.1385 HSQC= 2C80
11V_H3  / 2    2.202340  1*1*1  STAT=Y  PRED= 2.094 RANGE= 0.587 WIDTH(Y)= 1.475 RESP(Y)= -0.0067 HSQC= 2C81
11V_H4  / 2    1.027215  1*1*3  STAT=Y  PRED= 1.094 RANGE= 0.247 WIDTH(Y)= 1.062 RESP(Y)= -0.0235 HSQC= 2C82
11V_H5  / 2    0.995323  1*1*3  STAT=Y  PRED= 1.080 RANGE= 0.297 WIDTH(Y)= 3.467 RESP(Y)= 0.1087 HSQC= 2C83
12F_H2  / 2    4.866963  1*1*1  STAT=Y  PRED= 4.499 RANGE= 0.985 WIDTH(Y)= 1.271 RESP(Y)= 0.0288 HSQC= 2C86
12F_H3  / 2    5.339936  1*1*1  STAT=Y  PRED= 5.208 RANGE= 0.487 WIDTH(Y)= 2.981 RESP(Y)= 0.1089 HSQC= 2C87
12F_H5  / 2    7.242205  1*2*1  STAT=Y  PRED= 7.524 RANGE= 0.307 WIDTH(Y)= 6.488 RESP(Y)= 0.1056 HSQC= 2C89_93
12F_H6  / 2    7.254230  1*2*1  STAT=Y  PRED= 7.372 RANGE= 0.577 WIDTH(Y)= 1.301 RESP(Y)= 0.0525 HSQC= 2C90_92
12F_H7  / 2    7.200270  1*1*1  STAT=Y  PRED= 7.281 RANGE= 0.307 WIDTH(Y)= 4.125 RESP(Y)= 0.0478 HSQC= 2C91
13V_H2  / 2    4.400648  1*1*1  STAT=Y  PRED= 4.169 RANGE= 0.667 WIDTH(Y)= 1.648 RESP(Y)= -0.0065 HSQC= 2C97
13V_H3  / 2    1.969265  1*1*1  STAT=Y  PRED= 1.935 RANGE= 0.865 WIDTH(Y)= 2.788 RESP(Y)= -2.3800 HSQC= 2C99
13V_H4  / 2    0.936823  1*1*3  STAT=Y  PRED= 1.277 RANGE= 0.217 WIDTH(Y)= 2.537 RESP(Y)= 0.0982 HSQC= 2C100
13V_H5  / 2    0.919067  1*1*3  STAT=Y  PRED= 0.933 RANGE= 0.277 WIDTH(Y)= 1.735 RESP(Y)= 0.0798 HSQC= 2C101

COUPLING CONSTANTS(HZ): fixed
J115_217   7.7969   J 10Trp_H8 10Trp_H9   STAT=Y  PRED= 8.100 RANGE= 0.890
J115_218   8.1808   J 10Trp_H8 10Trp_H7   STAT=Y  PRED= 7.850 RANGE= 0.800
J122_123   9.1737   J 01Val_H2 01Val_H3   STAT=Y  PRED= 12.510 RANGE= 4.000
J123_124   6.5890   J 01Val_H3 01Val_H6   STAT=Y  PRED= 6.640 RANGE= 0.200
J123_127   6.6205   J 01Val_H3 01Val_H7   STAT=Y  PRED= 6.640 RANGE= 0.200
J131_132   8.7545   J 02Val_H2 02Val_H3   STAT=Y  PRED= 12.600 RANGE= 6.000
```

Appendix H (continued)

J132_133 6.7841 J 02Val_H3 02Val_H4 STAT=Y PRED= 6.640 RANGE= 0.200
J132_136 6.7206 J 02Val_H3 02Val_H5 STAT=Y PRED= 6.640 RANGE= 0.200
J142_143 11.2297 J 03Ile_H2 03Ile_H3 STAT=Y PRED= 13.150 RANGE= 4.000
J143_144 0.4614 J 03Ile_H3 03IleH4A STAT=Y PRED= 1.950 RANGE= 3.000
J143_145 2.9276 J 03Ile_H3 03IleH4B STAT=Y PRED= 12.660 RANGE= 2.800
J143_146 6.6276 J 03Ile_H3 03Ile_H6 STAT=Y PRED= 6.640 RANGE= 0.200
J144_145 -12.2168 J 03IleH4A 03IleH4B STAT=Y PRED= -13.400 RANGE= 0.600
J144_149 7.2855 J 03IleH4A 03Ile_H5 STAT=Y PRED= 7.440 RANGE= 0.150
J145_149 7.6340 J 03IleH4B 03Ile_H5 STAT=Y PRED= 7.440 RANGE= 0.150
J153_154 2.3441 J 04Thr_H2 04Thr_H3 STAT=Y PRED= 2.690 RANGE= 6.600
J154_155 6.5134 J 04Thr_H3 04Thr_H4 STAT=Y PRED= 6.250 RANGE= 0.600
J161_162 3.7259 J 05Thr_H2 05Thr_H3 STAT=Y PRED= 2.440 RANGE= 4.400
J162_164 6.4691 J 05Thr_H3 05Thr_H4 STAT=Y PRED= 6.250 RANGE= 0.600
J168_169 8.9180 J 06Val_H2 06Val_H3 STAT=Y PRED= 2.980 RANGE= 6.600
J169_170 6.6944 J 06Val_H3 06Val_H4 STAT=Y PRED= 6.640 RANGE= 0.200
J169_173 7.0316 J 06Val_H3 06Val_H5 STAT=Y PRED= 6.640 RANGE= 0.200
J179_180 6.2437 J 07Leu_H2 07LeuH3A STAT=Y PRED= 3.040 RANGE= 6.000
J179_181 8.3839 J 07Leu_H2 07LeuH3B STAT=Y PRED= 13.950 RANGE= 4.000
J180_181 -13.3047 J 07LeuH3A 07LeuH3B STAT=Y PRED= -14.710 RANGE= 1.600
J180_182 8.2119 J 07LeuH3A 07Leu_H4 STAT=Y PRED= 12.990 RANGE= 2.560
J181_182 5.7896 J 07LeuH3B 07Leu_H4 STAT=Y PRED= 2.270 RANGE= 3.000
J182_183 6.5482 J 07Leu_H4 07Leu_H5 STAT=Y PRED= 6.640 RANGE= 0.200
J182_186 6.5879 J 07Leu_H4 07Leu_H6 STAT=Y PRED= 6.640 RANGE= 0.200
J190_191 8.8736 J 08Val_H2 08Val_H3 STAT=Y PRED= 12.880 RANGE= 6.000
J191_192 6.5520 J 08Val_H3 08Val_H4 STAT=Y PRED= 6.640 RANGE= 0.200
J191_195 6.7834 J 08Val_H3 08Val_H5 STAT=Y PRED= 6.640 RANGE= 0.200
J201_202 7.6281 J 09Val_H2 09Val_H3 STAT=Y PRED= 12.960 RANGE= 4.000
J202_203 6.4961 J 09Val_H3 09Val_H4 STAT=Y PRED= 6.640 RANGE= 0.200
J202_206 6.7760 J 09Val_H3 09Val_H5 STAT=Y PRED= 6.640 RANGE= 0.200
J212_213 11.1630 J 10Trp_H2 10TrpH3A STAT=Y PRED= 12.890 RANGE= 4.000
J212_214 4.7143 J 10Trp_H2 10TrpH3B STAT=Y PRED= 1.900 RANGE= 4.400
J213_214 -13.7295 J 10TrpH3A 10TrpH3B STAT=Y PRED= -16.760 RANGE= 2.560
J215_218 0.4880 J 10Trp_H5 10Trp_H7 STAT=Y PRED= -0.300 RANGE= 0.500
J217_218 0.6708 J 10Trp_H9 10Trp_H7 STAT=Y PRED= 1.020 RANGE= 1.200
J223_224 7.9094 J 11Val_H2 11Val_H3 STAT=Y PRED= 3.450 RANGE= 9.000
J224_225 6.7483 J 11Val_H3 11Val_H4 STAT=Y PRED= 6.640 RANGE= 0.200
J224_228 6.8064 J 11Val_H3 11Val_H5 STAT=Y PRED= 6.640 RANGE= 0.200
J232_233 1.9005 J 12Phe_H2 12Phe_H3 STAT=Y PRED= 1.900 RANGE= 6.600
J234_238 1.3335 J 12Phe_H5 12Phe_H5 STAT=Y PRED= 1.980 RANGE= 1.200
J234_235 7.6508 J 12Phe_H5 12Phe_H6 STAT=Y PRED= 7.660 RANGE= 0.340
J234_237 0.7769 J 12Phe_H6 12Phe_H5 STAT=Y PRED= 0.550 RANGE= 0.750
J234_236 1.2760 J 12Phe_H5 12Phe_H7 STAT=Y PRED= 1.260 RANGE= 1.200
J235_237 1.7027 J 12Phe_H6 12Phe_H6 STAT=Y PRED= 1.480 RANGE= 1.200
J235_236 7.4760 J 12Phe_H6 12Phe_H7 STAT=Y PRED= 7.400 RANGE= 0.240
J241_242 8.8924 J 13Val_H2 13Val_H3 STAT=Y PRED= 12.320 RANGE= 6.000
J242_243 6.8372 J 13Val_H3 13Val_H4 STAT=Y PRED= 6.640 RANGE= 0.200
J242_246 6.4162 J 13Val_H3 13Val_H5 STAT=Y PRED= 6.640 RANGE= 0.200
115_217 7.7969 J 10Y_H8 10Y_H9 STAT=Y PRED= 8.100 RANGE= 0.890
115_218 8.1808 J 10Y_H8 10Y_H7 STAT=Y PRED= 7.850 RANGE= 0.800
122_123 9.1737 J 01V_H2 01V_H3 STAT=Y PRED= 12.510 RANGE= 4.000

Appendix H (continued)

123_124 6.5890 J 01V_H3 01V_H6 STAT=Y PRED= 6.640 RANGE= 0.200
123_127 6.6205 J 01V_H3 01V_H7 STAT=Y PRED= 6.640 RANGE= 0.200
131_132 8.7545 J 02V_H2 02V_H3 STAT=Y PRED= 12.600 RANGE= 6.000
132_133 6.7841 J 02V_H3 02V_H4 STAT=Y PRED= 6.640 RANGE= 0.200
132_136 6.7206 J 02V_H3 02V_H5 STAT=Y PRED= 6.640 RANGE= 0.200
142_143 11.2297 J 03I_H2 03I_H3 STAT=Y PRED= 13.150 RANGE= 4.000
143_144 0.4614 J 03I_H3 03IH4A STAT=Y PRED= 1.950 RANGE= 3.000
143_145 2.9276 J 03I_H3 03IH4B STAT=Y PRED= 12.660 RANGE= 2.800
143_146 6.6276 J 03I_H3 03I_H6 STAT=Y PRED= 6.640 RANGE= 0.200
144_145 -12.2168 J 03IH4A 03IH4B STAT=Y PRED= -13.400 RANGE= 0.600
144_149 7.2855 J 03IH4A 03I_H5 STAT=Y PRED= 7.440 RANGE= 0.150
145_149 7.6340 J 03IH4B 03I_H5 STAT=Y PRED= 7.440 RANGE= 0.150
153_154 2.3441 J 04T_H2 04T_H3 STAT=Y PRED= 2.690 RANGE= 6.600
154_155 6.5134 J 04T_H3 04T_H4 STAT=Y PRED= 6.250 RANGE= 0.600
161_162 3.7259 J 05T_H2 05T_H3 STAT=Y PRED= 2.440 RANGE= 4.400
162_164 6.4691 J 05T_H3 05T_H4 STAT=Y PRED= 6.250 RANGE= 0.600
168_169 8.9180 J 06V_H2 06V_H3 STAT=Y PRED= 2.980 RANGE= 6.600
169_170 6.6944 J 06V_H3 06V_H4 STAT=Y PRED= 6.640 RANGE= 0.200
169_173 7.0316 J 06V_H3 06V_H5 STAT=Y PRED= 6.640 RANGE= 0.200
179_180 6.2437 J 07L_H2 07LH3A STAT=Y PRED= 3.040 RANGE= 6.000
179_181 8.3839 J 07L_H2 07LH3B STAT=Y PRED= 13.950 RANGE= 4.000
180_181 -13.3047 J 07LH3A 07LH3B STAT=Y PRED= -14.710 RANGE= 1.600
180_182 8.2119 J 07LH3A 07L_H4 STAT=Y PRED= 12.990 RANGE= 2.560
181_182 5.7896 J 07LH3B 07L_H4 STAT=Y PRED= 2.270 RANGE= 3.000
182_183 6.5482 J 07L_H4 07L_H5 STAT=Y PRED= 6.640 RANGE= 0.200
182_186 6.5879 J 07L_H4 07L_H6 STAT=Y PRED= 6.640 RANGE= 0.200
190_191 8.8736 J 08V_H2 08V_H3 STAT=Y PRED= 12.880 RANGE= 6.000
191_192 6.5520 J 08V_H3 08V_H4 STAT=Y PRED= 6.640 RANGE= 0.200
191_195 6.7834 J 08V_H3 08V_H5 STAT=Y PRED= 6.640 RANGE= 0.200
201_202 7.6281 J 09V_H2 09V_H3 STAT=Y PRED= 12.960 RANGE= 4.000
202_203 6.4961 J 09V_H3 09V_H4 STAT=Y PRED= 6.640 RANGE= 0.200
202_206 6.7760 J 09V_H3 09V_H5 STAT=Y PRED= 6.640 RANGE= 0.200
212_213 11.1630 J 10Y_H2 10YH3A STAT=Y PRED= 12.890 RANGE= 4.000
212_214 4.7143 J 10Y_H2 10YH3B STAT=Y PRED= 1.900 RANGE= 4.400
213_214 -13.7295 J 10YH3A 10YH3B STAT=Y PRED= -16.760 RANGE= 2.560
215_218 0.4880 J 10Y_H5 10Y_H7 STAT=Y PRED= -0.300 RANGE= 0.500
217_218 0.6708 J 10Y_H9 10Y_H7 STAT=Y PRED= 1.020 RANGE= 1.200
223_224 7.9094 J 11V_H2 11V_H3 STAT=Y PRED= 3.450 RANGE= 9.000
224_225 6.7483 J 11V_H3 11V_H4 STAT=Y PRED= 6.640 RANGE= 0.200
224_228 6.8064 J 11V_H3 11V_H5 STAT=Y PRED= 6.640 RANGE= 0.200
232_233 1.9005 J 12F_H2 12F_H3 STAT=Y PRED= 1.900 RANGE= 6.600
234_238 1.3335 J 12F_H5 12F_H5 STAT=Y PRED= 1.980 RANGE= 1.200
234_235 7.6508 J 12F_H5 12F_H6 STAT=Y PRED= 7.660 RANGE= 0.340
234_237 0.7769 J 12F_H6 12F_H5 STAT=Y PRED= 0.550 RANGE= 0.750
234_236 1.2760 J 12F_H5 12F_H7 STAT=Y PRED= 1.260 RANGE= 1.200
235_237 1.7027 J 12F_H6 12F_H6 STAT=Y PRED= 1.480 RANGE= 1.200
235_236 7.4760 J 12F_H6 12F_H7 STAT=Y PRED= 7.400 RANGE= 0.240
241_242 8.8924 J 13V_H2 13V_H3 STAT=Y PRED= 12.320 RANGE= 6.000
242_243 6.8372 J 13V_H3 13V_H4 STAT=Y PRED= 6.640 RANGE= 0.200
242_246 6.4162 J 13V_H3 13V_H5 STAT=Y PRED= 6.640 RANGE= 0.200

Appendix H (continued)

CONTROL PARAMETERS:
Solvent = none (def. 99% enriched)
1.000 = Concentration (vol%, def=1.0%)
0.00100000 = Minimum line-intensity
0.00100000 = Diagonalization criterium (not in use)
600.13201900 = FIELD(1H,MHz), used to transform shifts to ppms
11.63298481 = Left frequency (ppm)
-4.33373638 = Right frequency (ppm)
0.000 = Acquisition time (s, for QMTLS)
0.542 = Line-width (for modes D, P & T, 0=use defaults)
0.031750000 = Data-point resolution (Hz)
8.461 = GAUSSIAN (%, 0=use default from INF)
-9.471 = Dispersion contribution (%, 0=use default from INF)
0.00000000 = Decoupling frequency (for DORES)

CONSTRAINTS (in equations X0 = 1.0)...use no empty lines
EQUAL 01Val_H2 = 13Val_H2
EQUAL 06Val_H5 = 11Val_H4
EQUAL 07Leu_H5 = 07Leu_H6
EQUAL 01V_H2 = 13V_H2
EQUAL 06V_H5 = 11V_H4
EQUAL 07L_H5 = 07L_H6
IGNORE(HZ): 2900.885 to 2887.442
IGNORE(HZ): 1991.286 to 1980.638
IGNORE(HZ): 1165.333 to 1158.472
IGNORE(HZ): 779.618 to 766.330
IGNORE(HZ): 1376.676 to 1343.069
IGNORE(HZ): 2900.600 to 2868.152

END of FILE

Appendix I. The PMS file of common amino acids between deoxyecumicin and ecumicin.

* NEW: the lines beginning by * are comment lines !
* To keep all the chemical shifts fixed during iteration
* replace "CHEMICAL SHIFTS(HZ):" by "..SHIFTS(HZ): fixed"
* The couplings can be fixed in the same way

NMR-data: C:\Users\jgnapo_2\Desktop\Wei_H14_XRays\H14_withoutGO
#$œ Date 5. 3.2014; Time 5:32:40 perch.pms

CHEMICAL SHIFTS(PPM):
PROTON 2*SPIN= 1 SPECIES=1H POPULATION(Y)= 0.64679
10Trp_H8/ 1 6.983053 1*1*1 STAT=Y PRED= 7.318 RANGE= 0.197 WIDTH(Y)= 2.918 RESP(Y)= 0.0950 HSQC= C74
01ValH45/ 1 2.313729 1*1*6 STAT=Y PRED= 2.370 RANGE= 0.307 WIDTH(Y)= 2.374 RESP(Y)= 0.1269 HSQC= C1_2
01Val_H2/ 1 2.667577 1*1*1 STAT=Y PRED= 4.169 RANGE= 0.637 WIDTH(Y)= 2.140 RESP(Y)= 0.1182 HSQC= C4
01Val_H3/ 1 2.050022 1*1*1 STAT=Y PRED= 1.952 RANGE= 0.815 WIDTH(Y)= 2.950 RESP(Y)= 0.1124 HSQC= C5
01Val_H6/ 1 0.851269 1*1*3 STAT=Y PRED= 0.509 RANGE= 0.865 WIDTH(Y)= 3.418 RESP(Y)= 0.1182 HSQC= C6
01Val_H7/ 1 0.981248 1*1*3 STAT=Y PRED= 0.818 RANGE= 0.357 WIDTH(Y)= 2.537 RESP(Y)= 0.1144 HSQC= C7
02Val_H2/ 1 4.673890 1*1*1 STAT=Y PRED= 4.508 RANGE= 0.805 WIDTH(Y)= 4.074 RESP(Y)= 0.1462 HSQC= C10
02Val_H3/ 1 2.085055 1*1*1 STAT=Y PRED= 2.155 RANGE= 0.775 WIDTH(Y)= 2.449 RESP(Y)= 0.1053 HSQC= C12
02Val_H4/ 1 0.982708 1*1*3 STAT=Y PRED= 1.038 RANGE= 0.277 WIDTH(Y)= 2.759 RESP(Y)= 0.1228 HSQC= C13
02Val_H5/ 1 1.045184 1*1*3 STAT=Y PRED= 0.943 RANGE= 0.247 WIDTH(Y)= 2.640 RESP(Y)= 0.1342 HSQC= C14
03Ile_H7/ 1 3.227709 1*1*3 STAT=Y PRED= 3.196 RANGE= 0.367 WIDTH(Y)= 2.776 RESP(Y)= 0.1592 HSQC= C15
03Ile_H2/ 1 4.944549 1*1*1 STAT=Y PRED= 4.617 RANGE= 1.628 WIDTH(Y)= 1.993 RESP(Y)= 0.0997 HSQC= C17
03Ile_H3/ 1 1.938019 1*1*1 STAT=Y PRED= 2.032 RANGE= 0.705 WIDTH(Y)= 3.112 RESP(Y)= 0.1704 HSQC= C19
03IleH4A/ 1 0.924796 1*1*1 STAT=Y PRED= 1.465 RANGE= 0.697 WIDTH(Y)= 5.496 RESP(Y)= 0.9453 HSQC= C20
03IleH4B/ 1 1.301495 1*1*1 STAT=Y PRED= 1.175 RANGE= 0.587 WIDTH(Y)= 3.721 RESP(Y)= 0.3274 HSQC= C20
03Ile_H6/ 1 0.753003 1*1*3 STAT=Y PRED= 0.723 RANGE= 0.397 WIDTH(Y)= 3.460 RESP(Y)= 0.1267 HSQC= C21
03Ile_H5/ 1 0.723527 1*1*3 STAT=Y PRED= 0.880 RANGE= 0.217 WIDTH(Y)= 2.511 RESP(Y)= 0.1077 HSQC= C22
04Thr_H2/ 1 5.133407 1*1*1 STAT=Y PRED= 4.668 RANGE= 1.015 WIDTH(Y)= 2.338 RESP(Y)= 0.1201 HSQC= C24
04Thr_H3/ 1 5.783119 1*1*1 STAT=Y PRED= 4.010 RANGE= 0.477 WIDTH(Y)= 3.356 RESP(Y)= 0.0954 HSQC= C25
04Thr_H4/ 1 1.314106 1*1*3 STAT=Y PRED= 1.270 RANGE= 0.497 WIDTH(Y)= 2.339 RESP(Y)= 0.1237 HSQC= C27
05Thr_H5/ 1 3.320271 1*1*3 STAT=Y PRED= 3.257 RANGE= 0.397 WIDTH(Y)= 2.864 RESP(Y)= 0.1330 HSQC= C29
05Thr_H2/ 1 5.027764 1*1*1 STAT=Y PRED= 4.099 RANGE= 1.025 WIDTH(Y)= 2.437 RESP(Y)= 0.1146 HSQC= C31
05Thr_H3/ 1 4.434703 1*1*1 STAT=Y PRED= 4.345 RANGE= 0.717 WIDTH(Y)= 2.793 RESP(Y)= 0.1177 HSQC= C32
05Thr_H4/ 1 0.885803 1*1*3 STAT=Y PRED= 1.252 RANGE= 0.297 WIDTH(Y)= 3.099 RESP(Y)= 0.1331 HSQC= C34
06Val_H2/ 1 4.825834 1*1*1 STAT=Y PRED= 4.525 RANGE= 1.405 WIDTH(Y)= 5.324 RESP(Y)= 0.1511 HSQC= C37
06Val_H3/ 1 2.363811 1*1*1 STAT=Y PRED= 1.975 RANGE= 1.015 WIDTH(Y)= 3.643 RESP(Y)= 0.1139 HSQC= C38
06Val_H4/ 1 1.096438 1*1*3 STAT=Y PRED= 0.938 RANGE= 0.217 WIDTH(Y)= 3.235 RESP(Y)= 0.0950 HSQC= C39
06Val_H5/ 1 0.981084 1*1*3 STAT=Y PRED= 1.094 RANGE= 0.387 WIDTH(Y)= 3.327 RESP(Y)= 0.1145 HSQC= C40
07Leu_H7/ 1 3.263047 1*1*3 STAT=Y PRED= 3.110 RANGE= 0.375 WIDTH(Y)= 2.476 RESP(Y)= 0.1144 HSQC= C42
07Leu_H2/ 1 5.168766 1*1*1 STAT=Y PRED= 5.342 RANGE= 1.085 WIDTH(Y)= 2.976 RESP(Y)= 0.1164 HSQC= C44
07LeuH3A/ 1 1.426201 1*1*1 STAT=Y PRED= 1.444 RANGE= 0.427 WIDTH(Y)= 2.845 RESP(Y)= 0.0645 HSQC= C45
07LeuH3B/ 1 1.263367 1*1*1 STAT=Y PRED= 1.914 RANGE= 0.367 WIDTH(Y)= 3.300 RESP(Y)= 0.0250 HSQC= C45
07Leu_H4/ 1 0.929673 1*1*1 STAT=Y PRED= 1.630 RANGE= 0.627 WIDTH(Y)= 0.635 RESP(Y)= 0.0262 HSQC= C46
07Leu_H5/ 1 0.321895 1*1*3 STAT=Y PRED= 0.972 RANGE= 0.315 WIDTH(Y)= 2.804 RESP(Y)= 0.0994 HSQC= C47
07Leu_H6/ 1 0.224427 1*1*3 STAT=Y PRED= 0.972 RANGE= 0.147 WIDTH(Y)= 2.934 RESP(Y)= 0.1019 HSQC= C48
08Val_H2/ 1 4.601908 1*1*1 STAT=Y PRED= 4.489 RANGE= 0.895 WIDTH(Y)= 2.859 RESP(Y)= 0.0784 HSQC= C51
08Val_H3/ 1 2.035456 1*1*1 STAT=Y PRED= 1.995 RANGE= 0.485 WIDTH(Y)= 2.821 RESP(Y)= 0.0823 HSQC= C52
08Val_H4/ 1 0.905401 1*1*3 STAT=Y PRED= 1.060 RANGE= 0.237 WIDTH(Y)= 5.457 RESP(Y)= 0.0482 HSQC= C53
08Val_H5/ 1 0.867810 1*1*3 STAT=Y PRED= 0.999 RANGE= 0.227 WIDTH(Y)= 3.597 RESP(Y)= 0.1328 HSQC= C54
09Val_H6/ 1 3.146274 1*1*3 STAT=Y PRED= 3.169 RANGE= 0.465 WIDTH(Y)= 2.526 RESP(Y)= 0.1119 HSQC= C56

Appendix I (continued)

09Val_H2/ 1 3.054073 1*1*1 STAT=Y PRED= 5.153 RANGE= 0.717 WIDTH(Y)= 3.037 RESP(Y)= 0.1144 HSQC= C58
09Val_H3/ 1 2.593761 1*1*1 STAT=Y PRED= 2.524 RANGE= 0.407 WIDTH(Y)= 2.512 RESP(Y)= 0.0810 HSQC= C59
09Val_H4/ 1 1.097701 1*1*3 STAT=Y PRED= 1.319 RANGE= 0.227 WIDTH(Y)= 5.464 RESP(Y)= 0.0726 HSQC= C60
09Val_H5/ 1 0.976341 1*1*3 STAT=Y PRED= 1.075 RANGE= 0.237 WIDTH(Y)= 3.101 RESP(Y)= 0.0961 HSQC= C61
10TrpH13/ 1 2.165324 1*1*3 STAT=Y PRED= 2.936 RANGE= 0.895 WIDTH(Y)= 2.521 RESP(Y)= 0.1165 HSQC= C63
10Trp_H2/ 1 4.094748 1*1*1 STAT=Y PRED= 5.043 RANGE= 1.765 WIDTH(Y)= 2.790 RESP(Y)= 0.0653 HSQC= C65
10TrpH3A/ 1 3.545626 1*1*1 STAT=Y PRED= 3.613 RANGE= 0.467 WIDTH(Y)= 3.303 RESP(Y)= -0.0090 HSQC= C66
10TrpH3B/ 1 3.690903 1*1*1 STAT=Y PRED= 3.367 RANGE= 0.627 WIDTH(Y)= 2.655 RESP(Y)= 0.0939 HSQC= C66
10Trp_H5/ 1 6.699103 1*1*1 STAT=Y PRED= 6.772 RANGE= 0.275 WIDTH(Y)= 2.961 RESP(Y)= 0.0950 HSQC= C68
10Trp_H9/ 1 6.442889 1*1*1 STAT=Y PRED= 7.089 RANGE= 0.217 WIDTH(Y)= 3.286 RESP(Y)= 0.0964 HSQC= C73
10Trp_H7/ 1 6.921954 1*1*1 STAT=Y PRED= 7.333 RANGE= 0.307 WIDTH(Y)= 2.283 RESP(Y)= 0.0883 HSQC= C75
10TrpH12/ 1 3.818211 1*1*3 STAT=Y PRED= 4.072 RANGE= 0.247 WIDTH(Y)= 2.165 RESP(Y)= 0.1143 HSQC= C77
11Val_H2/ 1 4.368919 1*1*1 STAT=Y PRED= 4.303 RANGE= 1.445 WIDTH(Y)= 2.482 RESP(Y)= 0.0966 HSQC= C80
11Val_H3/ 1 2.195172 1*1*1 STAT=Y PRED= 2.094 RANGE= 0.587 WIDTH(Y)= 3.768 RESP(Y)= 0.1307 HSQC= C81
11Val_H4/ 1 1.026649 1*1*3 STAT=Y PRED= 1.094 RANGE= 0.247 WIDTH(Y)= 3.019 RESP(Y)= 0.1535 HSQC= C82
11Val_H5/ 1 0.984184 1*1*3 STAT=Y PRED= 1.080 RANGE= 0.297 WIDTH(Y)= 3.657 RESP(Y)= 0.1309 HSQC= C83
13Val_H2/ 1 4.406966 1*1*1 STAT=Y PRED= 4.169 RANGE= 0.667 WIDTH(Y)= 3.030 RESP(Y)= 0.1506 HSQC= C97
13Val_H3/ 1 1.969060 1*1*1 STAT=Y PRED= 1.935 RANGE= 0.865 WIDTH(Y)= 3.185 RESP(Y)= 1.0000 HSQC= C99
13Val_H4/ 1 0.936791 1*1*3 STAT=Y PRED= 1.277 RANGE= 0.217 WIDTH(Y)= 4.983 RESP(Y)= 0.0408 HSQC= C100
13Val_H5/ 1 0.920725 1*1*3 STAT=Y PRED= 0.933 RANGE= 0.277 WIDTH(Y)= 2.396 RESP(Y)= 0.0898 HSQC= C101
PROTON 2*SPIN= 1 SPECIES=1H POPULATION(Y)= 0.35321
10Y_H8 / 2 6.981128 1*1*1 STAT=Y PRED= 7.318 RANGE= 0.197 WIDTH(Y)= 1.362 RESP(Y)= 0.1077 HSQC= 2C74
01VH45 / 2 2.316357 1*1*6 STAT=Y PRED= 2.370 RANGE= 0.307 WIDTH(Y)= 2.312 RESP(Y)= 0.0837 HSQC= 2C1_2
01V_H2 / 2 2.670690 1*1*1 STAT=Y PRED= 4.169 RANGE= 0.637 WIDTH(Y)= 2.428 RESP(Y)= 0.0649 HSQC= 2C4
01V_H3 / 2 2.042286 1*1*1 STAT=Y PRED= 1.952 RANGE= 0.815 WIDTH(Y)= 2.318 RESP(Y)= 0.1573 HSQC= 2C5
01V_H6 / 2 0.847521 1*1*3 STAT=Y PRED= 0.509 RANGE= 0.865 WIDTH(Y)= 4.120 RESP(Y)= 0.1144 HSQC= 2C6
01V_H7 / 2 0.979456 1*1*3 STAT=Y PRED= 0.818 RANGE= 0.357 WIDTH(Y)= 1.806 RESP(Y)= 0.0934 HSQC= 2C7
02V_H2 / 2 4.672940 1*1*1 STAT=Y PRED= 4.508 RANGE= 0.805 WIDTH(Y)= 1.704 RESP(Y)= 0.0590 HSQC= 2C10
02V_H3 / 2 2.102035 1*1*1 STAT=Y PRED= 2.155 RANGE= 0.775 WIDTH(Y)= 2.216 RESP(Y)= 0.0766 HSQC= 2C12
02V_H4 / 2 1.001765 1*1*3 STAT=Y PRED= 1.038 RANGE= 0.277 WIDTH(Y)= 4.785 RESP(Y)= 0.0968 HSQC= 2C13
02V_H5 / 2 1.054994 1*1*3 STAT=Y PRED= 0.943 RANGE= 0.247 WIDTH(Y)= 1.835 RESP(Y)= 0.0425 HSQC= 2C14
03I_H7 / 2 3.227585 1*1*3 STAT=Y PRED= 3.196 RANGE= 0.367 WIDTH(Y)= 4.020 RESP(Y)= 0.0410 HSQC= 2C15
03I_H2 / 2 4.917218 1*1*1 STAT=Y PRED= 4.617 RANGE= 1.628 WIDTH(Y)= 1.218 RESP(Y)= 0.0198 HSQC= 2C17
03I_H3 / 2 1.966822 1*1*1 STAT=Y PRED= 2.032 RANGE= 0.705 WIDTH(Y)= 3.820 RESP(Y)= 1.0000 HSQC= 2C19
03IH4A / 2 0.961339 1*1*1 STAT=Y PRED= 1.465 RANGE= 0.697 WIDTH(Y)= 5.241 RESP(Y)= 0.4654 HSQC= 2C20
03IH4B / 2 1.258661 1*1*1 STAT=Y PRED= 1.175 RANGE= 0.587 WIDTH(Y)= 2.889 RESP(Y)= 0.1943 HSQC= 2C20
03I_H6 / 2 0.750814 1*1*3 STAT=Y PRED= 0.723 RANGE= 0.397 WIDTH(Y)= 1.500 RESP(Y)= 0.0724 HSQC= 2C21
03I_H5 / 2 0.752205 1*1*3 STAT=Y PRED= 0.880 RANGE= 0.217 WIDTH(Y)= 4.341 RESP(Y)= 0.0972 HSQC= 2C22
04T_H2 / 2 5.166397 1*1*1 STAT=Y PRED= 4.668 RANGE= 1.015 WIDTH(Y)= 1.968 RESP(Y)= 0.0520 HSQC= 2C24
04T_H3 / 2 5.783803 1*1*1 STAT=Y PRED= 4.010 RANGE= 0.477 WIDTH(Y)= 3.202 RESP(Y)= 0.1104 HSQC= 2C25
04T_H4 / 2 1.316886 1*1*3 STAT=Y PRED= 1.270 RANGE= 0.497 WIDTH(Y)= 2.401 RESP(Y)= 0.0773 HSQC= 2C27
05T_H5 / 2 3.326836 1*1*3 STAT=Y PRED= 3.257 RANGE= 0.397 WIDTH(Y)= 5.251 RESP(Y)= 0.1276 HSQC= 2C29
05T_H2 / 2 5.011839 1*1*1 STAT=Y PRED= 4.099 RANGE= 1.025 WIDTH(Y)= 4.062 RESP(Y)= 0.0389 HSQC= 2C31
05T_H3 / 2 4.452619 1*1*1 STAT=Y PRED= 4.345 RANGE= 0.717 WIDTH(Y)= 3.220 RESP(Y)= 0.1222 HSQC= 2C32
05T_H4 / 2 0.915828 1*1*3 STAT=Y PRED= 1.252 RANGE= 0.297 WIDTH(Y)= 2.010 RESP(Y)= 0.0685 HSQC= 2C34
06V_H2 / 2 4.847775 1*1*1 STAT=Y PRED= 4.525 RANGE= 1.405 WIDTH(Y)= 5.287 RESP(Y)= 0.2609 HSQC= 2C37
06V_H3 / 2 2.348346 1*1*1 STAT=Y PRED= 1.975 RANGE= 1.015 WIDTH(Y)= 2.039 RESP(Y)= 0.0383 HSQC= 2C38
06V_H4 / 2 1.094360 1*1*3 STAT=Y PRED= 0.938 RANGE= 0.217 WIDTH(Y)= 1.431 RESP(Y)= 0.0937 HSQC= 2C39
06V_H5 / 2 0.975087 1*1*3 STAT=Y PRED= 1.094 RANGE= 0.387 WIDTH(Y)= 2.216 RESP(Y)= 0.1134 HSQC= 2C40
07L_H7 / 2 3.256784 1*1*3 STAT=Y PRED= 3.110 RANGE= 0.375 WIDTH(Y)= 2.112 RESP(Y)= 0.0273 HSQC= 2C42

Appendix I (continued)

07L_H2 / 2 5.107801 1*1*1 STAT=Y PRED= 5.342 RANGE= 1.085 WIDTH(Y)= 2.095 RESP(Y)= 0.0187 HSQC= 2C44
07LH3A / 2 1.453160 1*1*1 STAT=Y PRED= 1.444 RANGE= 0.427 WIDTH(Y)= 1.776 RESP(Y)= -0.0322 HSQC= 2C45
07LH3B / 2 1.233198 1*1*1 STAT=Y PRED= 1.914 RANGE= 0.367 WIDTH(Y)= 3.329 RESP(Y)= 0.0476 HSQC= 2C45
07L_H4 / 2 0.959553 1*1*1 STAT=Y PRED= 1.630 RANGE= 0.627 WIDTH(Y)= 1.082 RESP(Y)= 0.0916 HSQC= 2C46
07L_H5 / 2 0.333644 1*1*3 STAT=Y PRED= 0.972 RANGE= 0.315 WIDTH(Y)= 3.344 RESP(Y)= 0.0304 HSQC= 2C47
07L_H6 / 2 0.183852 1*1*3 STAT=Y PRED= 0.972 RANGE= 0.147 WIDTH(Y)= 3.257 RESP(Y)= 0.0424 HSQC= 2C48
08V_H2 / 2 4.585484 1*1*1 STAT=Y PRED= 4.489 RANGE= 0.895 WIDTH(Y)= 2.825 RESP(Y)= 0.1093 HSQC= 2C51
08V_H3 / 2 2.027966 1*1*1 STAT=Y PRED= 1.995 RANGE= 0.485 WIDTH(Y)= 2.883 RESP(Y)= 0.0132 HSQC= 2C52
08V_H4 / 2 0.914194 1*1*3 STAT=Y PRED= 1.060 RANGE= 0.237 WIDTH(Y)= 1.405 RESP(Y)= 0.0548 HSQC= 2C53
08V_H5 / 2 0.850989 1*1*3 STAT=Y PRED= 0.999 RANGE= 0.227 WIDTH(Y)= 2.119 RESP(Y)= 0.0754 HSQC= 2C54
09V_H6 / 2 3.139138 1*1*3 STAT=Y PRED= 3.169 RANGE= 0.465 WIDTH(Y)= 2.316 RESP(Y)= 0.0307 HSQC= 2C56
09V_H2 / 2 3.069536 1*1*1 STAT=Y PRED= 5.153 RANGE= 0.717 WIDTH(Y)= 2.567 RESP(Y)= 0.0053 HSQC= 2C58
09V_H3 / 2 2.583162 1*1*1 STAT=Y PRED= 2.524 RANGE= 0.407 WIDTH(Y)= 1.843 RESP(Y)= 0.0169 HSQC= 2C59
09V_H4 / 2 1.095853 1*1*3 STAT=Y PRED= 1.319 RANGE= 0.227 WIDTH(Y)= 1.796 RESP(Y)= 0.1107 HSQC= 2C60
09V_H5 / 2 0.977932 1*1*3 STAT=Y PRED= 1.075 RANGE= 0.237 WIDTH(Y)= 1.536 RESP(Y)= 0.0873 HSQC= 2C61
10YH13 / 2 2.158367 1*1*3 STAT=Y PRED= 2.936 RANGE= 0.895 WIDTH(Y)= 2.136 RESP(Y)= 0.0317 HSQC= 2C63
10Y_H2 / 2 4.095302 1*1*1 STAT=Y PRED= 5.043 RANGE= 1.765 WIDTH(Y)= 2.597 RESP(Y)= 0.0913 HSQC= 2C65
10YH3A / 2 3.547008 1*1*1 STAT=Y PRED= 3.613 RANGE= 0.467 WIDTH(Y)= 2.191 RESP(Y)= 0.2121 HSQC= 2C66
10YH3B / 2 3.696022 1*1*1 STAT=Y PRED= 3.367 RANGE= 0.627 WIDTH(Y)= 2.734 RESP(Y)= 0.0558 HSQC= 2C66
10Y_H5 / 2 6.697081 1*1*1 STAT=Y PRED= 6.772 RANGE= 0.275 WIDTH(Y)= 1.582 RESP(Y)= 0.0880 HSQC= 2C68
10Y_H9 / 2 6.439998 1*1*1 STAT=Y PRED= 7.089 RANGE= 0.217 WIDTH(Y)= 1.251 RESP(Y)= 0.0951 HSQC= 2C73
10Y_H7 / 2 6.920387 1*1*1 STAT=Y PRED= 7.333 RANGE= 0.307 WIDTH(Y)= 0.777 RESP(Y)= 0.0925 HSQC= 2C75
10YH12 / 2 3.828094 1*1*3 STAT=Y PRED= 4.072 RANGE= 0.247 WIDTH(Y)= 2.057 RESP(Y)= 0.0490 HSQC= 2C77
11V_H2 / 2 4.526543 1*1*1 STAT=Y PRED= 4.303 RANGE= 1.445 WIDTH(Y)= 6.717 RESP(Y)= 0.1385 HSQC= 2C80
11V_H3 / 2 2.202340 1*1*1 STAT=Y PRED= 2.094 RANGE= 0.587 WIDTH(Y)= 1.475 RESP(Y)= -0.0067 HSQC= 2C81
11V_H4 / 2 1.027215 1*1*3 STAT=Y PRED= 1.094 RANGE= 0.247 WIDTH(Y)= 1.062 RESP(Y)= -0.0235 HSQC= 2C82
11V_H5 / 2 0.995323 1*1*3 STAT=Y PRED= 1.080 RANGE= 0.297 WIDTH(Y)= 3.467 RESP(Y)= 0.1087 HSQC= 2C83
12F_H2 / 2 4.866963 1*1*1 STAT=Y PRED= 4.499 RANGE= 0.985 WIDTH(Y)= 1.271 RESP(Y)= 0.0288 HSQC= 2C86
12F_H3 / 2 5.339936 1*1*1 STAT=Y PRED= 5.208 RANGE= 0.487 WIDTH(Y)= 2.981 RESP(Y)= 0.1089 HSQC= 2C87
12F_H5 / 2 7.242205 1*2*1 STAT=Y PRED= 7.524 RANGE= 0.307 WIDTH(Y)= 6.488 RESP(Y)= 0.1056 HSQC= 2C89_93
12F_H6 / 2 7.254230 1*2*1 STAT=Y PRED= 7.372 RANGE= 0.577 WIDTH(Y)= 1.301 RESP(Y)= 0.0525 HSQC= 2C90_92
12F_H7 / 2 7.200270 1*1*1 STAT=Y PRED= 7.281 RANGE= 0.307 WIDTH(Y)= 4.125 RESP(Y)= 0.0478 HSQC= 2C91
13V_H2 / 2 4.400648 1*1*1 STAT=Y PRED= 4.169 RANGE= 0.667 WIDTH(Y)= 1.648 RESP(Y)= -0.0065 HSQC= 2C97
13V_H3 / 2 1.969265 1*1*1 STAT=Y PRED= 1.935 RANGE= 0.865 WIDTH(Y)= 2.788 RESP(Y)= -2.3800 HSQC= 2C99
13V_H4 / 2 0.936823 1*1*3 STAT=Y PRED= 1.277 RANGE= 0.217 WIDTH(Y)= 2.537 RESP(Y)= 0.0982 HSQC= 2C100
13V_H5 / 2 0.919067 1*1*3 STAT=Y PRED= 0.933 RANGE= 0.277 WIDTH(Y)= 1.735 RESP(Y)= 0.0798 HSQC= 2C101

COUPLING CONSTANTS(HZ): fixed
J115_217 7.7969 J 10Trp_H8 10Trp_H9 STAT=Y PRED= 8.100 RANGE= 0.890
J115_218 8.1808 J 10Trp_H8 10Trp_H7 STAT=Y PRED= 7.850 RANGE= 0.800
J122_123 9.1737 J 01Val_H2 01Val_H3 STAT=Y PRED= 12.510 RANGE= 4.000
J123_124 6.5890 J 01Val_H3 01Val_H6 STAT=Y PRED= 6.640 RANGE= 0.200
J123_127 6.6205 J 01Val_H3 01Val_H7 STAT=Y PRED= 6.640 RANGE= 0.200
J131_132 8.7545 J 02Val_H2 02Val_H3 STAT=Y PRED= 12.600 RANGE= 6.000
J132_133 6.7841 J 02Val_H3 02Val_H4 STAT=Y PRED= 6.640 RANGE= 0.200
J132_136 6.7206 J 02Val_H3 02Val_H5 STAT=Y PRED= 6.640 RANGE= 0.200
J142_143 11.2297 J 03Ile_H2 03Ile_H3 STAT=Y PRED= 13.150 RANGE= 4.000
J143_144 0.4614 J 03Ile_H3 03IleH4A STAT=Y PRED= 1.950 RANGE= 3.000
J143_145 2.9276 J 03Ile_H3 03IleH4B STAT=Y PRED= 12.660 RANGE= 2.800
J143_146 6.6276 J 03Ile_H3 03Ile_H6 STAT=Y PRED= 6.640 RANGE= 0.200

Appendix I (continued)

J144_145 -12.2168 J 03IleH4A 03IleH4B STAT=Y PRED= -13.400 RANGE= 0.600
J144_149 7.2855 J 03IleH4A 03Ile_H5 STAT=Y PRED= 7.440 RANGE= 0.150
J145_149 7.6340 J 03IleH4B 03Ile_H5 STAT=Y PRED= 7.440 RANGE= 0.150
J153_154 2.3441 J 04Thr_H2 04Thr_H3 STAT=Y PRED= 2.690 RANGE= 6.600
J154_155 6.5134 J 04Thr_H3 04Thr_H4 STAT=Y PRED= 6.250 RANGE= 0.600
J161_162 3.7259 J 05Thr_H2 05Thr_H3 STAT=Y PRED= 2.440 RANGE= 4.400
J162_164 6.4691 J 05Thr_H3 05Thr_H4 STAT=Y PRED= 6.250 RANGE= 0.600
J168_169 8.9180 J 06Val_H2 06Val_H3 STAT=Y PRED= 2.980 RANGE= 6.600
J169_170 6.6944 J 06Val_H3 06Val_H4 STAT=Y PRED= 6.640 RANGE= 0.200
J169_173 7.0316 J 06Val_H3 06Val_H5 STAT=Y PRED= 6.640 RANGE= 0.200
J179_180 6.2437 J 07Leu_H2 07LeuH3A STAT=Y PRED= 3.040 RANGE= 6.000
J179_181 8.3839 J 07Leu_H2 07LeuH3B STAT=Y PRED= 13.950 RANGE= 4.000
J180_181 -13.3047 J 07LeuH3A 07LeuH3B STAT=Y PRED= -14.710 RANGE= 1.600
J180_182 8.2119 J 07LeuH3A 07Leu_H4 STAT=Y PRED= 12.990 RANGE= 2.560
J181_182 5.7896 J 07LeuH3B 07Leu_H4 STAT=Y PRED= 2.270 RANGE= 3.000
J182_183 6.5482 J 07Leu_H4 07Leu_H5 STAT=Y PRED= 6.640 RANGE= 0.200
J182_186 6.5879 J 07Leu_H4 07Leu_H6 STAT=Y PRED= 6.640 RANGE= 0.200
J190_191 8.8736 J 08Val_H2 08Val_H3 STAT=Y PRED= 12.880 RANGE= 6.000
J191_192 6.5520 J 08Val_H3 08Val_H4 STAT=Y PRED= 6.640 RANGE= 0.200
J191_195 6.7834 J 08Val_H3 08Val_H5 STAT=Y PRED= 6.640 RANGE= 0.200
J201_202 7.6281 J 09Val_H2 09Val_H3 STAT=Y PRED= 12.960 RANGE= 4.000
J202_203 6.4961 J 09Val_H3 09Val_H4 STAT=Y PRED= 6.640 RANGE= 0.200
J202_206 6.7760 J 09Val_H3 09Val_H5 STAT=Y PRED= 6.640 RANGE= 0.200
J212_213 11.1630 J 10Trp_H2 10TrpH3A STAT=Y PRED= 12.890 RANGE= 4.000
J212_214 4.7143 J 10Trp_H2 10TrpH3B STAT=Y PRED= 1.900 RANGE= 4.400
J213_214 -13.7295 J 10TrpH3A 10TrpH3B STAT=Y PRED= -16.760 RANGE= 2.560
J215_218 0.4880 J 10Trp_H5 10Trp_H7 STAT=Y PRED= -0.300 RANGE= 0.500
J217_218 0.6708 J 10Trp_H9 10Trp_H7 STAT=Y PRED= 1.020 RANGE= 1.200
J223_224 7.9094 J 11Val_H2 11Val_H3 STAT=Y PRED= 3.450 RANGE= 9.000
J224_225 6.7483 J 11Val_H3 11Val_H4 STAT=Y PRED= 6.640 RANGE= 0.200
J224_228 6.8064 J 11Val_H3 11Val_H5 STAT=Y PRED= 6.640 RANGE= 0.200
J241_242 8.8924 J 13Val_H2 13Val_H3 STAT=Y PRED= 12.320 RANGE= 6.000
J242_243 6.8372 J 13Val_H3 13Val_H4 STAT=Y PRED= 6.640 RANGE= 0.200
J242_246 6.4162 J 13Val_H3 13Val_H5 STAT=Y PRED= 6.640 RANGE= 0.200
115_217 7.7969 J 10Y_H8 10Y_H9 STAT=Y PRED= 8.100 RANGE= 0.890
115_218 8.1808 J 10Y_H8 10Y_H7 STAT=Y PRED= 7.850 RANGE= 0.800
122_123 9.1737 J 01V_H2 01V_H3 STAT=Y PRED= 12.510 RANGE= 4.000
123_124 6.5890 J 01V_H3 01V_H6 STAT=Y PRED= 6.640 RANGE= 0.200
123_127 6.6205 J 01V_H3 01V_H7 STAT=Y PRED= 6.640 RANGE= 0.200
131_132 8.7545 J 02V_H2 02V_H3 STAT=Y PRED= 12.600 RANGE= 6.000
132_133 6.7841 J 02V_H3 02V_H4 STAT=Y PRED= 6.640 RANGE= 0.200
132_136 6.7206 J 02V_H3 02V_H5 STAT=Y PRED= 6.640 RANGE= 0.200
142_143 11.2297 J 03I_H2 03I_H3 STAT=Y PRED= 13.150 RANGE= 4.000
143_144 0.4614 J 03I_H3 03IH4A STAT=Y PRED= 1.950 RANGE= 3.000
143_145 2.9276 J 03I_H3 03IH4B STAT=Y PRED= 12.660 RANGE= 2.800
143_146 6.6276 J 03I_H3 03I_H6 STAT=Y PRED= 6.640 RANGE= 0.200
144_145 -12.2168 J 03IH4A 03IH4B STAT=Y PRED= -13.400 RANGE= 0.600
144_149 7.2855 J 03IH4A 03I_H5 STAT=Y PRED= 7.440 RANGE= 0.150
145_149 7.6340 J 03IH4B 03I_H5 STAT=Y PRED= 7.440 RANGE= 0.150
153_154 2.3441 J 04T_H2 04T_H3 STAT=Y PRED= 2.690 RANGE= 6.600

Appendix I (continued)

```
 154_155    6.5134   J 04T_H3   04T_H4    STAT=Y  PRED= 6.250 RANGE= 0.600
 161_162    3.7259   J 05T_H2   05T_H3    STAT=Y  PRED= 2.440 RANGE= 4.400
 162_164    6.4691   J 05T_H3   05T_H4    STAT=Y  PRED= 6.250 RANGE= 0.600
 168_169    8.9180   J 06V_H2   06V_H3    STAT=Y  PRED= 2.980 RANGE= 6.600
 169_170    6.6944   J 06V_H3   06V_H4    STAT=Y  PRED= 6.640 RANGE= 0.200
 169_173    7.0316   J 06V_H3   06V_H5    STAT=Y  PRED= 6.640 RANGE= 0.200
 179_180    6.2437   J 07L_H2   07LH3A    STAT=Y  PRED= 3.040 RANGE= 6.000
 179_181    8.3839   J 07L_H2   07LH3B    STAT=Y  PRED= 13.950 RANGE= 4.000
 180_181  -13.3047   J 07LH3A   07LH3B    STAT=Y  PRED= -14.710 RANGE= 1.600
 180_182    8.2119   J 07LH3A   07L_H4    STAT=Y  PRED= 12.990 RANGE= 2.560
 181_182    5.7896   J 07LH3B   07L_H4    STAT=Y  PRED= 2.270 RANGE= 3.000
 182_183    6.5482   J 07L_H4   07L_H5    STAT=Y  PRED= 6.640 RANGE= 0.200
 182_186    6.5879   J 07L_H4   07L_H6    STAT=Y  PRED= 6.640 RANGE= 0.200
 190_191    8.8736   J 08V_H2   08V_H3    STAT=Y  PRED= 12.880 RANGE= 6.000
 191_192    6.5520   J 08V_H3   08V_H4    STAT=Y  PRED= 6.640 RANGE= 0.200
 191_195    6.7834   J 08V_H3   08V_H5    STAT=Y  PRED= 6.640 RANGE= 0.200
 201_202    7.6281   J 09V_H2   09V_H3    STAT=Y  PRED= 12.960 RANGE= 4.000
 202_203    6.4961   J 09V_H3   09V_H4    STAT=Y  PRED= 6.640 RANGE= 0.200
 202_206    6.7760   J 09V_H3   09V_H5    STAT=Y  PRED= 6.640 RANGE= 0.200
 212_213   11.1630   J 10Y_H2   10YH3A    STAT=Y  PRED= 12.890 RANGE= 4.000
 212_214    4.7143   J 10Y_H2   10YH3B    STAT=Y  PRED= 1.900 RANGE= 4.400
 213_214  -13.7295   J 10YH3A   10YH3B    STAT=Y  PRED= -16.760 RANGE= 2.560
 215_218    0.4880   J 10Y_H5   10Y_H7    STAT=Y  PRED= -0.300 RANGE= 0.500
 217_218    0.6708   J 10Y_H9   10Y_H7    STAT=Y  PRED= 1.020 RANGE= 1.200
 223_224    7.9094   J 11V_H2   11V_H3    STAT=Y  PRED= 3.450 RANGE= 9.000
 224_225    6.7483   J 11V_H3   11V_H4    STAT=Y  PRED= 6.640 RANGE= 0.200
 224_228    6.8064   J 11V_H3   11V_H5    STAT=Y  PRED= 6.640 RANGE= 0.200
 232_233    1.9005   J 12F_H2   12F_H3    STAT=Y  PRED= 1.900 RANGE= 6.600
 234_238    1.3335   J 12F_H5   12F_H5    STAT=Y  PRED= 1.980 RANGE= 1.200
 234_235    7.6508   J 12F_H5   12F_H6    STAT=Y  PRED= 7.660 RANGE= 0.340
 234_237    0.7769   J 12F_H6   12F_H5    STAT=Y  PRED= 0.550 RANGE= 0.750
 234_236    1.2760   J 12F_H5   12F_H7    STAT=Y  PRED= 1.260 RANGE= 1.200
 235_237    1.7027   J 12F_H6   12F_H6    STAT=Y  PRED= 1.480 RANGE= 1.200
 235_236    7.4760   J 12F_H6   12F_H7    STAT=Y  PRED= 7.400 RANGE= 0.240
 241_242    8.8924   J 13V_H2   13V_H3    STAT=Y  PRED= 12.320 RANGE= 6.000
 242_243    6.8372   J 13V_H3   13V_H4    STAT=Y  PRED= 6.640 RANGE= 0.200
 242_246    6.4162   J 13V_H3   13V_H5    STAT=Y  PRED= 6.640 RANGE= 0.200

CONTROL PARAMETERS:
      Solvent =  none (def. 99% enriched)
        1.000 =  Concentration (vol%, def=1.0%)
   0.00100000 =  Minimum line-intensity
   0.00100000 =  Diagonalization criterium (not in use)
 600.13201900 =  FIELD(1H,MHz), used to transform shifts to ppms
  11.63298481 =  Left frequency (ppm)
  -4.33373638 =  Right frequency (ppm)
        0.000 =  Acquisition time (s, for QMTLS)
        0.542 =  Line-width (for modes D, P & T, 0=use defaults)
  0.031750000 =  Data-point resolution (Hz)
        8.461 =  GAUSSIAN (%, 0=use default from INF)
```

Appendix I (continued)

```
     -9.471 =  Dispersion contribution (%, 0=use default from INF)
  0.00000000 =  Decoupling frequency (for DORES)

CONSTRAINTS (in equations X0 = 1.0)...use no empty lines
 EQUAL 01Val_H2 = 13Val_H2
 EQUAL 06Val_H5 = 11Val_H4
 EQUAL 07Leu_H5 = 07Leu_H6
 EQUAL 01V_H2   = 13V_H2
 EQUAL 06V_H5   = 11V_H4
 EQUAL 07L_H5   = 07L_H6
 IGNORE(HZ):  2900.885 to  2887.442
 IGNORE(HZ):  1991.286 to  1980.638
 IGNORE(HZ):  1165.333 to  1158.472
 IGNORE(HZ):   779.618 to   766.330
 IGNORE(HZ):  1376.676 to  1343.069
 IGNORE(HZ):  2900.600 to  2868.152

END of FILE
```

Appendix J. The PMS file of deoxyecumicin.

* NEW: the lines beginning by * are comment lines !
* To keep all the chemical shifts fixed during iteration
* replace "CHEMICAL SHIFTS(HZ):" by "..SHIFTS(HZ): fixed"
* The couplings can be fixed in the same way

NMR-data: C:\Users\jgnapo_2\Desktop\Wei_H14_XRays\H14_withoutGO
#$œ Date 10. 3.2014; Time 12:40:21 perch.pms

CHEMICAL SHIFTS(PPM):
PROTON 2*SPIN= 1 SPECIES=1H POPULATION(Y)= 0.99595
10Trp_H8/ 1 6.983127 1*1*1 STAT=Y PRED= 7.318 RANGE= 0.197 WIDTH(Y)= 2.896 RESP(Y)= 0.0009 HSQC= C74
01ValH45/ 1 2.313733 1*1*6 STAT=Y PRED= 2.370 RANGE= 0.307 WIDTH(Y)= 2.393 RESP(Y)= 0.0011 HSQC= C1_2
01Val_H2/ 1 2.667573 1*1*1 STAT=Y PRED= 4.169 RANGE= 0.637 WIDTH(Y)= 2.157 RESP(Y)= 0.0011 HSQC= C4
01Val_H3/ 1 2.049619 1*1*1 STAT=Y PRED= 1.952 RANGE= 0.815 WIDTH(Y)= 3.479 RESP(Y)= 0.0036 HSQC= C5
01Val_H6/ 1 0.851275 1*1*3 STAT=Y PRED= 0.509 RANGE= 0.865 WIDTH(Y)= 3.500 RESP(Y)= 0.0011 HSQC= C6
01Val_H7/ 1 0.981228 1*1*3 STAT=Y PRED= 0.818 RANGE= 0.357 WIDTH(Y)= 2.543 RESP(Y)= 0.0010 HSQC= C7
02Val_H2/ 1 4.673981 1*1*1 STAT=Y PRED= 4.508 RANGE= 0.805 WIDTH(Y)= 4.068 RESP(Y)= 0.0011 HSQC= C10
02Val_H3/ 1 2.085289 1*1*1 STAT=Y PRED= 2.155 RANGE= 0.775 WIDTH(Y)= 2.679 RESP(Y)= 0.0028 HSQC= C12
02Val_H4/ 1 0.982726 1*1*3 STAT=Y PRED= 1.038 RANGE= 0.277 WIDTH(Y)= 2.778 RESP(Y)= 0.0011 HSQC= C13
02Val_H5/ 1 1.045196 1*1*3 STAT=Y PRED= 0.943 RANGE= 0.247 WIDTH(Y)= 2.675 RESP(Y)= 0.0012 HSQC= C14
03Ile_H7/ 1 3.227581 1*1*3 STAT=Y PRED= 3.196 RANGE= 0.367 WIDTH(Y)= 2.264 RESP(Y)= 0.0011 HSQC= C15
03Ile_H2/ 1 4.944588 1*1*1 STAT=Y PRED= 4.617 RANGE= 1.628 WIDTH(Y)= 2.004 RESP(Y)= 0.0008 HSQC= C17
03Ile_H3/ 1 1.937799 1*1*1 STAT=Y PRED= 2.155 RANGE= 0.775 WIDTH(Y)= 2.761 RESP(Y)= 0.0028 HSQC= C19
03IleH4A/ 1 0.924717 1*1*1 STAT=Y PRED= 1.465 RANGE= 0.697 WIDTH(Y)= 5.377 RESP(Y)= 0.0065 HSQC= C20
03IleH4B/ 1 1.301602 1*1*1 STAT=Y PRED= 1.175 RANGE= 0.587 WIDTH(Y)= 3.737 RESP(Y)= 0.0032 HSQC= C20
03Ile_H6/ 1 0.753025 1*1*3 STAT=Y PRED= 0.723 RANGE= 0.397 WIDTH(Y)= 3.462 RESP(Y)= 0.0011 HSQC= C21
03Ile_H5/ 1 0.723546 1*1*3 STAT=Y PRED= 0.880 RANGE= 0.217 WIDTH(Y)= 2.491 RESP(Y)= 0.0009 HSQC= C22
04Thr_H2/ 1 5.133473 1*1*1 STAT=Y PRED= 4.668 RANGE= 1.015 WIDTH(Y)= 2.378 RESP(Y)= 0.0011 HSQC= C24
04Thr_H3/ 1 5.783248 1*1*1 STAT=Y PRED= 4.010 RANGE= 0.477 WIDTH(Y)= 3.357 RESP(Y)= 0.0009 HSQC= C25
04Thr_H4/ 1 1.314130 1*1*3 STAT=Y PRED= 1.270 RANGE= 0.497 WIDTH(Y)= 2.361 RESP(Y)= 0.0011 HSQC= C27
05Thr_H5/ 1 3.320489 1*1*3 STAT=Y PRED= 3.257 RANGE= 0.397 WIDTH(Y)= 3.305 RESP(Y)= 0.0014 HSQC= C29
05Thr_H2/ 1 5.027812 1*1*1 STAT=Y PRED= 4.099 RANGE= 1.025 WIDTH(Y)= 2.465 RESP(Y)= 0.0010 HSQC= C31
05Thr_H3/ 1 4.434779 1*1*1 STAT=Y PRED= 4.345 RANGE= 0.717 WIDTH(Y)= 2.800 RESP(Y)= 0.0010 HSQC= C32
05Thr_H4/ 1 0.885813 1*1*3 STAT=Y PRED= 1.252 RANGE= 0.297 WIDTH(Y)= 3.124 RESP(Y)= 0.0011 HSQC= C34
06Val_H2/ 1 4.825834 1*1*1 STAT=Y PRED= 4.525 RANGE= 1.405 WIDTH(Y)= 5.324 RESP(Y)= 0.0013 HSQC= C37
06Val_H3/ 1 2.363909 1*1*1 STAT=Y PRED= 1.975 RANGE= 1.015 WIDTH(Y)= 3.582 RESP(Y)= 0.0012 HSQC= C38
06Val_H4/ 1 1.096410 1*1*3 STAT=Y PRED= 0.938 RANGE= 0.217 WIDTH(Y)= 3.176 RESP(Y)= 0.0009 HSQC= C39
06Val_H5/ 1 0.981078 1*1*3 STAT=Y PRED= 1.094 RANGE= 0.387 WIDTH(Y)= 3.351 RESP(Y)= 0.0010 HSQC= C40
07Leu_H7/ 1 3.263216 1*1*3 STAT=Y PRED= 3.110 RANGE= 0.375 WIDTH(Y)= 2.594 RESP(Y)= 0.0010 HSQC= C42
07Leu_H2/ 1 5.168798 1*1*1 STAT=Y PRED= 5.342 RANGE= 1.085 WIDTH(Y)= 3.065 RESP(Y)= 0.0011 HSQC= C44
07LeuH3A/ 1 1.426128 1*1*1 STAT=Y PRED= 1.444 RANGE= 0.427 WIDTH(Y)= 2.832 RESP(Y)= 0.0006 HSQC= C45
07LeuH3B/ 1 1.263496 1*1*1 STAT=Y PRED= 1.914 RANGE= 0.367 WIDTH(Y)= 3.294 RESP(Y)= 0.0004 HSQC= C45
07Leu_H4/ 1 0.929710 1*1*1 STAT=Y PRED= 1.630 RANGE= 0.627 WIDTH(Y)= 0.539 RESP(Y)= 0.0003 HSQC= C46
07Leu_H5/ 1 0.321845 1*1*3 STAT=Y PRED= 0.972 RANGE= 0.315 WIDTH(Y)= 2.630 RESP(Y)= 0.0009 HSQC= C47
07Leu_H6/ 1 0.224479 1*1*3 STAT=Y PRED= 0.972 RANGE= 0.147 WIDTH(Y)= 2.858 RESP(Y)= 0.0009 HSQC= C48
08Val_H2/ 1 4.601863 1*1*1 STAT=Y PRED= 4.489 RANGE= 0.895 WIDTH(Y)= 2.819 RESP(Y)= 0.0006 HSQC= C51
08Val_H3/ 1 2.033263 1*1*1 STAT=Y PRED= 1.995 RANGE= 0.485 WIDTH(Y)= 2.835 RESP(Y)= 0.0010 HSQC= C52
08Val_H4/ 1 0.905792 1*1*3 STAT=Y PRED= 1.060 RANGE= 0.237 WIDTH(Y)= 5.464 RESP(Y)= 0.0004 HSQC= C53
08Val_H5/ 1 0.867816 1*1*3 STAT=Y PRED= 0.999 RANGE= 0.227 WIDTH(Y)= 3.578 RESP(Y)= 0.0011 HSQC= C54
09Val_H6/ 1 3.146454 1*1*3 STAT=Y PRED= 3.169 RANGE= 0.465 WIDTH(Y)= 2.506 RESP(Y)= 0.0010 HSQC= C56

Appendix J (continued)

09Val_H2/ 1 3.054257 1*1*1 STAT=Y PRED= 5.153 RANGE= 0.717 WIDTH(Y)= 2.691 RESP(Y)= 0.0009 HSQC= C58
09Val_H3/ 1 2.593771 1*1*1 STAT=Y PRED= 2.524 RANGE= 0.407 WIDTH(Y)= 2.508 RESP(Y)= 0.0009 HSQC= C59
09Val_H4/ 1 1.097742 1*1*3 STAT=Y PRED= 1.319 RANGE= 0.227 WIDTH(Y)= 5.458 RESP(Y)= 0.0007 HSQC= C60
09Val_H5/ 1 0.976341 1*1*3 STAT=Y PRED= 1.075 RANGE= 0.237 WIDTH(Y)= 3.108 RESP(Y)= 0.0009 HSQC= C61
10TrpH13/ 1 2.165339 1*1*3 STAT=Y PRED= 2.936 RANGE= 0.895 WIDTH(Y)= 2.547 RESP(Y)= 0.0011 HSQC= C63
10Trp_H2/ 1 4.094824 1*1*1 STAT=Y PRED= 5.043 RANGE= 1.765 WIDTH(Y)= 2.783 RESP(Y)= 0.0006 HSQC= C65
10TrpH3A/ 1 3.545602 1*1*1 STAT=Y PRED= 3.613 RANGE= 0.467 WIDTH(Y)= 5.358 RESP(Y)= -0.0005 HSQC= C66
10TrpH3B/ 1 3.691009 1*1*1 STAT=Y PRED= 3.367 RANGE= 0.627 WIDTH(Y)= 2.597 RESP(Y)= 0.0007 HSQC= C66
10Trp_H5/ 1 6.699203 1*1*1 STAT=Y PRED= 6.772 RANGE= 0.275 WIDTH(Y)= 2.870 RESP(Y)= 0.0009 HSQC= C68
10Trp_H9/ 1 6.442990 1*1*1 STAT=Y PRED= 7.089 RANGE= 0.217 WIDTH(Y)= 3.147 RESP(Y)= 0.0009 HSQC= C73
10Trp_H7/ 1 6.922025 1*1*1 STAT=Y PRED= 7.333 RANGE= 0.307 WIDTH(Y)= 2.237 RESP(Y)= 0.0008 HSQC= C75
10TrpH12/ 1 3.818301 1*1*3 STAT=Y PRED= 4.072 RANGE= 0.247 WIDTH(Y)= 2.130 RESP(Y)= 0.0010 HSQC= C77
11Val_H2/ 1 4.368950 1*1*1 STAT=Y PRED= 4.303 RANGE= 1.445 WIDTH(Y)= 2.525 RESP(Y)= 0.0008 HSQC= C80
11Val_H3/ 1 2.195260 1*1*1 STAT=Y PRED= 2.094 RANGE= 0.587 WIDTH(Y)= 4.033 RESP(Y)= 0.0030 HSQC= C81
11Val_H4/ 1 1.026640 1*1*3 STAT=Y PRED= 1.094 RANGE= 0.247 WIDTH(Y)= 3.031 RESP(Y)= 0.0013 HSQC= C82
11Val_H5/ 1 0.984237 1*1*3 STAT=Y PRED= 1.080 RANGE= 0.297 WIDTH(Y)= 3.676 RESP(Y)= 0.0012 HSQC= C83
12Phe_H2/ 1 4.797429 1*1*1 STAT=Y PRED= 4.499 RANGE= 0.985 WIDTH(Y)= 3.000 RESP(Y)= 0.0001 HSQC= C86
12PheH3A/ 1 3.349700 1*1*1 STAT=Y PRED= 5.208 RANGE= 0.487 WIDTH(Y)= 4.506 RESP(Y)= 0.0024 HSQC= C87
12PheH3B/ 1 2.841282 1*1*1 STAT=Y PRED= 5.208 RANGE= 0.487 WIDTH(Y)= 3.142 RESP(Y)= 0.0011 HSQC= C87
12Phe_H5/ 1 7.092791 1*2*1 STAT=Y PRED= 7.524 RANGE= 0.307 WIDTH(Y)= 2.685 RESP(Y)= 0.0012 HSQC= C89_93
12Phe_H6/ 1 7.202492 1*2*1 STAT=Y PRED= 7.372 RANGE= 0.577 WIDTH(Y)= 2.221 RESP(Y)= 0.0012 HSQC= C90_92
12Phe_H7/ 1 7.149534 1*1*1 STAT=Y PRED= 7.281 RANGE= 0.307 WIDTH(Y)= 2.409 RESP(Y)= 0.0011 HSQC= C91
13Val_H2/ 1 4.407003 1*1*1 STAT=Y PRED= 4.169 RANGE= 0.667 WIDTH(Y)= 3.065 RESP(Y)= 0.0013 HSQC= C97
13Val_H3/ 1 1.969079 1*1*1 STAT=Y PRED= 2.155 RANGE= 0.775 WIDTH(Y)= 2.734 RESP(Y)= 0.0028 HSQC= C99
13Val_H4/ 1 0.936815 1*1*3 STAT=Y PRED= 1.277 RANGE= 0.217 WIDTH(Y)= 4.948 RESP(Y)= 0.0005 HSQC= C100
13Val_H5/ 1 0.920700 1*1*3 STAT=Y PRED= 0.933 RANGE= 0.277 WIDTH(Y)= 2.376 RESP(Y)= 0.0008 HSQC= C101
PROTON 2*SPIN= 1 SPECIES=1H POPULATION(Y)= 0.00405
10Y_H8 / 2 6.981169 1*1*1 STAT=Y PRED= 7.318 RANGE= 0.197 WIDTH(Y)= 1.240 RESP(Y)= 0.1087 HSQC= 2C74
01VH45 / 2 2.316380 1*1*6 STAT=Y PRED= 2.370 RANGE= 0.307 WIDTH(Y)= 2.345 RESP(Y)= 0.0915 HSQC= 2C1_2
01V_H2 / 2 2.670761 1*1*1 STAT=Y PRED= 4.169 RANGE= 0.637 WIDTH(Y)= 2.441 RESP(Y)= 0.0878 HSQC= 2C4
01V_H3 / 2 2.041860 1*1*1 STAT=Y PRED= 1.952 RANGE= 0.815 WIDTH(Y)= 2.603 RESP(Y)= 1.0000 HSQC= 2C5
01V_H6 / 2 0.847609 1*1*3 STAT=Y PRED= 0.509 RANGE= 0.865 WIDTH(Y)= 4.125 RESP(Y)= 0.0903 HSQC= 2C6
01V_H7 / 2 0.979431 1*1*3 STAT=Y PRED= 0.818 RANGE= 0.357 WIDTH(Y)= 1.827 RESP(Y)= 0.0930 HSQC= 2C7
02V_H2 / 2 4.673002 1*1*1 STAT=Y PRED= 4.508 RANGE= 0.805 WIDTH(Y)= 1.647 RESP(Y)= 0.0720 HSQC= 2C10
02V_H3 / 2 2.102303 1*1*1 STAT=Y PRED= 2.155 RANGE= 0.775 WIDTH(Y)= 2.534 RESP(Y)= 0.5716 HSQC= 2C12
02V_H4 / 2 1.001924 1*1*3 STAT=Y PRED= 1.038 RANGE= 0.277 WIDTH(Y)= 4.776 RESP(Y)= 0.0962 HSQC= 2C13
02V_H5 / 2 1.054995 1*1*3 STAT=Y PRED= 0.943 RANGE= 0.247 WIDTH(Y)= 1.830 RESP(Y)= 0.0455 HSQC= 2C14
03I_H7 / 2 3.229634 1*1*3 STAT=Y PRED= 3.196 RANGE= 0.367 WIDTH(Y)= 2.493 RESP(Y)= 0.0772 HSQC= 2C15
03I_H2 / 2 4.917235 1*1*1 STAT=Y PRED= 4.617 RANGE= 1.628 WIDTH(Y)= 1.200 RESP(Y)= 0.0144 HSQC= 2C17
03I_H3 / 2 1.967471 1*1*1 STAT=Y PRED= 2.155 RANGE= 0.775 WIDTH(Y)= 2.440 RESP(Y)= 0.0028 HSQC= 2C19
03IH4A / 2 0.960566 1*1*1 STAT=Y PRED= 1.465 RANGE= 0.697 WIDTH(Y)= 5.242 RESP(Y)= 0.3864 HSQC= 2C20
03IH4B / 2 1.258721 1*1*1 STAT=Y PRED= 1.175 RANGE= 0.587 WIDTH(Y)= 2.894 RESP(Y)= 0.2199 HSQC= 2C20
03I_H6 / 2 0.750817 1*1*3 STAT=Y PRED= 0.723 RANGE= 0.397 WIDTH(Y)= 1.505 RESP(Y)= 0.0739 HSQC= 2C21
03I_H5 / 2 0.752284 1*1*3 STAT=Y PRED= 0.880 RANGE= 0.217 WIDTH(Y)= 4.337 RESP(Y)= 0.0773 HSQC= 2C22
04T_H2 / 2 5.166381 1*1*1 STAT=Y PRED= 4.668 RANGE= 1.015 WIDTH(Y)= 1.957 RESP(Y)= 0.0515 HSQC= 2C24
04T_H3 / 2 5.783879 1*1*1 STAT=Y PRED= 4.010 RANGE= 0.477 WIDTH(Y)= 3.200 RESP(Y)= 0.1195 HSQC= 2C25
04T_H4 / 2 1.316963 1*1*3 STAT=Y PRED= 1.270 RANGE= 0.497 WIDTH(Y)= 2.534 RESP(Y)= 0.0859 HSQC= 2C27
05T_H5 / 2 3.327995 1*1*3 STAT=Y PRED= 3.257 RANGE= 0.397 WIDTH(Y)= 3.073 RESP(Y)= 0.0363 HSQC= 2C29
05T_H2 / 2 5.011838 1*1*1 STAT=Y PRED= 4.099 RANGE= 1.025 WIDTH(Y)= 4.062 RESP(Y)= 0.0356 HSQC= 2C31
05T_H3 / 2 4.452621 1*1*1 STAT=Y PRED= 4.345 RANGE= 0.717 WIDTH(Y)= 3.220 RESP(Y)= 0.1146 HSQC= 2C32

Appendix J (continued)

05T_H4 / 2 0.915797 1*1*3 STAT=Y PRED= 1.252 RANGE= 0.297 WIDTH(Y)= 1.994 RESP(Y)= 0.0807 HSQC= 2C34
06V_H2 / 2 4.846700 1*1*1 STAT=Y PRED= 4.525 RANGE= 1.405 WIDTH(Y)= 5.284 RESP(Y)= 0.2697 HSQC= 2C37
06V_H3 / 2 2.348382 1*1*1 STAT=Y PRED= 1.975 RANGE= 1.015 WIDTH(Y)= 2.075 RESP(Y)= 0.1127 HSQC= 2C38
06V_H4 / 2 1.094360 1*1*3 STAT=Y PRED= 0.938 RANGE= 0.217 WIDTH(Y)= 1.439 RESP(Y)= 0.0976 HSQC= 2C39
06V_H5 / 2 0.975054 1*1*3 STAT=Y PRED= 1.094 RANGE= 0.387 WIDTH(Y)= 2.239 RESP(Y)= 0.1058 HSQC= 2C40
07L_H7 / 2 3.256745 1*1*3 STAT=Y PRED= 3.110 RANGE= 0.375 WIDTH(Y)= 1.320 RESP(Y)= 0.0221 HSQC= 2C42
07L_H2 / 2 5.107801 1*1*1 STAT=Y PRED= 5.342 RANGE= 1.085 WIDTH(Y)= 2.095 RESP(Y)= 0.0230 HSQC= 2C44
07LH3A / 2 1.453162 1*1*1 STAT=Y PRED= 1.444 RANGE= 0.427 WIDTH(Y)= 1.773 RESP(Y)= -0.0287 HSQC= 2C45
07LH3B / 2 1.233026 1*1*1 STAT=Y PRED= 1.914 RANGE= 0.367 WIDTH(Y)= 3.326 RESP(Y)= 0.1443 HSQC= 2C45
07L_H4 / 2 0.959514 1*1*1 STAT=Y PRED= 1.630 RANGE= 0.627 WIDTH(Y)= 0.775 RESP(Y)= 0.1110 HSQC= 2C46
07L_H5 / 2 0.334238 1*1*3 STAT=Y PRED= 0.972 RANGE= 0.315 WIDTH(Y)= 2.595 RESP(Y)= 0.0434 HSQC= 2C47
07L_H6 / 2 0.183833 1*1*3 STAT=Y PRED= 0.972 RANGE= 0.147 WIDTH(Y)= 3.217 RESP(Y)= 0.0547 HSQC= 2C48
08V_H2 / 2 4.585611 1*1*1 STAT=Y PRED= 4.489 RANGE= 0.895 WIDTH(Y)= 2.822 RESP(Y)= 0.1024 HSQC= 2C51
08V_H3 / 2 2.029978 1*1*1 STAT=Y PRED= 1.995 RANGE= 0.485 WIDTH(Y)= 2.913 RESP(Y)= -0.3870 HSQC= 2C52
08V_H4 / 2 0.914187 1*1*3 STAT=Y PRED= 1.060 RANGE= 0.237 WIDTH(Y)= 1.395 RESP(Y)= 0.0628 HSQC= 2C53
08V_H5 / 2 0.850989 1*1*3 STAT=Y PRED= 0.999 RANGE= 0.227 WIDTH(Y)= 2.029 RESP(Y)= 0.0746 HSQC= 2C54
09V_H6 / 2 3.139199 1*1*3 STAT=Y PRED= 3.169 RANGE= 0.465 WIDTH(Y)= 1.628 RESP(Y)= 0.0265 HSQC= 2C56
09V_H2 / 2 3.069517 1*1*1 STAT=Y PRED= 5.153 RANGE= 0.717 WIDTH(Y)= 2.567 RESP(Y)= -0.0094 HSQC= 2C58
09V_H3 / 2 2.583169 1*1*1 STAT=Y PRED= 2.524 RANGE= 0.407 WIDTH(Y)= 1.846 RESP(Y)= 0.0160 HSQC= 2C59
09V_H4 / 2 1.095810 1*1*3 STAT=Y PRED= 1.319 RANGE= 0.227 WIDTH(Y)= 1.802 RESP(Y)= 0.1114 HSQC= 2C60
09V_H5 / 2 0.977948 1*1*3 STAT=Y PRED= 1.075 RANGE= 0.237 WIDTH(Y)= 1.548 RESP(Y)= 0.0896 HSQC= 2C61
10YH13 / 2 2.158338 1*1*3 STAT=Y PRED= 2.936 RANGE= 0.895 WIDTH(Y)= 2.199 RESP(Y)= 0.0604 HSQC= 2C63
10Y_H2 / 2 4.095381 1*1*1 STAT=Y PRED= 5.043 RANGE= 1.765 WIDTH(Y)= 2.592 RESP(Y)= 0.1029 HSQC= 2C65
10YH3A / 2 3.547086 1*1*1 STAT=Y PRED= 3.613 RANGE= 0.467 WIDTH(Y)= 2.799 RESP(Y)= 0.3072 HSQC= 2C66
10YH3B / 2 3.696060 1*1*1 STAT=Y PRED= 3.367 RANGE= 0.627 WIDTH(Y)= 2.750 RESP(Y)= 0.0468 HSQC= 2C66
10Y_H5 / 2 6.697101 1*1*1 STAT=Y PRED= 6.772 RANGE= 0.275 WIDTH(Y)= 1.339 RESP(Y)= 0.0867 HSQC= 2C68
10Y_H9 / 2 6.440030 1*1*1 STAT=Y PRED= 7.089 RANGE= 0.217 WIDTH(Y)= 1.098 RESP(Y)= 0.0981 HSQC= 2C73
10Y_H7 / 2 6.920404 1*1*1 STAT=Y PRED= 7.333 RANGE= 0.307 WIDTH(Y)= 0.708 RESP(Y)= 0.0939 HSQC= 2C75
10YH12 / 2 3.828175 1*1*3 STAT=Y PRED= 4.072 RANGE= 0.247 WIDTH(Y)= 2.100 RESP(Y)= 0.0522 HSQC= 2C77
11V_H2 / 2 4.526543 1*1*1 STAT=Y PRED= 4.303 RANGE= 1.445 WIDTH(Y)= 6.717 RESP(Y)= 0.1162 HSQC= 2C80
11V_H3 / 2 2.202439 1*1*1 STAT=Y PRED= 2.094 RANGE= 0.587 WIDTH(Y)= 1.728 RESP(Y)= 0.1032 HSQC= 2C81
11V_H4 / 2 1.027208 1*1*3 STAT=Y PRED= 1.094 RANGE= 0.247 WIDTH(Y)= 1.038 RESP(Y)= -0.0280 HSQC= 2C82
11V_H5 / 2 0.995367 1*1*3 STAT=Y PRED= 1.080 RANGE= 0.297 WIDTH(Y)= 3.600 RESP(Y)= 0.1139 HSQC= 2C83
12F_H2 / 2 4.867004 1*1*1 STAT=Y PRED= 4.499 RANGE= 0.985 WIDTH(Y)= 1.209 RESP(Y)= 0.0249 HSQC= 2C86
12F_H3 / 2 5.340083 1*1*1 STAT=Y PRED= 5.208 RANGE= 0.487 WIDTH(Y)= 2.979 RESP(Y)= 0.0488 HSQC= 2C87
12F_H5 / 2 7.242371 1*2*1 STAT=Y PRED= 7.524 RANGE= 0.307 WIDTH(Y)= 6.488 RESP(Y)= 0.1084 HSQC= 2C89_93
12F_H6 / 2 7.254249 1*2*1 STAT=Y PRED= 7.372 RANGE= 0.577 WIDTH(Y)= 1.256 RESP(Y)= 0.0554 HSQC= 2C90_92
12F_H7 / 2 7.200272 1*1*1 STAT=Y PRED= 7.281 RANGE= 0.307 WIDTH(Y)= 4.125 RESP(Y)= 0.0296 HSQC= 2C91
13V_H2 / 2 4.400648 1*1*1 STAT=Y PRED= 4.169 RANGE= 0.667 WIDTH(Y)= 1.648 RESP(Y)= -0.0127 HSQC= 2C97
13V_H3 / 2 1.969239 1*1*1 STAT=Y PRED= 2.155 RANGE= 0.775 WIDTH(Y)= 2.441 RESP(Y)= 0.0028 HSQC= 2C99
13V_H4 / 2 0.936908 1*1*3 STAT=Y PRED= 1.277 RANGE= 0.217 WIDTH(Y)= 2.557 RESP(Y)= 0.1065 HSQC= 2C100
13V_H5 / 2 0.919029 1*1*3 STAT=Y PRED= 0.933 RANGE= 0.277 WIDTH(Y)= 1.757 RESP(Y)= 0.0855 HSQC= 2C101

COUPLING CONSTANTS(HZ):

J115_217 7.8341 J 10Trp_H8 10Trp_H9 STAT=Y PRED= 8.100 RANGE= 0.890
J115_218 8.2541 J 10Trp_H8 10Trp_H7 STAT=Y PRED= 7.850 RANGE= 0.800
J122_123 9.1318 J 01Val_H2 01Val_H3 STAT=Y PRED= 12.510 RANGE= 4.000
J123_124 6.5353 J 01Val_H3 01Val_H6 STAT=Y PRED= 6.640 RANGE= 0.200
J123_127 6.6822 J 01Val_H3 01Val_H7 STAT=Y PRED= 6.640 RANGE= 0.200
J131_132 8.6888 J 02Val_H2 02Val_H3 STAT=Y PRED= 12.600 RANGE= 6.000

Appendix J (continued)

J132_133 6.7974 J 02Val_H3 02Val_H4 STAT=Y PRED= 6.640 RANGE= 0.200
J132_136 6.7565 J 02Val_H3 02Val_H5 STAT=Y PRED= 6.640 RANGE= 0.200
J142_143 11.2672 J 03Ile_H2 03Ile_H3 STAT=Y PRED= 13.150 RANGE= 4.000
J143_144 0.4733 J 03Ile_H3 03IleH4A STAT=Y PRED= 1.950 RANGE= 3.000
J143_145 2.9143 J 03Ile_H3 03IleH4B STAT=Y PRED= 12.660 RANGE= 2.800
J143_146 6.5943 J 03Ile_H3 03Ile_H6 STAT=Y PRED= 6.640 RANGE= 0.200
J144_145 -12.2434 J 03IleH4A 03IleH4B STAT=Y PRED= -13.400 RANGE= 0.600
J144_149 7.3933 J 03IleH4A 03Ile_H5 STAT=Y PRED= 7.440 RANGE= 0.150
J145_149 7.4542 J 03IleH4B 03Ile_H5 STAT=Y PRED= 7.440 RANGE= 0.150
J153_154 2.3157 J 04Thr_H2 04Thr_H3 STAT=Y PRED= 2.690 RANGE= 6.600
J154_155 6.4896 J 04Thr_H3 04Thr_H4 STAT=Y PRED= 6.250 RANGE= 0.600
J161_162 3.6722 J 05Thr_H2 05Thr_H3 STAT=Y PRED= 2.440 RANGE= 4.400
J162_164 6.3652 J 05Thr_H3 05Thr_H4 STAT=Y PRED= 6.250 RANGE= 0.600
J168_169 8.7168 J 06Val_H2 06Val_H3 STAT=Y PRED= 2.980 RANGE= 6.600
J169_170 6.6194 J 06Val_H3 06Val_H4 STAT=Y PRED= 6.640 RANGE= 0.200
J169_173 6.9510 J 06Val_H3 06Val_H5 STAT=Y PRED= 6.640 RANGE= 0.200
J179_180 6.4093 J 07Leu_H2 07LeuH3A STAT=Y PRED= 3.040 RANGE= 6.000
J179_181 8.3999 J 07Leu_H2 07LeuH3B STAT=Y PRED= 13.950 RANGE= 4.000
J180_181 -13.3061 J 07LeuH3A 07LeuH3B STAT=Y PRED= -14.710 RANGE= 1.600
J180_182 8.0994 J 07LeuH3A 07Leu_H4 STAT=Y PRED= 12.990 RANGE= 2.560
J181_182 5.8496 J 07LeuH3B 07Leu_H4 STAT=Y PRED= 2.270 RANGE= 3.000
J182_183 6.4860 J 07Leu_H4 07Leu_H5 STAT=Y PRED= 6.640 RANGE= 0.200
J182_186 6.6355 J 07Leu_H4 07Leu_H6 STAT=Y PRED= 6.640 RANGE= 0.200
J190_191 8.9242 J 08Val_H2 08Val_H3 STAT=Y PRED= 12.880 RANGE= 6.000
J191_192 7.2063 J 08Val_H3 08Val_H4 STAT=Y PRED= 6.640 RANGE= 0.200
J191_195 6.7157 J 08Val_H3 08Val_H5 STAT=Y PRED= 6.640 RANGE= 0.200
J201_202 7.6441 J 09Val_H2 09Val_H3 STAT=Y PRED= 12.960 RANGE= 4.000
J202_203 6.3139 J 09Val_H3 09Val_H4 STAT=Y PRED= 6.640 RANGE= 0.200
J202_206 6.9207 J 09Val_H3 09Val_H5 STAT=Y PRED= 6.640 RANGE= 0.200
J212_213 10.9847 J 10Trp_H2 10TrpH3A STAT=Y PRED= 12.890 RANGE= 4.000
J212_214 4.6743 J 10Trp_H2 10TrpH3B STAT=Y PRED= 1.900 RANGE= 4.400
J213_214 -13.9317 J 10TrpH3A 10TrpH3B STAT=Y PRED= -16.760 RANGE= 2.560
J215_218 0.4627 J 10Trp_H5 10Trp_H7 STAT=Y PRED= -0.300 RANGE= 0.500
J217_218 0.5746 J 10Trp_H9 10Trp_H7 STAT=Y PRED= 1.020 RANGE= 1.200
J223_224 8.4170 J 11Val_H2 11Val_H3 STAT=Y PRED= 3.450 RANGE= 9.000
J224_225 6.7699 J 11Val_H3 11Val_H4 STAT=Y PRED= 6.640 RANGE= 0.200
J224_228 6.7801 J 11Val_H3 11Val_H5 STAT=Y PRED= 6.640 RANGE= 0.200
F23 13.1202 J 12Phe_H2 12PheH3A STAT=Y PRED= 1.900 RANGE= 6.600
F23b 10.5559 J 12Phe_H2 12PheH3B STAT=Y PRED= 1.900 RANGE= 6.600
F33 -13.9160 J 12PheH3A 12PheH3B STAT=Y PRED= 1.900 RANGE= 6.600
J234_238 1.4186 J 12Phe_H5 12Phe_H5 STAT=Y PRED= 1.980 RANGE= 1.200
J234_235 7.7010 J 12Phe_H5 12Phe_H6 STAT=Y PRED= 7.660 RANGE= 0.340
J234_237 0.6922 J 12Phe_H6 12Phe_H5 STAT=Y PRED= 0.550 RANGE= 0.750
J234_236 1.1263 J 12Phe_H5 12Phe_H7 STAT=Y PRED= 1.260 RANGE= 1.200
J235_237 1.5635 J 12Phe_H6 12Phe_H6 STAT=Y PRED= 1.480 RANGE= 1.200
J235_236 7.4519 J 12Phe_H6 12Phe_H7 STAT=Y PRED= 7.400 RANGE= 0.240
J241_242 8.8938 J 13Val_H2 13Val_H3 STAT=Y PRED= 12.320 RANGE= 6.000
J242_243 6.7287 J 13Val_H3 13Val_H4 STAT=Y PRED= 6.640 RANGE= 0.200
J242_246 6.4490 J 13Val_H3 13Val_H5 STAT=Y PRED= 6.640 RANGE= 0.200
115_217 7.8190 J 10Y_H8 10Y_H9 STAT=Y PRED= 8.100 RANGE= 0.890

Appendix J (continued)

115_218 8.1817 J 10Y_H8 10Y_H7 STAT=Y PRED= 7.850 RANGE= 0.800
122_123 9.2123 J 01V_H2 01V_H3 STAT=Y PRED= 12.510 RANGE= 4.000
123_124 6.9596 J 01V_H3 01V_H6 STAT=Y PRED= 6.640 RANGE= 0.200
123_127 6.6826 J 01V_H3 01V_H7 STAT=Y PRED= 6.640 RANGE= 0.200
131_132 8.7392 J 02V_H2 02V_H3 STAT=Y PRED= 12.600 RANGE= 6.000
132_133 6.7456 J 02V_H3 02V_H4 STAT=Y PRED= 6.640 RANGE= 0.200
132_136 6.6587 J 02V_H3 02V_H5 STAT=Y PRED= 6.640 RANGE= 0.200
142_143 11.3172 J 03I_H2 03I_H3 STAT=Y PRED= 13.150 RANGE= 4.000
143_144 0.4615 J 03I_H3 03IH4A STAT=Y PRED= 1.950 RANGE= 3.000
143_145 2.7273 J 03I_H3 03IH4B STAT=Y PRED= 12.660 RANGE= 2.800
143_146 6.5602 J 03I_H3 03I_H6 STAT=Y PRED= 6.640 RANGE= 0.200
144_145 -12.4414 J 03IH4A 03IH4B STAT=Y PRED= -13.400 RANGE= 0.600
144_149 7.3376 J 03IH4A 03I_H5 STAT=Y PRED= 7.440 RANGE= 0.150
145_149 7.4487 J 03IH4B 03I_H5 STAT=Y PRED= 7.440 RANGE= 0.150
153_154 2.3513 J 04T_H2 04T_H3 STAT=Y PRED= 2.690 RANGE= 6.600
154_155 6.4912 J 04T_H3 04T_H4 STAT=Y PRED= 6.250 RANGE= 0.600
161_162 3.7198 J 05T_H2 05T_H3 STAT=Y PRED= 2.440 RANGE= 4.400
162_164 6.4861 J 05T_H3 05T_H4 STAT=Y PRED= 6.250 RANGE= 0.600
168_169 9.5371 J 06V_H2 06V_H3 STAT=Y PRED= 2.980 RANGE= 6.600
169_170 6.6359 J 06V_H3 06V_H4 STAT=Y PRED= 6.640 RANGE= 0.200
169_173 7.0196 J 06V_H3 06V_H5 STAT=Y PRED= 6.640 RANGE= 0.200
179_180 6.2454 J 07L_H2 07LH3A STAT=Y PRED= 3.040 RANGE= 6.000
179_181 8.3655 J 07L_H2 07LH3B STAT=Y PRED= 13.950 RANGE= 4.000
180_181 -13.2862 J 07LH3A 07LH3B STAT=Y PRED= -14.710 RANGE= 1.600
180_182 8.1966 J 07LH3A 07L_H4 STAT=Y PRED= 12.990 RANGE= 2.560
181_182 5.6475 J 07LH3B 07L_H4 STAT=Y PRED= 2.270 RANGE= 3.000
182_183 6.1444 J 07L_H4 07L_H5 STAT=Y PRED= 6.640 RANGE= 0.200
182_186 6.7639 J 07L_H4 07L_H6 STAT=Y PRED= 6.640 RANGE= 0.200
190_191 9.1785 J 08V_H2 08V_H3 STAT=Y PRED= 12.880 RANGE= 6.000
191_192 6.5252 J 08V_H3 08V_H4 STAT=Y PRED= 6.640 RANGE= 0.200
191_195 6.6198 J 08V_H3 08V_H5 STAT=Y PRED= 6.640 RANGE= 0.200
201_202 7.6271 J 09V_H2 09V_H3 STAT=Y PRED= 12.960 RANGE= 4.000
202_203 6.5511 J 09V_H3 09V_H4 STAT=Y PRED= 6.640 RANGE= 0.200
202_206 6.7993 J 09V_H3 09V_H5 STAT=Y PRED= 6.640 RANGE= 0.200
212_213 11.2213 J 10Y_H2 10YH3A STAT=Y PRED= 12.890 RANGE= 4.000
212_214 4.5999 J 10Y_H2 10YH3B STAT=Y PRED= 1.900 RANGE= 4.400
213_214 -13.7036 J 10YH3A 10YH3B STAT=Y PRED= -16.760 RANGE= 2.560
215_218 0.4722 J 10Y_H5 10Y_H7 STAT=Y PRED= -0.300 RANGE= 0.500
217_218 0.6202 J 10Y_H9 10Y_H7 STAT=Y PRED= 1.020 RANGE= 1.200
223_224 8.0434 J 11V_H2 11V_H3 STAT=Y PRED= 3.450 RANGE= 9.000
224_225 6.7574 J 11V_H3 11V_H4 STAT=Y PRED= 6.640 RANGE= 0.200
224_228 7.0071 J 11V_H3 11V_H5 STAT=Y PRED= 6.640 RANGE= 0.200
232_233 1.7657 J 12F_H2 12F_H3 STAT=Y PRED= 1.900 RANGE= 6.600
234_238 1.3347 J 12F_H5 12F_H5 STAT=Y PRED= 1.980 RANGE= 1.200
234_235 7.6929 J 12F_H5 12F_H6 STAT=Y PRED= 7.660 RANGE= 0.340
234_237 0.7971 J 12F_H6 12F_H5 STAT=Y PRED= 0.550 RANGE= 0.750
234_236 1.2586 J 12F_H5 12F_H7 STAT=Y PRED= 1.260 RANGE= 1.200
235_237 1.7100 J 12F_H6 12F_H6 STAT=Y PRED= 1.480 RANGE= 1.200
235_236 7.4191 J 12F_H6 12F_H7 STAT=Y PRED= 7.400 RANGE= 0.240
241_242 8.8889 J 13V_H2 13V_H3 STAT=Y PRED= 12.320 RANGE= 6.000

Appendix J (continued)

```
 242_243    6.9574   J 13V_H3   13V_H4    STAT=Y  PRED= 6.640 RANGE= 0.200
 242_246    6.5087   J 13V_H3   13V_H5    STAT=Y  PRED= 6.640 RANGE= 0.200

CONTROL PARAMETERS:
      Solvent =  none (def. 99% enriched)
        1.000 =  Concentration (vol%, def=1.0%)
   0.00100000 =  Minimum line-intensity
   0.00100000 =  Diagonalization criterium (not in use)
 600.13201900 =  FIELD(1H,MHz), used to transform shifts to ppms
  11.63298481 =  Left frequency (ppm)
  -4.33373638 =  Right frequency (ppm)
       10.000 =  Acquisition time (s, for QMTLS)
        0.000 =  Line-width (for modes D, P & T, 0=use defaults)
  0.026949999 =  Data-point resolution (Hz)
        5.466 =  GAUSSIAN (%, 0=use default from INF)
      -10.108 =  Dispersion contribution (%, 0=use default from INF)
   0.00000000 =  Decoupling frequency (for DORES)

CONSTRAINTS (in equations X0 = 1.0)...use no empty lines
 EQUAL 01Val_H2 = 13Val_H2
 EQUAL 06Val_H5 = 11Val_H4
 EQUAL 07Leu_H5 = 07Leu_H6
 EQUAL 01V_H2   = 13V_H2
 EQUAL 06V_H5   = 11V_H4
 EQUAL 07L_H5   = 07L_H6
 EQUAL 12PheH3A = 12PheH3B
 IGNORE(HZ):  2900.885 to  2887.442
 IGNORE(HZ):  1991.286 to  1980.638
 IGNORE(HZ):  1165.333 to  1158.472
 IGNORE(HZ):   779.618 to   766.330
 IGNORE(HZ):  1376.676 to  1343.069
 IGNORE(HZ):  2900.600 to  2868.152
 IGNORE(HZ):  1700.282 to  1696.127

END of FILE
```

Appendix K. PMS file for deoxyecumicin. ^{1}H NMR spectrum obtained with Bruker Avance 600 instrument; sample contains residual acid.

* NEW: the lines beginning by * are comment lines !
* To keep all the chemical shifts fixed during iteration
* replace "CHEMICAL SHIFTS(HZ):" by "..SHIFTS(HZ): fixed"
* The couplings can be fixed in the same way

NMR-data: C:\Users\wgao\Documents\My Box Files\ITR Lab work\Lab Data\ECUM\H
#$œ Date 9.11.2013; Time 11:48:50 perch.pms

CHEMICAL SHIFTS(PPM):
PROTON 2*SPIN= 1 SPECIES=1H POPULATION(Y)= 1.00000
H74 / 1 6.980223 1*1*1 STAT=Y PRED= 7.031 RANGE= 0.240 WIDTH(N)= 2.026 RESP(Y)= 0.1072 HSQC= C74
H1_2 / 1 2.537946 1*1*6 STAT=Y PRED= 2.302 RANGE= 0.325 WIDTH(Y)= 4.785 RESP(Y)= 0.1140 HSQC= C1_2
H4 / 1 3.062813 1*1*1 STAT=Y PRED= 3.393 RANGE= 0.557 WIDTH(Y)= 2.675 RESP(Y)= 0.1107 HSQC= C4
H5 / 1 2.174726 1*1*1 STAT=Y PRED= 2.069 RANGE= 0.855 WIDTH(Y)= 3.745 RESP(Y)= 0.0774 HSQC= C5
H6 / 1 0.867986 1*1*3 STAT=Y PRED= 0.895 RANGE= 0.562 WIDTH(Y)= 3.092 RESP(Y)= 0.1048 HSQC= C6
H7 / 1 1.024909 1*1*3 STAT=Y PRED= 0.900 RANGE= 0.312 WIDTH(Y)= 2.926 RESP(Y)= 0.1057 HSQC= C7
H9 / 1 7.175999 1*1*1 STAT=Y PRED= 7.176 RANGE= 1.673 WIDTH(Y)= 21.040 RESP(Y)= 0.0096
H10 / 1 4.680628 1*1*1 STAT=Y PRED= 4.483 RANGE= 0.790 WIDTH(Y)= 2.432 RESP(Y)= 0.1035 HSQC= C10
H12 / 1 2.107298 1*1*1 STAT=Y PRED= 2.307 RANGE= 0.900 WIDTH(Y)= 2.914 RESP(Y)= 0.1031 HSQC= C12
H13 / 1 1.051311 1*1*3 STAT=Y PRED= 1.066 RANGE= 0.267 WIDTH(Y)= 2.524 RESP(Y)= 0.1090 HSQC= C13
H14 / 1 1.020821 1*1*3 STAT=Y PRED= 0.890 RANGE= 0.277 WIDTH(Y)= 3.396 RESP(Y)= 0.1288 HSQC= C14
H15 / 1 3.233304 1*1*3 STAT=Y PRED= 3.279 RANGE= 0.380 WIDTH(Y)= 2.308 RESP(Y)= 0.1113 HSQC= C15
H17 / 1 4.948305 1*1*1 STAT=Y PRED= 4.819 RANGE= 0.920 WIDTH(Y)= 2.111 RESP(Y)= 0.0965 HSQC= C17
H19 / 1 1.939506 1*1*1 STAT=Y PRED= 2.097 RANGE= 0.722 WIDTH(Y)= 4.009 RESP(Y)= 0.0506 HSQC= C19
H20A / 1 0.985820 1*1*1 STAT=Y PRED= 1.126 RANGE= 0.687 WIDTH(Y)= 7.317 RESP(Y)= 1.0000 HSQC= C20
H20B / 1 1.245980 1*1*1 STAT=Y PRED= 1.095 RANGE= 0.512 WIDTH(Y)= 4.213 RESP(Y)= 0.0807 HSQC= C20
H21 / 1 0.753237 1*1*3 STAT=Y PRED= 0.849 RANGE= 0.287 WIDTH(Y)= 2.972 RESP(Y)= 0.1229 HSQC= C21
H22 / 1 0.716440 1*1*3 STAT=Y PRED= 0.837 RANGE= 0.222 WIDTH(Y)= 2.224 RESP(Y)= 0.0891 HSQC= C22
H23 / 1 8.485799 1*1*1 STAT=Y PRED= 7.583 RANGE= 1.645 WIDTH(Y)= 2.500 RESP(Y)= 0.0466
H24 / 1 5.130787 1*1*1 STAT=Y PRED= 4.479 RANGE= 0.940 WIDTH(Y)= 1.919 RESP(Y)= 0.0890 HSQC= C24
H25 / 1 5.794303 1*1*1 STAT=Y PRED= 4.829 RANGE= 0.577 WIDTH(Y)= 2.484 RESP(Y)= 0.1014 HSQC= C25
H27 / 1 1.314599 1*1*3 STAT=Y PRED= 1.136 RANGE= 0.497 WIDTH(Y)= 2.863 RESP(Y)= 0.1149 HSQC= C27
H29 / 1 3.264873 1*1*3 STAT=Y PRED= 3.474 RANGE= 0.422 WIDTH(Y)= 2.302 RESP(Y)= 0.0931 HSQC= C29
H31 / 1 5.031622 1*1*1 STAT=Y PRED= 5.502 RANGE= 1.010 WIDTH(Y)= 2.175 RESP(Y)= 0.0916 HSQC= C31
H32 / 1 4.441880 1*1*1 STAT=Y PRED= 4.466 RANGE= 0.727 WIDTH(Y)= 2.567 RESP(Y)= 0.1036 HSQC= C32
H33 / 1 8.478019 1*1*1 STAT=Y PRED= 3.368 RANGE= 1.750 WIDTH(Y)= 16.040 RESP(Y)= 0.0466
H34 / 1 0.891519 1*1*3 STAT=Y PRED= 1.119 RANGE= 0.340 WIDTH(Y)= 3.099 RESP(Y)= 0.1310 HSQC= C34
H36 / 1 7.704351 1*1*1 STAT=Y PRED= 8.455 RANGE= 0.885 WIDTH(Y)= 2.944 RESP(Y)= 0.0870
H37 / 1 4.824639 1*1*1 STAT=Y PRED= 4.618 RANGE= 1.485 WIDTH(Y)= 2.827 RESP(Y)= 0.1009 HSQC= C37
H38 / 1 2.364756 1*1*1 STAT=Y PRED= 2.343 RANGE= 1.115 WIDTH(Y)= 3.475 RESP(Y)= 0.0962 HSQC= C38
H39 / 1 0.971743 1*1*3 STAT=Y PRED= 0.967 RANGE= 0.242 WIDTH(Y)= 2.866 RESP(Y)= 0.0640 HSQC= C39
H40 / 1 1.099781 1*1*3 STAT=Y PRED= 1.023 RANGE= 0.362 WIDTH(Y)= 3.127 RESP(Y)= 0.1108 HSQC= C40
H42 / 1 3.323220 1*1*3 STAT=Y PRED= 3.255 RANGE= 0.437 WIDTH(Y)= 2.539 RESP(Y)= 0.1059 HSQC= C42
H44 / 1 5.145381 1*1*1 STAT=Y PRED= 5.709 RANGE= 1.165 WIDTH(Y)= 3.674 RESP(Y)= 0.1108 HSQC= C44
H45A / 1 1.275939 1*1*1 STAT=Y PRED= 1.254 RANGE= 0.692 WIDTH(Y)= 4.055 RESP(Y)= 0.1301 HSQC= C45
H45B / 1 1.427323 1*1*1 STAT=Y PRED= 1.409 RANGE= 0.510 WIDTH(Y)= 3.027 RESP(Y)= 0.0909 HSQC= C45
H46 / 1 1.000125 1*1*1 STAT=Y PRED= 1.581 RANGE= 0.745 WIDTH(Y)= 5.911 RESP(Y)= 1.0000 HSQC= C46
H47 / 1 0.202034 1*1*3 STAT=Y PRED= 0.375 RANGE= 0.705 WIDTH(N)= 2.662 RESP(Y)= 0.0912 HSQC= C47
H48 / 1 0.313917 1*1*3 STAT=Y PRED= 0.462 RANGE= 0.682 WIDTH(N)= 2.655 RESP(Y)= 0.0905 HSQC= C48

Appendix K (continued)

H50 / 1 7.795019 1*1*1 STAT=Y PRED= 7.525 RANGE= 0.900 WIDTH(Y)= 3.114 RESP(Y)= 0.0952
H51 / 1 4.584670 1*1*1 STAT=Y PRED= 4.429 RANGE= 0.825 WIDTH(Y)= 2.281 RESP(Y)= 0.0914 HSQC= C51
H52 / 1 2.043174 1*1*1 STAT=Y PRED= 2.081 RANGE= 0.697 WIDTH(Y)= 3.343 RESP(Y)= 0.0913 HSQC= C52
H53 / 1 0.913967 1*1*3 STAT=Y PRED= 0.937 RANGE= 0.235 WIDTH(Y)= 2.898 RESP(Y)= 0.1142 HSQC= C53
H54 / 1 0.878982 1*1*3 STAT=Y PRED= 0.782 RANGE= 0.255 WIDTH(Y)= 3.234 RESP(Y)= 0.1034 HSQC= C54
H56 / 1 3.147105 1*1*3 STAT=Y PRED= 2.954 RANGE= 0.457 WIDTH(Y)= 2.275 RESP(Y)= 0.0913 HSQC= C56
H58 / 1 3.055236 1*1*1 STAT=Y PRED= 5.153 RANGE= 0.752 WIDTH(Y)= 4.308 RESP(Y)= 0.0834 HSQC= C58
H59 / 1 2.569991 1*1*1 STAT=Y PRED= 2.623 RANGE= 0.707 WIDTH(Y)= 4.141 RESP(Y)= 0.0397 HSQC= C59
H60 / 1 0.978884 1*1*3 STAT=Y PRED= 1.238 RANGE= 0.255 WIDTH(Y)= 3.086 RESP(Y)= 0.0986 HSQC= C60
H61 / 1 1.093004 1*1*3 STAT=Y PRED= 0.932 RANGE= 0.255 WIDTH(Y)= 2.259 RESP(Y)= 0.0954 HSQC= C61
H63 / 1 2.161684 1*1*3 STAT=Y PRED= 2.719 RANGE= 0.925 WIDTH(Y)= 2.164 RESP(Y)= 0.0904 HSQC= C63
H65 / 1 4.092313 1*1*1 STAT=Y PRED= 4.369 RANGE= 1.070 WIDTH(N)= 2.682 RESP(Y)= 0.0891 HSQC= C65
H66A / 1 3.542091 1*1*1 STAT=Y PRED= 3.100 RANGE= 0.375 WIDTH(N)= 2.631 RESP(Y)= 0.0959 HSQC= C66
H66B / 1 3.687640 1*1*1 STAT=Y PRED= 3.791 RANGE= 0.465 WIDTH(N)= 3.173 RESP(Y)= 0.0964 HSQC= C66
H68 / 1 6.695587 1*1*1 STAT=Y PRED= 6.634 RANGE= 0.667 WIDTH(N)= 1.568 RESP(Y)= 0.0943 HSQC= C68
H69 / 1 8.484703 1*1*1 STAT=Y PRED= 7.404 RANGE= 1.828 WIDTH(N)= 2.500 RESP(Y)= 0.0466
H73 / 1 6.437455 1*1*1 STAT=Y PRED= 6.592 RANGE= 0.447 WIDTH(N)= 2.345 RESP(Y)= 0.1060 HSQC= C73
H75 / 1 6.919230 1*1*1 STAT=Y PRED= 6.967 RANGE= 0.532 WIDTH(N)= 1.342 RESP(Y)= 0.0948 HSQC= C75
H77 / 1 3.813394 1*1*3 STAT=Y PRED= 3.866 RANGE= 0.210 WIDTH(N)= 2.068 RESP(Y)= 0.0953 HSQC= C77
H79 / 1 9.154038 1*1*1 STAT=Y PRED= 7.015 RANGE= 1.675 WIDTH(Y)= 3.345 RESP(Y)= 0.0899
H80 / 1 4.402499 1*1*1 STAT=Y PRED= 4.029 RANGE= 1.360 WIDTH(Y)= 2.728 RESP(Y)= 0.1073 HSQC= C80
H81 / 1 2.178353 1*1*1 STAT=Y PRED= 2.226 RANGE= 0.717 WIDTH(Y)= 3.721 RESP(Y)= 0.1453 HSQC= C81
H82 / 1 0.978312 1*1*3 STAT=Y PRED= 1.059 RANGE= 0.220 WIDTH(Y)= 3.081 RESP(Y)= 0.0913 HSQC= C82
H83 / 1 0.985578 1*1*3 STAT=Y PRED= 0.919 RANGE= 0.382 WIDTH(Y)= 2.523 RESP(Y)= 0.0835 HSQC= C83
H85 / 1 8.699132 1*1*1 STAT=Y PRED= 7.293 RANGE= 1.718 WIDTH(Y)= 3.218 RESP(Y)= 0.0760
H86 / 1 4.775819 1*1*1 STAT=Y PRED= 4.499 RANGE= 1.055 WIDTH(Y)= 3.036 RESP(Y)= 0.0804 HSQC= C86
H87 / 1 3.338017 1*1*1 STAT=Y PRED= 3.009 RANGE= 0.705 WIDTH(Y)= 8.847 RESP(Y)= 0.2940 HSQC= C87
H89_93/ 1 7.088374 1*2*1 STAT=Y PRED= 7.004 RANGE= 0.472 WIDTH(N)= 2.382 RESP(Y)= 0.1055 HSQC= C89_93
H90_92/ 1 7.205146 1*2*1 STAT=Y PRED= 7.144 RANGE= 0.305 WIDTH(N)= 2.167 RESP(Y)= 0.1085 HSQC= C90_92
H91 / 1 7.152829 1*1*1 STAT=Y PRED= 7.105 RANGE= 0.315 WIDTH(N)= 2.105 RESP(Y)= 0.1016 HSQC= C91
H96 / 1 9.039539 1*1*1 STAT=Y PRED= 10.454 RANGE= 1.750 WIDTH(Y)= 3.196 RESP(Y)= 0.0922
H97 / 1 4.359956 1*1*1 STAT=Y PRED= 4.349 RANGE= 0.732 WIDTH(Y)= 2.025 RESP(Y)= 0.0841 HSQC= C97
H99 / 1 1.962051 1*1*1 STAT=Y PRED= 2.081 RANGE= 0.870 WIDTH(Y)= 5.444 RESP(Y)= 0.2025 HSQC= C99
H100 / 1 0.920214 1*1*3 STAT=Y PRED= 1.028 RANGE= 0.202 WIDTH(Y)= 2.931 RESP(Y)= 0.1114 HSQC= C100
H101 / 1 0.936201 1*1*3 STAT=Y PRED= 0.914 RANGE= 0.355 WIDTH(Y)= 3.485 RESP(Y)= 0.1179 HSQC= C101
H87B / 1 2.836295 1*1*1 STAT=Y PRED= 2.914 RANGE= 0.387 WIDTH(Y)= 4.721 RESP(Y)= 0.1162 HSQC= C87

COUPLING CONSTANTS(HZ):
J114_215 0.1050 J H74 H69 STAT=N PRED= -0.150 RANGE= 0.360
J114_216 7.8171 J H74 H73 STAT=N PRED= 8.100 RANGE= 0.890
J114_217 8.1722 J H74 H75 STAT=N PRED= 7.850 RANGE= 0.800
J121_122 7.8164 J H4 H5 STAT=N PRED= 12.760 RANGE= 4.000
J122_123 8.5657 J H5 H6 STAT=Y PRED= 6.640 RANGE= 0.200
J122_126 6.6234 J H5 H7 STAT=Y PRED= 6.640 RANGE= 0.200
J130_131 8.7327 J H10 H12 STAT=N PRED= 13.120 RANGE= 6.000
J131_132 6.6028 J H12 H13 STAT=N PRED= 6.640 RANGE= 0.200
J131_135 6.6899 J H12 H14 STAT=N PRED= 6.640 RANGE= 0.200
J141_142 11.2668 J H17 H19 STAT=N PRED= 13.370 RANGE= 4.000
J142_143 1.9966 J H19 H20A STAT=Y PRED= 2.370 RANGE= 2.560
J142_144 9.2089 J H19 H20B STAT=Y PRED= 13.350 RANGE= 2.560

Appendix K (continued)

J142_145 6.5618 J H19 H21 STAT=N PRED= 6.640 RANGE= 0.200
J143_144 -13.9498 J H20A H20B STAT=N PRED= -13.400 RANGE= 0.600
J143_148 7.6189 J H20A H22 STAT=N PRED= 7.440 RANGE= 0.150
J144_148 7.2283 J H20B H22 STAT=N PRED= 7.440 RANGE= 0.150
J152_153 2.2367 J H24 H25 STAT=N PRED= 1.690 RANGE= 6.000
J153_154 6.4232 J H25 H27 STAT=N PRED= 6.250 RANGE= 0.600
J160_161 3.5823 J H31 H32 STAT=N PRED= 2.370 RANGE= 4.000
J161_163 6.4807 J H32 H34 STAT=N PRED= 6.250 RANGE= 0.600
J166_167 8.6706 J H36 H37 STAT=N PRED= 7.720 RANGE= 3.580
J167_168 9.1799 J H37 H38 STAT=N PRED= 2.320 RANGE= 6.000
139 0.0000 J H37 H40 STAT=Y
J168_169 6.5000 J H38 H39 STAT=N PRED= 6.640 RANGE= 0.200
J168_172 6.5658 J H38 H40 STAT=N PRED= 6.640 RANGE= 0.200
J178_179 7.7589 J H44 H45A STAT=N PRED= 13.740 RANGE= 4.000
J178_180 6.0896 J H44 H45B STAT=N PRED= 1.680 RANGE= 4.000
J179_180 -13.8589 J H45A H45B STAT=N PRED= -14.670 RANGE= 1.600
J179_181 6.6290 J H45A H46 STAT=N PRED= 12.620 RANGE= 2.560
J180_181 8.5309 J H45B H46 STAT=N PRED= 0.740 RANGE= 2.560
J181_182 6.5748 J H46 H47 STAT=N PRED= 6.640 RANGE= 0.200
J181_185 6.5359 J H46 H48 STAT=N PRED= 6.640 RANGE= 0.200
J188_189 9.6192 J H50 H51 STAT=N PRED= 6.950 RANGE= 3.580
J189_190 9.0469 J H51 H52 STAT=N PRED= 13.060 RANGE= 6.000
J190_191 6.7111 J H52 H53 STAT=N PRED= 6.640 RANGE= 0.200
J190_194 8.2495 J H52 H54 STAT=N PRED= 6.640 RANGE= 0.200
J200_201 7.8724 J H58 H59 STAT=N PRED= 12.900 RANGE= 4.000
J201_202 6.6137 J H59 H60 STAT=N PRED= 6.640 RANGE= 0.200
J201_205 6.6334 J H59 H61 STAT=N PRED= 6.640 RANGE= 0.200
J211_212 11.1542 J H65 H66A STAT=N PRED= 14.630 RANGE= 4.000
J211_213 4.6521 J H65 H66B STAT=N PRED= 3.970 RANGE= 5.190
J212_213 -13.7265 J H66A H66B STAT=N PRED= -16.790 RANGE= 2.560
J214_215 0.8550 J H68 H69 STAT=N PRED= 2.600 RANGE= 0.600
J214_217 0.7370 J H68 H75 STAT=N PRED= -0.300 RANGE= 0.500
J215_217 0.5550 J H69 H75 STAT=N PRED= -0.440 RANGE= 0.200
J216_217 0.0211 J H73 H75 STAT=N PRED= 1.020 RANGE= 1.200
J221_222 9.5449 J H79 H80 STAT=N PRED= 5.150 RANGE= 3.580
J222_223 8.3962 J H80 H81 STAT=N PRED= 2.490 RANGE= 6.000
J223_224 6.5000 J H81 H82 STAT=N PRED= 6.640 RANGE= 0.200
J223_227 6.8110 J H81 H83 STAT=N PRED= 6.640 RANGE= 0.200
J230_231 7.4526 J H85 H86 STAT=N PRED= 7.680 RANGE= 3.580
J231_232 3.5493 J H86 H87 STAT=Y PRED= 1.900 RANGE= 6.000
J231_247 10.6370 J H86 H87B STAT=Y PRED= 13.650 RANGE= 6.000
J232_247 -15.0065 J H87 H87B STAT=Y PRED= -16.860 RANGE= 2.560
J233_237 1.3171 J H89_93 H89_93 STAT=Y PRED= 1.980 RANGE= 1.200
J233_234 7.6457 J H89_93 H90_92 STAT=N PRED= 7.660 RANGE= 0.340
J233_236 0.3390 J H90_92 H89_93 STAT=N PRED= 0.550 RANGE= 0.750
J233_235 1.2389 J H89_93 H91 STAT=N PRED= 1.260 RANGE= 1.200
J234_236 1.1970 J H90_92 H90_92 STAT=Y PRED= 1.480 RANGE= 1.200
J234_235 7.3929 J H90_92 H91 STAT=N PRED= 7.400 RANGE= 0.240
J238_239 9.6727 J H96 H97 STAT=N PRED= 5.470 RANGE= 3.580
J239_240 9.2068 J H97 H99 STAT=N PRED= 2.170 RANGE= 6.000

Appendix K (continued)

```
J240_241    6.6627   J H99    H100     STAT=N  PRED= 6.640 RANGE= 0.200
J240_244    6.6239   J H99    H101     STAT=N  PRED= 6.640 RANGE= 0.200

CONTROL PARAMETERS:
      Solvent =  none (def. 99% enriched)
        1.000 =  Concentration (vol%, def=1.0%)
   0.00100000 =  Minimum line-intensity
   0.00100000 =  Diagonalization criterium (not in use)
   9.80927313 =  Left frequency (ppm)
  -0.84749699 =  Right frequency (ppm)
        0.000 =  Acquisition time (s, for QMTLS)
        1.342 =  Line-width (for modes D, P & T, 0=use defaults)
  0.034304897 =  Data-point resolution (Hz)
       -8.585 =  GAUSSIAN (%, 0=use default from INF)
        2.459 =  Dispersion contribution (%, 0=use default from INF)
   0.00000000 =  Decoupling frequency (for DORES)

CONSTRAINTS (in equations X0 = 1.0)...use no empty lines
 EQUAL H52     = H99
 EQUAL H15     = H42
 EQUAL H34     = H54
 EQUAL H7      = H14
 IGNORE(HZ):  4378.574 to  4338.051
 IGNORE(HZ):  4101.350 to  4087.378
 IGNORE(HZ):  4174.205 to  4159.567
 IGNORE(HZ):   139.592 to   127.469
 IGNORE(HZ):   105.836 to    43.732
 IGNORE(HZ):   206.358 to   196.660
 IGNORE(HZ):  2948.072 to  2915.954
 IGNORE(HZ):  1992.095 to  1977.811
 IGNORE(HZ):  2280.048 to  2260.483
 IGNORE(HZ):  2310.483 to  2293.092
 IGNORE(HZ):  2197.169 to  2143.637
 IGNORE(HZ):  3224.723 to  3112.827
 IGNORE(HZ):  3001.529 to  2981.184
 IGNORE(HZ):  2680.201 to  2673.619
 IGNORE(HZ):  2062.096 to  2043.375
 IGNORE(HZ):  1927.354 to  1906.212
 IGNORE(HZ):  2013.316 to  2011.423
 IGNORE(HZ):  2015.092 to  2010.880
 IGNORE(HZ):  1771.219 to  1761.243
 IGNORE(HZ):  1698.284 to  1692.520
 IGNORE(HZ):  1687.210 to  1673.161
 IGNORE(HZ):  1728.949 to  1718.680
 IGNORE(HZ):  1711.988 to  1706.777
 IGNORE(HZ):  1653.931 to  1574.032
 IGNORE(HZ):  1826.109 to  1817.029
 IGNORE(HZ):   370.616 to   258.204
 IGNORE(HZ):  1164.792 to  1161.934
 IGNORE(HZ):  5380.692 to  5346.095
```

Appendix K (continued)

IGNORE(HZ): 4898.320 to 4873.702
IGNORE(HZ): 5168.222 to 4999.603
IGNORE(HZ): 512.944 to 488.291
IGNORE(HZ): 728.696 to 676.356

END of FILE

Appendix L. HiFSA profile for deoxyecumicin. ^{1}H NMR spectrum obtained with Bruker Avance 600 instrument; sample contains minimum residual acid.

* NEW: the lines beginning by * are comment lines !
* To keep all the chemical shifts fixed during iteration
* replace "CHEMICAL SHIFTS(HZ):" by "..SHIFTS(HZ): fixed"
* The couplings can be fixed in the same way

NMR-data: C:\Users\wgao\Documents\My Box Files\ITR Lab work\Lab Data\ECUM\H
#$œ Date 9.11.2013; Time 10:59:15 perch.pms

CHEMICAL SHIFTS(PPM):
PROTON 2*SPIN= 1 SPECIES=1H POPULATION(Y)= 1.00000
H74 / 1 6.981545 1*1*1 STAT=Y PRED= 6.995 RANGE= 0.350 WIDTH(Y)= 3.026 RESP(Y)= 0.0974 HSQC= C74
H1_2 / 1 2.314022 1*1*6 STAT=Y PRED= 2.369 RANGE= 0.317 WIDTH(Y)= 2.666 RESP(Y)= 0.0873 HSQC= C1_2
H4 / 1 2.668059 1*1*1 STAT=Y PRED= 3.427 RANGE= 0.552 WIDTH(N)= 3.859 RESP(Y)= 0.0895 HSQC= C4
H5 / 1 2.072487 1*1*1 STAT=Y PRED= 2.062 RANGE= 0.840 WIDTH(Y)= 2.815 RESP(Y)= 0.0682 HSQC= C5
H6 / 1 0.980654 1*1*3 STAT=Y PRED= 0.981 RANGE= 0.545 WIDTH(Y)= 3.298 RESP(Y)= 1.0000 HSQC= C6
H7 / 1 0.850958 1*1*3 STAT=Y PRED= 0.970 RANGE= 0.305 WIDTH(Y)= 4.373 RESP(Y)= 0.1174 HSQC= C7
H10 / 1 4.673505 1*1*1 STAT=Y PRED= 4.486 RANGE= 0.810 WIDTH(N)= 3.800 RESP(Y)= 0.0974 HSQC= C10
H12 / 1 2.072487 1*1*1 STAT=Y PRED= 2.290 RANGE= 0.880 WIDTH(Y)= 3.624 RESP(Y)= 0.0181 HSQC= C12
H13 / 1 1.045027 1*1*3 STAT=Y PRED= 1.146 RANGE= 0.257 WIDTH(Y)= 3.423 RESP(Y)= 0.0875 HSQC= C13
H14 / 1 1.026845 1*1*3 STAT=Y PRED= 0.962 RANGE= 0.267 WIDTH(Y)= 3.211 RESP(Y)= 0.0536 HSQC= C14
H15 / 1 3.227934 1*1*3 STAT=Y PRED= 3.345 RANGE= 0.372 WIDTH(Y)= 3.144 RESP(Y)= 0.0927 HSQC= C15
H17 / 1 4.944629 1*1*1 STAT=Y PRED= 4.796 RANGE= 1.410 WIDTH(N)= 2.653 RESP(Y)= 0.0974 HSQC= C17
H19 / 1 1.949060 1*1*1 STAT=Y PRED= 2.085 RANGE= 0.702 WIDTH(Y)= 2.789 RESP(Y)= 0.0680 HSQC= C19
H20A / 1 1.000082 1*1*1 STAT=Y PRED= 1.234 RANGE= 0.667 WIDTH(Y)= 2.394 RESP(Y)= 0.1464 HSQC= C20
H20B / 1 1.266972 1*1*1 STAT=Y PRED= 1.205 RANGE= 0.495 WIDTH(Y)= 7.736 RESP(Y)= 0.1097 HSQC= C20
H21 / 1 0.752209 1*1*3 STAT=Y PRED= 0.940 RANGE= 0.277 WIDTH(Y)= 4.500 RESP(Y)= 0.1120 HSQC= C21
H22 / 1 0.723519 1*1*3 STAT=Y PRED= 0.920 RANGE= 0.212 WIDTH(Y)= 2.719 RESP(Y)= 0.0516 HSQC= C22
H24 / 1 5.133765 1*1*1 STAT=Y PRED= 4.668 RANGE= 0.965 WIDTH(N)= 3.199 RESP(Y)= 0.0974 HSQC= C24
H25 / 1 5.783595 1*1*1 STAT=Y PRED= 4.829 RANGE= 0.590 WIDTH(N)= 3.401 RESP(Y)= 0.0974 HSQC= C25
H27 / 1 1.314574 1*1*3 STAT=Y PRED= 1.222 RANGE= 0.482 WIDTH(Y)= 4.070 RESP(Y)= 0.1167 HSQC= C27
H29 / 1 3.320138 1*1*3 STAT=Y PRED= 3.517 RANGE= 0.420 WIDTH(Y)= 4.914 RESP(Y)= 0.1163 HSQC= C29
H31 / 1 5.027812 1*1*1 STAT=Y PRED= 5.502 RANGE= 1.040 WIDTH(Y)= 2.991 RESP(Y)= 0.0974 HSQC= C31
H32 / 1 4.435483 1*1*1 STAT=Y PRED= 4.432 RANGE= 0.775 WIDTH(N)= 3.315 RESP(Y)= 0.0974 HSQC= C32
H34 / 1 0.885967 1*1*3 STAT=Y PRED= 1.187 RANGE= 0.337 WIDTH(Y)= 4.661 RESP(Y)= 0.0893 HSQC= C34
H37 / 1 4.820000 1*1*1 STAT=Y PRED= 4.584 RANGE= 1.528 WIDTH(Y)= 3.572 RESP(Y)= 0.0974 HSQC= C37
H38 / 1 2.363237 1*1*1 STAT=Y PRED= 2.318 RANGE= 0.717 WIDTH(Y)= 3.480 RESP(Y)= 0.0016 HSQC= C38
H39 / 1 1.095611 1*1*3 STAT=Y PRED= 1.048 RANGE= 0.232 WIDTH(Y)= 2.768 RESP(Y)= 0.1013 HSQC= C39
H40 / 1 0.980654 1*1*3 STAT=Y PRED= 1.122 RANGE= 0.350 WIDTH(Y)= 3.023 RESP(Y)= 0.0469 HSQC= C40
H42 / 1 3.263198 1*1*3 STAT=Y PRED= 3.333 RANGE= 0.430 WIDTH(Y)= 3.066 RESP(Y)= 0.0634 HSQC= C42
H44 / 1 5.168322 1*1*1 STAT=Y PRED= 5.709 RANGE= 1.180 WIDTH(N)= 4.217 RESP(Y)= 0.0974 HSQC= C44
H45A / 1 1.291686 1*1*1 STAT=Y PRED= 1.343 RANGE= 0.675 WIDTH(Y)= 4.000 RESP(Y)= 0.0974 HSQC= C45
H45B / 1 1.425651 1*1*1 STAT=Y PRED= 1.409 RANGE= 0.500 WIDTH(N)= 3.874 RESP(Y)= 0.0333 HSQC= C45
H46 / 1 0.994195 1*1*1 STAT=Y PRED= 1.581 RANGE= 0.752 WIDTH(Y)= 1.678 RESP(Y)= 0.1800 HSQC= C46
H47 / 1 0.224197 1*1*3 STAT=Y PRED= 0.484 RANGE= 0.695 WIDTH(N)= 3.264 RESP(Y)= 0.0974 HSQC= C47
H48 / 1 0.321762 1*1*3 STAT=Y PRED= 0.573 RANGE= 0.670 WIDTH(N)= 3.276 RESP(Y)= 0.0974 HSQC= C48
H51 / 1 4.601548 1*1*1 STAT=Y PRED= 4.427 RANGE= 0.855 WIDTH(N)= 3.814 RESP(Y)= 0.0974 HSQC= C51
H52 / 1 2.038317 1*1*1 STAT=Y PRED= 2.038 RANGE= 1.020 WIDTH(Y)= 3.242 RESP(Y)= 0.1094 HSQC= C52
H53 / 1 0.914673 1*1*3 STAT=Y PRED= 1.016 RANGE= 0.222 WIDTH(Y)= 4.555 RESP(Y)= 0.1045 HSQC= C53
H54 / 1 0.867681 1*1*3 STAT=Y PRED= 0.877 RANGE= 0.242 WIDTH(Y)= 3.305 RESP(Y)= 0.0500 HSQC= C54
H56 / 1 3.146426 1*1*3 STAT=Y PRED= 3.023 RANGE= 0.457 WIDTH(Y)= 2.938 RESP(Y)= 0.0601 HSQC= C56
H58 / 1 3.054310 1*1*1 STAT=Y PRED= 5.153 RANGE= 0.775 WIDTH(N)= 3.193 RESP(Y)= 0.0593 HSQC= C58
H59 / 1 2.587787 1*1*1 STAT=Y PRED= 2.632 RANGE= 0.695 WIDTH(Y)= 1.880 RESP(Y)= 0.0226 HSQC= C59
H60 / 1 0.980654 1*1*3 STAT=Y PRED= 1.351 RANGE= 0.260 WIDTH(Y)= 2.439 RESP(Y)= 1.0000 HSQC= C60
H61 / 1 1.095611 1*1*3 STAT=Y PRED= 1.028 RANGE= 0.242 WIDTH(Y)= 7.389 RESP(Y)= 0.0466 HSQC= C61
H63 / 1 2.165281 1*1*3 STAT=Y PRED= 2.756 RANGE= 0.990 WIDTH(Y)= 3.049 RESP(Y)= 0.0635 HSQC= C63
H65 / 1 4.094945 1*1*1 STAT=Y PRED= 4.369 RANGE= 1.100 WIDTH(N)= 2.884 RESP(Y)= 0.0974 HSQC= C65

Appendix L (continued)

```
H66A  / 1    3.547159  1*1*1  STAT=Y  PRED= 3.113 RANGE= 0.455 WIDTH(N)= 2.455 RESP(Y)= 0.0974 HSQC= C66
H66B  / 1    3.691122  1*1*1  STAT=Y  PRED= 3.828 RANGE= 0.547 WIDTH(N)= 3.471 RESP(Y)= 0.0974 HSQC= C66
H68   / 1    6.697627  1*1*1  STAT=Y  PRED= 6.508 RANGE= 0.657 WIDTH(N)= 3.027 RESP(Y)= 0.0974 HSQC= C68
H73   / 1    6.440797  1*1*1  STAT=Y  PRED= 6.482 RANGE= 0.457 WIDTH(N)= 3.434 RESP(Y)= 0.0974 HSQC= C73
H75   / 1    6.920714  1*1*1  STAT=Y  PRED= 6.817 RANGE= 0.527 WIDTH(N)= 2.113 RESP(Y)= 0.0974 HSQC= C75
H77   / 1    3.818260  1*1*3  STAT=Y  PRED= 3.981 RANGE= 0.217 WIDTH(Y)= 2.508 RESP(Y)= 0.0974 HSQC= C77
H80   / 1    4.407037  1*1*1  STAT=Y  PRED= 3.999 RANGE= 1.400 WIDTH(N)= 3.314 RESP(Y)= 0.0974 HSQC= C80
H81   / 1    2.189621  1*1*1  STAT=Y  PRED= 2.166 RANGE= 0.692 WIDTH(Y)= 2.527 RESP(Y)= 0.0646 HSQC= C81
H82   / 1    0.980654  1*1*3  STAT=Y  PRED= 1.138 RANGE= 0.212 WIDTH(Y)= 2.210 RESP(Y)= 1.0000 HSQC= C82
H83   / 1    0.980654  1*1*3  STAT=Y  PRED= 1.004 RANGE= 0.372 WIDTH(Y)= 3.438 RESP(Y)= 1.0000 HSQC= C83
H86   / 1    4.780001  1*1*1  STAT=Y  PRED= 4.499 RANGE= 1.080 WIDTH(N)= 3.572 RESP(Y)= 0.0974 HSQC= C86
H87A  / 1    3.349996  1*1*1  STAT=Y  PRED= 2.988 RANGE= 0.725 WIDTH(Y)= 4.048 RESP(Y)= 0.1451 HSQC= C87
H89_93/ 1    7.092746  1*2*1  STAT=Y  PRED= 7.067 RANGE= 0.512 WIDTH(N)= 2.772 RESP(Y)= 0.0974 HSQC= C89_93
H90_92/ 1    7.202454  1*2*1  STAT=Y  PRED= 7.231 RANGE= 0.307 WIDTH(N)= 2.794 RESP(Y)= 0.0974 HSQC= C90_92
H91   / 1    7.149510  1*1*1  STAT=Y  PRED= 7.190 RANGE= 0.325 WIDTH(N)= 2.309 RESP(Y)= 0.0974 HSQC= C91
H97   / 1    4.368953  1*1*1  STAT=Y  PRED= 4.349 RANGE= 0.752 WIDTH(Y)= 2.684 RESP(Y)= 0.0974 HSQC= C97
H99   / 1    1.965944  1*1*1  STAT=Y  PRED= 2.027 RANGE= 0.840 WIDTH(Y)= 3.080 RESP(Y)= 0.0771 HSQC= C99
H100  / 1    0.936735  1*1*3  STAT=Y  PRED= 1.130 RANGE= 0.190 WIDTH(Y)= 5.537 RESP(Y)= 0.1417 HSQC= C100
H101  / 1    0.919918  1*1*3  STAT=Y  PRED= 1.022 RANGE= 0.340 WIDTH(Y)= 3.109 RESP(Y)= 0.0787 HSQC= C101
H87B  / 1    2.841229  1*1*1  STAT=Y  PRED= 2.895 RANGE= 0.402 WIDTH(Y)= 3.089 RESP(Y)= 0.0565 HSQC= C87

COUPLING CONSTANTS(HZ):
J114_216    7.8015   J H74    H73     STAT=Y  PRED= 8.100 RANGE= 0.890
J114_217    8.2269   J H74    H75     STAT=Y  PRED= 7.850 RANGE= 0.800
J121_122    9.0291   J H4     H5      STAT=N  PRED= 12.760 RANGE= 4.000
J122_123    7.3334   J H5     H6      STAT=Y  PRED= 6.640 RANGE= 0.200
J122_126    6.6627   J H5     H7      STAT=N  PRED= 6.640 RANGE= 0.200
J130_131    8.3724   J H10    H12     STAT=N  PRED= 13.120 RANGE= 6.000
J131_132    6.4851   J H12    H13     STAT=N  PRED= 6.640 RANGE= 0.200
J131_135    6.5771   J H12    H14     STAT=N  PRED= 6.640 RANGE= 0.200
J141_142   11.3176   J H17    H19     STAT=N  PRED= 13.370 RANGE= 4.000
J142_143    2.1101   J H19    H20A    STAT=Y  PRED= 2.370 RANGE= 2.560
J142_144    7.0034   J H19    H20B    STAT=Y  PRED= 13.350 RANGE= 2.560
J142_145    6.2950   J H19    H21     STAT=N  PRED= 6.640 RANGE= 0.200
J143_144  -14.8081   J H20A   H20B    STAT=Y  PRED= -13.400 RANGE= 0.600
J143_148    7.0992   J H20A   H22     STAT=N  PRED= 7.440 RANGE= 0.150
J144_148    7.7363   J H20B   H22     STAT=N  PRED= 7.440 RANGE= 0.150
J152_153    2.1231   J H24    H25     STAT=N  PRED= 1.690 RANGE= 6.000
J153_154    6.5372   J H25    H27     STAT=N  PRED= 6.250 RANGE= 0.600
J160_161    3.6337   J H31    H32     STAT=N  PRED= 2.370 RANGE= 4.000
J161_163    7.1261   J H32    H34     STAT=N  PRED= 6.250 RANGE= 0.600
J167_168    9.2199   J H37    H38     STAT=Y  PRED= 2.320 RANGE= 6.000
J168_169    6.5961   J H38    H39     STAT=N  PRED= 6.640 RANGE= 0.200
J168_172    6.5000   J H38    H40     STAT=N  PRED= 6.640 RANGE= 0.200
J178_179    7.4347   J H44    H45A    STAT=N  PRED= 13.740 RANGE= 4.000
J178_180    7.4245   J H44    H45B    STAT=N  PRED= 1.680 RANGE= 4.000
J179_180  -14.0543   J H45A   H45B    STAT=N  PRED= -14.670 RANGE= 1.600
J179_181    1.8651   J H45A   H46     STAT=Y  PRED= 12.620 RANGE= 2.560
J180_181    5.7789   J H45B   H46     STAT=N  PRED= 0.740 RANGE= 2.560
J181_182    6.6422   J H46    H47     STAT=N  PRED= 6.640 RANGE= 0.200
J181_185    6.6420   J H46    H48     STAT=N  PRED= 6.640 RANGE= 0.200
J189_190    9.2177   J H51    H52     STAT=N  PRED= 13.060 RANGE= 6.000
J190_191    6.4052   J H52    H53     STAT=N  PRED= 6.640 RANGE= 0.200
J190_194    6.2006   J H52    H54     STAT=N  PRED= 6.640 RANGE= 0.200
J200_201    7.5980   J H58    H59     STAT=N  PRED= 12.900 RANGE= 4.000
J201_202    6.9722   J H59    H60     STAT=Y  PRED= 6.640 RANGE= 0.200
J201_205    6.5089   J H59    H61     STAT=N  PRED= 6.640 RANGE= 0.200
```

Appendix L (continued)

```
J211_212   11.1745   J H65    H66A     STAT=N  PRED= 14.630 RANGE= 4.000
J211_213    4.4921   J H65    H66B     STAT=N  PRED= 3.970 RANGE= 5.190
J212_213  -13.5926   J H66A   H66B     STAT=N  PRED= -16.790 RANGE= 2.560
J214_217   -0.8664   J H68    H75      STAT=N  PRED= -0.300 RANGE= 0.500
J216_217    0.8982   J H73    H75      STAT=N  PRED= 1.020 RANGE= 1.200
J222_223    8.3338   J H80    H81      STAT=N  PRED= 2.490 RANGE= 6.000
J223_224    6.0273   J H81    H82      STAT=Y  PRED= 6.640 RANGE= 0.200
J223_227    7.9583   J H81    H83      STAT=Y  PRED= 6.640 RANGE= 0.200
J231_232   12.1466   J H86    H87A     STAT=N  PRED= 1.900 RANGE= 6.000
J231_247   10.5990   J H86    H87B     STAT=Y  PRED= 13.650 RANGE= 6.000
J232_247  -14.1309   J H87A   H87B     STAT=Y  PRED= -16.860 RANGE= 2.560
J233_237    1.8622   J H89_93 H89_93   STAT=N  PRED= 1.980 RANGE= 1.200
J233_234    7.8885   J H89_93 H90_92   STAT=N  PRED= 7.660 RANGE= 0.340
J233_236    0.3817   J H90_92 H89_93   STAT=N  PRED= 0.550 RANGE= 0.750
J233_235    1.2933   J H89_93 H91      STAT=N  PRED= 1.260 RANGE= 1.200
J234_236    1.9768   J H90_92 H90_92   STAT=N  PRED= 1.480 RANGE= 1.200
J234_235    7.3828   J H90_92 H91      STAT=N  PRED= 7.400 RANGE= 0.240
J239_240    8.9483   J H97    H99      STAT=N  PRED= 2.170 RANGE= 6.000
J240_241    7.2690   J H99    H100     STAT=N  PRED= 6.640 RANGE= 0.200
J240_244    6.8270   J H99    H101     STAT=N  PRED= 6.640 RANGE= 0.200

CONTROL PARAMETERS:
      Solvent =  none (def. 99% enriched)
        1.000 =  Concentration (vol%, def=1.0%)
   0.00100000 =  Minimum line-intensity
   0.00100000 =  Diagonalization criterium (not in use)
  21.00281198 =  Left frequency (ppm)
  -1.03819279 =  Right frequency (ppm)
        0.000 =  Acquisition time (s, for QMTLS)
        1.678 =  Line-width (for modes D, P & T, 0=use defaults)
  0.025229526 =  Data-point resolution (Hz)
        9.112 =  GAUSSIAN (%, 0=use default from INF)
      -15.455 =  Dispersion contribution (%, 0=use default from INF)
   0.00000000 =  Decoupling frequency (for DORES)

CONSTRAINTS (in equations X0 = 1.0)...use no empty lines
 EQUAL H6      = H40     = H60     = H82     = H83
 EQUAL H39     = H61
 IGNORE(HZ):  1991.405 to  1976.279
 IGNORE(HZ):  2935.734 to  2811.994
 IGNORE(HZ):   156.837 to   142.993
 IGNORE(HZ):   206.949 to   200.305
 IGNORE(HZ):   126.104 to   117.798
 IGNORE(HZ):  4470.507 to  4335.175
 IGNORE(HZ):  2740.981 to  2668.467
 IGNORE(HZ):  3011.610 to  2981.179
 IGNORE(HZ):  2283.646 to  2235.644
 IGNORE(HZ):  2352.770 to  2294.207
 IGNORE(HZ):  1701.013 to  1695.150
 IGNORE(HZ):  1931.046 to  1905.728
 IGNORE(HZ):  1885.459 to  1878.157
 IGNORE(HZ):  1956.050 to  1941.793
 IGNORE(HZ):  1165.938 to  1157.356
 IGNORE(HZ):  1296.639 to  1287.398
 IGNORE(HZ):  1395.961 to  1377.543
 IGNORE(HZ):   782.178 to   766.344
 IGNORE(HZ):   831.783 to   797.901
```

Appendix L (continued)

IGNORE(HZ): 740.988 to 736.116
IGNORE(HZ): 639.296 to 634.457
IGNORE(HZ): 542.122 to 537.446
IGNORE(HZ): 576.018 to 569.875

END of FILE

Appendix M. Pseudo HiFSA profile of norecumicin.

* NEW: the lines beginning by * are comment lines !
* To keep all the chemical shifts fixed during iteration
* replace "CHEMICAL SHIFTS(HZ):" by "..SHIFTS(HZ): fixed"
* The couplings can be fixed in the same way

NMR-data: C:\Users\jgnapo_2\Desktop\Wei_H14_XRays\H14_withoutGO
#$œ Date 9. 3.2014; Time 16:45:19 perch.pms

CHEMICAL SHIFTS(PPM):
PROTON 2*SPIN= 1 SPECIES=1H POPULATION(Y)= 1.00000

10Trp_H8/ 1 6.981596 1*1*1 STAT=Y PRED= 7.318 RANGE= 0.197 WIDTH(Y)= 1.523 RESP(Y)= 0.2608 HSQC= C74
01ValH45/ 1 2.516666 1*1*6 STAT=Y PRED= 2.370 RANGE= 0.307 WIDTH(Y)= 2.856 RESP(Y)= 0.2493 HSQC= C1_2
01Val_H2/ 1 3.013303 1*1*1 STAT=Y PRED= 4.169 RANGE= 0.637 WIDTH(Y)= 3.518 RESP(Y)= 0.2345 HSQC= C4
01Val_H3/ 1 2.024337 1*1*1 STAT=Y PRED= 1.952 RANGE= 0.815 WIDTH(Y)= 2.927 RESP(Y)= 0.1328 HSQC= C5
01Val_H6/ 1 0.858642 1*1*3 STAT=Y PRED= 0.509 RANGE= 0.865 WIDTH(Y)= 2.967 RESP(Y)= 0.2806 HSQC= C6
01Val_H7/ 1 0.980523 1*1*3 STAT=Y PRED= 0.818 RANGE= 0.357 WIDTH(Y)= 2.368 RESP(Y)= 0.2336 HSQC= C7
02Val_H2/ 1 4.701697 1*1*1 STAT=Y PRED= 4.508 RANGE= 0.805 WIDTH(Y)= 2.622 RESP(Y)= 0.2975 HSQC= C10
02Val_H3/ 1 2.122249 1*1*1 STAT=Y PRED= 2.155 RANGE= 0.775 WIDTH(Y)= 1.936 RESP(Y)= 0.1885 HSQC= C12
02Val_H4/ 1 1.017845 1*1*3 STAT=Y PRED= 1.038 RANGE= 0.277 WIDTH(Y)= 2.625 RESP(Y)= 0.2382 HSQC= C13
02Val_H5/ 1 1.058053 1*1*3 STAT=Y PRED= 0.943 RANGE= 0.247 WIDTH(Y)= 2.275 RESP(Y)= 0.2664 HSQC= C14
04Thr_H2/ 1 5.171477 1*1*1 STAT=Y PRED= 4.668 RANGE= 1.015 WIDTH(Y)= 2.077 RESP(Y)= 0.2366 HSQC= C24
04Thr_H3/ 1 5.779328 1*1*1 STAT=Y PRED= 4.010 RANGE= 0.477 WIDTH(Y)= 2.195 RESP(Y)= 0.2224 HSQC= C25
04Thr_H4/ 1 1.314112 1*1*3 STAT=Y PRED= 1.270 RANGE= 0.497 WIDTH(Y)= 2.753 RESP(Y)= 0.2655 HSQC= C27
05Thr_H5/ 1 3.320648 1*1*3 STAT=Y PRED= 3.257 RANGE= 0.397 WIDTH(Y)= 2.279 RESP(Y)= 0.2567 HSQC= C29
05Thr_H2/ 1 5.004684 1*1*1 STAT=Y PRED= 4.099 RANGE= 1.025 WIDTH(Y)= 2.210 RESP(Y)= 0.2626 HSQC= C31
05Thr_H3/ 1 4.424087 1*1*1 STAT=Y PRED= 4.345 RANGE= 0.717 WIDTH(Y)= 2.228 RESP(Y)= 0.2252 HSQC= C32
05Thr_H4/ 1 0.911489 1*1*3 STAT=Y PRED= 1.252 RANGE= 0.297 WIDTH(Y)= 2.670 RESP(Y)= 0.2653 HSQC= C34
06Val_H2/ 1 4.843812 1*1*1 STAT=Y PRED= 4.525 RANGE= 1.405 WIDTH(Y)= 5.217 RESP(Y)= 0.2653 HSQC= C37
06Val_H3/ 1 2.348846 1*1*1 STAT=Y PRED= 1.975 RANGE= 1.015 WIDTH(Y)= 2.576 RESP(Y)= 0.2022 HSQC= C38
06Val_H4/ 1 1.087437 1*1*3 STAT=Y PRED= 0.938 RANGE= 0.217 WIDTH(Y)= 1.945 RESP(Y)= 0.1796 HSQC= C39
06Val_H5/ 1 0.992826 1*1*3 STAT=Y PRED= 1.094 RANGE= 0.387 WIDTH(Y)= 2.420 RESP(Y)= 0.1919 HSQC= C40
07Leu_H7/ 1 3.256346 1*1*3 STAT=Y PRED= 3.110 RANGE= 0.375 WIDTH(Y)= 2.208 RESP(Y)= 0.2294 HSQC= C42
07Leu_H2/ 1 5.094221 1*1*1 STAT=Y PRED= 5.342 RANGE= 1.085 WIDTH(Y)= 2.729 RESP(Y)= 0.2035 HSQC= C44
07LeuH3A/ 1 1.462779 1*1*1 STAT=Y PRED= 1.444 RANGE= 0.427 WIDTH(Y)= 2.201 RESP(Y)= 0.1329 HSQC= C45
07LeuH3B/ 1 1.226268 1*1*1 STAT=Y PRED= 1.914 RANGE= 0.367 WIDTH(Y)= 3.770 RESP(Y)= 0.2733 HSQC= C45
07Leu_H4/ 1 0.938876 1*1*1 STAT=Y PRED= 1.630 RANGE= 0.627 WIDTH(Y)= 3.004 RESP(Y)= 0.4584 HSQC= C46
07Leu_H5/ 1 0.336312 1*1*3 STAT=Y PRED= 0.972 RANGE= 0.315 WIDTH(Y)= 2.494 RESP(Y)= 0.2101 HSQC= C47
07Leu_H6/ 1 0.161633 1*1*3 STAT=Y PRED= 0.972 RANGE= 0.147 WIDTH(Y)= 2.600 RESP(Y)= 0.2075 HSQC= C48
08Val_H2/ 1 4.601765 1*1*1 STAT=Y PRED= 4.489 RANGE= 0.895 WIDTH(Y)= 3.315 RESP(Y)= 0.2216 HSQC= C51
08Val_H3/ 1 1.985653 1*1*1 STAT=Y PRED= 1.995 RANGE= 0.485 WIDTH(Y)= 2.957 RESP(Y)= 0.1668 HSQC= C52
08Val_H4/ 1 0.920357 1*1*3 STAT=Y PRED= 1.060 RANGE= 0.237 WIDTH(Y)= 2.316 RESP(Y)= 0.2133 HSQC= C53
08Val_H5/ 1 0.888145 1*1*3 STAT=Y PRED= 0.999 RANGE= 0.227 WIDTH(Y)= 2.753 RESP(Y)= 0.3213 HSQC= C54
09Val_H6/ 1 3.131909 1*1*3 STAT=Y PRED= 3.169 RANGE= 0.465 WIDTH(Y)= 2.455 RESP(Y)= 0.2275 HSQC= C56
09Val_H2/ 1 3.053726 1*1*1 STAT=Y PRED= 5.153 RANGE= 0.717 WIDTH(Y)= 3.143 RESP(Y)= 0.2025 HSQC= C58
09Val_H3/ 1 2.580776 1*1*1 STAT=Y PRED= 2.524 RANGE= 0.407 WIDTH(Y)= 2.626 RESP(Y)= 0.2161 HSQC= C59
09Val_H4/ 1 1.093409 1*1*3 STAT=Y PRED= 1.319 RANGE= 0.227 WIDTH(Y)= 2.669 RESP(Y)= 0.3378 HSQC= C60
09Val_H5/ 1 0.976814 1*1*3 STAT=Y PRED= 1.075 RANGE= 0.237 WIDTH(Y)= 2.677 RESP(Y)= 0.1936 HSQC= C61
10TrpH13/ 1 2.154822 1*1*3 STAT=Y PRED= 2.936 RANGE= 0.895 WIDTH(Y)= 2.817 RESP(Y)= 0.2545 HSQC= C63
10Trp_H2/ 1 4.101427 1*1*1 STAT=Y PRED= 5.043 RANGE= 1.765 WIDTH(Y)= 2.697 RESP(Y)= 0.1932 HSQC= C65
10TrpH3A/ 1 3.546010 1*1*1 STAT=Y PRED= 3.613 RANGE= 0.467 WIDTH(Y)= 1.896 RESP(Y)= 0.1965 HSQC= C66

Appendix M (continued)

10TrpH3B/ 1 3.696461 1*1*1 STAT=Y PRED= 3.367 RANGE= 0.627 WIDTH(Y)= 2.594 RESP(Y)= 0.2199 HSQC= C66
10Trp_H5/ 1 6.700103 1*1*1 STAT=Y PRED= 6.772 RANGE= 0.275 WIDTH(Y)= 1.916 RESP(Y)= 0.2409 HSQC= C68
10Trp_H9/ 1 6.441885 1*1*1 STAT=Y PRED= 7.089 RANGE= 0.217 WIDTH(Y)= 1.656 RESP(Y)= 0.2523 HSQC= C73
10Trp_H7/ 1 6.922224 1*1*1 STAT=Y PRED= 7.333 RANGE= 0.307 WIDTH(Y)= 1.163 RESP(Y)= 0.2299 HSQC= C75
10TrpH12/ 1 3.826462 1*1*3 STAT=Y PRED= 4.072 RANGE= 0.247 WIDTH(Y)= 1.703 RESP(Y)= 0.2281 HSQC= C77
11Val_H2/ 1 4.527542 1*1*1 STAT=Y PRED= 4.303 RANGE= 1.445 WIDTH(Y)= 2.167 RESP(Y)= 0.2288 HSQC= C80
11Val_H3/ 1 2.188102 1*1*1 STAT=Y PRED= 2.094 RANGE= 0.587 WIDTH(Y)= 4.425 RESP(Y)= 0.2651 HSQC= C81
11Val_H4/ 1 1.027242 1*1*3 STAT=Y PRED= 1.094 RANGE= 0.247 WIDTH(Y)= 2.591 RESP(Y)= 0.2551 HSQC= C82
11Val_H5/ 1 1.000423 1*1*3 STAT=Y PRED= 1.080 RANGE= 0.297 WIDTH(Y)= 2.219 RESP(Y)= 0.2097 HSQC= C83
12Phe_H2/ 1 4.841653 1*1*1 STAT=Y PRED= 4.499 RANGE= 0.985 WIDTH(Y)= 3.593 RESP(Y)= 0.2523 HSQC= C86
12Phe_H3/ 1 5.326092 1*1*1 STAT=Y PRED= 5.208 RANGE= 0.487 WIDTH(Y)= 2.098 RESP(Y)= 0.2226 HSQC= C87
12Phe_H5/ 1 7.230609 1*2*1 STAT=Y PRED= 7.524 RANGE= 0.307 WIDTH(Y)= 1.433 RESP(Y)= 0.2480 HSQC= C89_93
12Phe_H6/ 1 7.250066 1*2*1 STAT=Y PRED= 7.372 RANGE= 0.577 WIDTH(Y)= 1.876 RESP(Y)= 0.2658 HSQC= C90_92
12Phe_H7/ 1 7.196979 1*1*1 STAT=Y PRED= 7.281 RANGE= 0.307 WIDTH(Y)= 1.828 RESP(Y)= 0.2695 HSQC= C91
13Val_H2/ 1 4.407490 1*1*1 STAT=Y PRED= 4.169 RANGE= 0.667 WIDTH(Y)= 1.764 RESP(Y)= 0.2459 HSQC= C97
13Val_H3/ 1 1.965710 1*1*1 STAT=Y PRED= 1.935 RANGE= 0.865 WIDTH(Y)= 1.999 RESP(Y)= 0.2069 HSQC= C99
13Val_H4/ 1 0.935848 1*1*3 STAT=Y PRED= 1.277 RANGE= 0.217 WIDTH(Y)= 3.028 RESP(Y)= 0.3033 HSQC= C100
13Val_H5/ 1 0.925029 1*1*3 STAT=Y PRED= 0.933 RANGE= 0.277 WIDTH(Y)= 2.510 RESP(Y)= 0.2573 HSQC= C101

COUPLING CONSTANTS(HZ): fixed
J115_217 7.7969 J 10Trp_H8 10Trp_H9 STAT=Y PRED= 8.100 RANGE= 0.890
J115_218 8.1808 J 10Trp_H8 10Trp_H7 STAT=Y PRED= 7.850 RANGE= 0.800
J122_123 9.1737 J 01Val_H2 01Val_H3 STAT=Y PRED= 12.510 RANGE= 4.000
J123_124 6.5890 J 01Val_H3 01Val_H6 STAT=Y PRED= 6.640 RANGE= 0.200
J123_127 6.6205 J 01Val_H3 01Val_H7 STAT=Y PRED= 6.640 RANGE= 0.200
J131_132 8.7545 J 02Val_H2 02Val_H3 STAT=Y PRED= 12.600 RANGE= 6.000
J132_133 6.7841 J 02Val_H3 02Val_H4 STAT=Y PRED= 6.640 RANGE= 0.200
J132_136 6.7206 J 02Val_H3 02Val_H5 STAT=Y PRED= 6.640 RANGE= 0.200
J153_154 2.3441 J 04Thr_H2 04Thr_H3 STAT=Y PRED= 2.690 RANGE= 6.600
J154_155 6.5134 J 04Thr_H3 04Thr_H4 STAT=Y PRED= 6.250 RANGE= 0.600
J161_162 3.7259 J 05Thr_H2 05Thr_H3 STAT=Y PRED= 2.440 RANGE= 4.400
J162_164 6.4691 J 05Thr_H3 05Thr_H4 STAT=Y PRED= 6.250 RANGE= 0.600
J168_169 8.9180 J 06Val_H2 06Val_H3 STAT=Y PRED= 2.980 RANGE= 6.600
J169_170 6.6944 J 06Val_H3 06Val_H4 STAT=Y PRED= 6.640 RANGE= 0.200
J169_173 7.0316 J 06Val_H3 06Val_H5 STAT=Y PRED= 6.640 RANGE= 0.200
J179_180 6.2437 J 07Leu_H2 07LeuH3A STAT=Y PRED= 3.040 RANGE= 6.000
J179_181 8.3839 J 07Leu_H2 07LeuH3B STAT=Y PRED= 13.950 RANGE= 4.000
J180_181 -13.3047 J 07LeuH3A 07LeuH3B STAT=Y PRED= -14.710 RANGE= 1.600
J180_182 8.2119 J 07LeuH3A 07Leu_H4 STAT=Y PRED= 12.990 RANGE= 2.560
J181_182 5.7896 J 07LeuH3B 07Leu_H4 STAT=Y PRED= 2.270 RANGE= 3.000
J182_183 6.5482 J 07Leu_H4 07Leu_H5 STAT=Y PRED= 6.640 RANGE= 0.200
J182_186 6.5879 J 07Leu_H4 07Leu_H6 STAT=Y PRED= 6.640 RANGE= 0.200
J190_191 8.8736 J 08Val_H2 08Val_H3 STAT=Y PRED= 12.880 RANGE= 6.000
J191_192 6.5520 J 08Val_H3 08Val_H4 STAT=Y PRED= 6.640 RANGE= 0.200
J191_195 6.7834 J 08Val_H3 08Val_H5 STAT=Y PRED= 6.640 RANGE= 0.200
J201_202 7.6281 J 09Val_H2 09Val_H3 STAT=Y PRED= 12.960 RANGE= 4.000
J202_203 6.4961 J 09Val_H3 09Val_H4 STAT=Y PRED= 6.640 RANGE= 0.200
J202_206 6.7760 J 09Val_H3 09Val_H5 STAT=Y PRED= 6.640 RANGE= 0.200
J212_213 11.1630 J 10Trp_H2 10TrpH3A STAT=Y PRED= 12.890 RANGE= 4.000
J212_214 4.7143 J 10Trp_H2 10TrpH3B STAT=Y PRED= 1.900 RANGE= 4.400

Appendix M (continued)

```
J213_214  -13.7295   J 10TrpH3A 10TrpH3B   STAT=Y  PRED= -16.760 RANGE= 2.560
J215_218    0.4880   J 10Trp_H5 10Trp_H7   STAT=Y  PRED= -0.300 RANGE= 0.500
J217_218    0.6708   J 10Trp_H9 10Trp_H7   STAT=Y  PRED= 1.020 RANGE= 1.200
J223_224    7.9094   J 11Val_H2 11Val_H3   STAT=Y  PRED= 3.450 RANGE= 9.000
J224_225    6.7483   J 11Val_H3 11Val_H4   STAT=Y  PRED= 6.640 RANGE= 0.200
J224_228    6.8064   J 11Val_H3 11Val_H5   STAT=Y  PRED= 6.640 RANGE= 0.200
J232_233    1.9005   J 12Phe_H2 12Phe_H3   STAT=Y  PRED= 1.900 RANGE= 6.600
J234_238    1.3335   J 12Phe_H5 12Phe_H5   STAT=Y  PRED= 1.980 RANGE= 1.200
J234_235    7.6508   J 12Phe_H5 12Phe_H6   STAT=Y  PRED= 7.660 RANGE= 0.340
J234_237    0.7769   J 12Phe_H6 12Phe_H5   STAT=Y  PRED= 0.550 RANGE= 0.750
J234_236    1.2760   J 12Phe_H5 12Phe_H7   STAT=Y  PRED= 1.260 RANGE= 1.200
J235_237    1.7027   J 12Phe_H6 12Phe_H6   STAT=Y  PRED= 1.480 RANGE= 1.200
J235_236    7.4760   J 12Phe_H6 12Phe_H7   STAT=Y  PRED= 7.400 RANGE= 0.240
J241_242    8.8924   J 13Val_H2 13Val_H3   STAT=Y  PRED= 12.320 RANGE= 6.000
J242_243    6.8372   J 13Val_H3 13Val_H4   STAT=Y  PRED= 6.640 RANGE= 0.200
J242_246    6.4162   J 13Val_H3 13Val_H5   STAT=Y  PRED= 6.640 RANGE= 0.200

CONTROL PARAMETERS:
      Solvent =  none (def. 99% enriched)
        1.000 =  Concentration (vol%, def=1.0%)
   0.00100000 =  Minimum line-intensity
   0.00100000 =  Diagonalization criterium (not in use)
 600.13000500 =  FIELD(1H,MHz), used to transform shifts to ppms
  11.63298479 =  Left frequency (ppm)
  -4.33373628 =  Right frequency (ppm)
       10.000 =  Acquisition time (s, for QMTLS)
        0.000 =  Line-width (for modes D, P & T, 0=use defaults)
  0.058337236 =  Data-point resolution (Hz)
      -3.018 =  GAUSSIAN (%, 0=use default from INF)
      -6.775 =  Dispersion contribution (%, 0=use default from INF)
   0.00000000 =  Decoupling frequency (for DORES)

CONSTRAINTS (in equations X0 = 1.0)...use no empty lines
 EQUAL 01Val_H2 = 13Val_H2
 EQUAL 06Val_H5 = 11Val_H4
 EQUAL 07Leu_H5 = 07Leu_H6
 IGNORE(HZ):  2904.119 to  2866.556
 IGNORE(HZ):  1990.683 to  1980.117

END of FILE
```

Appendix N. The PMS file of common amino acids between norecumicin and ecumicin.

* NEW: the lines beginning by * are comment lines !
* To keep all the chemical shifts fixed during iteration
* replace "CHEMICAL SHIFTS(HZ):" by "..SHIFTS(HZ): fixed"
* The couplings can be fixed in the same way

NMR-data: C:\Users\jgnapo_2\Desktop\Wei_H14_XRays\H14_withoutGO
#$œ Date 9. 3.2014; Time 16:45:19 perch.pms

CHEMICAL SHIFTS(PPM):
PROTON 2*SPIN= 1 SPECIES=1H POPULATION(Y)= 1.00000
10Trp_H8/ 1 6.981596 1*1*1 STAT=Y PRED= 7.318 RANGE= 0.197 WIDTH(Y)= 1.523 RESP(Y)= 0.2608 HSQC= C74
01ValH45/ 1 2.516666 1*1*6 STAT=Y PRED= 2.370 RANGE= 0.307 WIDTH(Y)= 2.856 RESP(Y)= 0.2493 HSQC= C1_2
01Val_H2/ 1 3.013303 1*1*1 STAT=Y PRED= 4.169 RANGE= 0.637 WIDTH(Y)= 3.518 RESP(Y)= 0.2345 HSQC= C4
01Val_H3/ 1 2.024337 1*1*1 STAT=Y PRED= 1.952 RANGE= 0.815 WIDTH(Y)= 2.927 RESP(Y)= 0.1328 HSQC= C5
01Val_H6/ 1 0.858642 1*1*3 STAT=Y PRED= 0.509 RANGE= 0.865 WIDTH(Y)= 2.967 RESP(Y)= 0.2806 HSQC= C6
01Val_H7/ 1 0.980523 1*1*3 STAT=Y PRED= 0.818 RANGE= 0.357 WIDTH(Y)= 2.368 RESP(Y)= 0.2336 HSQC= C7
02Val_H2/ 1 4.701697 1*1*1 STAT=Y PRED= 4.508 RANGE= 0.805 WIDTH(Y)= 2.622 RESP(Y)= 0.2975 HSQC= C10
02Val_H3/ 1 2.122249 1*1*1 STAT=Y PRED= 2.155 RANGE= 0.775 WIDTH(Y)= 1.936 RESP(Y)= 0.1885 HSQC= C12
02Val_H4/ 1 1.017845 1*1*3 STAT=Y PRED= 1.038 RANGE= 0.277 WIDTH(Y)= 2.625 RESP(Y)= 0.2382 HSQC= C13
02Val_H5/ 1 1.058053 1*1*3 STAT=Y PRED= 0.943 RANGE= 0.247 WIDTH(Y)= 2.275 RESP(Y)= 0.2664 HSQC= C14
04Thr_H2/ 1 5.171477 1*1*1 STAT=Y PRED= 4.668 RANGE= 1.015 WIDTH(Y)= 2.077 RESP(Y)= 0.2366 HSQC= C24
04Thr_H3/ 1 5.779328 1*1*1 STAT=Y PRED= 4.010 RANGE= 0.477 WIDTH(Y)= 2.195 RESP(Y)= 0.2224 HSQC= C25
04Thr_H4/ 1 1.314112 1*1*3 STAT=Y PRED= 1.270 RANGE= 0.497 WIDTH(Y)= 2.753 RESP(Y)= 0.2655 HSQC= C27
05Thr_H5/ 1 3.320648 1*1*3 STAT=Y PRED= 3.257 RANGE= 0.397 WIDTH(Y)= 2.279 RESP(Y)= 0.2567 HSQC= C29
05Thr_H2/ 1 5.004684 1*1*1 STAT=Y PRED= 4.099 RANGE= 1.025 WIDTH(Y)= 2.210 RESP(Y)= 0.2626 HSQC= C31
05Thr_H3/ 1 4.424087 1*1*1 STAT=Y PRED= 4.345 RANGE= 0.717 WIDTH(Y)= 2.228 RESP(Y)= 0.2252 HSQC= C32
05Thr_H4/ 1 0.911489 1*1*3 STAT=Y PRED= 1.252 RANGE= 0.297 WIDTH(Y)= 2.670 RESP(Y)= 0.2653 HSQC= C34
06Val_H2/ 1 4.843812 1*1*1 STAT=Y PRED= 4.525 RANGE= 1.405 WIDTH(Y)= 5.217 RESP(Y)= 0.2653 HSQC= C37
06Val_H3/ 1 2.348846 1*1*1 STAT=Y PRED= 1.975 RANGE= 1.015 WIDTH(Y)= 2.576 RESP(Y)= 0.2022 HSQC= C38
06Val_H4/ 1 1.087437 1*1*3 STAT=Y PRED= 0.938 RANGE= 0.217 WIDTH(Y)= 1.945 RESP(Y)= 0.1796 HSQC= C39
06Val_H5/ 1 0.992826 1*1*3 STAT=Y PRED= 1.094 RANGE= 0.387 WIDTH(Y)= 2.420 RESP(Y)= 0.1919 HSQC= C40
07Leu_H7/ 1 3.256346 1*1*3 STAT=Y PRED= 3.110 RANGE= 0.375 WIDTH(Y)= 2.208 RESP(Y)= 0.2294 HSQC= C42
07Leu_H2/ 1 5.094221 1*1*1 STAT=Y PRED= 5.342 RANGE= 1.085 WIDTH(Y)= 2.729 RESP(Y)= 0.2035 HSQC= C44
07LeuH3A/ 1 1.462779 1*1*1 STAT=Y PRED= 1.444 RANGE= 0.427 WIDTH(Y)= 2.201 RESP(Y)= 0.1329 HSQC= C45
07LeuH3B/ 1 1.226268 1*1*1 STAT=Y PRED= 1.914 RANGE= 0.367 WIDTH(Y)= 3.770 RESP(Y)= 0.2733 HSQC= C45
07Leu_H4/ 1 0.938876 1*1*1 STAT=Y PRED= 1.630 RANGE= 0.627 WIDTH(Y)= 3.004 RESP(Y)= 0.4584 HSQC= C46
07Leu_H5/ 1 0.336312 1*1*3 STAT=Y PRED= 0.972 RANGE= 0.315 WIDTH(Y)= 2.494 RESP(Y)= 0.2101 HSQC= C47
07Leu_H6/ 1 0.161633 1*1*3 STAT=Y PRED= 0.972 RANGE= 0.147 WIDTH(Y)= 2.600 RESP(Y)= 0.2075 HSQC= C48
08Val_H2/ 1 4.601765 1*1*1 STAT=Y PRED= 4.489 RANGE= 0.895 WIDTH(Y)= 3.315 RESP(Y)= 0.2216 HSQC= C51
08Val_H3/ 1 1.985653 1*1*1 STAT=Y PRED= 1.995 RANGE= 0.485 WIDTH(Y)= 2.957 RESP(Y)= 0.1668 HSQC= C52
08Val_H4/ 1 0.920357 1*1*3 STAT=Y PRED= 1.060 RANGE= 0.237 WIDTH(Y)= 2.316 RESP(Y)= 0.2133 HSQC= C53
08Val_H5/ 1 0.888145 1*1*3 STAT=Y PRED= 0.999 RANGE= 0.227 WIDTH(Y)= 2.753 RESP(Y)= 0.3213 HSQC= C54
09Val_H6/ 1 3.131909 1*1*3 STAT=Y PRED= 3.169 RANGE= 0.465 WIDTH(Y)= 2.455 RESP(Y)= 0.2275 HSQC= C56
09Val_H2/ 1 3.053726 1*1*1 STAT=Y PRED= 5.153 RANGE= 0.717 WIDTH(Y)= 3.143 RESP(Y)= 0.2025 HSQC= C58
09Val_H3/ 1 2.580776 1*1*1 STAT=Y PRED= 2.524 RANGE= 0.407 WIDTH(Y)= 2.626 RESP(Y)= 0.2161 HSQC= C59
09Val_H4/ 1 1.093409 1*1*3 STAT=Y PRED= 1.319 RANGE= 0.227 WIDTH(Y)= 2.669 RESP(Y)= 0.3378 HSQC= C60
09Val_H5/ 1 0.976814 1*1*3 STAT=Y PRED= 1.075 RANGE= 0.237 WIDTH(Y)= 2.677 RESP(Y)= 0.1936 HSQC= C61
10TrpH13/ 1 2.154822 1*1*3 STAT=Y PRED= 2.936 RANGE= 0.895 WIDTH(Y)= 2.817 RESP(Y)= 0.2545 HSQC= C63
10Trp_H2/ 1 4.101427 1*1*1 STAT=Y PRED= 5.043 RANGE= 1.765 WIDTH(Y)= 2.697 RESP(Y)= 0.1932 HSQC= C65
10TrpH3A/ 1 3.546010 1*1*1 STAT=Y PRED= 3.613 RANGE= 0.467 WIDTH(Y)= 1.896 RESP(Y)= 0.1965 HSQC= C66

Appendix N (continued)

10TrpH3B/ 1 3.696461 1*1*1 STAT=Y PRED= 3.367 RANGE= 0.627 WIDTH(Y)= 2.594 RESP(Y)= 0.2199 HSQC= C66
10Trp_H5/ 1 6.700103 1*1*1 STAT=Y PRED= 6.772 RANGE= 0.275 WIDTH(Y)= 1.916 RESP(Y)= 0.2409 HSQC= C68
10Trp_H9/ 1 6.441885 1*1*1 STAT=Y PRED= 7.089 RANGE= 0.217 WIDTH(Y)= 1.656 RESP(Y)= 0.2523 HSQC= C73
10Trp_H7/ 1 6.922224 1*1*1 STAT=Y PRED= 7.333 RANGE= 0.307 WIDTH(Y)= 1.163 RESP(Y)= 0.2299 HSQC= C75
10TrpH12/ 1 3.826462 1*1*3 STAT=Y PRED= 4.072 RANGE= 0.247 WIDTH(Y)= 1.703 RESP(Y)= 0.2281 HSQC= C77
11Val_H2/ 1 4.527542 1*1*1 STAT=Y PRED= 4.303 RANGE= 1.445 WIDTH(Y)= 2.167 RESP(Y)= 0.2288 HSQC= C80
11Val_H3/ 1 2.188102 1*1*1 STAT=Y PRED= 2.094 RANGE= 0.587 WIDTH(Y)= 4.425 RESP(Y)= 0.2651 HSQC= C81
11Val_H4/ 1 1.027242 1*1*3 STAT=Y PRED= 1.094 RANGE= 0.247 WIDTH(Y)= 2.591 RESP(Y)= 0.2551 HSQC= C82
11Val_H5/ 1 1.000423 1*1*3 STAT=Y PRED= 1.080 RANGE= 0.297 WIDTH(Y)= 2.219 RESP(Y)= 0.2097 HSQC= C83
12Phe_H2/ 1 4.841653 1*1*1 STAT=Y PRED= 4.499 RANGE= 0.985 WIDTH(Y)= 3.593 RESP(Y)= 0.2523 HSQC= C86
12Phe_H3/ 1 5.326092 1*1*1 STAT=Y PRED= 5.208 RANGE= 0.487 WIDTH(Y)= 2.098 RESP(Y)= 0.2226 HSQC= C87
12Phe_H5/ 1 7.230609 1*2*1 STAT=Y PRED= 7.524 RANGE= 0.307 WIDTH(Y)= 1.433 RESP(Y)= 0.2480 HSQC= C89_93
12Phe_H6/ 1 7.250066 1*2*1 STAT=Y PRED= 7.372 RANGE= 0.577 WIDTH(Y)= 1.876 RESP(Y)= 0.2658 HSQC= C90_92
12Phe_H7/ 1 7.196979 1*1*1 STAT=Y PRED= 7.281 RANGE= 0.307 WIDTH(Y)= 1.828 RESP(Y)= 0.2695 HSQC= C91
13Val_H2/ 1 4.407490 1*1*1 STAT=Y PRED= 4.169 RANGE= 0.667 WIDTH(Y)= 1.764 RESP(Y)= 0.2459 HSQC= C97
13Val_H3/ 1 1.965710 1*1*1 STAT=Y PRED= 1.935 RANGE= 0.865 WIDTH(Y)= 1.999 RESP(Y)= 0.2069 HSQC= C99
13Val_H4/ 1 0.935848 1*1*3 STAT=Y PRED= 1.277 RANGE= 0.217 WIDTH(Y)= 3.028 RESP(Y)= 0.3033 HSQC= C100
13Val_H5/ 1 0.925029 1*1*3 STAT=Y PRED= 0.933 RANGE= 0.277 WIDTH(Y)= 2.510 RESP(Y)= 0.2573 HSQC= C101

COUPLING CONSTANTS(HZ): fixed
J115_217 7.7969 J 10Trp_H8 10Trp_H9 STAT=Y PRED= 8.100 RANGE= 0.890
J115_218 8.1808 J 10Trp_H8 10Trp_H7 STAT=Y PRED= 7.850 RANGE= 0.800
J122_123 9.1737 J 01Val_H2 01Val_H3 STAT=Y PRED= 12.510 RANGE= 4.000
J123_124 6.5890 J 01Val_H3 01Val_H6 STAT=Y PRED= 6.640 RANGE= 0.200
J123_127 6.6205 J 01Val_H3 01Val_H7 STAT=Y PRED= 6.640 RANGE= 0.200
J131_132 8.7545 J 02Val_H2 02Val_H3 STAT=Y PRED= 12.600 RANGE= 6.000
J132_133 6.7841 J 02Val_H3 02Val_H4 STAT=Y PRED= 6.640 RANGE= 0.200
J132_136 6.7206 J 02Val_H3 02Val_H5 STAT=Y PRED= 6.640 RANGE= 0.200
J153_154 2.3441 J 04Thr_H2 04Thr_H3 STAT=Y PRED= 2.690 RANGE= 6.600
J154_155 6.5134 J 04Thr_H3 04Thr_H4 STAT=Y PRED= 6.250 RANGE= 0.600
J161_162 3.7259 J 05Thr_H2 05Thr_H3 STAT=Y PRED= 2.440 RANGE= 4.400
J162_164 6.4691 J 05Thr_H3 05Thr_H4 STAT=Y PRED= 6.250 RANGE= 0.600
J168_169 8.9180 J 06Val_H2 06Val_H3 STAT=Y PRED= 2.980 RANGE= 6.600
J169_170 6.6944 J 06Val_H3 06Val_H4 STAT=Y PRED= 6.640 RANGE= 0.200
J169_173 7.0316 J 06Val_H3 06Val_H5 STAT=Y PRED= 6.640 RANGE= 0.200
J179_180 6.2437 J 07Leu_H2 07LeuH3A STAT=Y PRED= 3.040 RANGE= 6.000
J179_181 8.3839 J 07Leu_H2 07LeuH3B STAT=Y PRED= 13.950 RANGE= 4.000
J180_181 -13.3047 J 07LeuH3A 07LeuH3B STAT=Y PRED= -14.710 RANGE= 1.600
J180_182 8.2119 J 07LeuH3A 07Leu_H4 STAT=Y PRED= 12.990 RANGE= 2.560
J181_182 5.7896 J 07LeuH3B 07Leu_H4 STAT=Y PRED= 2.270 RANGE= 3.000
J182_183 6.5482 J 07Leu_H4 07Leu_H5 STAT=Y PRED= 6.640 RANGE= 0.200
J182_186 6.5879 J 07Leu_H4 07Leu_H6 STAT=Y PRED= 6.640 RANGE= 0.200
J190_191 8.8736 J 08Val_H2 08Val_H3 STAT=Y PRED= 12.880 RANGE= 6.000
J191_192 6.5520 J 08Val_H3 08Val_H4 STAT=Y PRED= 6.640 RANGE= 0.200
J191_195 6.7834 J 08Val_H3 08Val_H5 STAT=Y PRED= 6.640 RANGE= 0.200
J201_202 7.6281 J 09Val_H2 09Val_H3 STAT=Y PRED= 12.960 RANGE= 4.000
J202_203 6.4961 J 09Val_H3 09Val_H4 STAT=Y PRED= 6.640 RANGE= 0.200
J202_206 6.7760 J 09Val_H3 09Val_H5 STAT=Y PRED= 6.640 RANGE= 0.200
J212_213 11.1630 J 10Trp_H2 10TrpH3A STAT=Y PRED= 12.890 RANGE= 4.000
J212_214 4.7143 J 10Trp_H2 10TrpH3B STAT=Y PRED= 1.900 RANGE= 4.400

Appendix N (continued)

```
J213_214  -13.7295   J 10TrpH3A 10TrpH3B   STAT=Y  PRED= -16.760 RANGE= 2.560
J215_218    0.4880   J 10Trp_H5 10Trp_H7   STAT=Y  PRED= -0.300 RANGE= 0.500
J217_218    0.6708   J 10Trp_H9 10Trp_H7   STAT=Y  PRED= 1.020 RANGE= 1.200
J223_224    7.9094   J 11Val_H2 11Val_H3   STAT=Y  PRED= 3.450 RANGE= 9.000
J224_225    6.7483   J 11Val_H3 11Val_H4   STAT=Y  PRED= 6.640 RANGE= 0.200
J224_228    6.8064   J 11Val_H3 11Val_H5   STAT=Y  PRED= 6.640 RANGE= 0.200
J232_233    1.9005   J 12Phe_H2 12Phe_H3   STAT=Y  PRED= 1.900 RANGE= 6.600
J234_238    1.3335   J 12Phe_H5 12Phe_H5   STAT=Y  PRED= 1.980 RANGE= 1.200
J234_235    7.6508   J 12Phe_H5 12Phe_H6   STAT=Y  PRED= 7.660 RANGE= 0.340
J234_237    0.7769   J 12Phe_H6 12Phe_H5   STAT=Y  PRED= 0.550 RANGE= 0.750
J234_236    1.2760   J 12Phe_H5 12Phe_H7   STAT=Y  PRED= 1.260 RANGE= 1.200
J235_237    1.7027   J 12Phe_H6 12Phe_H6   STAT=Y  PRED= 1.480 RANGE= 1.200
J235_236    7.4760   J 12Phe_H6 12Phe_H7   STAT=Y  PRED= 7.400 RANGE= 0.240
J241_242    8.8924   J 13Val_H2 13Val_H3   STAT=Y  PRED= 12.320 RANGE= 6.000
J242_243    6.8372   J 13Val_H3 13Val_H4   STAT=Y  PRED= 6.640 RANGE= 0.200
J242_246    6.4162   J 13Val_H3 13Val_H5   STAT=Y  PRED= 6.640 RANGE= 0.200

CONTROL PARAMETERS:
      Solvent =  none (def. 99% enriched)
        1.000 =  Concentration (vol%, def=1.0%)
   0.00100000 =  Minimum line-intensity
   0.00100000 =  Diagonalization criterium (not in use)
 600.13000500 =  FIELD(1H,MHz), used to transform shifts to ppms
  11.63298479 =  Left frequency (ppm)
  -4.33373628 =  Right frequency (ppm)
       10.000 =  Acquisition time (s, for QMTLS)
        0.000 =  Line-width (for modes D, P & T, 0=use defaults)
  0.058337236 =  Data-point resolution (Hz)
      -3.018 =  GAUSSIAN (%, 0=use default from INF)
      -6.775 =  Dispersion contribution (%, 0=use default from INF)
   0.00000000 =  Decoupling frequency (for DORES)

CONSTRAINTS (in equations X0 = 1.0)...use no empty lines
 EQUAL 01Val_H2 = 13Val_H2
 EQUAL 06Val_H5 = 11Val_H4
 EQUAL 07Leu_H5 = 07Leu_H6
 IGNORE(HZ):  2904.119 to  2866.556
 IGNORE(HZ):  1990.683 to  1980.117

END of FILE
```

Appendix O. PMS file for norecumicin. ^{1}H spectrum obtained with Bruker Avance 600, sample contains residual acid.

```
* NEW: the lines beginning by * are comment lines !
* To keep all the chemical shifts fixed during iteration
* replace "CHEMICAL SHIFTS(HZ):" by "..SHIFTS(HZ): fixed"
* The couplings can be fixed in the same way

NMR-data: C:\Users\wgao\Documents\My Box Files\ITR Lab work\Lab Data\ECUM\R
#$œ  Date  6.10.2013;  Time 15:43:40     perch.pms

CHEMICAL SHIFTS(PPM):
PROTON   2*SPIN= 1 SPECIES=1H    POPULATION(Y)=   1.00000
 H74   / 1    6.981610  1*1*1  STAT=Y  PRED= 7.023 RANGE= 0.367 WIDTH(Y)= 1.571 RESP(Y)= 0.0131 HSQC= C74
 H1_2  / 1    2.516674  1*1*6  STAT=Y  PRED= 2.406 RANGE= 0.300 WIDTH(Y)= 2.912 RESP(Y)= 0.0121 HSQC= C1_2
 H4    / 1    3.053736  1*1*1  STAT=Y  PRED= 3.396 RANGE= 0.622 WIDTH(Y)= 3.394 RESP(Y)= 0.0109 HSQC= C4
 H5    / 1    2.580793  1*1*1  STAT=Y  PRED= 2.135 RANGE= 0.727 WIDTH(Y)= 2.749 RESP(Y)= 0.0123 HSQC= C5
 H6    / 1    0.992730  1*1*3  STAT=Y  PRED= 1.015 RANGE= 0.495 WIDTH(Y)= 2.786 RESP(Y)= 0.0112 HSQC= C6
 H7    / 1    0.858647  1*1*3  STAT=Y  PRED= 0.973 RANGE= 0.295 WIDTH(Y)= 2.999 RESP(Y)= 0.0138 HSQC= C7
 H10   / 1    4.701699  1*1*1  STAT=Y  PRED= 4.573 RANGE= 0.767 WIDTH(Y)= 2.283 RESP(Y)= 0.0125 HSQC= C10
 H12   / 1    2.122312  1*1*1  STAT=Y  PRED= 2.176 RANGE= 0.730 WIDTH(Y)= 2.318 RESP(Y)= 0.0104 HSQC= C12
 H13   / 1    1.000294  1*1*3  STAT=Y  PRED= 1.069 RANGE= 0.255 WIDTH(Y)= 2.654 RESP(Y)= 0.0148 HSQC= C13
 H14   / 1    1.058060  1*1*3  STAT=Y  PRED= 0.977 RANGE= 0.230 WIDTH(Y)= 2.267 RESP(Y)= 0.0129 HSQC= C14
 H15   / 1    3.243363  1*1*3  STAT=Y  PRED= 3.422 RANGE= 0.402 WIDTH(Y)= 1.906 RESP(Y)= 0.0125 HSQC= C15
 H17   / 1    4.858555  1*1*1  STAT=Y  PRED= 5.157 RANGE= 1.515 WIDTH(Y)= 2.047 RESP(Y)= 0.0105 HSQC= C17
 H19   / 1    2.348921  1*1*1  STAT=Y  PRED= 2.269 RANGE= 0.360 WIDTH(Y)= 2.940 RESP(Y)= 0.0119 HSQC= C19
 H20   / 1    1.087407  1*1*3  STAT=Y  PRED= 1.123 RANGE= 0.290 WIDTH(Y)= 1.788 RESP(Y)= 0.0076 HSQC= C20
 H21   / 1    0.980430  1*1*3  STAT=Y  PRED= 0.958 RANGE= 0.227 WIDTH(Y)= 2.694 RESP(Y)= 0.0156 HSQC= C21
 H24   / 1    5.171459  1*1*1  STAT=Y  PRED= 4.479 RANGE= 0.965 WIDTH(Y)= 1.932 RESP(Y)= 0.0111 HSQC= C24
 H25   / 1    5.779368  1*1*1  STAT=Y  PRED= 5.009 RANGE= 0.620 WIDTH(Y)= 2.444 RESP(Y)= 0.0118 HSQC= C25
 H27   / 1    1.314121  1*1*3  STAT=Y  PRED= 1.213 RANGE= 0.447 WIDTH(Y)= 2.780 RESP(Y)= 0.0130 HSQC= C27
 H29   / 1    3.320643  1*1*3  STAT=Y  PRED= 3.479 RANGE= 0.425 WIDTH(Y)= 2.223 RESP(Y)= 0.0122 HSQC= C29
 H31   / 1    5.004686  1*1*1  STAT=Y  PRED= 5.502 RANGE= 1.070 WIDTH(Y)= 2.083 RESP(Y)= 0.0123 HSQC= C31
 H32   / 1    4.424222  1*1*1  STAT=Y  PRED= 4.397 RANGE= 0.657 WIDTH(Y)= 2.116 RESP(Y)= 0.0115 HSQC= C32
 H34   / 1    0.920493  1*1*3  STAT=Y  PRED= 1.243 RANGE= 0.290 WIDTH(Y)= 2.515 RESP(Y)= 0.0133 HSQC= C34
 H37   / 1    4.829998  1*1*1  STAT=Y  PRED= 4.457 RANGE= 1.495 WIDTH(Y)= 2.484 RESP(Y)= 1.0000 HSQC= C37
 H38   / 1    2.198484  1*1*1  STAT=Y  PRED= 2.091 RANGE= 0.617 WIDTH(Y)= 2.556 RESP(Y)= 0.0157 HSQC= C38
 H39   / 1    0.814786  1*1*3  STAT=Y  PRED= 0.984 RANGE= 0.242 WIDTH(Y)= 2.552 RESP(Y)= 0.0146 HSQC= C39
 H40   / 1    0.796176  1*1*3  STAT=Y  PRED= 1.026 RANGE= 0.367 WIDTH(Y)= 2.590 RESP(Y)= 0.0134 HSQC= C40
 H42   / 1    3.256352  1*1*3  STAT=Y  PRED= 3.426 RANGE= 0.427 WIDTH(Y)= 2.182 RESP(Y)= 0.0110 HSQC= C42
 H44   / 1    5.094328  1*1*1  STAT=Y  PRED= 4.381 RANGE= 1.015 WIDTH(Y)= 3.986 RESP(Y)= 0.0113 HSQC= C44
 H45A  / 1    1.226350  1*1*1  STAT=Y  PRED= 1.393 RANGE= 0.552 WIDTH(Y)= 3.114 RESP(Y)= 0.0102 HSQC= C45
 H45B  / 1    1.462857  1*1*1  STAT=Y  PRED= 1.155 RANGE= 0.542 WIDTH(Y)= 2.648 RESP(Y)= 0.0086 HSQC= C45
 H46   / 1    0.959179  1*1*1  STAT=Y  PRED= 1.649 RANGE= 0.445 WIDTH(Y)= 4.066 RESP(Y)= 0.0190 HSQC= C46
```

Appendix O (continued)

H47 / 1 0.161642 1*1*3 STAT=Y PRED= 0.889 RANGE= 0.302 WIDTH(Y)= 2.626 RESP(Y)= 0.0101 HSQC= C47
H48 / 1 0.336322 1*1*3 STAT=Y PRED= 0.760 RANGE= 0.300 WIDTH(Y)= 2.513 RESP(Y)= 0.0102 HSQC= C48
H51 / 1 4.601812 1*1*1 STAT=Y PRED= 4.432 RANGE= 0.870 WIDTH(Y)= 3.361 RESP(Y)= 0.0108 HSQC= C51
H52 / 1 2.012364 1*1*1 STAT=Y PRED= 1.936 RANGE= 0.482 WIDTH(Y)= 3.295 RESP(Y)= 0.0116 HSQC= C52
H53 / 1 0.911690 1*1*3 STAT=Y PRED= 1.015 RANGE= 0.225 WIDTH(Y)= 2.566 RESP(Y)= 0.0128 HSQC= C53
H54 / 1 0.888145 1*1*3 STAT=Y PRED= 0.840 RANGE= 0.247 WIDTH(Y)= 2.770 RESP(Y)= 0.0156 HSQC= C54
H56 / 1 3.131896 1*1*3 STAT=Y PRED= 3.099 RANGE= 0.437 WIDTH(Y)= 2.341 RESP(Y)= 0.0107 HSQC= C56
H58 / 1 3.013246 1*1*1 STAT=Y PRED= 5.151 RANGE= 0.762 WIDTH(Y)= 3.510 RESP(Y)= 0.0121 HSQC= C58
H59 / 1 2.177188 1*1*1 STAT=Y PRED= 2.677 RANGE= 0.632 WIDTH(Y)= 1.956 RESP(Y)= 0.0109 HSQC= C59
H60 / 1 0.976714 1*1*3 STAT=Y PRED= 1.286 RANGE= 0.250 WIDTH(Y)= 2.513 RESP(Y)= 0.0096 HSQC= C60
H61 / 1 1.093404 1*1*3 STAT=Y PRED= 1.021 RANGE= 0.245 WIDTH(Y)= 2.830 RESP(Y)= 0.0173 HSQC= C61
H63 / 1 2.154836 1*1*3 STAT=Y PRED= 2.815 RANGE= 1.050 WIDTH(Y)= 2.546 RESP(Y)= 0.0111 HSQC= C63
H65 / 1 4.101423 1*1*1 STAT=Y PRED= 4.369 RANGE= 1.085 WIDTH(Y)= 3.038 RESP(Y)= 0.0108 HSQC= C65
H66A / 1 3.546031 1*1*1 STAT=Y PRED= 2.991 RANGE= 0.450 WIDTH(Y)= 2.153 RESP(Y)= 0.0109 HSQC= C66
H66B / 1 3.696470 1*1*1 STAT=Y PRED= 3.850 RANGE= 0.557 WIDTH(Y)= 2.880 RESP(Y)= 0.0122 HSQC= C66
H68 / 1 6.700107 1*1*1 STAT=Y PRED= 6.561 RANGE= 0.662 WIDTH(Y)= 1.670 RESP(Y)= 0.0115 HSQC= C68
H73 / 1 6.922230 1*1*1 STAT=Y PRED= 6.532 RANGE= 0.512 WIDTH(Y)= 1.072 RESP(Y)= 0.0113 HSQC= C73
H75 / 1 6.441898 1*1*1 STAT=Y PRED= 6.819 RANGE= 0.542 WIDTH(Y)= 1.831 RESP(Y)= 0.0129 HSQC= C75
H77 / 1 3.826467 1*1*3 STAT=Y PRED= 4.111 RANGE= 0.272 WIDTH(Y)= 1.666 RESP(Y)= 0.0108 HSQC= C77
H80 / 1 4.527536 1*1*1 STAT=Y PRED= 4.239 RANGE= 1.445 WIDTH(Y)= 2.218 RESP(Y)= 0.0114 HSQC= C80
H81 / 1 2.168089 1*1*1 STAT=Y PRED= 2.213 RANGE= 0.692 WIDTH(Y)= 2.592 RESP(Y)= 0.0114 HSQC= C81
H82 / 1 1.027228 1*1*3 STAT=Y PRED= 1.063 RANGE= 0.232 WIDTH(Y)= 2.636 RESP(Y)= 0.0123 HSQC= C82
H83 / 1 1.017840 1*1*3 STAT=Y PRED= 1.034 RANGE= 0.382 WIDTH(Y)= 2.754 RESP(Y)= 0.0126 HSQC= C83
H86 / 1 4.889740 1*1*1 STAT=Y PRED= 4.479 RANGE= 1.030 WIDTH(Y)= 2.056 RESP(Y)= 0.0105 HSQC= C86
H87 / 1 5.326115 1*1*1 STAT=Y PRED= 5.208 RANGE= 0.567 WIDTH(Y)= 2.228 RESP(Y)= 0.0111 HSQC= C87
H89_93/ 1 7.250017 1*2*1 STAT=Y PRED= 7.330 RANGE= 0.542 WIDTH(Y)= 2.128 RESP(Y)= 0.0130 HSQC= C89_93
H90_92/ 1 7.230658 1*2*1 STAT=Y PRED= 7.270 RANGE= 0.342 WIDTH(Y)= 1.356 RESP(Y)= 0.0116 HSQC= C90_92
H91 / 1 7.196820 1*1*1 STAT=Y PRED= 7.244 RANGE= 0.347 WIDTH(Y)= 1.791 RESP(Y)= 0.0134 HSQC= C91
H97 / 1 4.407524 1*1*1 STAT=Y PRED= 4.423 RANGE= 1.155 WIDTH(Y)= 1.821 RESP(Y)= 0.0120 HSQC= C97
H99 / 1 1.964895 1*1*1 STAT=Y PRED= 2.095 RANGE= 0.660 WIDTH(Y)= 2.317 RESP(Y)= 0.0139 HSQC= C99
H100 / 1 0.936018 1*1*3 STAT=Y PRED= 0.968 RANGE= 0.225 WIDTH(Y)= 3.101 RESP(Y)= 0.0173 HSQC= C100
H101 / 1 0.924866 1*1*3 STAT=Y PRED= 1.001 RANGE= 0.307 WIDTH(Y)= 2.098 RESP(Y)= 0.0094 HSQC= C101

COUPLING CONSTANTS(HZ):

J114_213 8.2279 J H74 H73 STAT=Y PRED= 8.100 RANGE= 0.440
J114_214 7.7897 J H74 H75 STAT=Y PRED= 7.850 RANGE= 0.400
J121_122 7.5305 J H4 H5 STAT=Y PRED= 12.640 RANGE= 2.000
J122_123 6.8006 J H5 H6 STAT=Y PRED= 6.640 RANGE= 0.100
J122_126 6.7841 J H5 H7 STAT=Y PRED= 6.640 RANGE= 0.100
J130_131 8.6187 J H10 H12 STAT=Y PRED= 12.660 RANGE= 2.000
J131_132 6.8023 J H12 H13 STAT=Y PRED= 6.640 RANGE= 0.100
J131_135 6.6113 J H12 H14 STAT=Y PRED= 6.640 RANGE= 0.100

Appendix O (continued)

J141_142 8.8773 J H17 H19 STAT=Y PRED= 12.990 RANGE= 2.000
J142_143 6.6581 J H19 H20 STAT=Y PRED= 6.640 RANGE= 0.100
J142_145 6.9193 J H19 H21 STAT=Y PRED= 6.640 RANGE= 0.100
J149_150 2.1893 J H24 H25 STAT=Y PRED= 1.510 RANGE= 2.200
J150_151 6.4103 J H25 H27 STAT=Y PRED= 6.250 RANGE= 0.300
J157_158 4.0972 J H31 H32 STAT=Y PRED= 2.250 RANGE= 2.200
J158_160 6.5969 J H32 H34 STAT=Y PRED= 6.250 RANGE= 0.300
J164_165 8.3584 J H37 H38 STAT=Y PRED= 2.920 RANGE= 2.200
J165_166 6.5096 J H38 H39 STAT=Y PRED= 6.640 RANGE= 0.100
J165_169 6.5456 J H38 H40 STAT=Y PRED= 6.640 RANGE= 0.100
66 7.2622 J H44 H45A STAT=Y
68 8.0000 J H44 H45B STAT=Y
65 8.4615 J H44 H45B STAT=Y
64 -13.5770 J H45A H45B STAT=Y
72 6.3059 J H45A H46 STAT=Y
74 5.0898 J H45B H46 STAT=Y
96 6.5705 J H46 H47 STAT=Y
97 6.6223 J H46 H48 STAT=Y
98 8.7487 J H51 H52 STAT=Y
99 6.8195 J H52 H53 STAT=Y
100 6.6274 J H52 H54 STAT=Y
101 7.7962 J H58 H59 STAT=Y
79 6.8078 J H59 H60 STAT=Y
80 6.5148 J H59 H61 STAT=Y
82 11.1714 J H65 H66A STAT=Y
84 4.5879 J H65 H66B STAT=Y
86 -13.6833 J H66A H66B STAT=Y
83 0.8885 J H68 H73 STAT=Y
88 0.5332 J H73 H75 STAT=Y
102 7.6741 J H80 H81 STAT=Y
109 6.8423 J H81 H82 STAT=Y
111 6.6048 J H81 H83 STAT=Y
113 1.8362 J H86 H87 STAT=Y
91 0.7381 J H89_93 H89_93 STAT=Y
121 1.2129 J H89_93 H90_92 STAT=Y
122 7.8847 J H90_92 H89_93 STAT=Y
118 7.4096 J H89_93 H91 STAT=Y
108 0.4925 J H90_92 H90_92 STAT=Y
115 1.3733 J H90_92 H91 STAT=Y
126 8.7094 J H97 H99 STAT=Y
71 6.3788 J H99 H100 STAT=Y
78 6.0000 J H99 H101 STAT=Y

Appendix O (continued)

67	6.9054	J H99	H101	STAT=Y
69	6.1030	J H99	H101	STAT=Y

Appendix P. PMS file for norecumicin. ^{1}H spectrum obtained with Bruker Avance II 900, sample contains residual acid.

* NEW: the lines beginning by * are comment lines !
* To keep all the chemical shifts fixed during iteration
* replace CHEMICAL SHIFTS(HZ): by ..SHIFTS(HZ): fixed
* The couplings can be fixed in the same way

NMR-data: C:\Users\wgao\Documents\My Box Files\ITR Lab work\Lab Data\ECUM\R
#$œ Date 6.11.2013; Time 0:11:38 perch.pms

CHEMICAL SHIFTS(PPM):
PROTON 2*SPIN= 1 SPECIES=1H POPULATION(Y)= 1
H74 / 1 6.981637 1*1*1 STAT=Y PRED= 6.997 RANGE= 0.339 WIDTH(Y)= 1.055 RESP(Y)= 0.2123 HSQC= C74
H1_2 / 1 2.315267 1*1*6 STAT=Y PRED= 2.401 RANGE= 0.299 WIDTH(Y)= 2.238 RESP(Y)= 0.2204 HSQC= C1_2
H4 / 1 2.675387 1*1*1 STAT=Y PRED= 3.396 RANGE= 0.587 WIDTH(Y)= 1.919 RESP(Y)= 0.1772 HSQC= C4
H5 / 1 2.042623 1*1*1 STAT=Y PRED= 1.998 RANGE= 0.577 WIDTH(Y)= 3.585 RESP(Y)= 0.1863 HSQC= C5
H6 / 1 1.092514 1*1*3 STAT=Y PRED= 1.018 RANGE= 0.559 WIDTH(Y)= 1.268 RESP(Y)= 0.0977 HSQC= C6
H7 / 1 0.845893 1*1*3 STAT=Y PRED= 0.973 RANGE= 0.299 WIDTH(Y)= 1.848 RESP(Y)= 0.1955 HSQC= C7
H10 / 1 4.672014 1*1*1 STAT=Y PRED= 4.503 RANGE= 0.799 WIDTH(Y)= 1.744 RESP(Y)= 0.1932 HSQC= C10
H12 / 1 2.102824 1*1*1 STAT=Y PRED= 2.256 RANGE= 0.879 WIDTH(Y)= 1.759 RESP(Y)= 0.1754 HSQC= C12
H13 / 1 0.977216 1*1*3 STAT=Y PRED= 1.093 RANGE= 0.267 WIDTH(Y)= 4.265 RESP(Y)= 0.211 HSQC= C13
H14 / 1 1.055758 1*1*3 STAT=Y PRED= 0.982 RANGE= 0.259 WIDTH(Y)= 1.8 RESP(Y)= 0.1971 HSQC= C14
H15 / 1 3.248635 1*1*3 STAT=Y PRED= 3.516 RANGE= 0.408 WIDTH(Y)= 1.231 RESP(Y)= 0.1501 HSQC= C15
H17 / 1 4.834013 1*1*1 STAT=Y PRED= 4.885 RANGE= 0.965 WIDTH(Y)= 1.502 RESP(Y)= 0.1686 HSQC= C17
H19 / 1 2.175649 1*1*1 STAT=Y PRED= 2.203 RANGE= 0.636 WIDTH(Y)= 1.759 RESP(Y)= 0.1662 HSQC= C19
H20 / 1 0.809878 1*1*3 STAT=Y PRED= 1.044 RANGE= 0.269 WIDTH(Y)= 2.011 RESP(Y)= 0.2062 HSQC= C20
H21 / 1 0.793833 1*1*3 STAT=Y PRED= 0.922 RANGE= 0.279 WIDTH(Y)= 1.775 RESP(Y)= 0.1592 HSQC= C21
H24 / 1 5.173976 1*1*1 STAT=Y PRED= 4.479 RANGE= 0.997 WIDTH(Y)= 1.61 RESP(Y)= 0.1689 HSQC= C24
H25 / 1 5.785936 1*1*1 STAT=Y PRED= 5.139 RANGE= 0.649 WIDTH(Y)= 1.975 RESP(Y)= 0.1597 HSQC= C25
H27 / 1 1.313048 1*1*3 STAT=Y PRED= 1.257 RANGE= 0.468 WIDTH(Y)= 2.455 RESP(Y)= 0.266 HSQC= C27
H29 / 1 3.323236 1*1*3 STAT=Y PRED= 3.532 RANGE= 0.429 WIDTH(Y)= 1.679 RESP(Y)= 0.1779 HSQC= C29
H31 / 1 5.0085 1*1*1 STAT=Y PRED= 5.502 RANGE= 1.009 WIDTH(Y)= 1.524 RESP(Y)= 0.1565 HSQC= C31
H32 / 1 4.426267 1*1*1 STAT=Y PRED= 4.52 RANGE= 0.788 WIDTH(Y)= 1.555 RESP(Y)= 0.1813 HSQC= C32
H34 / 1 0.919684 1*1*3 STAT=Y PRED= 1.18 RANGE= 0.329 WIDTH(Y)= 1.959 RESP(Y)= 0.146 HSQC= C34
H37 / 1 4.853292 1*1*1 STAT=Y PRED= 4.533 RANGE= 1.529 WIDTH(Y)= 2.621 RESP(Y)= 0.2469 HSQC= C37
H38 / 1 2.351437 1*1*1 STAT=Y PRED= 2.382 RANGE= 1.089 WIDTH(Y)= 2.665 RESP(Y)= 0.2619 HSQC= C38
H39 / 1 1.093803 1*1*3 STAT=Y PRED= 1.071 RANGE= 0.249 WIDTH(Y)= 1.742 RESP(Y)= 0.1408 HSQC= C39
H40 / 1 0.978045 1*1*3 STAT=Y PRED= 1.128 RANGE= 0.359 WIDTH(Y)= 1.895 RESP(Y)= 0.1916 HSQC= C40
H42 / 1 3.260269 1*1*3 STAT=Y PRED= 3.359 RANGE= 0.428 WIDTH(Y)= 1.551 RESP(Y)= 0.1699 HSQC= C42
H44 / 1 5.08441 1*1*1 STAT=Y PRED= 5.342 RANGE= 1.199 WIDTH(Y)= 2.284 RESP(Y)= 0.1459 HSQC= C44
H45A / 1 1.218894 1*1*1 STAT=Y PRED= 1.407 RANGE= 0.689 WIDTH(Y)= 5.653 RESP(Y)= 0.1914 HSQC= C45
H45B / 1 1.465951 1*1*1 STAT=Y PRED= 1.554 RANGE= 0.529 WIDTH(Y)= 2.509 RESP(Y)= 0.1232 HSQC= C45
H46 / 1 0.991833 1*1*1 STAT=Y PRED= 0.977 RANGE= 0.749 WIDTH(Y)= 1.8 RESP(Y)= 1 HSQC= C46
H47 / 1 0.148023 1*1*3 STAT=Y PRED= 0.591 RANGE= 0.638 WIDTH(Y)= 2.043 RESP(Y)= 0.1325 HSQC= C47
H48 / 1 0.335707 1*1*3 STAT=Y PRED= 0.367 RANGE= 0.729 WIDTH(Y)= 2.182 RESP(Y)= 0.1497 HSQC= C48
H51 / 1 4.595735 1*1*1 STAT=Y PRED= 4.458 RANGE= 0.827 WIDTH(Y)= 1.641 RESP(Y)= 0.186 HSQC= C51
H52 / 1 2.027228 1*1*1 STAT=Y PRED= 1.951 RANGE= 0.929 WIDTH(Y)= 2.545 RESP(Y)= 0.1885 HSQC= C52
H53 / 1 0.912431 1*1*3 STAT=Y PRED= 1.059 RANGE= 0.229 WIDTH(Y)= 2.525 RESP(Y)= 0.2445 HSQC= C53
H54 / 1 0.85921 1*1*3 STAT=Y PRED= 0.965 RANGE= 0.209 WIDTH(Y)= 2.833 RESP(Y)= 0.2512 HSQC= C54
H56 / 1 3.137783 1*1*3 STAT=Y PRED= 3.034 RANGE= 0.459 WIDTH(Y)= 2.284 RESP(Y)= 0.179 HSQC= C56
H58 / 1 3.063932 1*1*1 STAT=Y PRED= 5.153 RANGE= 0.788 WIDTH(Y)= 2.848 RESP(Y)= 0.1778 HSQC= C58

Appendix P (continued)

H59 / 1 2.581881 1*1*1 STAT=Y PRED= 2.507 RANGE= 0.669 WIDTH(Y)= 1.398 RESP(Y)= 0.1405 HSQC= C59
H60 / 1 0.980146 1*1*3 STAT=Y PRED= 1.377 RANGE= 0.277 WIDTH(Y)= 2.217 RESP(Y)= 0.1991 HSQC= C60
H61 / 1 1.093888 1*1*3 STAT=Y PRED= 1.041 RANGE= 0.259 WIDTH(Y)= 1.836 RESP(Y)= 0.1426 HSQC= C61
H63 / 1 2.156422 1*1*3 STAT=Y PRED= 2.847 RANGE= 0.905 WIDTH(Y)= 1.961 RESP(Y)= 0.1718 HSQC= C63
H65 / 1 4.104257 1*1*1 STAT=Y PRED= 3.979 RANGE= 1.079 WIDTH(Y)= 2.494 RESP(Y)= 0.1731 HSQC= C65
H66A / 1 3.544928 1*1*1 STAT=Y PRED= 3.235 RANGE= 0.409 WIDTH(Y)= 1.941 RESP(Y)= 0.1891 HSQC= C66
H66B / 1 3.693397 1*1*1 STAT=Y PRED= 3.808 RANGE= 0.559 WIDTH(Y)= 2.194 RESP(Y)= 0.1725 HSQC= C66
H68 / 1 6.698177 1*1*1 STAT=Y PRED= 6.518 RANGE= 0.499 WIDTH(Y)= 1.251 RESP(Y)= 0.1798 HSQC= C68
H73 / 1 6.91749 1*1*1 STAT=Y PRED= 6.499 RANGE= 0.457 WIDTH(Y)= 0.905 RESP(Y)= 0.1837 HSQC= C73
H75 / 1 6.44215 1*1*1 STAT=Y PRED= 6.805 RANGE= 0.536 WIDTH(Y)= 0.914 RESP(Y)= 0.1921 HSQC= C75
H77 / 1 3.826912 1*1*3 STAT=Y PRED= 4.025 RANGE= 0.229 WIDTH(Y)= 1.302 RESP(Y)= 0.1782 HSQC= C77
H80 / 1 4.536292 1*1*1 STAT=Y PRED= 4.071 RANGE= 1.409 WIDTH(Y)= 2.138 RESP(Y)= 0.189 HSQC= C80
H81 / 1 2.190577 1*1*1 STAT=Y PRED= 2.387 RANGE= 0.719 WIDTH(Y)= 2.468 RESP(Y)= 0.2188 HSQC= C81
H82 / 1 1.026756 1*1*3 STAT=Y PRED= 1.146 RANGE= 0.216 WIDTH(Y)= 2.887 RESP(Y)= 0.2231 HSQC= C82
H83 / 1 0.993264 1*1*3 STAT=Y PRED= 1.049 RANGE= 0.379 WIDTH(Y)= 2.919 RESP(Y)= 0.2384 HSQC= C83
H86 / 1 4.883879 1*1*1 STAT=Y PRED= 4.609 RANGE= 0.959 WIDTH(Y)= 5.821 RESP(Y)= 0.0693 HSQC= C86
H87 / 1 5.325957 1*1*1 STAT=Y PRED= 5.208 RANGE= 0.629 WIDTH(Y)= 1.722 RESP(Y)= 0.1462 HSQC= C87
H89_93/ 1 7.229176 1*2*1 STAT=Y PRED= 7.298 RANGE= 0.519 WIDTH(Y)= 2.373 RESP(Y)= 0.219 HSQC= C89_93
H90_92/ 1 7.252244 1*2*1 STAT=Y PRED= 7.298 RANGE= 0.319 WIDTH(Y)= 1.869 RESP(Y)= 0.216 HSQC= C90_92
H91 / 1 7.198397 1*1*1 STAT=Y PRED= 7.266 RANGE= 0.316 WIDTH(Y)= 2.299 RESP(Y)= 0.2317 HSQC= C91
H97 / 1 4.402209 1*1*1 STAT=Y PRED= 4.349 RANGE= 0.737 WIDTH(Y)= 1.416 RESP(Y)= 0.1873 HSQC= C97
H99 / 1 1.963344 1*1*1 STAT=Y PRED= 1.986 RANGE= 0.899 WIDTH(Y)= 3.964 RESP(Y)= 0.218 HSQC= C99
H100 / 1 0.937003 1*1*3 STAT=Y PRED= 1.122 RANGE= 0.189 WIDTH(Y)= 3.436 RESP(Y)= 0.337 HSQC= C100
H101 / 1 0.922406 1*1*3 STAT=Y PRED= 1.109 RANGE= 0.389 WIDTH(Y)= 2.275 RESP(Y)= 0.2212 HSQC= C101

COUPLING CONSTANTS(HZ):
J114_213 8.1721 J H74 H73 STAT=Y PRED= 8.1 RANGE= 0.89
J114_214 7.7521 J H74 H75 STAT=Y PRED= 7.85 RANGE= 0.8
J121_122 9.1891 J H4 H5 STAT=Y PRED= 12.64 RANGE= 4
J122_123 6.7525 J H5 H6 STAT=Y PRED= 6.64 RANGE= 0.2
J122_126 6.4614 J H5 H7 STAT=Y PRED= 6.64 RANGE= 0.2
J130_131 8.7553 J H10 H12 STAT=Y PRED= 13.12 RANGE= 6
J131_132 6.7759 J H12 H13 STAT=Y PRED= 6.64 RANGE= 0.2
J131_135 6.6949 J H12 H14 STAT=Y PRED= 6.64 RANGE= 0.2
J141_142 11.0683 J H17 H19 STAT=Y PRED= 13.17 RANGE= 4
J142_143 6.4231 J H19 H20 STAT=Y PRED= 6.64 RANGE= 0.2
J142_145 6.6072 J H19 H21 STAT=Y PRED= 6.64 RANGE= 0.2
J149_150 2.2939 J H24 H25 STAT=Y PRED= 1.92 RANGE= 6
J150_151 6.5059 J H25 H27 STAT=Y PRED= 6.25 RANGE= 0.6
J157_158 4.0145 J H31 H32 STAT=Y PRED= 2.33 RANGE= 4
J158_160 6.6081 J H32 H34 STAT=Y PRED= 6.25 RANGE= 0.6
J164_165 8.9166 J H37 H38 STAT=Y PRED= 1.9 RANGE= 6
J165_166 7.2268 J H38 H39 STAT=Y PRED= 6.64 RANGE= 0.2
J165_169 6.842 J H38 H40 STAT=Y PRED= 6.64 RANGE= 0.2
J175_176 6.7714 J H44 H45A STAT=Y PRED= 14.07 RANGE= 4
J175_177 8.5864 J H44 H45B STAT=Y PRED= 2.1 RANGE= 4
J176_177 -13.5731 J H45A H45B STAT=Y PRED= -14.65 RANGE= 1.6
J176_178 0.0005 J H45A H46 STAT=Y PRED= 12.06 RANGE= 2.56
J177_178 6.7331 J H45B H46 STAT=Y PRED= 0.52 RANGE= 2.56
J178_179 6.6152 J H46 H47 STAT=Y PRED= 6.64 RANGE= 0.2

Appendix P (continued)

J178_182 6.5684 J H46 H48 STAT=Y PRED= 6.64 RANGE= 0.2
J186_187 8.9068 J H51 H52 STAT=Y PRED= 12.95 RANGE= 6
J187_188 6.8268 J H52 H53 STAT=Y PRED= 6.64 RANGE= 0.2
J187_191 6.816 J H52 H54 STAT=Y PRED= 6.64 RANGE= 0.2
J197_198 7.5799 J H58 H59 STAT=Y PRED= 13.15 RANGE= 4
J198_199 7.1553 J H59 H60 STAT=Y PRED= 6.64 RANGE= 0.2
J198_202 6.1175 J H59 H61 STAT=Y PRED= 6.64 RANGE= 0.2
J208_209 11.1727 J H65 H66A STAT=Y PRED= 14.45 RANGE= 4
J208_210 4.6701 J H65 H66B STAT=Y PRED= 4.6 RANGE= 5.19
J209_210 -13.7236 J H66A H66B STAT=Y PRED= -16.77 RANGE= 2.56
J211_214 0.8069 J H68 H75 STAT=Y PRED= -0.3 RANGE= 0.5
J213_214 0.5682 J H73 H75 STAT=Y PRED= 1.02 RANGE= 1.2
J219_220 7.8638 J H80 H81 STAT=Y PRED= 2.52 RANGE= 6
J220_221 6.8073 J H81 H82 STAT=Y PRED= 6.64 RANGE= 0.2
J220_224 6.66 J H81 H83 STAT=Y PRED= 6.64 RANGE= 0.2
J228_229 1.5907 J H86 H87 STAT=Y PRED= 1.78 RANGE= 6
J230_234 0.7001 J H89_93 H89_93 STAT=Y PRED= 1.98 RANGE= 1.2
J230_231 7.7218 J H89_93 H90_92 STAT=Y PRED= 7.66 RANGE= 0.34
J230_233 -0.7838 J H90_92 H89_93 STAT=Y PRED= 0.55 RANGE= 0.75
J230_232 1.0008 J H89_93 H91 STAT=Y PRED= 1.26 RANGE= 1.2
J231_233 0.2049 J H90_92 H90_92 STAT=Y PRED= 1.48 RANGE= 1.2
J231_232 7.5034 J H90_92 H91 STAT=Y PRED= 7.4 RANGE= 0.24
J237_238 8.8253 J H97 H99 STAT=Y PRED= 1.96 RANGE= 6
J238_239 6.7253 J H99 H100 STAT=Y PRED= 6.64 RANGE= 0.2
J238_242 6.7906 J H99 H101 STAT=Y PRED= 6.64 RANGE= 0.2

CONTROL PARAMETERS:
Solvent = none (def. 99% enriched)
1 = Concentration "(vol%," def=1.0%)
0.001 = Minimum line-intensity
0.001 = Diagonalization criterium (not in use)
22.5356505 = Left frequency (ppm)
-7.57782696 = Right frequency (ppm)
0 = Acquisition time "(s," for QMTLS)
0.979 = Line-width (for modes "D," P & "T," 0=use defaults)
0.051689764 = Data-point resolution (Hz)
-53.963 = GAUSSIAN "(%," 0=use default from INF)
-4.14 = Dispersion contribution "(%," 0=use default from INF)
0 = Decoupling frequency (for DORES)

CONSTRAINTS (in equations X0 = 1.0)...use no empty lines
EQUAL H89_93 = H90_92
EQUAL H34 = H101
EQUAL H6 = H40
IGNORE(HZ): 4408.628 to 4380.755
IGNORE(HZ): 2148.223 to 2141.235
IGNORE(HZ): 1749.832 to 1734.72
IGNORE(HZ): 863.941 to 850.993

END of FILE

Appendix Q. The pseudo HiFSA profile of nordeoxyecumicin.

* NEW: the lines beginning by * are comment lines !
* To keep all the chemical shifts fixed during iteration
* replace "CHEMICAL SHIFTS(HZ):" by "..SHIFTS(HZ): fixed"
* The couplings can be fixed in the same way

NMR-data: C:\Users\jgnapo_2\Desktop\Wei_H14_XRays\H14_withoutGO
#$œ Date 11. 3.2014; Time 14:51:36 perch.pms

CHEMICAL SHIFTS(PPM):
PROTON 2*SPIN= 1 SPECIES=1H POPULATION(Y)= 1.00000
10Trp_H8/ 1 6.980083 1*1*1 STAT=Y PRED= 7.318 RANGE= 0.199 WIDTH(Y)= 1.482 RESP(Y)= 1.0000 HSQC= C74
01ValH45/ 1 2.382027 1*1*6 STAT=Y PRED= 2.370 RANGE= 0.307 WIDTH(Y)= 2.911 RESP(Y)= 1.0000 HSQC= C1_2
01Val_H2/ 1 2.790095 1*1*1 STAT=Y PRED= 4.169 RANGE= 0.639 WIDTH(Y)= 3.272 RESP(Y)= 1.0000 HSQC= C4
01Val_H3/ 1 2.085970 1*1*1 STAT=Y PRED= 1.952 RANGE= 0.819 WIDTH(Y)= 2.474 RESP(Y)= 1.0000 HSQC= C5
01Val_H6/ 1 0.858112 1*1*3 STAT=Y PRED= 0.509 RANGE= 0.869 WIDTH(Y)= 2.072 RESP(Y)= 1.0000 HSQC= C6
01Val_H7/ 1 0.983837 1*1*3 STAT=Y PRED= 0.818 RANGE= 0.359 WIDTH(Y)= 2.723 RESP(Y)= 1.0000 HSQC= C7
02Val_H2/ 1 4.670478 1*1*1 STAT=Y PRED= 4.508 RANGE= 0.809 WIDTH(Y)= 2.043 RESP(Y)= 1.0000 HSQC= C10
02Val_H3/ 1 2.092087 1*1*1 STAT=Y PRED= 2.155 RANGE= 0.779 WIDTH(Y)= 2.563 RESP(Y)= 1.0000 HSQC= C12
02Val_H4/ 1 0.989331 1*1*3 STAT=Y PRED= 1.038 RANGE= 0.279 WIDTH(Y)= 2.337 RESP(Y)= 1.0000 HSQC= C13
02Val_H5/ 1 1.048558 1*1*3 STAT=Y PRED= 0.943 RANGE= 0.249 WIDTH(Y)= 2.196 RESP(Y)= 1.0000 HSQC= C14
03Ile_H7/ 1 3.248591 1*1*3 STAT=Y PRED= 3.196 RANGE= 0.369 WIDTH(Y)= 1.586 RESP(Y)= 1.0000 HSQC= C15
03Ile_H2/ 1 4.856972 1*1*1 STAT=Y PRED= 4.617 RANGE= 1.628 WIDTH(Y)= 1.651 RESP(Y)= 1.0000 HSQC= C17
03Ile_H3/ 1 1.959403 1*1*1 STAT=Y PRED= 2.032 RANGE= 0.706 WIDTH(Y)= 2.932 RESP(Y)= 1.0000 HSQC= C19
03IleH4A/ 1 0.997587 1*1*1 STAT=Y PRED= 1.465 RANGE= 0.699 WIDTH(Y)= 5.273 RESP(Y)= 1.0000 HSQC= C20
03IleH4B/ 1 1.237746 1*1*1 STAT=Y PRED= 1.175 RANGE= 0.589 WIDTH(Y)= 2.301 RESP(Y)= 1.0000 HSQC= C20
03Ile_H6/ 1 0.799634 1*1*3 STAT=Y PRED= 0.723 RANGE= 0.398 WIDTH(Y)= 3.103 RESP(Y)= 1.0000 HSQC= C21
03Ile_H5/ 1 0.788668 1*1*3 STAT=Y PRED= 0.880 RANGE= 0.219 WIDTH(Y)= 3.443 RESP(Y)= 1.0000 HSQC= C22
04Thr_H2/ 1 5.152384 1*1*1 STAT=Y PRED= 4.668 RANGE= 1.016 WIDTH(Y)= 1.696 RESP(Y)= 1.0000 HSQC= C24
04Thr_H3/ 1 5.791048 1*1*1 STAT=Y PRED= 4.010 RANGE= 0.479 WIDTH(Y)= 2.108 RESP(Y)= 1.0000 HSQC= C25
04Thr_H4/ 1 1.310071 1*1*3 STAT=Y PRED= 1.270 RANGE= 0.499 WIDTH(Y)= 2.697 RESP(Y)= 1.0000 HSQC= C27
05Thr_H5/ 1 3.315986 1*1*3 STAT=Y PRED= 3.257 RANGE= 0.399 WIDTH(Y)= 2.173 RESP(Y)= 1.0000 HSQC= C29
05Thr_H2/ 1 5.016060 1*1*1 STAT=Y PRED= 4.099 RANGE= 1.025 WIDTH(Y)= 1.989 RESP(Y)= 1.0000 HSQC= C31
05Thr_H3/ 1 4.407756 1*1*1 STAT=Y PRED= 4.345 RANGE= 0.719 WIDTH(Y)= 2.103 RESP(Y)= 1.0000 HSQC= C32
05Thr_H4/ 1 0.885540 1*1*3 STAT=Y PRED= 1.252 RANGE= 0.299 WIDTH(Y)= 2.631 RESP(Y)= 1.0000 HSQC= C34
06Val_H2/ 1 4.835997 1*1*1 STAT=Y PRED= 4.525 RANGE= 1.409 WIDTH(Y)= 2.169 RESP(Y)= 1.0000 HSQC= C37
06Val_H3/ 1 2.362962 1*1*1 STAT=Y PRED= 1.975 RANGE= 1.019 WIDTH(Y)= 1.690 RESP(Y)= 1.0000 HSQC= C38
06Val_H4/ 1 1.093811 1*1*3 STAT=Y PRED= 0.938 RANGE= 0.219 WIDTH(Y)= 1.705 RESP(Y)= 1.0000 HSQC= C39
06Val_H5/ 1 0.979053 1*1*3 STAT=Y PRED= 1.094 RANGE= 0.389 WIDTH(Y)= 2.534 RESP(Y)= 1.0000 HSQC= C40
07Leu_H7/ 1 3.264509 1*1*3 STAT=Y PRED= 3.110 RANGE= 0.376 WIDTH(Y)= 2.000 RESP(Y)= 1.0000 HSQC= C42
07Leu_H2/ 1 5.132161 1*1*1 STAT=Y PRED= 5.342 RANGE= 1.085 WIDTH(Y)= 2.356 RESP(Y)= 1.0000 HSQC= C44
07LeuH3A/ 1 1.435249 1*1*1 STAT=Y PRED= 1.444 RANGE= 0.429 WIDTH(Y)= 2.481 RESP(Y)= 1.0000 HSQC= C45
07LeuH3B/ 1 1.277112 1*1*1 STAT=Y PRED= 1.914 RANGE= 0.369 WIDTH(Y)= 2.146 RESP(Y)= 1.0000 HSQC= C45
07Leu_H4/ 1 0.934474 1*1*1 STAT=Y PRED= 1.630 RANGE= 0.627 WIDTH(Y)= 4.066 RESP(Y)= 1.0000 HSQC= C46
07Leu_H5/ 1 0.317861 1*1*3 STAT=Y PRED= 0.972 RANGE= 0.316 WIDTH(Y)= 2.266 RESP(Y)= 1.0000 HSQC= C47
07Leu_H6/ 1 0.193218 1*1*3 STAT=Y PRED= 0.972 RANGE= 0.149 WIDTH(Y)= 2.156 RESP(Y)= 1.0000 HSQC= C48
08Val_H2/ 1 4.581116 1*1*1 STAT=Y PRED= 4.489 RANGE= 0.899 WIDTH(Y)= 2.019 RESP(Y)= 1.0000 HSQC= C51
08Val_H3/ 1 2.044991 1*1*1 STAT=Y PRED= 1.995 RANGE= 0.486 WIDTH(Y)= 2.865 RESP(Y)= 1.0000 HSQC= C52
08Val_H4/ 1 0.914530 1*1*3 STAT=Y PRED= 1.060 RANGE= 0.237 WIDTH(Y)= 2.509 RESP(Y)= 1.0000 HSQC= C53
08Val_H5/ 1 0.867141 1*1*3 STAT=Y PRED= 0.999 RANGE= 0.229 WIDTH(Y)= 2.710 RESP(Y)= 1.0000 HSQC= C54
09Val_H6/ 1 3.145877 1*1*3 STAT=Y PRED= 3.169 RANGE= 0.466 WIDTH(Y)= 1.753 RESP(Y)= 1.0000 HSQC= C56

Appendix Q (continued)

09Val_H2/ 1 3.061973 1*1*1 STAT=Y PRED= 5.153 RANGE= 0.719 WIDTH(Y)= 2.193 RESP(Y)= 1.0000 HSQC= C58
09Val_H3/ 1 2.591202 1*1*1 STAT=Y PRED= 2.524 RANGE= 0.407 WIDTH(Y)= 1.993 RESP(Y)= 1.0000 HSQC= C59
09Val_H4/ 1 1.098319 1*1*3 STAT=Y PRED= 1.319 RANGE= 0.227 WIDTH(Y)= 2.256 RESP(Y)= 1.0000 HSQC= C60
09Val_H5/ 1 0.974702 1*1*3 STAT=Y PRED= 1.075 RANGE= 0.239 WIDTH(Y)= 3.198 RESP(Y)= 1.0000 HSQC= C61
10TrpH13/ 1 2.162239 1*1*3 STAT=Y PRED= 2.936 RANGE= 0.895 WIDTH(Y)= 1.827 RESP(Y)= 1.0000 HSQC= C63
10Trp_H2/ 1 4.095875 1*1*1 STAT=Y PRED= 5.043 RANGE= 1.765 WIDTH(Y)= 1.827 RESP(Y)= 1.0000 HSQC= C65
10TrpH3A/ 1 3.543711 1*1*1 STAT=Y PRED= 3.613 RANGE= 0.469 WIDTH(Y)= 1.849 RESP(Y)= 1.0000 HSQC= C66
10TrpH3B/ 1 3.687611 1*1*1 STAT=Y PRED= 3.367 RANGE= 0.629 WIDTH(Y)= 2.347 RESP(Y)= 1.0000 HSQC= C66
10Trp_H5/ 1 6.695141 1*1*1 STAT=Y PRED= 6.772 RANGE= 0.276 WIDTH(Y)= 1.972 RESP(Y)= 1.0000 HSQC= C68
10Trp_H9/ 1 6.438058 1*1*1 STAT=Y PRED= 7.089 RANGE= 0.219 WIDTH(Y)= 1.603 RESP(Y)= 1.0000 HSQC= C73
10Trp_H7/ 1 6.917695 1*1*1 STAT=Y PRED= 7.333 RANGE= 0.309 WIDTH(Y)= 1.010 RESP(Y)= 1.0000 HSQC= C75
10TrpH12/ 1 3.815845 1*1*3 STAT=Y PRED= 4.072 RANGE= 0.249 WIDTH(Y)= 1.471 RESP(Y)= 1.0000 HSQC= C77
11Val_H2/ 1 4.364417 1*1*1 STAT=Y PRED= 4.303 RANGE= 1.449 WIDTH(Y)= 2.746 RESP(Y)= 1.0000 HSQC= C80
11Val_H3/ 1 2.175687 1*1*1 STAT=Y PRED= 2.094 RANGE= 0.589 WIDTH(Y)= 3.217 RESP(Y)= 1.0000 HSQC= C81
11Val_H4/ 1 1.025555 1*1*3 STAT=Y PRED= 1.094 RANGE= 0.249 WIDTH(Y)= 2.731 RESP(Y)= 1.0000 HSQC= C82
11Val_H5/ 1 0.981855 1*1*3 STAT=Y PRED= 1.080 RANGE= 0.299 WIDTH(Y)= 2.129 RESP(Y)= 1.0000 HSQC= C83
12Phe_H2/ 1 4.807927 1*1*1 STAT=Y PRED= 4.499 RANGE= 0.989 WIDTH(Y)= 3.024 RESP(Y)= 1.0000 HSQC= C86
12Phe_H3/ 1 5.343847 1*1*1 STAT=Y PRED= 5.208 RANGE= 0.489 WIDTH(Y)= 1.884 RESP(Y)= 1.0000 HSQC= C87
12Phe_H5/ 1 7.077278 1*2*1 STAT=Y PRED= 7.524 RANGE= 0.309 WIDTH(Y)= 1.739 RESP(Y)= 1.0000 HSQC= C89_93
12Phe_H6/ 1 7.201157 1*2*1 STAT=Y PRED= 7.372 RANGE= 0.579 WIDTH(Y)= 1.252 RESP(Y)= 1.0000 HSQC= C90_92
12Phe_H7/ 1 7.149803 1*1*1 STAT=Y PRED= 7.281 RANGE= 0.309 WIDTH(Y)= 1.566 RESP(Y)= 1.0000 HSQC= C91
13Val_H2/ 1 4.406030 1*1*1 STAT=Y PRED= 4.169 RANGE= 0.669 WIDTH(Y)= 2.705 RESP(Y)= 1.0000 HSQC= C97
13Val_H3/ 1 1.959947 1*1*1 STAT=Y PRED= 1.935 RANGE= 0.869 WIDTH(Y)= 2.194 RESP(Y)= 1.0000 HSQC= C99
13Val_H4/ 1 0.922552 1*1*3 STAT=Y PRED= 1.277 RANGE= 0.219 WIDTH(Y)= 2.328 RESP(Y)= 1.0000 HSQC= C100
13Val_H5/ 1 0.938313 1*1*3 STAT=Y PRED= 0.933 RANGE= 0.278 WIDTH(Y)= 2.894 RESP(Y)= 1.0000 HSQC= C101

COUPLING CONSTANTS(HZ): fixed
J115_217 7.7969 J 10Trp_H8 10Trp_H9 STAT=Y PRED= 8.100 RANGE= 0.890
J115_218 8.1808 J 10Trp_H8 10Trp_H7 STAT=Y PRED= 7.850 RANGE= 0.800
J122_123 9.1737 J 01Val_H2 01Val_H3 STAT=Y PRED= 12.510 RANGE= 4.000
J123_124 6.5890 J 01Val_H3 01Val_H6 STAT=Y PRED= 6.640 RANGE= 0.200
J123_127 6.6205 J 01Val_H3 01Val_H7 STAT=Y PRED= 6.640 RANGE= 0.200
J131_132 8.7545 J 02Val_H2 02Val_H3 STAT=Y PRED= 12.600 RANGE= 6.000
J132_133 6.7841 J 02Val_H3 02Val_H4 STAT=Y PRED= 6.640 RANGE= 0.200
J132_136 6.7206 J 02Val_H3 02Val_H5 STAT=Y PRED= 6.640 RANGE= 0.200
J142_143 11.2297 J 03Ile_H2 03Ile_H3 STAT=Y PRED= 13.150 RANGE= 4.000
J143_144 0.4614 J 03Ile_H3 03IleH4A STAT=Y PRED= 1.950 RANGE= 3.000
J143_145 2.9276 J 03Ile_H3 03IleH4B STAT=Y PRED= 12.660 RANGE= 2.800
J143_146 6.6276 J 03Ile_H3 03Ile_H6 STAT=Y PRED= 6.640 RANGE= 0.200
J144_145 -12.2168 J 03IleH4A 03IleH4B STAT=Y PRED= -13.400 RANGE= 0.600
J144_149 7.2855 J 03IleH4A 03Ile_H5 STAT=Y PRED= 7.440 RANGE= 0.150
J145_149 7.6340 J 03IleH4B 03Ile_H5 STAT=Y PRED= 7.440 RANGE= 0.150
J153_154 2.3441 J 04Thr_H2 04Thr_H3 STAT=Y PRED= 2.690 RANGE= 6.600
J154_155 6.5134 J 04Thr_H3 04Thr_H4 STAT=Y PRED= 6.250 RANGE= 0.600
J161_162 3.7259 J 05Thr_H2 05Thr_H3 STAT=Y PRED= 2.440 RANGE= 4.400
J162_164 6.4691 J 05Thr_H3 05Thr_H4 STAT=Y PRED= 6.250 RANGE= 0.600
J168_169 8.9180 J 06Val_H2 06Val_H3 STAT=Y PRED= 2.980 RANGE= 6.600
J169_170 6.6944 J 06Val_H3 06Val_H4 STAT=Y PRED= 6.640 RANGE= 0.200
J169_173 7.0316 J 06Val_H3 06Val_H5 STAT=Y PRED= 6.640 RANGE= 0.200
J179_180 6.2437 J 07Leu_H2 07LeuH3A STAT=Y PRED= 3.040 RANGE= 6.000

Appendix Q (continued)

```
 J179_181    8.3839   J 07Leu_H2 07LeuH3B   STAT=Y  PRED= 13.950 RANGE= 4.000
 J180_181  -13.3047   J 07LeuH3A 07LeuH3B   STAT=Y  PRED= -14.710 RANGE= 1.600
 J180_182    8.2119   J 07LeuH3A 07Leu_H4   STAT=Y  PRED= 12.990 RANGE= 2.560
 J181_182    5.7896   J 07LeuH3B 07Leu_H4   STAT=Y  PRED= 2.270 RANGE= 3.000
 J182_183    6.5482   J 07Leu_H4 07Leu_H5   STAT=Y  PRED= 6.640 RANGE= 0.200
 J182_186    6.5879   J 07Leu_H4 07Leu_H6   STAT=Y  PRED= 6.640 RANGE= 0.200
 J190_191    8.8736   J 08Val_H2 08Val_H3   STAT=Y  PRED= 12.880 RANGE= 6.000
 J191_192    6.5520   J 08Val_H3 08Val_H4   STAT=Y  PRED= 6.640 RANGE= 0.200
 J191_195    6.7834   J 08Val_H3 08Val_H5   STAT=Y  PRED= 6.640 RANGE= 0.200
 J201_202    7.6281   J 09Val_H2 09Val_H3   STAT=Y  PRED= 12.960 RANGE= 4.000
 J202_203    6.4961   J 09Val_H3 09Val_H4   STAT=Y  PRED= 6.640 RANGE= 0.200
 J202_206    6.7760   J 09Val_H3 09Val_H5   STAT=Y  PRED= 6.640 RANGE= 0.200
 J212_213   11.1630   J 10Trp_H2 10TrpH3A   STAT=Y  PRED= 12.890 RANGE= 4.000
 J212_214    4.7143   J 10Trp_H2 10TrpH3B   STAT=Y  PRED= 1.900 RANGE= 4.400
 J213_214  -13.7295   J 10TrpH3A 10TrpH3B   STAT=Y  PRED= -16.760 RANGE= 2.560
 J215_218    0.4880   J 10Trp_H5 10Trp_H7   STAT=Y  PRED= -0.300 RANGE= 0.500
 J217_218    0.6708   J 10Trp_H9 10Trp_H7   STAT=Y  PRED= 1.020 RANGE= 1.200
 J223_224    7.9094   J 11Val_H2 11Val_H3   STAT=Y  PRED= 3.450 RANGE= 9.000
 J224_225    6.7483   J 11Val_H3 11Val_H4   STAT=Y  PRED= 6.640 RANGE= 0.200
 J224_228    6.8064   J 11Val_H3 11Val_H5   STAT=Y  PRED= 6.640 RANGE= 0.200
 J232_233    1.9005   J 12Phe_H2 12Phe_H3   STAT=Y  PRED= 1.900 RANGE= 6.600
 J234_238    1.3335   J 12Phe_H5 12Phe_H5   STAT=Y  PRED= 1.980 RANGE= 1.200
 J234_235    7.6508   J 12Phe_H5 12Phe_H6   STAT=Y  PRED= 7.660 RANGE= 0.340
 J234_237    0.7769   J 12Phe_H6 12Phe_H5   STAT=Y  PRED= 0.550 RANGE= 0.750
 J234_236    1.2760   J 12Phe_H5 12Phe_H7   STAT=Y  PRED= 1.260 RANGE= 1.200
 J235_237    1.7027   J 12Phe_H6 12Phe_H6   STAT=Y  PRED= 1.480 RANGE= 1.200
 J235_236    7.4760   J 12Phe_H6 12Phe_H7   STAT=Y  PRED= 7.400 RANGE= 0.240
 J241_242    8.8924   J 13Val_H2 13Val_H3   STAT=Y  PRED= 12.320 RANGE= 6.000
 J242_243    6.8372   J 13Val_H3 13Val_H4   STAT=Y  PRED= 6.640 RANGE= 0.200
 J242_246    6.4162   J 13Val_H3 13Val_H5   STAT=Y  PRED= 6.640 RANGE= 0.200

CONTROL PARAMETERS:
      Solvent =  none (def. 99% enriched)
        1.000 =  Concentration (vol%, def=1.0%)
   0.00100000 =  Minimum line-intensity
   0.00100000 =  Diagonalization criterium (not in use)
 899.93597400 =  FIELD(1H,MHz), used to transform shifts to ppms
  11.63298469 =  Left frequency (ppm)
  -4.33373631 =  Right frequency (ppm)
        0.000 =  Acquisition time (s, for QMTLS)
        0.831 =  Line-width (for modes D, P & T, 0=use defaults)
  0.051689764 =  Data-point resolution (Hz)
      -14.840 =  GAUSSIAN (%, 0=use default from INF)
       -4.829 =  Dispersion contribution (%, 0=use default from INF)
   0.00000000 =  Decoupling frequency (for DORES)

CONSTRAINTS (in equations X0 = 1.0)...use no empty lines
 EQUAL 01Val_H2 = 13Val_H2
 EQUAL 06Val_H5 = 11Val_H4
 EQUAL 07Leu_H5 = 07Leu_H6
```

Appendix Q (continued)

IGNORE(HZ): 2062.779 to 2027.293
IGNORE(HZ): 5188.061 to 5161.182
IGNORE(HZ): 4803.141 to 4787.420
IGNORE(HZ): 4827.557 to 4786.824
IGNORE(HZ): 4420.654 to 4385.691
IGNORE(HZ): 2983.196 to 2962.773
IGNORE(HZ): 1746.134 to 1739.063
IGNORE(HZ): 3055.453 to 2997.906
IGNORE(HZ): 2582.749 to 2525.202
IGNORE(HZ): 8440.896 to 6880.013
IGNORE(HZ): 1170.100 to 1157.055
IGNORE(HZ): 2140.689 to 2134.734

END of FILE

Appendix R. The HiFSA profile of common amino acids between nordeoxyecumicin and ecumicin.

* NEW: the lines beginning by * are comment lines !
* To keep all the chemical shifts fixed during iteration
* replace "CHEMICAL SHIFTS(HZ):" by "..SHIFTS(HZ): fixed"
* The couplings can be fixed in the same way

NMR-data: C:\Users\jgnapo_2\Desktop\Wei_H14_XRays\H14_withoutGO
#$œ Date 11. 3.2014; Time 14:51:36 perch.pms

CHEMICAL SHIFTS(PPM):
PROTON 2*SPIN= 1 SPECIES=1H POPULATION(Y)= 1.00000
10Trp_H8/ 1 6.980083 1*1*1 STAT=Y PRED= 7.318 RANGE= 0.199 WIDTH(Y)= 1.482 RESP(Y)= 1.0000 HSQC= C74
01ValH45/ 1 2.382027 1*1*6 STAT=Y PRED= 2.370 RANGE= 0.307 WIDTH(Y)= 2.911 RESP(Y)= 1.0000 HSQC= C1_2
01Val_H2/ 1 2.790095 1*1*1 STAT=Y PRED= 4.169 RANGE= 0.639 WIDTH(Y)= 3.272 RESP(Y)= 1.0000 HSQC= C4
01Val_H3/ 1 2.085970 1*1*1 STAT=Y PRED= 1.952 RANGE= 0.819 WIDTH(Y)= 2.474 RESP(Y)= 1.0000 HSQC= C5
01Val_H6/ 1 0.858112 1*1*3 STAT=Y PRED= 0.509 RANGE= 0.869 WIDTH(Y)= 2.072 RESP(Y)= 1.0000 HSQC= C6
01Val_H7/ 1 0.983837 1*1*3 STAT=Y PRED= 0.818 RANGE= 0.359 WIDTH(Y)= 2.723 RESP(Y)= 1.0000 HSQC= C7
02Val_H2/ 1 4.670478 1*1*1 STAT=Y PRED= 4.508 RANGE= 0.809 WIDTH(Y)= 2.043 RESP(Y)= 1.0000 HSQC= C10
02Val_H3/ 1 2.092087 1*1*1 STAT=Y PRED= 2.155 RANGE= 0.779 WIDTH(Y)= 2.563 RESP(Y)= 1.0000 HSQC= C12
02Val_H4/ 1 0.989331 1*1*3 STAT=Y PRED= 1.038 RANGE= 0.279 WIDTH(Y)= 2.337 RESP(Y)= 1.0000 HSQC= C13
02Val_H5/ 1 1.048558 1*1*3 STAT=Y PRED= 0.943 RANGE= 0.249 WIDTH(Y)= 2.196 RESP(Y)= 1.0000 HSQC= C14
03Ile_H7/ 1 3.248591 1*1*3 STAT=Y PRED= 3.196 RANGE= 0.369 WIDTH(Y)= 1.586 RESP(Y)= 1.0000 HSQC= C15
03Ile_H2/ 1 4.856972 1*1*1 STAT=Y PRED= 4.617 RANGE= 1.628 WIDTH(Y)= 1.651 RESP(Y)= 1.0000 HSQC= C17
03Ile_H3/ 1 1.959403 1*1*1 STAT=Y PRED= 2.032 RANGE= 0.706 WIDTH(Y)= 2.932 RESP(Y)= 1.0000 HSQC= C19
03IleH4A/ 1 0.997587 1*1*1 STAT=Y PRED= 1.465 RANGE= 0.699 WIDTH(Y)= 5.273 RESP(Y)= 1.0000 HSQC= C20
03IleH4B/ 1 1.237746 1*1*1 STAT=Y PRED= 1.175 RANGE= 0.589 WIDTH(Y)= 2.301 RESP(Y)= 1.0000 HSQC= C20
03Ile_H6/ 1 0.799634 1*1*3 STAT=Y PRED= 0.723 RANGE= 0.398 WIDTH(Y)= 3.103 RESP(Y)= 1.0000 HSQC= C21
03Ile_H5/ 1 0.788668 1*1*3 STAT=Y PRED= 0.880 RANGE= 0.219 WIDTH(Y)= 3.443 RESP(Y)= 1.0000 HSQC= C22
04Thr_H2/ 1 5.152384 1*1*1 STAT=Y PRED= 4.668 RANGE= 1.016 WIDTH(Y)= 1.696 RESP(Y)= 1.0000 HSQC= C24
04Thr_H3/ 1 5.791048 1*1*1 STAT=Y PRED= 4.010 RANGE= 0.479 WIDTH(Y)= 2.108 RESP(Y)= 1.0000 HSQC= C25
04Thr_H4/ 1 1.310071 1*1*3 STAT=Y PRED= 1.270 RANGE= 0.499 WIDTH(Y)= 2.697 RESP(Y)= 1.0000 HSQC= C27
05Thr_H5/ 1 3.315986 1*1*3 STAT=Y PRED= 3.257 RANGE= 0.399 WIDTH(Y)= 2.173 RESP(Y)= 1.0000 HSQC= C29
05Thr_H2/ 1 5.016060 1*1*1 STAT=Y PRED= 4.099 RANGE= 1.025 WIDTH(Y)= 1.989 RESP(Y)= 1.0000 HSQC= C31
05Thr_H3/ 1 4.407756 1*1*1 STAT=Y PRED= 4.345 RANGE= 0.719 WIDTH(Y)= 2.103 RESP(Y)= 1.0000 HSQC= C32
05Thr_H4/ 1 0.885540 1*1*3 STAT=Y PRED= 1.252 RANGE= 0.299 WIDTH(Y)= 2.631 RESP(Y)= 1.0000 HSQC= C34
06Val_H2/ 1 4.835997 1*1*1 STAT=Y PRED= 4.525 RANGE= 1.409 WIDTH(Y)= 2.169 RESP(Y)= 1.0000 HSQC= C37
06Val_H3/ 1 2.362962 1*1*1 STAT=Y PRED= 1.975 RANGE= 1.019 WIDTH(Y)= 1.690 RESP(Y)= 1.0000 HSQC= C38
06Val_H4/ 1 1.093811 1*1*3 STAT=Y PRED= 0.938 RANGE= 0.219 WIDTH(Y)= 1.705 RESP(Y)= 1.0000 HSQC= C39
06Val_H5/ 1 0.979053 1*1*3 STAT=Y PRED= 1.094 RANGE= 0.389 WIDTH(Y)= 2.534 RESP(Y)= 1.0000 HSQC= C40
07Leu_H7/ 1 3.264509 1*1*3 STAT=Y PRED= 3.110 RANGE= 0.376 WIDTH(Y)= 2.000 RESP(Y)= 1.0000 HSQC= C42
07Leu_H2/ 1 5.132161 1*1*1 STAT=Y PRED= 5.342 RANGE= 1.085 WIDTH(Y)= 2.356 RESP(Y)= 1.0000 HSQC= C44
07LeuH3A/ 1 1.435249 1*1*1 STAT=Y PRED= 1.444 RANGE= 0.429 WIDTH(Y)= 2.481 RESP(Y)= 1.0000 HSQC= C45
07LeuH3B/ 1 1.277112 1*1*1 STAT=Y PRED= 1.914 RANGE= 0.369 WIDTH(Y)= 2.146 RESP(Y)= 1.0000 HSQC= C45
07Leu_H4/ 1 0.934474 1*1*1 STAT=Y PRED= 1.630 RANGE= 0.627 WIDTH(Y)= 4.066 RESP(Y)= 1.0000 HSQC= C46
07Leu_H5/ 1 0.317861 1*1*3 STAT=Y PRED= 0.972 RANGE= 0.316 WIDTH(Y)= 2.266 RESP(Y)= 1.0000 HSQC= C47
07Leu_H6/ 1 0.193218 1*1*3 STAT=Y PRED= 0.972 RANGE= 0.149 WIDTH(Y)= 2.156 RESP(Y)= 1.0000 HSQC= C48
08Val_H2/ 1 4.581116 1*1*1 STAT=Y PRED= 4.489 RANGE= 0.899 WIDTH(Y)= 2.019 RESP(Y)= 1.0000 HSQC= C51
08Val_H3/ 1 2.044991 1*1*1 STAT=Y PRED= 1.995 RANGE= 0.486 WIDTH(Y)= 2.865 RESP(Y)= 1.0000 HSQC= C52
08Val_H4/ 1 0.914530 1*1*3 STAT=Y PRED= 1.060 RANGE= 0.237 WIDTH(Y)= 2.509 RESP(Y)= 1.0000 HSQC= C53
08Val_H5/ 1 0.867141 1*1*3 STAT=Y PRED= 0.999 RANGE= 0.229 WIDTH(Y)= 2.710 RESP(Y)= 1.0000 HSQC= C54

Appendix R (continued)

09Val_H6/ 1 3.145877 1*1*3 STAT=Y PRED= 3.169 RANGE= 0.466 WIDTH(Y)= 1.753 RESP(Y)= 1.0000 HSQC= C56
09Val_H2/ 1 3.061973 1*1*1 STAT=Y PRED= 5.153 RANGE= 0.719 WIDTH(Y)= 2.193 RESP(Y)= 1.0000 HSQC= C58
09Val_H3/ 1 2.591202 1*1*1 STAT=Y PRED= 2.524 RANGE= 0.407 WIDTH(Y)= 1.993 RESP(Y)= 1.0000 HSQC= C59
09Val_H4/ 1 1.098319 1*1*3 STAT=Y PRED= 1.319 RANGE= 0.227 WIDTH(Y)= 2.256 RESP(Y)= 1.0000 HSQC= C60
09Val_H5/ 1 0.974702 1*1*3 STAT=Y PRED= 1.075 RANGE= 0.239 WIDTH(Y)= 3.198 RESP(Y)= 1.0000 HSQC= C61
10TrpH13/ 1 2.162239 1*1*3 STAT=Y PRED= 2.936 RANGE= 0.895 WIDTH(Y)= 1.827 RESP(Y)= 1.0000 HSQC= C63
10Trp_H2/ 1 4.095875 1*1*1 STAT=Y PRED= 5.043 RANGE= 1.765 WIDTH(Y)= 1.827 RESP(Y)= 1.0000 HSQC= C65
10TrpH3A/ 1 3.543711 1*1*1 STAT=Y PRED= 3.613 RANGE= 0.469 WIDTH(Y)= 1.849 RESP(Y)= 1.0000 HSQC= C66
10TrpH3B/ 1 3.687611 1*1*1 STAT=Y PRED= 3.367 RANGE= 0.629 WIDTH(Y)= 2.347 RESP(Y)= 1.0000 HSQC= C66
10Trp_H5/ 1 6.695141 1*1*1 STAT=Y PRED= 6.772 RANGE= 0.276 WIDTH(Y)= 1.972 RESP(Y)= 1.0000 HSQC= C68
10Trp_H9/ 1 6.438058 1*1*1 STAT=Y PRED= 7.089 RANGE= 0.219 WIDTH(Y)= 1.603 RESP(Y)= 1.0000 HSQC= C73
10Trp_H7/ 1 6.917695 1*1*1 STAT=Y PRED= 7.333 RANGE= 0.309 WIDTH(Y)= 1.010 RESP(Y)= 1.0000 HSQC= C75
10TrpH12/ 1 3.815845 1*1*3 STAT=Y PRED= 4.072 RANGE= 0.249 WIDTH(Y)= 1.471 RESP(Y)= 1.0000 HSQC= C77
11Val_H2/ 1 4.364417 1*1*1 STAT=Y PRED= 4.303 RANGE= 1.449 WIDTH(Y)= 2.746 RESP(Y)= 1.0000 HSQC= C80
11Val_H3/ 1 2.175687 1*1*1 STAT=Y PRED= 2.094 RANGE= 0.589 WIDTH(Y)= 3.217 RESP(Y)= 1.0000 HSQC= C81
11Val_H4/ 1 1.025555 1*1*3 STAT=Y PRED= 1.094 RANGE= 0.249 WIDTH(Y)= 2.731 RESP(Y)= 1.0000 HSQC= C82
11Val_H5/ 1 0.981855 1*1*3 STAT=Y PRED= 1.080 RANGE= 0.299 WIDTH(Y)= 2.129 RESP(Y)= 1.0000 HSQC= C83
13Val_H2/ 1 4.406030 1*1*1 STAT=Y PRED= 4.169 RANGE= 0.669 WIDTH(Y)= 2.705 RESP(Y)= 1.0000 HSQC= C97
13Val_H3/ 1 1.959947 1*1*1 STAT=Y PRED= 1.935 RANGE= 0.869 WIDTH(Y)= 2.194 RESP(Y)= 1.0000 HSQC= C99
13Val_H4/ 1 0.922552 1*1*3 STAT=Y PRED= 1.277 RANGE= 0.219 WIDTH(Y)= 2.328 RESP(Y)= 1.0000 HSQC= C100
13Val_H5/ 1 0.938313 1*1*3 STAT=Y PRED= 0.933 RANGE= 0.278 WIDTH(Y)= 2.894 RESP(Y)= 1.0000 HSQC= C101

COUPLING CONSTANTS(HZ): fixed

J115_217 7.7969 J 10Trp_H8 10Trp_H9 STAT=Y PRED= 8.100 RANGE= 0.890
J115_218 8.1808 J 10Trp_H8 10Trp_H7 STAT=Y PRED= 7.850 RANGE= 0.800
J122_123 9.1737 J 01Val_H2 01Val_H3 STAT=Y PRED= 12.510 RANGE= 4.000
J123_124 6.5890 J 01Val_H3 01Val_H6 STAT=Y PRED= 6.640 RANGE= 0.200
J123_127 6.6205 J 01Val_H3 01Val_H7 STAT=Y PRED= 6.640 RANGE= 0.200
J131_132 8.7545 J 02Val_H2 02Val_H3 STAT=Y PRED= 12.600 RANGE= 6.000
J132_133 6.7841 J 02Val_H3 02Val_H4 STAT=Y PRED= 6.640 RANGE= 0.200
J132_136 6.7206 J 02Val_H3 02Val_H5 STAT=Y PRED= 6.640 RANGE= 0.200
J142_143 11.2297 J 03Ile_H2 03Ile_H3 STAT=Y PRED= 13.150 RANGE= 4.000
J143_144 0.4614 J 03Ile_H3 03IleH4A STAT=Y PRED= 1.950 RANGE= 3.000
J143_145 2.9276 J 03Ile_H3 03IleH4B STAT=Y PRED= 12.660 RANGE= 2.800
J143_146 6.6276 J 03Ile_H3 03Ile_H6 STAT=Y PRED= 6.640 RANGE= 0.200
J144_145 -12.2168 J 03IleH4A 03IleH4B STAT=Y PRED= -13.400 RANGE= 0.600
J144_149 7.2855 J 03IleH4A 03Ile_H5 STAT=Y PRED= 7.440 RANGE= 0.150
J145_149 7.6340 J 03IleH4B 03Ile_H5 STAT=Y PRED= 7.440 RANGE= 0.150
J153_154 2.3441 J 04Thr_H2 04Thr_H3 STAT=Y PRED= 2.690 RANGE= 6.600
J154_155 6.5134 J 04Thr_H3 04Thr_H4 STAT=Y PRED= 6.250 RANGE= 0.600
J161_162 3.7259 J 05Thr_H2 05Thr_H3 STAT=Y PRED= 2.440 RANGE= 4.400
J162_164 6.4691 J 05Thr_H3 05Thr_H4 STAT=Y PRED= 6.250 RANGE= 0.600
J168_169 8.9180 J 06Val_H2 06Val_H3 STAT=Y PRED= 2.980 RANGE= 6.600
J169_170 6.6944 J 06Val_H3 06Val_H4 STAT=Y PRED= 6.640 RANGE= 0.200
J169_173 7.0316 J 06Val_H3 06Val_H5 STAT=Y PRED= 6.640 RANGE= 0.200
J179_180 6.2437 J 07Leu_H2 07LeuH3A STAT=Y PRED= 3.040 RANGE= 6.000
J179_181 8.3839 J 07Leu_H2 07LeuH3B STAT=Y PRED= 13.950 RANGE= 4.000
J180_181 -13.3047 J 07LeuH3A 07LeuH3B STAT=Y PRED= -14.710 RANGE= 1.600
J180_182 8.2119 J 07LeuH3A 07Leu_H4 STAT=Y PRED= 12.990 RANGE= 2.560
J181_182 5.7896 J 07LeuH3B 07Leu_H4 STAT=Y PRED= 2.270 RANGE= 3.000

Appendix R (continued)

```
 J182_183    6.5482   J 07Leu_H4 07Leu_H5   STAT=Y  PRED= 6.640 RANGE= 0.200
 J182_186    6.5879   J 07Leu_H4 07Leu_H6   STAT=Y  PRED= 6.640 RANGE= 0.200
 J190_191    8.8736   J 08Val_H2 08Val_H3   STAT=Y  PRED= 12.880 RANGE= 6.000
 J191_192    6.5520   J 08Val_H3 08Val_H4   STAT=Y  PRED= 6.640 RANGE= 0.200
 J191_195    6.7834   J 08Val_H3 08Val_H5   STAT=Y  PRED= 6.640 RANGE= 0.200
 J201_202    7.6281   J 09Val_H2 09Val_H3   STAT=Y  PRED= 12.960 RANGE= 4.000
 J202_203    6.4961   J 09Val_H3 09Val_H4   STAT=Y  PRED= 6.640 RANGE= 0.200
 J202_206    6.7760   J 09Val_H3 09Val_H5   STAT=Y  PRED= 6.640 RANGE= 0.200
 J212_213   11.1630   J 10Trp_H2 10TrpH3A   STAT=Y  PRED= 12.890 RANGE= 4.000
 J212_214    4.7143   J 10Trp_H2 10TrpH3B   STAT=Y  PRED= 1.900 RANGE= 4.400
 J213_214  -13.7295   J 10TrpH3A 10TrpH3B   STAT=Y  PRED= -16.760 RANGE= 2.560
 J215_218    0.4880   J 10Trp_H5 10Trp_H7   STAT=Y  PRED= -0.300 RANGE= 0.500
 J217_218    0.6708   J 10Trp_H9 10Trp_H7   STAT=Y  PRED= 1.020 RANGE= 1.200
 J223_224    7.9094   J 11Val_H2 11Val_H3   STAT=Y  PRED= 3.450 RANGE= 9.000
 J224_225    6.7483   J 11Val_H3 11Val_H4   STAT=Y  PRED= 6.640 RANGE= 0.200
 J224_228    6.8064   J 11Val_H3 11Val_H5   STAT=Y  PRED= 6.640 RANGE= 0.200
 J241_242    8.8924   J 13Val_H2 13Val_H3   STAT=Y  PRED= 12.320 RANGE= 6.000
 J242_243    6.8372   J 13Val_H3 13Val_H4   STAT=Y  PRED= 6.640 RANGE= 0.200
 J242_246    6.4162   J 13Val_H3 13Val_H5   STAT=Y  PRED= 6.640 RANGE= 0.200

CONTROL PARAMETERS:
      Solvent =  none (def. 99% enriched)
        1.000 =  Concentration (vol%, def=1.0%)
   0.00100000 =  Minimum line-intensity
   0.00100000 =  Diagonalization criterium (not in use)
 899.93597400 =  FIELD(1H,MHz), used to transform shifts to ppms
  11.63298469 =  Left frequency (ppm)
  -4.33373631 =  Right frequency (ppm)
        0.000 =  Acquisition time (s, for QMTLS)
        0.831 =  Line-width (for modes D, P & T, 0=use defaults)
  0.051689764 =  Data-point resolution (Hz)
      -14.840 =  GAUSSIAN (%, 0=use default from INF)
       -4.829 =  Dispersion contribution (%, 0=use default from INF)
   0.00000000 =  Decoupling frequency (for DORES)

CONSTRAINTS (in equations X0 = 1.0)...use no empty lines
 EQUAL 01Val_H2 = 13Val_H2
 EQUAL 06Val_H5 = 11Val_H4
 EQUAL 07Leu_H5 = 07Leu_H6
 IGNORE(HZ):  2062.779 to  2027.293
 IGNORE(HZ):  5188.061 to  5161.182
 IGNORE(HZ):  4803.141 to  4787.420
 IGNORE(HZ):  4827.557 to  4786.824
 IGNORE(HZ):  4420.654 to  4385.691
 IGNORE(HZ):  2983.196 to  2962.773
 IGNORE(HZ):  1746.134 to  1739.063
 IGNORE(HZ):  3055.453 to  2997.906
 IGNORE(HZ):  2582.749 to  2525.202
 IGNORE(HZ):  8440.896 to  6880.013
 IGNORE(HZ):  1170.100 to  1157.055
```

Appendix R (continued)

IGNORE(HZ): 2140.689 to 2134.734
END of FILE

Appendix S. The third HiFSA profile for the structure elucidation of nordeoxyecumicin.

* NEW: the lines beginning by * are comment lines !
* To keep all the chemical shifts fixed during iteration
* replace "CHEMICAL SHIFTS(HZ):" by "..SHIFTS(HZ): fixed"
* The couplings can be fixed in the same way

NMR-data: C:\Users\jgnapo_2\Desktop\Wei_H14_XRays\H14_withoutGO
#$œ Date 11. 3.2014; Time 14:51:36 perch.pms

CHEMICAL SHIFTS(PPM):
PROTON 2*SPIN= 1 SPECIES=1H POPULATION(Y)= 1.00000

10Trp_H8/ 1 6.980083 1*1*1 STAT=Y PRED= 7.318 RANGE= 0.199 WIDTH(Y)= 1.482 RESP(Y)= 1.0000 HSQC= C74
01ValH45/ 1 2.382027 1*1*6 STAT=Y PRED= 2.370 RANGE= 0.307 WIDTH(Y)= 2.911 RESP(Y)= 1.0000 HSQC= C1_2
01Val_H2/ 1 2.790095 1*1*1 STAT=Y PRED= 4.169 RANGE= 0.639 WIDTH(Y)= 3.272 RESP(Y)= 1.0000 HSQC= C4
01Val_H3/ 1 2.085970 1*1*1 STAT=Y PRED= 1.952 RANGE= 0.819 WIDTH(Y)= 2.474 RESP(Y)= 1.0000 HSQC= C5
01Val_H6/ 1 0.858112 1*1*3 STAT=Y PRED= 0.509 RANGE= 0.869 WIDTH(Y)= 2.072 RESP(Y)= 1.0000 HSQC= C6
01Val_H7/ 1 0.983837 1*1*3 STAT=Y PRED= 0.818 RANGE= 0.359 WIDTH(Y)= 2.723 RESP(Y)= 1.0000 HSQC= C7
02Val_H2/ 1 4.670478 1*1*1 STAT=Y PRED= 4.508 RANGE= 0.809 WIDTH(Y)= 2.043 RESP(Y)= 1.0000 HSQC= C10
02Val_H3/ 1 2.092087 1*1*1 STAT=Y PRED= 2.155 RANGE= 0.779 WIDTH(Y)= 2.563 RESP(Y)= 1.0000 HSQC= C12
02Val_H4/ 1 0.989331 1*1*3 STAT=Y PRED= 1.038 RANGE= 0.279 WIDTH(Y)= 2.337 RESP(Y)= 1.0000 HSQC= C13
02Val_H5/ 1 1.048558 1*1*3 STAT=Y PRED= 0.943 RANGE= 0.249 WIDTH(Y)= 2.196 RESP(Y)= 1.0000 HSQC= C14
04Thr_H2/ 1 5.152384 1*1*1 STAT=Y PRED= 4.668 RANGE= 1.016 WIDTH(Y)= 1.696 RESP(Y)= 1.0000 HSQC= C24
04Thr_H3/ 1 5.791048 1*1*1 STAT=Y PRED= 4.010 RANGE= 0.479 WIDTH(Y)= 2.108 RESP(Y)= 1.0000 HSQC= C25
04Thr_H4/ 1 1.310071 1*1*3 STAT=Y PRED= 1.270 RANGE= 0.499 WIDTH(Y)= 2.697 RESP(Y)= 1.0000 HSQC= C27
05Thr_H5/ 1 3.315986 1*1*3 STAT=Y PRED= 3.257 RANGE= 0.399 WIDTH(Y)= 2.173 RESP(Y)= 1.0000 HSQC= C29
05Thr_H2/ 1 5.016060 1*1*1 STAT=Y PRED= 4.099 RANGE= 1.025 WIDTH(Y)= 1.989 RESP(Y)= 1.0000 HSQC= C31
05Thr_H3/ 1 4.407756 1*1*1 STAT=Y PRED= 4.345 RANGE= 0.719 WIDTH(Y)= 2.103 RESP(Y)= 1.0000 HSQC= C32
05Thr_H4/ 1 0.885540 1*1*3 STAT=Y PRED= 1.252 RANGE= 0.299 WIDTH(Y)= 2.631 RESP(Y)= 1.0000 HSQC= C34
06Val_H2/ 1 4.835997 1*1*1 STAT=Y PRED= 4.525 RANGE= 1.409 WIDTH(Y)= 2.169 RESP(Y)= 1.0000 HSQC= C37
06Val_H3/ 1 2.362962 1*1*1 STAT=Y PRED= 1.975 RANGE= 1.019 WIDTH(Y)= 1.690 RESP(Y)= 1.0000 HSQC= C38
06Val_H4/ 1 1.093811 1*1*3 STAT=Y PRED= 0.938 RANGE= 0.219 WIDTH(Y)= 1.705 RESP(Y)= 1.0000 HSQC= C39
06Val_H5/ 1 0.979053 1*1*3 STAT=Y PRED= 1.094 RANGE= 0.389 WIDTH(Y)= 2.534 RESP(Y)= 1.0000 HSQC= C40
07Leu_H7/ 1 3.264509 1*1*3 STAT=Y PRED= 3.110 RANGE= 0.376 WIDTH(Y)= 2.000 RESP(Y)= 1.0000 HSQC= C42
07Leu_H2/ 1 5.132161 1*1*1 STAT=Y PRED= 5.342 RANGE= 1.085 WIDTH(Y)= 2.356 RESP(Y)= 1.0000 HSQC= C44
07LeuH3A/ 1 1.435249 1*1*1 STAT=Y PRED= 1.444 RANGE= 0.429 WIDTH(Y)= 2.481 RESP(Y)= 1.0000 HSQC= C45
07LeuH3B/ 1 1.277112 1*1*1 STAT=Y PRED= 1.914 RANGE= 0.369 WIDTH(Y)= 2.146 RESP(Y)= 1.0000 HSQC= C45
07Leu_H4/ 1 0.934474 1*1*1 STAT=Y PRED= 1.630 RANGE= 0.627 WIDTH(Y)= 4.066 RESP(Y)= 1.0000 HSQC= C46
07Leu_H5/ 1 0.317861 1*1*3 STAT=Y PRED= 0.972 RANGE= 0.316 WIDTH(Y)= 2.266 RESP(Y)= 1.0000 HSQC= C47
07Leu_H6/ 1 0.193218 1*1*3 STAT=Y PRED= 0.972 RANGE= 0.149 WIDTH(Y)= 2.156 RESP(Y)= 1.0000 HSQC= C48
08Val_H2/ 1 4.581116 1*1*1 STAT=Y PRED= 4.489 RANGE= 0.899 WIDTH(Y)= 2.019 RESP(Y)= 1.0000 HSQC= C51
08Val_H3/ 1 2.044991 1*1*1 STAT=Y PRED= 1.995 RANGE= 0.486 WIDTH(Y)= 2.865 RESP(Y)= 1.0000 HSQC= C52
08Val_H4/ 1 0.914530 1*1*3 STAT=Y PRED= 1.060 RANGE= 0.237 WIDTH(Y)= 2.509 RESP(Y)= 1.0000 HSQC= C53
08Val_H5/ 1 0.867141 1*1*3 STAT=Y PRED= 0.999 RANGE= 0.229 WIDTH(Y)= 2.710 RESP(Y)= 1.0000 HSQC= C54
09Val_H6/ 1 3.145877 1*1*3 STAT=Y PRED= 3.169 RANGE= 0.466 WIDTH(Y)= 1.753 RESP(Y)= 1.0000 HSQC= C56
09Val_H2/ 1 3.061973 1*1*1 STAT=Y PRED= 5.153 RANGE= 0.719 WIDTH(Y)= 2.193 RESP(Y)= 1.0000 HSQC= C58
09Val_H3/ 1 2.591202 1*1*1 STAT=Y PRED= 2.524 RANGE= 0.407 WIDTH(Y)= 1.993 RESP(Y)= 1.0000 HSQC= C59
09Val_H4/ 1 1.098319 1*1*3 STAT=Y PRED= 1.319 RANGE= 0.227 WIDTH(Y)= 2.256 RESP(Y)= 1.0000 HSQC= C60
09Val_H5/ 1 0.974702 1*1*3 STAT=Y PRED= 1.075 RANGE= 0.239 WIDTH(Y)= 3.198 RESP(Y)= 1.0000 HSQC= C61
10TrpH13/ 1 2.162239 1*1*3 STAT=Y PRED= 2.936 RANGE= 0.895 WIDTH(Y)= 1.827 RESP(Y)= 1.0000 HSQC= C63
10Trp_H2/ 1 4.095875 1*1*1 STAT=Y PRED= 5.043 RANGE= 1.765 WIDTH(Y)= 1.827 RESP(Y)= 1.0000 HSQC= C65
10TrpH3A/ 1 3.543711 1*1*1 STAT=Y PRED= 3.613 RANGE= 0.469 WIDTH(Y)= 1.849 RESP(Y)= 1.0000 HSQC= C66

Appendix S (continued)

```
10TrpH3B/ 1    3.687611  1*1*1  STAT=Y  PRED= 3.367 RANGE= 0.629 WIDTH(Y)= 2.347 RESP(Y)= 1.0000 HSQC= C66
10Trp_H5/ 1    6.695141  1*1*1  STAT=Y  PRED= 6.772 RANGE= 0.276 WIDTH(Y)= 1.972 RESP(Y)= 1.0000 HSQC= C68
10Trp_H9/ 1    6.438058  1*1*1  STAT=Y  PRED= 7.089 RANGE= 0.219 WIDTH(Y)= 1.603 RESP(Y)= 1.0000 HSQC= C73
10Trp_H7/ 1    6.917695  1*1*1  STAT=Y  PRED= 7.333 RANGE= 0.309 WIDTH(Y)= 1.010 RESP(Y)= 1.0000 HSQC= C75
10TrpH12/ 1    3.815845  1*1*3  STAT=Y  PRED= 4.072 RANGE= 0.249 WIDTH(Y)= 1.471 RESP(Y)= 1.0000 HSQC= C77
11Val_H2/ 1    4.364417  1*1*1  STAT=Y  PRED= 4.303 RANGE= 1.449 WIDTH(Y)= 2.746 RESP(Y)= 1.0000 HSQC= C80
11Val_H3/ 1    2.175687  1*1*1  STAT=Y  PRED= 2.094 RANGE= 0.589 WIDTH(Y)= 3.217 RESP(Y)= 1.0000 HSQC= C81
11Val_H4/ 1    1.025555  1*1*3  STAT=Y  PRED= 1.094 RANGE= 0.249 WIDTH(Y)= 2.731 RESP(Y)= 1.0000 HSQC= C82
11Val_H5/ 1    0.981855  1*1*3  STAT=Y  PRED= 1.080 RANGE= 0.299 WIDTH(Y)= 2.129 RESP(Y)= 1.0000 HSQC= C83
13Val_H2/ 1    4.406030  1*1*1  STAT=Y  PRED= 4.169 RANGE= 0.669 WIDTH(Y)= 2.705 RESP(Y)= 1.0000 HSQC= C97
13Val_H3/ 1    1.959947  1*1*1  STAT=Y  PRED= 1.935 RANGE= 0.869 WIDTH(Y)= 2.194 RESP(Y)= 1.0000 HSQC= C99
13Val_H4/ 1    0.922552  1*1*3  STAT=Y  PRED= 1.277 RANGE= 0.219 WIDTH(Y)= 2.328 RESP(Y)= 1.0000 HSQC= C100
13Val_H5/ 1    0.938313  1*1*3  STAT=Y  PRED= 0.933 RANGE= 0.278 WIDTH(Y)= 2.894 RESP(Y)= 1.0000 HSQC= C101

COUPLING CONSTANTS(HZ): fixed
J115_217    7.7969   J 10Trp_H8 10Trp_H9   STAT=Y  PRED= 8.100 RANGE= 0.890
J115_218    8.1808   J 10Trp_H8 10Trp_H7   STAT=Y  PRED= 7.850 RANGE= 0.800
J122_123    9.1737   J 01Val_H2 01Val_H3   STAT=Y  PRED= 12.510 RANGE= 4.000
J123_124    6.5890   J 01Val_H3 01Val_H6   STAT=Y  PRED= 6.640 RANGE= 0.200
J123_127    6.6205   J 01Val_H3 01Val_H7   STAT=Y  PRED= 6.640 RANGE= 0.200
J131_132    8.7545   J 02Val_H2 02Val_H3   STAT=Y  PRED= 12.600 RANGE= 6.000
J132_133    6.7841   J 02Val_H3 02Val_H4   STAT=Y  PRED= 6.640 RANGE= 0.200
J132_136    6.7206   J 02Val_H3 02Val_H5   STAT=Y  PRED= 6.640 RANGE= 0.200
J153_154    2.3441   J 04Thr_H2 04Thr_H3   STAT=Y  PRED= 2.690 RANGE= 6.600
J154_155    6.5134   J 04Thr_H3 04Thr_H4   STAT=Y  PRED= 6.250 RANGE= 0.600
J161_162    3.7259   J 05Thr_H2 05Thr_H3   STAT=Y  PRED= 2.440 RANGE= 4.400
J162_164    6.4691   J 05Thr_H3 05Thr_H4   STAT=Y  PRED= 6.250 RANGE= 0.600
J168_169    8.9180   J 06Val_H2 06Val_H3   STAT=Y  PRED= 2.980 RANGE= 6.600
J169_170    6.6944   J 06Val_H3 06Val_H4   STAT=Y  PRED= 6.640 RANGE= 0.200
J169_173    7.0316   J 06Val_H3 06Val_H5   STAT=Y  PRED= 6.640 RANGE= 0.200
J179_180    6.2437   J 07Leu_H2 07LeuH3A   STAT=Y  PRED= 3.040 RANGE= 6.000
J179_181    8.3839   J 07Leu_H2 07LeuH3B   STAT=Y  PRED= 13.950 RANGE= 4.000
J180_181  -13.3047   J 07LeuH3A 07LeuH3B   STAT=Y  PRED= -14.710 RANGE= 1.600
J180_182    8.2119   J 07LeuH3A 07Leu_H4   STAT=Y  PRED= 12.990 RANGE= 2.560
J181_182    5.7896   J 07LeuH3B 07Leu_H4   STAT=Y  PRED= 2.270 RANGE= 3.000
J182_183    6.5482   J 07Leu_H4 07Leu_H5   STAT=Y  PRED= 6.640 RANGE= 0.200
J182_186    6.5879   J 07Leu_H4 07Leu_H6   STAT=Y  PRED= 6.640 RANGE= 0.200
J190_191    8.8736   J 08Val_H2 08Val_H3   STAT=Y  PRED= 12.880 RANGE= 6.000
J191_192    6.5520   J 08Val_H3 08Val_H4   STAT=Y  PRED= 6.640 RANGE= 0.200
J191_195    6.7834   J 08Val_H3 08Val_H5   STAT=Y  PRED= 6.640 RANGE= 0.200
J201_202    7.6281   J 09Val_H2 09Val_H3   STAT=Y  PRED= 12.960 RANGE= 4.000
J202_203    6.4961   J 09Val_H3 09Val_H4   STAT=Y  PRED= 6.640 RANGE= 0.200
J202_206    6.7760   J 09Val_H3 09Val_H5   STAT=Y  PRED= 6.640 RANGE= 0.200
J212_213   11.1630   J 10Trp_H2 10TrpH3A   STAT=Y  PRED= 12.890 RANGE= 4.000
J212_214    4.7143   J 10Trp_H2 10TrpH3B   STAT=Y  PRED= 1.900 RANGE= 4.400
J213_214  -13.7295   J 10TrpH3A 10TrpH3B   STAT=Y  PRED= -16.760 RANGE= 2.560
J215_218    0.4880   J 10Trp_H5 10Trp_H7   STAT=Y  PRED= -0.300 RANGE= 0.500
J217_218    0.6708   J 10Trp_H9 10Trp_H7   STAT=Y  PRED= 1.020 RANGE= 1.200
J223_224    7.9094   J 11Val_H2 11Val_H3   STAT=Y  PRED= 3.450 RANGE= 9.000
J224_225    6.7483   J 11Val_H3 11Val_H4   STAT=Y  PRED= 6.640 RANGE= 0.200
```

Appendix S (continued)

```
J224_228   6.8064  J 11Val_H3 11Val_H5   STAT=Y  PRED= 6.640 RANGE= 0.200
J241_242   8.8924  J 13Val_H2 13Val_H3   STAT=Y  PRED= 12.320 RANGE= 6.000
J242_243   6.8372  J 13Val_H3 13Val_H4   STAT=Y  PRED= 6.640 RANGE= 0.200
J242_246   6.4162  J 13Val_H3 13Val_H5   STAT=Y  PRED= 6.640 RANGE= 0.200

CONTROL PARAMETERS:
      Solvent =  none (def. 99% enriched)
        1.000 =  Concentration (vol%, def=1.0%)
   0.00100000 =  Minimum line-intensity
   0.00100000 =  Diagonalization criterium (not in use)
 899.93597400 =  FIELD(1H,MHz), used to transform shifts to ppms
  11.63298469 =  Left frequency (ppm)
  -4.33373631 =  Right frequency (ppm)
        0.000 =  Acquisition time (s, for QMTLS)
        0.831 =  Line-width (for modes D, P & T, 0=use defaults)
  0.051689764 =  Data-point resolution (Hz)
      -14.840 =  GAUSSIAN (%, 0=use default from INF)
       -4.829 =  Dispersion contribution (%, 0=use default from INF)
   0.00000000 =  Decoupling frequency (for DORES)

CONSTRAINTS (in equations X0 = 1.0)...use no empty lines
 EQUAL 01Val_H2 = 13Val_H2
 EQUAL 06Val_H5 = 11Val_H4
 EQUAL 07Leu_H5 = 07Leu_H6
 IGNORE(HZ):  2062.779 to  2027.293
 IGNORE(HZ):  5188.061 to  5161.182
 IGNORE(HZ):  4803.141 to  4787.420
 IGNORE(HZ):  4827.557 to  4786.824
 IGNORE(HZ):  4420.654 to  4385.691
 IGNORE(HZ):  2983.196 to  2962.773
 IGNORE(HZ):  1746.134 to  1739.063
 IGNORE(HZ):  3055.453 to  2997.906
 IGNORE(HZ):  2582.749 to  2525.202
 IGNORE(HZ):  8440.896 to  6880.013
 IGNORE(HZ):  1170.100 to  1157.055
 IGNORE(HZ):  2140.689 to  2134.734

END of FILE
```

Appendix T. HiFSA profile for nordeoxyecumicin.

* NEW: the lines beginning by * are comment lines !
* To keep all the chemical shifts fixed during iteration
* replace "CHEMICAL SHIFTS(HZ):" by "..SHIFTS(HZ): fixed"
* The couplings can be fixed in the same way

NMR-data: c:\users\wgao\documents\my box files\itr lab work\lab data\ecum\h
#$œ Date 22.10.2013; Time 0:24: 7 perch.pms

CHEMICAL SHIFTS(PPM):
PROTON 2*SPIN= 1 SPECIES=1H POPULATION(Y)= 1.00000
10_8 / 1 6.980051 1*1*1 STAT=Y PRED= 7.038 RANGE= 0.359 WIDTH(Y)= 1.497 RESP(Y)= 0.7080 HSQC= C74
01_45/ 1 2.381990 1*1*6 STAT=Y PRED= 2.392 RANGE= 0.299 WIDTH(Y)= 2.860 RESP(Y)= 0.2734 HSQC= C1_2
01_2 / 1 2.790014 1*1*1 STAT=Y PRED= 3.405 RANGE= 0.619 WIDTH(Y)= 4.435 RESP(Y)= 0.2913 HSQC= C4
01_3 / 1 2.085613 1*1*1 STAT=Y PRED= 2.136 RANGE= 0.679 WIDTH(Y)= 2.162 RESP(Y)= 0.2768 HSQC= C5
01_6 / 1 1.048498 1*1*3 STAT=Y PRED= 1.043 RANGE= 0.319 WIDTH(Y)= 2.133 RESP(Y)= 0.2949 HSQC= C6
01_7 / 1 0.983378 1*1*3 STAT=Y PRED= 0.974 RANGE= 0.289 WIDTH(Y)= 4.333 RESP(Y)= 0.3642 HSQC= C7
02_1 / 1 4.670441 1*1*1 STAT=Y PRED= 4.567 RANGE= 0.789 WIDTH(Y)= 2.110 RESP(Y)= 0.2884 HSQC= C10
02_2 / 1 2.091080 1*1*1 STAT=Y PRED= 2.190 RANGE= 0.529 WIDTH(Y)= 2.444 RESP(Y)= 0.2415 HSQC= C12
02_3 / 1 0.858080 1*1*3 STAT=Y PRED= 0.995 RANGE= 0.296 WIDTH(Y)= 2.451 RESP(Y)= 0.3445 HSQC= C13
02_4 / 1 0.989294 1*1*3 STAT=Y PRED= 0.992 RANGE= 0.229 WIDTH(Y)= 1.960 RESP(Y)= 0.2619 HSQC= C14
03_1 / 1 3.248566 1*1*3 STAT=Y PRED= 3.434 RANGE= 0.389 WIDTH(Y)= 1.613 RESP(Y)= 0.2633 HSQC= C15
03_2 / 1 4.405998 1*1*1 STAT=Y PRED= 5.167 RANGE= 1.479 WIDTH(Y)= 2.013 RESP(Y)= 0.2424 HSQC= C17
03_3 / 1 2.175670 1*1*1 STAT=Y PRED= 2.281 RANGE= 0.559 WIDTH(Y)= 1.456 RESP(Y)= 0.1780 HSQC= C19
03_4 / 1 1.025492 1*1*3 STAT=Y PRED= 1.200 RANGE= 0.239 WIDTH(Y)= 2.336 RESP(Y)= 0.2561 HSQC= C20
03_5 / 1 0.982180 1*1*3 STAT=Y PRED= 0.981 RANGE= 0.218 WIDTH(Y)= 3.611 RESP(Y)= 0.4370 HSQC= C21
04_2 / 1 5.152366 1*1*1 STAT=Y PRED= 4.667 RANGE= 0.908 WIDTH(Y)= 1.741 RESP(Y)= 0.2528 HSQC= C24
04_3 / 1 5.790968 1*1*1 STAT=Y PRED= 4.010 RANGE= 0.509 WIDTH(Y)= 2.204 RESP(Y)= 0.2831 HSQC= C25
04_4 / 1 1.310031 1*1*3 STAT=Y PRED= 1.285 RANGE= 0.506 WIDTH(Y)= 2.540 RESP(Y)= 0.3087 HSQC= C27
05_5 / 1 3.315962 1*1*3 STAT=Y PRED= 3.609 RANGE= 0.699 WIDTH(Y)= 2.477 RESP(Y)= 0.3476 HSQC= C29
05_2 / 1 5.016013 1*1*1 STAT=Y PRED= 5.502 RANGE= 1.049 WIDTH(Y)= 2.005 RESP(Y)= 0.2690 HSQC= C31
05_3 / 1 4.407548 1*1*1 STAT=Y PRED= 4.319 RANGE= 0.689 WIDTH(Y)= 2.014 RESP(Y)= 0.2336 HSQC= C32
05_4 / 1 0.885527 1*1*3 STAT=Y PRED= 1.360 RANGE= 0.319 WIDTH(Y)= 2.395 RESP(Y)= 0.2556 HSQC= C34
06_2 / 1 4.835998 1*1*1 STAT=Y PRED= 4.379 RANGE= 1.517 WIDTH(Y)= 2.611 RESP(Y)= 0.3034 HSQC= C37
06_3 / 1 2.363256 1*1*1 STAT=Y PRED= 2.041 RANGE= 0.946 WIDTH(Y)= 2.281 RESP(Y)= 0.2290 HSQC= C38
06_4 / 1 1.098314 1*1*3 STAT=Y PRED= 1.097 RANGE= 0.219 WIDTH(Y)= 2.259 RESP(Y)= 0.2517 HSQC= C39
06_5 / 1 0.974424 1*1*3 STAT=Y PRED= 1.139 RANGE= 0.596 WIDTH(Y)= 2.463 RESP(Y)= 0.2047 HSQC= C40
07_7 / 1 3.264465 1*1*3 STAT=Y PRED= 3.081 RANGE= 0.369 WIDTH(Y)= 1.821 RESP(Y)= 0.2311 HSQC= C42
07_2 / 1 5.132089 1*1*1 STAT=Y PRED= 5.262 RANGE= 1.455 WIDTH(Y)= 5.093 RESP(Y)= 0.2449 HSQC= C44
07_3A/ 1 1.439474 1*1*1 STAT=Y PRED= 1.679 RANGE= 0.559 WIDTH(Y)= 2.624 RESP(Y)= 0.0705 HSQC= C45
07_3b/ 1 1.283980 1*1*1 STAT=Y PRED= 1.648 RANGE= 0.409 WIDTH(Y)= 3.159 RESP(Y)= 0.2154 HSQC= C45
07_4 / 1 0.957258 1*1*1 STAT=Y PRED= 1.601 RANGE= 0.306 WIDTH(Y)= 3.783 RESP(Y)= 0.6315 HSQC= C46
07_5 / 1 0.317826 1*1*3 STAT=Y PRED= 0.907 RANGE= 0.179 WIDTH(Y)= 2.009 RESP(Y)= 0.1805 HSQC= C47
07_6 / 1 0.193188 1*1*3 STAT=Y PRED= 0.968 RANGE= 0.139 WIDTH(Y)= 1.948 RESP(Y)= 0.1762 HSQC= C48
08_2 / 1 4.581076 1*1*1 STAT=Y PRED= 4.504 RANGE= 0.799 WIDTH(Y)= 1.881 RESP(Y)= 0.2032 HSQC= C51
08_3 / 1 2.044776 1*1*1 STAT=Y PRED= 2.027 RANGE= 0.559 WIDTH(Y)= 2.514 RESP(Y)= 0.1672 HSQC= C52
08_4 / 1 0.914653 1*1*3 STAT=Y PRED= 1.017 RANGE= 0.229 WIDTH(Y)= 2.628 RESP(Y)= 0.3167 HSQC= C53
08_5 / 1 0.867111 1*1*3 STAT=Y PRED= 0.953 RANGE= 0.248 WIDTH(Y)= 2.304 RESP(Y)= 0.2119 HSQC= C54
09_6 / 1 3.145838 1*1*3 STAT=Y PRED= 3.072 RANGE= 0.438 WIDTH(Y)= 1.814 RESP(Y)= 0.2221 HSQC= C56
09_2 / 1 3.061940 1*1*1 STAT=Y PRED= 4.369 RANGE= 0.719 WIDTH(Y)= 2.026 RESP(Y)= 0.2100 HSQC= C58
09_3 / 1 2.591147 1*1*1 STAT=Y PRED= 1.984 RANGE= 0.548 WIDTH(Y)= 1.540 RESP(Y)= 0.1623 HSQC= C59
09_4 / 1 1.093782 1*1*3 STAT=Y PRED= 1.268 RANGE= 0.266 WIDTH(Y)= 1.744 RESP(Y)= 0.2490 HSQC= C60
09_5 / 1 0.978830 1*1*3 STAT=Y PRED= 1.308 RANGE= 0.249 WIDTH(Y)= 2.514 RESP(Y)= 0.2373 HSQC= C61
10_12/ 1 2.162206 1*1*3 STAT=Y PRED= 2.713 RANGE= 1.035 WIDTH(Y)= 1.748 RESP(Y)= 0.2152 HSQC= C63
10_2 / 1 4.095847 1*1*1 STAT=Y PRED= 4.672 RANGE= 1.228 WIDTH(Y)= 1.856 RESP(Y)= 0.2198 HSQC= C65
10_3A/ 1 3.687573 1*1*1 STAT=Y PRED= 3.077 RANGE= 0.539 WIDTH(Y)= 2.260 RESP(Y)= 0.2171 HSQC= C66
10_3B/ 1 3.543671 1*1*1 STAT=Y PRED= 3.785 RANGE= 0.649 WIDTH(Y)= 1.691 RESP(Y)= 0.2175 HSQC= C66
10_5 / 1 6.695087 1*1*1 STAT=Y PRED= 6.538 RANGE= 0.579 WIDTH(Y)= 1.562 RESP(Y)= 0.6801 HSQC= C68

Appendix T (continued)

```
10_7 / 1    6.917655  1*1*1  STAT=Y  PRED= 6.543 RANGE= 0.509 WIDTH(Y)= 0.953 RESP(Y)= 0.6625 HSQC= C73
10_9 / 1    6.438059  1*1*1  STAT=Y  PRED= 6.829 RANGE= 0.547 WIDTH(Y)= 2.648 RESP(Y)= 1.0000 HSQC= C75
10_13/ 1    3.815815  1*1*3  STAT=Y  PRED= 4.118 RANGE= 0.259 WIDTH(Y)= 1.465 RESP(Y)= 0.2251 HSQC= C77
11_2 / 1    4.856934  1*1*1  STAT=Y  PRED= 4.113 RANGE= 1.459 WIDTH(Y)= 2.436 RESP(Y)= 0.3478 HSQC= C80
11_3 / 1    2.160599  1*1*1  STAT=Y  PRED= 2.065 RANGE= 0.659 WIDTH(Y)= 3.341 RESP(Y)= 0.3837 HSQC= C81
11_4 / 1    0.799702  1*1*3  STAT=Y  PRED= 1.033 RANGE= 0.229 WIDTH(Y)= 2.052 RESP(Y)= 0.2334 HSQC= C82
11_5 / 1    0.792423  1*1*3  STAT=Y  PRED= 1.004 RANGE= 0.328 WIDTH(Y)= 2.376 RESP(Y)= 0.2934 HSQC= C83
12_2 / 1    4.802115  1*1*1  STAT=Y  PRED= 4.609 RANGE= 1.079 WIDTH(Y)= 2.633 RESP(Y)= 0.2268 HSQC= C86
12_3A/ 1    2.833268  1*1*1  STAT=Y  PRED= 3.421 RANGE= 0.649 WIDTH(Y)= 2.155 RESP(Y)= 0.2106 HSQC= C87
12_59/ 1    7.077218  1*2*1  STAT=Y  PRED= 7.297 RANGE= 0.288 WIDTH(Y)= 2.337 RESP(Y)= 0.1628 HSQC= C89_93
12_68/ 1    7.201033  1*2*1  STAT=Y  PRED= 7.334 RANGE= 0.359 WIDTH(Y)= 2.244 RESP(Y)= 0.1779 HSQC= C90_92
12_7 / 1    7.149698  1*1*1  STAT=Y  PRED= 7.105 RANGE= 0.557 WIDTH(Y)= 1.917 RESP(Y)= 0.1760 HSQC= C91
13_2 / 1    4.364383  1*1*1  STAT=Y  PRED= 4.361 RANGE= 0.999 WIDTH(Y)= 1.625 RESP(Y)= 0.2303 HSQC= C97
13_3 / 1    1.959862  1*1*1  STAT=Y  PRED= 2.106 RANGE= 0.769 WIDTH(Y)= 2.389 RESP(Y)= 0.2408 HSQC= C99
13_4 / 1    0.922262  1*1*3  STAT=Y  PRED= 0.999 RANGE= 0.209 WIDTH(Y)= 3.549 RESP(Y)= 0.4069 HSQC= C100
13_5 / 1    0.938226  1*1*3  STAT=Y  PRED= 1.048 RANGE= 0.309 WIDTH(Y)= 3.173 RESP(Y)= 0.3371 HSQC= C101
12_3B/ 1    3.320084  1*1*1  STAT=Y  PRED= 2.911 RANGE= 0.569 WIDTH(Y)= 1.900 RESP(Y)= 0.0034 HSQC= C87

COUPLING CONSTANTS(HZ):
J113_212    8.1745   J 10_8  10_7    STAT=Y  PRED= 8.100 RANGE= 0.440
J113_213    7.8016   J 10_8  10_9    STAT=Y  PRED= 7.850 RANGE= 0.400
J120_121    8.7591   J 01_2  01_3    STAT=Y  PRED= 12.610 RANGE= 2.000
J121_122    6.7208   J 01_3  01_6    STAT=Y  PRED= 6.640 RANGE= 0.100
J121_125    6.9969   J 01_3  01_7    STAT=Y  PRED= 6.640 RANGE= 0.100
J129_130    8.7379   J 02_1  02_2    STAT=Y  PRED= 12.550 RANGE= 2.000
J130_131    6.5721   J 02_2  02_3    STAT=Y  PRED= 6.640 RANGE= 0.100
J130_134    6.9835   J 02_2  02_4    STAT=Y  PRED= 6.640 RANGE= 0.100
J140_141    8.4567   J 03_2  03_3    STAT=Y  PRED= 12.920 RANGE= 2.000
J141_142    6.7309   J 03_3  03_4    STAT=Y  PRED= 6.640 RANGE= 0.100
J141_144    6.8080   J 03_3  03_5    STAT=Y  PRED= 6.640 RANGE= 0.100
J148_149    2.3275   J 04_2  04_3    STAT=Y  PRED= 1.890 RANGE= 2.200
J149_150    6.3517   J 04_3  04_4    STAT=Y  PRED= 6.250 RANGE= 0.300
J156_157    3.8542   J 05_2  05_3    STAT=Y  PRED= 2.690 RANGE= 2.200
J157_159    6.4578   J 05_3  05_4    STAT=Y  PRED= 6.250 RANGE= 0.300
J163_164    9.0622   J 06_2  06_3    STAT=Y  PRED= 2.190 RANGE= 2.200
J164_165    6.6724   J 06_3  06_4    STAT=Y  PRED= 6.640 RANGE= 0.100
J164_168    6.4514   J 06_3  06_5    STAT=Y  PRED= 6.640 RANGE= 0.100
65          7.9245   J 07_2  07_3A   STAT=Y
66          7.1393   J 07_2  07_3b   STAT=Y
67        -12.1243   J 07_3A 07_3b   STAT=Y
69          4.1553   J 07_3A 07_4    STAT=Y
68          5.7412   J 07_3b 07_4    STAT=Y
70          6.5432   J 07_4  07_5    STAT=Y
71          6.5848   J 07_4  07_6    STAT=Y
72          9.1745   J 08_2  08_3    STAT=Y
73          7.1305   J 08_3  08_4    STAT=Y
74          6.7408   J 08_3  08_5    STAT=Y
75          7.7414   J 09_2  09_3    STAT=Y
76          6.6102   J 09_3  09_4    STAT=Y
77          6.9848   J 09_3  09_5    STAT=Y
78          4.7322   J 10_2  10_3A   STAT=Y
79         11.1769   J 10_2  10_3B   STAT=Y
80        -13.7052   J 10_3A 10_3B   STAT=Y
88          0.8060   J 10_5  10_7    STAT=Y
96          0.3325   J 10_7  10_9    STAT=Y
115         0.0000   J 10_7  11_4    STAT=Y
81         11.0321   J 11_2  11_3    STAT=Y
```

Appendix T (continued)

```
 82        6.5908   J 11_3  11_4    STAT=Y
 83        6.5747   J 11_3  11_5    STAT=Y
 84       10.8450   J 12_2  12_3A   STAT=Y
 85        2.6476   J 12_2  12_3B   STAT=Y
 86      -14.3372   J 12_3A 12_3B   STAT=Y
 89        1.1327   J 12_59 12_59   STAT=Y
 87        6.7692   J 12_68 12_59   STAT=Y
 90        1.3139   J 12_59 12_7    STAT=Y
 91        0.8000   J 12_68 12_68   STAT=N
 92        7.5501   J 12_68 12_7    STAT=Y
 93        9.0700   J 13_2  13_3    STAT=Y
 94        7.3088   J 13_3  13_4    STAT=Y
 95        6.5502   J 13_3  13_5    STAT=Y

CONTROL PARAMETERS:
      Solvent =  none (def. 99% enriched)
        1.000 =  Concentration (vol%, def=1.0%)
   0.00100000 =  Minimum line-intensity
   0.00100000 =  Diagonalization criterium (not in use)
  19.94827676 =  Left frequency (ppm)
 -10.16527177 =  Right frequency (ppm)
        0.000 =  Acquisition time (s, for QMTLS)
        0.953 =  Line-width (for modes D, P & T, 0=use defaults)
  0.051689764 =  Data-point resolution (Hz)
      -10.743 =  GAUSSIAN (%, 0=use default from INF)
       -1.131 =  Dispersion contribution (%, 0=use default from INF)
   0.00000000 =  Decoupling frequency (for DORES)

CONSTRAINTS (in equations X0 = 1.0)...use no empty lines
 EQUAL 01_7     = 11_5
 IGNORE(HZ):  4420.245 to  4403.372
 IGNORE(HZ):  8408.396 to  7438.706
 IGNORE(HZ):  7065.850 to  6602.454
 IGNORE(HZ):   693.905 to   347.597
 IGNORE(HZ):  6567.991 to  6505.517
 IGNORE(HZ):  6266.729 to  6249.375
 IGNORE(HZ):  6161.217 to  6143.169
 IGNORE(HZ):  5712.794 to  5691.969
 IGNORE(HZ):  5612.142 to  5585.069
 IGNORE(HZ):   208.209 to   192.436
 IGNORE(HZ):   319.443 to   304.224
 IGNORE(HZ):  4855.530 to  4640.748
 IGNORE(HZ):  4423.222 to  4386.769
 IGNORE(HZ):  4506.542 to  4422.180
 IGNORE(HZ):  4307.615 to  4210.754
 IGNORE(HZ):  4188.883 to  4129.517
 IGNORE(HZ):  3913.405 to  3822.794
 IGNORE(HZ):  3447.827 to  3436.074
 IGNORE(HZ):  3424.112 to  3336.805
 IGNORE(HZ):  3336.596 to  3330.929
 IGNORE(HZ):  3305.115 to  3206.686
 IGNORE(HZ):  2971.684 to  2944.401
 IGNORE(HZ):  2740.773 to  2569.304
 IGNORE(HZ):  2480.527 to  2357.919
 IGNORE(HZ):  2299.068 to  2160.113
 IGNORE(HZ):  2913.740 to  2840.993
 IGNORE(HZ):  2819.741 to  2770.698
```

Appendix T (continued)

IGNORE(HZ): 2545.530 to 2541.669
IGNORE(HZ): 2502.010 to 2494.201
IGNORE(HZ): 756.636 to 730.312
IGNORE(HZ): 1030.592 to 995.465
IGNORE(HZ): 965.986 to 950.276
IGNORE(HZ): 915.149 to 897.497
IGNORE(HZ): 814.887 to 802.354
IGNORE(HZ): 765.550 to 754.959
IGNORE(HZ): 166.406 to 44.347
IGNORE(HZ): 1747.539 to 1322.914
IGNORE(HZ): 6570.428 to 6493.058
IGNORE(HZ): 6468.784 to 6447.545
IGNORE(HZ): 6420.238 to 6380.036
IGNORE(HZ): 6358.796 to 6331.489
IGNORE(HZ): 6250.326 to 6235.155
IGNORE(HZ): 6213.157 to 6068.277
IGNORE(HZ): 5755.001 to 5571.435
IGNORE(HZ): 2533.823 to 2520.305
IGNORE(HZ): 1265.970 to 1184.888
IGNORE(HZ): 1128.549 to 1060.981
IGNORE(HZ): 1060.743 to 1023.628
IGNORE(HZ): 5804.091 to 5799.604
IGNORE(HZ): 5795.457 to 5792.134
IGNORE(HZ): 5998.250 to 5835.601
IGNORE(HZ): 3048.532 to 2992.469
IGNORE(HZ): 2983.319 to 2971.591
IGNORE(HZ): 2141.298 to 2134.353
IGNORE(HZ): 2935.604 to 2929.610
IGNORE(HZ): 2921.501 to 2913.745
IGNORE(HZ): 2828.073 to 2819.612
IGNORE(HZ): 2914.375 to 2912.431
IGNORE(HZ): 6295.260 to 6292.522
IGNORE(HZ): 6287.388 to 6284.993
IGNORE(HZ): 6279.517 to 6276.779
IGNORE(HZ): 3980.261 to 3974.877

END of FILE

Appendix U Pseudo HiFSA profile of homoecumicin-11I.

* NEW: the lines beginning by * are comment lines !
* To keep all the chemical shifts fixed during iteration
* replace "CHEMICAL SHIFTS(HZ):" by "..SHIFTS(HZ): fixed"
* The couplings can be fixed in the same way

NMR-data: C:\Users\jgnapo_2\Desktop\Wei_H14_XRays\H14_withoutGO
#$œ Date 22. 2.2012; Time 18:15:36 perch.8th

CHEMICAL SHIFTS(PPM):
PROTON 2*SPIN= 1 SPECIES=1H POPULATION(Y)= 1.00000

10Trp_H8/ 1 6.981702 1*1*1 STAT=Y PRED= 7.318 RANGE= 0.199 WIDTH(Y)= 1.215 RESP(Y)= 0.2294 HSQC= C74
01ValH45/ 1 2.312749 1*1*6 STAT=Y PRED= 2.370 RANGE= 0.307 WIDTH(Y)= 1.536 RESP(Y)= 0.1971 HSQC= C1_2
01Val_H2/ 1 2.671561 1*1*1 STAT=Y PRED= 4.169 RANGE= 0.639 WIDTH(Y)= 1.557 RESP(Y)= 0.1955 HSQC= C4
01Val_H3/ 1 2.042384 1*1*1 STAT=Y PRED= 1.952 RANGE= 0.819 WIDTH(Y)= 1.561 RESP(Y)= 0.1582 HSQC= C5
01Val_H6/ 1 0.847135 1*1*3 STAT=Y PRED= 0.509 RANGE= 0.869 WIDTH(Y)= 1.598 RESP(Y)= 0.2195 HSQC= C6
01Val_H7/ 1 0.978236 1*1*3 STAT=Y PRED= 0.818 RANGE= 0.359 WIDTH(Y)= 1.688 RESP(Y)= 0.1917 HSQC= C7
02Val_H2/ 1 4.669057 1*1*1 STAT=Y PRED= 4.508 RANGE= 0.809 WIDTH(Y)= 1.467 RESP(Y)= 0.1935 HSQC= C10
02Val_H3/ 1 2.101399 1*1*1 STAT=Y PRED= 2.155 RANGE= 0.779 WIDTH(Y)= 1.561 RESP(Y)= 0.1880 HSQC= C12
02Val_H4/ 1 0.992199 1*1*3 STAT=Y PRED= 1.038 RANGE= 0.279 WIDTH(Y)= 1.468 RESP(Y)= 0.1493 HSQC= C13
02Val_H5/ 1 1.055401 1*1*3 STAT=Y PRED= 0.943 RANGE= 0.249 WIDTH(Y)= 1.538 RESP(Y)= 0.2055 HSQC= C14
03Ile_H7/ 1 3.233925 1*1*3 STAT=Y PRED= 3.196 RANGE= 0.369 WIDTH(Y)= 1.536 RESP(Y)= 0.2005 HSQC= C15
03Ile_H2/ 1 4.918283 1*1*1 STAT=Y PRED= 4.617 RANGE= 1.628 WIDTH(Y)= 1.466 RESP(Y)= 0.1936 HSQC= C17
03Ile_H3/ 1 1.957476 1*1*1 STAT=Y PRED= 2.032 RANGE= 0.706 WIDTH(Y)= 2.929 RESP(Y)= 0.1562 HSQC= C19
03IleH4A/ 1 0.989134 1*1*1 STAT=Y PRED= 1.465 RANGE= 0.699 WIDTH(Y)= 5.275 RESP(Y)= 1.0000 HSQC= C20
03IleH4B/ 1 1.255324 1*1*1 STAT=Y PRED= 1.175 RANGE= 0.589 WIDTH(Y)= 2.795 RESP(Y)= 0.1091 HSQC= C20
03Ile_H6/ 1 0.753945 1*1*3 STAT=Y PRED= 0.723 RANGE= 0.398 WIDTH(Y)= 1.613 RESP(Y)= 0.1953 HSQC= C21
03Ile_H5/ 1 0.743889 1*1*3 STAT=Y PRED= 0.880 RANGE= 0.219 WIDTH(Y)= 1.391 RESP(Y)= 0.1663 HSQC= C22
04Thr_H2/ 1 5.166937 1*1*1 STAT=Y PRED= 4.668 RANGE= 1.016 WIDTH(Y)= 1.377 RESP(Y)= 0.1774 HSQC= C24
04Thr_H3/ 1 5.783161 1*1*1 STAT=Y PRED= 4.010 RANGE= 0.479 WIDTH(Y)= 1.941 RESP(Y)= 0.1822 HSQC= C25
04Thr_H4/ 1 1.313144 1*1*3 STAT=Y PRED= 1.270 RANGE= 0.499 WIDTH(Y)= 1.818 RESP(Y)= 0.2026 HSQC= C27
05Thr_H5/ 1 3.329509 1*1*3 STAT=Y PRED= 3.257 RANGE= 0.399 WIDTH(Y)= 1.439 RESP(Y)= 0.1781 HSQC= C29
05Thr_H2/ 1 5.017583 1*1*1 STAT=Y PRED= 4.099 RANGE= 1.025 WIDTH(Y)= 1.500 RESP(Y)= 0.1944 HSQC= C31
05Thr_H3/ 1 4.457478 1*1*1 STAT=Y PRED= 4.345 RANGE= 0.719 WIDTH(Y)= 1.572 RESP(Y)= 0.1838 HSQC= C32
05Thr_H4/ 1 0.911837 1*1*3 STAT=Y PRED= 1.252 RANGE= 0.299 WIDTH(Y)= 1.939 RESP(Y)= 0.1922 HSQC= C34
06Val_H2/ 1 4.842224 1*1*1 STAT=Y PRED= 4.525 RANGE= 1.409 WIDTH(Y)= 1.382 RESP(Y)= 0.1523 HSQC= C37
06Val_H3/ 1 2.350353 1*1*1 STAT=Y PRED= 1.975 RANGE= 1.019 WIDTH(Y)= 1.789 RESP(Y)= 0.1830 HSQC= C38
06Val_H4/ 1 1.092268 1*1*3 STAT=Y PRED= 0.938 RANGE= 0.219 WIDTH(Y)= 1.894 RESP(Y)= 0.1902 HSQC= C39
06Val_H5/ 1 0.979285 1*1*3 STAT=Y PRED= 1.094 RANGE= 0.389 WIDTH(Y)= 2.275 RESP(Y)= 0.1940 HSQC= C40
07Leu_H7/ 1 3.258856 1*1*3 STAT=Y PRED= 3.110 RANGE= 0.376 WIDTH(Y)= 1.459 RESP(Y)= 0.1758 HSQC= C42
07Leu_H2/ 1 5.110377 1*1*1 STAT=Y PRED= 5.342 RANGE= 1.085 WIDTH(Y)= 2.240 RESP(Y)= 0.1736 HSQC= C44
07LeuH3A/ 1 1.452263 1*1*1 STAT=Y PRED= 1.444 RANGE= 0.429 WIDTH(Y)= 1.805 RESP(Y)= 0.1253 HSQC= C45
07LeuH3B/ 1 1.238825 1*1*1 STAT=Y PRED= 1.914 RANGE= 0.369 WIDTH(Y)= 3.321 RESP(Y)= 0.2550 HSQC= C45
07Leu_H4/ 1 0.957012 1*1*1 STAT=Y PRED= 1.630 RANGE= 0.627 WIDTH(Y)= 1.520 RESP(Y)= 0.1513 HSQC= C46
07Leu_H5/ 1 0.330648 1*1*3 STAT=Y PRED= 0.972 RANGE= 0.316 WIDTH(Y)= 1.961 RESP(Y)= 0.1633 HSQC= C47
07Leu_H6/ 1 0.168240 1*1*3 STAT=Y PRED= 0.972 RANGE= 0.149 WIDTH(Y)= 1.885 RESP(Y)= 0.1544 HSQC= C48
08Val_H2/ 1 4.594366 1*1*1 STAT=Y PRED= 4.489 RANGE= 0.899 WIDTH(Y)= 1.578 RESP(Y)= 0.1883 HSQC= C51
08Val_H3/ 1 2.026705 1*1*1 STAT=Y PRED= 1.995 RANGE= 0.486 WIDTH(Y)= 2.872 RESP(Y)= 0.1833 HSQC= C52
08Val_H4/ 1 0.915098 1*1*3 STAT=Y PRED= 1.060 RANGE= 0.237 WIDTH(Y)= 1.731 RESP(Y)= 0.1845 HSQC= C53
08Val_H5/ 1 0.858580 1*1*3 STAT=Y PRED= 0.999 RANGE= 0.229 WIDTH(Y)= 2.065 RESP(Y)= 0.1899 HSQC= C54
09Val_H6/ 1 3.139923 1*1*3 STAT=Y PRED= 3.169 RANGE= 0.466 WIDTH(Y)= 1.931 RESP(Y)= 0.1698 HSQC= C56

Appendix U (continued)

09Val_H2/ 1 3.065448 1*1*1 STAT=Y PRED= 5.153 RANGE= 0.719 WIDTH(Y)= 2.597 RESP(Y)= 0.1650 HSQC= C58
09Val_H3/ 1 2.582945 1*1*1 STAT=Y PRED= 2.524 RANGE= 0.407 WIDTH(Y)= 1.736 RESP(Y)= 0.1528 HSQC= C59
09Val_H4/ 1 1.093807 1*1*3 STAT=Y PRED= 1.319 RANGE= 0.227 WIDTH(Y)= 1.741 RESP(Y)= 0.1953 HSQC= C60
09Val_H5/ 1 0.975890 1*1*3 STAT=Y PRED= 1.075 RANGE= 0.239 WIDTH(Y)= 2.379 RESP(Y)= 0.1859 HSQC= C61
10TrpH13/ 1 2.157320 1*1*3 STAT=Y PRED= 2.936 RANGE= 0.895 WIDTH(Y)= 1.862 RESP(Y)= 0.1713 HSQC= C63
10Trp_H2/ 1 4.102017 1*1*1 STAT=Y PRED= 5.043 RANGE= 1.765 WIDTH(Y)= 2.064 RESP(Y)= 0.1681 HSQC= C65
10TrpH3A/ 1 3.544888 1*1*1 STAT=Y PRED= 3.613 RANGE= 0.469 WIDTH(Y)= 1.516 RESP(Y)= 0.1749 HSQC= C66
10TrpH3B/ 1 3.693826 1*1*1 STAT=Y PRED= 3.367 RANGE= 0.629 WIDTH(Y)= 2.118 RESP(Y)= 0.1765 HSQC= C66
10Trp_H5/ 1 6.698373 1*1*1 STAT=Y PRED= 6.772 RANGE= 0.276 WIDTH(Y)= 1.649 RESP(Y)= 0.2013 HSQC= C68
10Trp_H9/ 1 6.441824 1*1*1 STAT=Y PRED= 7.089 RANGE= 0.219 WIDTH(Y)= 1.143 RESP(Y)= 0.2128 HSQC= C73
10Trp_H7/ 1 6.918050 1*1*1 STAT=Y PRED= 7.333 RANGE= 0.309 WIDTH(Y)= 0.719 RESP(Y)= 0.1990 HSQC= C75
10TrpH12/ 1 3.825517 1*1*3 STAT=Y PRED= 4.072 RANGE= 0.249 WIDTH(Y)= 1.244 RESP(Y)= 0.1876 HSQC= C77
11Val_H2/ 1 4.528581 1*1*1 STAT=Y PRED= 4.303 RANGE= 1.449 WIDTH(Y)= 1.849 RESP(Y)= 0.1834 HSQC= C80
11Val_H3/ 1 2.200081 1*1*1 STAT=Y PRED= 2.094 RANGE= 0.589 WIDTH(Y)= 1.854 RESP(Y)= 0.1757 HSQC= C81
11Val_H4/ 1 1.028241 1*1*3 STAT=Y PRED= 1.094 RANGE= 0.249 WIDTH(Y)= 2.106 RESP(Y)= 0.1836 HSQC= C82
11Val_H5/ 1 0.989118 1*1*3 STAT=Y PRED= 1.080 RANGE= 0.299 WIDTH(Y)= 1.787 RESP(Y)= 0.1359 HSQC= C83
12Phe_H2/ 1 4.853691 1*1*1 STAT=Y PRED= 4.499 RANGE= 0.989 WIDTH(Y)= 1.261 RESP(Y)= 0.1673 HSQC= C86
12Phe_H3/ 1 5.343847 1*1*1 STAT=Y PRED= 5.208 RANGE= 0.489 WIDTH(Y)= 1.884 RESP(Y)= 0.1897 HSQC= C87
12Phe_H5/ 1 7.239588 1*2*1 STAT=Y PRED= 7.524 RANGE= 0.309 WIDTH(Y)= 2.042 RESP(Y)= 0.2024 HSQC= C89_93
12Phe_H6/ 1 7.255487 1*2*1 STAT=Y PRED= 7.372 RANGE= 0.579 WIDTH(Y)= 1.207 RESP(Y)= 0.2038 HSQC= C90_92
12Phe_H7/ 1 7.200632 1*1*1 STAT=Y PRED= 7.281 RANGE= 0.309 WIDTH(Y)= 1.557 RESP(Y)= 0.2174 HSQC= C91
13Val_H2/ 1 4.396080 1*1*1 STAT=Y PRED= 4.169 RANGE= 0.669 WIDTH(Y)= 1.205 RESP(Y)= 0.1804 HSQC= C97
13Val_H3/ 1 1.967817 1*1*1 STAT=Y PRED= 1.935 RANGE= 0.869 WIDTH(Y)= 1.973 RESP(Y)= 0.2062 HSQC= C99
13Val_H4/ 1 0.934963 1*1*3 STAT=Y PRED= 1.277 RANGE= 0.219 WIDTH(Y)= 2.666 RESP(Y)= 0.2386 HSQC= C100
13Val_H5/ 1 0.919356 1*1*3 STAT=Y PRED= 0.933 RANGE= 0.278 WIDTH(Y)= 2.083 RESP(Y)= 0.2256 HSQC= C101

COUPLING CONSTANTS(HZ): fixed
J115_217 7.7969 J 10Trp_H8 10Trp_H9 STAT=Y PRED= 8.100 RANGE= 0.890
J115_218 8.1808 J 10Trp_H8 10Trp_H7 STAT=Y PRED= 7.850 RANGE= 0.800
J122_123 9.1737 J 01Val_H2 01Val_H3 STAT=Y PRED= 12.510 RANGE= 4.000
J123_124 6.5890 J 01Val_H3 01Val_H6 STAT=Y PRED= 6.640 RANGE= 0.200
J123_127 6.6205 J 01Val_H3 01Val_H7 STAT=Y PRED= 6.640 RANGE= 0.200
J131_132 8.7545 J 02Val_H2 02Val_H3 STAT=Y PRED= 12.600 RANGE= 6.000
J132_133 6.7841 J 02Val_H3 02Val_H4 STAT=Y PRED= 6.640 RANGE= 0.200
J132_136 6.7206 J 02Val_H3 02Val_H5 STAT=Y PRED= 6.640 RANGE= 0.200
J142_143 11.2297 J 03Ile_H2 03Ile_H3 STAT=Y PRED= 13.150 RANGE= 4.000
J143_144 0.4614 J 03Ile_H3 03IleH4A STAT=Y PRED= 1.950 RANGE= 3.000
J143_145 2.9276 J 03Ile_H3 03IleH4B STAT=Y PRED= 12.660 RANGE= 2.800
J143_146 6.6276 J 03Ile_H3 03Ile_H6 STAT=Y PRED= 6.640 RANGE= 0.200
J144_145 -12.2168 J 03IleH4A 03IleH4B STAT=Y PRED= -13.400 RANGE= 0.600
J144_149 7.2855 J 03IleH4A 03Ile_H5 STAT=Y PRED= 7.440 RANGE= 0.150
J145_149 7.6340 J 03IleH4B 03Ile_H5 STAT=Y PRED= 7.440 RANGE= 0.150
J153_154 2.3441 J 04Thr_H2 04Thr_H3 STAT=Y PRED= 2.690 RANGE= 6.600
J154_155 6.5134 J 04Thr_H3 04Thr_H4 STAT=Y PRED= 6.250 RANGE= 0.600
J161_162 3.7259 J 05Thr_H2 05Thr_H3 STAT=Y PRED= 2.440 RANGE= 4.400
J162_164 6.4691 J 05Thr_H3 05Thr_H4 STAT=Y PRED= 6.250 RANGE= 0.600
J168_169 8.9180 J 06Val_H2 06Val_H3 STAT=Y PRED= 2.980 RANGE= 6.600
J169_170 6.6944 J 06Val_H3 06Val_H4 STAT=Y PRED= 6.640 RANGE= 0.200
J169_173 7.0316 J 06Val_H3 06Val_H5 STAT=Y PRED= 6.640 RANGE= 0.200
J179_180 6.2437 J 07Leu_H2 07LeuH3A STAT=Y PRED= 3.040 RANGE= 6.000

Appendix U (continued)

```
J179_181    8.3839   J 07Leu_H2 07LeuH3B   STAT=Y  PRED= 13.950 RANGE= 4.000
J180_181  -13.3047   J 07LeuH3A 07LeuH3B   STAT=Y  PRED= -14.710 RANGE= 1.600
J180_182    8.2119   J 07LeuH3A 07Leu_H4   STAT=Y  PRED= 12.990 RANGE= 2.560
J181_182    5.7896   J 07LeuH3B 07Leu_H4   STAT=Y  PRED= 2.270 RANGE= 3.000
J182_183    6.5482   J 07Leu_H4 07Leu_H5   STAT=Y  PRED= 6.640 RANGE= 0.200
J182_186    6.5879   J 07Leu_H4 07Leu_H6   STAT=Y  PRED= 6.640 RANGE= 0.200
J190_191    8.8736   J 08Val_H2 08Val_H3   STAT=Y  PRED= 12.880 RANGE= 6.000
J191_192    6.5520   J 08Val_H3 08Val_H4   STAT=Y  PRED= 6.640 RANGE= 0.200
J191_195    6.7834   J 08Val_H3 08Val_H5   STAT=Y  PRED= 6.640 RANGE= 0.200
J201_202    7.6281   J 09Val_H2 09Val_H3   STAT=Y  PRED= 12.960 RANGE= 4.000
J202_203    6.4961   J 09Val_H3 09Val_H4   STAT=Y  PRED= 6.640 RANGE= 0.200
J202_206    6.7760   J 09Val_H3 09Val_H5   STAT=Y  PRED= 6.640 RANGE= 0.200
J212_213   11.1630   J 10Trp_H2 10TrpH3A   STAT=Y  PRED= 12.890 RANGE= 4.000
J212_214    4.7143   J 10Trp_H2 10TrpH3B   STAT=Y  PRED= 1.900 RANGE= 4.400
J213_214  -13.7295   J 10TrpH3A 10TrpH3B   STAT=Y  PRED= -16.760 RANGE= 2.560
J215_218    0.4880   J 10Trp_H5 10Trp_H7   STAT=Y  PRED= -0.300 RANGE= 0.500
J217_218    0.6708   J 10Trp_H9 10Trp_H7   STAT=Y  PRED= 1.020 RANGE= 1.200
J223_224    7.9094   J 11Val_H2 11Val_H3   STAT=Y  PRED= 3.450 RANGE= 9.000
J224_225    6.7483   J 11Val_H3 11Val_H4   STAT=Y  PRED= 6.640 RANGE= 0.200
J224_228    6.8064   J 11Val_H3 11Val_H5   STAT=Y  PRED= 6.640 RANGE= 0.200
J232_233    1.9005   J 12Phe_H2 12Phe_H3   STAT=Y  PRED= 1.900 RANGE= 6.600
J234_238    1.3335   J 12Phe_H5 12Phe_H5   STAT=Y  PRED= 1.980 RANGE= 1.200
J234_235    7.6508   J 12Phe_H5 12Phe_H6   STAT=Y  PRED= 7.660 RANGE= 0.340
J234_237    0.7769   J 12Phe_H6 12Phe_H5   STAT=Y  PRED= 0.550 RANGE= 0.750
J234_236    1.2760   J 12Phe_H5 12Phe_H7   STAT=Y  PRED= 1.260 RANGE= 1.200
J235_237    1.7027   J 12Phe_H6 12Phe_H6   STAT=Y  PRED= 1.480 RANGE= 1.200
J235_236    7.4760   J 12Phe_H6 12Phe_H7   STAT=Y  PRED= 7.400 RANGE= 0.240
J241_242    8.8924   J 13Val_H2 13Val_H3   STAT=Y  PRED= 12.320 RANGE= 6.000
J242_243    6.8372   J 13Val_H3 13Val_H4   STAT=Y  PRED= 6.640 RANGE= 0.200
J242_246    6.4162   J 13Val_H3 13Val_H5   STAT=Y  PRED= 6.640 RANGE= 0.200

CONTROL PARAMETERS:
      Solvent =  none (def. 99% enriched)
        1.000 =  Concentration (vol%, def=1.0%)
   0.00100000 =  Minimum line-intensity
   0.00100000 =  Diagonalization criterium (not in use)
  11.63298470 =  Left frequency (ppm)
  -4.33373638 =  Right frequency (ppm)
        0.000 =  Acquisition time (s, for QMTLS)
        0.715 =  Line-width (for modes D, P & T, 0=use defaults)
  0.103379714 =  Data-point resolution (Hz)
       28.306 =  GAUSSIAN (%, 0=use default from INF)
      -10.087 =  Dispersion contribution (%, 0=use default from INF)
   0.00000000 =  Decoupling frequency (for DORES)

CONSTRAINTS (in equations X0 = 1.0)...use no empty lines
 EQUAL 01Val_H2 = 13Val_H2
 EQUAL 06Val_H5 = 11Val_H4
 EQUAL 07Leu_H5 = 07Leu_H6
 IGNORE(HZ):   940.350 to   936.356
```

Appendix U (continued)

IGNORE(HZ): 2062.779 to 2027.293
IGNORE(HZ): 1175.285 to 1149.842
IGNORE(HZ): 1232.768 to 1209.210
IGNORE(HZ): 5188.061 to 5161.182
IGNORE(HZ): 4803.141 to 4787.420
IGNORE(HZ): 812.060 to 780.231

END of FILE

Appendix V. Pseudo HiFSA profile of homoecumicin-11I with one major impurity.

* NEW: the lines beginning by * are comment lines !
* To keep all the chemical shifts fixed during iteration
* replace "CHEMICAL SHIFTS(HZ):" by "..SHIFTS(HZ): fixed"
* The couplings can be fixed in the same way

NMR-data: C:\Users\jgnapo_2\Desktop\Wei_H14_XRays\H14_withoutGO
#$œ Date 20. 3.2014; Time 18:24:18 perch.pms

CHEMICAL SHIFTS(PPM):
PROTON 2*SPIN= 1 SPECIES=1H POPULATION(Y)= 0.68139

10Trp_H8/ 1 6.982643 1*1*1 STAT=Y PRED= 7.318 RANGE= 0.199 WIDTH(Y)= 1.531 RESP(Y)= 0.0434 HSQC= C74
01ValH45/ 1 2.331868 1*1*6 STAT=Y PRED= 2.370 RANGE= 0.306 WIDTH(Y)= 1.848 RESP(Y)= 0.0482 HSQC= C1_2
01Val_H2/ 1 2.705504 1*1*1 STAT=Y PRED= 4.169 RANGE= 0.636 WIDTH(Y)= 2.131 RESP(Y)= 0.0559 HSQC= C4
01Val_H3/ 1 2.049241 1*1*1 STAT=Y PRED= 1.952 RANGE= 0.817 WIDTH(Y)= 1.698 RESP(Y)= 0.0308 HSQC= C5
01Val_H6/ 1 0.852217 1*1*3 STAT=Y PRED= 0.509 RANGE= 0.867 WIDTH(Y)= 2.669 RESP(Y)= 0.0457 HSQC= C6
01Val_H7/ 1 0.977892 1*1*3 STAT=Y PRED= 0.818 RANGE= 0.356 WIDTH(Y)= 2.044 RESP(Y)= 0.0321 HSQC= C7
02Val_H2/ 1 4.670294 1*1*1 STAT=Y PRED= 4.508 RANGE= 0.807 WIDTH(Y)= 2.163 RESP(Y)= 0.0371 HSQC= C10
02Val_H3/ 1 2.107461 1*1*1 STAT=Y PRED= 2.155 RANGE= 0.777 WIDTH(Y)= 2.465 RESP(Y)= 0.0434 HSQC= C12
02Val_H4/ 1 0.996897 1*1*3 STAT=Y PRED= 1.038 RANGE= 0.279 WIDTH(Y)= 2.445 RESP(Y)= 0.0433 HSQC= C13
02Val_H5/ 1 1.059276 1*1*3 STAT=Y PRED= 0.943 RANGE= 0.249 WIDTH(Y)= 2.523 RESP(Y)= 0.0426 HSQC= C14
03Ile_H7/ 1 3.235379 1*1*3 STAT=Y PRED= 3.196 RANGE= 0.366 WIDTH(Y)= 2.575 RESP(Y)= 0.0473 HSQC= C15
03Ile_H2/ 1 4.914213 1*1*1 STAT=Y PRED= 4.617 RANGE= 1.627 WIDTH(Y)= 1.966 RESP(Y)= 0.0358 HSQC= C17
03Ile_H3/ 1 1.951239 1*1*1 STAT=Y PRED= 2.032 RANGE= 0.706 WIDTH(Y)= 2.986 RESP(Y)= 0.0484 HSQC= C19
03IleH4A/ 1 0.999098 1*1*1 STAT=Y PRED= 1.465 RANGE= 0.697 WIDTH(Y)= 6.181 RESP(Y)= 0.0500 HSQC= C20
03IleH4B/ 1 1.257083 1*1*1 STAT=Y PRED= 1.175 RANGE= 0.586 WIDTH(Y)= 2.801 RESP(Y)= 0.0344 HSQC= C20
03Ile_H6/ 1 0.756753 1*1*3 STAT=Y PRED= 0.723 RANGE= 0.396 WIDTH(Y)= 2.578 RESP(Y)= 0.0596 HSQC= C21
03Ile_H5/ 1 0.756000 1*1*3 STAT=Y PRED= 0.880 RANGE= 0.219 WIDTH(Y)= 2.951 RESP(Y)= 0.0493 HSQC= C22
04Thr_H2/ 1 5.168841 1*1*1 STAT=Y PRED= 4.668 RANGE= 1.013 WIDTH(Y)= 1.970 RESP(Y)= 0.0547 HSQC= C24
04Thr_H3/ 1 5.775699 1*1*1 STAT=Y PRED= 4.010 RANGE= 0.476 WIDTH(Y)= 2.145 RESP(Y)= 0.0372 HSQC= C25
04Thr_H4/ 1 1.311053 1*1*3 STAT=Y PRED= 1.270 RANGE= 0.496 WIDTH(Y)= 2.430 RESP(Y)= 0.0569 HSQC= C27
05Thr_H5/ 1 3.325073 1*1*3 STAT=Y PRED= 3.257 RANGE= 0.396 WIDTH(Y)= 2.259 RESP(Y)= 0.0476 HSQC= C29
05Thr_H2/ 1 4.998962 1*1*1 STAT=Y PRED= 4.099 RANGE= 1.023 WIDTH(Y)= 2.180 RESP(Y)= 0.0564 HSQC= C31
05Thr_H3/ 1 4.446938 1*1*1 STAT=Y PRED= 4.345 RANGE= 0.717 WIDTH(Y)= 3.186 RESP(Y)= 0.0551 HSQC= C32
05Thr_H4/ 1 0.912007 1*1*3 STAT=Y PRED= 1.252 RANGE= 0.299 WIDTH(Y)= 3.049 RESP(Y)= 0.0798 HSQC= C34
06Val_H2/ 1 4.863868 1*1*1 STAT=Y PRED= 4.525 RANGE= 1.407 WIDTH(Y)= 1.373 RESP(Y)= 0.0346 HSQC= C37
06Val_H3/ 1 2.363577 1*1*1 STAT=Y PRED= 1.975 RANGE= 1.017 WIDTH(Y)= 3.747 RESP(Y)= 0.0848 HSQC= C38
06Val_H4/ 1 1.087533 1*1*3 STAT=Y PRED= 0.938 RANGE= 0.219 WIDTH(Y)= 2.234 RESP(Y)= 0.0414 HSQC= C39
06Val_H5/ 1 0.984692 1*1*3 STAT=Y PRED= 1.094 RANGE= 0.386 WIDTH(Y)= 3.674 RESP(Y)= 0.0493 HSQC= C40
07Leu_H7/ 1 3.264469 1*1*3 STAT=Y PRED= 3.110 RANGE= 0.376 WIDTH(Y)= 1.765 RESP(Y)= 0.0399 HSQC= C42
07Leu_H2/ 1 5.132368 1*1*1 STAT=Y PRED= 5.342 RANGE= 1.083 WIDTH(Y)= 3.155 RESP(Y)= 0.0510 HSQC= C44
07LeuH3A/ 1 1.479530 1*1*1 STAT=Y PRED= 1.444 RANGE= 0.426 WIDTH(Y)= 2.570 RESP(Y)= 0.0493 HSQC= C45
07LeuH3B/ 1 1.231176 1*1*1 STAT=Y PRED= 1.914 RANGE= 0.366 WIDTH(Y)= 3.280 RESP(Y)= 0.0500 HSQC= C45
07Leu_H4/ 1 0.947227 1*1*1 STAT=Y PRED= 1.630 RANGE= 0.626 WIDTH(Y)= 0.965 RESP(Y)= 0.0509 HSQC= C46
07Leu_H5/ 1 0.363945 1*1*3 STAT=Y PRED= 0.972 RANGE= 0.316 WIDTH(Y)= 2.119 RESP(Y)= 0.0338 HSQC= C47
07Leu_H6/ 1 0.180620 1*1*3 STAT=Y PRED= 0.972 RANGE= 0.149 WIDTH(Y)= 2.566 RESP(Y)= 0.0366 HSQC= C48
08Val_H2/ 1 4.609611 1*1*1 STAT=Y PRED= 4.489 RANGE= 0.897 WIDTH(Y)= 2.553 RESP(Y)= 0.0556 HSQC= C51
08Val_H3/ 1 2.007773 1*1*1 STAT=Y PRED= 1.995 RANGE= 0.486 WIDTH(Y)= 2.850 RESP(Y)= 0.0533 HSQC= C52
08Val_H4/ 1 0.915823 1*1*3 STAT=Y PRED= 1.060 RANGE= 0.236 WIDTH(Y)= 2.169 RESP(Y)= 0.0519 HSQC= C53
08Val_H5/ 1 0.859328 1*1*3 STAT=Y PRED= 0.999 RANGE= 0.229 WIDTH(Y)= 2.452 RESP(Y)= 0.0385 HSQC= C54
09Val_H6/ 1 3.135974 1*1*3 STAT=Y PRED= 3.169 RANGE= 0.466 WIDTH(Y)= 2.404 RESP(Y)= 0.0393 HSQC= C56

Appendix V (continued)

09Val_H2/ 1 3.075521 1*1*1 STAT=Y PRED= 5.153 RANGE= 0.717 WIDTH(Y)= 2.468 RESP(Y)= 0.0439 HSQC= C58
09Val_H3/ 1 2.575990 1*1*1 STAT=Y PRED= 2.524 RANGE= 0.406 WIDTH(Y)= 2.500 RESP(Y)= 0.0313 HSQC= C59
09Val_H4/ 1 1.094712 1*1*3 STAT=Y PRED= 1.319 RANGE= 0.226 WIDTH(Y)= 3.272 RESP(Y)= 0.0345 HSQC= C60
09Val_H5/ 1 0.960940 1*1*3 STAT=Y PRED= 1.075 RANGE= 0.239 WIDTH(Y)= 2.928 RESP(Y)= 0.0372 HSQC= C61
10TrpH13/ 1 2.157534 1*1*3 STAT=Y PRED= 2.936 RANGE= 0.893 WIDTH(Y)= 1.955 RESP(Y)= 0.0418 HSQC= C63
10Trp_H2/ 1 4.118428 1*1*1 STAT=Y PRED= 5.043 RANGE= 1.764 WIDTH(Y)= 1.931 RESP(Y)= 0.0313 HSQC= C65
10TrpH3A/ 1 3.562472 1*1*1 STAT=Y PRED= 3.613 RANGE= 0.466 WIDTH(Y)= 3.217 RESP(Y)= 0.0533 HSQC= C66
10TrpH3B/ 1 3.690038 1*1*1 STAT=Y PRED= 3.367 RANGE= 0.626 WIDTH(Y)= 3.161 RESP(Y)= 0.0570 HSQC= C66
10Trp_H5/ 1 6.701943 1*1*1 STAT=Y PRED= 6.772 RANGE= 0.276 WIDTH(Y)= 1.783 RESP(Y)= 0.0411 HSQC= C68
10Trp_H9/ 1 6.443520 1*1*1 STAT=Y PRED= 7.089 RANGE= 0.219 WIDTH(Y)= 1.488 RESP(Y)= 0.0385 HSQC= C73
10Trp_H7/ 1 6.919385 1*1*1 STAT=Y PRED= 7.333 RANGE= 0.309 WIDTH(Y)= 1.091 RESP(Y)= 0.0548 HSQC= C75
10TrpH12/ 1 3.830224 1*1*3 STAT=Y PRED= 4.072 RANGE= 0.249 WIDTH(Y)= 1.508 RESP(Y)= 0.0416 HSQC= C77
11Val_H2/ 1 4.645899 1*1*1 STAT=Y PRED= 4.303 RANGE= 1.447 WIDTH(Y)= 2.214 RESP(Y)= 0.0424 HSQC= C80
11Val_H3/ 1 2.199515 1*1*1 STAT=Y PRED= 2.094 RANGE= 0.586 WIDTH(Y)= 1.854 RESP(Y)= 0.0317 HSQC= C81
11Val_H4/ 1 1.034837 1*1*3 STAT=Y PRED= 1.094 RANGE= 0.249 WIDTH(Y)= 3.830 RESP(Y)= 0.0218 HSQC= C82
11Val_H5/ 1 0.982491 1*1*3 STAT=Y PRED= 1.080 RANGE= 0.299 WIDTH(Y)= 1.785 RESP(Y)= 0.0662 HSQC= C83
12Phe_H2/ 1 4.919632 1*1*1 STAT=Y PRED= 4.499 RANGE= 0.987 WIDTH(Y)= 1.906 RESP(Y)= 0.0448 HSQC= C86
12Phe_H3/ 1 5.318783 1*1*1 STAT=Y PRED= 5.208 RANGE= 0.486 WIDTH(Y)= 1.884 RESP(Y)= 0.0429 HSQC= C87
12Phe_H5/ 1 7.228980 1*2*1 STAT=Y PRED= 7.524 RANGE= 0.309 WIDTH(Y)= 3.515 RESP(Y)= 0.0585 HSQC= C89_93
12Phe_H6/ 1 7.249518 1*2*1 STAT=Y PRED= 7.372 RANGE= 0.576 WIDTH(Y)= 1.860 RESP(Y)= 0.0573 HSQC= C90_92
12Phe_H7/ 1 7.195551 1*1*1 STAT=Y PRED= 7.281 RANGE= 0.309 WIDTH(Y)= 2.804 RESP(Y)= 0.0426 HSQC= C91
13Val_H2/ 1 4.408571 1*1*1 STAT=Y PRED= 4.169 RANGE= 0.667 WIDTH(Y)= 1.919 RESP(Y)= 0.0593 HSQC= C97
13Val_H3/ 1 1.966492 1*1*1 STAT=Y PRED= 1.935 RANGE= 0.867 WIDTH(Y)= 2.061 RESP(Y)= 0.0389 HSQC= C99
13Val_H4/ 1 0.929692 1*1*3 STAT=Y PRED= 1.277 RANGE= 0.219 WIDTH(Y)= 1.516 RESP(Y)= 0.0436 HSQC= C100
13Val_H5/ 1 0.922088 1*1*3 STAT=Y PRED= 0.933 RANGE= 0.276 WIDTH(Y)= 1.551 RESP(Y)= 0.0395 HSQC= C101
PROTON 2*SPIN= 1 SPECIES=1H POPULATION(Y)= 0.31861
10Y_H8 / 2 6.982487 1*1*1 STAT=Y PRED= 7.318 RANGE= 0.196 WIDTH(Y)= 1.715 RESP(Y)= 0.0372 HSQC= 2C74
01VH45 / 2 2.327979 1*1*6 STAT=Y PRED= 2.370 RANGE= 0.306 WIDTH(Y)= 3.925 RESP(Y)= 0.0242 HSQC= 2C1_2
01V_H2 / 2 2.700743 1*1*1 STAT=Y PRED= 4.169 RANGE= 0.636 WIDTH(Y)= 2.601 RESP(Y)= 0.0242 HSQC= 2C4
01V_H3 / 2 2.053752 1*1*1 STAT=Y PRED= 1.952 RANGE= 0.813 WIDTH(Y)= 2.327 RESP(Y)= 0.0242 HSQC= 2C5
01V_H6 / 2 0.847319 1*1*3 STAT=Y PRED= 0.509 RANGE= 0.863 WIDTH(Y)= 4.263 RESP(Y)= 0.0242 HSQC= 2C6
01V_H7 / 2 0.980928 1*1*3 STAT=Y PRED= 0.818 RANGE= 0.356 WIDTH(Y)= 2.396 RESP(Y)= 0.0242 HSQC= 2C7
02V_H2 / 2 4.666752 1*1*1 STAT=Y PRED= 4.508 RANGE= 0.803 WIDTH(Y)= 2.306 RESP(Y)= 0.0242 HSQC= 2C10
02V_H3 / 2 2.107949 1*1*1 STAT=Y PRED= 2.155 RANGE= 0.773 WIDTH(Y)= 3.331 RESP(Y)= 0.0242 HSQC= 2C12
02V_H4 / 2 1.006437 1*1*3 STAT=Y PRED= 1.038 RANGE= 0.276 WIDTH(Y)= 5.857 RESP(Y)= 0.0242 HSQC= 2C13
02V_H5 / 2 1.055337 1*1*3 STAT=Y PRED= 0.943 RANGE= 0.246 WIDTH(Y)= 4.052 RESP(Y)= 0.0242 HSQC= 2C14
03I_H7 / 2 3.242864 1*1*3 STAT=Y PRED= 3.196 RANGE= 0.366 WIDTH(Y)= 1.999 RESP(Y)= 0.0242 HSQC= 2C15
03I_H2 / 2 4.919119 1*1*1 STAT=Y PRED= 4.617 RANGE= 1.627 WIDTH(Y)= 3.875 RESP(Y)= 0.0385 HSQC= 2C17
03I_H3 / 2 1.969041 1*1*1 STAT=Y PRED= 2.155 RANGE= 0.773 WIDTH(Y)= 2.500 RESP(Y)= 0.0242 HSQC= 2C19
03IH4A / 2 0.935337 1*1*1 STAT=Y PRED= 1.465 RANGE= 0.697 WIDTH(Y)= 3.187 RESP(Y)= 0.0242 HSQC= 2C20
03IH4B / 2 1.260340 1*1*1 STAT=Y PRED= 1.175 RANGE= 0.586 WIDTH(Y)= 2.898 RESP(Y)= 0.0242 HSQC= 2C20
03I_H6 / 2 0.753797 1*1*3 STAT=Y PRED= 0.723 RANGE= 0.396 WIDTH(Y)= 1.677 RESP(Y)= 0.0217 HSQC= 2C21
03I_H5 / 2 0.790245 1*1*3 STAT=Y PRED= 0.880 RANGE= 0.216 WIDTH(Y)= 4.150 RESP(Y)= 0.0242 HSQC= 2C22
04T_H2 / 2 5.161237 1*1*1 STAT=Y PRED= 4.668 RANGE= 1.013 WIDTH(Y)= 2.253 RESP(Y)= 0.0296 HSQC= 2C24
04T_H3 / 2 5.783822 1*1*1 STAT=Y PRED= 4.010 RANGE= 0.476 WIDTH(Y)= 3.150 RESP(Y)= 0.0242 HSQC= 2C25
04T_H4 / 2 1.314452 1*1*3 STAT=Y PRED= 1.270 RANGE= 0.496 WIDTH(Y)= 4.501 RESP(Y)= 0.0242 HSQC= 2C27
05T_H5 / 2 3.329480 1*1*3 STAT=Y PRED= 3.257 RANGE= 0.396 WIDTH(Y)= 8.377 RESP(Y)= 0.0242 HSQC= 2C29
05T_H2 / 2 5.010823 1*1*1 STAT=Y PRED= 4.099 RANGE= 1.023 WIDTH(Y)= 4.736 RESP(Y)= 0.0242 HSQC= 2C31
05T_H3 / 2 4.448158 1*1*1 STAT=Y PRED= 4.345 RANGE= 0.717 WIDTH(Y)= 2.538 RESP(Y)= 0.0242 HSQC= 2C32
05T_H4 / 2 0.902516 1*1*3 STAT=Y PRED= 1.252 RANGE= 0.296 WIDTH(Y)= 5.903 RESP(Y)= 0.0242 HSQC= 2C34

Appendix V (continued)

06V_H2 / 2 4.858994 1*1*1 STAT=Y PRED= 4.525 RANGE= 1.404 WIDTH(Y)= 7.646 RESP(Y)= 0.0242 HSQC= 2C37
06V_H3 / 2 2.350618 1*1*1 STAT=Y PRED= 1.975 RANGE= 1.013 WIDTH(Y)= 0.266 RESP(Y)= 0.0242 HSQC= 2C38
06V_H4 / 2 1.109455 1*1*3 STAT=Y PRED= 0.938 RANGE= 0.216 WIDTH(Y)= 3.012 RESP(Y)= 0.0242 HSQC= 2C39
06V_H5 / 2 0.975957 1*1*3 STAT=Y PRED= 1.094 RANGE= 0.386 WIDTH(Y)= 2.654 RESP(Y)= 0.0242 HSQC= 2C40
07L_H7 / 2 3.258284 1*1*3 STAT=Y PRED= 3.110 RANGE= 0.373 WIDTH(Y)= 2.124 RESP(Y)= 0.0242 HSQC= 2C42
07L_H2 / 2 5.108018 1*1*1 STAT=Y PRED= 5.342 RANGE= 1.083 WIDTH(Y)= 2.130 RESP(Y)= 0.0242 HSQC= 2C44
07LH3A / 2 1.479333 1*1*1 STAT=Y PRED= 1.444 RANGE= 0.426 WIDTH(Y)= 1.890 RESP(Y)= 0.0242 HSQC= 2C45
07LH3B / 2 1.231226 1*1*1 STAT=Y PRED= 1.914 RANGE= 0.366 WIDTH(Y)= 3.308 RESP(Y)= 0.0242 HSQC= 2C45
07L_H4 / 2 0.955455 1*1*1 STAT=Y PRED= 1.630 RANGE= 0.626 WIDTH(Y)= 3.746 RESP(Y)= 0.0242 HSQC= 2C46
07L_H5 / 2 0.337172 1*1*3 STAT=Y PRED= 0.972 RANGE= 0.313 WIDTH(Y)= 2.985 RESP(Y)= 0.0242 HSQC= 2C47
07L_H6 / 2 0.170287 1*1*3 STAT=Y PRED= 0.972 RANGE= 0.146 WIDTH(Y)= 3.209 RESP(Y)= 0.0255 HSQC= 2C48
08V_H2 / 2 4.583431 1*1*1 STAT=Y PRED= 4.489 RANGE= 0.893 WIDTH(Y)= 4.045 RESP(Y)= 0.0242 HSQC= 2C51
08V_H3 / 2 2.034768 1*1*1 STAT=Y PRED= 1.995 RANGE= 0.483 WIDTH(Y)= 2.931 RESP(Y)= 0.0218 HSQC= 2C52
08V_H4 / 2 0.912094 1*1*3 STAT=Y PRED= 1.060 RANGE= 0.236 WIDTH(Y)= 1.807 RESP(Y)= 0.0385 HSQC= 2C53
08V_H5 / 2 0.867362 1*1*3 STAT=Y PRED= 0.999 RANGE= 0.226 WIDTH(Y)= 5.085 RESP(Y)= 0.0242 HSQC= 2C54
09V_H6 / 2 3.135922 1*1*3 STAT=Y PRED= 3.169 RANGE= 0.463 WIDTH(Y)= 2.284 RESP(Y)= 0.0242 HSQC= 2C56
09V_H2 / 2 3.069404 1*1*1 STAT=Y PRED= 5.153 RANGE= 0.717 WIDTH(Y)= 2.568 RESP(Y)= 0.0242 HSQC= 2C58
09V_H3 / 2 2.574331 1*1*1 STAT=Y PRED= 2.524 RANGE= 0.406 WIDTH(Y)= 2.994 RESP(Y)= 0.0242 HSQC= 2C59
09V_H4 / 2 1.109455 1*1*3 STAT=Y PRED= 1.319 RANGE= 0.226 WIDTH(Y)= 4.091 RESP(Y)= 0.0242 HSQC= 2C60
09V_H5 / 2 0.980536 1*1*3 STAT=Y PRED= 1.075 RANGE= 0.236 WIDTH(Y)= 1.921 RESP(Y)= 0.0242 HSQC= 2C61
10YH13 / 2 2.159626 1*1*3 STAT=Y PRED= 2.936 RANGE= 0.893 WIDTH(Y)= 4.052 RESP(Y)= 0.0304 HSQC= 2C63
10Y_H2 / 2 4.096628 1*1*1 STAT=Y PRED= 5.043 RANGE= 1.764 WIDTH(Y)= 2.600 RESP(Y)= 0.0242 HSQC= 2C65
10YH3A / 2 3.550258 1*1*1 STAT=Y PRED= 3.613 RANGE= 0.466 WIDTH(Y)= 2.945 RESP(Y)= 0.0242 HSQC= 2C66
10YH3B / 2 3.693523 1*1*1 STAT=Y PRED= 3.367 RANGE= 0.626 WIDTH(Y)= 2.200 RESP(Y)= 0.0242 HSQC= 2C66
10Y_H5 / 2 6.698463 1*1*1 STAT=Y PRED= 6.772 RANGE= 0.273 WIDTH(Y)= 1.735 RESP(Y)= 0.0209 HSQC= 2C68
10Y_H9 / 2 6.443096 1*1*1 STAT=Y PRED= 7.089 RANGE= 0.216 WIDTH(Y)= 1.345 RESP(Y)= 0.0242 HSQC= 2C73
10Y_H7 / 2 6.920633 1*1*1 STAT=Y PRED= 7.333 RANGE= 0.306 WIDTH(Y)= 0.543 RESP(Y)= 0.0242 HSQC= 2C75
10YH12 / 2 3.826339 1*1*3 STAT=Y PRED= 4.072 RANGE= 0.246 WIDTH(Y)= 1.765 RESP(Y)= 0.0284 HSQC= 2C77
11V_H2 / 2 4.527447 1*1*1 STAT=Y PRED= 4.303 RANGE= 1.444 WIDTH(Y)= 6.713 RESP(Y)= 0.0242 HSQC= 2C80
11V_H3 / 2 2.202592 1*1*1 STAT=Y PRED= 2.094 RANGE= 0.586 WIDTH(Y)= 1.728 RESP(Y)= 0.0242 HSQC= 2C81
11V_H4 / 2 1.028591 1*1*3 STAT=Y PRED= 1.094 RANGE= 0.246 WIDTH(Y)= 1.845 RESP(Y)= 0.0242 HSQC= 2C82
11V_H5 / 2 0.998058 1*1*3 STAT=Y PRED= 1.080 RANGE= 0.296 WIDTH(Y)= 6.575 RESP(Y)= 0.0242 HSQC= 2C83
12F_H2 / 2 4.917910 1*1*1 STAT=Y PRED= 4.499 RANGE= 0.983 WIDTH(Y)= 1.668 RESP(Y)= 0.0242 HSQC= 2C86
12F_H3 / 2 5.349701 1*1*1 STAT=Y PRED= 5.208 RANGE= 0.486 WIDTH(Y)= 2.979 RESP(Y)= 0.0242 HSQC= 2C87
12F_H5 / 2 7.241031 1*2*1 STAT=Y PRED= 7.524 RANGE= 0.306 WIDTH(Y)= 6.498 RESP(Y)= 0.0242 HSQC= 2C89_93
12F_H6 / 2 7.254214 1*2*1 STAT=Y PRED= 7.372 RANGE= 0.576 WIDTH(Y)= 1.698 RESP(Y)= 0.0242 HSQC= 2C90_92
12F_H7 / 2 7.200107 1*1*1 STAT=Y PRED= 7.281 RANGE= 0.306 WIDTH(Y)= 4.116 RESP(Y)= 0.0242 HSQC= 2C91
13V_H2 / 2 4.398304 1*1*1 STAT=Y PRED= 4.169 RANGE= 0.667 WIDTH(Y)= 2.132 RESP(Y)= 0.0242 HSQC= 2C97
13V_H3 / 2 1.969133 1*1*1 STAT=Y PRED= 2.155 RANGE= 0.773 WIDTH(Y)= 2.476 RESP(Y)= 0.0242 HSQC= 2C99
13V_H4 / 2 0.933567 1*1*3 STAT=Y PRED= 1.277 RANGE= 0.216 WIDTH(Y)= 1.198 RESP(Y)= 0.0203 HSQC= 2C100
13V_H5 / 2 0.919851 1*1*3 STAT=Y PRED= 0.933 RANGE= 0.276 WIDTH(Y)= 2.074 RESP(Y)= 0.0242 HSQC= 2C101

COUPLING CONSTANTS(HZ): fixed

J115_217 7.7969 J 10Trp_H8 10Trp_H9 STAT=Y PRED= 8.100 RANGE= 0.890
J115_218 8.1808 J 10Trp_H8 10Trp_H7 STAT=Y PRED= 7.850 RANGE= 0.800
J122_123 9.1737 J 01Val_H2 01Val_H3 STAT=Y PRED= 12.510 RANGE= 4.000
J123_124 6.5890 J 01Val_H3 01Val_H6 STAT=Y PRED= 6.640 RANGE= 0.200
J123_127 6.6205 J 01Val_H3 01Val_H7 STAT=Y PRED= 6.640 RANGE= 0.200
J131_132 8.7545 J 02Val_H2 02Val_H3 STAT=Y PRED= 12.600 RANGE= 6.000
J132_133 6.7841 J 02Val_H3 02Val_H4 STAT=Y PRED= 6.640 RANGE= 0.200

Appendix V (continued)

J132_136 6.7206 J 02Val_H3 02Val_H5 STAT=Y PRED= 6.640 RANGE= 0.200
J142_143 11.2297 J 03Ile_H2 03Ile_H3 STAT=Y PRED= 13.150 RANGE= 4.000
J143_144 0.4614 J 03Ile_H3 03IleH4A STAT=Y PRED= 1.950 RANGE= 3.000
J143_145 2.9276 J 03Ile_H3 03IleH4B STAT=Y PRED= 12.660 RANGE= 2.800
J143_146 6.6276 J 03Ile_H3 03Ile_H6 STAT=Y PRED= 6.640 RANGE= 0.200
J144_145 -12.2168 J 03IleH4A 03IleH4B STAT=Y PRED= -13.400 RANGE= 0.600
J144_149 7.2855 J 03IleH4A 03Ile_H5 STAT=Y PRED= 7.440 RANGE= 0.150
J145_149 7.6340 J 03IleH4B 03Ile_H5 STAT=Y PRED= 7.440 RANGE= 0.150
J153_154 2.3441 J 04Thr_H2 04Thr_H3 STAT=Y PRED= 2.690 RANGE= 6.600
J154_155 6.5134 J 04Thr_H3 04Thr_H4 STAT=Y PRED= 6.250 RANGE= 0.600
J161_162 3.7259 J 05Thr_H2 05Thr_H3 STAT=Y PRED= 2.440 RANGE= 4.400
J162_164 6.4691 J 05Thr_H3 05Thr_H4 STAT=Y PRED= 6.250 RANGE= 0.600
J168_169 8.9180 J 06Val_H2 06Val_H3 STAT=Y PRED= 2.980 RANGE= 6.600
J169_170 6.6944 J 06Val_H3 06Val_H4 STAT=Y PRED= 6.640 RANGE= 0.200
J169_173 7.0316 J 06Val_H3 06Val_H5 STAT=Y PRED= 6.640 RANGE= 0.200
J179_180 6.2437 J 07Leu_H2 07LeuH3A STAT=Y PRED= 3.040 RANGE= 6.000
J179_181 8.3839 J 07Leu_H2 07LeuH3B STAT=Y PRED= 13.950 RANGE= 4.000
J180_181 -13.3047 J 07LeuH3A 07LeuH3B STAT=Y PRED= -14.710 RANGE= 1.600
J180_182 8.2119 J 07LeuH3A 07Leu_H4 STAT=Y PRED= 12.990 RANGE= 2.560
J181_182 5.7896 J 07LeuH3B 07Leu_H4 STAT=Y PRED= 2.270 RANGE= 3.000
J182_183 6.5482 J 07Leu_H4 07Leu_H5 STAT=Y PRED= 6.640 RANGE= 0.200
J182_186 6.5879 J 07Leu_H4 07Leu_H6 STAT=Y PRED= 6.640 RANGE= 0.200
J190_191 8.8736 J 08Val_H2 08Val_H3 STAT=Y PRED= 12.880 RANGE= 6.000
J191_192 6.5520 J 08Val_H3 08Val_H4 STAT=Y PRED= 6.640 RANGE= 0.200
J191_195 6.7834 J 08Val_H3 08Val_H5 STAT=Y PRED= 6.640 RANGE= 0.200
J201_202 7.6281 J 09Val_H2 09Val_H3 STAT=Y PRED= 12.960 RANGE= 4.000
J202_203 6.4961 J 09Val_H3 09Val_H4 STAT=Y PRED= 6.640 RANGE= 0.200
J202_206 6.7760 J 09Val_H3 09Val_H5 STAT=Y PRED= 6.640 RANGE= 0.200
J212_213 11.1630 J 10Trp_H2 10TrpH3A STAT=Y PRED= 12.890 RANGE= 4.000
J212_214 4.7143 J 10Trp_H2 10TrpH3B STAT=Y PRED= 1.900 RANGE= 4.400
J213_214 -13.7295 J 10TrpH3A 10TrpH3B STAT=Y PRED= -16.760 RANGE= 2.560
J215_218 0.4880 J 10Trp_H5 10Trp_H7 STAT=Y PRED= -0.300 RANGE= 0.500
J217_218 0.6708 J 10Trp_H9 10Trp_H7 STAT=Y PRED= 1.020 RANGE= 1.200
J223_224 7.9094 J 11Val_H2 11Val_H3 STAT=Y PRED= 3.450 RANGE= 9.000
J224_225 6.7483 J 11Val_H3 11Val_H4 STAT=Y PRED= 6.640 RANGE= 0.200
J224_228 6.8064 J 11Val_H3 11Val_H5 STAT=Y PRED= 6.640 RANGE= 0.200
J232_233 1.9005 J 12Phe_H2 12Phe_H3 STAT=Y PRED= 1.900 RANGE= 6.600
J234_238 1.3335 J 12Phe_H5 12Phe_H5 STAT=Y PRED= 1.980 RANGE= 1.200
J234_235 7.6508 J 12Phe_H5 12Phe_H6 STAT=Y PRED= 7.660 RANGE= 0.340
J234_237 0.7769 J 12Phe_H6 12Phe_H5 STAT=Y PRED= 0.550 RANGE= 0.750
J234_236 1.2760 J 12Phe_H5 12Phe_H7 STAT=Y PRED= 1.260 RANGE= 1.200
J235_237 1.7027 J 12Phe_H6 12Phe_H6 STAT=Y PRED= 1.480 RANGE= 1.200
J235_236 7.4760 J 12Phe_H6 12Phe_H7 STAT=Y PRED= 7.400 RANGE= 0.240
J241_242 8.8924 J 13Val_H2 13Val_H3 STAT=Y PRED= 12.320 RANGE= 6.000
J242_243 6.8372 J 13Val_H3 13Val_H4 STAT=Y PRED= 6.640 RANGE= 0.200
J242_246 6.4162 J 13Val_H3 13Val_H5 STAT=Y PRED= 6.640 RANGE= 0.200
115_217 7.8190 J 10Y_H8 10Y_H9 STAT=Y PRED= 8.100 RANGE= 0.890
115_218 8.1817 J 10Y_H8 10Y_H7 STAT=Y PRED= 7.850 RANGE= 0.800
122_123 9.2123 J 01V_H2 01V_H3 STAT=Y PRED= 12.510 RANGE= 4.000
123_124 6.9596 J 01V_H3 01V_H6 STAT=Y PRED= 6.640 RANGE= 0.200

Appendix V (continued)

123_127 6.6826 J 01V_H3 01V_H7 STAT=Y PRED= 6.640 RANGE= 0.200
131_132 8.7392 J 02V_H2 02V_H3 STAT=Y PRED= 12.600 RANGE= 6.000
132_133 6.7456 J 02V_H3 02V_H4 STAT=Y PRED= 6.640 RANGE= 0.200
132_136 6.6587 J 02V_H3 02V_H5 STAT=Y PRED= 6.640 RANGE= 0.200
142_143 11.3172 J 03I_H2 03I_H3 STAT=Y PRED= 13.150 RANGE= 4.000
143_144 0.4615 J 03I_H3 03IH4A STAT=Y PRED= 1.950 RANGE= 3.000
143_145 2.7273 J 03I_H3 03IH4B STAT=Y PRED= 12.660 RANGE= 2.800
143_146 6.5602 J 03I_H3 03I_H6 STAT=Y PRED= 6.640 RANGE= 0.200
144_145 -12.4414 J 03IH4A 03IH4B STAT=Y PRED= -13.400 RANGE= 0.600
144_149 7.3376 J 03IH4A 03I_H5 STAT=Y PRED= 7.440 RANGE= 0.150
145_149 7.4487 J 03IH4B 03I_H5 STAT=Y PRED= 7.440 RANGE= 0.150
153_154 2.3513 J 04T_H2 04T_H3 STAT=Y PRED= 2.690 RANGE= 6.600
154_155 6.4912 J 04T_H3 04T_H4 STAT=Y PRED= 6.250 RANGE= 0.600
161_162 3.7198 J 05T_H2 05T_H3 STAT=Y PRED= 2.440 RANGE= 4.400
162_164 6.4861 J 05T_H3 05T_H4 STAT=Y PRED= 6.250 RANGE= 0.600
168_169 9.5371 J 06V_H2 06V_H3 STAT=Y PRED= 2.980 RANGE= 6.600
169_170 6.6359 J 06V_H3 06V_H4 STAT=Y PRED= 6.640 RANGE= 0.200
169_173 7.0196 J 06V_H3 06V_H5 STAT=Y PRED= 6.640 RANGE= 0.200
179_180 6.2454 J 07L_H2 07LH3A STAT=Y PRED= 3.040 RANGE= 6.000
179_181 8.3655 J 07L_H2 07LH3B STAT=Y PRED= 13.950 RANGE= 4.000
180_181 -13.2862 J 07LH3A 07LH3B STAT=Y PRED= -14.710 RANGE= 1.600
180_182 8.1966 J 07LH3A 07L_H4 STAT=Y PRED= 12.990 RANGE= 2.560
181_182 5.6475 J 07LH3B 07L_H4 STAT=Y PRED= 2.270 RANGE= 3.000
182_183 6.1444 J 07L_H4 07L_H5 STAT=Y PRED= 6.640 RANGE= 0.200
182_186 6.7639 J 07L_H4 07L_H6 STAT=Y PRED= 6.640 RANGE= 0.200
190_191 9.1785 J 08V_H2 08V_H3 STAT=Y PRED= 12.880 RANGE= 6.000
191_192 6.5252 J 08V_H3 08V_H4 STAT=Y PRED= 6.640 RANGE= 0.200
191_195 6.6198 J 08V_H3 08V_H5 STAT=Y PRED= 6.640 RANGE= 0.200
201_202 7.6271 J 09V_H2 09V_H3 STAT=Y PRED= 12.960 RANGE= 4.000
202_203 6.5511 J 09V_H3 09V_H4 STAT=Y PRED= 6.640 RANGE= 0.200
202_206 6.7993 J 09V_H3 09V_H5 STAT=Y PRED= 6.640 RANGE= 0.200
212_213 11.2213 J 10Y_H2 10YH3A STAT=Y PRED= 12.890 RANGE= 4.000
212_214 4.5999 J 10Y_H2 10YH3B STAT=Y PRED= 1.900 RANGE= 4.400
213_214 -13.7036 J 10YH3A 10YH3B STAT=Y PRED= -16.760 RANGE= 2.560
215_218 0.4722 J 10Y_H5 10Y_H7 STAT=Y PRED= -0.300 RANGE= 0.500
217_218 0.6202 J 10Y_H9 10Y_H7 STAT=Y PRED= 1.020 RANGE= 1.200
223_224 8.0434 J 11V_H2 11V_H3 STAT=Y PRED= 3.450 RANGE= 9.000
224_225 6.7574 J 11V_H3 11V_H4 STAT=Y PRED= 6.640 RANGE= 0.200
224_228 7.0071 J 11V_H3 11V_H5 STAT=Y PRED= 6.640 RANGE= 0.200
232_233 1.7657 J 12F_H2 12F_H3 STAT=Y PRED= 1.900 RANGE= 6.600
234_238 1.3347 J 12F_H5 12F_H5 STAT=Y PRED= 1.980 RANGE= 1.200
234_235 7.6929 J 12F_H5 12F_H6 STAT=Y PRED= 7.660 RANGE= 0.340
234_237 0.7971 J 12F_H6 12F_H5 STAT=Y PRED= 0.550 RANGE= 0.750
234_236 1.2586 J 12F_H5 12F_H7 STAT=Y PRED= 1.260 RANGE= 1.200
235_237 1.7100 J 12F_H6 12F_H6 STAT=Y PRED= 1.480 RANGE= 1.200
235_236 7.4191 J 12F_H6 12F_H7 STAT=Y PRED= 7.400 RANGE= 0.240
241_242 8.8889 J 13V_H2 13V_H3 STAT=Y PRED= 12.320 RANGE= 6.000
242_243 6.9574 J 13V_H3 13V_H4 STAT=Y PRED= 6.640 RANGE= 0.200
242_246 6.5087 J 13V_H3 13V_H5 STAT=Y PRED= 6.640 RANGE= 0.200

Appendix V (continued)

CONTROL PARAMETERS:
Solvent = none (def. 99% enriched)
1.000 = Concentration (vol%, def=1.0%)
0.00100000 = Minimum line-intensity
0.00100000 = Diagonalization criterium (not in use)
700.15197800 = FIELD(1H,MHz), used to transform shifts to ppms
11.63296542 = Left frequency (ppm)
-4.33374659 = Right frequency (ppm)
10.000 = Acquisition time (s, for QMTLS)
0.000 = Line-width (for modes D, P & T, 0=use defaults)
0.032885446 = Data-point resolution (Hz)
4.282 = GAUSSIAN (%, 0=use default from INF)
-6.865 = Dispersion contribution (%, 0=use default from INF)
0.00000000 = Decoupling frequency (for DORES)

CONSTRAINTS (in equations X0 = 1.0)...use no empty lines
EQUAL 01Val_H2 = 13Val_H2
EQUAL 06Val_H5 = 11Val_H4
EQUAL 07Leu_H5 = 07Leu_H6
EQUAL 06V_H4 = 09V_H4
IGNORE(HZ): 940.350 to 936.356
IGNORE(HZ): 2062.779 to 2027.293
IGNORE(HZ): 1175.285 to 1149.842
IGNORE(HZ): 1232.768 to 1209.210
IGNORE(HZ): 5188.061 to 5161.182
IGNORE(HZ): 4803.141 to 4787.420
IGNORE(HZ): 812.060 to 780.231
IGNORE(HZ): 1357.932 to 1354.940
IGNORE(HZ): 2348.723 to 2336.269
IGNORE(HZ): 1881.398 to 1875.582
IGNORE(HZ): 1995.608 to 1930.572
IGNORE(HZ): 2521.183 to 2514.310
IGNORE(HZ): 2560.840 to 2552.380
IGNORE(HZ): 2393.755 to 2377.364
IGNORE(HZ): 2254.166 to 2238.832
IGNORE(HZ): 2324.489 to 2302.282
IGNORE(HZ): 3471.125 to 3355.287

END of FILE

Appendix W. HiFSA profile of homoecumicin-11I.

* NEW: the lines beginning by * are comment lines !
* To keep all the chemical shifts fixed during iteration
* replace "CHEMICAL SHIFTS(HZ):" by "..SHIFTS(HZ): fixed"
* The couplings can be fixed in the same way

NMR-data: C:\Users\jgnapo_2\Desktop\Wei_H14_XRays\H14_withoutGO
#$œ Date 27. 3.2014; Time 16:58:31 perch.pms

CHEMICAL SHIFTS(PPM):
PROTON 2*SPIN= 1 SPECIES=1H POPULATION(Y)= 0.79121
10Trp_H8/ 1 6.982643 1*1*1 STAT=N PRED= 7.318 RANGE= 0.199 WIDTH(Y)= 1.215 RESP(Y)= 1.0000 HSQC= C74
01ValH45/ 1 2.331280 1*1*6 STAT=N PRED= 2.370 RANGE= 0.306 WIDTH(Y)= 1.536 RESP(Y)= 1.0000 HSQC= C1_2
01Val_H2/ 1 2.705188 1*1*1 STAT=N PRED= 4.169 RANGE= 0.636 WIDTH(Y)= 1.557 RESP(Y)= 1.0000 HSQC= C4
01Val_H3/ 1 2.044179 1*1*1 STAT=N PRED= 1.952 RANGE= 0.817 WIDTH(Y)= 1.561 RESP(Y)= 1.0000 HSQC= C5
01Val_H6/ 1 0.849588 1*1*3 STAT=N PRED= 0.509 RANGE= 0.867 WIDTH(Y)= 1.598 RESP(Y)= 1.0000 HSQC= C6
01Val_H7/ 1 0.980989 1*1*3 STAT=N PRED= 0.818 RANGE= 0.356 WIDTH(Y)= 1.688 RESP(Y)= 1.0000 HSQC= C7
02Val_H2/ 1 4.670147 1*1*1 STAT=N PRED= 4.508 RANGE= 0.807 WIDTH(Y)= 1.467 RESP(Y)= 1.0000 HSQC= C10
02Val_H3/ 1 2.108243 1*1*1 STAT=N PRED= 2.155 RANGE= 0.777 WIDTH(Y)= 1.561 RESP(Y)= 1.0000 HSQC= C12
02Val_H4/ 1 0.981760 1*1*3 STAT=N PRED= 1.038 RANGE= 0.279 WIDTH(Y)= 1.468 RESP(Y)= 1.0000 HSQC= C13
02Val_H5/ 1 1.058864 1*1*3 STAT=N PRED= 0.943 RANGE= 0.249 WIDTH(Y)= 1.538 RESP(Y)= 1.0000 HSQC= C14
03Ile_H7/ 1 3.235337 1*1*3 STAT=N PRED= 3.196 RANGE= 0.366 WIDTH(Y)= 1.536 RESP(Y)= 1.0000 HSQC= C15
03Ile_H2/ 1 4.907493 1*1*1 STAT=N PRED= 4.617 RANGE= 1.627 WIDTH(Y)= 1.466 RESP(Y)= 1.0000 HSQC= C17
03Ile_H3/ 1 1.951705 1*1*1 STAT=N PRED= 2.032 RANGE= 0.706 WIDTH(Y)= 2.929 RESP(Y)= 1.0000 HSQC= C19
03IleH4A/ 1 0.904202 1*1*1 STAT=N PRED= 1.465 RANGE= 0.697 WIDTH(Y)= 5.275 RESP(Y)= 1.0000 HSQC= C20
03IleH4B/ 1 1.244466 1*1*1 STAT=N PRED= 1.175 RANGE= 0.586 WIDTH(Y)= 2.795 RESP(Y)= 1.0000 HSQC= C20
03Ile_H6/ 1 0.760037 1*1*3 STAT=N PRED= 0.723 RANGE= 0.396 WIDTH(Y)= 1.613 RESP(Y)= 1.0000 HSQC= C21
03Ile_H5/ 1 0.750330 1*1*3 STAT=N PRED= 0.880 RANGE= 0.219 WIDTH(Y)= 1.391 RESP(Y)= 1.0000 HSQC= C22
04Thr_H2/ 1 5.168532 1*1*1 STAT=N PRED= 4.668 RANGE= 1.013 WIDTH(Y)= 1.377 RESP(Y)= 1.0000 HSQC= C24
04Thr_H3/ 1 5.779659 1*1*1 STAT=N PRED= 4.010 RANGE= 0.476 WIDTH(Y)= 1.941 RESP(Y)= 1.0000 HSQC= C25
04Thr_H4/ 1 1.311416 1*1*3 STAT=N PRED= 1.270 RANGE= 0.496 WIDTH(Y)= 1.818 RESP(Y)= 1.0000 HSQC= C27
05Thr_H5/ 1 3.325329 1*1*3 STAT=N PRED= 3.257 RANGE= 0.396 WIDTH(Y)= 1.439 RESP(Y)= 1.0000 HSQC= C29
05Thr_H2/ 1 4.999806 1*1*1 STAT=N PRED= 4.099 RANGE= 1.023 WIDTH(Y)= 1.500 RESP(Y)= 1.0000 HSQC= C31
05Thr_H3/ 1 4.444347 1*1*1 STAT=N PRED= 4.345 RANGE= 0.717 WIDTH(Y)= 1.572 RESP(Y)= 1.0000 HSQC= C32
05Thr_H4/ 1 0.911618 1*1*3 STAT=N PRED= 1.252 RANGE= 0.299 WIDTH(Y)= 1.939 RESP(Y)= 1.0000 HSQC= C34
06Val_H2/ 1 4.863987 1*1*1 STAT=N PRED= 4.525 RANGE= 1.407 WIDTH(Y)= 1.382 RESP(Y)= 1.0000 HSQC= C37
06Val_H3/ 1 2.341573 1*1*1 STAT=N PRED= 1.975 RANGE= 1.017 WIDTH(Y)= 1.789 RESP(Y)= 1.0000 HSQC= C38
06Val_H4/ 1 1.086573 1*1*3 STAT=N PRED= 0.938 RANGE= 0.219 WIDTH(Y)= 1.894 RESP(Y)= 1.0000 HSQC= C39
06Val_H5/ 1 0.985855 1*1*3 STAT=N PRED= 1.094 RANGE= 0.386 WIDTH(Y)= 2.275 RESP(Y)= 1.0000 HSQC= C40
07Leu_H7/ 1 3.264425 1*1*3 STAT=N PRED= 3.110 RANGE= 0.376 WIDTH(Y)= 1.459 RESP(Y)= 1.0000 HSQC= C42
07Leu_H2/ 1 5.132251 1*1*1 STAT=N PRED= 5.342 RANGE= 1.083 WIDTH(Y)= 2.240 RESP(Y)= 1.0000 HSQC= C44
07LeuH3A/ 1 1.470249 1*1*1 STAT=N PRED= 1.444 RANGE= 0.426 WIDTH(Y)= 1.805 RESP(Y)= 1.0000 HSQC= C45
07LeuH3B/ 1 1.231458 1*1*1 STAT=N PRED= 1.914 RANGE= 0.366 WIDTH(Y)= 3.321 RESP(Y)= 1.0000 HSQC= C45
07Leu_H4/ 1 0.927464 1*1*1 STAT=N PRED= 1.630 RANGE= 0.626 WIDTH(Y)= 1.520 RESP(Y)= 1.0000 HSQC= C46
07Leu_H5/ 1 0.363847 1*1*3 STAT=N PRED= 0.972 RANGE= 0.316 WIDTH(Y)= 1.961 RESP(Y)= 1.0000 HSQC= C47
07Leu_H6/ 1 0.180380 1*1*3 STAT=N PRED= 0.972 RANGE= 0.149 WIDTH(Y)= 1.885 RESP(Y)= 1.0000 HSQC= C48
08Val_H2/ 1 4.609585 1*1*1 STAT=N PRED= 4.489 RANGE= 0.897 WIDTH(Y)= 1.578 RESP(Y)= 1.0000 HSQC= C51
08Val_H3/ 1 1.987696 1*1*1 STAT=N PRED= 1.995 RANGE= 0.486 WIDTH(Y)= 2.872 RESP(Y)= 1.0000 HSQC= C52
08Val_H4/ 1 0.928532 1*1*3 STAT=N PRED= 1.060 RANGE= 0.236 WIDTH(Y)= 1.731 RESP(Y)= 1.0000 HSQC= C53
08Val_H5/ 1 0.861982 1*1*3 STAT=N PRED= 0.999 RANGE= 0.229 WIDTH(Y)= 2.065 RESP(Y)= 1.0000 HSQC= C54
09Val_H6/ 1 3.135917 1*1*3 STAT=N PRED= 3.169 RANGE= 0.466 WIDTH(Y)= 1.931 RESP(Y)= 1.0000 HSQC= C56

Appendix W (continued)

09Val_H2/ 1 3.065174 1*1*1 STAT=N PRED= 5.153 RANGE= 0.717 WIDTH(Y)= 2.597 RESP(Y)= 1.0000 HSQC= C58
09Val_H3/ 1 2.575838 1*1*1 STAT=N PRED= 2.524 RANGE= 0.406 WIDTH(Y)= 1.736 RESP(Y)= 1.0000 HSQC= C59
09Val_H4/ 1 1.094566 1*1*3 STAT=N PRED= 1.319 RANGE= 0.226 WIDTH(Y)= 1.741 RESP(Y)= 1.0000 HSQC= C60
09Val_H5/ 1 0.983397 1*1*3 STAT=N PRED= 1.075 RANGE= 0.239 WIDTH(Y)= 2.379 RESP(Y)= 1.0000 HSQC= C61
10TrpH13/ 1 2.157614 1*1*3 STAT=N PRED= 2.936 RANGE= 0.893 WIDTH(Y)= 1.862 RESP(Y)= 1.0000 HSQC= C63
10Trp_H2/ 1 4.114944 1*1*1 STAT=N PRED= 5.043 RANGE= 1.764 WIDTH(Y)= 2.064 RESP(Y)= 1.0000 HSQC= C65
10TrpH3A/ 1 3.564700 1*1*1 STAT=N PRED= 3.613 RANGE= 0.466 WIDTH(Y)= 1.516 RESP(Y)= 1.0000 HSQC= C66
10TrpH3B/ 1 3.692019 1*1*1 STAT=N PRED= 3.367 RANGE= 0.626 WIDTH(Y)= 2.118 RESP(Y)= 1.0000 HSQC= C66
10Trp_H5/ 1 6.701771 1*1*1 STAT=N PRED= 6.772 RANGE= 0.276 WIDTH(Y)= 1.649 RESP(Y)= 1.0000 HSQC= C68
10Trp_H9/ 1 6.443403 1*1*1 STAT=N PRED= 7.089 RANGE= 0.219 WIDTH(Y)= 1.143 RESP(Y)= 1.0000 HSQC= C73
10Trp_H7/ 1 6.919434 1*1*1 STAT=N PRED= 7.333 RANGE= 0.309 WIDTH(Y)= 0.719 RESP(Y)= 1.0000 HSQC= C75
10TrpH12/ 1 3.830106 1*1*3 STAT=N PRED= 4.072 RANGE= 0.249 WIDTH(Y)= 1.244 RESP(Y)= 1.0000 HSQC= C77
11Ile_H2/ 1 4.645948 1*1*1 STAT=N PRED= 4.303 RANGE= 1.447 WIDTH(Y)= 1.849 RESP(Y)= 1.0000 HSQC= C80
11Ile_H3/ 1 1.963073 1*1*1 STAT=N PRED= 2.094 RANGE= 0.586 WIDTH(Y)= 1.854 RESP(Y)= 1.0000 HSQC= C81
11IleH4A/ 1 1.577140 1*1*3 STAT=N PRED= 1.094 RANGE= 0.249 WIDTH(Y)= 2.106 RESP(Y)= 1.0000 HSQC= C82
11IleH4B/ 1 1.222059 1*1*3 STAT=N PRED= 1.080 RANGE= 0.299 WIDTH(Y)= 1.787 RESP(Y)= 1.0000 HSQC= C82
11Ile_H5/ 1 0.915100 1*1*3 STAT=N PRED= 1.080 RANGE= 0.299 WIDTH(Y)= 1.787 RESP(Y)= 1.0000 HSQC= C83
11Ile_H6/ 1 0.990779 1*1*3 STAT=N PRED= 1.080 RANGE= 0.299 WIDTH(Y)= 1.787 RESP(Y)= 1.0000 HSQC= C84
12Phe_H2/ 1 4.920692 1*1*1 STAT=N PRED= 4.499 RANGE= 0.987 WIDTH(Y)= 1.261 RESP(Y)= 1.0000 HSQC= C86
12Phe_H3/ 1 5.318327 1*1*1 STAT=N PRED= 5.208 RANGE= 0.486 WIDTH(Y)= 1.884 RESP(Y)= 1.0000 HSQC= C87
12Phe_H5/ 1 7.229493 1*2*1 STAT=N PRED= 7.524 RANGE= 0.309 WIDTH(Y)= 2.042 RESP(Y)= 1.0000 HSQC= C89_93
12Phe_H6/ 1 7.249523 1*2*1 STAT=N PRED= 7.372 RANGE= 0.576 WIDTH(Y)= 1.207 RESP(Y)= 1.0000 HSQC= C90_92
12Phe_H7/ 1 7.195963 1*1*1 STAT=N PRED= 7.281 RANGE= 0.309 WIDTH(Y)= 1.557 RESP(Y)= 1.0000 HSQC= C91
13Val_H2/ 1 4.408276 1*1*1 STAT=N PRED= 4.169 RANGE= 0.667 WIDTH(Y)= 1.205 RESP(Y)= 1.0000 HSQC= C97
13Val_H3/ 1 1.962989 1*1*1 STAT=N PRED= 1.935 RANGE= 0.867 WIDTH(Y)= 1.973 RESP(Y)= 1.0000 HSQC= C99
13Val_H4/ 1 0.944236 1*1*3 STAT=N PRED= 1.277 RANGE= 0.219 WIDTH(Y)= 2.666 RESP(Y)= 1.0000 HSQC= C100
13Val_H5/ 1 0.915347 1*1*3 STAT=N PRED= 0.933 RANGE= 0.276 WIDTH(Y)= 2.083 RESP(Y)= 1.0000 HSQC= C101
PROTON 2*SPIN= 1 SPECIES=1H POPULATION(Y)= 0.20879
10Y_H8 / 2 6.985259 1*1*1 STAT=Y PRED= 7.318 RANGE= 0.196 WIDTH(Y)= 1.715 RESP(Y)= 1.0000 HSQC= 2C74
01VH45 / 2 2.326612 1*1*6 STAT=Y PRED= 2.370 RANGE= 0.306 WIDTH(Y)= 3.925 RESP(Y)= 1.0000 HSQC= 2C1_2
01V_H2 / 2 2.699528 1*1*1 STAT=Y PRED= 4.169 RANGE= 0.636 WIDTH(Y)= 2.601 RESP(Y)= 1.0000 HSQC= 2C4
01V_H3 / 2 2.052235 1*1*1 STAT=Y PRED= 1.952 RANGE= 0.813 WIDTH(Y)= 2.327 RESP(Y)= 1.0000 HSQC= 2C5
01V_H6 / 2 0.844488 1*1*3 STAT=Y PRED= 0.509 RANGE= 0.863 WIDTH(Y)= 4.263 RESP(Y)= 1.0000 HSQC= 2C6
01V_H7 / 2 0.975325 1*1*3 STAT=Y PRED= 0.818 RANGE= 0.356 WIDTH(Y)= 2.396 RESP(Y)= 1.0000 HSQC= 2C7
02V_H2 / 2 4.666002 1*1*1 STAT=Y PRED= 4.508 RANGE= 0.803 WIDTH(Y)= 2.306 RESP(Y)= 1.0000 HSQC= 2C10
02V_H3 / 2 2.102348 1*1*1 STAT=Y PRED= 2.155 RANGE= 0.773 WIDTH(Y)= 3.331 RESP(Y)= 1.0000 HSQC= 2C12
02V_H4 / 2 1.020790 1*1*3 STAT=Y PRED= 1.038 RANGE= 0.276 WIDTH(Y)= 5.857 RESP(Y)= 1.0000 HSQC= 2C13
02V_H5 / 2 1.036172 1*1*3 STAT=Y PRED= 0.943 RANGE= 0.246 WIDTH(Y)= 4.052 RESP(Y)= 1.0000 HSQC= 2C14
03I_H7 / 2 3.241211 1*1*3 STAT=Y PRED= 3.196 RANGE= 0.366 WIDTH(Y)= 1.999 RESP(Y)= 1.0000 HSQC= 2C15
03I_H2 / 2 4.918370 1*1*1 STAT=Y PRED= 4.617 RANGE= 1.627 WIDTH(Y)= 3.875 RESP(Y)= 1.0000 HSQC= 2C17
03I_H3 / 2 1.968469 1*1*1 STAT=Y PRED= 2.155 RANGE= 0.773 WIDTH(Y)= 2.500 RESP(Y)= 1.0000 HSQC= 2C19
03IH4A / 2 0.902958 1*1*1 STAT=Y PRED= 1.465 RANGE= 0.697 WIDTH(Y)= 3.187 RESP(Y)= 1.0000 HSQC= 2C20
03IH4B / 2 1.285777 1*1*1 STAT=Y PRED= 1.175 RANGE= 0.586 WIDTH(Y)= 2.898 RESP(Y)= 1.0000 HSQC= 2C20
03I_H6 / 2 0.749462 1*1*3 STAT=Y PRED= 0.723 RANGE= 0.396 WIDTH(Y)= 1.677 RESP(Y)= 1.0000 HSQC= 2C21
03I_H5 / 2 0.789981 1*1*3 STAT=Y PRED= 0.880 RANGE= 0.216 WIDTH(Y)= 4.150 RESP(Y)= 1.0000 HSQC= 2C22
04T_H2 / 2 5.159046 1*1*1 STAT=Y PRED= 4.668 RANGE= 1.013 WIDTH(Y)= 2.253 RESP(Y)= 1.0000 HSQC= 2C24
04T_H3 / 2 5.795922 1*1*1 STAT=Y PRED= 4.010 RANGE= 0.476 WIDTH(Y)= 3.150 RESP(Y)= 1.0000 HSQC= 2C25
04T_H4 / 2 1.316114 1*1*3 STAT=Y PRED= 1.270 RANGE= 0.496 WIDTH(Y)= 2.500 RESP(Y)= 1.0000 HSQC= 2C27
05T_H5 / 2 3.330396 1*1*3 STAT=Y PRED= 3.257 RANGE= 0.396 WIDTH(Y)= 8.377 RESP(Y)= 1.0000 HSQC= 2C29
05T_H2 / 2 5.016384 1*1*1 STAT=Y PRED= 4.099 RANGE= 1.023 WIDTH(Y)= 4.736 RESP(Y)= 1.0000 HSQC= 2C31

Appendix W (continued)

```
05T_H3  / 2    4.462465  1*1*1  STAT=Y  PRED= 4.345 RANGE= 0.717 WIDTH(Y)= 2.538 RESP(Y)= 1.0000 HSQC= 2C32
05T_H4  / 2    0.880590  1*1*3  STAT=Y  PRED= 1.252 RANGE= 0.296 WIDTH(Y)= 5.903 RESP(Y)= 1.0000 HSQC= 2C34
06V_H2  / 2    4.846034  1*1*1  STAT=Y  PRED= 4.525 RANGE= 1.404 WIDTH(Y)= 7.646 RESP(Y)= 1.0000 HSQC= 2C37
06V_H3  / 2    2.354183  1*1*1  STAT=Y  PRED= 1.975 RANGE= 1.013 WIDTH(Y)= 0.266 RESP(Y)= 1.0000 HSQC= 2C38
06V_H4  / 2    1.110907  1*1*3  STAT=Y  PRED= 0.938 RANGE= 0.216 WIDTH(Y)= 3.012 RESP(Y)= 1.0000 HSQC= 2C39
06V_H5  / 2    0.923585  1*1*3  STAT=Y  PRED= 1.094 RANGE= 0.386 WIDTH(Y)= 2.654 RESP(Y)= 1.0000 HSQC= 2C40
07L_H7  / 2    3.250897  1*1*3  STAT=Y  PRED= 3.110 RANGE= 0.373 WIDTH(Y)= 2.124 RESP(Y)= 1.0000 HSQC= 2C42
07L_H2  / 2    5.104425  1*1*1  STAT=Y  PRED= 5.342 RANGE= 1.083 WIDTH(Y)= 2.130 RESP(Y)= 1.0000 HSQC= 2C44
07LH3A  / 2    1.506878  1*1*1  STAT=Y  PRED= 1.444 RANGE= 0.426 WIDTH(Y)= 1.890 RESP(Y)= 1.0000 HSQC= 2C45
07LH3B  / 2    1.232980  1*1*1  STAT=Y  PRED= 1.914 RANGE= 0.366 WIDTH(Y)= 3.308 RESP(Y)= 1.0000 HSQC= 2C45
07L_H4  / 2    0.905984  1*1*1  STAT=Y  PRED= 1.630 RANGE= 0.626 WIDTH(Y)= 3.746 RESP(Y)= 1.0000 HSQC= 2C46
07L_H5  / 2    0.336687  1*1*3  STAT=Y  PRED= 0.972 RANGE= 0.313 WIDTH(Y)= 2.985 RESP(Y)= 1.0000 HSQC= 2C47
07L_H6  / 2    0.163898  1*1*3  STAT=Y  PRED= 0.972 RANGE= 0.146 WIDTH(Y)= 3.209 RESP(Y)= 1.0000 HSQC= 2C48
08V_H2  / 2    4.582563  1*1*1  STAT=Y  PRED= 4.489 RANGE= 0.893 WIDTH(Y)= 4.045 RESP(Y)= 1.0000 HSQC= 2C51
08V_H3  / 2    2.035162  1*1*1  STAT=Y  PRED= 1.995 RANGE= 0.483 WIDTH(Y)= 2.931 RESP(Y)= 1.0000 HSQC= 2C52
08V_H4  / 2    0.895459  1*1*3  STAT=Y  PRED= 1.060 RANGE= 0.236 WIDTH(Y)= 1.807 RESP(Y)= 1.0000 HSQC= 2C53
08V_H5  / 2    0.855337  1*1*3  STAT=Y  PRED= 0.999 RANGE= 0.226 WIDTH(Y)= 5.085 RESP(Y)= 1.0000 HSQC= 2C54
09V_H6  / 2    3.149425  1*1*3  STAT=Y  PRED= 3.169 RANGE= 0.463 WIDTH(Y)= 2.284 RESP(Y)= 1.0000 HSQC= 2C56
09V_H2  / 2    3.082134  1*1*1  STAT=Y  PRED= 5.153 RANGE= 0.717 WIDTH(Y)= 2.568 RESP(Y)= 1.0000 HSQC= 2C58
09V_H3  / 2    2.571644  1*1*1  STAT=Y  PRED= 2.524 RANGE= 0.406 WIDTH(Y)= 2.994 RESP(Y)= 1.0000 HSQC= 2C59
09V_H4  / 2    1.110907  1*1*3  STAT=Y  PRED= 1.319 RANGE= 0.226 WIDTH(Y)= 4.091 RESP(Y)= 1.0000 HSQC= 2C60
09V_H5  / 2    0.950395  1*1*3  STAT=Y  PRED= 1.075 RANGE= 0.236 WIDTH(Y)= 1.921 RESP(Y)= 1.0000 HSQC= 2C61
10YH13  / 2    2.168525  1*1*3  STAT=Y  PRED= 2.936 RANGE= 0.893 WIDTH(Y)= 4.052 RESP(Y)= 1.0000 HSQC= 2C63
10Y_H2  / 2    4.085846  1*1*1  STAT=Y  PRED= 5.043 RANGE= 1.764 WIDTH(Y)= 2.600 RESP(Y)= 1.0000 HSQC= 2C65
10YH3A  / 2    3.552700  1*1*1  STAT=Y  PRED= 3.613 RANGE= 0.466 WIDTH(Y)= 2.945 RESP(Y)= 1.0000 HSQC= 2C66
10YH3B  / 2    3.682365  1*1*1  STAT=Y  PRED= 3.367 RANGE= 0.626 WIDTH(Y)= 2.200 RESP(Y)= 1.0000 HSQC= 2C66
10Y_H5  / 2    6.694561  1*1*1  STAT=Y  PRED= 6.772 RANGE= 0.273 WIDTH(Y)= 1.735 RESP(Y)= 1.0000 HSQC= 2C68
10Y_H9  / 2    6.450117  1*1*1  STAT=Y  PRED= 7.089 RANGE= 0.216 WIDTH(Y)= 1.345 RESP(Y)= 1.0000 HSQC= 2C73
10Y_H7  / 2    6.925836  1*1*1  STAT=Y  PRED= 7.333 RANGE= 0.306 WIDTH(Y)= 0.543 RESP(Y)= 1.0000 HSQC= 2C75
10YH12  / 2    3.813110  1*1*3  STAT=Y  PRED= 4.072 RANGE= 0.246 WIDTH(Y)= 1.765 RESP(Y)= 1.0000 HSQC= 2C77
11V_H2  / 2    4.527238  1*1*1  STAT=Y  PRED= 4.303 RANGE= 1.444 WIDTH(Y)= 6.713 RESP(Y)= 1.0000 HSQC= 2C80
11V_H3  / 2    2.202615  1*1*1  STAT=Y  PRED= 2.094 RANGE= 0.586 WIDTH(Y)= 1.728 RESP(Y)= 1.0000 HSQC= 2C81
11V_H4  / 2    1.007226  1*1*3  STAT=Y  PRED= 1.094 RANGE= 0.246 WIDTH(Y)= 1.845 RESP(Y)= 1.0000 HSQC= 2C82
11V_H5  / 2    1.010476  1*1*3  STAT=Y  PRED= 1.080 RANGE= 0.296 WIDTH(Y)= 6.575 RESP(Y)= 1.0000 HSQC= 2C83
12F_H2  / 2    4.919442  1*1*1  STAT=Y  PRED= 4.499 RANGE= 0.983 WIDTH(Y)= 1.668 RESP(Y)= 1.0000 HSQC= 2C86
12F_H3  / 2    5.349017  1*1*1  STAT=Y  PRED= 5.208 RANGE= 0.486 WIDTH(Y)= 2.979 RESP(Y)= 1.0000 HSQC= 2C87
12F_H5  / 2    7.241206  1*2*1  STAT=Y  PRED= 7.524 RANGE= 0.306 WIDTH(Y)= 6.498 RESP(Y)= 1.0000 HSQC= 2C89_93
12F_H6  / 2    7.266658  1*2*1  STAT=Y  PRED= 7.372 RANGE= 0.576 WIDTH(Y)= 1.698 RESP(Y)= 1.0000 HSQC= 2C90_92
12F_H7  / 2    7.202917  1*1*1  STAT=Y  PRED= 7.281 RANGE= 0.306 WIDTH(Y)= 4.116 RESP(Y)= 1.0000 HSQC= 2C91
13V_H2  / 2    4.398051  1*1*1  STAT=Y  PRED= 4.169 RANGE= 0.667 WIDTH(Y)= 2.132 RESP(Y)= 1.0000 HSQC= 2C97
13V_H3  / 2    1.967932  1*1*1  STAT=Y  PRED= 2.155 RANGE= 0.773 WIDTH(Y)= 2.476 RESP(Y)= 1.0000 HSQC= 2C99
13V_H4  / 2    0.921909  1*1*3  STAT=Y  PRED= 1.277 RANGE= 0.216 WIDTH(Y)= 1.198 RESP(Y)= 1.0000 HSQC= 2C100
13V_H5  / 2    0.908608  1*1*3  STAT=Y  PRED= 0.933 RANGE= 0.276 WIDTH(Y)= 2.074 RESP(Y)= 1.0000 HSQC= 2C101

COUPLING CONSTANTS(HZ): fixed
J115_217    7.7969   J 10Trp_H8 10Trp_H9   STAT=Y  PRED= 8.100 RANGE= 0.890
J115_218    8.1808   J 10Trp_H8 10Trp_H7   STAT=Y  PRED= 7.850 RANGE= 0.800
J122_123    9.1737   J 01Val_H2 01Val_H3   STAT=Y  PRED= 12.510 RANGE= 4.000
J123_124    6.5890   J 01Val_H3 01Val_H6   STAT=Y  PRED= 6.640 RANGE= 0.200
J123_127    6.6205   J 01Val_H3 01Val_H7   STAT=Y  PRED= 6.640 RANGE= 0.200
```

Appendix W (continued)

J131_132 8.7545 J 02Val_H2 02Val_H3 STAT=Y PRED= 12.600 RANGE= 6.000
J132_133 6.7841 J 02Val_H3 02Val_H4 STAT=Y PRED= 6.640 RANGE= 0.200
J132_136 6.7206 J 02Val_H3 02Val_H5 STAT=Y PRED= 6.640 RANGE= 0.200
J142_143 11.2297 J 03Ile_H2 03Ile_H3 STAT=Y PRED= 13.150 RANGE= 4.000
J143_144 0.4614 J 03Ile_H3 03IleH4A STAT=Y PRED= 1.950 RANGE= 3.000
J143_145 2.9276 J 03Ile_H3 03IleH4B STAT=Y PRED= 12.660 RANGE= 2.800
J143_146 6.6276 J 03Ile_H3 03Ile_H6 STAT=Y PRED= 6.640 RANGE= 0.200
J144_145 -12.2168 J 03IleH4A 03IleH4B STAT=Y PRED= -13.400 RANGE= 0.600
J144_149 7.2855 J 03IleH4A 03Ile_H5 STAT=Y PRED= 7.440 RANGE= 0.150
J145_149 7.6340 J 03IleH4B 03Ile_H5 STAT=Y PRED= 7.440 RANGE= 0.150
J153_154 2.3441 J 04Thr_H2 04Thr_H3 STAT=Y PRED= 2.690 RANGE= 6.600
J154_155 6.5134 J 04Thr_H3 04Thr_H4 STAT=Y PRED= 6.250 RANGE= 0.600
J161_162 3.7259 J 05Thr_H2 05Thr_H3 STAT=Y PRED= 2.440 RANGE= 4.400
J162_164 6.4691 J 05Thr_H3 05Thr_H4 STAT=Y PRED= 6.250 RANGE= 0.600
J168_169 8.9180 J 06Val_H2 06Val_H3 STAT=Y PRED= 2.980 RANGE= 6.600
J169_170 6.6944 J 06Val_H3 06Val_H4 STAT=Y PRED= 6.640 RANGE= 0.200
J169_173 7.0316 J 06Val_H3 06Val_H5 STAT=Y PRED= 6.640 RANGE= 0.200
J179_180 6.2437 J 07Leu_H2 07LeuH3A STAT=Y PRED= 3.040 RANGE= 6.000
J179_181 8.3839 J 07Leu_H2 07LeuH3B STAT=Y PRED= 13.950 RANGE= 4.000
J180_181 -13.3047 J 07LeuH3A 07LeuH3B STAT=Y PRED= -14.710 RANGE= 1.600
J180_182 8.2119 J 07LeuH3A 07Leu_H4 STAT=Y PRED= 12.990 RANGE= 2.560
J181_182 5.7896 J 07LeuH3B 07Leu_H4 STAT=Y PRED= 2.270 RANGE= 3.000
J182_183 6.5482 J 07Leu_H4 07Leu_H5 STAT=Y PRED= 6.640 RANGE= 0.200
J182_186 6.5879 J 07Leu_H4 07Leu_H6 STAT=Y PRED= 6.640 RANGE= 0.200
J190_191 8.8736 J 08Val_H2 08Val_H3 STAT=Y PRED= 12.880 RANGE= 6.000
J191_192 6.5520 J 08Val_H3 08Val_H4 STAT=Y PRED= 6.640 RANGE= 0.200
J191_195 6.7834 J 08Val_H3 08Val_H5 STAT=Y PRED= 6.640 RANGE= 0.200
237 0.0000 J 08Val_H4 09Val_H4 STAT=Y
J201_202 7.6281 J 09Val_H2 09Val_H3 STAT=Y PRED= 12.960 RANGE= 4.000
J202_203 6.4961 J 09Val_H3 09Val_H4 STAT=Y PRED= 6.640 RANGE= 0.200
J202_206 6.7760 J 09Val_H3 09Val_H5 STAT=Y PRED= 6.640 RANGE= 0.200
J212_213 11.1630 J 10Trp_H2 10TrpH3A STAT=Y PRED= 12.890 RANGE= 4.000
J212_214 4.7143 J 10Trp_H2 10TrpH3B STAT=Y PRED= 1.900 RANGE= 4.400
J213_214 -13.7295 J 10TrpH3A 10TrpH3B STAT=Y PRED= -16.760 RANGE= 2.560
J215_218 0.4880 J 10Trp_H5 10Trp_H7 STAT=Y PRED= -0.300 RANGE= 0.500
J217_218 0.6708 J 10Trp_H9 10Trp_H7 STAT=Y PRED= 1.020 RANGE= 1.200
J223_224 7.1764 J 11Ile_H2 11Ile_H3 STAT=Y PRED= 3.450 RANGE= 9.000
J224_225 11.6481 J 11Ile_H3 11IleH4A STAT=Y PRED= 6.640 RANGE= 0.200
J224225B 8.6548 J 11Ile_H3 11IleH4B STAT=Y PRED= 6.640 RANGE= 0.200
J224_228 6.8064 J 11Ile_H3 11Ile_H5 STAT=N PRED= 6.640 RANGE= 0.200
J225AB -15.2022 J 11IleH4A 11IleH4B STAT=Y PRED= 6.640 RANGE= 0.200
225_229 6.5064 J 11IleH4A 11Ile_H6 STAT=N PRED= 6.640 RANGE= 0.200
225B229 6.8064 J 11IleH4B 11Ile_H6 STAT=N PRED= 6.640 RANGE= 0.200
J232_233 1.9005 J 12Phe_H2 12Phe_H3 STAT=Y PRED= 1.900 RANGE= 6.600
J234_238 1.3335 J 12Phe_H5 12Phe_H5 STAT=Y PRED= 1.980 RANGE= 1.200
J234_235 7.6508 J 12Phe_H5 12Phe_H6 STAT=Y PRED= 7.660 RANGE= 0.340
J234_237 0.7769 J 12Phe_H6 12Phe_H5 STAT=Y PRED= 0.550 RANGE= 0.750
J234_236 1.2760 J 12Phe_H5 12Phe_H7 STAT=Y PRED= 1.260 RANGE= 1.200
J235_237 1.7027 J 12Phe_H6 12Phe_H6 STAT=Y PRED= 1.480 RANGE= 1.200
J235_236 7.4760 J 12Phe_H6 12Phe_H7 STAT=Y PRED= 7.400 RANGE= 0.240

Appendix W (continued)

J241_242 8.8924 J 13Val_H2 13Val_H3 STAT=Y PRED= 12.320 RANGE= 6.000
J242_243 6.8372 J 13Val_H3 13Val_H4 STAT=Y PRED= 6.640 RANGE= 0.200
J242_246 6.4162 J 13Val_H3 13Val_H5 STAT=Y PRED= 6.640 RANGE= 0.200
115_217 7.8190 J 10Y_H8 10Y_H9 STAT=Y PRED= 8.100 RANGE= 0.890
115_218 8.1817 J 10Y_H8 10Y_H7 STAT=Y PRED= 7.850 RANGE= 0.800
122_123 9.2123 J 01V_H2 01V_H3 STAT=Y PRED= 12.510 RANGE= 4.000
123_124 6.9596 J 01V_H3 01V_H6 STAT=Y PRED= 6.640 RANGE= 0.200
123_127 6.6826 J 01V_H3 01V_H7 STAT=Y PRED= 6.640 RANGE= 0.200
131_132 8.7392 J 02V_H2 02V_H3 STAT=Y PRED= 12.600 RANGE= 6.000
132_133 6.7456 J 02V_H3 02V_H4 STAT=Y PRED= 6.640 RANGE= 0.200
132_136 6.6587 J 02V_H3 02V_H5 STAT=Y PRED= 6.640 RANGE= 0.200
142_143 11.3172 J 03I_H2 03I_H3 STAT=Y PRED= 13.150 RANGE= 4.000
143_144 0.4615 J 03I_H3 03IH4A STAT=Y PRED= 1.950 RANGE= 3.000
143_145 2.7273 J 03I_H3 03IH4B STAT=Y PRED= 12.660 RANGE= 2.800
143_146 6.5602 J 03I_H3 03I_H6 STAT=Y PRED= 6.640 RANGE= 0.200
144_145 -12.4414 J 03IH4A 03IH4B STAT=Y PRED= -13.400 RANGE= 0.600
144_149 7.3376 J 03IH4A 03I_H5 STAT=Y PRED= 7.440 RANGE= 0.150
145_149 7.4487 J 03IH4B 03I_H5 STAT=Y PRED= 7.440 RANGE= 0.150
153_154 2.3513 J 04T_H2 04T_H3 STAT=Y PRED= 2.690 RANGE= 6.600
154_155 6.4912 J 04T_H3 04T_H4 STAT=Y PRED= 6.250 RANGE= 0.600
161_162 3.7198 J 05T_H2 05T_H3 STAT=Y PRED= 2.440 RANGE= 4.400
162_164 6.4861 J 05T_H3 05T_H4 STAT=Y PRED= 6.250 RANGE= 0.600
168_169 9.5371 J 06V_H2 06V_H3 STAT=Y PRED= 2.980 RANGE= 6.600
169_170 6.6359 J 06V_H3 06V_H4 STAT=Y PRED= 6.640 RANGE= 0.200
169_173 7.0196 J 06V_H3 06V_H5 STAT=Y PRED= 6.640 RANGE= 0.200
179_180 6.2454 J 07L_H2 07LH3A STAT=Y PRED= 3.040 RANGE= 6.000
179_181 8.3655 J 07L_H2 07LH3B STAT=Y PRED= 13.950 RANGE= 4.000
180_181 -13.2862 J 07LH3A 07LH3B STAT=Y PRED= -14.710 RANGE= 1.600
180_182 8.1966 J 07LH3A 07L_H4 STAT=Y PRED= 12.990 RANGE= 2.560
181_182 5.6475 J 07LH3B 07L_H4 STAT=Y PRED= 2.270 RANGE= 3.000
182_183 6.1444 J 07L_H4 07L_H5 STAT=Y PRED= 6.640 RANGE= 0.200
182_186 6.7639 J 07L_H4 07L_H6 STAT=Y PRED= 6.640 RANGE= 0.200
190_191 9.1785 J 08V_H2 08V_H3 STAT=Y PRED= 12.880 RANGE= 6.000
191_192 6.5252 J 08V_H3 08V_H4 STAT=Y PRED= 6.640 RANGE= 0.200
191_195 6.6198 J 08V_H3 08V_H5 STAT=Y PRED= 6.640 RANGE= 0.200
201_202 7.6271 J 09V_H2 09V_H3 STAT=Y PRED= 12.960 RANGE= 4.000
202_203 6.5511 J 09V_H3 09V_H4 STAT=Y PRED= 6.640 RANGE= 0.200
202_206 6.7993 J 09V_H3 09V_H5 STAT=Y PRED= 6.640 RANGE= 0.200
212_213 11.2213 J 10Y_H2 10YH3A STAT=Y PRED= 12.890 RANGE= 4.000
212_214 4.5999 J 10Y_H2 10YH3B STAT=Y PRED= 1.900 RANGE= 4.400
213_214 -13.7036 J 10YH3A 10YH3B STAT=Y PRED= -16.760 RANGE= 2.560
215_218 0.4722 J 10Y_H5 10Y_H7 STAT=Y PRED= -0.300 RANGE= 0.500
217_218 0.6202 J 10Y_H9 10Y_H7 STAT=Y PRED= 1.020 RANGE= 1.200
223_224 8.0434 J 11V_H2 11V_H3 STAT=Y PRED= 3.450 RANGE= 9.000
224_225 6.7574 J 11V_H3 11V_H4 STAT=Y PRED= 6.640 RANGE= 0.200
224_228 7.0071 J 11V_H3 11V_H5 STAT=Y PRED= 6.640 RANGE= 0.200
232_233 1.7657 J 12F_H2 12F_H3 STAT=Y PRED= 1.900 RANGE= 6.600
234_238 1.3347 J 12F_H5 12F_H5 STAT=Y PRED= 1.980 RANGE= 1.200
234_235 7.6929 J 12F_H5 12F_H6 STAT=Y PRED= 7.660 RANGE= 0.340
234_237 0.7971 J 12F_H6 12F_H5 STAT=Y PRED= 0.550 RANGE= 0.750

Appendix W (continued)

```
 234_236    1.2586  J 12F_H5  12F_H7    STAT=Y  PRED= 1.260 RANGE= 1.200
 235_237    1.7100  J 12F_H6  12F_H6    STAT=Y  PRED= 1.480 RANGE= 1.200
 235_236    7.4191  J 12F_H6  12F_H7    STAT=Y  PRED= 7.400 RANGE= 0.240
 241_242    8.8889  J 13V_H2  13V_H3    STAT=Y  PRED= 12.320 RANGE= 6.000
 242_243    6.9574  J 13V_H3  13V_H4    STAT=Y  PRED= 6.640 RANGE= 0.200
 242_246    6.5087  J 13V_H3  13V_H5    STAT=Y  PRED= 6.640 RANGE= 0.200

CONTROL PARAMETERS:
      Solvent =  none (def. 99% enriched)
        1.000 =  Concentration (vol%, def=1.0%)
   0.00100000 =  Minimum line-intensity
   0.00100000 =  Diagonalization criterium (not in use)
 700.15197800 =  FIELD(1H,MHz), used to transform shifts to ppms
  11.63296542 =  Left frequency (ppm)
  -4.33374659 =  Right frequency (ppm)
       10.000 =  Acquisition time (s, for QMTLS)
        0.000 =  Line-width (for modes D, P & T, 0=use defaults)
  0.103379714 =  Data-point resolution (Hz)
       28.306 =  GAUSSIAN (%, 0=use default from INF)
      -10.087 =  Dispersion contribution (%, 0=use default from INF)
   0.00000000 =  Decoupling frequency (for DORES)

CONSTRAINTS (in equations X0 = 1.0)...use no empty lines
 EQUAL 01Val_H2 = 13Val_H2
 EQUAL 07Leu_H5 = 07Leu_H6
 EQUAL 06V_H4   = 09V_H4
  0.000 * 1.0 =
  1.000 * 1.0 = -0.486 * 1.0
 IGNORE(HZ):  3440.373 to  3420.437
 IGNORE(HZ):  2324.017 to  2307.608
 IGNORE(HZ):  2348.713 to  2338.757
 IGNORE(HZ):  2159.525 to  2154.754
 IGNORE(HZ):  2527.813 to  2513.502

PSEUDO SPECTRUM(IN PPM):
      1     0.9916      0.4857      1.5672      0.0000      0.0000      0.0000     1    2

END of FILE
```

Appendix X Pseudo HiFSA profile of homoecumicin-13I.

* NEW: the lines beginning by * are comment lines !
* To keep all the chemical shifts fixed during iteration
* replace "CHEMICAL SHIFTS(HZ):" by "..SHIFTS(HZ): fixed"
* The couplings can be fixed in the same way

NMR-data: C:\Users\jgnapo_2\Desktop\Wei_H14_XRays\H14_withoutGO
#$œ Date 26. 3.2014; Time 16:54:39 perch.pms

CHEMICAL SHIFTS(PPM):
PROTON 2*SPIN= 1 SPECIES=1H POPULATION(Y)= 1.00000
10Trp_H8/ 1 6.982300 1*1*1 STAT=Y PRED= 7.318 RANGE= 0.199 WIDTH(Y)= 1.391 RESP(Y)= 0.2499 HSQC= C74
01ValH45/ 1 2.325486 1*1*6 STAT=Y PRED= 2.370 RANGE= 0.306 WIDTH(Y)= 2.341 RESP(Y)= 0.2609 HSQC= C1_2
01Val_H2/ 1 2.689443 1*1*1 STAT=Y PRED= 4.169 RANGE= 0.636 WIDTH(Y)= 2.099 RESP(Y)= 0.2445 HSQC= C4
01Val_H3/ 1 2.050273 1*1*1 STAT=Y PRED= 1.952 RANGE= 0.817 WIDTH(Y)= 1.964 RESP(Y)= 0.2048 HSQC= C5
01Val_H6/ 1 0.848583 1*1*3 STAT=Y PRED= 0.509 RANGE= 0.867 WIDTH(Y)= 2.754 RESP(Y)= 0.3661 HSQC= C6
01Val_H7/ 1 0.976069 1*1*3 STAT=Y PRED= 0.818 RANGE= 0.356 WIDTH(Y)= 2.516 RESP(Y)= 0.2935 HSQC= C7
02Val_H2/ 1 4.666031 1*1*1 STAT=Y PRED= 4.508 RANGE= 0.807 WIDTH(Y)= 2.226 RESP(Y)= 0.3212 HSQC= C10
02Val_H3/ 1 2.099686 1*1*1 STAT=Y PRED= 2.155 RANGE= 0.777 WIDTH(Y)= 1.592 RESP(Y)= 0.1225 HSQC= C12
02Val_H4/ 1 0.995731 1*1*3 STAT=Y PRED= 1.038 RANGE= 0.279 WIDTH(Y)= 2.593 RESP(Y)= 0.3074 HSQC= C13
02Val_H5/ 1 1.053976 1*1*3 STAT=Y PRED= 0.943 RANGE= 0.249 WIDTH(Y)= 2.769 RESP(Y)= 0.2988 HSQC= C14
03Ile_H7/ 1 3.233986 1*1*3 STAT=Y PRED= 3.196 RANGE= 0.366 WIDTH(Y)= 1.973 RESP(Y)= 0.2946 HSQC= C15
03Ile_H2/ 1 4.909803 1*1*1 STAT=Y PRED= 4.617 RANGE= 1.627 WIDTH(Y)= 0.917 RESP(Y)= 0.0165 HSQC= C17
03Ile_H3/ 1 1.949727 1*1*1 STAT=Y PRED= 2.032 RANGE= 0.706 WIDTH(Y)= 2.928 RESP(Y)= 0.1984 HSQC= C19
03IleH4A/ 1 0.955262 1*1*1 STAT=Y PRED= 1.465 RANGE= 0.697 WIDTH(Y)= 5.271 RESP(Y)= 0.7171 HSQC= C20
03IleH4B/ 1 1.300446 1*1*1 STAT=Y PRED= 1.175 RANGE= 0.586 WIDTH(Y)= 3.437 RESP(Y)= 1.0000 HSQC= C20
03Ile_H6/ 1 0.758828 1*1*3 STAT=Y PRED= 0.723 RANGE= 0.396 WIDTH(Y)= 3.625 RESP(Y)= 0.2298 HSQC= C21
03Ile_H5/ 1 0.748416 1*1*3 STAT=Y PRED= 0.880 RANGE= 0.219 WIDTH(Y)= 2.596 RESP(Y)= 0.3360 HSQC= C22
04Thr_H2/ 1 5.160303 1*1*1 STAT=Y PRED= 4.668 RANGE= 1.013 WIDTH(Y)= 1.944 RESP(Y)= 0.2039 HSQC= C24
04Thr_H3/ 1 5.772164 1*1*1 STAT=Y PRED= 4.010 RANGE= 0.476 WIDTH(Y)= 2.178 RESP(Y)= 0.1929 HSQC= C25
04Thr_H4/ 1 1.310477 1*1*3 STAT=Y PRED= 1.270 RANGE= 0.496 WIDTH(Y)= 2.232 RESP(Y)= 0.2650 HSQC= C27
05Thr_H5/ 1 3.328914 1*1*3 STAT=Y PRED= 3.257 RANGE= 0.396 WIDTH(Y)= 1.939 RESP(Y)= 0.2217 HSQC= C29
05Thr_H2/ 1 5.008152 1*1*1 STAT=Y PRED= 4.099 RANGE= 1.023 WIDTH(Y)= 1.966 RESP(Y)= 0.2225 HSQC= C31
05Thr_H3/ 1 4.456075 1*1*1 STAT=Y PRED= 4.345 RANGE= 0.717 WIDTH(Y)= 1.723 RESP(Y)= 0.1169 HSQC= C32
05Thr_H4/ 1 0.910990 1*1*3 STAT=Y PRED= 1.252 RANGE= 0.299 WIDTH(Y)= 2.545 RESP(Y)= 0.3855 HSQC= C34
06Val_H2/ 1 4.843301 1*1*1 STAT=Y PRED= 4.525 RANGE= 1.407 WIDTH(Y)= 3.308 RESP(Y)= 0.2485 HSQC= C37
06Val_H3/ 1 2.334956 1*1*1 STAT=Y PRED= 1.975 RANGE= 1.017 WIDTH(Y)= 2.237 RESP(Y)= 0.9433 HSQC= C38
06Val_H4/ 1 1.090340 1*1*3 STAT=Y PRED= 0.938 RANGE= 0.219 WIDTH(Y)= 3.058 RESP(Y)= 0.2411 HSQC= C39
06Val_H5/ 1 0.980112 1*1*3 STAT=Y PRED= 1.094 RANGE= 0.386 WIDTH(Y)= 2.638 RESP(Y)= 0.4050 HSQC= C40
07Leu_H7/ 1 3.260594 1*1*3 STAT=Y PRED= 3.110 RANGE= 0.376 WIDTH(Y)= 1.459 RESP(Y)= 0.0165 HSQC= C42
07Leu_H2/ 1 5.115604 1*1*1 STAT=Y PRED= 5.342 RANGE= 1.083 WIDTH(Y)= 2.263 RESP(Y)= 0.1409 HSQC= C44
07LeuH3A/ 1 1.458194 1*1*1 STAT=Y PRED= 1.444 RANGE= 0.426 WIDTH(Y)= 1.804 RESP(Y)= 0.0954 HSQC= C45
07LeuH3B/ 1 1.240396 1*1*1 STAT=Y PRED= 1.914 RANGE= 0.366 WIDTH(Y)= 3.418 RESP(Y)= 0.5776 HSQC= C45
07Leu_H4/ 1 0.948729 1*1*1 STAT=Y PRED= 1.630 RANGE= 0.626 WIDTH(Y)= 1.591 RESP(Y)= 0.3976 HSQC= C46
07Leu_H5/ 1 0.336579 1*1*3 STAT=Y PRED= 0.972 RANGE= 0.316 WIDTH(Y)= 1.927 RESP(Y)= 0.1112 HSQC= C47
07Leu_H6/ 1 0.169265 1*1*3 STAT=Y PRED= 0.972 RANGE= 0.149 WIDTH(Y)= 2.146 RESP(Y)= 0.1472 HSQC= C48
08Val_H2/ 1 4.608955 1*1*1 STAT=Y PRED= 4.489 RANGE= 0.897 WIDTH(Y)= 2.504 RESP(Y)= 0.3706 HSQC= C51
08Val_H3/ 1 2.026078 1*1*1 STAT=Y PRED= 1.995 RANGE= 0.486 WIDTH(Y)= 2.865 RESP(Y)= 0.1330 HSQC= C52
08Val_H4/ 1 0.916733 1*1*3 STAT=Y PRED= 1.060 RANGE= 0.236 WIDTH(Y)= 2.787 RESP(Y)= 0.3265 HSQC= C53
08Val_H5/ 1 0.861414 1*1*3 STAT=Y PRED= 0.999 RANGE= 0.229 WIDTH(Y)= 3.739 RESP(Y)= 0.3647 HSQC= C54
09Val_H6/ 1 3.145550 1*1*3 STAT=Y PRED= 3.169 RANGE= 0.466 WIDTH(Y)= 2.245 RESP(Y)= 0.1668 HSQC= C56

Appendix X (continued)

09Val_H2/ 1 3.075107 1*1*1 STAT=Y PRED= 5.153 RANGE= 0.717 WIDTH(Y)= 2.595 RESP(Y)= 0.1097 HSQC= C58
09Val_H3/ 1 2.584340 1*1*1 STAT=Y PRED= 2.524 RANGE= 0.406 WIDTH(Y)= 1.736 RESP(Y)= 0.0440 HSQC= C59
09Val_H4/ 1 1.096271 1*1*3 STAT=Y PRED= 1.319 RANGE= 0.226 WIDTH(Y)= 2.466 RESP(Y)= 0.3535 HSQC= C60
09Val_H5/ 1 0.983017 1*1*3 STAT=Y PRED= 1.075 RANGE= 0.239 WIDTH(Y)= 3.139 RESP(Y)= 0.4629 HSQC= C61
10TrpH13/ 1 2.156808 1*1*3 STAT=Y PRED= 2.936 RANGE= 0.893 WIDTH(Y)= 2.121 RESP(Y)= 0.2379 HSQC= C63
10Trp_H2/ 1 4.101338 1*1*1 STAT=Y PRED= 5.043 RANGE= 1.764 WIDTH(Y)= 2.065 RESP(Y)= 0.1026 HSQC= C65
10TrpH3A/ 1 3.560378 1*1*1 STAT=Y PRED= 3.613 RANGE= 0.466 WIDTH(Y)= 2.811 RESP(Y)= 0.3108 HSQC= C66
10TrpH3B/ 1 3.690898 1*1*1 STAT=Y PRED= 3.367 RANGE= 0.626 WIDTH(Y)= 3.457 RESP(Y)= 0.4505 HSQC= C66
10Trp_H5/ 1 6.698271 1*1*1 STAT=Y PRED= 6.772 RANGE= 0.276 WIDTH(Y)= 2.324 RESP(Y)= 0.2339 HSQC= C68
10Trp_H9/ 1 6.442417 1*1*1 STAT=Y PRED= 7.089 RANGE= 0.219 WIDTH(Y)= 1.328 RESP(Y)= 0.2327 HSQC= C73
10Trp_H7/ 1 6.918811 1*1*1 STAT=Y PRED= 7.333 RANGE= 0.309 WIDTH(Y)= 0.829 RESP(Y)= 0.2255 HSQC= C75
10TrpH12/ 1 3.826345 1*1*3 STAT=Y PRED= 4.072 RANGE= 0.249 WIDTH(Y)= 1.650 RESP(Y)= 0.1915 HSQC= C77
11Val_H2/ 1 4.526279 1*1*1 STAT=Y PRED= 4.303 RANGE= 1.447 WIDTH(Y)= 2.292 RESP(Y)= 0.2292 HSQC= C80
11Val_H3/ 1 2.199630 1*1*1 STAT=Y PRED= 2.094 RANGE= 0.586 WIDTH(Y)= 1.854 RESP(Y)= 0.0784 HSQC= C81
11Val_H4/ 1 1.034276 1*1*3 STAT=Y PRED= 1.094 RANGE= 0.249 WIDTH(Y)= 3.110 RESP(Y)= 0.2484 HSQC= C82
11Val_H5/ 1 0.990614 1*1*3 STAT=Y PRED= 1.080 RANGE= 0.299 WIDTH(Y)= 2.756 RESP(Y)= 0.4210 HSQC= C83
12Phe_H2/ 1 4.883889 1*1*1 STAT=Y PRED= 4.499 RANGE= 0.987 WIDTH(Y)= 1.808 RESP(Y)= 0.2375 HSQC= C86
12Phe_H3/ 1 5.348825 1*1*1 STAT=Y PRED= 5.208 RANGE= 0.486 WIDTH(Y)= 1.838 RESP(Y)= 0.1386 HSQC= C87
12Phe_H5/ 1 7.239202 1*2*1 STAT=Y PRED= 7.524 RANGE= 0.309 WIDTH(Y)= 3.875 RESP(Y)= 0.3256 HSQC= C89_93
12Phe_H6/ 1 7.254924 1*2*1 STAT=Y PRED= 7.372 RANGE= 0.576 WIDTH(Y)= 1.677 RESP(Y)= 0.2221 HSQC= C90_92
12Phe_H7/ 1 7.201947 1*1*1 STAT=Y PRED= 7.281 RANGE= 0.309 WIDTH(Y)= 2.328 RESP(Y)= 0.2990 HSQC= C91
13Val_H2/ 1 4.407512 1*1*1 STAT=Y PRED= 4.169 RANGE= 0.667 WIDTH(Y)= 1.186 RESP(Y)= 0.0476 HSQC= C97
13Val_H3/ 1 1.974802 1*1*1 STAT=Y PRED= 1.935 RANGE= 0.867 WIDTH(Y)= 1.972 RESP(Y)= 0.1451 HSQC= C99
13Val_H4/ 1 0.930030 1*1*3 STAT=Y PRED= 1.277 RANGE= 0.219 WIDTH(Y)= 3.632 RESP(Y)= 0.3219 HSQC= C100
13Val_H5/ 1 0.914495 1*1*3 STAT=Y PRED= 0.933 RANGE= 0.276 WIDTH(Y)= 2.863 RESP(Y)= 0.4180 HSQC= C101

COUPLING CONSTANTS(HZ): fixed
J115_217 7.7969 J 10Trp_H8 10Trp_H9 STAT=Y PRED= 8.100 RANGE= 0.890
J115_218 8.1808 J 10Trp_H8 10Trp_H7 STAT=Y PRED= 7.850 RANGE= 0.800
J122_123 9.1737 J 01Val_H2 01Val_H3 STAT=Y PRED= 12.510 RANGE= 4.000
J123_124 6.5890 J 01Val_H3 01Val_H6 STAT=Y PRED= 6.640 RANGE= 0.200
J123_127 6.6205 J 01Val_H3 01Val_H7 STAT=Y PRED= 6.640 RANGE= 0.200
J131_132 8.7545 J 02Val_H2 02Val_H3 STAT=Y PRED= 12.600 RANGE= 6.000
J132_133 6.7841 J 02Val_H3 02Val_H4 STAT=Y PRED= 6.640 RANGE= 0.200
J132_136 6.7206 J 02Val_H3 02Val_H5 STAT=Y PRED= 6.640 RANGE= 0.200
J142_143 11.2297 J 03Ile_H2 03Ile_H3 STAT=Y PRED= 13.150 RANGE= 4.000
J143_144 0.4614 J 03Ile_H3 03IleH4A STAT=Y PRED= 1.950 RANGE= 3.000
J143_145 2.9276 J 03Ile_H3 03IleH4B STAT=Y PRED= 12.660 RANGE= 2.800
J143_146 6.6276 J 03Ile_H3 03Ile_H6 STAT=Y PRED= 6.640 RANGE= 0.200
J144_145 -12.2168 J 03IleH4A 03IleH4B STAT=Y PRED= -13.400 RANGE= 0.600
J144_149 7.2855 J 03IleH4A 03Ile_H5 STAT=Y PRED= 7.440 RANGE= 0.150
J145_149 7.6340 J 03IleH4B 03Ile_H5 STAT=Y PRED= 7.440 RANGE= 0.150
J153_154 2.3441 J 04Thr_H2 04Thr_H3 STAT=Y PRED= 2.690 RANGE= 6.600
J154_155 6.5134 J 04Thr_H3 04Thr_H4 STAT=Y PRED= 6.250 RANGE= 0.600
J161_162 3.7259 J 05Thr_H2 05Thr_H3 STAT=Y PRED= 2.440 RANGE= 4.400
J162_164 6.4691 J 05Thr_H3 05Thr_H4 STAT=Y PRED= 6.250 RANGE= 0.600
J168_169 8.9180 J 06Val_H2 06Val_H3 STAT=Y PRED= 2.980 RANGE= 6.600
J169_170 6.6944 J 06Val_H3 06Val_H4 STAT=Y PRED= 6.640 RANGE= 0.200
J169_173 7.0316 J 06Val_H3 06Val_H5 STAT=Y PRED= 6.640 RANGE= 0.200
J179_180 6.2437 J 07Leu_H2 07LeuH3A STAT=Y PRED= 3.040 RANGE= 6.000

Appendix X (continued)

```
J179_181    8.3839   J 07Leu_H2 07LeuH3B   STAT=Y  PRED= 13.950 RANGE= 4.000
J180_181  -13.3047   J 07LeuH3A 07LeuH3B   STAT=Y  PRED= -14.710 RANGE= 1.600
J180_182    8.2119   J 07LeuH3A 07Leu_H4   STAT=Y  PRED= 12.990 RANGE= 2.560
J181_182    5.7896   J 07LeuH3B 07Leu_H4   STAT=Y  PRED= 2.270 RANGE= 3.000
J182_183    6.5482   J 07Leu_H4 07Leu_H5   STAT=Y  PRED= 6.640 RANGE= 0.200
J182_186    6.5879   J 07Leu_H4 07Leu_H6   STAT=Y  PRED= 6.640 RANGE= 0.200
J190_191    8.8736   J 08Val_H2 08Val_H3   STAT=Y  PRED= 12.880 RANGE= 6.000
J191_192    6.5520   J 08Val_H3 08Val_H4   STAT=Y  PRED= 6.640 RANGE= 0.200
J191_195    6.7834   J 08Val_H3 08Val_H5   STAT=Y  PRED= 6.640 RANGE= 0.200
J201_202    7.6281   J 09Val_H2 09Val_H3   STAT=Y  PRED= 12.960 RANGE= 4.000
J202_203    6.4961   J 09Val_H3 09Val_H4   STAT=Y  PRED= 6.640 RANGE= 0.200
J202_206    6.7760   J 09Val_H3 09Val_H5   STAT=Y  PRED= 6.640 RANGE= 0.200
J212_213   11.1630   J 10Trp_H2 10TrpH3A   STAT=Y  PRED= 12.890 RANGE= 4.000
J212_214    4.7143   J 10Trp_H2 10TrpH3B   STAT=Y  PRED= 1.900 RANGE= 4.400
J213_214  -13.7295   J 10TrpH3A 10TrpH3B   STAT=Y  PRED= -16.760 RANGE= 2.560
J215_218    0.4880   J 10Trp_H5 10Trp_H7   STAT=Y  PRED= -0.300 RANGE= 0.500
J217_218    0.6708   J 10Trp_H9 10Trp_H7   STAT=Y  PRED= 1.020 RANGE= 1.200
J223_224    7.9094   J 11Val_H2 11Val_H3   STAT=Y  PRED= 3.450 RANGE= 9.000
J224_225    6.7483   J 11Val_H3 11Val_H4   STAT=Y  PRED= 6.640 RANGE= 0.200
J224_228    6.8064   J 11Val_H3 11Val_H5   STAT=Y  PRED= 6.640 RANGE= 0.200
J232_233    1.9005   J 12Phe_H2 12Phe_H3   STAT=Y  PRED= 1.900 RANGE= 6.600
J234_238    1.3335   J 12Phe_H5 12Phe_H5   STAT=Y  PRED= 1.980 RANGE= 1.200
J234_235    7.6508   J 12Phe_H5 12Phe_H6   STAT=Y  PRED= 7.660 RANGE= 0.340
J234_237    0.7769   J 12Phe_H6 12Phe_H5   STAT=Y  PRED= 0.550 RANGE= 0.750
J234_236    1.2760   J 12Phe_H5 12Phe_H7   STAT=Y  PRED= 1.260 RANGE= 1.200
J235_237    1.7027   J 12Phe_H6 12Phe_H6   STAT=Y  PRED= 1.480 RANGE= 1.200
J235_236    7.4760   J 12Phe_H6 12Phe_H7   STAT=Y  PRED= 7.400 RANGE= 0.240
J241_242    8.8924   J 13Val_H2 13Val_H3   STAT=Y  PRED= 12.320 RANGE= 6.000
J242_243    6.8372   J 13Val_H3 13Val_H4   STAT=Y  PRED= 6.640 RANGE= 0.200
J242_246    6.4162   J 13Val_H3 13Val_H5   STAT=Y  PRED= 6.640 RANGE= 0.200

CONTROL PARAMETERS:
      Solvent =  none (def. 99% enriched)
        1.000 =  Concentration (vol%, def=1.0%)
   0.00100000 =  Minimum line-intensity
   0.00100000 =  Diagonalization criterium (not in use)
 700.15197800 =  FIELD(1H,MHz), used to transform shifts to ppms
  11.63296961 =  Left frequency (ppm)
  -4.33374415 =  Right frequency (ppm)
        0.000 =  Acquisition time (s, for QMTLS)
        0.719 =  Line-width (for modes D, P & T, 0=use defaults)
  0.065771143 =  Data-point resolution (Hz)
       28.306 =  GAUSSIAN (%, 0=use default from INF)
      -10.087 =  Dispersion contribution (%, 0=use default from INF)
   0.00000000 =  Decoupling frequency (for DORES)

CONSTRAINTS (in equations X0 = 1.0)...use no empty lines
 EQUAL 01Val_H2 = 13Val_H2
 EQUAL 06Val_H5 = 11Val_H4
 EQUAL 07Leu_H5 = 07Leu_H6
```

Appendix X (continued)

IGNORE(HZ): 3441.747 to 3420.668
IGNORE(HZ): 2323.920 to 2309.428
IGNORE(HZ): 2328.672 to 2324.470
IGNORE(HZ): 2288.657 to 2282.788
IGNORE(HZ): 2392.691 to 2378.287
IGNORE(HZ): 2251.845 to 2238.507
IGNORE(HZ): 2197.427 to 2189.958

END of FILE

Appendix Y. Pseudo HiFSA profile of homoecumicin-13I with major impurity.

* NEW: the lines beginning by * are comment lines !
* To keep all the chemical shifts fixed during iteration
* replace "CHEMICAL SHIFTS(HZ):" by "..SHIFTS(HZ): fixed"
* The couplings can be fixed in the same way

NMR-data: C:\Users\jgnapo_2\Desktop\Wei_H14_XRays\H14_withoutGO
#$œ Date 27. 3.2014; Time 17:53:21 perch.pms

CHEMICAL SHIFTS(PPM):
PROTON 2*SPIN= 1 SPECIES=1H POPULATION(Y)= 0.71163
10Trp_H8/ 1 6.982325 1*1*1 STAT=Y PRED= 7.318 RANGE= 0.199 WIDTH(Y)= 1.215 RESP(Y)= 1.0000 HSQC= C74
01ValH45/ 1 2.325486 1*1*6 STAT=Y PRED= 2.370 RANGE= 0.306 WIDTH(Y)= 1.536 RESP(Y)= 1.0000 HSQC= C1_2
01Val_H2/ 1 2.690219 1*1*1 STAT=Y PRED= 4.169 RANGE= 0.636 WIDTH(Y)= 1.557 RESP(Y)= 1.0000 HSQC= C4
01Val_H3/ 1 2.051284 1*1*1 STAT=Y PRED= 1.952 RANGE= 0.817 WIDTH(Y)= 1.561 RESP(Y)= 1.0000 HSQC= C5
01Val_H6/ 1 0.848433 1*1*3 STAT=Y PRED= 0.509 RANGE= 0.867 WIDTH(Y)= 1.598 RESP(Y)= 1.0000 HSQC= C6
01Val_H7/ 1 0.976475 1*1*3 STAT=Y PRED= 0.818 RANGE= 0.356 WIDTH(Y)= 1.688 RESP(Y)= 1.0000 HSQC= C7
02Val_H2/ 1 4.665068 1*1*1 STAT=Y PRED= 4.508 RANGE= 0.807 WIDTH(Y)= 1.467 RESP(Y)= 1.0000 HSQC= C10
02Val_H3/ 1 2.099755 1*1*1 STAT=Y PRED= 2.155 RANGE= 0.777 WIDTH(Y)= 1.561 RESP(Y)= 1.0000 HSQC= C12
02Val_H4/ 1 0.994696 1*1*3 STAT=Y PRED= 1.038 RANGE= 0.279 WIDTH(Y)= 1.468 RESP(Y)= 1.0000 HSQC= C13
02Val_H5/ 1 1.054013 1*1*3 STAT=Y PRED= 0.943 RANGE= 0.249 WIDTH(Y)= 1.538 RESP(Y)= 1.0000 HSQC= C14
03Ile_H7/ 1 3.233986 1*1*3 STAT=Y PRED= 3.196 RANGE= 0.366 WIDTH(Y)= 1.536 RESP(Y)= 1.0000 HSQC= C15
03Ile_H2/ 1 4.911071 1*1*1 STAT=Y PRED= 4.617 RANGE= 1.627 WIDTH(Y)= 1.466 RESP(Y)= 1.0000 HSQC= C17
03Ile_H3/ 1 1.949735 1*1*1 STAT=Y PRED= 2.032 RANGE= 0.706 WIDTH(Y)= 2.929 RESP(Y)= 1.0000 HSQC= C19
03IleH4A/ 1 0.955039 1*1*1 STAT=Y PRED= 1.465 RANGE= 0.697 WIDTH(Y)= 5.275 RESP(Y)= 1.0000 HSQC= C20
03IleH4B/ 1 1.296763 1*1*1 STAT=Y PRED= 1.175 RANGE= 0.586 WIDTH(Y)= 2.795 RESP(Y)= 1.0000 HSQC= C20
03Ile_H6/ 1 0.757782 1*1*3 STAT=Y PRED= 0.723 RANGE= 0.396 WIDTH(Y)= 1.613 RESP(Y)= 1.0000 HSQC= C21
03Ile_H5/ 1 0.748021 1*1*3 STAT=Y PRED= 0.880 RANGE= 0.219 WIDTH(Y)= 1.391 RESP(Y)= 1.0000 HSQC= C22
04Thr_H2/ 1 5.161027 1*1*1 STAT=Y PRED= 4.668 RANGE= 1.013 WIDTH(Y)= 1.377 RESP(Y)= 1.0000 HSQC= C24
04Thr_H3/ 1 5.772637 1*1*1 STAT=Y PRED= 4.010 RANGE= 0.476 WIDTH(Y)= 1.941 RESP(Y)= 1.0000 HSQC= C25
04Thr_H4/ 1 1.310504 1*1*3 STAT=Y PRED= 1.270 RANGE= 0.496 WIDTH(Y)= 1.818 RESP(Y)= 1.0000 HSQC= C27
05Thr_H5/ 1 3.329093 1*1*3 STAT=Y PRED= 3.257 RANGE= 0.396 WIDTH(Y)= 1.439 RESP(Y)= 1.0000 HSQC= C29
05Thr_H2/ 1 5.008056 1*1*1 STAT=Y PRED= 4.099 RANGE= 1.023 WIDTH(Y)= 1.500 RESP(Y)= 1.0000 HSQC= C31
05Thr_H3/ 1 4.466749 1*1*1 STAT=Y PRED= 4.345 RANGE= 0.717 WIDTH(Y)= 1.572 RESP(Y)= 1.0000 HSQC= C32
05Thr_H4/ 1 0.910868 1*1*3 STAT=Y PRED= 1.252 RANGE= 0.299 WIDTH(Y)= 1.939 RESP(Y)= 1.0000 HSQC= C34
06Val_H2/ 1 4.843536 1*1*1 STAT=Y PRED= 4.525 RANGE= 1.407 WIDTH(Y)= 1.382 RESP(Y)= 1.0000 HSQC= C37
06Val_H3/ 1 2.335187 1*1*1 STAT=Y PRED= 1.975 RANGE= 1.017 WIDTH(Y)= 1.789 RESP(Y)= 1.0000 HSQC= C38
06Val_H4/ 1 1.090452 1*1*3 STAT=Y PRED= 0.938 RANGE= 0.219 WIDTH(Y)= 1.894 RESP(Y)= 1.0000 HSQC= C39
06Val_H5/ 1 0.980823 1*1*3 STAT=Y PRED= 1.094 RANGE= 0.386 WIDTH(Y)= 2.275 RESP(Y)= 1.0000 HSQC= C40
07Leu_H7/ 1 3.260594 1*1*3 STAT=Y PRED= 3.110 RANGE= 0.376 WIDTH(Y)= 1.459 RESP(Y)= 1.0000 HSQC= C42
07Leu_H2/ 1 5.116104 1*1*1 STAT=Y PRED= 5.342 RANGE= 1.083 WIDTH(Y)= 2.240 RESP(Y)= 1.0000 HSQC= C44
07LeuH3A/ 1 1.458188 1*1*1 STAT=Y PRED= 1.444 RANGE= 0.426 WIDTH(Y)= 1.805 RESP(Y)= 1.0000 HSQC= C45
07LeuH3B/ 1 1.237573 1*1*1 STAT=Y PRED= 1.914 RANGE= 0.366 WIDTH(Y)= 3.321 RESP(Y)= 1.0000 HSQC= C45
07Leu_H4/ 1 0.948812 1*1*1 STAT=Y PRED= 1.630 RANGE= 0.626 WIDTH(Y)= 1.520 RESP(Y)= 1.0000 HSQC= C46
07Leu_H5/ 1 0.336591 1*1*3 STAT=Y PRED= 0.972 RANGE= 0.316 WIDTH(Y)= 1.961 RESP(Y)= 1.0000 HSQC= C47
07Leu_H6/ 1 0.168976 1*1*3 STAT=Y PRED= 0.972 RANGE= 0.149 WIDTH(Y)= 1.885 RESP(Y)= 1.0000 HSQC= C48
08Val_H2/ 1 4.608604 1*1*1 STAT=Y PRED= 4.489 RANGE= 0.897 WIDTH(Y)= 1.578 RESP(Y)= 1.0000 HSQC= C51
08Val_H3/ 1 2.026205 1*1*1 STAT=Y PRED= 1.995 RANGE= 0.486 WIDTH(Y)= 2.872 RESP(Y)= 1.0000 HSQC= C52
08Val_H4/ 1 0.916425 1*1*3 STAT=Y PRED= 1.060 RANGE= 0.236 WIDTH(Y)= 1.731 RESP(Y)= 1.0000 HSQC= C53
08Val_H5/ 1 0.861363 1*1*3 STAT=Y PRED= 0.999 RANGE= 0.229 WIDTH(Y)= 2.065 RESP(Y)= 1.0000 HSQC= C54
09Val_H6/ 1 3.145503 1*1*3 STAT=Y PRED= 3.169 RANGE= 0.466 WIDTH(Y)= 1.931 RESP(Y)= 1.0000 HSQC= C56

Appendix Y (continued)

09Val_H2/ 1 3.074915 1*1*1 STAT=Y PRED= 5.153 RANGE= 0.717 WIDTH(Y)= 2.597 RESP(Y)= 1.0000 HSQC= C58
09Val_H3/ 1 2.584340 1*1*1 STAT=Y PRED= 2.524 RANGE= 0.406 WIDTH(Y)= 1.736 RESP(Y)= 1.0000 HSQC= C59
09Val_H4/ 1 1.096137 1*1*3 STAT=Y PRED= 1.319 RANGE= 0.226 WIDTH(Y)= 1.741 RESP(Y)= 1.0000 HSQC= C60
09Val_H5/ 1 0.982470 1*1*3 STAT=Y PRED= 1.075 RANGE= 0.239 WIDTH(Y)= 2.379 RESP(Y)= 1.0000 HSQC= C61
10TrpH13/ 1 2.156847 1*1*3 STAT=Y PRED= 2.936 RANGE= 0.893 WIDTH(Y)= 1.862 RESP(Y)= 1.0000 HSQC= C63
10Trp_H2/ 1 4.101575 1*1*1 STAT=Y PRED= 5.043 RANGE= 1.764 WIDTH(Y)= 2.064 RESP(Y)= 1.0000 HSQC= C65
10TrpH3A/ 1 3.560440 1*1*1 STAT=Y PRED= 3.613 RANGE= 0.466 WIDTH(Y)= 1.516 RESP(Y)= 1.0000 HSQC= C66
10TrpH3B/ 1 3.690935 1*1*1 STAT=Y PRED= 3.367 RANGE= 0.626 WIDTH(Y)= 2.118 RESP(Y)= 1.0000 HSQC= C66
10Trp_H5/ 1 6.698385 1*1*1 STAT=Y PRED= 6.772 RANGE= 0.276 WIDTH(Y)= 1.649 RESP(Y)= 1.0000 HSQC= C68
10Trp_H9/ 1 6.442449 1*1*1 STAT=Y PRED= 7.089 RANGE= 0.219 WIDTH(Y)= 1.143 RESP(Y)= 1.0000 HSQC= C73
10Trp_H7/ 1 6.918830 1*1*1 STAT=Y PRED= 7.333 RANGE= 0.309 WIDTH(Y)= 0.719 RESP(Y)= 1.0000 HSQC= C75
10TrpH12/ 1 3.826612 1*1*3 STAT=Y PRED= 4.072 RANGE= 0.249 WIDTH(Y)= 1.244 RESP(Y)= 1.0000 HSQC= C77
11Val_H2/ 1 4.524897 1*1*1 STAT=Y PRED= 4.303 RANGE= 1.447 WIDTH(Y)= 1.849 RESP(Y)= 1.0000 HSQC= C80
11Val_H3/ 1 2.199630 1*1*1 STAT=Y PRED= 2.094 RANGE= 0.586 WIDTH(Y)= 1.854 RESP(Y)= 1.0000 HSQC= C81
11Val_H4/ 1 1.034271 1*1*3 STAT=Y PRED= 1.094 RANGE= 0.249 WIDTH(Y)= 2.106 RESP(Y)= 1.0000 HSQC= C82
11Val_H5/ 1 0.989808 1*1*3 STAT=Y PRED= 1.080 RANGE= 0.299 WIDTH(Y)= 1.787 RESP(Y)= 1.0000 HSQC= C83
12Phe_H2/ 1 4.882842 1*1*1 STAT=Y PRED= 4.499 RANGE= 0.987 WIDTH(Y)= 1.261 RESP(Y)= 1.0000 HSQC= C86
12Phe_H3/ 1 5.348787 1*1*1 STAT=Y PRED= 5.208 RANGE= 0.486 WIDTH(Y)= 1.884 RESP(Y)= 1.0000 HSQC= C87
12Phe_H5/ 1 7.238322 1*2*1 STAT=Y PRED= 7.524 RANGE= 0.309 WIDTH(Y)= 2.042 RESP(Y)= 1.0000 HSQC= C89_93
12Phe_H6/ 1 7.255114 1*2*1 STAT=Y PRED= 7.372 RANGE= 0.576 WIDTH(Y)= 1.207 RESP(Y)= 1.0000 HSQC= C90_92
12Phe_H7/ 1 7.202197 1*1*1 STAT=Y PRED= 7.281 RANGE= 0.309 WIDTH(Y)= 1.557 RESP(Y)= 1.0000 HSQC= C91
13Val_H2/ 1 4.514692 1*1*1 STAT=Y PRED= 4.169 RANGE= 0.667 WIDTH(Y)= 1.205 RESP(Y)= 1.0000 HSQC= C97
13Val_H3/ 1 1.974671 1*1*1 STAT=Y PRED= 1.935 RANGE= 0.867 WIDTH(Y)= 1.973 RESP(Y)= 1.0000 HSQC= C99
13Val_H4/ 1 0.929643 1*1*3 STAT=Y PRED= 1.277 RANGE= 0.219 WIDTH(Y)= 2.666 RESP(Y)= 1.0000 HSQC= C100
13Val_H5/ 1 0.913883 1*1*3 STAT=Y PRED= 0.933 RANGE= 0.276 WIDTH(Y)= 2.083 RESP(Y)= 1.0000 HSQC= C101
PROTON 2*SPIN= 1 SPECIES=1H POPULATION(Y)= 0.28837
10Y_H8 / 2 6.982643 1*1*1 STAT=N PRED= 7.318 RANGE= 0.199 WIDTH(Y)= 1.215 RESP(Y)= 1.0000 HSQC= C74
01VH45 / 2 2.331280 1*1*6 STAT=N PRED= 2.370 RANGE= 0.306 WIDTH(Y)= 1.536 RESP(Y)= 1.0000 HSQC= C1_2
01V_H2 / 2 2.705188 1*1*1 STAT=N PRED= 4.169 RANGE= 0.636 WIDTH(Y)= 1.557 RESP(Y)= 1.0000 HSQC= C4
01V_H3 / 2 2.044179 1*1*1 STAT=N PRED= 1.952 RANGE= 0.817 WIDTH(Y)= 1.561 RESP(Y)= 1.0000 HSQC= C5
01V_H6 / 2 0.849588 1*1*3 STAT=N PRED= 0.509 RANGE= 0.867 WIDTH(Y)= 1.598 RESP(Y)= 1.0000 HSQC= C6
01V_H7 / 2 0.980989 1*1*3 STAT=N PRED= 0.818 RANGE= 0.356 WIDTH(Y)= 1.688 RESP(Y)= 1.0000 HSQC= C7
02V_H2 / 2 4.670147 1*1*1 STAT=N PRED= 4.508 RANGE= 0.807 WIDTH(Y)= 1.467 RESP(Y)= 1.0000 HSQC= C10
02V_H3 / 2 2.108243 1*1*1 STAT=N PRED= 2.155 RANGE= 0.777 WIDTH(Y)= 1.561 RESP(Y)= 1.0000 HSQC= C12
02V_H4 / 2 0.981760 1*1*3 STAT=N PRED= 1.038 RANGE= 0.279 WIDTH(Y)= 1.468 RESP(Y)= 1.0000 HSQC= C13
02V_H5 / 2 1.058864 1*1*3 STAT=N PRED= 0.943 RANGE= 0.249 WIDTH(Y)= 1.538 RESP(Y)= 1.0000 HSQC= C14
03I_H7 / 2 3.235337 1*1*3 STAT=N PRED= 3.196 RANGE= 0.366 WIDTH(Y)= 1.536 RESP(Y)= 1.0000 HSQC= C15
03I_H2 / 2 4.907493 1*1*1 STAT=N PRED= 4.617 RANGE= 1.627 WIDTH(Y)= 1.466 RESP(Y)= 1.0000 HSQC= C17
03I_H3 / 2 1.951705 1*1*1 STAT=N PRED= 2.032 RANGE= 0.706 WIDTH(Y)= 2.929 RESP(Y)= 1.0000 HSQC= C19
03IH4A / 2 0.904202 1*1*1 STAT=N PRED= 1.465 RANGE= 0.697 WIDTH(Y)= 5.275 RESP(Y)= 1.0000 HSQC= C20
03IH4B / 2 1.244466 1*1*1 STAT=N PRED= 1.175 RANGE= 0.586 WIDTH(Y)= 2.795 RESP(Y)= 1.0000 HSQC= C20
03I_H6 / 2 0.760037 1*1*3 STAT=N PRED= 0.723 RANGE= 0.396 WIDTH(Y)= 1.613 RESP(Y)= 1.0000 HSQC= C21
03I_H5 / 2 0.750330 1*1*3 STAT=N PRED= 0.880 RANGE= 0.219 WIDTH(Y)= 1.391 RESP(Y)= 1.0000 HSQC= C22
04T_H2 / 2 5.168532 1*1*1 STAT=N PRED= 4.668 RANGE= 1.013 WIDTH(Y)= 1.377 RESP(Y)= 1.0000 HSQC= C24
04T_H3 / 2 5.779659 1*1*1 STAT=N PRED= 4.010 RANGE= 0.476 WIDTH(Y)= 1.941 RESP(Y)= 1.0000 HSQC= C25
04T_H4 / 2 1.311416 1*1*3 STAT=N PRED= 1.270 RANGE= 0.496 WIDTH(Y)= 1.818 RESP(Y)= 1.0000 HSQC= C27
05T_H5 / 2 3.325329 1*1*3 STAT=N PRED= 3.257 RANGE= 0.396 WIDTH(Y)= 1.439 RESP(Y)= 1.0000 HSQC= C29
05T_H2 / 2 4.999806 1*1*1 STAT=N PRED= 4.099 RANGE= 1.023 WIDTH(Y)= 1.500 RESP(Y)= 1.0000 HSQC= C31
05T_H3 / 2 4.444347 1*1*1 STAT=N PRED= 4.345 RANGE= 0.717 WIDTH(Y)= 1.572 RESP(Y)= 1.0000 HSQC= C32
05T_H4 / 2 0.911618 1*1*3 STAT=N PRED= 1.252 RANGE= 0.299 WIDTH(Y)= 1.939 RESP(Y)= 1.0000 HSQC= C34

Appendix Y (continued)

06V_H2 / 2 4.863987 1*1*1 STAT=N PRED= 4.525 RANGE= 1.407 WIDTH(Y)= 1.382 RESP(Y)= 1.0000 HSQC= C37
06V_H3 / 2 2.341573 1*1*1 STAT=N PRED= 1.975 RANGE= 1.017 WIDTH(Y)= 1.789 RESP(Y)= 1.0000 HSQC= C38
06V_H4 / 2 1.086573 1*1*3 STAT=N PRED= 0.938 RANGE= 0.219 WIDTH(Y)= 1.894 RESP(Y)= 1.0000 HSQC= C39
06V_H5 / 2 0.985855 1*1*3 STAT=N PRED= 1.094 RANGE= 0.386 WIDTH(Y)= 2.275 RESP(Y)= 1.0000 HSQC= C40
07L_H7 / 2 3.264425 1*1*3 STAT=N PRED= 3.110 RANGE= 0.376 WIDTH(Y)= 1.459 RESP(Y)= 1.0000 HSQC= C42
07L_H2 / 2 5.132251 1*1*1 STAT=N PRED= 5.342 RANGE= 1.083 WIDTH(Y)= 2.240 RESP(Y)= 1.0000 HSQC= C44
07LH3A / 2 1.470249 1*1*1 STAT=N PRED= 1.444 RANGE= 0.426 WIDTH(Y)= 1.805 RESP(Y)= 1.0000 HSQC= C45
07LH3B / 2 1.231458 1*1*1 STAT=N PRED= 1.914 RANGE= 0.366 WIDTH(Y)= 3.321 RESP(Y)= 1.0000 HSQC= C45
07L_H4 / 2 0.927464 1*1*1 STAT=N PRED= 1.630 RANGE= 0.626 WIDTH(Y)= 1.520 RESP(Y)= 1.0000 HSQC= C46
07L_H5 / 2 0.363847 1*1*3 STAT=N PRED= 0.972 RANGE= 0.316 WIDTH(Y)= 1.961 RESP(Y)= 1.0000 HSQC= C47
07L_H6 / 2 0.180380 1*1*3 STAT=N PRED= 0.972 RANGE= 0.149 WIDTH(Y)= 1.885 RESP(Y)= 1.0000 HSQC= C48
08V_H2 / 2 4.595474 1*1*1 STAT=N PRED= 4.489 RANGE= 0.897 WIDTH(Y)= 1.578 RESP(Y)= 1.0000 HSQC= C51
08V_H3 / 2 1.987696 1*1*1 STAT=N PRED= 1.995 RANGE= 0.486 WIDTH(Y)= 2.872 RESP(Y)= 1.0000 HSQC= C52
08V_H4 / 2 0.928532 1*1*3 STAT=N PRED= 1.060 RANGE= 0.236 WIDTH(Y)= 1.731 RESP(Y)= 1.0000 HSQC= C53
08V_H5 / 2 0.861982 1*1*3 STAT=N PRED= 0.999 RANGE= 0.229 WIDTH(Y)= 2.065 RESP(Y)= 1.0000 HSQC= C54
09V_H6 / 2 3.135917 1*1*3 STAT=N PRED= 3.169 RANGE= 0.466 WIDTH(Y)= 1.931 RESP(Y)= 1.0000 HSQC= C56
09V_H2 / 2 3.065174 1*1*1 STAT=N PRED= 5.153 RANGE= 0.717 WIDTH(Y)= 2.597 RESP(Y)= 1.0000 HSQC= C58
09V_H3 / 2 2.575838 1*1*1 STAT=N PRED= 2.524 RANGE= 0.406 WIDTH(Y)= 1.736 RESP(Y)= 1.0000 HSQC= C59
09V_H4 / 2 1.094566 1*1*3 STAT=N PRED= 1.319 RANGE= 0.226 WIDTH(Y)= 1.741 RESP(Y)= 1.0000 HSQC= C60
09V_H5 / 2 0.983397 1*1*3 STAT=N PRED= 1.075 RANGE= 0.239 WIDTH(Y)= 2.379 RESP(Y)= 1.0000 HSQC= C61
10YH13 / 2 2.157614 1*1*3 STAT=N PRED= 2.936 RANGE= 0.893 WIDTH(Y)= 1.862 RESP(Y)= 1.0000 HSQC= C63
10Y_H2 / 2 4.114944 1*1*1 STAT=N PRED= 5.043 RANGE= 1.764 WIDTH(Y)= 2.064 RESP(Y)= 1.0000 HSQC= C65
10YH3A / 2 3.564700 1*1*1 STAT=N PRED= 3.613 RANGE= 0.466 WIDTH(Y)= 1.516 RESP(Y)= 1.0000 HSQC= C66
10YH3B / 2 3.692019 1*1*1 STAT=N PRED= 3.367 RANGE= 0.626 WIDTH(Y)= 2.118 RESP(Y)= 1.0000 HSQC= C66
10Y_H5 / 2 6.701771 1*1*1 STAT=N PRED= 6.772 RANGE= 0.276 WIDTH(Y)= 1.649 RESP(Y)= 1.0000 HSQC= C68
10Y_H9 / 2 6.443403 1*1*1 STAT=N PRED= 7.089 RANGE= 0.219 WIDTH(Y)= 1.143 RESP(Y)= 1.0000 HSQC= C73
10Y_H7 / 2 6.919434 1*1*1 STAT=N PRED= 7.333 RANGE= 0.309 WIDTH(Y)= 0.719 RESP(Y)= 1.0000 HSQC= C75
10YH12 / 2 3.830106 1*1*3 STAT=N PRED= 4.072 RANGE= 0.249 WIDTH(Y)= 1.244 RESP(Y)= 1.0000 HSQC= C77
11I_H2 / 2 4.645948 1*1*1 STAT=N PRED= 4.303 RANGE= 1.447 WIDTH(Y)= 1.849 RESP(Y)= 1.0000 HSQC= C80
11I_H3 / 2 1.963073 1*1*1 STAT=N PRED= 2.094 RANGE= 0.586 WIDTH(Y)= 1.854 RESP(Y)= 1.0000 HSQC= C81
11IH4A / 2 1.577140 1*1*3 STAT=N PRED= 1.094 RANGE= 0.249 WIDTH(Y)= 2.106 RESP(Y)= 1.0000 HSQC= C82
11IH4B / 2 1.222059 1*1*3 STAT=N PRED= 1.080 RANGE= 0.299 WIDTH(Y)= 1.787 RESP(Y)= 1.0000 HSQC= C82
11I_H5 / 2 0.915100 1*1*3 STAT=N PRED= 1.080 RANGE= 0.299 WIDTH(Y)= 1.787 RESP(Y)= 1.0000 HSQC= C83
11I_H6 / 2 0.990779 1*1*3 STAT=N PRED= 1.080 RANGE= 0.299 WIDTH(Y)= 1.787 RESP(Y)= 1.0000 HSQC= C84
12F_H2 / 2 4.920692 1*1*1 STAT=N PRED= 4.499 RANGE= 0.987 WIDTH(Y)= 1.261 RESP(Y)= 1.0000 HSQC= C86
12F_H3 / 2 5.318327 1*1*1 STAT=N PRED= 5.208 RANGE= 0.486 WIDTH(Y)= 1.884 RESP(Y)= 1.0000 HSQC= C87
12F_H5 / 2 7.229493 1*2*1 STAT=N PRED= 7.524 RANGE= 0.309 WIDTH(Y)= 2.042 RESP(Y)= 1.0000 HSQC= C89_93
12F_H6 / 2 7.249523 1*2*1 STAT=N PRED= 7.372 RANGE= 0.576 WIDTH(Y)= 1.207 RESP(Y)= 1.0000 HSQC= C90_92
12F_H7 / 2 7.195963 1*1*1 STAT=N PRED= 7.281 RANGE= 0.309 WIDTH(Y)= 1.557 RESP(Y)= 1.0000 HSQC= C91
13V_H2 / 2 4.408276 1*1*1 STAT=N PRED= 4.169 RANGE= 0.667 WIDTH(Y)= 1.205 RESP(Y)= 1.0000 HSQC= C97
13V_H3 / 2 1.962989 1*1*1 STAT=N PRED= 1.935 RANGE= 0.867 WIDTH(Y)= 1.973 RESP(Y)= 1.0000 HSQC= C99
13V_H4 / 2 0.944236 1*1*3 STAT=N PRED= 1.277 RANGE= 0.219 WIDTH(Y)= 2.666 RESP(Y)= 1.0000 HSQC= C100
13V_H5 / 2 0.915347 1*1*3 STAT=N PRED= 0.933 RANGE= 0.276 WIDTH(Y)= 2.083 RESP(Y)= 1.0000 HSQC= C101

COUPLING CONSTANTS(HZ): fixed

J115_217 7.7969 J 10Trp_H8 10Trp_H9 STAT=Y PRED= 8.100 RANGE= 0.890
J115_218 8.1808 J 10Trp_H8 10Trp_H7 STAT=Y PRED= 7.850 RANGE= 0.800
J122_123 9.1737 J 01Val_H2 01Val_H3 STAT=Y PRED= 12.510 RANGE= 4.000
J123_124 6.5890 J 01Val_H3 01Val_H6 STAT=Y PRED= 6.640 RANGE= 0.200
J123_127 6.6205 J 01Val_H3 01Val_H7 STAT=Y PRED= 6.640 RANGE= 0.200

Appendix Y (continued)

J131_132 8.7545 J 02Val_H2 02Val_H3 STAT=Y PRED= 12.600 RANGE= 6.000
J132_133 6.7841 J 02Val_H3 02Val_H4 STAT=Y PRED= 6.640 RANGE= 0.200
J132_136 6.7206 J 02Val_H3 02Val_H5 STAT=Y PRED= 6.640 RANGE= 0.200
J142_143 11.2297 J 03Ile_H2 03Ile_H3 STAT=Y PRED= 13.150 RANGE= 4.000
J143_144 0.4614 J 03Ile_H3 03IleH4A STAT=Y PRED= 1.950 RANGE= 3.000
J143_145 2.9276 J 03Ile_H3 03IleH4B STAT=Y PRED= 12.660 RANGE= 2.800
J143_146 6.6276 J 03Ile_H3 03Ile_H6 STAT=Y PRED= 6.640 RANGE= 0.200
J144_145 -12.2168 J 03IleH4A 03IleH4B STAT=Y PRED= -13.400 RANGE= 0.600
J144_149 7.2855 J 03IleH4A 03Ile_H5 STAT=Y PRED= 7.440 RANGE= 0.150
J145_149 7.6340 J 03IleH4B 03Ile_H5 STAT=Y PRED= 7.440 RANGE= 0.150
J153_154 2.3441 J 04Thr_H2 04Thr_H3 STAT=Y PRED= 2.690 RANGE= 6.600
J154_155 6.5134 J 04Thr_H3 04Thr_H4 STAT=Y PRED= 6.250 RANGE= 0.600
J161_162 3.7259 J 05Thr_H2 05Thr_H3 STAT=Y PRED= 2.440 RANGE= 4.400
J162_164 6.4691 J 05Thr_H3 05Thr_H4 STAT=Y PRED= 6.250 RANGE= 0.600
J168_169 8.9180 J 06Val_H2 06Val_H3 STAT=Y PRED= 2.980 RANGE= 6.600
J169_170 6.6944 J 06Val_H3 06Val_H4 STAT=Y PRED= 6.640 RANGE= 0.200
J169_173 7.0316 J 06Val_H3 06Val_H5 STAT=Y PRED= 6.640 RANGE= 0.200
J179_180 6.2437 J 07Leu_H2 07LeuH3A STAT=Y PRED= 3.040 RANGE= 6.000
J179_181 8.3839 J 07Leu_H2 07LeuH3B STAT=Y PRED= 13.950 RANGE= 4.000
J180_181 -13.3047 J 07LeuH3A 07LeuH3B STAT=Y PRED= -14.710 RANGE= 1.600
J180_182 8.2119 J 07LeuH3A 07Leu_H4 STAT=Y PRED= 12.990 RANGE= 2.560
J181_182 5.7896 J 07LeuH3B 07Leu_H4 STAT=Y PRED= 2.270 RANGE= 3.000
J182_183 6.5482 J 07Leu_H4 07Leu_H5 STAT=Y PRED= 6.640 RANGE= 0.200
J182_186 6.5879 J 07Leu_H4 07Leu_H6 STAT=Y PRED= 6.640 RANGE= 0.200
J190_191 8.8736 J 08Val_H2 08Val_H3 STAT=Y PRED= 12.880 RANGE= 6.000
J191_192 6.5520 J 08Val_H3 08Val_H4 STAT=Y PRED= 6.640 RANGE= 0.200
J191_195 6.7834 J 08Val_H3 08Val_H5 STAT=Y PRED= 6.640 RANGE= 0.200
J201_202 7.6281 J 09Val_H2 09Val_H3 STAT=Y PRED= 12.960 RANGE= 4.000
J202_203 6.4961 J 09Val_H3 09Val_H4 STAT=Y PRED= 6.640 RANGE= 0.200
J202_206 6.7760 J 09Val_H3 09Val_H5 STAT=Y PRED= 6.640 RANGE= 0.200
J212_213 11.1630 J 10Trp_H2 10TrpH3A STAT=Y PRED= 12.890 RANGE= 4.000
J212_214 4.7143 J 10Trp_H2 10TrpH3B STAT=Y PRED= 1.900 RANGE= 4.400
J213_214 -13.7295 J 10TrpH3A 10TrpH3B STAT=Y PRED= -16.760 RANGE= 2.560
J215_218 0.4880 J 10Trp_H5 10Trp_H7 STAT=Y PRED= -0.300 RANGE= 0.500
J217_218 0.6708 J 10Trp_H9 10Trp_H7 STAT=Y PRED= 1.020 RANGE= 1.200
J223_224 7.9094 J 11Val_H2 11Val_H3 STAT=Y PRED= 3.450 RANGE= 9.000
J224_225 6.7483 J 11Val_H3 11Val_H4 STAT=Y PRED= 6.640 RANGE= 0.200
J224_228 6.8064 J 11Val_H3 11Val_H5 STAT=Y PRED= 6.640 RANGE= 0.200
J232_233 1.9005 J 12Phe_H2 12Phe_H3 STAT=Y PRED= 1.900 RANGE= 6.600
J234_238 1.3335 J 12Phe_H5 12Phe_H5 STAT=Y PRED= 1.980 RANGE= 1.200
J234_235 7.6508 J 12Phe_H5 12Phe_H6 STAT=Y PRED= 7.660 RANGE= 0.340
J234_237 0.7769 J 12Phe_H6 12Phe_H5 STAT=Y PRED= 0.550 RANGE= 0.750
J234_236 1.2760 J 12Phe_H5 12Phe_H7 STAT=Y PRED= 1.260 RANGE= 1.200
J235_237 1.7027 J 12Phe_H6 12Phe_H6 STAT=Y PRED= 1.480 RANGE= 1.200
J235_236 7.4760 J 12Phe_H6 12Phe_H7 STAT=Y PRED= 7.400 RANGE= 0.240
J241_242 8.8924 J 13Val_H2 13Val_H3 STAT=Y PRED= 12.320 RANGE= 6.000
J242_243 6.8372 J 13Val_H3 13Val_H4 STAT=Y PRED= 6.640 RANGE= 0.200
J242_246 6.4162 J 13Val_H3 13Val_H5 STAT=Y PRED= 6.640 RANGE= 0.200
115_217 7.7969 J 10Y_H8 10Y_H9 STAT=Y PRED= 8.100 RANGE= 0.890
115_218 8.1808 J 10Y_H8 10Y_H7 STAT=Y PRED= 7.850 RANGE= 0.800

Appendix Y (continued)

122_123 9.1737 J 01V_H2 01V_H3 STAT=Y PRED= 12.510 RANGE= 4.000
123_124 6.5890 J 01V_H3 01V_H6 STAT=Y PRED= 6.640 RANGE= 0.200
123_127 6.6205 J 01V_H3 01V_H7 STAT=Y PRED= 6.640 RANGE= 0.200
131_132 8.7545 J 02V_H2 02V_H3 STAT=Y PRED= 12.600 RANGE= 6.000
132_133 6.7841 J 02V_H3 02V_H4 STAT=Y PRED= 6.640 RANGE= 0.200
132_136 6.7206 J 02V_H3 02V_H5 STAT=Y PRED= 6.640 RANGE= 0.200
142_143 11.2297 J 03I_H2 03I_H3 STAT=Y PRED= 13.150 RANGE= 4.000
143_144 0.4614 J 03I_H3 03IH4A STAT=Y PRED= 1.950 RANGE= 3.000
143_145 2.9276 J 03I_H3 03IH4B STAT=Y PRED= 12.660 RANGE= 2.800
143_146 6.6276 J 03I_H3 03I_H6 STAT=Y PRED= 6.640 RANGE= 0.200
144_145 -12.2168 J 03IH4A 03IH4B STAT=Y PRED= -13.400 RANGE= 0.600
144_149 7.2855 J 03IH4A 03I_H5 STAT=Y PRED= 7.440 RANGE= 0.150
145_149 7.6340 J 03IH4B 03I_H5 STAT=Y PRED= 7.440 RANGE= 0.150
153_154 2.3441 J 04T_H2 04T_H3 STAT=Y PRED= 2.690 RANGE= 6.600
154_155 6.5134 J 04T_H3 04T_H4 STAT=Y PRED= 6.250 RANGE= 0.600
161_162 3.7259 J 05T_H2 05T_H3 STAT=Y PRED= 2.440 RANGE= 4.400
162_164 6.4691 J 05T_H3 05T_H4 STAT=Y PRED= 6.250 RANGE= 0.600
243 0.0000 J 05T_H3 08V_H2 STAT=Y
168_169 8.9180 J 06V_H2 06V_H3 STAT=Y PRED= 2.980 RANGE= 6.600
169_170 6.6944 J 06V_H3 06V_H4 STAT=Y PRED= 6.640 RANGE= 0.200
169_173 7.0316 J 06V_H3 06V_H5 STAT=Y PRED= 6.640 RANGE= 0.200
179_180 6.2437 J 07L_H2 07LH3A STAT=Y PRED= 3.040 RANGE= 6.000
179_181 8.3839 J 07L_H2 07LH3B STAT=Y PRED= 13.950 RANGE= 4.000
180_181 -13.3047 J 07LH3A 07LH3B STAT=Y PRED= -14.710 RANGE= 1.600
180_182 8.2119 J 07LH3A 07L_H4 STAT=Y PRED= 12.990 RANGE= 2.560
181_182 5.7896 J 07LH3B 07L_H4 STAT=Y PRED= 2.270 RANGE= 3.000
182_183 6.5482 J 07L_H4 07L_H5 STAT=Y PRED= 6.640 RANGE= 0.200
182_186 6.5879 J 07L_H4 07L_H6 STAT=Y PRED= 6.640 RANGE= 0.200
190_191 8.8736 J 08V_H2 08V_H3 STAT=Y PRED= 12.880 RANGE= 6.000
191_192 6.5520 J 08V_H3 08V_H4 STAT=Y PRED= 6.640 RANGE= 0.200
191_195 6.7834 J 08V_H3 08V_H5 STAT=Y PRED= 6.640 RANGE= 0.200
201_202 7.6281 J 09V_H2 09V_H3 STAT=Y PRED= 12.960 RANGE= 4.000
202_203 6.4961 J 09V_H3 09V_H4 STAT=Y PRED= 6.640 RANGE= 0.200
202_206 6.7760 J 09V_H3 09V_H5 STAT=Y PRED= 6.640 RANGE= 0.200
212_213 11.1630 J 10Y_H2 10YH3A STAT=Y PRED= 12.890 RANGE= 4.000
212_214 4.7143 J 10Y_H2 10YH3B STAT=Y PRED= 1.900 RANGE= 4.400
213_214 -13.7295 J 10YH3A 10YH3B STAT=Y PRED= -16.760 RANGE= 2.560
215_218 0.4880 J 10Y_H5 10Y_H7 STAT=Y PRED= -0.300 RANGE= 0.500
217_218 0.6708 J 10Y_H9 10Y_H7 STAT=Y PRED= 1.020 RANGE= 1.200
223_224 7.1764 J 11I_H2 11I_H3 STAT=Y PRED= 3.450 RANGE= 9.000
224_225 11.6481 J 11I_H3 11IH4A STAT=Y PRED= 6.640 RANGE= 0.200
224225B 8.6548 J 11I_H3 11IH4B STAT=Y PRED= 6.640 RANGE= 0.200
224_228 6.8064 J 11I_H3 11I_H5 STAT=N PRED= 6.640 RANGE= 0.200
225AB -15.2022 J 11IH4A 11IH4B STAT=Y PRED= 6.640 RANGE= 0.200
25_229 6.5064 J 11IH4A 11I_H6 STAT=N PRED= 6.640 RANGE= 0.200
25B229 6.8064 J 11IH4B 11I_H6 STAT=N PRED= 6.640 RANGE= 0.200
232_233 1.9005 J 12F_H2 12F_H3 STAT=Y PRED= 1.900 RANGE= 6.600
234_238 1.3335 J 12F_H5 12F_H5 STAT=Y PRED= 1.980 RANGE= 1.200
234_235 7.6508 J 12F_H5 12F_H6 STAT=Y PRED= 7.660 RANGE= 0.340
234_237 0.7769 J 12F_H6 12F_H5 STAT=Y PRED= 0.550 RANGE= 0.750

Appendix Y (continued)

```
 234_236    1.2760   J 12F_H5   12F_H7    STAT=Y  PRED= 1.260 RANGE= 1.200
 235_237    1.7027   J 12F_H6   12F_H6    STAT=Y  PRED= 1.480 RANGE= 1.200
 235_236    7.4760   J 12F_H6   12F_H7    STAT=Y  PRED= 7.400 RANGE= 0.240
 241_242    8.8924   J 13V_H2   13V_H3    STAT=Y  PRED= 12.320 RANGE= 6.000
 242_243    6.8372   J 13V_H3   13V_H4    STAT=Y  PRED= 6.640 RANGE= 0.200
 242_246    6.4162   J 13V_H3   13V_H5    STAT=Y  PRED= 6.640 RANGE= 0.200

CONTROL PARAMETERS:
      Solvent =  none (def. 99% enriched)
        1.000 =  Concentration (vol%, def=1.0%)
   0.00100000 =  Minimum line-intensity
   0.00100000 =  Diagonalization criterium (not in use)
 700.15197800 =  FIELD(1H,MHz), used to transform shifts to ppms
  11.63296542 =  Left frequency (ppm)
  -4.33374659 =  Right frequency (ppm)
      10.000 =  Acquisition time (s, for QMTLS)
       0.000 =  Line-width (for modes D, P & T, 0=use defaults)
  0.094246347 =  Data-point resolution (Hz)
      28.306 =  GAUSSIAN (%, 0=use default from INF)
     -10.087 =  Dispersion contribution (%, 0=use default from INF)
   0.00000000 =  Decoupling frequency (for DORES)

CONSTRAINTS (in equations X0 = 1.0)...use no empty lines
 EQUAL 01Val_H2 = 13Val_H2
 EQUAL 06Val_H5 = 11Val_H4
 EQUAL 07Leu_H5 = 07Leu_H6
 IGNORE(HZ):  3441.747 to  3420.668
 IGNORE(HZ):  2323.920 to  2309.428
 IGNORE(HZ):  2328.672 to  2324.470
 IGNORE(HZ):  2288.657 to  2282.788
 IGNORE(HZ):  2392.691 to  2378.287
 IGNORE(HZ):  2251.845 to  2238.507
 IGNORE(HZ):  2197.427 to  2189.958

PSEUDO SPECTRUM(IN PPM):
      1     4.5945      0.0110      2.1609      0.0000      0.0000      0.0000     1    1

END of FILE
```

Appendix Z. The HiFSA profile of homoecumicin-11I.

* NEW: the lines beginning by * are comment lines !
* To keep all the chemical shifts fixed during iteration
* replace "CHEMICAL SHIFTS(HZ):" by "..SHIFTS(HZ): fixed"
* The couplings can be fixed in the same way

NMR-data: C:\Users\jgnapo_2\Desktop\Wei_H14_XRays\H14_withoutGO
#$œ Date 28. 3.2014; Time 16: 8:12 perch.pms

CHEMICAL SHIFTS(PPM):
PROTON 2*SPIN= 1 SPECIES=1H POPULATION(Y)= 0.71163
10Trp_H8/ 1 6.982325 1*1*1 STAT=Y PRED= 7.318 RANGE= 0.199 WIDTH(Y)= 1.215 RESP(Y)= 1.0000 HSQC= C74
01ValH45/ 1 2.325486 1*1*6 STAT=Y PRED= 2.370 RANGE= 0.306 WIDTH(Y)= 1.536 RESP(Y)= 1.0000 HSQC= C1_2
01Val_H2/ 1 2.690219 1*1*1 STAT=Y PRED= 4.169 RANGE= 0.636 WIDTH(Y)= 1.557 RESP(Y)= 1.0000 HSQC= C4
01Val_H3/ 1 2.051284 1*1*1 STAT=Y PRED= 1.952 RANGE= 0.817 WIDTH(Y)= 1.561 RESP(Y)= 1.0000 HSQC= C5
01Val_H6/ 1 0.848433 1*1*3 STAT=Y PRED= 0.509 RANGE= 0.867 WIDTH(Y)= 1.598 RESP(Y)= 1.0000 HSQC= C6
01Val_H7/ 1 0.976475 1*1*3 STAT=Y PRED= 0.818 RANGE= 0.356 WIDTH(Y)= 1.688 RESP(Y)= 1.0000 HSQC= C7
02Val_H2/ 1 4.665068 1*1*1 STAT=Y PRED= 4.508 RANGE= 0.807 WIDTH(Y)= 1.467 RESP(Y)= 1.0000 HSQC= C10
02Val_H3/ 1 2.099755 1*1*1 STAT=Y PRED= 2.155 RANGE= 0.777 WIDTH(Y)= 1.561 RESP(Y)= 1.0000 HSQC= C12
02Val_H4/ 1 0.994696 1*1*3 STAT=Y PRED= 1.038 RANGE= 0.279 WIDTH(Y)= 1.468 RESP(Y)= 1.0000 HSQC= C13
02Val_H5/ 1 1.054013 1*1*3 STAT=Y PRED= 0.943 RANGE= 0.249 WIDTH(Y)= 1.538 RESP(Y)= 1.0000 HSQC= C14
03Ile_H7/ 1 3.233986 1*1*3 STAT=Y PRED= 3.196 RANGE= 0.366 WIDTH(Y)= 1.536 RESP(Y)= 1.0000 HSQC= C15
03Ile_H2/ 1 4.911071 1*1*1 STAT=Y PRED= 4.617 RANGE= 1.627 WIDTH(Y)= 1.466 RESP(Y)= 1.0000 HSQC= C17
03Ile_H3/ 1 1.949735 1*1*1 STAT=Y PRED= 2.032 RANGE= 0.706 WIDTH(Y)= 2.929 RESP(Y)= 1.0000 HSQC= C19
03IleH4A/ 1 0.955039 1*1*1 STAT=Y PRED= 1.465 RANGE= 0.697 WIDTH(Y)= 5.275 RESP(Y)= 1.0000 HSQC= C20
03IleH4B/ 1 1.296763 1*1*1 STAT=Y PRED= 1.175 RANGE= 0.586 WIDTH(Y)= 2.795 RESP(Y)= 1.0000 HSQC= C20
03Ile_H6/ 1 0.757782 1*1*3 STAT=Y PRED= 0.723 RANGE= 0.396 WIDTH(Y)= 1.613 RESP(Y)= 1.0000 HSQC= C21
03Ile_H5/ 1 0.748021 1*1*3 STAT=Y PRED= 0.880 RANGE= 0.219 WIDTH(Y)= 1.391 RESP(Y)= 1.0000 HSQC= C22
04Thr_H2/ 1 5.161027 1*1*1 STAT=Y PRED= 4.668 RANGE= 1.013 WIDTH(Y)= 1.377 RESP(Y)= 1.0000 HSQC= C24
04Thr_H3/ 1 5.772637 1*1*1 STAT=Y PRED= 4.010 RANGE= 0.476 WIDTH(Y)= 1.941 RESP(Y)= 1.0000 HSQC= C25
04Thr_H4/ 1 1.310504 1*1*3 STAT=Y PRED= 1.270 RANGE= 0.496 WIDTH(Y)= 1.818 RESP(Y)= 1.0000 HSQC= C27
05Thr_H5/ 1 3.329093 1*1*3 STAT=Y PRED= 3.257 RANGE= 0.396 WIDTH(Y)= 1.439 RESP(Y)= 1.0000 HSQC= C29
05Thr_H2/ 1 5.008056 1*1*1 STAT=Y PRED= 4.099 RANGE= 1.023 WIDTH(Y)= 1.500 RESP(Y)= 1.0000 HSQC= C31
05Thr_H3/ 1 4.466749 1*1*1 STAT=Y PRED= 4.345 RANGE= 0.717 WIDTH(Y)= 1.572 RESP(Y)= 1.0000 HSQC= C32
05Thr_H4/ 1 0.910868 1*1*3 STAT=Y PRED= 1.252 RANGE= 0.299 WIDTH(Y)= 1.939 RESP(Y)= 1.0000 HSQC= C34
13Ile_H2/ 1 4.839938 1*1*1 STAT=Y PRED= 4.525 RANGE= 1.407 WIDTH(Y)= 1.382 RESP(Y)= 1.0000 HSQC= C37
13Ile_H3/ 1 1.785187 1*1*1 STAT=Y PRED= 1.975 RANGE= 1.017 WIDTH(Y)= 1.789 RESP(Y)= 1.0000 HSQC= C38
13IleH4A/ 1 1.400452 1*1*3 STAT=Y PRED= 0.938 RANGE= 0.219 WIDTH(Y)= 1.894 RESP(Y)= 1.0000 HSQC= C39
13IleH4B/ 1 1.120452 1*1*3 STAT=Y PRED= 0.938 RANGE= 0.219 WIDTH(Y)= 1.894 RESP(Y)= 1.0000 HSQC= C39
13Ile_H5/ 1 0.910823 1*1*3 STAT=Y PRED= 1.094 RANGE= 0.386 WIDTH(Y)= 2.275 RESP(Y)= 1.0000 HSQC= C40
13Ile_H6/ 1 0.910823 1*1*3 STAT=Y PRED= 1.094 RANGE= 0.386 WIDTH(Y)= 2.275 RESP(Y)= 1.0000 HSQC= C41
07Leu_H7/ 1 3.260594 1*1*3 STAT=Y PRED= 3.110 RANGE= 0.376 WIDTH(Y)= 1.459 RESP(Y)= 1.0000 HSQC= C42
07Leu_H2/ 1 5.116104 1*1*1 STAT=Y PRED= 5.342 RANGE= 1.083 WIDTH(Y)= 2.240 RESP(Y)= 1.0000 HSQC= C44
07LeuH3A/ 1 1.458188 1*1*1 STAT=Y PRED= 1.444 RANGE= 0.426 WIDTH(Y)= 1.805 RESP(Y)= 1.0000 HSQC= C45
07LeuH3B/ 1 1.237573 1*1*1 STAT=Y PRED= 1.914 RANGE= 0.366 WIDTH(Y)= 3.321 RESP(Y)= 1.0000 HSQC= C45
07Leu_H4/ 1 0.948812 1*1*1 STAT=Y PRED= 1.630 RANGE= 0.626 WIDTH(Y)= 1.520 RESP(Y)= 1.0000 HSQC= C46
07Leu_H5/ 1 0.336591 1*1*3 STAT=Y PRED= 0.972 RANGE= 0.316 WIDTH(Y)= 1.961 RESP(Y)= 1.0000 HSQC= C47
07Leu_H6/ 1 0.168976 1*1*3 STAT=Y PRED= 0.972 RANGE= 0.149 WIDTH(Y)= 1.885 RESP(Y)= 1.0000 HSQC= C48
08Val_H2/ 1 4.608604 1*1*1 STAT=Y PRED= 4.489 RANGE= 0.897 WIDTH(Y)= 1.578 RESP(Y)= 1.0000 HSQC= C51
08Val_H3/ 1 2.026205 1*1*1 STAT=Y PRED= 1.995 RANGE= 0.486 WIDTH(Y)= 2.872 RESP(Y)= 1.0000 HSQC= C52
08Val_H4/ 1 0.916425 1*1*3 STAT=Y PRED= 1.060 RANGE= 0.236 WIDTH(Y)= 1.731 RESP(Y)= 1.0000 HSQC= C53

Appendix Z (continued)

08Val_H5/ 1 0.861363 1*1*3 STAT=Y PRED= 0.999 RANGE= 0.229 WIDTH(Y)= 2.065 RESP(Y)= 1.0000 HSQC= C54
09Val_H6/ 1 3.145503 1*1*3 STAT=Y PRED= 3.169 RANGE= 0.466 WIDTH(Y)= 1.931 RESP(Y)= 1.0000 HSQC= C56
09Val_H2/ 1 3.074915 1*1*1 STAT=Y PRED= 5.153 RANGE= 0.717 WIDTH(Y)= 2.597 RESP(Y)= 1.0000 HSQC= C58
09Val_H3/ 1 2.584340 1*1*1 STAT=Y PRED= 2.524 RANGE= 0.406 WIDTH(Y)= 1.736 RESP(Y)= 1.0000 HSQC= C59
09Val_H4/ 1 1.096137 1*1*3 STAT=Y PRED= 1.319 RANGE= 0.226 WIDTH(Y)= 1.741 RESP(Y)= 1.0000 HSQC= C60
09Val_H5/ 1 0.982470 1*1*3 STAT=Y PRED= 1.075 RANGE= 0.239 WIDTH(Y)= 2.379 RESP(Y)= 1.0000 HSQC= C61
10TrpH13/ 1 2.156847 1*1*3 STAT=Y PRED= 2.936 RANGE= 0.893 WIDTH(Y)= 1.862 RESP(Y)= 1.0000 HSQC= C63
10Trp_H2/ 1 4.101575 1*1*1 STAT=Y PRED= 5.043 RANGE= 1.764 WIDTH(Y)= 2.064 RESP(Y)= 1.0000 HSQC= C65
10TrpH3A/ 1 3.560440 1*1*1 STAT=Y PRED= 3.613 RANGE= 0.466 WIDTH(Y)= 1.516 RESP(Y)= 1.0000 HSQC= C66
10TrpH3B/ 1 3.690935 1*1*1 STAT=Y PRED= 3.367 RANGE= 0.626 WIDTH(Y)= 2.118 RESP(Y)= 1.0000 HSQC= C66
10Trp_H5/ 1 6.698385 1*1*1 STAT=Y PRED= 6.772 RANGE= 0.276 WIDTH(Y)= 1.649 RESP(Y)= 1.0000 HSQC= C68
10Trp_H9/ 1 6.442449 1*1*1 STAT=Y PRED= 7.089 RANGE= 0.219 WIDTH(Y)= 1.143 RESP(Y)= 1.0000 HSQC= C73
10Trp_H7/ 1 6.918830 1*1*1 STAT=Y PRED= 7.333 RANGE= 0.309 WIDTH(Y)= 0.719 RESP(Y)= 1.0000 HSQC= C75
10TrpH12/ 1 3.826612 1*1*3 STAT=Y PRED= 4.072 RANGE= 0.249 WIDTH(Y)= 1.244 RESP(Y)= 1.0000 HSQC= C77
11Val_H2/ 1 4.524897 1*1*1 STAT=Y PRED= 4.303 RANGE= 1.447 WIDTH(Y)= 1.849 RESP(Y)= 1.0000 HSQC= C80
11Val_H3/ 1 2.199630 1*1*1 STAT=Y PRED= 2.094 RANGE= 0.586 WIDTH(Y)= 1.854 RESP(Y)= 1.0000 HSQC= C81
11Val_H4/ 1 1.034271 1*1*3 STAT=Y PRED= 1.094 RANGE= 0.249 WIDTH(Y)= 2.106 RESP(Y)= 1.0000 HSQC= C82
11Val_H5/ 1 0.989808 1*1*3 STAT=Y PRED= 1.080 RANGE= 0.299 WIDTH(Y)= 1.787 RESP(Y)= 1.0000 HSQC= C83
12Phe_H2/ 1 4.839108 1*1*1 STAT=Y PRED= 4.499 RANGE= 0.987 WIDTH(Y)= 1.261 RESP(Y)= 1.0000 HSQC= C86
12Phe_H3/ 1 5.348787 1*1*1 STAT=Y PRED= 5.208 RANGE= 0.486 WIDTH(Y)= 1.884 RESP(Y)= 1.0000 HSQC= C87
12Phe_H5/ 1 7.238322 1*2*1 STAT=Y PRED= 7.524 RANGE= 0.309 WIDTH(Y)= 2.042 RESP(Y)= 1.0000 HSQC= C89_93
12Phe_H6/ 1 7.255114 1*2*1 STAT=Y PRED= 7.372 RANGE= 0.576 WIDTH(Y)= 1.207 RESP(Y)= 1.0000 HSQC= C90_92
12Phe_H7/ 1 7.202197 1*1*1 STAT=Y PRED= 7.281 RANGE= 0.309 WIDTH(Y)= 1.557 RESP(Y)= 1.0000 HSQC= C91
06Val_H2/ 1 4.514692 1*1*1 STAT=Y PRED= 4.169 RANGE= 0.667 WIDTH(Y)= 1.205 RESP(Y)= 1.0000 HSQC= C97
06Val_H3/ 1 1.974671 1*1*1 STAT=Y PRED= 1.935 RANGE= 0.867 WIDTH(Y)= 1.973 RESP(Y)= 1.0000 HSQC= C99
06Val_H4/ 1 0.929643 1*1*3 STAT=Y PRED= 1.277 RANGE= 0.219 WIDTH(Y)= 2.666 RESP(Y)= 1.0000 HSQC= C100
06Val_H5/ 1 0.913883 1*1*3 STAT=Y PRED= 0.933 RANGE= 0.276 WIDTH(Y)= 2.083 RESP(Y)= 1.0000 HSQC= C101
PROTON 2*SPIN= 1 SPECIES=1H POPULATION(Y)= 0.28837
10Y_H8 / 2 6.982643 1*1*1 STAT=N PRED= 7.318 RANGE= 0.199 WIDTH(Y)= 1.215 RESP(Y)= 1.0000 HSQC= C74
01VH45 / 2 2.331280 1*1*6 STAT=N PRED= 2.370 RANGE= 0.306 WIDTH(Y)= 1.536 RESP(Y)= 1.0000 HSQC= C1_2
01V_H2 / 2 2.705188 1*1*1 STAT=N PRED= 4.169 RANGE= 0.636 WIDTH(Y)= 1.557 RESP(Y)= 1.0000 HSQC= C4
01V_H3 / 2 2.044179 1*1*1 STAT=N PRED= 1.952 RANGE= 0.817 WIDTH(Y)= 1.561 RESP(Y)= 1.0000 HSQC= C5
01V_H6 / 2 0.849588 1*1*3 STAT=N PRED= 0.509 RANGE= 0.867 WIDTH(Y)= 1.598 RESP(Y)= 1.0000 HSQC= C6
01V_H7 / 2 0.980989 1*1*3 STAT=N PRED= 0.818 RANGE= 0.356 WIDTH(Y)= 1.688 RESP(Y)= 1.0000 HSQC= C7
02V_H2 / 2 4.670147 1*1*1 STAT=N PRED= 4.508 RANGE= 0.807 WIDTH(Y)= 1.467 RESP(Y)= 1.0000 HSQC= C10
02V_H3 / 2 2.108243 1*1*1 STAT=N PRED= 2.155 RANGE= 0.777 WIDTH(Y)= 1.561 RESP(Y)= 1.0000 HSQC= C12
02V_H4 / 2 0.981760 1*1*3 STAT=N PRED= 1.038 RANGE= 0.279 WIDTH(Y)= 1.468 RESP(Y)= 1.0000 HSQC= C13
02V_H5 / 2 1.058864 1*1*3 STAT=N PRED= 0.943 RANGE= 0.249 WIDTH(Y)= 1.538 RESP(Y)= 1.0000 HSQC= C14
03I_H7 / 2 3.235337 1*1*3 STAT=N PRED= 3.196 RANGE= 0.366 WIDTH(Y)= 1.536 RESP(Y)= 1.0000 HSQC= C15
03I_H2 / 2 4.907493 1*1*1 STAT=N PRED= 4.617 RANGE= 1.627 WIDTH(Y)= 1.466 RESP(Y)= 1.0000 HSQC= C17
03I_H3 / 2 1.951705 1*1*1 STAT=N PRED= 2.032 RANGE= 0.706 WIDTH(Y)= 2.929 RESP(Y)= 1.0000 HSQC= C19
03IH4A / 2 0.904202 1*1*1 STAT=N PRED= 1.465 RANGE= 0.697 WIDTH(Y)= 5.275 RESP(Y)= 1.0000 HSQC= C20
03IH4B / 2 1.244466 1*1*1 STAT=N PRED= 1.175 RANGE= 0.586 WIDTH(Y)= 2.795 RESP(Y)= 1.0000 HSQC= C20
03I_H6 / 2 0.760037 1*1*3 STAT=N PRED= 0.723 RANGE= 0.396 WIDTH(Y)= 1.613 RESP(Y)= 1.0000 HSQC= C21
03I_H5 / 2 0.750330 1*1*3 STAT=N PRED= 0.880 RANGE= 0.219 WIDTH(Y)= 1.391 RESP(Y)= 1.0000 HSQC= C22
04T_H2 / 2 5.168532 1*1*1 STAT=N PRED= 4.668 RANGE= 1.013 WIDTH(Y)= 1.377 RESP(Y)= 1.0000 HSQC= C24
04T_H3 / 2 5.779659 1*1*1 STAT=N PRED= 4.010 RANGE= 0.476 WIDTH(Y)= 1.941 RESP(Y)= 1.0000 HSQC= C25
04T_H4 / 2 1.311416 1*1*3 STAT=N PRED= 1.270 RANGE= 0.496 WIDTH(Y)= 1.818 RESP(Y)= 1.0000 HSQC= C27
05T_H5 / 2 3.325329 1*1*3 STAT=N PRED= 3.257 RANGE= 0.396 WIDTH(Y)= 1.439 RESP(Y)= 1.0000 HSQC= C29
05T_H2 / 2 4.999806 1*1*1 STAT=N PRED= 4.099 RANGE= 1.023 WIDTH(Y)= 1.500 RESP(Y)= 1.0000 HSQC= C31

Appendix Z (continued)

```
05T_H3  / 2    4.444347  1*1*1  STAT=N  PRED= 4.345 RANGE= 0.717 WIDTH(Y)= 1.572 RESP(Y)= 1.0000 HSQC= C32
05T_H4  / 2    0.911618  1*1*3  STAT=N  PRED= 1.252 RANGE= 0.299 WIDTH(Y)= 1.939 RESP(Y)= 1.0000 HSQC= C34
06V_H2  / 2    4.863987  1*1*1  STAT=N  PRED= 4.525 RANGE= 1.407 WIDTH(Y)= 1.382 RESP(Y)= 1.0000 HSQC= C37
06V_H3  / 2    2.341573  1*1*1  STAT=N  PRED= 1.975 RANGE= 1.017 WIDTH(Y)= 1.789 RESP(Y)= 1.0000 HSQC= C38
06V_H4  / 2    1.086573  1*1*3  STAT=N  PRED= 0.938 RANGE= 0.219 WIDTH(Y)= 1.894 RESP(Y)= 1.0000 HSQC= C39
06V_H5  / 2    0.985855  1*1*3  STAT=N  PRED= 1.094 RANGE= 0.386 WIDTH(Y)= 2.275 RESP(Y)= 1.0000 HSQC= C40
07L_H7  / 2    3.264425  1*1*3  STAT=N  PRED= 3.110 RANGE= 0.376 WIDTH(Y)= 1.459 RESP(Y)= 1.0000 HSQC= C42
07L_H2  / 2    5.132251  1*1*1  STAT=N  PRED= 5.342 RANGE= 1.083 WIDTH(Y)= 2.240 RESP(Y)= 1.0000 HSQC= C44
07LH3A  / 2    1.470249  1*1*1  STAT=N  PRED= 1.444 RANGE= 0.426 WIDTH(Y)= 1.805 RESP(Y)= 1.0000 HSQC= C45
07LH3B  / 2    1.231458  1*1*1  STAT=N  PRED= 1.914 RANGE= 0.366 WIDTH(Y)= 3.321 RESP(Y)= 1.0000 HSQC= C45
07L_H4  / 2    0.927464  1*1*1  STAT=N  PRED= 1.630 RANGE= 0.626 WIDTH(Y)= 1.520 RESP(Y)= 1.0000 HSQC= C46
07L_H5  / 2    0.363847  1*1*3  STAT=N  PRED= 0.972 RANGE= 0.316 WIDTH(Y)= 1.961 RESP(Y)= 1.0000 HSQC= C47
07L_H6  / 2    0.180380  1*1*3  STAT=N  PRED= 0.972 RANGE= 0.149 WIDTH(Y)= 1.885 RESP(Y)= 1.0000 HSQC= C48
08V_H2  / 2    4.595474  1*1*1  STAT=N  PRED= 4.489 RANGE= 0.897 WIDTH(Y)= 1.578 RESP(Y)= 1.0000 HSQC= C51
08V_H3  / 2    1.987696  1*1*1  STAT=N  PRED= 1.995 RANGE= 0.486 WIDTH(Y)= 2.872 RESP(Y)= 1.0000 HSQC= C52
08V_H4  / 2    0.928532  1*1*3  STAT=N  PRED= 1.060 RANGE= 0.236 WIDTH(Y)= 1.731 RESP(Y)= 1.0000 HSQC= C53
08V_H5  / 2    0.861982  1*1*3  STAT=N  PRED= 0.999 RANGE= 0.229 WIDTH(Y)= 2.065 RESP(Y)= 1.0000 HSQC= C54
09V_H6  / 2    3.135917  1*1*3  STAT=N  PRED= 3.169 RANGE= 0.466 WIDTH(Y)= 1.931 RESP(Y)= 1.0000 HSQC= C56
09V_H2  / 2    3.065174  1*1*1  STAT=N  PRED= 5.153 RANGE= 0.717 WIDTH(Y)= 2.597 RESP(Y)= 1.0000 HSQC= C58
09V_H3  / 2    2.575838  1*1*1  STAT=N  PRED= 2.524 RANGE= 0.406 WIDTH(Y)= 1.736 RESP(Y)= 1.0000 HSQC= C59
09V_H4  / 2    1.094566  1*1*3  STAT=N  PRED= 1.319 RANGE= 0.226 WIDTH(Y)= 1.741 RESP(Y)= 1.0000 HSQC= C60
09V_H5  / 2    0.983397  1*1*3  STAT=N  PRED= 1.075 RANGE= 0.239 WIDTH(Y)= 2.379 RESP(Y)= 1.0000 HSQC= C61
10YH13  / 2    2.157614  1*1*3  STAT=N  PRED= 2.936 RANGE= 0.893 WIDTH(Y)= 1.862 RESP(Y)= 1.0000 HSQC= C63
10Y_H2  / 2    4.114944  1*1*1  STAT=N  PRED= 5.043 RANGE= 1.764 WIDTH(Y)= 2.064 RESP(Y)= 1.0000 HSQC= C65
10YH3A  / 2    3.564700  1*1*1  STAT=N  PRED= 3.613 RANGE= 0.466 WIDTH(Y)= 1.516 RESP(Y)= 1.0000 HSQC= C66
10YH3B  / 2    3.692019  1*1*1  STAT=N  PRED= 3.367 RANGE= 0.626 WIDTH(Y)= 2.118 RESP(Y)= 1.0000 HSQC= C66
10Y_H5  / 2    6.701771  1*1*1  STAT=N  PRED= 6.772 RANGE= 0.276 WIDTH(Y)= 1.649 RESP(Y)= 1.0000 HSQC= C68
10Y_H9  / 2    6.443403  1*1*1  STAT=N  PRED= 7.089 RANGE= 0.219 WIDTH(Y)= 1.143 RESP(Y)= 1.0000 HSQC= C73
10Y_H7  / 2    6.919434  1*1*1  STAT=N  PRED= 7.333 RANGE= 0.309 WIDTH(Y)= 0.719 RESP(Y)= 1.0000 HSQC= C75
10YH12  / 2    3.830106  1*1*3  STAT=N  PRED= 4.072 RANGE= 0.249 WIDTH(Y)= 1.244 RESP(Y)= 1.0000 HSQC= C77
11I_H2  / 2    4.645948  1*1*1  STAT=N  PRED= 4.303 RANGE= 1.447 WIDTH(Y)= 1.849 RESP(Y)= 1.0000 HSQC= C80
11I_H3  / 2    1.963073  1*1*1  STAT=N  PRED= 2.094 RANGE= 0.586 WIDTH(Y)= 1.854 RESP(Y)= 1.0000 HSQC= C81
11IH4A  / 2    1.577140  1*1*3  STAT=N  PRED= 1.094 RANGE= 0.249 WIDTH(Y)= 2.106 RESP(Y)= 1.0000 HSQC= C82
11IH4B  / 2    1.222059  1*1*3  STAT=N  PRED= 1.080 RANGE= 0.299 WIDTH(Y)= 1.787 RESP(Y)= 1.0000 HSQC= C82
11I_H5  / 2    0.915100  1*1*3  STAT=N  PRED= 1.080 RANGE= 0.299 WIDTH(Y)= 1.787 RESP(Y)= 1.0000 HSQC= C83
11I_H6  / 2    0.990779  1*1*3  STAT=N  PRED= 1.080 RANGE= 0.299 WIDTH(Y)= 1.787 RESP(Y)= 1.0000 HSQC= C84
12F_H2  / 2    4.920692  1*1*1  STAT=N  PRED= 4.499 RANGE= 0.987 WIDTH(Y)= 1.261 RESP(Y)= 1.0000 HSQC= C86
12F_H3  / 2    5.318327  1*1*1  STAT=N  PRED= 5.208 RANGE= 0.486 WIDTH(Y)= 1.884 RESP(Y)= 1.0000 HSQC= C87
12F_H5  / 2    7.229493  1*2*1  STAT=N  PRED= 7.524 RANGE= 0.309 WIDTH(Y)= 2.042 RESP(Y)= 1.0000 HSQC= C89_93
12F_H6  / 2    7.249523  1*2*1  STAT=N  PRED= 7.372 RANGE= 0.576 WIDTH(Y)= 1.207 RESP(Y)= 1.0000 HSQC= C90_92
12F_H7  / 2    7.195963  1*1*1  STAT=N  PRED= 7.281 RANGE= 0.309 WIDTH(Y)= 1.557 RESP(Y)= 1.0000 HSQC= C91
13V_H2  / 2    4.408276  1*1*1  STAT=N  PRED= 4.169 RANGE= 0.667 WIDTH(Y)= 1.205 RESP(Y)= 1.0000 HSQC= C97
13V_H3  / 2    1.962989  1*1*1  STAT=N  PRED= 1.935 RANGE= 0.867 WIDTH(Y)= 1.973 RESP(Y)= 1.0000 HSQC= C99
13V_H4  / 2    0.944236  1*1*3  STAT=N  PRED= 1.277 RANGE= 0.219 WIDTH(Y)= 2.666 RESP(Y)= 1.0000 HSQC= C100
13V_H5  / 2    0.915347  1*1*3  STAT=N  PRED= 0.933 RANGE= 0.276 WIDTH(Y)= 2.083 RESP(Y)= 1.0000 HSQC= C101

COUPLING CONSTANTS(HZ):
J115_217    7.7969   J 10Trp_H8 10Trp_H9   STAT=N  PRED= 8.100 RANGE= 0.890
J115_218    8.1808   J 10Trp_H8 10Trp_H7   STAT=N  PRED= 7.850 RANGE= 0.800
J122_123    9.1737   J 01Val_H2 01Val_H3   STAT=N  PRED= 12.510 RANGE= 4.000
```

Appendix Z (continued)

J123_124 6.5890 J 01Val_H3 01Val_H6 STAT=N PRED= 6.640 RANGE= 0.200
J123_127 6.6205 J 01Val_H3 01Val_H7 STAT=N PRED= 6.640 RANGE= 0.200
J131_132 8.7545 J 02Val_H2 02Val_H3 STAT=N PRED= 12.600 RANGE= 6.000
J132_133 6.7841 J 02Val_H3 02Val_H4 STAT=N PRED= 6.640 RANGE= 0.200
J132_136 6.7206 J 02Val_H3 02Val_H5 STAT=N PRED= 6.640 RANGE= 0.200
J142_143 11.2297 J 03Ile_H2 03Ile_H3 STAT=N PRED= 13.150 RANGE= 4.000
J143_144 0.4614 J 03Ile_H3 03IleH4A STAT=N PRED= 1.950 RANGE= 3.000
J143_145 2.9276 J 03Ile_H3 03IleH4B STAT=N PRED= 12.660 RANGE= 2.800
J143_146 6.6276 J 03Ile_H3 03Ile_H6 STAT=N PRED= 6.640 RANGE= 0.200
J144_145 -12.2168 J 03IleH4A 03IleH4B STAT=N PRED= -13.400 RANGE= 0.600
J144_149 7.2855 J 03IleH4A 03Ile_H5 STAT=N PRED= 7.440 RANGE= 0.150
J145_149 7.6340 J 03IleH4B 03Ile_H5 STAT=N PRED= 7.440 RANGE= 0.150
J153_154 2.3441 J 04Thr_H2 04Thr_H3 STAT=N PRED= 2.690 RANGE= 6.600
J154_155 6.5134 J 04Thr_H3 04Thr_H4 STAT=N PRED= 6.250 RANGE= 0.600
J161_162 3.7259 J 05Thr_H2 05Thr_H3 STAT=N PRED= 2.440 RANGE= 4.400
J162_164 6.4691 J 05Thr_H3 05Thr_H4 STAT=N PRED= 6.250 RANGE= 0.600
J168_169 8.9180 J 13Ile_H2 13Ile_H3 STAT=Y PRED= 2.980 RANGE= 6.600
J169_170 6.6944 J 13Ile_H3 13IleH4A STAT=Y PRED= 6.640 RANGE= 0.200
J169_171 7.0316 J 13Ile_H3 13IleH4B STAT=Y PRED= 6.640 RANGE= 0.200
J169_172 7.0316 J 13Ile_H3 13Ile_H5 STAT=Y PRED= 6.640 RANGE= 0.200
J170_171 -14.0000 J 13IleH4A 13IleH4B STAT=Y PRED= -14.000 RANGE= 0.200
J170_173 7.0316 J 13IleH4A 13Ile_H6 STAT=Y PRED= 6.640 RANGE= 0.200
J171_173 7.0316 J 13IleH4B 13Ile_H6 STAT=Y PRED= 6.640 RANGE= 0.200
J179_180 6.2437 J 07Leu_H2 07LeuH3A STAT=N PRED= 3.040 RANGE= 6.000
J179_181 8.3839 J 07Leu_H2 07LeuH3B STAT=N PRED= 13.950 RANGE= 4.000
J180_181 -13.3047 J 07LeuH3A 07LeuH3B STAT=N PRED= -14.710 RANGE= 1.600
J180_182 8.2119 J 07LeuH3A 07Leu_H4 STAT=N PRED= 12.990 RANGE= 2.560
J181_182 5.7896 J 07LeuH3B 07Leu_H4 STAT=N PRED= 2.270 RANGE= 3.000
J182_183 6.5482 J 07Leu_H4 07Leu_H5 STAT=N PRED= 6.640 RANGE= 0.200
J182_186 6.5879 J 07Leu_H4 07Leu_H6 STAT=N PRED= 6.640 RANGE= 0.200
J190_191 8.8736 J 08Val_H2 08Val_H3 STAT=N PRED= 12.880 RANGE= 6.000
J191_192 6.5520 J 08Val_H3 08Val_H4 STAT=N PRED= 6.640 RANGE= 0.200
J191_195 6.7834 J 08Val_H3 08Val_H5 STAT=N PRED= 6.640 RANGE= 0.200
J201_202 7.6281 J 09Val_H2 09Val_H3 STAT=N PRED= 12.960 RANGE= 4.000
J202_203 6.4961 J 09Val_H3 09Val_H4 STAT=N PRED= 6.640 RANGE= 0.200
J202_206 6.7760 J 09Val_H3 09Val_H5 STAT=N PRED= 6.640 RANGE= 0.200
J212_213 11.1630 J 10Trp_H2 10TrpH3A STAT=N PRED= 12.890 RANGE= 4.000
J212_214 4.7143 J 10Trp_H2 10TrpH3B STAT=N PRED= 1.900 RANGE= 4.400
J213_214 -13.7295 J 10TrpH3A 10TrpH3B STAT=N PRED= -16.760 RANGE= 2.560
J215_218 0.4880 J 10Trp_H5 10Trp_H7 STAT=N PRED= -0.300 RANGE= 0.500
J217_218 0.6708 J 10Trp_H9 10Trp_H7 STAT=N PRED= 1.020 RANGE= 1.200
J223_224 7.9094 J 11Val_H2 11Val_H3 STAT=N PRED= 3.450 RANGE= 9.000
J224_225 6.7483 J 11Val_H3 11Val_H4 STAT=N PRED= 6.640 RANGE= 0.200
J224_228 6.8064 J 11Val_H3 11Val_H5 STAT=N PRED= 6.640 RANGE= 0.200
J232_233 1.9005 J 12Phe_H2 12Phe_H3 STAT=N PRED= 1.900 RANGE= 6.600
J234_238 1.3335 J 12Phe_H5 12Phe_H5 STAT=N PRED= 1.980 RANGE= 1.200
J234_235 7.6508 J 12Phe_H5 12Phe_H6 STAT=N PRED= 7.660 RANGE= 0.340
J234_237 0.7769 J 12Phe_H6 12Phe_H5 STAT=N PRED= 0.550 RANGE= 0.750
J234_236 1.2760 J 12Phe_H5 12Phe_H7 STAT=N PRED= 1.260 RANGE= 1.200
J235_237 1.7027 J 12Phe_H6 12Phe_H6 STAT=N PRED= 1.480 RANGE= 1.200

Appendix Z (continued)

J235_236 7.4760 J 12Phe_H6 12Phe_H7 STAT=N PRED= 7.400 RANGE= 0.240
J241_242 8.8924 J 06Val_H2 06Val_H3 STAT=N PRED= 12.320 RANGE= 6.000
J242_243 6.8372 J 06Val_H3 06Val_H4 STAT=N PRED= 6.640 RANGE= 0.200
J242_246 6.4162 J 06Val_H3 06Val_H5 STAT=N PRED= 6.640 RANGE= 0.200
115_217 7.7969 J 10Y_H8 10Y_H9 STAT=N PRED= 8.100 RANGE= 0.890
115_218 8.1808 J 10Y_H8 10Y_H7 STAT=N PRED= 7.850 RANGE= 0.800
122_123 9.1737 J 01V_H2 01V_H3 STAT=N PRED= 12.510 RANGE= 4.000
123_124 6.5890 J 01V_H3 01V_H6 STAT=N PRED= 6.640 RANGE= 0.200
123_127 6.6205 J 01V_H3 01V_H7 STAT=N PRED= 6.640 RANGE= 0.200
131_132 8.7545 J 02V_H2 02V_H3 STAT=N PRED= 12.600 RANGE= 6.000
132_133 6.7841 J 02V_H3 02V_H4 STAT=N PRED= 6.640 RANGE= 0.200
132_136 6.7206 J 02V_H3 02V_H5 STAT=N PRED= 6.640 RANGE= 0.200
142_143 11.2297 J 03I_H2 03I_H3 STAT=N PRED= 13.150 RANGE= 4.000
143_144 0.4614 J 03I_H3 03IH4A STAT=N PRED= 1.950 RANGE= 3.000
143_145 2.9276 J 03I_H3 03IH4B STAT=N PRED= 12.660 RANGE= 2.800
143_146 6.6276 J 03I_H3 03I_H6 STAT=N PRED= 6.640 RANGE= 0.200
144_145 -12.2168 J 03IH4A 03IH4B STAT=N PRED= -13.400 RANGE= 0.600
144_149 7.2855 J 03IH4A 03I_H5 STAT=N PRED= 7.440 RANGE= 0.150
145_149 7.6340 J 03IH4B 03I_H5 STAT=N PRED= 7.440 RANGE= 0.150
153_154 2.3441 J 04T_H2 04T_H3 STAT=N PRED= 2.690 RANGE= 6.600
154_155 6.5134 J 04T_H3 04T_H4 STAT=N PRED= 6.250 RANGE= 0.600
161_162 3.7259 J 05T_H2 05T_H3 STAT=N PRED= 2.440 RANGE= 4.400
162_164 6.4691 J 05T_H3 05T_H4 STAT=N PRED= 6.250 RANGE= 0.600
168_169 8.9180 J 06V_H2 06V_H3 STAT=N PRED= 2.980 RANGE= 6.600
169_170 6.6944 J 06V_H3 06V_H4 STAT=N PRED= 6.640 RANGE= 0.200
169_173 7.0316 J 06V_H3 06V_H5 STAT=N PRED= 6.640 RANGE= 0.200
179_180 6.2437 J 07L_H2 07LH3A STAT=N PRED= 3.040 RANGE= 6.000
179_181 8.3839 J 07L_H2 07LH3B STAT=N PRED= 13.950 RANGE= 4.000
180_181 -13.3047 J 07LH3A 07LH3B STAT=N PRED= -14.710 RANGE= 1.600
180_182 8.2119 J 07LH3A 07L_H4 STAT=N PRED= 12.990 RANGE= 2.560
181_182 5.7896 J 07LH3B 07L_H4 STAT=N PRED= 2.270 RANGE= 3.000
182_183 6.5482 J 07L_H4 07L_H5 STAT=N PRED= 6.640 RANGE= 0.200
182_186 6.5879 J 07L_H4 07L_H6 STAT=N PRED= 6.640 RANGE= 0.200
190_191 8.8736 J 08V_H2 08V_H3 STAT=N PRED= 12.880 RANGE= 6.000
191_192 6.5520 J 08V_H3 08V_H4 STAT=N PRED= 6.640 RANGE= 0.200
191_195 6.7834 J 08V_H3 08V_H5 STAT=N PRED= 6.640 RANGE= 0.200
201_202 7.6281 J 09V_H2 09V_H3 STAT=N PRED= 12.960 RANGE= 4.000
202_203 6.4961 J 09V_H3 09V_H4 STAT=N PRED= 6.640 RANGE= 0.200
202_206 6.7760 J 09V_H3 09V_H5 STAT=N PRED= 6.640 RANGE= 0.200
212_213 11.1630 J 10Y_H2 10YH3A STAT=N PRED= 12.890 RANGE= 4.000
212_214 4.7143 J 10Y_H2 10YH3B STAT=N PRED= 1.900 RANGE= 4.400
213_214 -13.7295 J 10YH3A 10YH3B STAT=N PRED= -16.760 RANGE= 2.560
215_218 0.4880 J 10Y_H5 10Y_H7 STAT=N PRED= -0.300 RANGE= 0.500
217_218 0.6708 J 10Y_H9 10Y_H7 STAT=N PRED= 1.020 RANGE= 1.200
223_224 7.1764 J 11I_H2 11I_H3 STAT=N PRED= 3.450 RANGE= 9.000
224_225 11.6481 J 11I_H3 11IH4A STAT=N PRED= 6.640 RANGE= 0.200
224225B 8.6548 J 11I_H3 11IH4B STAT=N PRED= 6.640 RANGE= 0.200
224_228 6.8064 J 11I_H3 11I_H5 STAT=N PRED= 6.640 RANGE= 0.200
225AB -15.2022 J 11IH4A 11IH4B STAT=N PRED= 6.640 RANGE= 0.200
25_229 6.5064 J 11IH4A 11I_H6 STAT=N PRED= 6.640 RANGE= 0.200

Appendix Z (continued)

```
 25B229     6.8064   J 11IH4B   11I_H6    STAT=N  PRED= 6.640 RANGE= 0.200
 232_233    1.9005   J 12F_H2   12F_H3    STAT=N  PRED= 1.900 RANGE= 6.600
 234_238    1.3335   J 12F_H5   12F_H5    STAT=N  PRED= 1.980 RANGE= 1.200
 234_235    7.6508   J 12F_H5   12F_H6    STAT=N  PRED= 7.660 RANGE= 0.340
 234_237    0.7769   J 12F_H6   12F_H5    STAT=N  PRED= 0.550 RANGE= 0.750
 234_236    1.2760   J 12F_H5   12F_H7    STAT=N  PRED= 1.260 RANGE= 1.200
 235_237    1.7027   J 12F_H6   12F_H6    STAT=N  PRED= 1.480 RANGE= 1.200
 235_236    7.4760   J 12F_H6   12F_H7    STAT=N  PRED= 7.400 RANGE= 0.240
 241_242    8.8924   J 13V_H2   13V_H3    STAT=N  PRED= 12.320 RANGE= 6.000
 242_243    6.8372   J 13V_H3   13V_H4    STAT=N  PRED= 6.640 RANGE= 0.200
 242_246    6.4162   J 13V_H3   13V_H5    STAT=N  PRED= 6.640 RANGE= 0.200

CONTROL PARAMETERS:
      Solvent =  none (def. 99% enriched)
        1.000 =  Concentration (vol%, def=1.0%)
   0.00100000 =  Minimum line-intensity
   0.00100000 =  Diagonalization criterium (not in use)
 700.15197800 =  FIELD(1H,MHz), used to transform shifts to ppms
  11.63296542 =  Left frequency (ppm)
  -4.33374659 =  Right frequency (ppm)
      10.000 =  Acquisition time (s, for QMTLS)
       0.000 =  Line-width (for modes D, P & T, 0=use defaults)
  0.094246347 =  Data-point resolution (Hz)
      28.306 =  GAUSSIAN (%, 0=use default from INF)
     -10.087 =  Dispersion contribution (%, 0=use default from INF)
   0.00000000 =  Decoupling frequency (for DORES)

CONSTRAINTS (in equations X0 = 1.0)...use no empty lines
 EQUAL 01Val_H2 = 06Val_H2
 EQUAL 07Leu_H5 = 07Leu_H6
 EQUAL 13Ile_H5 = 13Ile_H6
  0.000 * 1.0 =
  1.000 * 1.0 = -0.011 * 1.0
 IGNORE(HZ):  3441.747 to  3420.668
 IGNORE(HZ):  2323.920 to  2309.428
 IGNORE(HZ):  2328.672 to  2324.470
 IGNORE(HZ):  2288.657 to  2282.788
 IGNORE(HZ):  2392.691 to  2378.287
 IGNORE(HZ):  2251.845 to  2238.507
 IGNORE(HZ):  2197.427 to  2189.958

PSEUDO SPECTRUM(IN PPM):
      1     4.5945      0.0110      2.1609      0.0000      0.0000      0.0000     1     1

END of FILE
```

VITA

Wei Gao

826 S Claremont Ave Apt. 3, Chicago IL 60612
Cell phone: (+1)312-330-4150 | E-mail: wgao3@uic.edu or weigao14@gmail.com

SUMMARY

Team-oriented, creative researcher with inter-disciplinary knowledge and technique skills spanning from chemistry to biology, and intense training on pharmacognosy, in particular, isolation and chemical characterization of secondary metabolites from nature products, is seeking a research position in the pharmaceutical or biopharmaceutical or natural product based industry.

EDUCATION

August 2008 – August 2014	**Doctor of Philosophy** in Medicinal Chemistry University of Illinois at Chicago College of Pharmacy, Chicago, Illinois Cumulative GPA 4.0/4.0
August 2004 – June 2008	**Bachelor of Science** in Basic Pharmacy China Pharmaceutical University Nanjing, Jiangsu, China Cumulative GPA 89.5/100

RESEARCH EXPERIENCE

Institute for Tuberculosis Research, University of Illinois at Chicago
2009 – 2014, Graduate researcher

High-throughput screening of an actinomycete extract library using antimicrobial and cytotoxicity assays, to identify and prioritize top hit extracts and their parent strains.

Bioassay-guided isolation of novel anti-*Mycobacterium tuberculosis* peptides from an actinomycete strain, using orthogonal separation schemes involving countercurrent chromatography and kinds of column chromatography.

Structure elucidation of new anti-TB peptides (approximately 1600 amu m.w.) by comprehensive spectroscopic analyses including LC-HR-MS, LC-MS^2, NMR and X-ray crystallography.

In vitro testing of active compounds, including antimicrobial and stability assays (the latter in simulated gastric fluid, simulated intestinal fluid, and microsomes).

Formulation development (simple suspension, as emulsions and in micelles) and in vivo (mouse) testing. Developed high-sensitivity analytical methods for the assay of active compound in blood and lung tissues of mice. Determined the pharmacokinetics and assessed likely efficacy.

Molecular target identification of the active compound by genome sequencing of lab-generated resistant *M. tuberculosis* strains.

TEACHING and TRAINING EXPERIENCE

College of Pharmacy, University of Illinois at Chicago
2009 – 2011, Teaching Assistant for professional level classes.

TECHNICAL SKILLS

Pharmacognosy

Wide range of natural product chemistry methods: extraction procedures; fractionation by countercurrent chromatography (including HSCCC and CPC), size exclusion, adsorption, and lipophilic affinity chromatographies; quantitative analysis by HPLC with detection by MS, UV/vis and orthogonally with qHNMR aided by quantum mechanics-based Full Spin Analysis (HiFSA). Structure determination by 1D and 2D NMR analyses together with HRMS, IR, UV and CD spectroscopy, and, where necessary chemical derivatization and/or degradation.

Analytical/Spectroscopic Skills

LC-HRMS and LC-MS^2: experienced user on Shimadzu's LC-single Quadruple mass analyzer, LC-IT-TOF, and AbSciex's LC-Qtrap 4000 (condition optimization, quantitative and qualitative analysis).
NMR: experienced user on Bruker's 400-DPX and 400-Avance, 1D/2D data (^{1}H, ^{13}C, ^{1}H-qNMR, HSQC, HMBC, COSY, TOCSY, ROESY) acquisition and processing.
Others: UV/Vis, infrared red (IR) and circular dichroism (CD).

Microbiology

Culturing of *M. tuberculosis* (H37Rv, Erdman, single drug resistant strains), *Mycobacterium smegmatis, Escherichia coli, Candida albicans, Staphylococcus aureus.* Evaluation of antimicrobial effects on these strains. Generation of drug-resistant *M. tuberculosis* strains. Ability to work in BSL-2 and BSL-3 lab.

Cell Culture

Toxicity test using the African Green Monkey kidney cell line (VERO).

Biochemistry

Mycobacterium DNA extraction, electroporation.

Drug Delivery

Preparation and assessment of polymeric micelles by dialysis.

***In vivo* (mice) Pharmacokinetics**

Blood (serum) and lung tissue sample processing by protein precipitation, and analysis by LC-MS^2.

Computational Skills

LC-MS/LC-MS^2 data processing: LabSolutions and Analyst® Software.
NMR data processing: MestreNova, Topspin, and PERCH NMR Tools (for ^{1}H iterative full spin analysis).
Other softwares: ChemDraw, ChemSketch, PRISM, GIMP, Microsoft Office (Word, Excel, PowerPoint, Outlook, OneNote), EndNote.
Languages: fluent in Mandarin Chinese (mother language) and English.

HONORS and AWARDS

December 2011	Invited speaker to US-Japan Cooperative Medical Science Program 46th Tuberculosis and Leprosy Research Conference, Omiya, Japan
February 2011	W.E. van Doren Scholarship
May 2011	American Society of Pharmacognosy Student Travel Award
2006-2008	Excellent Undergraduate Scholarships from China Pharmaceutical University
December 2007	Second Grade Scholarship endowed by Suzhou Capsugel Ltd.

PROFESSIONAL MEMBERSHIP

Student member of American Association for the Advancement of Science (AAAS), and the American Society of Pharmacognosy (ASP)

SCIENTIFIC ARTICLES and PRESENTATIONS

Publication

1. W. Gao, J. Kim, S. Chen, S. Cho, J. Choi, B. U. Jaki, Y. Jin, D. C. Lankin, J. Lee, S. Lee, J. B. McAlpine, J. G. Napolitano, S. G. Franzblau, J. Suh, G. F. Pauli. Discovery and Characterization of the TB Drug Lead Ecumicin. Accepted by *Organic Letters.* (2014)DOI:10.1021/ol5026603
2. E. M. Grzelak, M. Choules, C. H. Hwang, J. W. Nam, S. G. Mulugeta, J. B. McAlping, G. Cai, W. Gao, D. C. Lankin, J. G. Napolitano, J. W. Suh, S. H. Yang, J. Cheng, J. Kim, S. Cho, G.F. Pauli, S. G. Franzblau, B. U. Jaki. A new concept for anti-tuberculosis drug discovery. *Planta Medica* (2014)80:CL8.
3. W. Gao, J. G. Napolitano, J. Kim, I. Lee, J. Lee, J. Choi, M. F. Rodríguez-Brasco, B. U. Jaki, S. Cho, J. B. McAlpine, G. F. Pauli, J. Kim, J. Suh, S. G. Franzblau. New insights on the structure of the anti-TB peptide H14: Crystal structure, ^{1}H NMR full spin analysis, and biosynthetic pathway. *Planta Medica* (2012)78:PJ134.

Publications in preparation

1. W. Gao, J. Kim, J. R. Anderson, T. Akopian, S. Hong, H. Jin, O. Kandror, J. Kim, I. Lee, S. Lee, J. B. McAlpine, S. Mulugeta, S. Sunoqrot, Y. Wang, S. Yang, T. Yoon, A. L. Goldberg, G. F. Pauli, J. Suh, S. G. Franzblau, S. Cho. *The cyclic peptide ecumicin targeting clpC1 is active against Mycobacterium tuberculosis in vivo.* Submitted to *Antimicrobial Agents and Chemotherapy*.
2. W. Gao, J. G. Napolitano, D. C. Lankin, J. B. McAlpine, J. Kim, Y. Jin, J. Suh, S. Chen, Lee, G. F. Pauli. Complete ^{1}H NMR spectral analysis of ecumicin. To be submitted to *Magnetic Resonance in Chemistry.*
3. W. Gao, J. G. Napolitano, J. Bisson, D. C. Lankin, J. B. McAlpine, J. Suh, S. G. Franzblau, G. F. Pauli, NMR structure sequencing of structurally related oligo peptides. To be submitted to *Journal of Organic Chemistry.*

Patent

1. J. W. Kim, S. W. Lee, S. J. Park, J. W. Suh, I. A. Lee, T. M. Yoon, J. K. Choi, J. E. Lee, J. Y. Kim, Y. Y. Jin, S. G. Franzblau, S. Cho, W. Gao, G. F. Pauli, J. B. McAlpine, J.G. Napolitano, B. U. Jaki, B. Friesen, M. F. Rodriguez Brasco, D. C. Lankin, Cyclic Peptide from *Nonomuraea sp*., Process for the Production thereof, and Pharmaceutical Composition for the Prevention or Treatment of Mycobacteria Related Disease Comprising the Same (2012)WO2012144790A1

Oral presentations

1. E. M. Grzelak, M. Choules, C. H. Hwang, J. W. Nam, S. G. Mulugeta, J. B. McAlping, G. Cai, W. Gao, D. C. Lankin, J. G. Napolitano, J. W. Suh, S. H. Yang, J. Cheng, J. Kim, S. Cho, G.F. Pauli, S. G. Franzblau, B. U. Jaki. A new concept for anti-tuberculosis drug discovery. (2014) ASP 55th annual meeting.
2. W. Gao, M.F. Rodriguez Brasco, B. Jaki, , J. G. Napolitano, S. Cho, M. Choules, J.B. Friesen, D. Lankin, I. A. Lee, J. McAlpine, J.W. Suh, T. Yoon, S. Franzblau and G. Pauli, Novel Anti-tuberculosis Leads from a *Nonomuraea sp.* (2012) Annual MIKI meeting
3. W. Gao, M.F. Rodriguez Brasco, B. Jaki, , J. G. Napolitano, S. Cho, M. Choules, J.B. Friesen, D. Lankin, I. A. Lee, J. McAlpine, J.W. Suh, T. Yoon, S. Franzblau and G. Pauli, Discovery of Novel Anti-tuberculosis Peptides from *Nonomuraea sp.* (2011) ASP 52nd annual meeting
4. W. Gao, M.F. Rodriguez Brasco, B. Jaki, , J. G. Napolitano, S. Cho, M. Choules, J.B. Friesen, D. Lankin, I. A. Lee, J. McAlpine, J.W. Suh, T. Yoon, S. Franzblau and G. Pauli, Novel Anti-tuberculosis Leads from a *Nonomuraea sp.* (2011) US-Japan Cooperative Medical Science

Program Forty-Sixth Tuberculosis and Leprosy Research Conference, Omiya

Poster presentations

1. W. Gao, M. F. Rodriguez Brasco, B. Jaki, J. G. Napolitano, S. Cho, M. Choules, M. Kim, Y. Kim, I. A. Lee, D. Lankin, J. McAlpine, K. Peng, J. W. Suh, Y. Wang, T. Yoon, G. F. Pauli and S. G. Franzblau , Novel Anti-TB Peptides from *Nonomuraea sp.* (2012) University of Illinois at Chicago College of Pharmacy Research Day
2. W Gao, J.G. Napolitano, J.Y. Kim, I. A. Lee, J.E. Lee, J.K. Choi, J. W. Suh, M. F. Rodríguez-Brasco, B.U. Jaki, S. Cho, J.B. McAlpine, G.F. Pauli, and S.G. Franzblau. New Insights on The Structure of the Anti-Tb Peptide H14: Crystal Structure, ^{1}H NMR Full Spin Analysis, and Biosynthetic Pathway (2012) ASP 53rd annual meeting
3. W. Gao, M. F. Rodriguez Brasco, B. Jaki, B. Becker, S. Cho, J.B. Friesen, M. Kim, D. Lankin, I. A. Lee, J. McAlpine, J.W. Suh, T. Yoon, S. Franzblau and G. Pauli, Chemical Evaluation of Anti-tuberculosis Components in *Nonomuraea sp.* (2010) ASP 51st annual meeting